34th International Symposium on Archaeometry

3-7 May 2004

Zaragoza, Spain

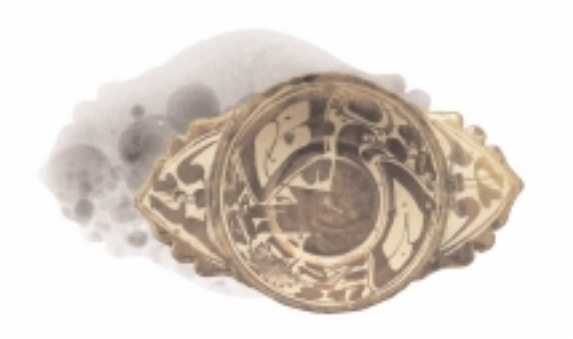

Institución «Fernando el Católico» (C.S.I.C.)
Excma. Diputación de Zaragoza

ZARAGOZA, 2006

CREDITS PREFACE COLLABORATORS INDEX ARTICLES

34th International Symposium on Archaeometry

3-7 May 2004, Zaragoza, Spain

The logo on the front cover represents a piece of lustre pottery from Muel (16th century), Museum of Zaragoza. The shadow is a TEM image of Cu nanocrystals forming the lustre layer.

START

Preface

On behalf of the organising committee and the University of Zaragoza I would like to welcome all participants to Zaragoza for the 34th International Symposium on Archaeometry.

We are very grateful to the institutions and individuals who assisted in making this conference possible and supported our work during its preparation. I would want to thank the financial supporters and in particular to the Aragonese Government, the University of Zaragoza and the Ministry of Science and Technology, for their important collaboration. Special thanks are due to Gres de Aragon and Euroarce that have supported the special session of this symposium: "Evolution and Technology of glazes".

Finally, Archaeometry 2004 would not have taken place without the collaboration and support of many other people, from Zaragoza and Barcelona, and I would like to thank them too, but there is not enough place in this page to write all their names.

I hope that all of you will enjoy this conference and the scientific work, but also that you will have enough time to visit and enjoy Zaragoza.

Josefina Pérez-Arantegui

Zaragoza, 2004

START

PUBLICACIÓN NÚMERO 2.621
DE LA
INSTITUCIÓN «FERNANDO EL CATÓLICO» (EXCMA. DIPUTACIÓN DE ZARAGOZA)
PLAZA DE ESPAÑA, 2 · 50071 ZARAGOZA (ESPAÑA)
TELS. [34] 976 28 88 78/79 · FAX [34] 976 28 88 69
ifc@dpz.es
www. ifc.dpz.es

ISBN: 84-7820-848-8
DEPÓSITO LEGAL: Z-1.368/2006
PREIMPRESIÓN: Ebro Composición, S.L. Zaragoza.
IMPRESIÓN: Sociedad Cooperativa, Librería General. Zaragoza.

IMPRESO EN ESPAÑA. UNIÓN EUROPEA.

34th INTERNATIONAL SYMPOSIUM ON ARCHAEOMETRY

3-7 May 2004, Zaragoza, Spain

Organising Institutions

Department of Analytical Chemistry of the University of Zaragoza
Patrimoni-UB Group of the University of Barcelona

Rectorado
Universidad de Zaragoza

Consejo Social
Universidad de Zaragoza

MINISTERIO DE CIENCIA Y TECNOLOGÍA

GOBIERNO DE ARAGON
Departamento de Ciencia, Tecnología y Universidad

GOBIERNO DE ARAGON
Departamento de Educación, Cultura y Deporte

Sponsors of the special session Evolution and Technology of Glazes

Gres Aragón

Lumineco

Collaborating institutions

AYUNTAMIENTO DE ZARAGOZA

CORTES DE ARAGÓN

DIPUTACIÓN DE ZARAGOZA

100 Años CAI

Bodegas Aragonesas

INSTITUCIÓN FERNANDO EL CATÓLICO

Z T

START

INDEX

INDEX

INDEX

1. FIELD ARCHAEOLOGY

INDEX

GEOPHYSICS AND ARCHAEOLOGY AT LA MESA SITE, CHICLANA DE LA FRONTERA, CÁDIZ (SPAIN)

Luis Barba Pingarrón
Laboratorio de Prospección Arqueológica. Instituto de Investigaciones Antropológicas. UNAM. México D.F. barba@servidor.unam.mx

Salvador Domínguez-Bella
Departamento de Cristalografía y Mineralogía. Facultad de Ciencias. Universidad de Cádiz. Puerto Real. 11510. Cádiz (Spain)

José Ramos Muñoz; Vicente Castañeda Fernández
Manuela Pérez Rodríguez and María Sánchez Aragón
Área de Prehistoria. Universidad de Cádiz. Facultad de Filosofía y Letras. 11001. Cádiz (Spain)

1. INTRODUCTION

La Mesa is a large archaeological site (80 Ha) with deep cultural roots (Neolithic, Copper and Bronze Age societies besides Roman and Islamic settlements). It is located near the modern town of Chiclana de la Frontera, in Southern Spain, in a strategic position along the Iro river valley lying on a promontory that dominates the natural pass and thus the trade between the coast and the hinterland.

An international project carried out jointly by teams from the University of Cadiz and the National University of Mexico undertook the pilot application of geophysical techniques on order to verify and extend the archaeological evidence provided by limited archaeological excavations.

2. OBJECTIVE

One of the goals of this project was to contribute to the understanding of the vertical and horizontal distribution of the numerous settlements at the site, by defining the spatial limits of each individual archaeological area. This would supply the corroboration needed for planning future excavations.

Finally, it was important to test the capability of many geophysical and geochemical techniques in that specific geological environment.

Figure 1. Location map of the archaeological site of La Mesa, at Chiclana de la Frontera, Cádiz, Spain.

3. METHODOLOGY AND PROSPECTING TECHNIQUES

When working on this site the first step was to carry out a systematic archaeological survey. We recovered archaeological materials, dated from Neolithic to Medieval times, which were later subjected to laboratory tests.

The topographic survey provided the base map to place the rest of the archaeological indicators.

For the magnetic survey, we used a GEOSCAN FM36 gradiometer, while for the electric survey we resorted to a Bradphys IV resistivity meter.

The work conditions for the gradiometer were four readings by meter along lines that were one meter apart. The electric readings were undertaken over the same lines with a Wenner array and a one meter electrode spacing.

Oblique aerial photographs using a light aircraft offered an overview of the whole site and showed some faint color traces suggesting buried archaeological remains in certain specific parts. Among others, scarce vegetation could be seen in the upper part, related to the Neolithic settlement area, while light-colored elongated areas trace the smashed walls surrounding this upper part and, finally, a rectangular structure, recently discovered at the southeastern corner of the field, seems to have been

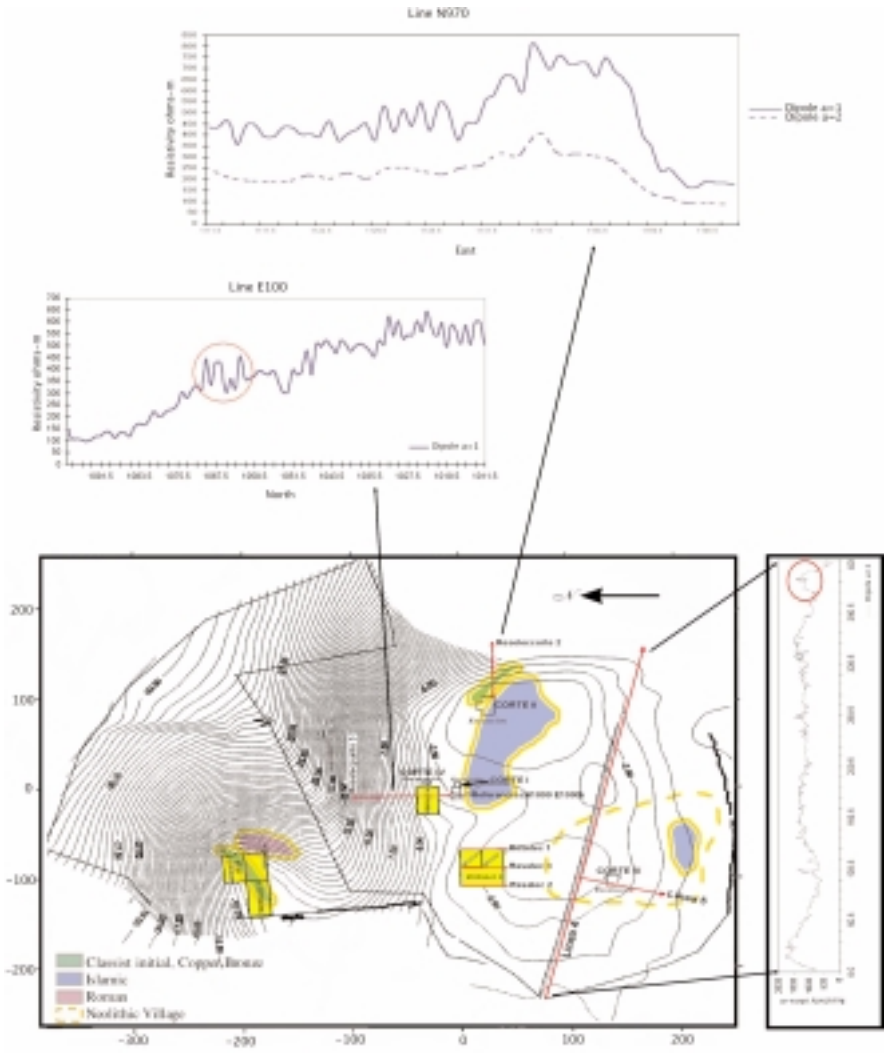

Figure 2. Topographic map showing in yellow the areas with surface material concentrations, in red electric resistivity lines and magnetic grids in yellow rectangles.

produced by the shallow alignment of the building materials. Unfortunately, aerial photographs were taken some weeks following the geophysical studies thus preventing the application of techniques in some of the features discovered later.

From the geophysical point of view, one of the outstanding information provided by the magnetic gradient studies permitted to detect the presence of

a faint circular induced magnetization anomaly interpreted as a ring-shaped ditch at the Neolithic settlement area.

On the other hand, extended electric resistivity lines ascertained the presence of a large defensive wall enclosing the Islamic settlement by the northern and eastern sides.

Magnetic gradient and electric resistivity surveys provided information confirming and somewhat extending the earlier archaeological findings. This is the case of the grid close to the excavated storage pit area where electric and magnetic results suggested the existence of more pits, enlarging the excavated area at least by 10 more meters.

4. FINAL COMMENTS

Taking into consideration the surface extension and the chronological depth of the archaeological site, compared with the shortness of time for the archaeological prospecting pilot project, it can be considered successful and very promising.

The combined interpretation of aerial photographs, geophysical, surface survey and archaeological excavation data, support the original idea that it was an important strategic site occupied by different societies during a large time frame. This seems to be mainly due to their access to a wide array of local resources and to their control of the movement between the inland and the costal zone.

In the concentration area of the Neolithic surface material, through magnetic gradient it was possible to define subtle circular anomalies that might have been produced by refilled trenches distinctive of the human settlements from that time.

During the Islamic era, the largest structures were built at the site, among them the perimeter walls and the already excavated storage pits. Geophysical results displayed high electric resistivity readings approaching the north and western walls, in addition to the clear electric and magnetic anomalies that could be seen along the west side of the storage pits excavated area.

The promising data recovered during fieldwork supported the proposal presented to the Andalusian government when we requested the funding we needed to study the entire area applying all the available geophysical techniques, and when putting together a joint project with the University of Cadiz, National University of Mexico and the University of Georgia (USA).

ACKNOWLEDGMENTS

We are grateful to Mr. Jose Mª Carrascal for his constant and enthusiastic support during the acquisition of data during field work and the acquirement of aerial pictures.

We appreciate the facilities provided by site owner Mr. Esteban Fernandez, and the help of Francisco Martinez y Andres Ciruela during different stages of the project.

REFERENCES

Ramos, José; Montañés, Manuel; Pérez, Manuela; Castañeda, Vicente; Herero, Nuria; García, María Eugenia y Cáceres, Isabel (editing and coordination).

1999. *Excavaciones arqueológicas en La Mesa (Chiclana de la Frontera, Cádiz). Temporada de 1998. Aproximación al estudio del proceso histórico de su ocupación*. Arqueología en Chiclana de la Frontera nº 1. Ayuntamiento de Chiclana de la Frontera. Fundación Vipren. Chiclana de la Frontera. Cadiz.

GEOPHYSICS AND ARCHAEOLOGY AT SANTA CRUZ ATIZAPAN, CENTRAL MEXICO

Luis Barba, Agustín Ortiz, Jorge Blancas, and Yoko Sugiura
Instituto de Investigaciones Antropológicas,
Universidad Nacional Autónoma de México

1. INTRODUCTION

The application of a suite of prospecting techniques for the study of archaeological sites from the surface, combined with reconnaissance and test pits made possible to obtain a better understanding for the distribution pattern, construction techniques and possible function of man-made "islands" occupied during the late Classic (550/650 AD) and the Epiclassic (650-900 AD) periods in the northeastern margin of the Chignahuapan Marsh, at Santa Cruz Atizapan, located in the Toluca Valley, Central Mexico (figure 1). The existence of more than a hundred mounds made virtually impossible to excavate the entire site. Considering limited time and financial resources, the geophysical survey of the site, in combination with the archaeological verification, was a practical and effective alternative.

The site of Santa Cruz Atizapan is divided in two areas: the central area is conformed by several monumental architectures, built on artificial terraces at the northeastern lakeshore of the Chignahuapan, whereas the sustaining area consists of more than a hundred man-made "islands" constructed in a marshland, covering a surface which exceeds a square kilometer.

Aerial photography taken by helium balloon produced a series of photographic mosaics of the terrain, while the topographic map was utilized to determine the size, location and distribution of the mounds. Magnetic gradient covered large surface extension, whereas georadar and electric resistivity were effective for verifying specific group of anomalies. Several test pits and one intensive-extensive archaeological excavation provided information difficult to be obtained by geophysical methods such as depth, chronology and characteristics of buried architectural features.

2. GEOPHYSICAL PROSPECTING SURVEYS

For the magnetic gradient survey, we used GEOSCAN FM36 gradiometer taking four readings by meter with one meter between lines. For those areas

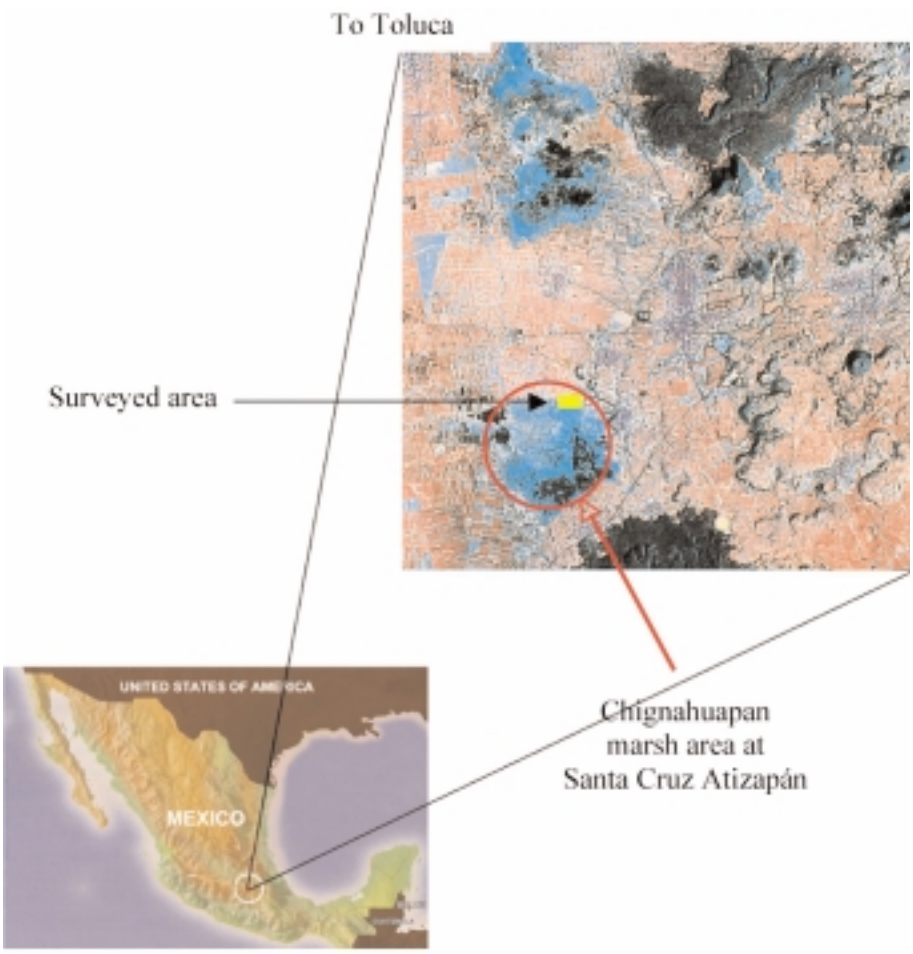

Figure 1. Location map. Surveyed area can be seen in yellow to the north of the Chignahuapan marsh.

where the anomalies were registered during the survey, radar and electric studies were conducted. Electric study was carried out employing BRADPHYS IV and GEOSCAN RM 15, using Wenner and pole-pole arrays. In addition, some electric pseudo-sections were registered, providing information of lateral and vertical variations of the electrical resistivity along lines at specific places. As a final stage of survey, GPR or georadar studies were carried out, using SIR System 2 with antennas of 300 AND 400 MHz from GSSI, to obtain detail information of areas with anomalies identified by the other techniques.

3. RESULTS

Magnetic survey registered a very good contrast between the low magnetic properties of the sediments and volcanic stones used for construction. Most of the small mounds located during the topographic survey have magnetic dipoles clusters interpreted as collapsed stone walls, although in some cases we have found that stones were not used as construction material.

Focus on the distribution pattern of the mounds, the topographic map seems to indicate that the smallest mounds are built far away from the lakeshore, in which predominates swampy and unstable soil condition, unsuitable for the construction of large mounds.

The most outstanding linear feature registered during magnetic survey was a buried stone concentration with nearly 300m long, which ran from southeast to northwest with two meters wide. We speculate that it could represent a dike, an aqueduct or some type of pathway, but we have to wait for its confirmation until the adequate excavation will be carried out.

3.1. Southern Complex

A cluster of 13 small mounds built, according to magnetic gradient images, with significant amount of small stones conforms the Southern Complex. In the present environmental conditions, this cluster is located at the edge of the marshland. Based on detailed analysis of electric and radar survey, we propose hypothetically that, over the natural lacustrine sediments a platform constructed by piling earth was built, and then superimposed floors and stonewalls formed the mounds.

3.2. Mound 20

It refers to one of the largest mounds, originally located in the marshland, which is the only one entirely excavated. Previous geophysical studies identified some of the late stage constructions uncovered by the excavations such as the circular wall foundation, the stone concentration in a roughly circular distribution that covers the northwestern edge of the mound and a the stone clusters forming a square shape surface. The excavation of this mound uncovered floors, some of which were identified by the radar study. Intensive, as well as extensive excavations uncovered seven well-defined floors, which were successively laid. The first five present rectangular layout, while the last two floors corresponding to the Epiclassic period are circular in form (figure 2).

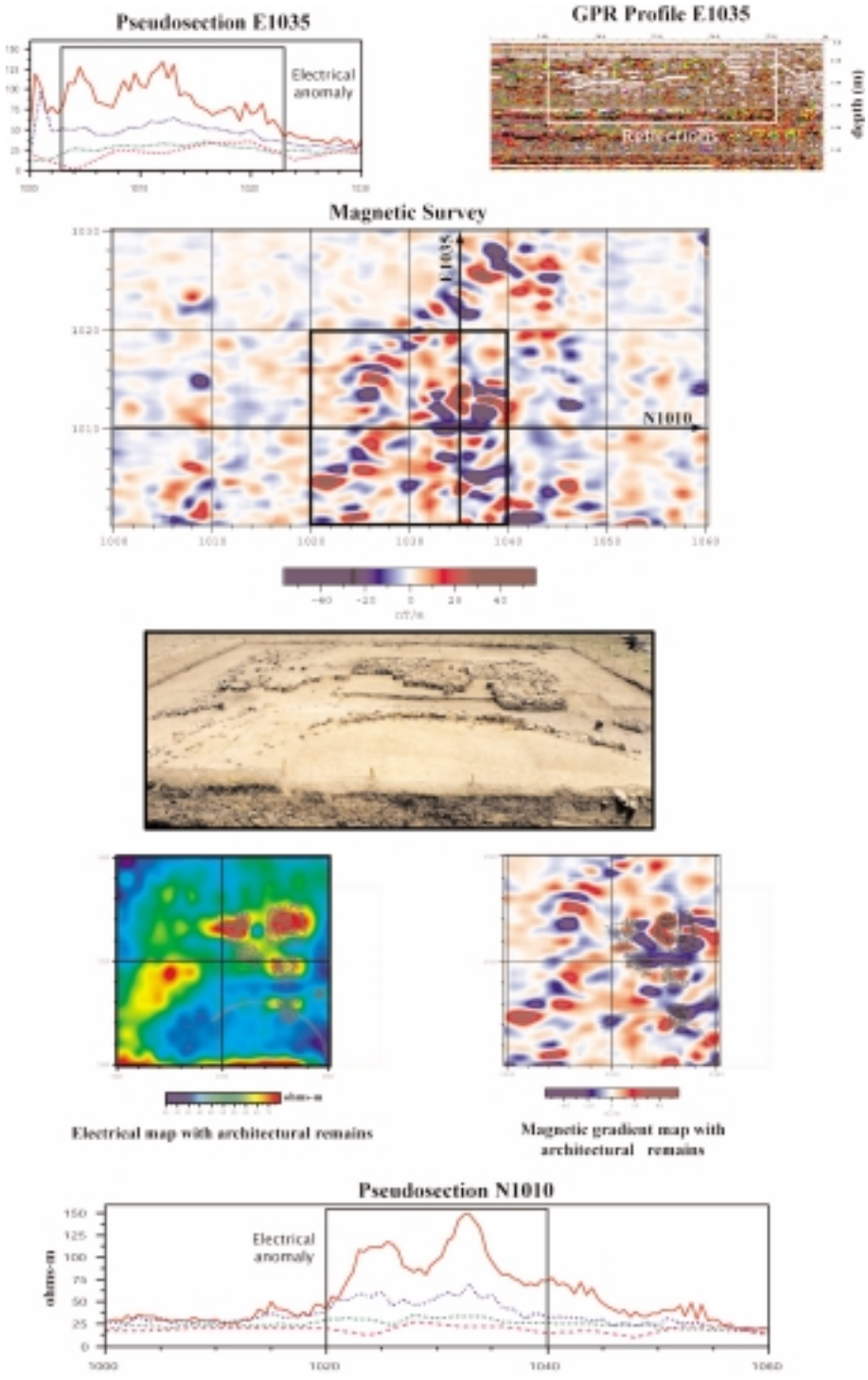

Figure 2. Geophysical results from Mound 20.

3.3. La Campana-Tepozoco

This corresponds to the civic-religious sector of the site, originally consistent of several monumental architectures and one pyramid called La Campana (The Bell). It is located roughly 500 m to the north of the lakeshore. Magnetic studies registered anomalies with circular tendency to the north of La Campana pyramid, which represented building stone foundations. Radar studies indicated that the magnetic anomalies were less than 1.3m in depth. Finally, archaeological excavation uncovered a partially destroyed stonewall of the circular structure 18m in diameter.

4. CONCLUSIONS

Spatial distribution patterns of the man-made "islands", their sizes, the proximity to the civic sector of the site, as well as the archaeological evidence obtained from geophysical data and excavations, indicated that the most of these mounds were constructed and used as domestic or habitational units, supporting one or two houses. Although the excavation of the Mound 20 provided evidence that this was built as public space.

Several field seasons of archaeological prospection and excavations, together with detailed laboratory analysis revealed that the inhabitants of the site of Santa Cruz Atizapan developed a complex internal social and political structure during the final stage of the Classic and the subsequent Epiclassic periods (550-900AD). In addition, the studies confirmed that these people had well organized labor force and technical capacity to solve specific environmental problems and to build many domestic mounds and some large architectures.

REMOTE SENSING AND FIELDWALKING SURVEY APPLIED TO THE STUDY OF ANCIENT LANDSCAPES: AN INTEGRATED APPROACH

Stefano Campana
Landscapes Archaeology, Dep. of Archaeology and History of Arts,
University of Siena at Grosseto
campana@unisi.it

Cristina Felici
Ph.d student, Dep. of Archaeology and History of Arts, University of Siena
felicicri@unisi.it

1. INTRODUCTION

In this paper we will discuss our experience with the gradual introduction of new methodologies and the problems of integrating different surveying techniques in the archaeological mapping of South Tuscan landscapes, specifically in the administrative areas of Grosseto and Siena.

The need to test new instruments and new approaches to surveying derives from a certain dissatisfaction with the results obtained through previous methods. The main problems encountered in the landscape analysis could be summarized as follow:

- degeneration of the surface finds due to more than half a century of ploughing.
- Low level of visibility, whether from the ground or from the air.
- The remaining land consists mainly of agricultural cultivation on heavy clay soils that are known to be an unfavourable surface for most remote sensing techniques.
- Areas with a higher level of visibility consist mainly of the alluvial plains of substantial rivers. In some of these areas, however, other problems arise from the great thickness of the layer of alluvium and from the impact of modern industry and residential development.

The strategy developed to face this situation is directed towards an integrated use of those remote sensing techniques that leave a wide choice to the archaeologist of times of the year to capture data capture and in particular

towards the study of the region of the electromagnetic spectrum not visible to the human eye (CAMPANA-FRANCOVICH 2003).

1.1. Aerial Survey

We started a programme of aerial survey in 2000 averaging 45 hours of flight per year collecting more than 12000 oblique air photographs. The use of exploratory aerial survey in Italy has only become possible in recent years. In ideal conditions this technique offers an extraordinary contribution to the search for new sites and for the continuous monitoring of the cultural heritage (fig. 1a). The flexibility of the method in allowing us to respond to the development of archaeological traces with extreme rapidity is of great benefit and importance. The archaeologist is free to choose conditions of lighting that range from soon after dawn to almost sunset as flying conditions (MUSSON *et al.* 2005).

1.2. Ikonos and Quickbird Satellite imagery

The introduction of satellite imagery was aimed in the first place at providing a total, continuous and objective view of a whole area at a particular moment of the year as planned by the archaeologist (CAMPANA 2002). The second feature is the capacity to provide multispectral data (and in particularly in the red and near-infrared region) to monitor plant health and to detect water-stress in vegetation where it cannot be seen by the naked eye (fig. 1b).

1.3. Historical vertical air photographs

Vertical aerial photographs, spanning with their wide temporal range, represent an irreplaceable source for the analysis of the Tuscan landscape (GUAITOLI 2003). Anyone interpreting the photographs through a digital photogrammetric workstation will see a 3D replica model of landscape as it was in 1938, 1954, 1976 or 1994. In addition to their historical content, vertical photographs are of course an important source for the conduct of "aerial reconnaissance" (fig. 1c).

1.4. Field walking survey

The technique of field-walking is aimed at the systematic investigation of sample areas and at the verification of the remotely sensed evidence. In the last 25 years of field-walking about 9000 sites have been detected in the provinces of Siena and Grosseto (FRANCOVICH-VALENTI 2001). Field survey constitutes therefore an important source for the archaeological study of settlement patterns. Nevertheless the collected information often turns out to be incomplete, confused and difficult to interpret because of post-depositional processes in the field, if not integrated with other sources of information (fig. 1d).

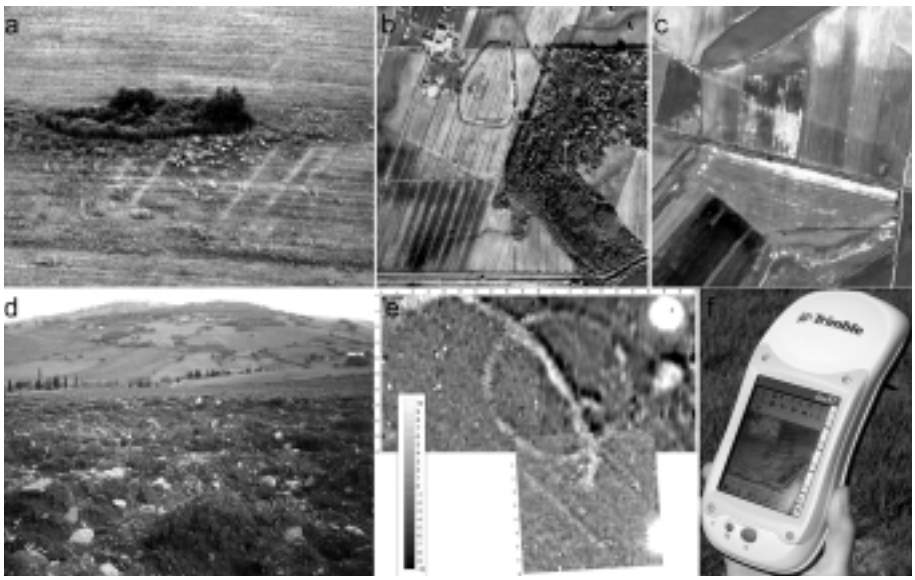

Figure 1. a) Oblique air photograph of the ancient roman city of Heba (GR); b) vertical air photograph of an early middle age village (LI); c) Quickbird-2 satellite imagery showing at the centre a linear feature corresponding to a roman road; d) artefact scatter recognized during field-waking survey in the Orcia valley; e) example of a double enclosure detected with the gradiometric survey; f) PDA computer showing on the screen the background layer of the result of the different remote sensing analysis and on the front the GPS position.

1.5 Magnetic survey

In 2003 we tested a system of data acquisition that allowed us to cover one hectare per day at a resolution of 60 cm along traverses which were each set 1 metre apart.

So far we have only acquired data for 15 hectares surveying 12 archaeological sites. The general trend arising from the results seems to confirm that the degree of detail, although not very high, is sufficient to show with a good approximation the position of the main features, depending on the characteristics of the materials to which the magnetometer is reacting (fig. 1e).

1.6 Field Data integration: PDA technology

The merging of PDA and GPS technologies goes far beyond the level of increased fieldwork efficiency, enabling data integration directly in the field and at best allowing the systematic application of strategies and methodologies developed in the past. These have only rarely been applied before because of the excessive amount of time required (Ryan-Van Leusen 2002). Best results

and a larger number of applications are possible only if the PDA mobile GIS system has the real time support of a GPS base station (fig. 1f).

2. CASE STUDY: PIEVE DI PAVA (SIENA)

The site of Pieve di Pava represents an important case study for us because we undertook an archaeological excavation there, between July and August 2004, which was the first chance to verify and compare the remotely sensed data with the observed stratigraphy. The case study is a good example of the integrated research strategy illustrated in the first part of our paper. The site had been discovered during the field-walking in 2000. We repeated the surface collection in 2001, 2002 and 2003 with significant results for the understanding of the function and chronology of the site. At that stage the surface data showed the presence of a roman settlement still alive in the late antiquity and the available documents revealed the existence of an early middle age church in the same area (FELICI 2003). The second step was the study of the vertical aerial photographs taken in the 1954, 1976 and 1996 (fig. 2a). Because of the geological characteristic of the area (heavy clay soil) the analysis of the vertical aerial photographs was negative. The same results come form the aerial survey that we began in the spring of 2002 and that we repeated over different seasons in 2003 and 2004 (fig. 2b/c).

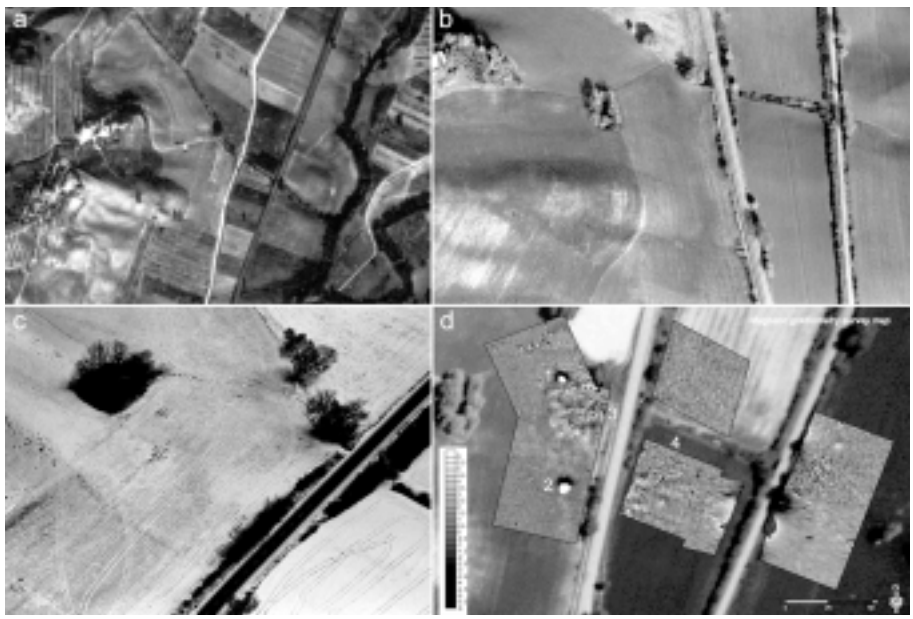

Figure 2. a) Vertical air photograph of year 1954; b) oblique air photograph of spring 2002; c) oblique air photograph of winter 2004; d) gradiometric survey with resolution of 1 m.

A real improvement of the site knowledge was granted by the gradiometric survey. Firstly we acquired data for 2 hectares at a resolution of 1 metre between traverses (fig. 2d). This level of detail allowed us to recognize the position of many features that greatly enrich the interpretation of the site, thus enabling us to distinguish with a good approximation two main areas features (fig. 2d n. 3 and n. 4), in one case elucidating site geometry (fig. 2d n. 3), and some strong dipoles (fig. 2d n. 1 and n. 2). Before the excavation we reduced the resolution to 25 cm along traverses and 50 cm apart in order to make a comparison. Notwithstanding an unquestionable enrichment of the data and the improvement in the resolution of the shapes, new features could not be detected. The excavation strategy had been planned following mainly the data of the magnetic survey. The correspondence after the first two months of excavation was impressive. On the dipole showed in fig. 2 n.1, an anomaly with values between -13 and +73 nT/m, we made a 3 by 3 m test excavation. At a depth of

Figure 3. a) Kiln; b) not yet identified productive activity; c) the church.

about 50 cm we found the remains of a kiln, characterized by the presence of bricks, some of them showing clear traces of exposure to high temperature (fig. 3a). The second dipole (-33/+98 nT/m) corresponded, at a depth of about 2 m, to a red clay stratification related to some kind of manufacturing activity that we still have to explore stratigraphically (fig. 3b). Taking into consideretion the value of the magnetic anomaly in relationship to its depth, it is possible to assume the presence of a high temperature activity related to some kind of furnace. Another significant confirmation of the interpretation of the magnetic data come from the lager area (20 by 10 meters) that we excavated (fig. 2d n. 3). The mosaic magnetogram showed numerous rectangular features with E-W orientation, which we interpreted as buildings. The northern side of the main anomaly, a rectangular feature measuring 20 by 10 meters with values between -3 and +6 nT/m, corresponds to the wall of a church, about 80 cm large, made of stones, bricks and mortar (fig. 3c).

ACKNOWLEDGMENTS

The authors are indebted to Prof. Salvatore Piro (ITABC – CNR) for their invaluable comments and criticisms on geophysical survey techniques and data processing. A special thanks are due to Claus Strøander by proofreading the translation of the text and to the team of the Landscapes Archaeology and Remote Sensing Laboratories of the University of Siena at Grosseto: F. Pericci, M. Corsi, E. Vaccaro.

REFERENCES

Campana, S., 2002. High resolution satellite imagery: a new source of information to the archaeological study of Italian landscapes? Case study of Tuscany. In Space Applications for Heritage Conservation, (Strasbourg, 5-8 Nov. 2002), CD-ROM.

Campana, S. and Francovich, R., 2003. Landscape Archaeology in Tuscany: Cultural resource management, remotely sensed techniques, GIS based data integration and interpretation. In The Recontruction of Archaeological Landscapes through Digital Technologies, (Boston, MA 1-3 novembre 2001), BAR SERIES 1151, pp. 15-28.

Felici, C., 2003. *Il caso della Val d'Orcia*, in *Chiese e insediamenti nelle campagne tra V e VI secolo*, Mantova, pp. 276-285.

Francovich, R., and Valenti, M., 2001. Cartografia archeologica, indagini sul campo ed informatizzazione. Il contributo senese alla conoscenza ed alla gestione della risorsa culturale del territorio. In La carta archeologica. Fra ricerca e pianificazione territoriale, Florence, 6-7 May 1999, Florence, pp. 83-116.

Guaitoli, M., 2003. Lo sguardo di Icaro. Rome.

Musson, C., Palmer, R. and Campana, S., 2005. *In volo nel passato*, Firenze.

Ryan, N. and Van Leusen, M., 2002. *Educating the Digital Fieldwork Assistant*, in Proceedings of CAA 2001, BAR International Series 1016, pp. 401-416.

GEOPHYSICAL SURVEY AND ARCHAEOLOGICAL VERIFICATION OF PREHISTORIC IRON PRODUCTION AREAS AND MEDIEVAL GLASS-WORKING SITES

Křivánek Roman
Institute of Archaeology of Academy of Sciences of Czech republic
Letenská 4, 118 01 Praha 1, Czech Republic
fax: +420-2-57532288, email: krivanek@arup.cas.cz

1. INTRODUCTION

The use of geophysical methods (magnetometry) for survey of different types of production areas has long tradition in bohemian archaeology. During more than last 20 years over 25 high medieval (mainly from 14th and 15th century AD) glass-works were surveyed by different magnetometric methods (various kinds of magnetometers and also kappameters). Since 2nd half of 90´s about 10 another prehistoric (from Iron Age, La Téne or Roman period) iron production areas were also surveyed or tested by magnetometric methods. All of these sites were surveyed by another field survey methods, nearly half of these sites were verified by archaeological excavation. This long-time cooperation of geophysicist and archaeologist helped to less expensive realization of rescue archaeological excavations or to evidence of unprotected archaeological sites. Subsequent cooperation of methods in more cases helped also to discovery of more efficient survey procedures of similar sites with typical production activity and better preliminary interpretation of particular production features before excavation.

2. POSSIBILITIES AND METHODOLOGY OF GEOPHYSICAL MEASUREMENTS

Magnetometric methods are the most suitable geophysical methods for field survey of production areas, particular detection of production and non-production features (furnaces or waste heaps), another sunken features (pits,…) and also for study of magnetic properties of different burned materials. Magnetic characteristics of all remains of production features are

mainly dependent on level of thermoremanent magnetization. Intensity (max. temperature), length of time of heating and also state of preservation of features are the main component for level of amplitudes of magnetic anomalies over burned materials. Some of differences in magnetic characteristics of different production features we can also observe during magnetometric surveys in the field. But possibilities of measurements are very dependent on type of field survey, methodology and on stage of present archaeological activities on production site. Different magnetometric field measurements (in different scale, aim and results of work) we can apply in 3 different stages of archaeoactivities on site: preliminary area prospection of site, detailed survey of particular situations and production features, detailed study of individual features in open archaeological situation. During the first stage according to the type of production site and terrain we can apply first survey of site by magnetometers in grid-net 1x0,25 m (Cs-magnetometer or fluxgate gradiometer prospection) to 1x1 m (protone magnetometers). This intensity of field data seems to be enough for basic identification of high magnetic production features and their concentrations. For particular survey of production features during the second stage we need for magnetometers more detailed grid-net 0,5x0,5 m to 0,25x0,25 m. In this scale of work we can also observe shape, dimensions or orientation of production features or separate more individual production features in group. During the third stage with use of kappameters in situ it is important to use grid-net 0,2x0,2 m or 0,1x0,1 m for detailed study of magnetic properties of choosen production features.

3. EXAMPLES OF RESULTS

3.1. Iron production areas

Detailed magnetometric survey within subsequent archaeological verification of iron production site (La Téne period) near Mšecké Žehrovice, distr. Rakovník documents efficient cooperation of more methods on arable fields in Central Bohemia (*Křivánek 2001*). For Cs-magnetometers survey has been chosen area identified by previous systematic field walking by typical big surface concentration of massive iron slags. In magnetometric result we can also identify a lot of these small point magnetic anomalies (+5-15 nT/m) from particular ploughed out slags in topsoil but we can also separate here some wider places of higher magnetic anomalies (+20-30 nT/m) with diameter approx. 1-3 m and negative border which could represent origin places of strongly burnt furnaces. Places of two highest magnetic anomalies were verified by limited trenches (archaeological excavation by Foster in 2001). The small subsurface/subsoil relic of iron-furnance was identified above one magnetic anomaly, the probable presence of iron-furnance above the second anomaly was not possible to verify and there was identified on the

level of subsoil only relic of burned soil (possible destruction of place, deep ploughing, intensive erosion). Detailed magnetometric research was copleted with surface artefact collection of slag and experimental research by metal detector (verified possibility of identification of slags only with higher content of iron). The result of combined geophysical and archaeological activities confirmed probable poor state of iron production site which has been ploughed over a long time.

Magnetometric surveys of polycultural prehistoric (Neolithic, La Téne, Roman period) and Early Medieval settlement and also iron production (La Téne) site near Hostivice, distr. Praha-západ is an example of various detailed measurements in open archaeological situation during rescue archaeological excavations by Pleinerova in 2002 NW of Prague. Results of Cs-magnetometer survey outside of open archaeological excavation confirmed presence of another mainly prehistoric sunken settlement features (magn. anomalies +5-10 nT/m) in similar concentration of features as on excavated area. Use of the same geophysical equipment inside of open excavation (with removed soil layer) helped then in more detailed scale to separate high burned concentrated material (over +15 nT/m), possible iron production features from another low magnetic sunken features. Presence of more small iron furnaces confirmed also archaeological excavation. Another detailed magnetometric measurement was also realized near another uncovered La Téne iron working center. The use of kappameters for detailed measurements in situ in open archaeological situation helped here to identify the most burned centers of one larger iron-production feature and different level of heating of two nearby small furnaces. Both small areas were also verified by kappameter measurements on vertical profiles where was possible to observe poor state of preservation of preserved only bottom (15-30 cm) sunken parts of iron-furnaces.

3.2. Medieval glass-working sites

Various and subsequent magnetometric measurements of high medieval glass-works Kyjov, distr. Děčín (14th/15th century AD) shows different role of magnetometric methods during different stages of prospection, survey and also excavation of glass-working site in Lusatian mountains region. The first prospection of site by protone magnetometers contributed to basic separation of more production features by amplitudes and dimension of magnetic anomalies: glass-furnaces with approx. +30-120 nT/m and diameter 2-4 m; glass waste heaps with approx. +5-15 nT/m and diameter over 10 m. Aditional detailed magnetic survey over production features could help to precise identification (dimensions, orientation, shape) of glass-furnaces and possible origin (main glass-furnace with highest magnetic anomalies; another cooling glass-furnaces with lower magnetic anomalies and often smaller dimensions) of glass-furnaces before excavations. The use of kappameter

measurements in situ above uncovered glass-furnace helped in first stage of excavation to identification of orientation of central heating channel where apparent magnetic susceptibility was higher than in perimeter rim of furnace. Archaeological excavations up to now (*Černá 2003b*) uncovered 2 different glass-furnaces, 1 glass waste heap and other non-production situations, third glass-furnace should be excavated in summer 2004.

Magnetometric survey of newly discovered high medieval glass-working site Gabrielina Hut', distr. Chomutov (from 14th century AD) is example of prospection of endangered site by new afforesting in Ore Mountains region (*K?ivánek 2003*). Measurements by protone magnetometers and kappameter were realized after the first finds of typical glass-working material. Only low magnetic unhomogenous anomalies (+5-15 nT/m) probably from recently redistributed glass-working material were discovered in area of new afforesting and recent terrain changes with glass-working finds (*Černá 2003a*). Two subrectangular high magnetic anomalies (about +100 nT/m) from glass-furnaces together with other low magnetic anomalies (+5 nT/m) from scattered production waste material were than identified not far in forested and more hilly terrain. The results of geophysical survey shows the centre of site within identified 2 high magnetic anomalies above glass-furnaces seems to be still in forested area outside of recent wood exploitation and new afforesting of disturbed terrain. From detailed magnetometric measurements we can say these furnaces should be still in subsurface in good state of preservation. Archaeological excavation of site will be applied in dependence on another new afforesting of central place of site with geophysicaly verified glass-furnaces.

4. CONCLUSION

Results of geophysical surveys of common small features with typical high magnetic burned materials of production sites have many similarities but also some specifics. Because magnetometric data from particular measurements share very often similar results we can summarize these results within types, amplitudes or the average surface extent of magnetic anomalies. 3 main types of archaeo-features (furnaces, waste heaps, another sunken features) within 3 different types of magnetic anomalies are very typical for all of production areas (*Křivánek 1995*). The furnaces have very significant positive magnetic anomaly, very limited area and typical negative border around. Prehistoric iron-furnaces have diameter 1-2 m, High Medieval glass-furnaces diameter 2-5 m. Amplitudes of magnetic anomalies over iron and glass furnaces are very different, common magnetic anomaly of glass-furnaces is much higher than magnetic anomaly of iron-furnaces. This fact we could probably connect not only with different dimensions, length and level of heating of raw material but also with specific length of use of production features. The main iron-production features have very often specific location in terrain, glass-working

sites have also typical geometry or orientation not far from water sources. The waste heaps have wide positive and often unhomogenous less magnetic anomaly. Their variable diameter 2-15 m depends on configuration of furnaces, length of use and state of preservation of site. Other subsurface relics of sunken archaeological features have lower positive magnetic anomalies. Their common diameter is 1-5 m and they are mainly connected with different settlement activities without burned materials.

Different magnetometers in different scale of field work we can use for identification of site and more detailed survey of particular production features. The first results of prospected production sites by continuous method of readings by Caesium magnetometers demonstrated the new possibilities of quick and efficient prospection of large (iron) production areas in agricultural lowland or flat field regions. The other examples of prospection of smaller production areas (glass-works) by protone magnetometers shows advantages of point measuring in conditions of afforested, variably sloped, less flat and more complicated terrains. The results of surveys of very small areas by detailed point measuring of magnetic susceptibility in situ by kappameter documents another possibilities of use of magnetic methods in open archaeological situations or during archaeological excavations.

REFERENCES

Černá, E. *2003a:* Neue Belege für die mittelalterliche Glaserzeugung im nordwestlichen Böhmen. *Glashütten im Gespräch*, Berichte und Materialien vom 2. Internationalen Symposium zur archäologischen Erforschung mittelalterlicher unf frühneuzeitlicher Glasghütten Europas, 57-64, Verlag Scmidt-Römhild, Lübeck.

Černá, E. 2003b: Das Fundgut einer mittelalterlichen Glashütte in Nord-Böhmen. Beitrage zur Mittelalterarchäologie in Österreich 19, 107-118.

Křivánek, R. 1995: Shrnutí výsledků geofyzikálních měření na místech zaniklých středověkých skláren – Geophysical measurements at the deserted medieval glass-works. In: Blažek, J.- Meduna, P. (eds.): *Archeologické výzkumy v SZ Čechách v letech 1983-1992* - Sborník ÚAPP SZČ Most, 279-308.

Křivánek, R. 2001: Přínos měření cesiovými magnetometry pro průzkum i výzkum archeologických lokalit v Čechách v letech 1999-2000 – Contribution of caesium magnetometer measurements in prospection and research of archaeological sites in 1999-2000. In: R. Nekuda - P. Kouřil - J. Unger (eds): Ve službách archeologie III – In service to Archaeology III, Brno, 114-131.

Křivánek, R. 2003: Geofyzikální průzkum zaniklé sklářské huti Gabrielina Huť, okr. Chomutov – Geophysical survey of abandoned glass-working site Gabrielina Hu', distr. Chomutov. *Historické sklo* 3, sborník pro dějiny skla, Městské muzeum Čelákovice, 119-126.

CHEMICAL RESIDUES OF HUMAN ACTIVITIES IN SAN VINCENZO AL VOLTURNO

Alessandra Pecci
Dipartimento di Archeologia e Storia delle Arti, Università di Siena

Federico Marazzi
Istituto Universitario Suor Orsola Benincasa, Napoli, Italia

1. INTRODUCTION

Human activities leave traces. Some of the traces, or by-products of these activities are composed of chemical compounds that are absorbed by the floors. Ethnoarchaeological experiments have demonstrated that the chemical compounds in floors do not have a random distribution and that there is a close relationship between certain types of human activities and the chemical enrichment of floors (Barba and Lazos 2000, Barba and Ortiz, 1992; Ortiz, Pecci and López Varela, in press). Thus, analyzing the chemical compounds absorbed in the floors it is possible to identify the acticivities that produced them. Furthermore, while archaeological objects move around, chemical compounds do not and stay where activities actually were carried out, suggesting an interesting way of studying "activity areas" and their spatial distribution (Barba and Lazos 2000).

2. THE PROJECT

San Vincenzo al Volturno (Molise, Italy) is at the moment one of the best known italian Early Medieval sites. According to the Chronicon Vulturnense, a document written in the early 12 th century, the monastery was founded near the Volturno watersprings between the end of the 7th and the beguinning of the 8th century a.C. It flourished quickly under the influence of the Dukes of Benevento and then of the Franks. Afterwords an earthquake, first, and an attack from the Arabs, in 881 destroyed it. In this occasion a big fire burnt almost all the monastery. During the 10th and 11th centuries it was rebuilt but then little by little it lost its properties and importance (Marazzi F. in press, Marazzi et al. 2003).

The archaeological project, carried out by the Sovrintendenza of the Molise Region and the Istituto Universitario of Suor Orsola Benincasa, in Naples, was

characterized by extensive and accurate excavations on a large-scale surface, that permitted to trace the historical development of the monastery.

This was the perfect occasion to test floor analysis techniques developped in Mexico on italian sites and understand their potential in the interpretation of Medioeval contexts.

3. METHODOLOGY

200 floor samples were obtained by drilling holes at the intersections of a square meter grid covering the site. The samples were analyzed in the Archaeometry Laboratory of the Medieval Area of the Archaeology Department of the University of Siena, using techniques developed by Barba, Rodríguez and Córdova (1991) in Mexico.

The analyses were used to detect the pH values and the presence of phosphates, protein residues and fatty acids in the floors. The mapping of the results was done using a GIS application (Arc View): to interpolate the results the kriging method was used.

At the interpretative stage, all the maps are considered together in order to evaluate the relations between the distributions of the different compounds. They are then related to the other archaeological materials found on the floors during excavation, such as ceramics, lithics and biological material, in order to trace the spatial distribution of activities. Chemical analysis were performed on one side on floor samples recovered from a room with a known function, the kitchen of the monastery, in order to establish the chemical patterns characteristics of the cooking activity. On the other side rooms with unknown functions were studied in order to find out the activities carried out there. This is the case of the room placed next to the kitchen and of room CF.

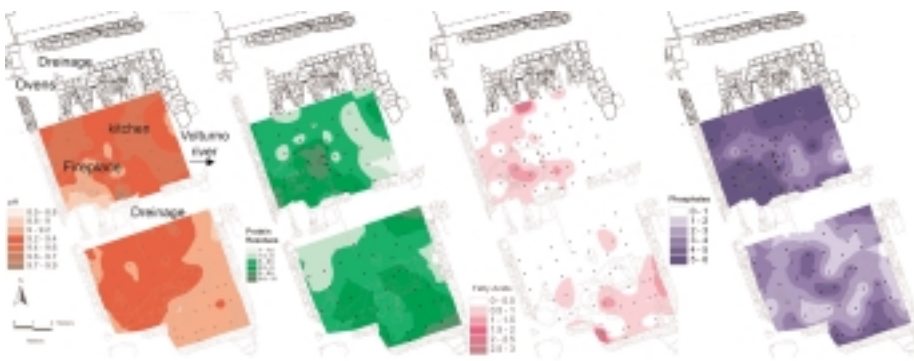

Figure 1. The results of the chemical analyses of the kitchens floors.

4. THE KITCHENS

The monastery kitchen was placed near the river in order to have easy access to the water. In the south-western corner of the room there was a big fireplace, made of bricks and clay. In the northern part there was a cooking platform, of which only four cavities - the firing chambers- are still in place. Next to the kitchen there was another room, called the "anti-kitchen" probably used to prepare or store the food.

The high values of Ph indicate the presence of ash in all the rooms. This suggests a big fire consumed the area. The evidence for this is the presence of charcoal fragments and ash in the floor. This fire was recognized to be the 881 fire described in the Chronicum Volturnense, related to the Arab attack to the monastery.

In previous studies relatively higher values of pH permitted to identify specific areas of heating, related to food preparation, even in cases where there were high global values of pH due to fire in the whole room (Pecci 2001). Here, the fireplace is instead characterized by relatively lower pH values. This can be due to the difference of the construction materials: the bricks of the fireplace may have absorbed less ash than the dirt floor that was very rich in charcoal fragments and ashes, probably produced by the fire and by the burnt material swan from the firing chambers of the ovens. Therefore we have to use different chemical compounds to identify the patterns that can be considered typical of the activities carried out in the kitchen. The results of the analysis of the phosphates, fatty acids and protein residues revealed interesting patterns. The phosphates, indicating the presence of organic material, were concentrated mainly on the fireplace and next to it. They were present also in the area in front of the ovens. These concentrations were related to the high values of fatty acids (indicating the presence of fats, oils, resins..) and protein residues (present in blood, meat, eggs..). This suggest that the monks may have intensely used the fireplace, the area around it and the ovens for food preparation.

Traces of activities were found also in the room next to the kitchen. Most of the room is characterized by average values of all chemical compounds. Ethnographic and archaeological studies showed that this pattern is typical of activities that do not leave chemical traces, such as sleeping and storing solid materials (Manzanilla and Barba 1990, Barba and Ortiz 1992). For this reason, part of the room may have been a storage area. In the Chronicon Volturnense it is in fact written that "frumentum et legumina in fluvium, qui secus effluit, disparserunt" suggesting that the cellaria were placed near the river. The southern part of the room - probably a small room - may have been used to carry out "dirty" activities related with the food preparation that left intense traces of fatty acids, protein residues and phosphates.

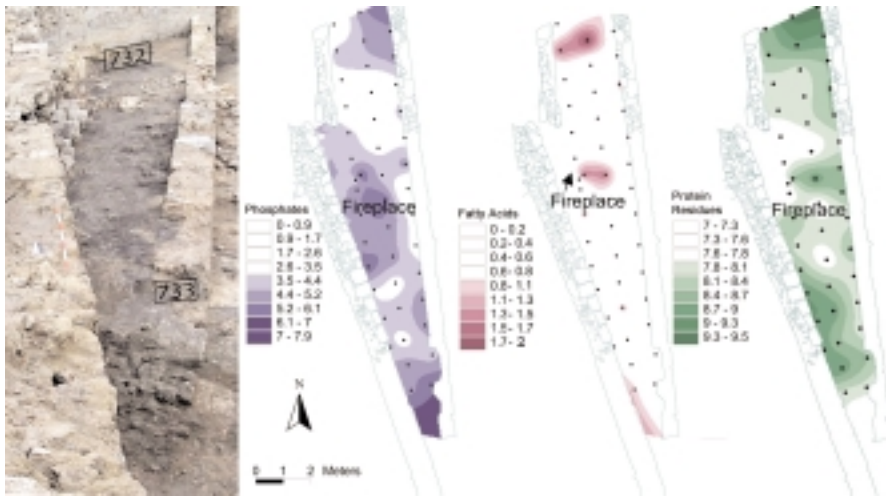

Figure 2. The results of the chemical analyses of Room CF floor.

5. ROOM CF

The room called CF is a long and narrow room, a sort of a "blind corridor". While it is easy to know the activities carried out in the kitchen, in room CF the strange form of the room and the small dimentions did not suggest any particular activity.

The chemical study of floors was carried out hoping that some suggestion could come to solve the problem. Two areas of concentration of chemical compounds were detected applying the interpolation of the results of the chemical analysis. They are particularly interesting, as they are characterized by the presence of phosphates, protein residues and fatty acids concentrations. This corresponds to the typical chemical patterns of the food preparation and consumption areas observed at ethnoarchaeological and archaeological level, as well as to the monastery kitchen (Barba and Ortiz 1992, Barba and Lazos 2000; Manzanilla and Barba 1990; Pecci and Ortiz 2003). Considered the type of room and the presence of real kitchens in the monastery, this hypothesis seemed to be quite strange. But it was supported by the presence of a fireplace in the central part of the room and of cooking vessels and table jars found during excavation. Their presence lead at first to think of a storage room. But considering together the archaeological findings and the chemical concentrations, the hypothesis that the fireplace was used to carry out food preparation activities started to make sense. CF may therefore have been used as a temporary kitchen during construction or restoration works in the monastery.

6. CONCLUSIONS

Although all the rooms studied suffered an important fire in the 9th century, it was possible to detect the presence of chemical residues in the floors. Studying the monastery kitchens it was possible to recognize the patterns that are typical of food preparation activities. It was also possible to give an interpretation of the activities carried out in rooms with an unknown function, such as the room next to the kitchen and room CF. Considered the type of room and the presence of real kitchens in the monastery, the cooking activities in room CF would have been imperceptible had one only studied the distribution of archaeological materials found on the floors.

Furthermore, the use of GIS has revealed to be an important instrument for the mapping of the results of the chemical analysis and their interpretation. GIS makes possible the storage of this type of data and its integration to the whole archaeological information recovered. Then it is interesting to point out that chemical analysis of floors may have an application for the intra site analysis and, used in combination with other techniques, constitute an effective archaeological tool for discerning ancient living patterns.

REFERENCES

Barba L., Lazos L., 2000. Chemical Analysis of Floors for the Identification of Activity Areas: A Review. Antropología y Técnica, 6:59-70.

Barba L., and Ortiz A., 1992 Análisis Químico de los Pisos de Ocupación: Un Caso Etnográfico en Tlaxcala, México. Latin American Antiquity, 3(1):63-82.

Barba L., Rodriguez R. and Córdova J.L., 1991. Manual de técnicas microquímicas de campo para la arqueología, Cuadernos de Investigación. IIA, UNAM, Mexico D.F.

Manzanilla L. and Barba L., 1990. The Study of Activities in Classic Households, Two Case Studies from Cobá and Teotihuacan. Ancient Mesoamerica 1(1):41-49.

Marazzi F. San Vincenzo al Volturno: evoluzione di un progetto monastico fra IX e XI secolo. In Il monachesimo italiano dall_età longobarda all'età ottoniana. Atti del VII Convegno di Studi Storici Benedettini,- Pontida (BS), 10 - 14 sett. 2003, Centro Storico Benedettino Italiano, in press.

Marazzi F., Filippone C., Petrone P.P., Galloway T., 2003. San Vincenzo al Volturno: scavi 2000-2002. Rapporto Preliminare. Archeologia Medievale 29: 209-274.

Ortiz A., Pecci A., and López Varela S., Ethnoarchaeological Study of chemical Residues in a "living" household in Mexico, Geoarchaeological and Bioarchaeological Studies. Vrije Universiteit, Amsterdam, in press.

Pecci A., 2001. The chemical analysis of floors. A case study in Teotihuacan, Proceedings of the 32th International Symposium of Archeometry, april 2000, Mexico, IIA, UNAM, Mexico (CD publication).

Pecci A. and Ortiz A., 2003. El estudio de estructuras arqueológicas del Centro de México a través del análisis químico de sus pisos. Quaderni di Thule, n. I, Atti del XXIII Convegno Internazionale di Americanistica (Perugia, 2001), Argo Editore, Perugia: 227-232.

2. DATING

INDEX

IRSL AND GLSL DATING STUDIES OF SAMPLES FROM NEOLITHIC SITE, ÇATALHÖYÜK-TURKEY

AKOĞLU, K.G.
Archaeometry Dept., METU, Ankara, Turkey, e-mail: gakoglu@yahoo.com

ÖZBAKAN, M.
Physics Dept., METU, Ankara, Turkey, e-mail: ozbakan@metu.edu.tr

ÖZER, A. M.
Archaeometry&Physics Dept., METU, Ankara, Turkey, e-mail: aymelek@metu.edu.tr

1. INTRODUCTION

Luminescence dating techniques, i.e. thermoluminescence (TL) and optically stimulated luminescence (OSL), have been widely used for dating inorganic materials such as bricks and sediments. In luminescence dating, quartz and feldspars are the minerals primarily concerned and comprises the measurement of the charge accumulated within the traps of the crystals of these minerals. The charges in these traps result from the decay of the naturally occuring radioelements such as, potassium-40, thorium-232 and uranium-238. Thus the luminescence dating is a method based on the storage of energy emitted by radioactivity.

The principle lies beneath the luminescence dating techniques is that the response of naturally-occuring minerals to environmental radiation is cumulative overtime. Independent measurements can determine both the total radiation dose received by the mineral and the environmental dose rate it experienced *in situ* (Huntley *et al*,1985). The age then can be deduced (Aitken, 1974). In other words, the basic principle of luminescence dating is to compare the dating signal with the signals obtained from portions to which known doses of nuclear radiation have been administered by a radioisotope source with a known activity. This comparison allows the evaluation of laboratory dose of nuclear radiation needed to induce luminescence equal to that acquired subsequent to the most recent bleaching event, paleodose (Aitken, 1998). In principle the age is then calculated using the equation:

Age = Paleodose / Annual Dose.

The annual dose represents the dose rate at which energy is absorbed from the flux of nuclear radiation emitted by the radioactive impurities of ^{232}Th, ^{238}U and ^{40}K in the material, as well as by cosmic rays and by ^{87}Rb to a minor extent. The annual dose, evaluated by assesment of the radioactivity of the material carried out both in the laboratory and on-site.

Çatalhöyük was first discovered by James Melaart in the late 1950s (Melaart, 1967) and excavated by him between 1961 and 1963. The site rapidly became famous internationally due to the size and dense occupation of the settlement, as well as the spectacular wall paintings and other arts that were uncovered inside the houses. Since 1993, an international team of archaeologists, led by Ian Hodder, has been carrying out new excavations and research.

Catalhöyük was phased by levels of buildings by Melaart. He also discovered 15 Neolithic levels numbered 0 (latest) to XIII (earliest), with two sub levels at VI level as VIA and VIB.

The buildings in the settlement were built of sun-dried mud brick, plaster, wood beams, and woven mats. Excavations today reveal a plan of rectangular houses built in a labyrinth-like arrangement. Each house has its own separate walls but is built next to each other.

Mud bricks are suitable materials for luminescence dating since they contain feldspars and quartz. Their production process involves direct exposure to light for drying.

In this note, we report OSL studies carried on mud brick samples from Çatalhöyük site. In the following paragraphs we report the results of the experiments performed to determine the ages of the mud brick samples using both with IRSL (Infra Red Stimulated Luminescence) and GLSL (Green Light Stimulated Luminescence) techniques.

2. EXPERIMENTAL STUDIES

Ten mud brick samples from different levels were collected and sent to the METU (Middle East Technical University), the Archaeometry Program of the Graduate School of Natural and Applied Sciences in 1998 and 1999. The collection of suitable samples must be done under very strictly controlled conditions during which the sample is exposed to no light, since the OSL signal is extremely sensitive to light.

Samples for measurements were taken by carefully scraping the surfaces of the bricks which may have been exposed to light during collection. Then they were treated with hydrochloric acid (HCl, 10%) and hydrogen peroxide (H_2O_2, 38%) to remove any organics, and thoroughly rinsed with distilled water, then with acetone in order to remove all traces of chemicals from the

previous treatments. Samples were subdivided into coarse grains (>90μm) and fine grains (<90μm). These were prepared following standard thermoluminescence (TL) dating procedures as described by Aitken (1985) and placed on aluminum discs.

Optically stimulated luminescence of samples were measured using ELSEC 9010 Optical Dating System. A broadband green light source was used as a stimulation source for quartz samples. An array of infrared diodes was used for the polymineral fine grains (Spooner *et. al* 1990) resulting in a signal mainly from feldspars. The "Natural Normalization" technique is used to normalize the data obtained after irradiation.

The Equivalent Dose (ED) was determined by the multiple aliquots additive dose (MAAD) technique, where the laboratory doses added to aliquots of the natural sample and the growth is extrapolated to zero luminescence signal to give the ED (Rees-Jones and Tite, 1997). Samples were irradiated by a $^{90}Sr/^{90}Y$ source which is delivering 0.0308Gy/sec.

In order to remove unwanted signals originating from shallow traps, which are filled during the laboratory irradiation but empty in natural samples, preheating was used. All quartz samples were preheated at 220°C for 5 minutes while the polymineral samples stimulated by infrared were at 160 °C for 2h. Water content was determined as a percentage of dry weight.

Uranium and thorium contribution to annual dose rate was estimated by low level alpha counting (ELSEC Low level alpha counter 7286) system, Potassium contribution was determined by the $K_2O\%$ content with Atomic Absorption Spectrometry (AAS). External gamma and cosmic ray components of annual dose rate by placing TLD discs (Al_2O_3:C) and kept for eight months in the site where samples were taken.

OSL ages of ten samples with their uncertainties, studied in this work are summarized in table 1. Here age refers to the time past since the samples' last exposure to light.

SAMPLE	LEVEL	IRSL AGE (1000 YRS)	GLSL AGE (1000 YRS)
S3727	VII	1.16 ± 0.10	1.14 ± 0.12
S3724	VII	8.50 ± 1.04	8.28 ± 1.09
S3707	VII	2.37 ± 0.23	2.80 ± 0.28
S3715	VII	1.37 ± 0.11	3.03 ± 0.49
S3716	VII	2.17 ± 0.17	4.28 ± 0.33
S4240	VII	3.07 ± 0.23	5.68 ± 0.92
S2817	VII	8.54 ± 0.69	8.45 ± 0.73
S5206	IX	7.72 ± 0.62	7.14 ± 0.57
N3830	VI-V	2.83 ± 0.22	5.38 ± 0.47
N3010	VI-V	2.79 ±0.27	6.34 ± 0.57

Table 1. IRSL & GLSL ages of mud brick samples from different levels.

3. RESULTS

IRSL & GLSL ages for samples S2817 and S3724 are in agreement with each other, those ages support the overall dating sequence derived from radiocarbon and dendrochronology (Newton and Kuniholm, 1999).

Although IRSL & GLSL ages of sample S5206 are in aggrement, the ages are slighltly younger than the radiocarbon ages given for Level IX (Cessford, 2001).

IRSL & GLSL ages for samples S4240, S3716, S3715, S3707, N3010 and N3830 are not in agreement. This disagreement may be explained by the different rates of eviction of electrons in quartz and feldspar minerals when they are exposed to light (Godfrey-Smith *et al.*1988) This exposure occured probably during collection of samples.

The IRSL & GLSL ages of sample S3727 are in agreement however they stay younger than the overall dating sequence in Çatalhöyük (Newton and Kuniholm, 1999). This could be explained by anomalous fading. In the context of luminescence dating anomalous fading was first noted in an attempt to date lava flows using the TL of both polymineral fine grains and extracted feldspars (Wintle, 1973). Since OSL uses the same or similar traps and centers to TL, it is expected to see the same phenomenon in OSL. In laboratory induced luminescence there are contributions from traps however, because of fading, they do not contribute to the natural signal; therefore the ratio of the natural luminescence to laboratory induced luminescence is lower than it should be, so the evaluated age (Aitken, 1998).

The OSL ages of this study can be considered to be broadly reliable. In order to be certain, the OSL dating studies for the same and different levels of the same site must be repeated for a large number of samples. Therefore, for Çatalhöyük, to establish a chronology for the site, based on direct dating of building materials, OSL technique can also be considered.

REFERENCES

Aitken, M.J., Huxtable, J., Wintle, A.G., and Browman, S.G.E., 1974, Age Determination by TL: review of progress at Oxford. Proceedings of the Fourth International Conference on Luminescence Dosimetry, Krakow, Poland, 1005-1010.

Aitken, M.J. 1985, Thermoluminescence Dating. Academic Press, London.

Aitken, M.J. 1998, An Introduction to Optical Dating. Oxford University Press, Oxford.

Cessford, C. 2001, A new dating Sequence for Çatalhöyük, Antiquity 75, 717-25.

Godfrey-Smith, D.I., Huntley, D.J. and Chen, W.H. 1988, Optical dating studies of quartz and feldspar sediment extracts, Quaternary Science Reviews 7, 373-80.

Huntley, D.J., Godfrey-Smith, D.I. and Thewalt, M.L.W., 1985, Optically Dating of Sediments, Nature, 313, 105-107.

Melaart, J., 1967, Çatalhüyük: A Neolithic Town in Anatolia. London: Thames&Hudson

Newton, W. M. and Kuniholm, P.I., 1999, Wiggles Worth Matching-making Radiocarbon Work. The Case of Catalhoyuk, Aegaeum 20, Annales d'archaeologie egenne de l'universite de Liege et UT-PASP, 527-536.

Rees-Jones, J. and Tite, M.S. 1997, Optical Dating Result for British Archaeological Sediments, Archaeometry 39, 177-88.

Spooner, N.A., Aitken, M.J., Smith, B.W., Franks, M. and McElroy, C. 1990. Archaeological Dating by Infrared Stimulated Luminescence Using a Diode Array, Radiation Protection Dosimetry 34, 83-86.

Wintle, A.G., 1973, Anamolous Fading of thermoluminescence in mineral samples, Nature, 245, 143-144.

PALEOMAGNETIC DATING OF POLLEN STRATIGRAPHY FROM LAKE SEDIMENT BASED ON PSV MASTER CURVE FROM CENTRAL FINLAND

Teija Alenius, Antti Ojala and Mia Tiljander
Geological Survey of Finland, Betonimiehentie 1, FIN-02150 Espoo, Finland teija.alenius@gsf.fi

The local settlement history was investigated by means of pollen analysis from the sediment of Lake Orijärvi, Mikkeli, central Finland, situated close to the Ion Age dwelling site. The aim of the work was to investigate the development of the environment, settlement history and onset of cultivation on the area.

Dating of the profile was based on paleomagnetic dating. Reference material for paleomagnetic dating is based on a carefully constructed and independent varve chronologies from three annually laminated (varved) lake sediment records from central southern Finland. Lakes Alimmainen Savijärvi, Nautajärvi and Korttajärvi were estimated to contain a varve chronological error of ±1 %, and cover the last ca. 10 000 years. They provide a strong and stable signal of paleosecular variation (PSV) i.e. paleomagnetic master curve, that was applied to assign age-depth transformation for a homogeneous sediment sequence from Lake Orijärvi, Mikkeli.

Varved sediment records provide a powerful tool for high-resolution absolute dating of sediment deposits and have, therefore, an important role in calibrating other soft sediment dating techniques. Paleomagnetic dating results from the sediment of lake Orijärvi provided a continuous and precise chronology and provide an excellent basis for the study of cultural-related pollen stratigraphy of Orijärvi sediments deposits.

REFERENCES

Ojala, A. E. K. & Saarnisto, M. 1999. Comparative varve counting and magnetic properties of the 8400-yr sequence of an annually laminated sediment in Lake Valkiajärvi, Central Finland. Journal of Paleolimnology 22, 335-348.

Ojala, A. E. K., Saarinen, T. & Salonen, V.-P. 2000. Preconditions for the formation of annually laminated lake sediments in southern and central Finland. Boreal Environment Research 5, 243-255.

Ojala, A. E. K. & Tiljander, M. 2003. Testing the fidelity of sediment chronology: comparison of varve and paleomagnetic results from Holocene lake sediments from central Finland. Quaternary Science Reviews 22, 1787-1803.

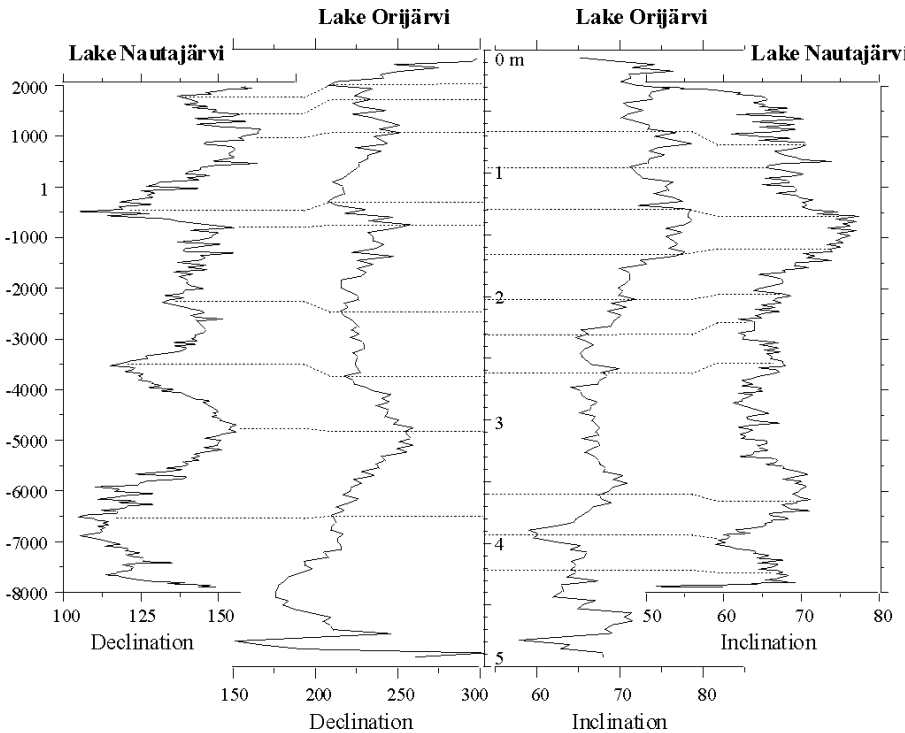

Figure 1. Comparison of Lake Nautajärvi and Lake Orijärvi (commune of Mikkeli) paleomagnetic secular variation curves (declination and inclination).

THERMOLUMINESCENCE AND ^{14}C DATING OF BRICK STRUCTURES IN S. LORENZO CHURCH IN MILANO. LATE ANTIQUE AND MEDIEVAL PHASES

Laura Fieni
Politecnico di Milano

A. Galli, M. Martini, E. Sibilia
INFM, sez. Milano-University of Milano Bicocca

T. Mannoni
I.S.C.M. Genova

ABSTRACT

The present study of the Laurentian complex in Milano has archaeological and archaeometric implications.

Through the archaeometric dating of several particular phases of the building history of the complex, especially those of tetraconc, S. Aquilino and S. Sisto chapels foundations, new reliable chronological and historiographic interpretations could be made, to better comprehend the meaning of the whole construction.

1. A FEW OBSERVATIONS ON THE USE AND INTERPRETATION OF ARCHAEOMETRIC DATA

The archaeometric methods we used are thermoluminescence (TL) dating (Aitken, 1985) and Radiocarbon (14-C), (Bowmann, 1990, Improta, 2002).

The first one was applied only to unbroken bricks and fictile tubes sampled in several wall structures of the complex. 14-C was used on wooden charcoal scrapes contained in the joint of mortars of walls. In absence of scrapes, calcium carbonates clots found in the mortars themselves were employed.

In general the dates obtained were interpreted taking into account the following principles:

1) Each date represents a *post quem* limit for the building phase they belong to.

2) The dates obtained from the wooden charcoal clots of mortars are in direct relation to the time of edification and, more precisely, to the moment in which the lime is produced, because it cannot be recycled.

Wooden charcoal, residuals of the calcinations of limestone, survived the phase of extinction and carbonation of the lime, remaining within the mortar even after its hardening.

The main limit in their use as dating agents is that their residual content of 14-C is related to the moment in which the fixation of CO_2 in the tree ended. This means that, if old wood and part of the heart of the trunk was used as combustible in the furnaces, a considerable backdating of the object could result.

3) The dating of the carbonates found in the composition of the mortars is in principle possible.

The main problem in this application is the separation of the carbonate of the binder from other possible carbonates aggregates, like sand. Furthermore, there is the problem of the possible solution and re-crystallization of the carbonate. caused by water. In this case the sample resulted "younger" because the date would refer to the re-crystallization itself. Consequently, 14-C date should be considered as *ante quem* limit for the age of the item. The problem of the re-crystallization of the nodule of carbonate is, of course, much more remarkable in case of open-air exposed structures.

4) The convergence of different dates obtained with TL method is not the determining factor to date a structure, referring instead to the date of bricks production.

5) The convergence of the dates obtained with the two methods from samples coming from the same stratigraphic unit notably increases the probability of dating the building of a structure. The age limit, more than a *post quem* term, tends to be the real date of construction.

2. DATING OF S. LORENZO CHURCH

Several specific dating problems of S.Lorenzo church are related to the way in which its construction was made, especially in Late Antique and Medieval periods (Fieni, 2002).

In the Late Antique period masonry techniques in Milan foresaw the use of new and not recycled bricks.TL dating results demonstrated instead that most of the bricks related to this phase were reused. Only a very small percentage of them were "purposely" made. Consequently, in order to date

the foundation of the monument, a dating campaign wider than initially thought was attempted.

14-C was applied principally to the wooden charcoal scraps frequently found in the thick mortar joints. The results of the two different dating methods, specific for two different kinds of materials, were in good agreement, and allowed to consider the derived *post quem* term the most probable date of construction. The multiplication of the coincidences enhanced the level of reliability of the datings obtained. For what concerns 14-C measurements, they were performed on clots embedded in the mortars, trying to obtain precise chronological limits, while TL dating gave *ante quem* terms, anyway convergent with the last crystallization of $CaCO_3$. In order to check if the age of carbonates were related to the hardening of the mortar or to subsequent transformations, the dating of a carbonatic clot and of a wooden charcoal scrape found spatially very close, was performed.

During the Late Antique period different distinct phases were discovered:

Phase I (s. 251, 127, 549, 575), included the tetraconc of S.Lorenzo, NW, NE, SW towers and S.Ippolito chapel. It was dated by 14-C on two wooden scrapes and one clot of $CaCO_3$. The TL age of the related bricks showed that they had all been recycled, already in this first phase.

The three 14-C dates do well overlap and, from a probabilistic point of view, indicate a narrow chronological period for the foundation of the tetraconc. It seems therefore reasonable to narrow the time range in which the foundation occurred, i..e. the twenty years period 390-410 A.D., that is much narrow and storiographically significant than the previous ones, estimated on historical ground (Fieni, 2002).

Phase II is characterised by the construction of S.Aquilino chapel (s. 304, 188, 415 of 14-C). The archaeometric data indicated the range 400-420 A.D., also confirming the validity of the dating of phase I. To date this second phase, both techniques could be used. 14-C results also played an important role in assessing the chronology of several others coheval stratigraphic units of the complex (US 613-616).

The results obtained for the S.Sisto chapel were instead unexpected, and not totally in agreement with the Milanese literary tradition. While the TL age of bricks, all of sesquipedalian module, is in agreement with the written sources that attribute the foundation to the bishop Lorenzo I, the 14-C dating of a scrap found in the vestibule of the chapel (s. 484), gave a later date for the foundation, probably in the Byzantine age (between 530-620 A.D., at 68% probability). This result would locate the construction significantly after the bishop's commission.

For the Late Antique period, the abundance of dating elements present in the walls and the possibility of crosschecking the results obtained with the two

techniques gave highly reliable chronological information for all the building of the complex, bringing to unexpected archaeological results. In particular, the absolute *post quem* chronological limit obtained for the construction of the S.Aquilino arcade, dated it much later than the foundation of the chapel, probably occurred during the first half of the VI century (phase III).

To date the Medieval phases of S.Lorenzo, we could rely only on 14-C analyses. The characteristic masonry techniques used during Middle Age did not include the use of new brick materials, neither in small quantities. TL dating of the medieval phases, applied on recycled bricks, could therefore simply establish generic *post quem* limits. Another peculiarity of the masonry techniques in this period is the extreme thinness of the mortars joints, which very rarely contain datable charcoal scraps. Consequently, it was necessary to use the carbonate clots extracted from the mortar joints, being careful to select points of construction never exposed to rain. Even being aware of the limitation intrinsic in dating such items, several dates have been obtained for the same stratigraphic unit or for the same phase of construction; all the results are characterized by a high level of convergence and overlapping.

In the cases attempted, the dating of carbonate clots coincided with that obtained from wooden scraps located very close. This good agreement gave more reliability to the 14-C results obtained on carbonates, and to the historical consideration that can be deduced on their basis.

For the Middle Age phases all the samples have been chosen on the basis of the stratigraphic analysis. Inside the church, a few carbonate clots coming from G and H pillars and from the column 1 have been dated. For what concerns the external walls, only three wooden charcoal scraps have been found in the WW side: one in the tetraconc (s. 216), one in the SW tower (s.237) and one on the SW tower (s. 387). In the towers were evidenced, and included in the stratigraphic analysis ringing works of small thickness (3-4 brick layers). Finally, in the SW tower, a restoration phase of the wall curtain has been recognised. Both phases were dated through the 14-C analysis of carbonate clots. The results showed a remarkable constructional continuity between high and low Middle Age.

TL was also applied to several fictile tubes, coming from the interior of tetraconc. The date obtained for the twelve samples could be divided into two groups. The first is composed by four samples dated to Xth century; the second by eight Romanesque samples. The TL dates are in good agreement with those obtained by 14-C on mortars from pillars and column and from wooden charcoal scraps from the tetraconc and the towers. These results indicated the existence of an important medieval phase of reconstruction of the S. Lorenzo complex , probably during the Ottonian reign.

Subsequent Romanesque phases of construction should have occurred, in agreement with the written sources: they correspond to the ringing works

in the towers Even a group of fictile tubes should belong to a Romanesque restoration of the church.

3. CONCLUSIONS

TL and 14-C dating methods, applied to bricks and organic items sampled from several structures of S.Lorenzo complex in Milano gave convergent results, which were very useful in assessing the history of the church and the complicated chronology of its building.. The applicability of these methods is subjected to the masonry techniques typical of each historical period and their results are significant only if obtained on the basis of the stratigraphic analysis.

REFERENCES

Aitken M.J. (1985) *Thermoluminescence dating*. Academic Press, London.

S. Bowmann,1990, *Radiocarbon dating*, London

L. Fieni, (2002), *La basilica di San Lorenzo Maggiore a Milano tra eta' tardoantica e medioevo: metodologie di indagine archeometrica per lo studio dell'elevato*, in: *Archeologia dell'Architettura*, n° VII, pg. 53-98

S. Improta, 2002, *Il metodo di datazione del Carbonio 14*, in: *Elementi di Archeometria. Metodi fisici per i beni culturali*, a cura di A. Castellano, M. Martini, E. Sibilia, Milano, pg. 83-112

TL DATING RESULTS		
Sample	**Description and USM**	**Dating (AD)**
D92	S.Aquilino 433	562Ú140 a.C.
D91	S.Aquilino 802	360Ú75
D90	S.Aquilino 425	530Ú135 a.C.
D70	S.Aquilino 613	410Ú160
D69	S.Aquilino 541	840Ú60
D67	S.Aquilino 531	35Ú135 a.C.
D66	S.Aquilino 531	30Ú180
D65	S.Aquilino 529	650Ú75
D64	S.Aquilino 531	245Ú170
D55	S.Aquilino 406	550Ú110
D54	S.Aquilino 406	275Ú150
D51	S.Aquilino 409	395Ú125 a.C.
D43	S.Ippolito 244	575Ú95
D40	S.Ippolito 655	605Ú100
D29	S.Ippolito 211	490Ú100
D190	S.Aquilino vault	350Ú95
D189	S.Aquilino arcade	320Ú100

TL DATING RESULTS		
Sample	**Description and USM**	**Dating (AD)**
D187	S.Ippolito vault	200Ú150 a. C.
D186	S.Ippolito vault	160Ú150 a.C.
D182	S. Aquilino – tomb	720Ú105
D180	S.Ippolito foundations	85Ú180
D179	S.Ippolito foundations	55Ú120
D178	Fictile tube	930Ú80
D176	Tower SW 263	580Ú70
D163	S. Aquilino vault 712	215Ú130
D162	S. Aquilino vault 712	600Ú100
D16	S.Sisto 204	520Ú130
D145	Tetraconc 2045	190Ú230 a.C.
D143	Tetraconc 1007	265Ú215 a.C.
D142	Tetraconc 1057	500Ú110
D114	Tetraconc 7001	95Ú300
D113	Tetraconc 7001	160Ú120 a.C.

14 C DATING				
sample	**date 1 sigma**	**building**	**USM**	**material**
127	390 (340-410)	Tetraconc pillar		ch
188	400 (350-420)	S.Aquilino	616	ch
216	970 (900-990)	Tetraconc	8030	ch
237	890 (870-960)	Torre SE	404	ch
251	400 (350-420)	Tetraconc	5055	ch
304	350 (260-400)	S.Aquilino	407	ch
358	1030 (1020-1060)/(1080-1150)	Tower SW	252	cl
387	890 (870-960)	Tower SE	304	ch
409	460-480-520 (430-540)	S.Aquilino arcade	712	cl
415	410 (390-430)	S.Aquilino mosaic		ch
453	bis 1050-1100-1140 (1030-1170)	Tower SE romanesque vault	211	ch
469	1040 (1030-1160)	Tower NE	104	cl
472	1160(1040-1190)	Tower SE int.	448	ch
484	560 (530-610)	S.Sisto	106	ch
508	1030 (1020-1060)/(1080-1150)	S.Ippolito vault	400	cl
543	390 (340 - 410)	S.Ippolito vault		ch
549	410 (390-430)	Tetraconc inner pillar		ch
567	910-920-960 (890-980)	Column 1		cl
568	900 (880-980)	Pillar G		cl
569	1010 (990 - 1020)	Pillar H		cl
571	340 (250-390)	S.Ippolito valut	102	cl
574	880 (790-900)	Torre SE gallery		cl
575	410 (390-430)	S.Aquilino vault	712	cl

ARTIFICIAL FLUORINE ENRICHMENT IN BONES: DIAGENESIS AS RESTRICTING FACTOR FOR EXPOSURE AGE DATING BY FLUORINE DIFFUSION

A. A.-M. Gaschen, U. Krähenbühl
Laboratory for Radio- and Environmental Chemistry, University of Bern, Switzerland

M. Döbeli
Institute for Particle Physics, ETH Zürich, Switzerland

A. Markwitz, B. Barry
Rafter Research Centre, Lower Hutt, New Zealand

ABSTRACT

Fossil fragments of bone and teeth take up fluorine from the surrounding soil when exposed to a humid environment. In cortical parts of long bone diaphysis a fluorine concentration profile can be observed, which decreases from the outer surface and the marrow cavity towards the inner parts of the bone. As the profile contains information on the exposure duration, several attempts to use fluorine profiling as a dating method have been undertaken [Coote 1992, Kottler et al. 2002]. The distribution of fluorine in a sample however is strongly influenced by environmentally induced processes of bone diagenesis, i.e. alteration in the structure and composition of the mineral and organic components of bone that may make the time information indistinct [Reiche et al. 2001].

For this study, pieces of fresh, intact bones have been exposed to fluorine solution simultaneously with fossil ones to exclude the influence of the site-dependent deterioration of samples on their fluorine distribution. On the basis of the resulting profile, the diffusion constant D of the material was determined and the dependency of the profile shape on exposure duration, temperature and fluorine concentration of the solution was examined. The artificial fluorine enrichment confirms the presumed diffusion-like character of the uptake and transport mechanism.

1. INTENTION

The aim of this work is to examine the uptake of fluorine ions into an intact bone matrix (fresh bovine femur diaphysis) by generating fluorine profiles

artificially. Bone can be described as a composite material of carbonated apatite with low crystallinity ("dahllite"), and protein, which is mainly collagen [Berna et al. 2004]. The fluorine ion replaces the hydroxyl-group in the mineral phase with the average composition $(Ca,Na,Mg)_5(HPO_4,PO_4,CO_3)_3$ (OH,CO_3). Geological time spans are needed for this process to obtain equilibrium and for the distribution to become uniform. Diffusion has been assumed to be the main uptake mechanism of fluorine, that may however be superimposed by other effects, for example percolation of solution through microfissures in fossil samples or via pores (e.g. Haversian canals). Only with an increased knowledge of the bone diagenesis, the uptake mechanism of elements originating from the surrounding soil and their resulting distribution in the sample can be understood [Oakley 1949, Nielsen-Marsh et al. 2000]. Studies on the uptake of U for age dating for example show similar significant influence of the environment in the burial site [Pike et al. 2002].

2. EXPERIMENTAL SECTION

Fluorine profiles have been generated by immersing about 0.5 g of the test samples in 20 ml of aqueous solution of NaF (p.a.). The fluorine content in the solution $[F]_{sol}$, the temperature T and the exposure duration t were systematically varied (table 1). Quantitative fluorine concentration profiles were measured with PIGE (Proton Induced Gamma-ray Emission) [Coote et al. 1981, Coote 1992, Kottler et al. 2002] by proton microscopy by scanning a finely focused 2.5 MeV proton ion beam over the targets from the periosteum towards the marrow cavity under high vacuum conditions (beam diameter < 25 mm, ion current density: 0.3 nA mm^{-2}, 75 x 75 mm BGO-detector positioned at 90°). The parameter Dt (D: diffusion constant, t: exposure time) that describes the depth of the diffusion front that penetrated into the sample was determined by fitting the data with an error function (erf), which simulates an undisturbed diffusion process. The diffusion constant D, which is a material constant, was derived from Dt. The total amount of fluorine was determined by fluorine selective electrode after completely dissolving the sample in HNO_3 (65%).

3. RESULTS AND DISCUSSION

a) Environmental effects on fluorine uptake and profile shape

The results of the artificial enrichment experiments show that the value Dt increases with time and temperature as expected but also with fluorine concentration in the surrounding medium $[F]_{sol}$, which has been described in [Gaschen et al. 2004]. The total fluorine content in the sample $[F]_{tot}$, the fluorine concentration on the sample surface $[F]_{sur}$ and the diffusion constant D_{art} are summarized in table 1. $[F]_{tot}$ is influenced by T, t and $[F]_{sol}$. As it is predicted for classical diffusion, D_{art} is independent on the exposure time, but increases

T [°C]	$[F]_{sol}$ [g/g]	t [d]	$[F]_{tot}$ [g/g]	$[F]_{sur}$ [at%]	D_{art} x 10^{-8} [mm²/s]	$\overline{D}_{art}$ x 10^{-8} [mm²/s]
5	100	7	379	0.13	1.8	
		14	412	0.60	1.6	2.2
		21	417	0.30	3.2	
5	500	7	1050	0.26	2.6	
		14	1218	1.32	4.6	4.7
		21	1462	0.50	6.8	
35	100	7	471	1.70	0.2	
		14	614	0.67	0.6	0.6
		21	686	0.43	0.9	
35	500	7	1460	1.86	0.5	
		14	2720	1.17	1.5	1.1
		21	3018	0.97	1.2	
35	1000	7	3246	1.10	3.3	
		14	5337	1.30	5.9	3.8
		21	5104	1.43	2.1	
65	100	7	998	0.94	1.4	
		14	965	1.71	0.7	1.0
		21	974	0.31	0.8	
65	500	7	2725	1.08	3.6	
		14	3743	2.78	3.3	3.4
		21	4401	0.90	3.3	

Table 1. Artificial fluorine enrichment in fresh bovine femur diaphysis (cow 2002). Total fluorine concentrations $[F]_{tot}$, surface fluorine concentrations $[F]_{sur}$ and diffusion constants D_{art} at different temperature and concentration of NaF-solution. Exposure times range from one to three weeks. As D shows considerable uncertainty, average values over time are considered.

with increasing temperature from 35 to 65 °C. Surprisingly high values are measured for D_{art} at 5 °C. Surface-fluorine is correlated with the fluorine concentration in the solution and the environmental temperature. It has to be noted that whereas $[F]_{sur}$ increases during the experiment where high

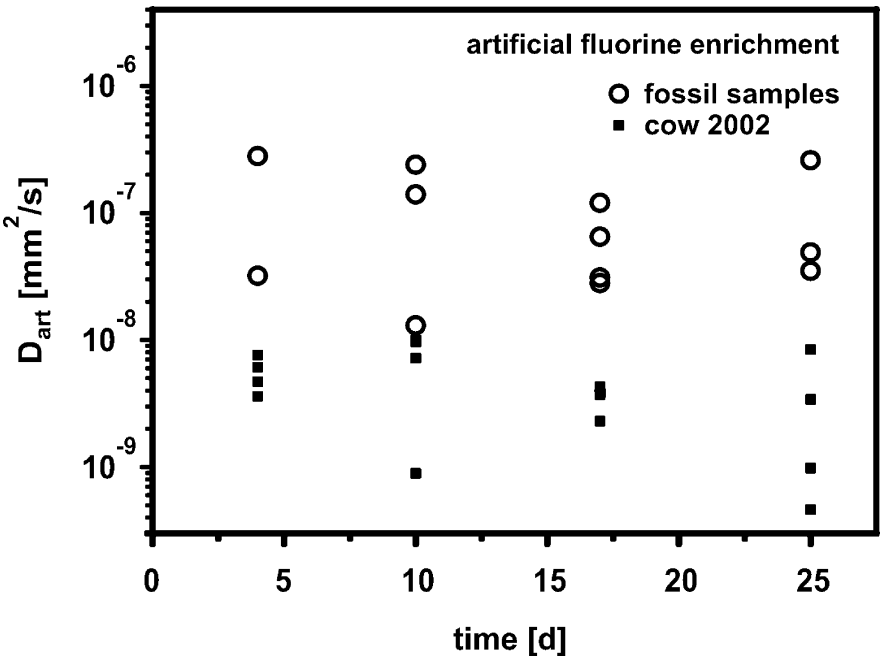

Figure 1. The diffusion constant D_{art} for artificially doped fossil samples of human origin is about 10 times higher than for doped fresh bovine bone samples and is not dependent on the exposition duration.

concentrations of fluorine are supplied (1000 ppm), it decreases with time in all other samples when the profile develops further into the body of the bone. Neither this behavior nor the decrease of *Dt* and *D* by decreasing $[F]_{sol}$ can be explained by classical diffusion, where an infinite reservoir of fluorine is assumed. Though it has been observed that the fluorine concentration in the vials decreased significantly during the experiments (up to 90%), which indicates that fluorine is readily taken up by the bone samples. This shortage of fluorine in the reservoir might have been responsible for the low values of *Dt* and *D* at low concentrations of $[F]_{sol}$ and the decrease of $[F]_{sur}$.

b) Artificial fluorine doping as model for fluorine uptake in nature

The diffusion constant shows generally higher values for artificially generated profiles (D_{art}) than for those developed in natural environments (D_{nat}). Furthermore, D_{art} for fossil bones is about ten times higher than D_{art} for fresh ones (refer to figures 1 & 2), which is probably due to the fact that the fossil bones were all of human origin, their diaphysis showing canals (Haversian systems) of typically 60 mm in diameter [Harsányi 1993], while in the bovine samples used in this study only much smaller pores were observed, if any. The major peculiarities

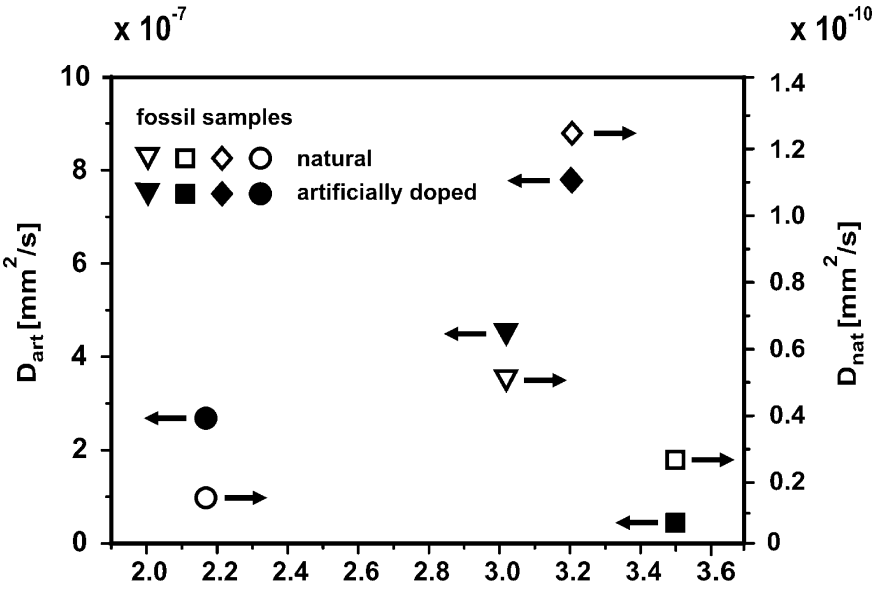

Figure 2. The degree of diagenesis of the sample is correlated with the uptake of fluorine. Note the different order of magnitude between D_{nat} and D_{art}. An explanation for "SF x CC" is given in the manuscript. Exposure times of fossil samples were determined by[14]

for a diagenetically altered bone are an increase in crystal size and perfection (described by the "splitting factor" SF of the IR phosphate double peak at 565 and 604 cm^{-1} [Nielsen-Marsh et al. 2000]) and a decrease of collagen content "CC", which is indicated by the intensity ratio of the carbonate and amide vibrations at 1452 cm^{-1} and 1650 cm^{-1}, respectively. The more the fossil bone underwent degradation, the more fluorine has been taken up. This is particularly the case for fossil samples considering their naturally developed fluorine profile as well as for the same samples that have been doped in the laboratory (figure 2. Sample "■□" has particular small pores sizes which reduced the transport of fluorine by pore water). The fact that a fossil sample doped in the laboratory shows an increased value of the diffusion constant by two to three orders of magnitude compared with a value calculated for the natural profile, cannot be fully explained by the reduced soil temperature and a lower fluorine concentration in the natural burial environment (0.1 mg g^{-1} in waters, several mg g^{-1} in soils). It is considered that D alters over a period of time. Because the bone was buried intact, the penetrating fluorine originating from the surrounding soil had encountered an intact bone structure with low diffusion constant values, e.g., in the Middle Ages, when short period had passed from burial. During the centenaries before excavation in 1993-97 the bone was already far degraded, showing considerably higher values for D. D_{nat} is therefore a function of several different values. When this same fossil sample is submerged in the laboratory, its structure is altered right from the

beginning. Thus the high diffusion constant D_{art} measured in laboratory corresponds to the physical quality of the bone at the time of excavation.

CONCLUDING REMARKS

Diffusion has been found to be one of many relevant mechanisms for fluorine uptake in bone. However the diffusion constant D is mainly characterized by the physical and chemical properties of the sample, which are exceedingly influenced by the soil conditions at the beginning of the burial and during the burial time. Because the bone undergoes diagenesis, D is not constant but changes during the time span as the profile develops. So far it is not possible to reconstruct these changes of D during bone history. Therefore the applicability of fluorine profiling as a dating technique for bones is limited.

ACKNOWLEDGEMENTS

The authors would like to thank Dr. S. Ulrich-Bochsler (Historical Anthropology, University of Bern), and Dr. M. Nussbaumer (Natural History Museum, Bern) for providing of samples. We are indebted to both the teams at ETH Zürich and Rafter Research Centre, Lower Hutt, for their help in ion beam measurements.

REFERENCES

Berna, F., Matthews, A. & Weiner, S., 2004, *Solubilities of bone mineral from archaeological sites: the recrystallization window.* J. Archaeol. Sci. 31, 867-882.

Coote, G. E. & Sparks, R. J., 1981, *Fluorine Concentration Profiles in Archaeological Bone: An Application of a Nuclear Microprobe.* New Zealand J. Archaeology, 3, 21-31.

Coote, G. E., 1992, *Ion beam analysis of fluorine: Its principles and applications.* Nucl. Instr. and Meth. B66, 191-204.

Gaschen, A. A.-M., Krähenbühl, U., Döbeli, M., Markwitz, A. & Barry, B., 2004, *Studies on Fluorine Diffusion in Archaeological Bones.* Bull. Soc. Suisse d'Anthrop. 10(1), 23-33.

Harsányi, L., *Differential diagnosis of human and animal bone,* in: G. Grupe, A. N. Garland (Eds.), Histology of Ancient Bone: Methods and Diagnosis. Springer Verlag, Berlin, 1993, 79-94.

Kottler, C., Döbeli, M., Krähenbühl, U. & Nussbaumer, M., 2002, *Exposure age dating by fluorine diffusion.* Nucl. Instr. Methods B188, 61-66.

Nielsen-Marsh C. M. & Hedges, R. E. M., 2000, *Patterns of Diagenesis in Bone I: The Effects of Site Environments.* J. Archaeol. Sci 27, 1139-1150.

Oakley, K. P., 1949, *The Fluorine-dating Method.* Yearbook Phys. Anthropol., 44-52.

Pike, A. W. G., Hedges, R. E. M. & Van Calsteren, P., 2002, *U-series dating of bone using the diffusion-adsorption model.* Geochim. Cosmochim. Acta 66, (24), 4273-4286.

Reiche, I. Vignaud, C., Favre-Quattropani, L., Charlet, L. & Menu, M., 2001, *Diffusion in Archaeological Bone.* Defect and Diffusion Forum Vols. 194-199, 953-960.

TL-DATING OF MOUSTERIAN OPEN AIR SITES OF THE ISLE VALLEY: LES FORÊTS AND PETIT BOST (DORDOGNE, FRANCE)

Pierre GUIBERT, Christelle LAHAYE, Matthieu DUTTINE, Françoise BECHTEL

Institut de Recherche sur les Archéomatériaux,
UMR 5060 CNRS – Université de Bordeaux 3
Centre de Recherche en Physique Appliquée à l'Archéologie (CRPAA)
Maison de l'Archéologie, 33607 Pessac Cedex, France.
Tel: 33-5 57 12 45 49; Fax: 33-5 57 12 45 50
e-mail: guibert@u-bordeaux3.fr

1. INTRODUCTION

Rescue archaeological works being carried out in France on the A89 highway path revealed numerous open air Palaeolithic sites in the Isle Valley (a tributary of the Dordogne), downstream from Périgueux, giving us the opportunity to improve our knowledge about the chronology of palaeolithic periods. Among the excavated sites, some attributed to the middle Palaeolithic are being dated by thermoluminescence; the results obtained (at the end of year 2003) at 2 sites are presented:

— Les Forêts (St. Martin de Gurçon, France): the Mousterian industry found out in a single archaeological level is remarkable by the evidence of a predominant discoid flaking method (Brenet and Folgado, 2003).

— Petit Bost (Neuvic sur l'Isle, France): 2 Middle Palaeolithic levels were identified, the oldest (level 2) was considered the most interesting for dating, because of lithic characteristics that belong both to the late Ancient Palaeolithic (Clactonian flakes) and to the Mousterian complex.

According to the basical principles of TL dating (Aitken, 1985), independent determination of the two following physical parameters is required : the equivalent dose accumulated in flints from natural irradiation since its past firing by palaeolithic people (named equivalent dose), and the annual dose which is the average (through time) dose accumulated in one year by the sample studied.

2. DETERMINATION OF EQUIVALENT DOSE

Sufficiently heated flint samples were selected for dating using TL saturation tests (Valladas, 1985). Those which passed the test were then investigated employing the additive dose and regeneration technique to measure the equivalent dose (Guibert et al., 1996). Methodological improvements of this classical technique were implemented: a study of the TL and EPR (Electron Paramagnetic Resonance) properties led us to define, for any sample studied, appropriate annealing conditions equivalent to the archaeological firing in order to obtain, after the laboratory re-annealing, the growth of TL the material is supposed to have after its ancient heating (Duttine et al., in press). These annealing conditions which are related to the thermal history of flints were approached by EPR using the informations provided by organic radicals, the type of which is related to the temperature attained by the material in the past, and by the thermal behaviour of E' centres population (oxygen vacancies having trapped an electron) (Robins et al., 1978; Toyoda et al., 1993). Complementary experiments by TL were performed on Petit Bost samples with the same aim. The appropriate laboratory annealing cycle was determined on the base of changes in TL sensitivity and in glow curves shapes with the annealing temperature in comparison with the TL properties of the archaeological material. All experiments were made on powdered material extracted from the inner part of samples (80-200 μm in grain size for beta equivalent dose determination and EPR measurements, 3-12 μm for alpha efficiency, but on annealed material). After grinding and sieving, carbonates were removed by a HCl(1M) solution and the surface of grains were then gently etched by a mixed HCl(1M), HF(0.5M) solution to avoid possible spurious signals resulting from grinding.

The TL glow curves were obtained using a home-made TL apparatus and heating in N_2 at a rate of 4 °C/s. The photomultiplier tube (EMI 9213 QKA) used for photon counting and a set composed of two Schott BG12 and one MTO Ta3 optical filters lead to a spectral window in the blue and UV region of TL. EPR measurements were performed using a Brüker spectrometer (ESP300E) which allows recording in the X band region (frequency 9.5 GHz) and at low temperatures (down to 100 K). Beta irradiations were performed with a ^{90}Sr beta source (1.85 GBq, AEA technology SIF1176 type) and alpha irraditions with a ^{241}Am source (21 MBq, Isotope Products Europe, APS G027 type).

3. DETERMINATION OF ANNUAL DOSE

Annual doses were determined from low background gamma spectroscopy measurements of both material being dated and surrounding sediments. Gamma spectrometry analyses were performed using a well Ge detector (Canberra-Eurisys, EGPC 200 P17, low background type: active Ge volume is 200cm^3 and well dimensions are 17 mm in diameter and 55 mm in length) The radiochemical composition was converted into annual dose using

the conversion factors by Adamiec and Aitken (1998). A disequilibrium in the U-series of the surroundings was observed. A statistical study of the distribution of U and Ra within sediment samples from les Forêts (according to a method already presented in Guibert et al. 1997) and complementary alpha spectroscopy experiments on some Petit Bost's sediment samples showed that in both sites, the disequilibrium was mainly due to the mobilization of uranium through the archaeological layers. Calculation of the time-averaged annual dose was achieved taking into account the existence of disequilibria.

At Petit Bost, the gamma dose rate was evaluated by a reconstruction technique because of the "lumpy" characteristics of the burial medium and its subsequent radiochemical inhomogeneity (Aitken et al., 1985; Guibert et al., 1998). The dated flints were collected from a heterogeneous context made of fine grain sediments and silicious gravels. An exhaustive excavation of a $1m^2$ gravel zone (50 cm deep) has been carried out in order to study the radioactivity distribution and gamma gradients, and finally to determine a realistic value of the gamma dose rate. As a result, around 7000 stones the dimensions of which were greater than 2 cm were sampled and referenced: X, Y, Z coordinates were recorded as well as their mass and nature of mineral. The "fine grain" sediment (clay, sand and gravels less than 2 cm) that embedded the gravels was statistically collected from this zone. The different types of material (i.e. different classes of radioactivity on the dosimetric point of view) that compose the burial medium and their properties relevant to dosimetry are given in table 2 as well as the average composition (mass % of each type of lithic material) of the gravel zone. The latter data were used to calculate the external gamma dose rate of Petit Bost flint samples, assuming a moisture content of 15±3% in mass of the fine grain sediment.

Sample reference	annealing temperature (°C)	beta Equivalent Dose (Gy)	alpha efficiency factor (k)
Les Forêts			
BDX 5177 (J8B #2)	380	158.8±9.8	0.118±0.011
BDX 5178 (L12C #1)	400	150.6±11.0	0.065±0.005
Petit Bost			
BDX 7519 (PB01 #6046)	400	327±40	0.043±0.003
BDX 7679 (PB01 #5241)	400	323±19	0.049±0.003

Table 1. Results of equivalent dose measurements (uncertainty: 1 σ); the duration of the thermal annealing cycle is 1 hour.

4. TL DATES

Table 3 reports the calculated annual dose components and ages for flints from both sites. Within each site, TL ages are not significantly different according to their uncertainty, so if we assume that the dated flint could be contemporaneous, error weighted means can be calculated.

The Mousterian industry with discoid flaking method uncovered at the open air site of Forêts is dated to 92.7 ± 4.5 ka (kiloyears, uncertainty 1s) before the present (2003), corresponding to the last half of oxygen isotopic stage OIS6.

If we consider that the Petit Bost's dated flints were intentionnally burnt and related to the assemblage Clactonian and Mousterian found out in the same layer (level 2), the mean age of 319 ± 20 ka (1s) before today (2003) is to be noticed. It is closed to the ESR dates obtained by ESR-US on horse teeth at the upper levels of la Micoque in Dordogne (Falguères et al., 1997) for the Micoquian 'Premousterian' culture. The chronological interval found at Petit Bost corresponds to the isotopic stage OIS9 - early OIS8, and it seems to date the very beginning of the Middle Palaeolithic and Mousterian periods.

nature of material	nb	K (%)	U(^{238}U) (ppm)	U(^{226}Ra) (ppm)	Th (ppm)	infinite matrix gamma dose rate (mGy/a)	mass % of material
fine grain sediment (Ø<2cm)	8	0.56±0.04	3.20±0.27	2.81±0.28	11.4±0.7	0.869±0.061	82.3
flint (m>10g)	13	0.034±0.017	0.74±0.68	0.74±0.68	0.45±0.21	0.114±0.074	6.3
quartz (m>10g)	5	0.002±0.002	0.010±0.003	0.010±0.003	0.026±0.007	0.0030±0.0004	5.4
undetermined (m>10g)	-	0.034±0.017	0.74±0.68	0.74±0.68	0.45±0.21	0.114±0.074	1.3
all type small gravels (m<10g, Ø>2cm)	6	0.14±0.04	1.48±0.32	1.20±0.25	3.4±1.2	0.333±0.091	4.6

Table 2. Radiochemical study of lithic components and mass composition of the burial medium test-zone excavated at Petit Bost site; nb is the number of independent analyses, uncertainty represents the standard deviation calculated from the dispersion observed for a given type of lithic material; the material called undetermined is assimilated to flint (laboratory examinations showed that most of these elements are cortical flint fragments). U(^{238}U) is the U content deduced from gamma rays from ^{234}Th and ^{235}U, U(^{226}Ra) from ^{214}Pb and ^{214}Bi (sample in sealed container, ^{222}Rn being in equilibrium with ^{226}Ra).

Sample reference	alpha (mGy/a)	beta (mGy/a) (mGy/a)	gamma internal (mGy/a)	gamma external	cosmic (mGy/a)	total (mGy/a)	TL-age (ka before present)
Les Forêts							
BDX 5177 (J8B #2)	0.465 ±0.046	0.243 ±0.012	0.021 ±0.001	0.866 ±0.028	0.175 ±0.018	1.770 ±0.060	90.3±5.0
BDX 5178 (L12C #1)	0.268 ±0.030	0.226 ±0.022	0.015 ±0.001	0.868 ±0.028	0.175 ±0.018	1.552 ±0.052	97.0±6.9
Petit Bost							
BDX 7519 (PB01 #6046)	0.057 ±0.009	0.106 ±0.009	0.007 ±0.001	0.641 ±0.040	0.155 ±0.016	0.967 ±0.047	338±43
BDX 7679 (PB01 #5241)	0.095 ±0.011	0.163 ±0.015	0.011 ±0.001	0.612 ±0.040	0.155 ±0.016	1.035 ±0.048	312±23

Table 3. Annual dose rates and TL-ages. Uncertainty: 1 standard deviation (including statistical and systematic uncertainties).

ACKNOWLEDGEMENTS

Financial support by Région Aquitaine, Ministère de la Culture (SRA Aquitaine), CNRS, INRAP, Université de Bordeaux 3.

REFERENCES

Adamiec G. et Aitken M.J., 1998, Dose-rate conversion factors: update. Ancient-TL 16(2), 37-49.

Aitken M.J., 1985, Thermoluminescence dating. Academic Press. London, 359pp.

Aitken M.J., Clark P.A., Gaffney C.F., Lovborg L., 1985, Beta and gamma gradients. Nuclear Tracks 10, 647-653.

Brenet M., Folgado M., 2003, Le débitage discoïde du gisement des Forêts à Saint Martin de Gurçon (Dordogne). British Archaeological Reports 1120, 153-178.

Duttine M., Guibert P., Perraut A., Lahaye C., Bechtel F., Villeneuve G., 2004 in press, Effects of thermal treatments on TL and EPR of flints and their importance in TL-dating: application to french Mousterian sites of Les Forêts (Dordogne) and Jiboui (Drôme). Radiation Measurements.

Falguères C., Bahain J.-J., Saleki H., 1997, U-series and ESR dating of teeth from Acheulean and Mousterian Levels at La Micoque (Dordogne, France). Journal of Archaeological Sciences 24, 537-545.

Guibert P., Vartanian E., Bechtel F., Schvoerer M., 1996, Non linear approach of TL response to dose: polynomial approximation. Ancient TL 14, 7-14.

Guibert P., Bechtel F., Schvoerer M., 1997, Déséquilibre des séries de l'uranium, implications sur la dose annuelle en datation par thermoluminescence: une étude à la Grotte XVI, Cénac et Saint-Julien, Dordogne (France). Quaternaire, 8, 377-389.

Guibert P., Bechtel F., Schvoerer M., Müller P., Balescu S., 1998, A new method for gamma dose-rate estimation of heterogeneous media in TL-dating. Radiation Measurements 29, 561-572.

Robins G.V., Seeley N.J., McNeil D.A.C., Symons M.C.R., 1978, Identification of ancient heat treatment in flint artefacts by EPR spectroscopy. Nature 276, 704.

Toyoda S., Ikeya M., Dunnell R.C., McCutcheon P.T., 1993, The use of electron spin resonance (ESR) for the determination of prehistoric lithic heat-treatment. Applied Radiation and Isotopes 44, 227-232.

Valladas H., 1985, Datation par TL de gisements moustériens du Sud de la France. Thèse Doctorat d'Etat, Univ. Paris VI, 178 pp.

AMS RADIOCARBON DATING OF PROTOCLASSIC MAYA LIME PLASTERS FROM AGUATECA, GUATEMALA

G. W. L. Hodgins
NSF-Arizona AMS Laboratory, University of Arizona

A.J. Vonarx
NSF-IGERT Graduate Program, Department of Anthropology, University of Arizona

and **B. Bachand**
Department of Anthropology, University of Arizona, Tucson, Arizona, USA 85721

1. INTRODUCTION

Lime plasters and mortars have widespread use in Mesoamerica. Their occurrence in a wide variety of contexts, the existence of many poorly dated, complex architectural structures, and an environment destructive to organic remains lead us to investigate the possibility of radiocarbon dating plaster surfaces. The principle of the method exploits the fact that plasters and mortars set by the incorporation of atmospheric CO_2 into newly-formed crystals of calcium carbonate (Gourdin and Kingery 1975).

There are two fundamental problems in dating mortars and plasters: contamination from carbonate containing aggregates such as limestone, and the post depositional precipitation of carbonates from ground water. The first problem has been discussed extensively in the literature (Stuiver and Smith 1965) Baxter and Walton (1970) Folk and Valastro (1976) Van Strydonck *et al.* (1986, 1989, 1992), Pachiaudi *et al.* (1986), Heinemeier *et al.* (1997), Sonninen and Jungner (2001). This is likely to be a common problem for dating Mesoamerican plasters as many sites are dominated by dolomitic limestone geology (ref). For the second problem, the suggested solution is to avoid samples likely to have been subject to water infiltration (Van Strydonck *et al.* (1986). An empirical method for identifying samples manifesting this second problem has not been developed.

Most sample preparation methods are variants on Folk and Valastro (1976). They exploit the friability, small particle size, and susceptibility to acid hydrolysis of newly-formed "cryptocrystalline $CaCO_3$" in mortars and plasters

compared to geologic carbonate in limestones particles. Baxter and Walton (1970), and Folk and Valastro (1976) recognized that ^{14}C measurements on the first 1/3rd of the gas released during hydroysis improved the method's accuracy. Subsequent methods have attempted to exploit their observations. Van Strydonck *et al.* (1986, 1992) limited acid availability and released only 10% of the carbonate CO_2. Heinemeier *et al.* (1997) collected both the first 30% and the last 70% of the released CO_2, dating both fractions. Sonninen and Jungner (2001) suggested that preparations of uniform particle size, specifically a 43-62 μm fraction, would accentuate differences in hydrolysis rates between limestone inclusions and mortar carbonates. Furthermore, control hydrolyses of limestone particles alone only would allow correction for early limestone CO_2 input.

We report on preliminary investigations into radiocarbon dating floor plasters from a Protoclassic Maya pyramid, Structure K6-1 at Aguateca, Guatemala (figure 1). The suggested age of the structure is 2100-1650 BP based upon associated ceramic finds (Bachand 2002). The plasters are stratigraphically

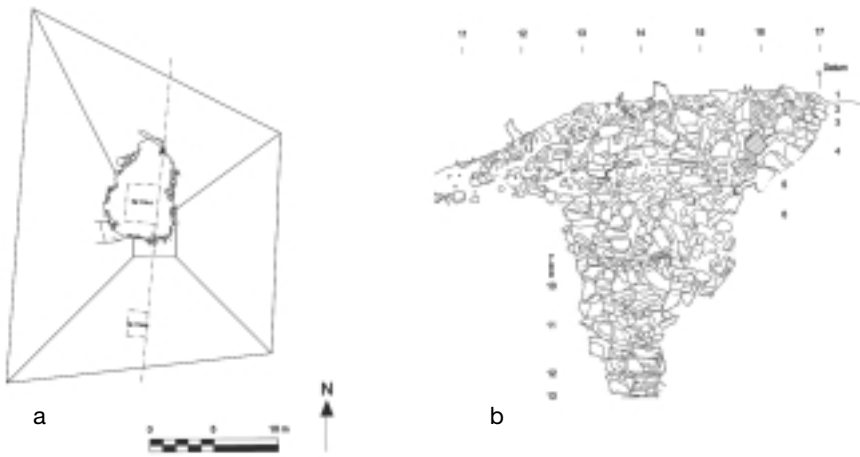

Figures 1a and b. 1a. Plan view of Pyramid K6-1 at Aguateca, Guatamala. The top of the pyramid was disturbed by looting. The dotted line locates the section shown in **b**. **1b:** A section view with one meter horizontal intervals. The vertical numbers from 1 to 13 designate horizons within the section. Plaster floor fragments for this study were obtained from layers 13, 9, and 7. Layer 13 is believed to be a plaza floor pre-dating the pyramid's construction.

related; the earliest is thought to derive from a plaza floor that pre-dates the pyramid's construction. The two later samples are thought to derive from the platforms of successive phases of pyramid construction. The samples were likely subject to water percolations. All were originally thought to contain species-identifiable charcoal inclusions that could be recovered for readiocarbon dating. While microscopic charcoal inclusions were visible in thin section, we were not able to recover charcoal in quantities sufficient for AMS dating.

2. METHODS

Petrographic thin sections of the three floor plasters were prepared following method outlined in Hansen (2000). Blue epoxy resin was used to impregnate plasters, which were cut, mounted on slides, and photomicrographed.

Plaster samples were prepared for hydrolysis according to Sonninen and Jungner (2001). This involved gentle crushing with a mortar and pestle and size fractionation by wet sieving to recover a 45-65 μm fraction. A slight modification involved wet sieving using CO_2-free water and subsequent drying under a nitrogen atmosphere. Hydrolysis of 50 mg samples was accomplished using 85% phosphoric acid, with CO_2 recovered as time-course fractions directly into liquid-nitrogen-cooled ampoules. The collection manifold geometry was changed between repetitions of the hydrolysis experiments to investigate the effect on yield and isotopic composition. The stable isotope compositions of the evolved gases were measured on a stable isotope mass spectrometer, with machine precision of ± 0.1‰. The total error is likely higher (± 0.3‰?), particularly in the earliest fractions due to kinetics. Radiocarbon measurements were carried out by accelerator mass spectrometry using established graphitization (Slota *et al.* 1987), and measurement methods (Donahue *et al.* 1990) .

3. RESULTS

The thin sections shown in figure 2 revealed marked differences in inclusion particle size distributions. The upper layers contained the progressively larger limestone inclusions. The percent carbon dioxide yield upon hydrolysis of 45-65 μm particle fractions of each plaster are shown in figure 3a. The $\delta^{13}C$ values of each fraction are shown in figure 3b. Radiocarbon measurements on some of the fractions are shown in table 1. A correction for limestone carbonate input was also applied to the earliest fractions (see discussion). This produced dates of 1994 ± 31, 2276 ± 32, and 2680 ± 32 for layers 1-7-1, 1-9-1, and 1-13-1 respectively.

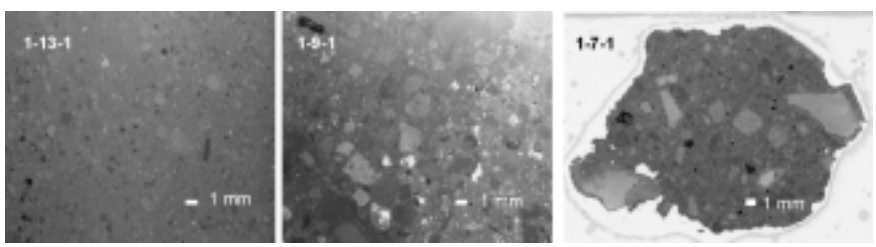

Figure 2. Thin sections of floor plasters from Pyramid K6-1 in layers 13, 9 and 7. The size and angularity of inclusions progressively increased from the basal layer 13 up through layers 9 and 7. The black inclusions, originally thought to be charcoal, were inorganic.

4. DISCUSSION

The high initial rate of plaster hydrolysis shown in figure 3 was predicted by previous investigators, including Heinemeier *et al*. (1997). Curve shapes are similar to those presented in Sonninen and Jungner (2001), but our rates appear slower by one order of magnitude. This may be partially explained by the fact that the Aguateca region is dominated by dolomitic limestone geology. This form of mineral carbonate is one of the least reactive to acid hydrolysis (Morse 1983, p.227). The fact that late fractions show $\delta^{13}C$ values approaching that of pure limestone (approx. +1‰) is consistent with all three samples containing substantial quantities of dolomitic limestone.

In all three samples an initial high rate of hydrolysis lasted approximately 5 minutes. This was followed by a second phase with a significantly lower rate, lasting many hours. The transition between the two phases occurred at approximately the same time for all three samples (between 5 and 40 minutes), but the proportions of fast and slow hydrolyzing carbonates differed between them. In sample 1-13-1 the transition to slower hydrolysis occurred after 60% CO_2 release, whereas for 1-7-1, the transition occurred after only 30% CO_2 release.

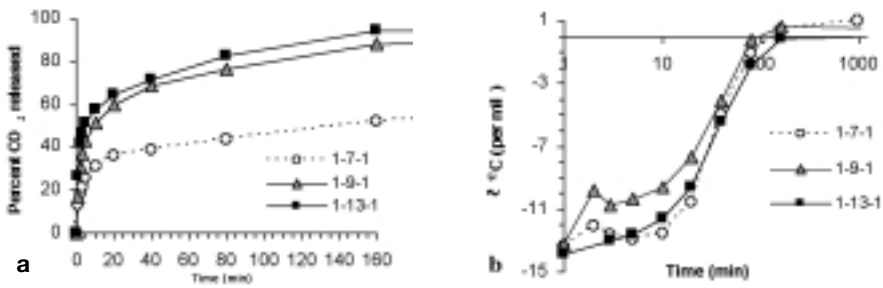

Figures 3a and b. **3a.** Hydrolysis of 50 mg of the (45-65 μm)-particle fractions of Pyramid K6-1 floor plasters. CO_2 samples were collected at 1, 2, 3, 5, 10, … 160, and 960 minutes. One hundred percent hydrolysis was reached by 960 minutes. Only the first 160 minutes of each reaction is shown. **3b**: Carbon stable isotope measurements on hydrolysis fractions. The results are plotted on a semi-log scale so that early time-points are distinguishable. Estimated error bars are covered by the symbols.

The early fractions are depleted in ^{13}C ($\delta^{13}C$ = -14 ‰). The reason for this depletion is not clear. The plaster carbonate is formed through the incorporation of atmospheric CO_2 ($\delta^{13}C$ = -7‰). It has been suggested that depletion is due to kinetic fractionation during plaster setting at non-equilibrium conditions (Letolle 1988).

In both 1-7-1 and 1-9-1 the two minute fractions were slightly enriched in ^{13}C relative to adjacent fractions. This enrichment was seen in replicate hydrolyses using different collection systems. We plan to look into this further. Unfortunately, the two minute samples from 1-13-1 were not measured.

Radiocarbon measurements on the evolved CO_2 are shown in table 1. These values were corrected for isotope fractionation. An attempt was made to correct dates for the first fractions for limestone contamination by assuming the hydrolysis kinetics of dolomitic limestone to be zero-order. This appears to be a reasonable assumption given the hydrolysis rates of the late fractions and hydrolysis curves of pure limestone shown in Sonninen and Jungner (2001). The corrections had the effect lowering the measured ages but not to within the expected window of 2100-1650 BP. If the archaeological age is correct, then the plaster dates overestimate age. This would be consistent with a post-burial incorporation of older carbon into the plaster matrix. If cycles of dissolution and precipitation occur as a consequence of episodic water infiltration, then one might expect that both limestone and plaster carbonate salts would be susceptible. The re-precipitation of limestone-derived carbonate ions on a plaster crystal might render the geologic carbonate acid labile. If the kinetics of hydrolysis of this fraction differs from that of the original plaster carbonate, then one might see evidence of re-precipitation in a fine-scale analysis of the stable isotope composition of early fractions.

5. CONCLUSIONS

The hydrolysis experiments we've presented essentially reproduce the results of previous investigations, but differ in rate and stable isotopic composition. Our samples were by no means protected from water infiltration and may have been remodeled in a manner that changes the relative hydrolysis rates of both the plaster and the geologic carbonate. Our future research will focus on plaster samples also containing organic inclusions to better assess the accuracy and viability of dating plasters through AMS.

Layer	1 min	2 min	3 min	80 min	160 min
1-7-1	2266 ± 31	2770 ± 70	2997 ± 82	19060 ± 400	29740 ± 910
1-9-1	2591 ± 32	3522 ± 33	4015 ± 59	22400 ± 380	31220 ± 400
1-13-1	2880 ± 32	n.d.	n.d.	18070 ± 170	24420 ± 180

Table 1. Radiocarbon dates derived from CO_2 samples released at various hydrolysis times. The dates are radiocarbon years BP corrected for fractionation using the $\delta^{13}C$ measurements shown in figure 3.

REFERENCES

Bachand, B. R. (2002) Estudio de la ocupación preclásica. En *Proyecto de restauración Aguateca segunda fase: Programa complementario*, editado por Oscar Sanchez, Takeshi Inomata y Erick Ponciano. Informe presentado al Instituto de Antropología e Historia de Guatemala.

Baxter, M. S., and Walton, A. (1970) Radiocarbon Dating of Mortars. *Nature* 225: 937-938.

Donahue, D.J., Linick, T.W. and Jull A.J.T. (1990) Isotope-ratio and background corrections for accelerator mass spectrometry radiocarbon measurements. *Radiocarbon* 32(2):135-142.

Folk, R. and Valastro, S. (1976) Successful Technique for Dating of Lime Mortar by Carbon 14. *Journal of Field Archaeology* 3(2):203-208.

Gourdin W. H., and Kingery W. D. (1975) The beginnings of Pyrotechnology: Neolithic and Egyptian Lime Plaster. *Journal of Field Archaeology* 2(1/2):133-150.

Hansen, E. (2000) Ancient Maya Burnt Lime Technology: Cultural Implications of Technological Styles. Ph. D. Dissertation. University of California, Los Angeles.

Heinemeier, J., Jungner, H., Lindroos, A., Ringbom, Å, von Konow, T., and Rud, N. (1997) AMS ^{14}C Dating of Lime Mortar. *Nuclear Instruments and Methods in Physics Research* B 123:487-495.

Letolle, R. (1988) Letter to Editor: *Radiocarbon* 30(1):129.

Morse, J. W. (1983) The Kinetics of Calcium Carbonate Dissolution and Precipitation. In *Carbonates: Mineralogy and Chemistry*, R. R.Reeder Ed., Mineralogical Society of America, Washington D. C. pp 227-299.

Pachiaudi C., Marechal, J., Van Strydonck, M., Dupas, M., and Dauchot-Dehon, M. (1986) Isotopic Fractionation of Carbon during CO_2 Absorption by Mortar. *Radiocarbon* 28(2A): 691-697.

Slota, P.J., Jull A.J.T., Linick, T.W., and Toolin, L.J. (1987) Preparation of small samples for ^{14}C accelerator targets by catalytic reduction of CO_2. *Radiocarbon* 29(2):303.

Sonninen, E., and Jungner, H. (2001) An Improvement in the Preparation of Mortars for Radiocarbon Dating. *Radiocarbon* 43(2A): 271-273.

Stuiver, M. and Smith, C. S. (1965) Radiocarbon Dating of Ancient Mortar and Plaster. In *International Conference on ^{14}C and tritium dating, 6th Proceedings: Clearinghouse for Federal Science and Technology Information*, edited by R. M. Chatters and E. A. Olson, pp. 338-341. National Bureau of Standards, US Department of Commerce, Washington, DC.

Van Strydonck, M., Dupas, M., Dauchot-Dehon, D., Pachiaudi, C. and Marechal J. (1986) The Influence of Contaminating (Fossil) Carbonate and the Variations of δ^{13}C in Mortar Dating. *Radiocarbon* 28(2A):702-710.

Van Strydonck, M., Dupas, M., and Keppens E. (1989) Isotopic Fractionation of Oxygen and Carbon in Lime Mortar Under Natural Environmental Conditions. *Radiocarbon* 31(3): 610-618.

Van Strydonck, M., Van Der Borg, K., De Jong, A., and Keppens E. (1992) Radiocarbon Dating of Lime Fractions and Organic Material from Buildings. *Radiocarbon*

ACCELERATOR MASS SPECTROMETRY DATING OF ARCHAEOLOGICAL SAMPLES FROM NOLA AREA (NAMPLES, ITALYCAMPANIA)

C. Lubritto*, F. Terrasi, A. D'Onofrio, C. Sabbarese, F. Marzaioli, I. Passariello, +D. Rogalla, M. Rubino
Dipartimento di Scienze Ambientali, Seconda Università di Napoli

N. De Cesare
Dipartimento di Scienze della Vita, Seconda Università di Napoli

M. Romano, L. Gialanella, V. Roca
Dipartimento di Scienze Fisiche and INFN Sezione di Napoli (Italy)

C. Rolfs
Institut für Physik mit Ionenstrahlen, Ruhr-Universität Bochum, Bochum (Germany)

C. Albore Livadie
Centre Camille Jullian, Aix-en-Provence (Francia)

G. Vecchio
Soprintendenza per i Beni Archeologici delle Province di Napoli e Caserta (Italy)

ABSTRACT

A systematic investigation on dates of samples from different archaeological sites related to Bronze age settlements in Campania region (Nola, S. Paolo Belsito, ecc.) has been undertaken, using the ^{14}C method. A significant marker in this context is the Avellino pumice eruption: charred wood and bone samples have been collected in layers both below and above the eruption material, with the aim of reconstructing the cronology of anthropic activity from the old bronze age to the middle bronze age, as well as the impact of the plinian eruption.

Samples were treated in the Mass Spectrometry Laboratory of the Environmental Science Department of the II University of Naples, and measured at the Accelerator Mass Spectrometry (AMS) facility set-up at the Dinamitron Tandem Laboratory of the Ruhr Universitaet in Bochum (D).

* corresponding author; e-mail: lubritto@sa.infn.it

+ Marie Curie fellow, contract N. HPMD-CT-2001-00088

1. INTRODUCTION: THE NOLA BRONZE AGE VILLAGE

In May 2001, in the immediate outskirts of Nola (an important city 25 km east from Naples), an early bronze age village, in locality Croce del Papa (CdP), was discovered buried by the products of a Plinian eruption of Vesuvius, the Avellino Pumices eruption of 3500 BP (Livadie Albore *et al* 2001). Three huts, originally part of a more extended settlement, were found six metres below the ground level, next to an enclosed area which included a threshing floor, some covered structures and an animal pen made out of wattle and daub (fig.1). The humidity of the soil conserved not only human footprints, but the hoof marks of domestic animals (sheeps, goats, cows and pigs) in the enclosures where they fled from at the time of the eruption (AA.VV. 2002). Nine pregnant goats were discovered in the animal fence (fig. 2). All other inhabitants escaped at the time of the eruption. After the fall of grey pumices that covered the huts without causing their collapse, a wave of mud penetrated slowly within the structures providing a counterforce to the pumices accumulated outside, and allowing their preservation. Recent excavations, in the place named Masseria Rossa (MR), few km apart from CdP, highlighted hut's remains above rearranged pumices of Avellino's eruption (AA.VV. 2002). This discover emphasizes the reinstallation of anthropic activity on the old environment after the eruption, that probably was mainly characterized by agriculture and stock farm activities characterizing the Palma Campania *facies*. Aim of this work is the historical reconstruction of this paleoenvironment by radiocarbon (^{14}C) dating of organic materials (bone, charcoal) collected in layers below and above the eruption materials. In particular, the main goal is to confirm the eruption date and to characterize the human resumption, in the lands involved by the eruption.

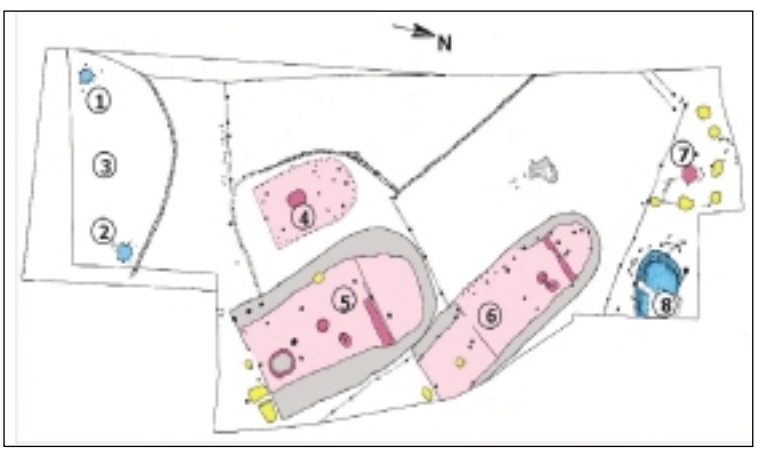

Figure 1. General plan of the site of Croce del Papa. 1,2 Wells; 3 Subcircular enclosure, threshing floor; 4 Hut 2; 5 Hut 3; 6 Hut 4; 7 Cage with goats; 8 Waterhole.

Figure 2. Animal pen with nine pregnant goats.

2. ^{14}C - AMS DATING

^{14}C is a radioactive isotope that enters as $^{14}CO_2$ in living photosynthetic organisms or, indirectly, as "organic ^{14}C" through the feeding in the etherothrophes. Therefore, ^{14}C concentrations inside the biosphere and the environment in which organism lives are the same (isotopic equilibrium). The metabolic processes, which continually bring carbon and realise the isotopic equilibrium, will be ended with the organism's death. From this time, ^{14}C content decreases according to the radioactive decay law and the isotopic ratio between ^{14}C and ^{12}C supplies information about the time elapsed since the metabolic activities ended (organism's death). In this work, radiocarbon dating is performed by Accelerator Mass Spectrometry (AMS): an ultrasensitive analytic technique which measures the abundance of the rare isotope (^{14}C) with respect to the corresponding abundant one (^{12}C). This isotopic ratio represents a very sensitive indicator of natural and anthropogenic processes that characterize past environment (Terrasi 2001). AMS technique offers the opportunity to use small amount of material (few milligrams) and to measure its isotopic ratio in a few minutes. Therefore, being a non destructive technique, AMS becomes an important tool to date rare and precious finds, like those of Nola archaeological site. Measurable age intervals (from hundreds to 50000 of years), together with the cited features, make the AMS a powerful tool for the study of an archaeological-environmental site.

2.1. Method and sample preparation

The AMS technique needs a set of physical and chemical pretreatments: their principal purpose is to isolate the carbon fraction and to eliminate carbon contaminating the sample. The physical and chemical pretreatments depend on the nature of the sample and on the organic fraction to be extract. The physical treatment includes the removal of obvious contaminants and the sample grinding. After these steps, the sample chemical pretreatment starts. Typically, the chemical treatments include the AAA method (Acid-Alkali-Acid) for charcoal, wood, peat and vegetation (Mook, Streurman 1983); collagen extraction from bone (Longin 1971); alpha-cellulose extraction from tree ring (Green 1963), and phosphoric acid method for shell and marine carbonates (Hoefs 1987). In fig. 3, it is shown the distribution of different kinds of samples, treated so far at the Mass Spectrometry Laboratory of the Environmental Science Department of the II University of Naples, and measured at the Accelerator Mass Spectrometry (AMS) system of the Ruhr Universitaet in Bochum (D) (Lubritto *et al* 2004). Moreover the pretreatments used for bone and charcoal samples, collected in CdP and S. Paolo Belsito (SPB), has been summarized in tab. 1.

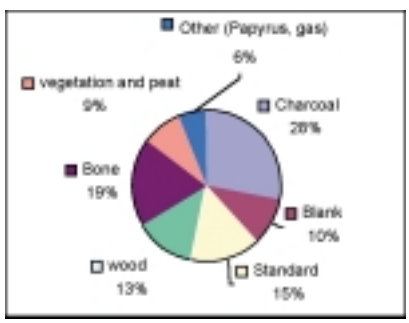

Figure 3. Cake diagram: % kind of samples treated in Mass Spectrometry Lab DSA SUN.

Sample's kind	Pretreatment's kind	Typic used mass (mg)
Charcoal	Treatment **AAA** (Acid/Alkali/Acid): **A**cid (HCl 3%) - **A**lkali (HCl 3%). (NaOH 3%)- **A**cid Between each phase, there are dilution with distilled water.	1-10
Bone	Bone is pulverized and immersed in an acid bath (HCl 0,6 N) at 0°C, where the organic fraction of the bone, collagen, is extracted. This cycle is repeated different times, depending from the bone preservation.	50-200

Table 1. Different pretreatments applied to bone and charcoal samples, collected in Croce del Papa and S. Paolo Belsito.

Then the sample has been dried and pyrolized by means of a quartz tube under a nitrogen (N_2) flow at 600°C. The pretreated sample is mixed with CuO and silver wires and put in a quartz test tube where a high vacuum with a membrane-turbomolecular pump system is achieved. Then, the test tube is sealed and heated to 900°C in order to oxidise the sample to CO_2. The CO_2 is cryogenically transferred to a "graphitization line" where it is reduced to graphite at 700°C. During the cryogenic transfer, the gas passes through a cold trap (dry ice-ethanol) in order to remove the water vapour impurities. The reaction takes place, tipically, during 4 hr in a 15 ml reaction chamber

filled with an hydrogen atmosphere at a partial pressure double than the CO_2 partial pressure and using iron powder catalyst (Dee *et al* 2000). The graphite, togheter with silver powder, is pressed into a target holder (an aluminum cylinder) and placed in the accelerator ion source of the Bochum Universitaet Accelerator Mass Spectrometry system (Lubritto *et al* 2004). The graphite, placed in the ion source, is converted to a single negatively charged ion beam by means of the sputtering process and injected, after the mass selection occurring in the injection magnet, into the Tandem Accelerator. Here, the carbon ions are accelerated in the first acceleration stage till the gas stripper where they are converted to positive ions. Subsequently, these cations are accelerated again from the stripper to the accelerator exit. The positive ion beam passes through further electric and magnetic selections in order to identificate and count the ^{14}C ions in a ΔE-E detector.

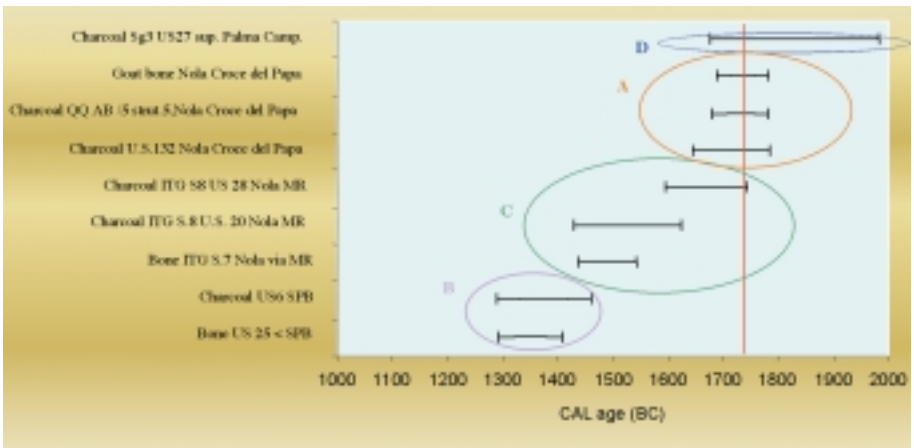

Figure 4. Calendarial intervals of Nola land's samples.

3. RESULTS AND CONCLUSIONS

To confirm the eruption date and to characterize the time of the human resumption, finds coming from CdP site (a goat bone found in the animal fence and two charcoals found near the goat's furnace), SPB site (bone and charcoal), MR site (bone and two charcoals) and Palma Campania site (charcoal) were measured. In figure 4, for each sample, the calendarial age intervals, obtained by the calibration software CALIB 3.0 (Stuiver, Reimer 1993) and expressed as Before Christ years (BC), with the corresponding statistical 1 sigma (s) error, are represented. In particular, measurements performed on the samples coming from CDP site , indicated in figure 4 by the circle A, give a more accurate indication about the date of the eruption, with respect to previous studies (Livadie Albore *et al* 1998), fixed to 1880 – 1680 B.C. and whose central value is represented in figure 4 by continuos vertical line. Indeed, the calendarial age interval, obtained

from the dating of a goat bone buried by eruption, fixs the eruption calendarial age interval to 1782-1686 BC. Results of measurements of sample coming from MR site (circle C) and SPB site (circle B) represent the calendarial age intervals characterizing the anthropic activity resumption, after the eruption, in the two sites. For SPB site, the human resumption happened in a time interval of about 250 years , while for the MR one, it happened around 150 years after the eruption. These results show an installation's fracture after the eruption: as a matter of fact the cultural development of the resumption in SPB e MR have the same characteristic as previous Palma Campania *facies*, as shown by the hut shapes and ceramic finds. Finally, the measurement of a charcoal coming from a layer, below the eruption one, at Palma Campania (circle D) demonstrates the existence of an older settlement abandoned shortly before the eruption.

REFERENCES

AA.VV., 2002. Nola Quattromila anni fa- Il villaggio del Bronzo Antico distrutto dal Vesuvio. Catalogo della mostra inaugurata a Nola il 20 giugno 2002. L'Arca e L'Arco s.r.l. Nola (Na).

Dee M., Bronk Ramsey C., 2000. Refinement of graphite target production at ORAU. *Nuclear Instrument and Methods in Physics Research* B, **172**, 449-450

Green J.W., 1963. *Methods of Carbohydrates Chemistry III* (Ed. R.I. Whistler). Academic Press, New York NK, pp.9-21.

Hoefs J., *Stable Isotope Geochemistry*. Third Edition, Springer-Verlag, Berlin, 1987.

Livadie Albore C., Castaldo N., Mastrolorenzo G., Vecchio G., 2001. Effetti delle eruzioni del Somma-Vesuvio sul territorio di Nola dall'età del Bronzo all'epoca romana tardiva. In: *Tephras-chronologie et archéologie, Congrès "Tèphrochronologie et coexistence hommes-volcans"*. Brivs-Charensac 24-29 agosto 1998, Dossiers de l'Archéo-Logis n°**1**, Clermont-Ferrand.

Livadie Albore C., Campatola L., Roca V., Romano M., Terrasi F., D'Onofrio A., Russo F., 1998. Sulla datazione dell'eruzione delle "Pomici di Avellino" e il suo impatto sui siti archeologici del Bronzo antico della Campania. IV Giornata delle Scienze della Terra e L'Archeometria. Ed.CUEN, pp.201-203.

Longin R., 1971. New method of collagen extraction for radiocarbon dating. *Nature* 230:241-2

Lubritto C., Rogalla D., Rubino M., Marzaioli F., Passariello I., Romano M., Spadaccini G., Casa G., Di Leva A., Gialanella L., Imbriani G., Calmieri A., Roca V., Rolfs C., Sabbarese C., Strieder F., Schuermann D., Terrasi F., 2004. Accelerator Mass Spectrometry at the 4 MV Dynamitron Tandem in Bochum. *Nuclear Instruments and Methods in Physics Research* B, **222**, 255-260.

Mook W.G. & Streurman H.J., 1983. Section B: The chemical aspects. *Physical and chemical aspects of radiocarbon dating*. PACT 8-**II.** 1. 47-53

Stuiver M., Reimer P.J., 1993. Extended ^{14}C Data Base and Revised CALIB 3.0 ^{14}C Age Calibration Program. *Radiocarbon* **35**, 215-230.

Terrasi F., 2001. Metodo di datazione mediante Spettrometria di Massa Ultrasensibile (AMS). In: *Elementi di Archeometria, metodi fisici per i beni culturali* (Castellano A., Martini M., Sibilia E., eds.) pp. 64-80. Egea

TOWARD A CHRONO-SERIATION METHOD BASED ON EUROPEAN TRADE WHITE BEADS IN NORTHEASTERN NORTH AMERICA

Jean-François Moreau
Université du Québec à Chicoutimi, Chicoutimi, Québec, Canada

R.G.V. Hancock
University of Toronto, Toronto, Canada

Marcel Moussette
CELAT, Université Laval, Québec, Canada

1. THE FUR TRADE AND THE CHRONOMETRY OF GLASS BEADS

Beginning in the late 16th century, Europeans began to trade a variety of goods, including glass beads, for furs trapped by the Amerindians. The beads have been systematically classified by archaeologists since the '60s, and by archaeometrists since the '90s. These beads are of Dutch, English or French trading origin; but many were probably made in The Netherlands (Karklins *et al.*2002). It has been shown that several elements follow a definite trend through time (Hancock *et al*. 1997, Sempowski *et al*. 2000, Moreau *et al*. 2002). This is notably the case for Sn, Sb, As, Mn and Ca (see figure 3). However the trend through time is quite less well defined for Al, Cl, Na and K. No definite explanations have been put forward to understand these chronological trends. However, economical (such as availability of minerals) and social (such as traditions in making beads) reasons are among reasonable hypotheses to be eventually tested. The difference in intervals for the time periods in figure 3 is the result of fairly unequal samples. Hence the two fifty years intervals of the 18th century total 15 and 8 beads while all other intervals (except 1900-1925) comprise generally well over 25 beads, most of them being 25 years intervals. One objective of this paper is thus to enhance the sample size for the 18th century.

2. LE PREMIER PALAIS DE L'INTENDANT ET LES MAGASINS DU ROY

While Québec City began with the early 17th century settling of Champlain, later 18th Century occupations are among the common

archaeological enterprises undertaken in the last forty years in Québec. The glass beads collections analysed here came from two archaeological contexts (Moussette 1994). The Premier Palais de l'Intendant, the residence of the French king's representative in New France, was erected around the beginning of the 18th century, the beads associated with the archaeological units of this Premier Palais may date to any time period from 1700 to 1750 as shown by several associated artifacts pertaining to later periods than the construction of the Palais. The second archaeological context is that of the Magasins du Roy (king's stores), erected by the middle of the 18th century and burned in 1760 when Québec was under English siege. Hence the beads from this context are neatly pinpointed to the 1750-1760 time period.

3. NEUTRON ACTIVATION RESULTS AND DISCUSSION

Following procedures largely described elsewhere (Moreau *et al*. 2002), these beads were submitted to neutron activation analysis (INAA) for nine elements (table 1). As shown in figure 1, the overall variation for any element is generally smaller and often much smaller for the Magasins du Roy (homogeneity of collections) than it is for the Premier Palais. Taking into

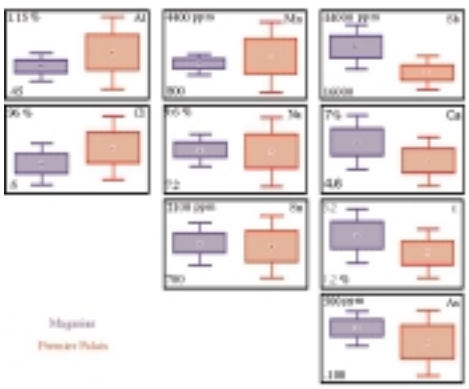

Figure 1. Québec's beads: mean and standard deviation.

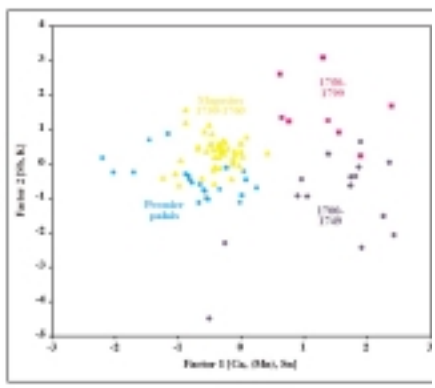

Figure 2. Factor analysis for Québec's and other 18th Century sites.

account both mean and standard deviation values, only three elements (Mn, Na, Sn) may be considered similar for both archaeological contexts while the values of Al and Cl are smaller for the Magasins compared to those of the Premier Palais, the reverse being observed for Sb, Ca, K and As. In figure 2, the factor analysis compares the beads from these two archaeological contexts to those two fifty years intervals collections that had been used for the chronometric trends already referred to in figure 3. While there is a split between the beads from Québec and the other sites along the horizontal axis,

			Al %	Ca %	Cl %	Mn ppm	K %	Na %	Sn ppm	As ppm	Sb ppm
Magasins	CeEt-30-13F8-12 1/C	213	0.72	5.7	0.75	2180	2.6	8.50	≤ 1650	≤ 160	33400
Magasins	CeEt-30-13F8-12 1/C	214	0.73	6.5	0.71	1980	2.5	8.75	≤ 1300	≤ 200	37600
Magasins	CeEt-30-13F8-12 1/C	215	0.76	6.0	0.76	2140	2.5	8.92	≤ 1590	≤ 200	35000
Magasins	CeEt-30-13C11-6	E01	0.75	6.5	0.69	1750	2.4	8.23	≤ 1150	≤ 210	35900
Magasins	CeEt-30-13C11-6	E02	0.71	6.0	0.75	2370	2.6	8.68	≤ 1560	≤ 170	33000
Magasins	CeEt-30-13C11-6	E03	0.68	6.7	0.84	2520	2.7	8.94	≤ 1630	≤ 220	32200
Magasins	CeEt-30-13C11-6	E04	0.69	6.1	0.76	2420	2.5	8.32	≤ 1190	≤ 220	31000
Magasins	CeEt-30-13C11-6	E05	0.73	6.5	0.76	2160	2.3	8.77	≤ 1190	≤ 210	35000
Magasins	CeEt-30-13C11-6	E06	0.66	5.9	0.68	2540	1.9	8.39	≤ 1340	≤ 180	29000
Magasins	CeEt-30-13C11-6	E07	0.67	6.1	0.73	2110	2.5	8.37	≤ 1210	≤ 210	32200
Magasins	CeEt-30-13C11-6	E08	0.71	5.8	0.73	2240	2.3	8.56	≤ 1270	≤ 220	34500
Magasins	CeEt-30-13C11-6	E09	0.74	5.2	0.77	2860	2.5	8.13	≤ 1740	≤ 200	20000
Magasins	CeEt-30-13C11-6	E10	0.69	6.2	0.73	2500	2.2	8.43	≤ 1340	≤ 210	29700
Magasins	CeEt-30-13C11-6	E11	0.72	5.9	0.74	2250	2.6	8.38	≤ 1360	≤ 250	32200
Magasins	CeEt-30-13C11-6	E12	0.73	6.3	0.74	2060	2.2	8.13	≤ 1350	≤ 190	31000
Magasins	CeEt-30-13C11-6	E13	0.73	6.0	0.70	2110	1.8	8.19	≤ 1290	≤ 190	32000
Magasins	CeEt-30-13C11-6	E14	0.69	6.0	0.62	1940	2.1	8.33	≤ 1330	≤ 260	36000
Magasins	CeEt-30-13C11-6	E15	0.71	6.1	0.77	2210	2.5	8.30	≤ 1500	≤ 230	32000
Magasins	CeEt-30-13C11-6	E16	0.74	6.0	0.73	2090	2.8	8.19	≤ 1240	≤ 250	34500
Magasins	CeEt-30-13C11-6	E17	0.70	5.9	0.67	1980	2.2	8.18	≤ 1250	≤ 270	34500
Magasins	CeEt-30-13C11-6	E18	0.72	5.9	0.73	2170	2.2	8.38	≤ 1510	≤ 290	33000
Magasins	CeEt-30-13C11-6	E19	0.69	5.8	0.70	2170	3,0	8.24	≤ 1520	≤ 320	34100
Magasins	CeEt-30-13C11-6	E20	0.38	5.7	0.69	2070	2.8	8.46	≤ 1210	≤ 290	34600
Magasins	CeEt-30-13F8-12 2/E	201	0.67	5.7	0.72	2570	2,0	8.28	≤ 1320	≤ 260	27500
Magasins	CeEt-30-13F8-12 2/E	202	0.73	6.4	0.70	1970	2.4	8.19	≤ 1410	≤ 260	32600
Magasins	CeEt-30-13F8-12 2/E	203	0.67	5.9	0.76	2420	2.2	8.18	≤ 1350	≤ 250	28800
Magasins	CeEt-30-13F8-12 2/E	204	0.68	6.1	0.74	2100	2.5	8.21	≤ 1330	≤ 260	33100
Magasins	CeEt-30-13F8-12 2/E	205	0.72	4.9	0.68	2200	2.1	8.33	≤ 1520	≤ 310	33900
Magasins	CeEt-30-13F8-12 2/E	206	0.71	6.4	0.70	2370	2.4	8.60	≤ 1380	≤ 310	31400
Magasins	CeEt-30-13F8-12 2/E	207	0.74	6.1	0.73	2390	2.2	8.09	≤ 1330	≤ 290	29500
Magasins	CeEt-30-13F8-12 2/E	208	0.73	5.7	0.69	1970	2.9	8.13	≤ 1390	≤ 330	32200
Magasins	CeEt-30-13F8-12 2/E	209	0.70	6.2	0.70	2210	2,0	8.56	≤ 1280	≤ 300	33200
Magasins	CeEt-30-13F8-12 2/E	210	0.68	6.2	0.77	1800	2.3	8.27	≤ 1400	≤ 350	34100
Magasins	CeEt-30-13F8-12 2/E	211	0.65	5.2	0.74	2390	1.6	8.30	≤ 1510	≤ 330	30800
Magasins	CeEt-30-13F8-12 2/E	212	0.75	6.5	0.72	2350	2,0	8.53	≤ 1580	≤ 330	32700
Magasins	CeEt-30-13F8-12 2/E	213	0.70	5.7	0.64	2060	2.8	8.31	≤ 1310	≤ 300	33100
Magasins	CeEt-30-13F8-12 2/E	214	0.70	6.6	0.82	2310	2.2	8.25	≤ 1390	≤ 310	30000
Magasins	CeEt-30-13F8-12 2/E	215	0.74	5.6	0.67	2350	2.7	8.20	≤ 1500	≤ 330	32600
Magasins	CeEt-30-13F8-12 2/E	216	0.76	6.1	0.72	2290	2,0	8.38	≤ 1280	≤ 320	32900
Magasins	CeEt-30-13F8-12 2/E	217	0.72	5.8	0.70	2300	2.8	8.44	≤ 1260	≤ 290	32900
Magasins	CeEt-30-13F8-12 2/E	218	0.72	6.0	0.70	2030	2.6	8.35	≤ 1350	≤ 320	35500
Magasins	CeEt-30-13F8-12 2/E	219	0.72	6.4	0.68	2130	2.4	8.52	≤ 1320	≤ 300	33300
Magasins	CeEt-30-13F8-12 2/E	220	0.73	6.1	0.68	1840	2.6	8.65	≤ 1910	≤ 420	40600
Magasins	CeEt-30-6C13-510	F21	0.79	5.9	0.67	2640	2.4	7.94	≤ 1680	≤ 260	20000
Magasins	CeEt-30-6C13-510	F22	0.68	5.8	0.68	2130	3,0	8.51	≤ 1750	≤ 400	34900
PremierPalais	CeEt-30-27C71	B01	1.03	5.5	0.91	3120	2.1	9.30	≤ 1700	≤ 74	26500
PremierPalais	CeEt-30-27C71	B02	0.93	4.8	0.83	2430	2,0	8.16	≤ 1380	≤ 70	23700
PremierPalais	CeEt-30-27C71	B03	0.96	5.3	0.81	2300	1.8	8.34	≤ 1380	≤ 64	24100
PremierPalais	CeEt-30-27C71	B04	0.92	5.0	0.83	1650	2,0	8.67	≤ 1120	≤ 69	26800
PremierPalais	CeEt-30-27C71	B05	0.97	5.6	0.75	2400	1.7	8.40	≤ 1300	≤ 73	22900
PremierPalais	CeEt-30-27C71	B06	0.91	5.5	0.79	2250	2.5	8.53	≤ 850	≤ 75	24500
PremierPalais	CeEt-30-27C71	B07	0.95	5.7	0.83	2430	1.6	8.22	≤ 1390	≤ 76	22600
PremierPalais	CeEt-30-27C71	B08	0.72	6.2	0.72	3130	1.6	7.97	≤ 1640	≤ 90	26700
PremierPalais	CeEt-30-27C71	B09	1.09	5.2	0.71	2220	2,0	8.33	≤ 1520	≤ 76	24600
PremierPalais	CeEt-30-27C71	B11	0.81	5.5	0.82	3970	1.8	9.35	≤ 1740	280	23400
PremierPalais	CeEt-30-27C71	B12	0.77	5.9	0.79	4030	2.1	8.67	≤ 1660	250	21900
PremierPalais	CeEt-30-17B39	C16	0.72	4.9	0.79	2210	1.8	8.10	≤ 1140	≤ 160	22700
PremierPalais	CeEt-30-17B39	C17	0.51	5.3	0.84	1980	1.9	7.93	≤ 1030	≤ 180	24900
PremierPalais	CeEt-30-17B27	D01	0.78	5.4	0.82	4110	1.9	8.89	≤ 1760	≤ 220	21800
PremierPalais	CeEt-30-17B27	D02	0.55	5.9	0.71	2270	1.9	8.54	≤ 1350	≤ 170	25600
PremierPalais	CeEt-30-17B27	D03	0.73	5.6	0.81	1830	2.4	7.74	≤ 1160	≤ 160	25400
PremierPalais	CeEt-30-17B27	D04	0.88	5.5	0.75	1830	1.9	7.92	≤ 1360	≤ 200	17300
PremierPalais	CeEt-30-17B27	D05	0.73	5.3	0.65	2660	2.3	7.95	≤ 1240	≤ 390	27000
PremierPalais	CeEt-30-17B27	D06	0.74	5.4	0.89	1850	1.8	8.67	≤ 1450	≤ 480	30800
PremierPalais	CeEt-30-17B27	D07	0.73	5.9	0.83	2690	1.7	8.23	≤ 1400	≤ 300	26100
PremierPalais	CeEt-30-17B27	D08	0.74	5.3	0.70	2020	2.4	7.52	≤ 1100	≤ 170	21600
PremierPalais	CeEt-30-17B27	D09	0.80	5.8	0.71	2010	2.6	7.70	≤ 1010	≤ 150	23400
Magasins	N		45	45	45	45	45	45	45	45	45
	μ		0.71	6.0	0.72	2214	2.4	8.37	1405	266	32396
	Sx		0.06	0.4	0.04	228	0.3	0.22	170	60	3576
PremierPalais	N		22	22	22	22	22	22	22	22	22
	μ		0.82	5.5	0.79	2517	2.0	8.32	1349	172	24277
	Sx		0.14	0.3	0.07	725	0.3	0.48	253	113	2691

Table 1. Neutron activation data for Beads from Premier Palais and Magasins du Roy

the vertical distribution respects quite well the time periods of each groups compared to the other. In figure 3, the trends in time expressed in mean and plus/minus one standard deviation for the five most significant elements is compared to the mean and plus/minus one standard deviation calculated for the Magasins du Roy's collections, symbolized by the three red lines. Moreover the violet vertical dotted line represents the 1750-1760 time interval of use of the Magasins du Roy.

4. CONCLUSIONS

The samples from the Premier Palais and the Magasins du Roy fit generally well with the previous beads studied by INAA. The definite short interval of the Magasins du Roy enable us to ascertain the chronometric trend for the elements in the third quarter of the 18th Century. Next steps will be to find collections for the three other quarters of century as well as testing if the blue beads from the Premier Palais and the Magasins du Roy also present good agreement with the general trends obtained from other sites.

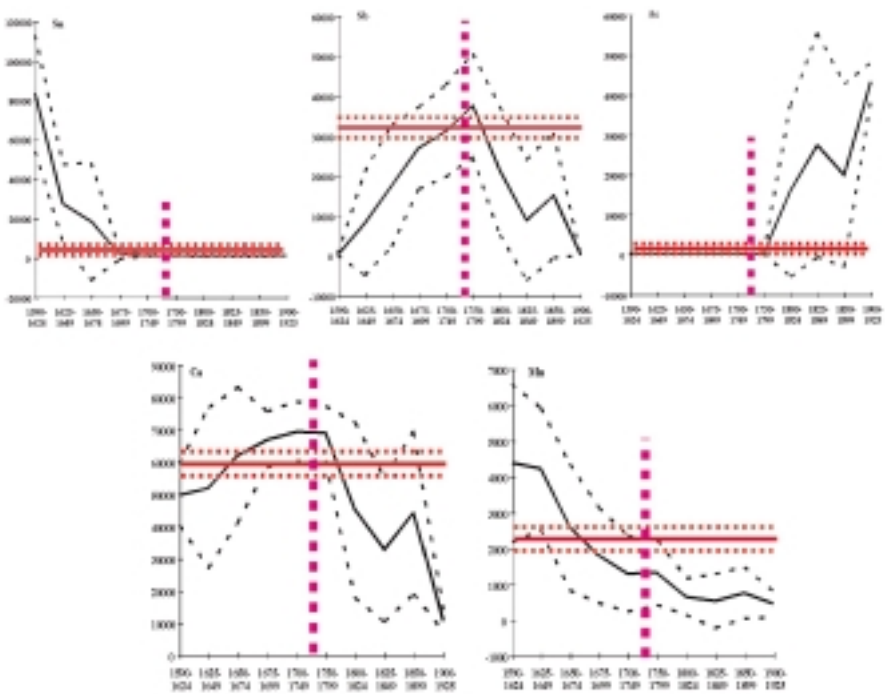

Figure 3. Québec's beads compared to trends observed for beads from 1600 to 1925.

REFERENCES

Hancock, R.G.V., S. Aufreiter and I. Kenyon, 1997, European White Glass Trade Beads as Chronological and Trade Markers, in P.B. Vandiver, J.R., Druzik, J.F. Merkel and J. Stewart (eds), *Materials Issues in Art and Archaeology V*, Pittsburgh, Pennsylvania, Materials Research Society, Symposium Proceedings Volume 462, p.181-191.

Karklins, K.; Hancock, R.G.V.; Baart, J.; Sempowski, M.L.; Moreau, J.-F.; Barham, D.; Aufreiter, S. & Kenyon, I., 2002, «Analysis of Glass Beads and Glass Recovered from an Early 17th-Century Glassmaking House in Amsterdam» in Jakes, Kathryn A.(dir), *Archaeological Chemistry. Materials, Methods, and Meaning*. American Chemical Society, Washington, DC, ACS Symposium Series 831, pp. 110-127.

Moreau, J.-F., Hancock, R.G.V., Aufreiter, S. & Kenyon, I., 2002, «Late French (1700-1750) to Early English (1750-1800) Regime White Glass Trade Beads From A Presumed Decorated Bag Found at the Ashuapmushuan Site (Eastern Central Québec), Canada» in Jerem, E. & Biro, K.T. (dir.), *Archaeometry 98. Proceedings of the 31st Symposium*, 2 volumes, British Archaeological Research, pp.613-619,(Coll. BAR International Series n° 1043)

Moussette, M., 1994, *Le site du Palais de l'intendant à Québec*. Septentrion, Sillery.

Sempowski, M.L.; Nohe, A.W.; Moreau, J.-F.; Kenyon, I.; Karklins, K.; Aufreiter, S., Hancock, R.G.V., 2000, «On the transition from tin-rich to antimony-rich European white soda-glass trade beads for the Senecas of Northeastern North America», *Journal of Radioanalytical and Nuclear Chemistry*, Vol. 244, No 3, pp. 559-566.

PETROGRAPHIC INVESTIGATIONS AND 14 C DATING FOR APPROXIMATING THE AGE OF LIME MORTARS

Danuta NAWROCKA
Institute of Geology, Department of Dynamic and Regional Geology,
Adam Mickiewicz University, ul. Maków Polnych 16, 61-606 Poznań, Poland.
e-mail: danutamich@go2.pl

Jacek MICHNIEWICZ
Institute of Geology, Department of Dynamic and Regional Geology,
Adam Mickiewicz University, ul. Maków Polnych 16, 61-606 Poznań, Poland.
e-mail: jacekm@amu.edu.pl

1. INTRODUCTION

Radiocarbon dating of lime mortars is based on setting the present ^{14}C concentration of CO_2 by mortar carbonates in the hardening process. If the mortars are made of completely burnt lime, radiocarbon dating gives the age of construction of the building.

1.1. The difficulties in radiocarbon dating of lime mortars

The problem with the estimation of the real radiocarbon age appears, when there are some unburnt fragments of carbonate rocks in the mortar. Then not all the $CaCO_3$ is transposed into CaO and the mentioned fragments give so called "dead carbon", what is the reason of significant exaggeration in the absolute age. The big difficulty is also the presence of aggregate, especially carbonatious one, which is hardly separable from the also carbonate binder. This kind of aggregate is partially or completely devoid of active isotope 14C, what makes the age determined by dating much older than the real one (cf. Folk, Valastro, 1979).

In this context, the application of petrographic studies that enable determination of mineral composition and percentage of aggregate turns to be particularly important. If in mortar some content of limestone fragments, which are the source of dead carbon, is identified, it needs to be eliminated, to make the sample destined for dating possibly clear. Practice shows, that

limestone fragments building aggregate can be very small in size and difficult to eliminate, so despite efforts to separate them, some amount may remain in the sample.

1.2. The difficulties in radiocarbon dating of charcoal fragments

The charcoal materials are probably most widely used material in radiocarbon dating. The dates obtained from the charcoal sample often give ages which are too old. The main source of this errors seems to be the fact, that the wood fragments could came from the old tree. Each year a tree grows a new layer of wood over the older wood, and the analyzing sample from inner part, could exist even hundreds years before the death of a tree.

2. Subject and aim of the study

This study is an attempt to evaluate and compare the methods of the age estimation of lime mortars using gas proportional counting method (GPC) and accelerator mass spectrometry technique (AMS). The dating by GPC has been performed in Gliwice Radiocarbon Laboratory, whereas by AMS in Pozna_ Radiocarbon Laboratory. As the benchmarks there were used samples of the mortars with the approximate age established by an archaeological research. Three groups of samples have been analysed. The first group comes from the Medieval church (XII cent. AD) situated on the terrain of the Wle_ Castle, SW Poland. The second one was collected at the north-western shore of the Dead Sea. These mortars are from the Roman period (II cent. BC - I cent. AD). They come from the settlement Khirbet Mazen and from the water supply system situated near the caves above Qumran. The third gruop is from the Byzanthine church (V-VI/VII cent. AD) in Hippos, the town situated at the top of the hill, about 350 m above water level of the Galilean Lake (III cent. B.C.-749 AD). It should be stressed, that the investigations are not the profound study aiming to solve the problems raised by archaeologists. They are the material, which enables the development of the methodology connected with the possibility of absolute age estimation of mortars on the basis of radiocarbon content.

3. SAMPLE MATERIAL AND PREPARATION FOR ^{14}C DATING

Mortar is a mixture of binder and aggregate, in different proportions. Petrographic investigations allowed to obtain the precise characteristics both the aggregate and the binder of the analysed mortars. The analysed mortars from south-western Poland, as well as from Palestine represent the type of lime mortars. The Palestinian mortars contain appreciable amount of aggregate (sometimes even exceeding 50%), whereas the Polish ones (e.g. K/160/4) are almost completely devoid of aggregate (fig. 1, 2).

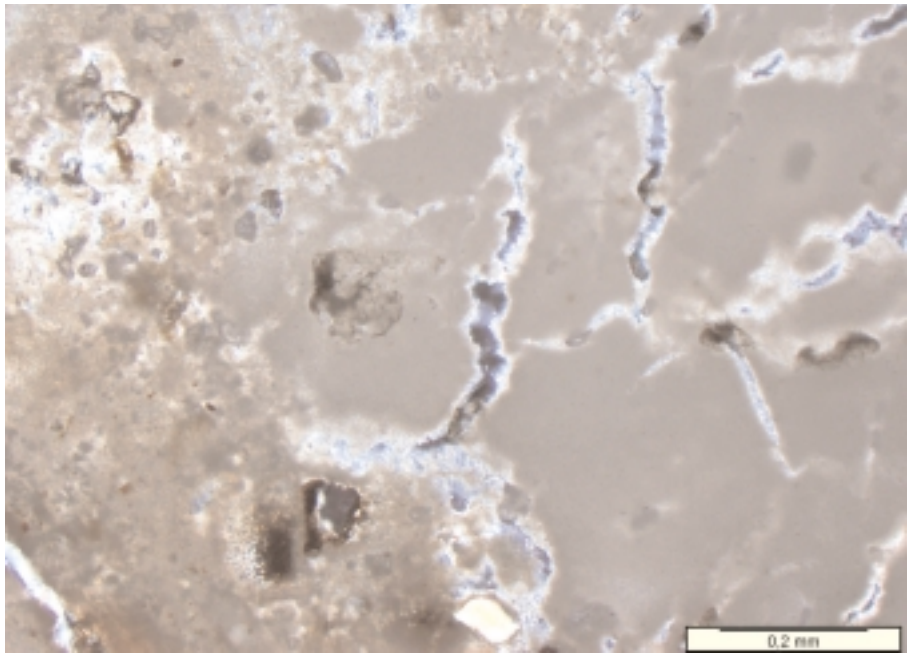

Figure 1. Microphotograph of sample K/160/4 from Wleń.

Two categories of the investigated material have been determined from these samples: the binder and the charcoal fragments from the mortars.

3.1. GPC-Gas counting

The first radiocarbon dating was performed for the mortar samples from the Medieval church in Wleń and for the Roman mortars from the settlements on the west bank of the Dead Sea (table 1). The conventional method was applied. To make the dating of the mortars reliable, it was necessary to remove the limestone components, clearly visible at the microphotographs of the Palestinian mortars (fig. 2). The mechanical separation basing on the fact, that the limestone in aggregate is stronger and more resistant than more porous mortar carbonate was carried out. The mortars were delicately crushed, and then repeatedly frozen and thawed. Most of the soft mortar carbonate was separated from the aggregate grains, and during binocular observations, required amount of sample material was collected. Carbon dioxide in the studied mortar samples was released by treatment of the sample with hydrochloric acid in the vacuum apparatus of the Gliwice Laboratory. Then, after purification process, 14C has been counted in a proportional counter.

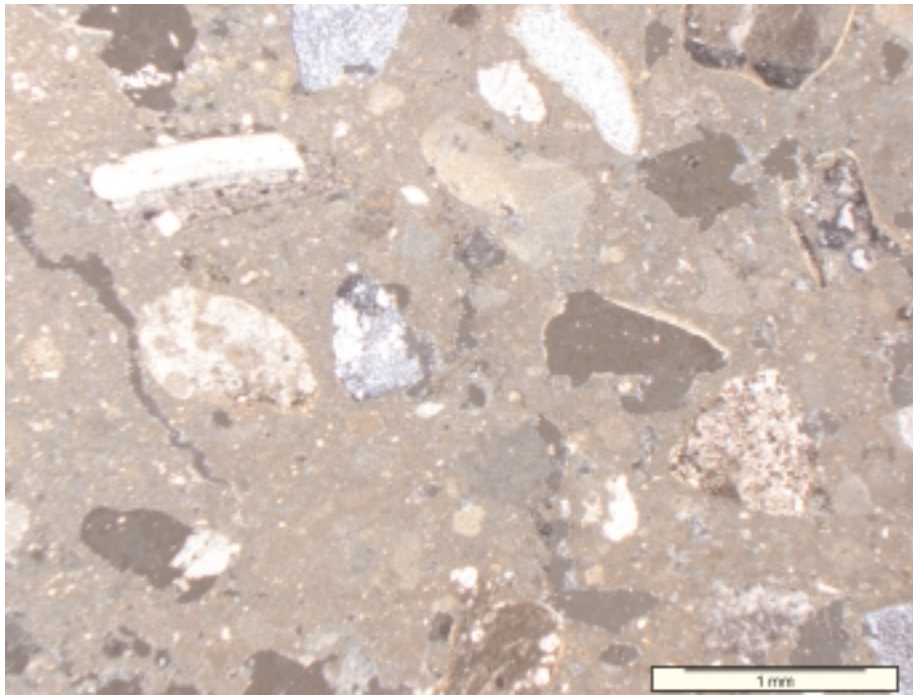

Figure 2. Microphotographs of the mortar QA/1997 from Khirbet Mazen. The variegated composition of the aggregate (quartz, snail shells, limestone grains) is visible.

3.2. AMS - accelerator mass spectrometry technique

Sometimes collected samples are too small for the conventional 14C dating. AMS radiocarbon dating requires less than 1 mg of carbon, what makes collecting of the sufficient amount of material for investigation much easier. From among the chosen group of the mortars, i. a. the charcoal fragments (Hip14, Hip2, K/157/1, K/160/4, Qm4) and the binder (Hip2sp, Hip10) allowing the comparison of the results were selected for dating by this method (table 2).

The next group of mortars, after delicate crushing in a porcelain mortar, sifting and XRD analysis of individual fractions is prepared for the radiocarbon dating. For this part of the material, in order to eliminate the dead carbon coming from the limestone fragments used as an aggregate, the difference in the course of reaction with acid will be applied. The separation of fractions from mortars for dating and the application of the dependence of the rate of reaction on grain size for a mortar and a limestone proposed by Soninen, Jungner (Soninen, Jungner,2001) seem to be promising for obtaining the reliable real ages.

4. RESULTS

Radiocarbon ages (obtained by GPC method) of the samples from medieval church in Wleń, which were devoid of lime aggregate confirm existing architectural-historical data. The obtained GPC radiocarbon results for the Roman mortars were far from expectations and historical premises, although they revealed some regularity. The samples, from which the sufficient amount of the binder could not be separated, were the mixture of binder and aggregate. Despite of efforts made to eliminate lime aggregate from binder (by freezing and thawing) and taking into consideration the $\delta^{13}C$ value in the binder alone and in the mixture of binder with aggregate, so called corrected conventional radiocarbon age was still significantly higher then the age obtained for the binder (table 1). It must be noted, that the age of the mixture is much more exaggerated, what confirms the enormous

Sample name	M	Lab. no	T_C [BP]	ΔT_C [years]	$\delta^{13}C$ [‰, PDB]	T_{CCA} [BP]	ΔT_{CCA} [years]	Cal. age [BC]/[AD]	Approximate age established by archeological research
QA/1997	S	15262	2810	130	-9,74	2810	130	[1127, 829]	140BC, 68AD
Q1/2000	S	15264	4360	220	(-9)[A]	4360	220	[3356, 2857]	140BC, 68AD
Q6/2000	S	15226	3250	120	-8,11	3250	120	[1642, 1410]	140BC, 68AD
Q1/2000	SK	15223	6640	110	-7,69	6210	180	[5324, 4917]	140BC, 68AD
Q2/2000	SK	15225	4730	90	-11,0[B]	7180	150	[3634, 3555][C]	140BC, 68AD
Q3/2000	SK	15228	8750	130	-7,37	7980	200	[7084, 6638]	140BC, 68AD
Q6/2000	SK	12313	9220	80	-6,13	6970	180	[5933, 5719]	140BC, 68AD
K1/93/W	S	15369	1030	80	-12,5			[890AD,1050AD	[1177AD,1230AD
K160/4/W	S	17105	940	130	-13,2			[980AD,1230AD]	[1177AD,1230AD

Table 1. ^{14}C dating results for lime mortars in comparison with historical data; gas proportional counting method.

Explanatory notes (table 1, 2):

A=estimated $\delta^{13}C$ values; B=estimated $\delta^{13}C$ value (-8.11 per milles) is higher than $\delta^{13}C$ value of the dated material (binder with aggregate). It resulted in T_{CCA} value higher than T_C; C=T_C age was calibrated; M=type of dated material; S=binder; SK=binder with aggregate; W=charcoal; T_C=Conventional radiocarbon age of dated mortar fraction; T_{CCA}=Conventional radiocarbon age of aggregate, obtained after correction for content of "old", radiocarbon-free aggregate. In case of binder sample dating, the age is identical with the T_c age; ΔT_C, ΔT_{CCA}=estimated errors of the given ages; Cal age=Calendary (calibrated) age interval on the confidence level of 68% (T_{CCA} was calibrated); Samples from the Roman period are indicated by Q and QA; from the Medieval by K, from the Byzantine by Hip.

influence of aggregate on the radiocarbon age. The dating results by AMS look much better than in the first stage (by GPC) and mainly fall into the age range expected from the historical context. The difference in the AMS dating results of the charcoal and the binder from the same sample (Hip2) should be connected with the above-mentioned constraints for dating of this kind of materials. The future analysis will be based on the separation of an fraction which is appropriate to the dating from mortar (cf. Heinemeier et al.,1997).

Sample name	M	Lab. no	^{14}C age	ΔT_C years BP	$\delta^{13}C$ [‰]	Cal. Age (95,4%) [BC/AD]	Cal. Age (68,2%) [BC]/[AD]	Approximate age established by archeological research
Hip 14	W	5088	2025	80	-42,9	400BC-250AD	160BC94,6%)130BC 120BC(63,6%)70AD	V-VI/VII cent.AD
Hip 2	W	5087	1570	70	-42,4	340AD-640A	410AD-570AD	V-VI/VII cent.AD
Hip 2 sp	S	5016	1295	30	-10,8	660AD-780AD	680AD(40,1%)725AD	V-VI/VII cent.AD 740AD(28,1%)775AD
Hip 10	S	7417	1245	35	-9,5	680AD-890AD	690AD(61,0%)820AD	V-VI/VII cent.AD 840AD(7,2%)860AD
K/157/1	W	5091	1035	30	-21,9	890AD-920AD 950AD-1040AD	988AD-1020AD	[1177AD,1230AD]
K/160/4	W	5092	1185	35	-26	720AD-750AD 770AD-970AD	780AD-890AD	[1177AD,1230AD]
Qm 4	W	5089	2165	30	-22,3	360BC-270BC 260BC-110BC	360BC(31,3%)290BC 240BC(36,9%)160BC	140BC, 68AD

Table 2. AMS radiocarbon dating results.

ACKNOWLEDGEMENTS

We sincerely thank Prof. Anna Pazdur from Gliwice Radiocarbon Laboratory for performing radiocarbon dating and help in the interpretation of results. We also thank Prof. Tomasz Goslar from Poznan Radiocarbon Laboratory. The research was supported by Polish Komitet Badan Naukowych, Grant no 3 P04D 05325 in the years 2003-2005.

REFERENCES

Folk R.L, Valastro S, 1979. Dating of lime mortar by ^{14}C. In: Berger R, Suess H, editors. *Radiocarbon Dating. (Proceedings of the Nonth International Conference Los Angeles and La Jolla 1976).* Berkeley, Los Angeles: University of California Press. 721-730.

Heinemeier J, Jungner H, Lindroos A, Ringbom A, von Konow T, Rud N, 1997. AMS ^{14}C dating of lime mortar. *Nuclear Insttruments and Methods in Physics Research* B 123: 487-495.

Sonninen E., Jungner H., 2001: An improvement in preparation of mortar for radiocarbon dating. *Radiocarbon* 43 (2A): 271-273.

SIMULATIONS OF THE STATISTICAL ARCHAEOMAGNETIC DATING METHOD

Rob Sternberg
Department of Earth and Environment, Franklin & Marshall College, Lancaster, PA 17604-3003, USA; Rob.Sternberg@FandM.edu

Jeffrey L. Eighmy
Department of Anthropology, Colorado State University, Ft. Collins, CO 80523-1787, USA; jeff.eighmy@colostate.edu

1. INTRODUCTION

Archaeomagnetic (AM) dating involves comparison of an archaeomagnetic direction to a master record of secular variation to derive an absolute date (Sternberg, 1997). This is similar to radiocarbon dating where a radiocarbon age is compared to a calibration curve to obtain a probabilistic calendric date. AM dating is complicated by the three-dimensional nature of the problem, and counterintuitive dating interpretations can result (Sternberg and McGuire, 1990). Here we systematically consider how these interactions influence the derivation of archaeomagnetic dates.

Archaeomagnetic secular variation (SV) curves constructed using statistical methods are also subject to 3D uncertainties. Statistical curves are commonly based on a moving-average technique. Lengyel and Eighmy (2002) showed the effects of incorrectly dated directions on a looping curve. If a point which actually dates to one segment of a looping curve is incorrectly dated to the opposite side of the loop, the curvature of the segment will be damped. Lengyel and Eighmy (2002) suggested how curves can be corrected for this problem.

As an example of archaeomagnetic dating, consider HV046, a fire pit from Homolovi II, an Anasazi archaeological site in northeastern Arizona, USA, with a tentative archaeological date of AD 1325-1425. Statistically comparing the AM virtual geomagnetic pole (VGP) direction point-by-point to Eighmy's (1991, table 2, with subsequent corrections) SV curve (fig. 1) using F-tests (Sternberg, 1989; Le Goff et al., 2002) yields an archaeomagnetic date with two options at the 5% significance level, AD 930-1370, and 1430-1645 (fig. 2). The B95 (geometric average of VGP semi-major axes dm and dp) for HV046 is a

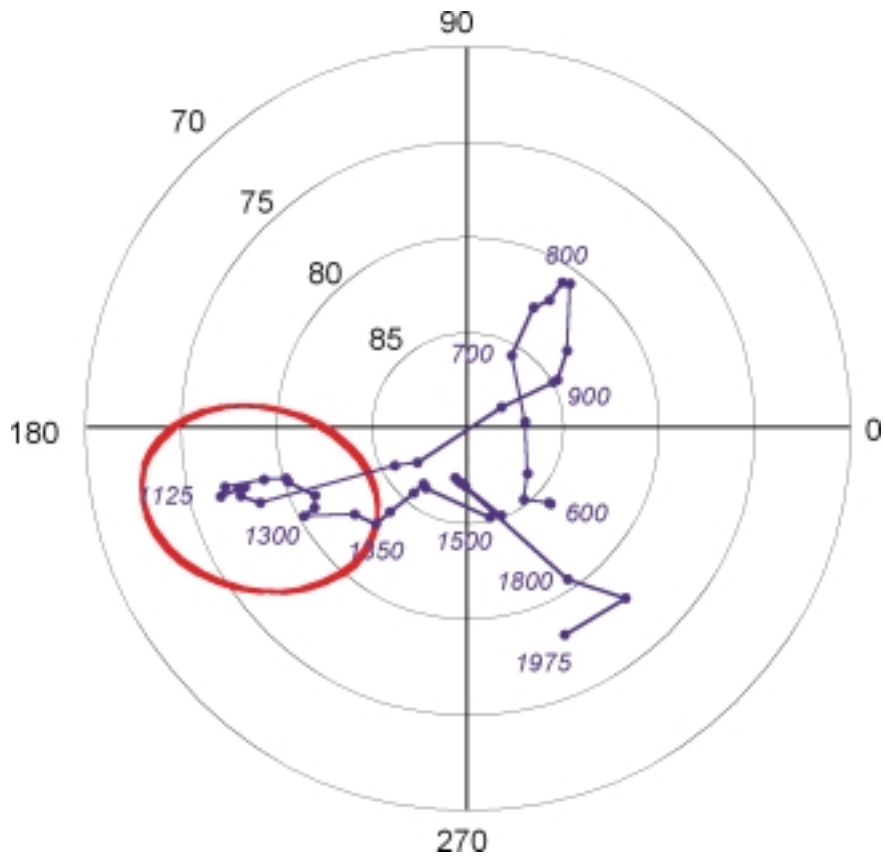

Figure 1. The oval of confidence of the VGP for the archaeomagnetic feature HV046 (red) is plotted with the U.S. Southwestern secular variation curve (blue; Eighmy, 1991, table 2). The plot is centered on the north geographic pole; several latitudes and the cardinal longitudes are shown. Several dates in years AD are shown for the curve.

mediocre 4.1∞. The oval of confidence for HV046 overlaps the curve from AD 1000-1350, yet the archaeomagnetic date is more inclusive because of the varying precision with which the time-averaged SV VGPs are known. The pre-1000 and post-1450 AM dating options arise because of the larger uncertainty (A95s>5∞) of the curve for those times (Eighmy, 1991, table 2), even though the HV046 oval is further away from the curve. It could be argued from the full probability curve (fig. 2) that the two options could be lumped into one larger option, with only one intervening point having a probability just below 5%.

In this paper, we seek to better understand the interaction of AM directions to be dated with SV curves through a series of simulations, using both hypothetical and actual SV curves.

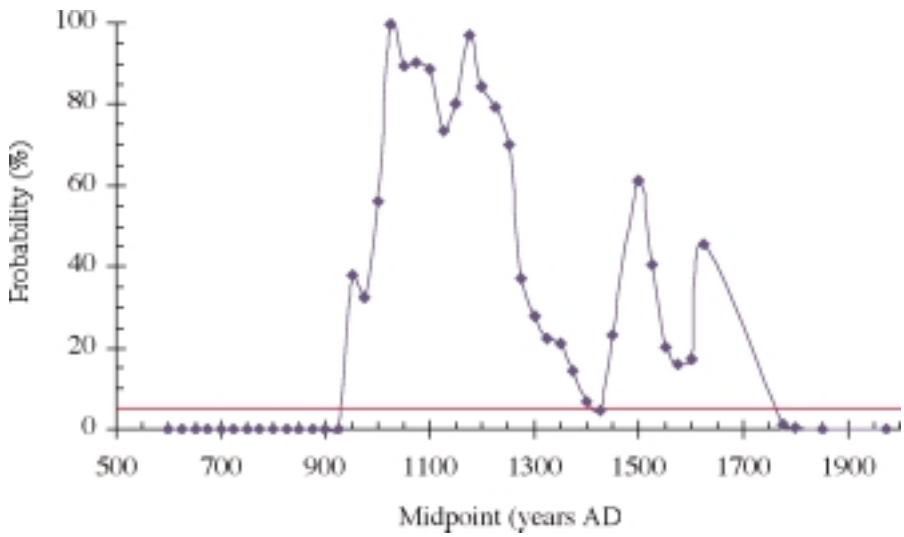

Figure 2. The dating probability plot for HV046 using the secular variation curve of Eighmy (1991), using methods like those in Le Goff et al. (2002). The red line represents the 5% significance level for dating probabilities.

2. SIMULATION METHOD

To better examine the interactions between a VGP to be dated and VGP secular variation curves, we have looked for 16 cases at how a grid of possible VGPs would date at the 5% significance level against the following secular variation curves: 1) a hypothetical linear curve; 2) a hypothetical circular curve; 3) a hypothetical cusped curve; 4) Lengyel & Eighmy's (2002) SW U.S. curve; 5) Sternberg's (1989) SW U.S. curve. The hypothetical curves represent typical SV rates at 50-year intervals. VGPs at each point on a 2∞ grid about the north geographic pole were dated against each curve. A95 and B95 angles were generally set to 2∞, but were varied for some cases. Using the probabilistic dating method (Le Goff et al., 2002), the dating probability was calculated for each point on the grid. An *Excel* spreadsheet with macros for looping was used for the basic calculations. The results for each simulation were summarized in terms of total number of both dated intervals and dating options for each point on the grid. An interval is a period of time represented by one point on the secular variation curve. A dating option is a continuous period of time composed of one or more consecutive dated intervals. These numbers were posted to a grid corresponding to the test VGPs to be dated, and then contoured using *Surfer* software.

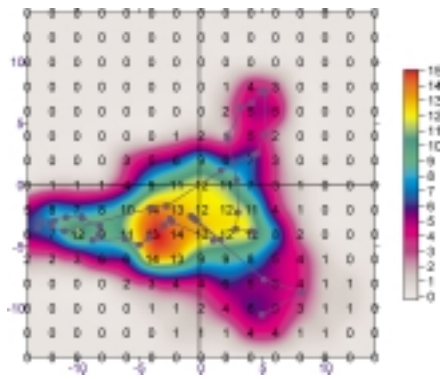

Figure 3. Posted and contoured values are the number of different dating intervals for a simulation based on VGPs over a grid and the SV curve of Eighmy (1991).

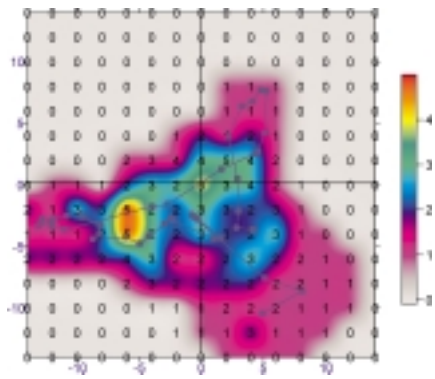

Figure 4. Posted and contoured values are the number of different dating options for a simulation based on VGPs over a grid and the SV curve of Eighmy (1991).

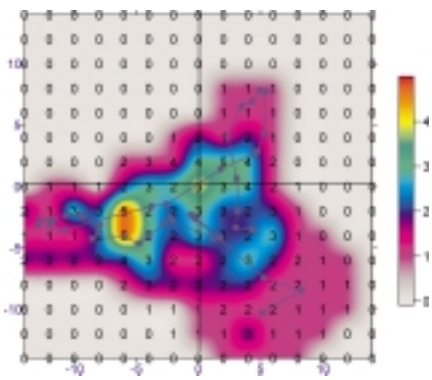

Figure 5. Posted and contoured values are the number of different dating intervals for a simulation based on VGPs over a grid and the SV curve of Sternberg (1989). The smoother SV curve with larger windows produces fewer options than the curve of Eighmy (1991).

3. RESULTS

Results for the hypothetical curves, not surprisingly, confirmed the observations that have been made about the counterintuitive results of the statistical method when applied to directions (Sternberg and McGuire, 1990; Le Goff et al., 2002). Points further from the curves dated to fewer intervals, giving an apparently better precision, if only the number of dated intervals was considered, but the peak probabilities were lower. Precision of SV curves typically decreases towards the endpoints due to

decreased density of data comprising the curve. Simulation of this effect showed, as expected, the corresponding increase in the number of dated intervals for VGPs near the curve endpoints. For the cusped or triangular-shaped SV curve, it was shown how VGPS near the cusp can have two dating options, one to either side of the cusp. Probability curves reflected the asymmetry of the VGP locations relative to the sides of the curve on either side of the cusp, with higher probabilities for the side of the curve closer to the VGP to be dated.

Results for the actual SV curves were instructive concerning the complicated interaction of VGPs with curves of varying smoothness and precision. For the SV curve of Eighmy (1991) VGPS near the curve generate as many as fifteen different dating intervals (fig. 3) spanning up to five different dating options (fig. 4). The effects of using a different SV curve are shown in figure 5, where the SV curve of Sternberg (1989) is used. The number of dating options is now no more than three, less than what is generated using the SV curve of Eighmy (1991). The curve of Eighmy is based on a greater number of data points, but is also less smooth because of shorter windows used for the moving averages. Longer windows gives a smoother curve with smallers A95s. Both these factors will lead to fewer dating options.

4. CONCLUSIONS

Whereas the results for the hypothetical curves were not surprising based on past experience, these simulations provide a tool for exploring the less obvious interactions of actual SV curves with directions to be dated. The statistical dating method in archaeomagnetism, when quoted at the 5% significance level, generates apparently paradoxical results, such that VGPs further from the SV curve yield more precise dates. For determining dates by the statistical method, reporting of complete probability curves (Le Goff et al., 2002) as shown in fig. 2 would compensate for this apparent anomaly. Probability curves are also useful in demonstrating that maximum dating probabilities do fall along the SV curve. Our analysis has shown that the number of dating options are reduced for smooth secular variation curves, so archaeomagnetists should optimize the number of data comprising a SV curve as well as the method used to construct the SV curve from the database.

ACKNOWLEDGMENTS

Thanks to Franklin & Marshall College and Colorado State University for sabbatical support for RS, and to F&M for travel support for RS.

REFERENCES

Eighmy, J.L., 1991. Archaeomagnetism: New data on the South-west U.S.A. master virtual geomagnetic pole curve. *Archaeometry*, 33 (2), 201-214.

Le Goff, M., Gallet, Y., Genevey, A., and Warmé, N, 2002. On archeomagnetic secular variation curves and archeomagnetic dating. *Physics of the Earth and Planetary Interiors*, 134, 203-211.

Lengyel, S.N., and Eighmy, J.L., 2002. A revision to the U.S. Southwest archaeomagnetic master curve. *Journal of Archaeological Science*, 29, 1423-1433.

Sternberg, R.S., 1989 Secular variation of archaeomagnetic direction in the American Southwest, A.D. 750-1425. *Journal of Geophysical Research*, 94 (B1), 527-546.

Sternberg, R.S., 1997. Archaeomagnetic dating. *In:* Taylor, R.E. and Aitken, M.J., eds. *Chronometric Dating in Archaeology*, New York, , Plenum Press, 323-356.

Sternberg, R.S., and McGuire, R.H., 1990. Techniques for constructing secular variation curves and for interpreting archaeomagnetic dates. *In:* Eighmy, J.L., and Sternberg, R.S, eds. *Archaeomagnetic Dating*, Tucson, University of Arizona Press, 109-138.

INVESTIGATION OF THE EFFECTS OF THE SAMPLING AND BREAKING TECHNIQUES ON THE TL SIGNAL AND MINERALOGICAL COMPOSITION OF THE 'FINE GRAINS'

N.C. Tsirliganis, Z. Loukou, D. Papadopoulou, G. Polymeris*
Cultural and Educational Technology Institute, Tsimiski 58, GR-67100 Xanthi, Greece
*Nuclear Physics Laboratory, Aristotle University of Thessaloniki, GR-540 06 Thessaloniki, Greece

G. Papathanasiou, P. Kotsanidis
Democritus University of Thrace, Department of Electrical and Computer Engineering, Physics Laboratory, Vas. Sofias 12, GR-67100 Xanthi, Greece

1. INTRODUCTION

Thermoluminescence (TL) is one of the most extensively used methods for dating heated archaeological ceramics as well as geological sedimentary materials (Aitken M.J.,1985). Various techniques have been developed for the application of the method for the absolute dating of ancient pottery. A commonly used technique that avoids inhomogeneities caused by non-uniform radiation fields inside grains is the *'fine grain' (FG) technique,* originally developed by D.W. Zimmerman (Zimmerman D.W.,1971). In this technique, only fine grains, typically less than 10 μm, are used for the dose determination, so that the alpha dose attenuation inside them is negligible and the absorbed dose is uniform and consists of the full contribution of all ionizing radiations. For the successful application of the technique, a critical step in the sample preparation is the extraction of the fine grains from the ceramic fabric without breaking apart and mixing with larger grains. Several 'extraction' techniques can be used but the most 'favored' over the years is crushing the shred in a vice.

The present work, studies the effects of different extraction techniques on the TL signal (glow-curve), the equivalent dose determination, as well as the mineralogical constituency of the fine grain fraction received and used for the age determination of ceramics.

2. EXPERIMENTAL PROCEDURE

2.1. Site and samples

A single large shred of a 4th century B.C. roof tile from an excavation in Northern Greece was used in the present measurements. A surface layer approximately 2 mm thick from each side was removed manually with a grindstone, and the remaining part was cut in ten pieces. A different sampling technique was used next for the extraction of the fine grains from each segment. The used sampling techniques are given in table 1.

No.	Sampling Technique	Sample Code
1	Manual grinding with a grindstone	*ST1*
2	Grinding with an electrical grindstone at low rpm	*ST2a*
3	Grinding with an electrical grindstone at high rpm	*ST2b*
4	Drilling with a carbide bit at low rpm	*ST3a*
5	Drilling with a carbide bit at medium rpm	*ST3b*
6	Drilling with a carbide bit at high rpm	*ST3c*
7	Manual 'drilling' the sample with a carbide bit	*ST4*
8	Scraping the sample with a metal scraper	*ST5*
9	Crushing the sample in an agate mortar and pestle	*ST6*
10	Crushing the sample in a vice (commonly used technique)	*ST7*

Table 1. Fine grain extraction techniques.

2.2. Thermoluminescence measurements

For the TL measurements the 2–8 μm fine grain fraction from each sample was separated and deposited on Al-disks using the well prescribed 2–20 minute sequence in an acetone suspension (Fleming S.J., 1979). All measurements were performed with a RISO TL/OSL reader (model TL/OSL-DA-15) equipped with a 0.085 Gy/s $^{90}Sr/^{90}Y$ β-source for irradiations. All TL measurements were performed using a combination of a Pilkington HA-3 heat absorbing filter and a 12 mm Corning 7-59 blue filter.

Both the natural TL signal and the signal after a specific artificial beta dose were measured for each sample. The various glow-curves were compared then with each other, in terms of shape and size. The equivalent doses were also determined in each case using the 'age-plateau' analysis (Fleming S.J., 1979).

2.3. X-Ray diffraction measurements

The mineralogical consistency of the fine grain fraction in each case was investigated using powder X-ray Diffraction (XRD). The X-ray diffraction measurements were performed with a Philips PW 1730/10 Diffractometer,

equipped with monochromator, Co-tube and Fe-filter. High-quality powder XRD spectra were obtained for all samples, under the following operational conditions: current 20 mA, voltage 40 kV, counting time 5 s every 0.02º (2θ).

In order to obtain a better comparison of the intensities of the same characteristic lines the operational conditions were maintained constant and a standard procedure was adopted for the preparation of the test specimens.

In powder XRD analysis, the measured peak area of a characteristic line of each mineral is a limited criterion for the calculation of the concentration of the particular mineral, as the crystalline structure, absorption, particle size and background are conditioned by the material itself. The relative intensities (peak areas) are sufficient, however, for comparison in order to obtain a trend in the behaviour of the samples originating from the same bulk sample using different sampling techniques.

3. RESULTS

3.1. TL Analysis

From the TL results presented in figures 1-2, it can be seen that the various extraction techniques affect both the shape and the size of the glow-curve. The equivalent dose estimated from the segment crushed in a vice (ST7) is the only one that agrees with the expected total dose from the known

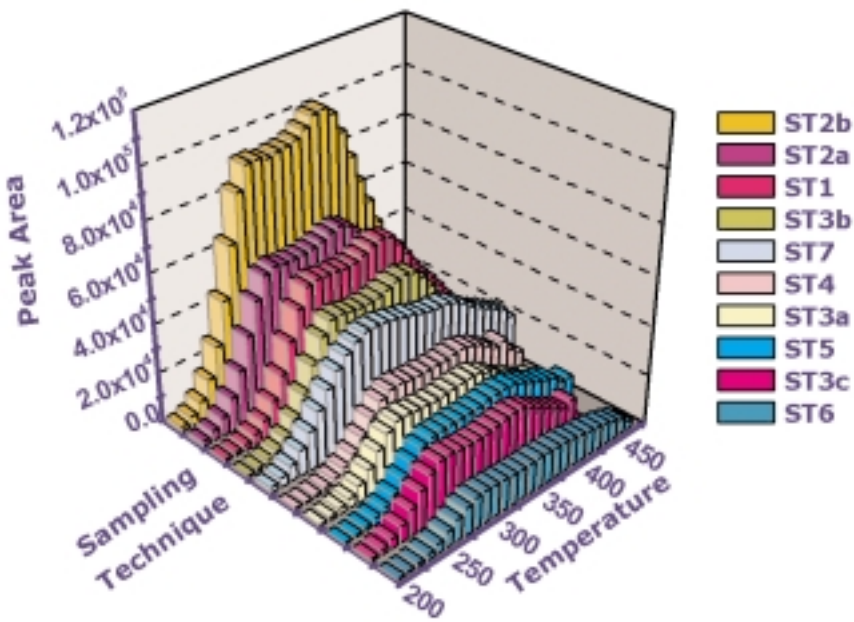

Figure 1. Natural dose TL glow-curve obtained for different fine grain extraction techniques.

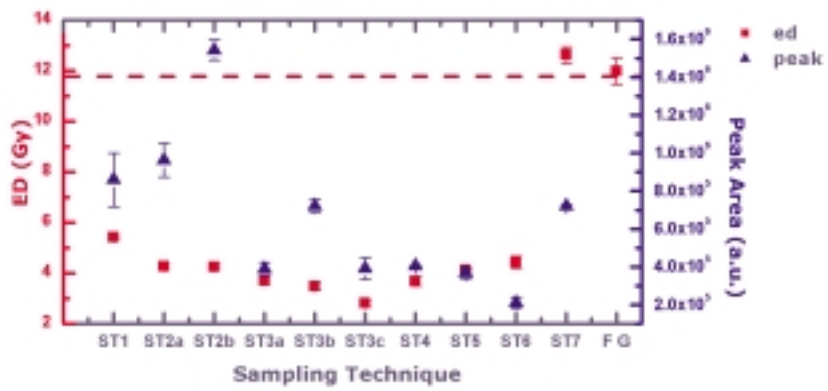

Figure 2. Peak Areas (peak) and estimated Equivalent Doses (ed) obtained for different fine grain extraction techniques.

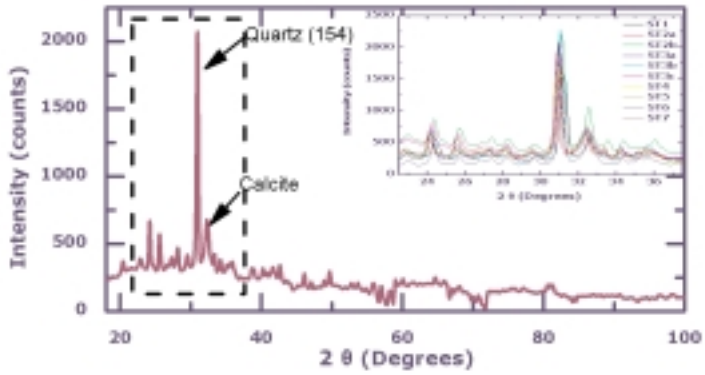

Figure 3. Diffractogram for sample ST7. The area of interest for all samples is shown in the insert.

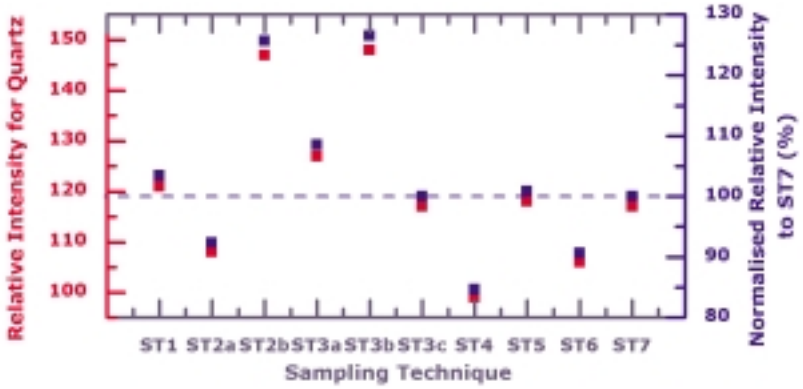

Figure 4. Relative Quartz content in different samples from XRD analysis.

archaeological age of the sample (figure 2). It is important to note that although the natural glow-curve from ST3a is similar in size (integral area) with ST7, the estimated Equivalent Dose is much lower than the expected (see figures 1 and 2). Sample ST2b exhibited a significantly higher integral value for both natural (figure 1) and natural+beta dose glow curves which was attributed to an artificial enrichment (see also XRD analysis, figure 4) of the quartz fraction due to dislocation of quartz particles present in the grindstone.

3.2. XRD Analysis

From the results given in figures 3 and 4, it can be seen that the various extraction techniques alter the relative mineralogical composition of the fine grain fraction. More specifically, in the case of quartz only two other methods (ST5–metal scraper and ST3c–high speed drilling) provide a fraction approximately equal to the fraction from ST7–vice (see figure 4).

4. CONCLUSIONS

The various sampling techniques for the extraction of the fine grain fraction for TL dating of ceramics has a significant effect on the shape and size of the obtained glow-curves and the relative mineralogical consistency of this fraction. This change can be attributed to the breaking of larger grains in various degrees for different minerals. Considering the changes in the relative mineralogical consistency and the respective behavior of the glow curve it is apparent that tribo-luminescence phenomena are taking place that either induce or bleach the luminescence signal.

The present results confirm that the crushing of a sample in a vice, though relatively inefficient since a large portion of the sample is finally discarded, is the most 'gentle' technique that leads to the most accurate age determination. At the same time crushing the sample with a mortar and pestle has the most serious effect on the size and shape of the glow-curve and leads to a significant underestimation of the age of the sample.

REFERENCES

Aitken, M.J. (1985) *Thermoluminescence Dating*. Academic Press Inc., London .

Fleming, S.J. (1979) *Thermoluminescence techniques in archaeology*. Clarendon Press, Oxford 4.

Zimmerman, D.W. (1971) Thermoluminescent dating using fine grains from pottery. *Archaeometry* 13 (1):29-52.

APPLICATION OF FINE-GRAIN TL AND SINGLE-ALIQUOT OSL DATING TECHNIQUES TO WELL AND NOT WELL FIRED ANCIENT CERAMIC MATERIALS

N.C. Tsirliganis, D. Tsiafaki, Z. Loukou, G. Polymeris*
Cultural and Educational Technology Institute, Tsimiski 58, GR-67100 Xanthi, Greece
*Nuclear Physics Laboratory, Aristotle University of Thessaloniki,
GR-540 06 Thessaloniki, Greece

1. INTRODUCTION

Luminescence signals from naturally occurring minerals have been used over the last forty years for dating both heated materials and unheated sediments. Thermoluminescence (TL) is the most widespread used method for dating heated materials in general (Aitken M.J.,1985) and especially archaeological artifacts like ceramics (Zimmerman D.W.,1971), while Optically Stimulated Luminescence (OSL) is used mostly for dating geological sediments (Aitken M.J.,1998). The major difference between the two methods is the zero-setting mechanism of the luminescence clock. In the case of sediments the luminescence was bleached during the exposure of the mineral grains to daylight during sediment transport and deposition. In the case of heated materials and especially ceramics, the luminescence signal was extinguished by the firing of the pottery. Various techniques and laboratory procedures have been developed for the application of the above methods. The most commonly used technique for dating pottery, using TL is the 'fine grain' (FG) technique (Zimmerman D.W.,1971) while for OSL dating the preferred method is the one prescribed in the 'single-aliquot regenerative-dose' (SAR) protocol (Aitken M.J.,1998).

The FG technique in TL dating, however, requires relatively large sample sizes and is limited to well-fired samples. The OSL techniques, on the other hand, usually demand smaller samples and give a higher age precision but so far these techniques have been mainly restricted to sediments.

The present work investigates the use of the above TL and OSL dating techniques for the age determination of 'well' and 'not-well' fired ancient ceramic materials of known age. The results obtained are compared on the bases of accuracy, age precision and applicability.

2. EXPERIMENTAL PROCEDURE

2.1. Site and samples

Three shreds (coded **WF1, WF2, WF3**) of 'well-fired' and three shreds (coded **NF1, NF2, NF3**) of 'not-well-fired' pottery from the excavation in Karabournaki were used in these measurements. Karabournaki is located in North Greece, on the edge of the promontory in the center of Thermaic Gulf (Thessaloniki area) and it preserves the remains of an ancient site including a settlement, a harbor and cemeteries. The occupation of the site appears to be continuous from the Late Bronze Age down to the Roman times, with the flourish of the "town", however, during the Archaic times (7th - 6th centuries B.C.). Typological assessment of ceramics put the age of the samples used in this study sometime between 650 and 550 BC (Tiverios, M. et al, 2003).

2.2. Sample preparation and equipment

An external layer with thickness approximately 2 mm was removed manually with a grindstone from each sample. The remaining part was broken in a vice and the resulting powder passed through a 20 μm sieve.

For the TL measurements the fine grain fraction from each sample was separated using the well-described 2/20 minute sequence in an acetone suspension (Zimmerman D.W., 1971). For the OSL measurements a 10-20 μm fine grain fraction was used from each sample and the SAR protocol was followed.

All samples were deposited on Al-discs and the measurements were performed using a RISO TL/OSL reader (model TL/OSL-DA-15) equipped with a high-power blue LED light source, a infrared solid state laser and a 0.085 Gy/s $^{90}Sr/^{90}Y$ β-source for irradiations.

2.3. TL measurements

TL measurements were performed using a combination of a Pilkington HA-3 heat absorbing and a Corning 7-59 blue filter, and a maximum heat temperature of 500 °C. The equivalent dose (D_e) was determined using both the glow-curve routine and the 'age-plateau' analysis (Fleming, S.J., 1979).

2.4. OSL measurements

OSL measurements were performed using a Hoya U-340 filter and the signals were integrated over the first 5 out of 250 channels of stimulation time. A background was subtracted based on the last 25 channels. For the estimation of D_e a modified SAR protocol was employed using the IR laser diode to stimulate and zero the IRSL signal from feldspars, prior to the use of

blue light that was used to stimulate and zero the signal from both quartz and feldspar grains. After the IR exposure a substantial OSL signal is observed from feldspar (Duller G.A.T. and Botter-Jensen L., 1993). The procedure thus permits the determination of a D_e from both the feldspar signal and the mixed quartz plus feldspar signal for a single aliquot, thus providing an 'intrinsic' merit. A minimum of three regenerative β-doses (namely 10.2, 30.6 and 51.0 Gy), were given to each aliquot. A 0 Gy β-dose was included to monitor recuperation. A repetition of the first regenerative dose, applied at the end of the measurement protocol, was used to monitor possible sensitivity changes. Following the measurement of each natural or regenerative dose signal, a fixed test dose (5.1 Gy) was used to monitor and correct possible sensitivity changes during the measurement procedure. OSL signals were bleached by IR stimulation for 100 s at 125 °C followed by blue light stimulation for 50 s at 125 °C. In both cases the pre-heat temperature was 200 °C (held for 10 s).

2.5. Age calculation

To provide a basis for assessing the reliability of each method, the expected total accumulated dose was estimated based on the known age of the samples. This dose was compared to the equivalent dose values. The average annual dose used in the above calculations was estimated using α-counting for the determination of U and Th and γ-spectroscopy for K-40. The estimated annual average dose was 0.0041 ± 5% Gy, and the corresponding total dose 10.5 – 10.9 Gy (archaeological age 650 – 550 B.C.).

3. RESULTS AND DISCUSSION

3.1. Fine Grain TL dating

The D_e values determined by the Fine Grain TL technique for the well-fired ceramics were found to be in good agreement among them and with the expected total accumulated dose. That was not the case for the not well-fired ceramics where the De values were related more to the geological age of the material itself (clay). As can be seen in figures 1a and 1b in the case of not well-fired ceramics the plateau is not well defined and the glow curve does not have a good shape.

3.2. Single-Aliquot OSL dating

In the case of OSL measurements the estimated $D_e$values were in good agreement among them and with the expected total accumulate dose. As can be seen in figures 2a and 2b in both cases the decay curves have good shape and give similar regenerative growth curves.

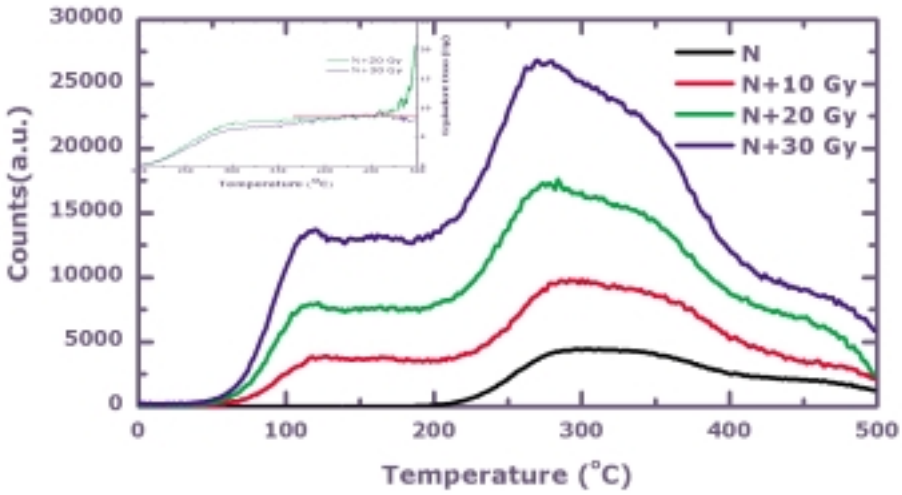

Figure 1a. Additive Dose Glow Curve of a '*well-fired*' ceramic sample.

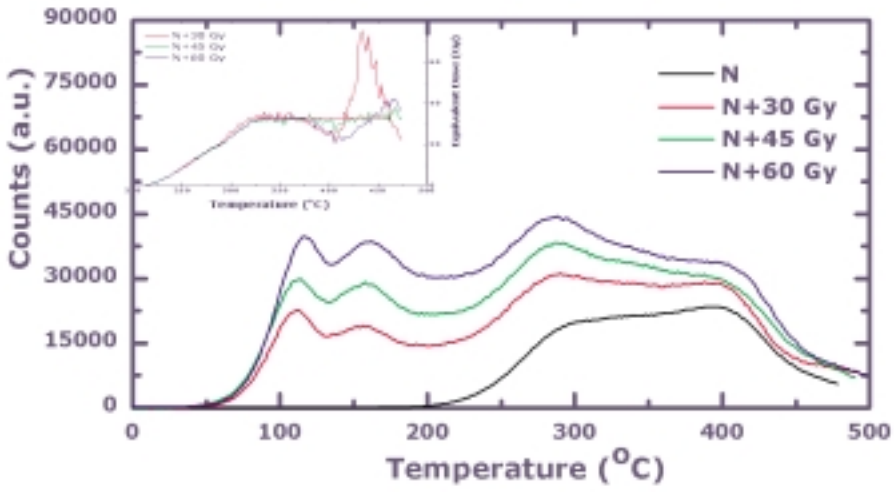

Figure 1b. Additive Dose Glow Curve of a '*not well-fired*' ceramic sample.

3.3. TL-OSL Comparison

D_e values for well-fired ceramics from both methods (TL, OSL) are in good agreement with each other and with the expected total accumulated dose value. For not well fired ceramics D_e values obtained with the OSL technique seem to over-estimating the total dose by 8-10% while the TL technique yields D_e values that are related more to the geological age of the material itself (clay) and not the artifact. The above values are summarized in table 1.

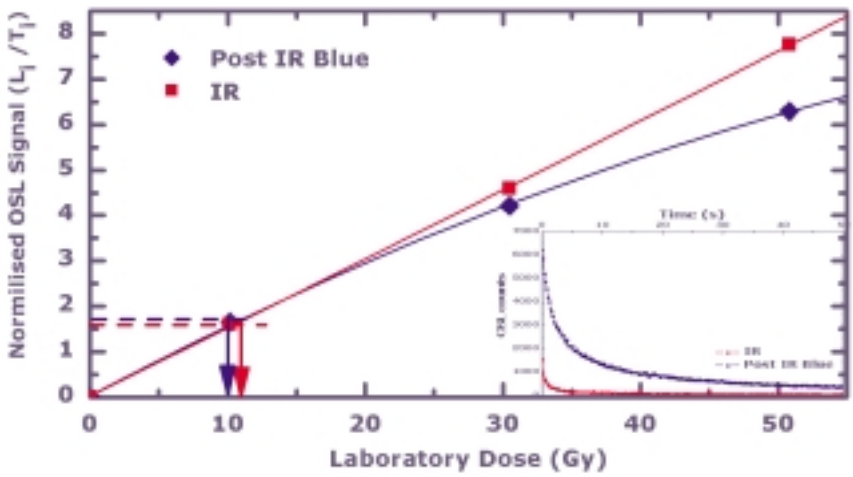

Figure 2a. Regenerative Growth Curve for a '*well-fired*' ceramic sample.

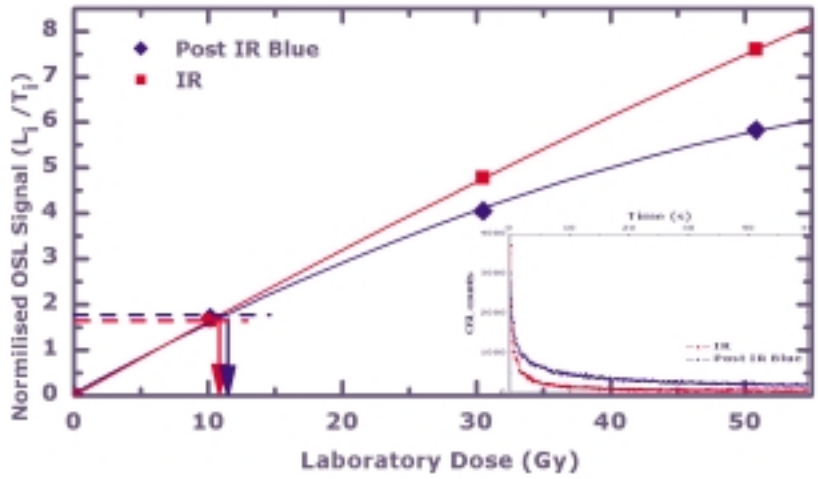

Figure 2b. Regenerative Growth Curve for a '*not well-fired*' ceramic sample.

4. CONCLUSIONS

Based on the above results, it can be seen that the application of the OSL method using the SAR protocol for dating well-fired ceramics yields in general similar results as the TL Fine Grain technique, while at the same time provides the advantages of the method (smaller sample size ect.). For not-well-fired shreds the TL method, yields values that are much higher than the age of the artifact and are more related to the geological age of the material itself (clay).

Sample No	Method Used	De (Gy)	SD (Gy)	Method Used	De (Gy)	SD (Gy)
WF1	Glow-curve routine	10.08	0.68	Post IR Blue LEDs	10.11	0.13
	Age-plateau analysis	10.40	0.34	IRSL	10.60	0.47
WF2	Glow-curve routine	10.88	0.57	Post IR Blue LEDs	10.23	0.46
	Age-plateau analysis	10.30	0.10	IRSL	9.04	0.36
WF3	Glow-curve routine	10.50	0.21	Post IR Blue LEDs	8.91	0.44
	Age-plateau analysis	8.39	0.46	IRSL	11.78	0.50
NF1	Glow-curve routine	16.37	5.21	Post IR Blue LEDs	11.54	0.91
	Age-plateau analysis	—	—	IRSL	11.25	0.93
NF2	Glow-curve routine	15.53	2.78	Post IR Blue LEDs	11.59	0.48
	Age-plateau analysis	—	—	IRSL	12.57	0.82
NF3	Glow-curve routine	20.97	0.94	Post IR Blue LEDs	11.61	0.39
	Age-plateau analysis	32.3	1.86	IRSL	11.37	0.81

Table 1. D_e values obtained by the TL and OSL methods (expected archaeological D_e= 10.5 - 10.9 Gy).

However, the OSL technique (SAR protocol) still provides age values that are closer to the real age of the artifact, although slightly overestimated.

As a conclusion, OSL appears to be a reliable alternative to TL for dating of ancient ceramics with certain advantages regarding the sample size and in the case of artifacts that were not well fired.

REFERENCES

Aitken, M.J. (1985) *Thermoluminescence Dating*. Academic Press INC. London.

Aitken, M.J. (1998) *An Introduction to Optical Dating*. Oxford Science Publications.

Duller, G.A.T., Botter-Jensen, L. (1993) Luminescence from potassium feldspars stimulated by infrared and green light *Radiation Protection Dosimetry* 47: 683-688.

Fleming, S.J. (1979) *Thermoluminescence techniques in archaeology*. Clarendon Press, Oxford 4

Tiverios, M., Manakidou, E., Tsiafakis, D., (2003) University excavations in Karabournaki, Thessaloniki 2000-2002 (in Greek), *Egnatia* 7: 327-351

Zimmerman, D.W. (1971) Thermoluminescent dating using fine grains from pottery. *Archaeometry* 13 (1):29-52.

EXPLORATION OF THE POSSIBILITIES TO DATE MEDIEVAL BUILDING CONSTRUCTION BY OSL: THE CASE OF THE BRICKBUILT CITADEL OF TERMEZ (UZBEKISTAN)

Emmanuelle Vieillevigne, Pierre Guibert, Françoise Bechtel
Institut de Recherche sur les Archéomatériaux, UMR 5060 CNRS
Université Bordeaux 3.
Centre de Recherche en Physique Appliquée à l'Archéologie (CRP2A),
Maison de l'Archéologie, 33607 Pessac cedex, France.
Corresponding author: evieille@etu.u-bordeaux3.fr

Usually, dating a structure built of burnt bricks by luminescence (thermoluminescence, optically stimulated luminescence) means dating the making of materials. Since bricks recycling is possible, interpretation problems could arise. This led us to use optically stimulated luminescence in a less "conventional" way to investigate the potentials to date the moment of construction.

Within the framework of Termez medieval citadel (Uzbekistan) luminescence dating, we were interested in the brick laying in the walls: exposing to light their surface before embedding in masonries makes it possible to empty the optical traps of the crystals present on material surface. Consequently, if we were able to extract those crystals, we could know the sealing time and thus obtain a direct dating of the construction of the architectural structures. This is the purpose of this work.

1. THE UZBEK CITADEL OF TERMEZ

Termez, an uzbek city in the centre of Central Asia, was founded during the Hellenic era. Some historians believe that Alexander the Great had been there. Its geographic position along the Amou Darya river, at the crossroads of Iranian, Mesopotamian, Indian and Chinese cultures, allowed it to become one of the medieval Tokharestan capitals. The city was destroyed in 1220 by Gengis Khan (Leriche *et al.*, 2001).

Termez archaeological site extended on about 500 hectares, which represents also a great and large site in Central Asia. Besides various antique monuments built in adobe bricks and daub, the citadel, about 10 hectares in area, present architectural vestiges built in adobe bricks and strong fortifications built in burnt bricks, that constitutes the predominant material during the islamic era (VIIth-XIVth centuries).

2. TOWARDS THE BRICKS SURFACE DATING

For this surface dating study, we had to proceed in several steps. First, TL has been studied on several samples. As we used polymineral fine grains (quartz and feldspars), a careful study of the feldspars fading was necessary in order to avoid the underestimating of the equivalent dose (ED) (Zimmerman, 1971; Sanderson, 1988; Visocekas *et al*., 1994; Zink, 1996). For this TL study, an additive dose and regeneration procedure is carried out. A thermal annealing precedes the regeneration experiments, in order to determine the appropriate growth curve function. This procedure consists in fitting the first TL reading experimental points with the growth curve deduced from the regeneration experiments performed with the thermally annealed material (Guibert *et al*., 1996). This procedure must be carried out for every sample studied, in order to avoid most changes in luminescence properties, which would distort the ED-values and, as a consequence, the dates themselves (Roque *et al*., 2004). After the first TL studies were achieved (Vieillevigne *et al*., *in press*), we carried out different OSL experiments to attempt at brick surface dating.

2.1. First step: comparison between TL and OSL to date the brick firing

To test OSL response, we compared TL and OSL dates obtained on brick cores. OSL dates are generally younger than TL dates for the same sample (fig. 1). The OSL signal was generally of very low intensity because of a poor quartz content, as shown in the figures 2 and 3, however OSL sensitivity varies from sample to sample. Because of these weak OSL signals and of the feldspar presence, we have also tested the IRSL of few samples but we had to overcome the well known fading phenomenon (fig. 1). Although OSL results were found less accurate than TL ones, we estimated that OSL signals were significant and so experiments were kept on.

2.2. Second step: measurement of the solar bleaching depth

In practice, solar bleaching should have affected a volume of material and not only the very superficial crystals. In order to evaluate the depth of material affected by solar bleaching, freshly cut pieces of the studied bricks were exposed to the daylight. The exposed face has then been eroded by steps

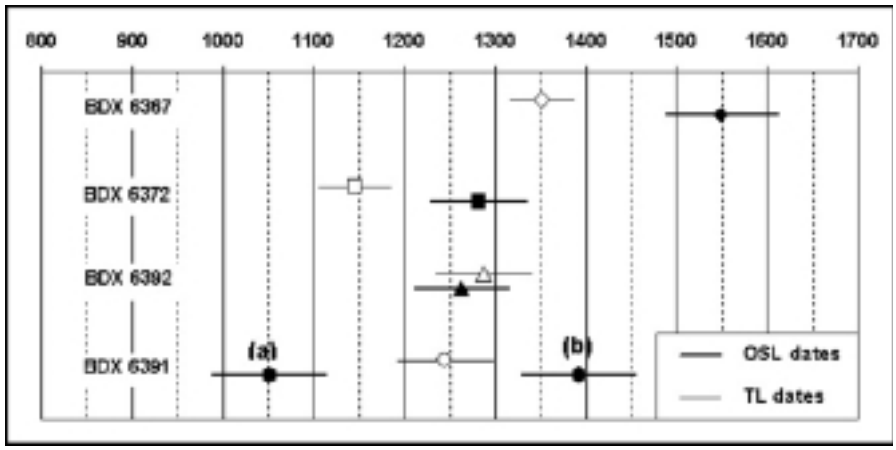

Figure 1. Comparison between TL and OSL dates (in black) for four bricks samples from Termez citadel. Brick BDX 6391 was studied by IRSL: the two dates (a and b) correspond to distinct models for fading corrections (tunnel afterglow model (a) and isothermal decay model with a stable level (b)).

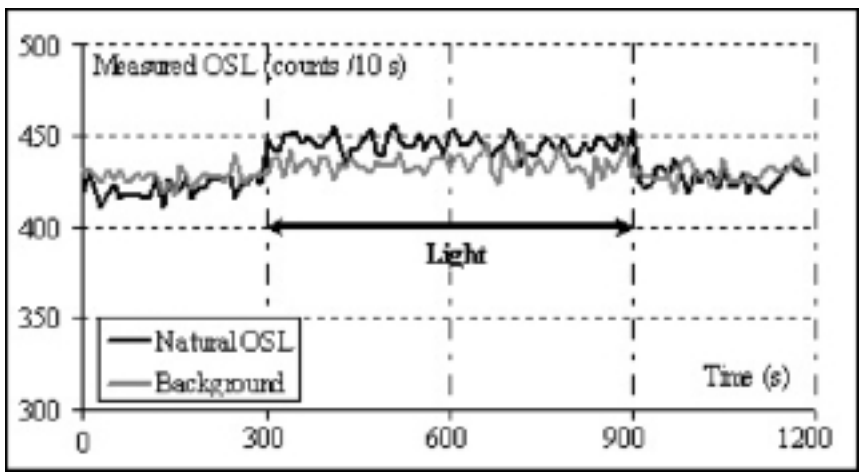

Figure 2. Brick BDX 6367. An example of the low OSL signal intensity is shown here. The natural OSL signal and its background are not very different. For these averaged curves, the stimulation wavelength was fixed at 450±10 nm. OSL is detected in the range 250-400 nm (combination of the spectral transmittance of optical filters, 2 Schott DUG11, and spectral efficiency of photomultiplier EMI 9813 QKA).

of 0.2 mm with a law speed disc saw. The remaining OSL of every subsample obtained has been measured.

The first results (fig. 4, 5) have shown that bleaching light penetrates into the brick at a depth that varies from sample to sample: from 0.4 mm to 1 mm

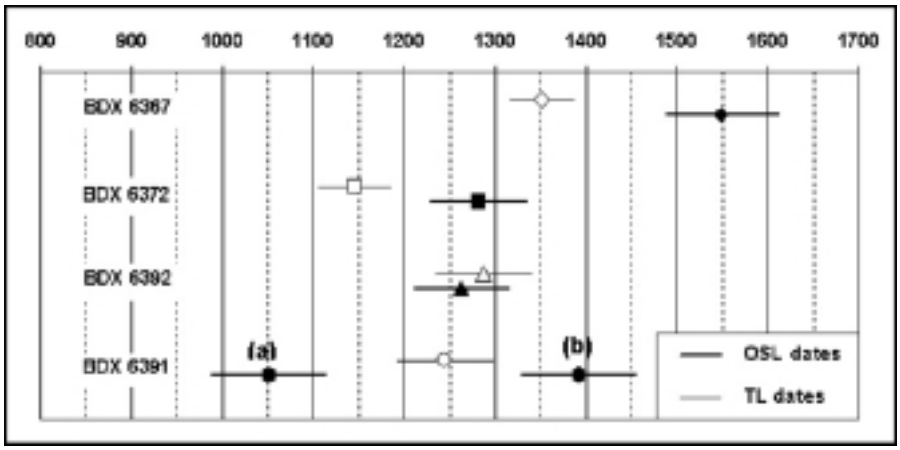

Figure 3. Brick BDX 6392. For the same curves, we could observe that both signals are quite different and so the results are more accurate. The OSL experimental conditions were the same as those described at figure 2.

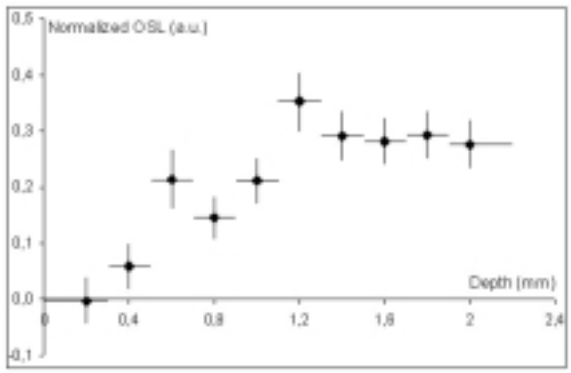

Figure 4. Brick BDX 6392. This graph showed that the bleached depth of this brick is around 0.4 mm. This experiment was carried out by OSL. The daylight exposition time was 2 weeks.

respectively with bricks BDX 6392 and BDX 6387. Such effects of daylight in the interior of other materials were observed also for granites or gabbro (Haberman *et al.*, 2000; Greilich, 2004). It is then possible to sample the material anciently bleached at the superficial layer of bricks, since the bleached volume is sufficient to carry on further OSL measurements.

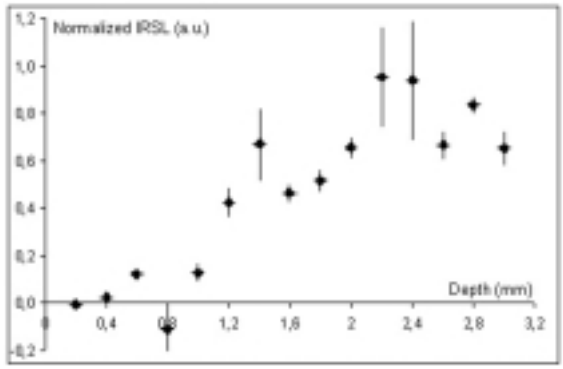

Figure 5. Brick BDX 6387. We can observe that the bleached depth obtained by IRSL is around 1 mm. This brick has been exposed to daylight for 1 week.

2.3. Third step: how to take out the superficially layer, anciently bleached, of a brick with irregular surface?

As the surface of bricks is commonly irregular and covered by mortar, a particularly careful sampling must be performed. First, the mortar is removed by a mechanical and manual method using a scalpel, taking care to not remove fragments from the brick surface. Then because of the irregular topography, punctual sampling is practiced every 5 mm (order of magnitude of the blade dimensions) at the brick surface. The thickness of each point sample is controlled by a micrometer.

3. CONCLUSION: FIRST ATTEMPT AT SURFACE DATING

A surface dating has been attempted by OSL. The same difficulties than those for core dating by OSL were encountered. The rough value of paleodose was 1.2 ± 1.8 Gy (1.). This high uncertainty only provides an age inferior to 970 years (2) which is not contradictory to the firing age (856 ± 41 years).

The IRSL signals from these samples being more significant, a further investigation using IRSL rather than OSL could be envisaged in order to lead to more substantial results. Nevertheless first results are encouraging (the methodology and the practical aspects of surface dating have been established) and we need to carry on investigations with other bricks from different origins to validate this method.

REFERENCES

Greilich, K.-S. (2004) *Über die Datierung von Gesteinsoberflächen mittels optisch stimulierter Lumineszenz*, Dissertation, University of Heidelberg, Germany, 162 p.

Guibert, P., Vartanian, E., Bechtel, F., Schvoerer, M. (1996) Non linear approach of TL response to dose: polynomial approximation, *Ancient TL*, 14, 2, 7-14.

Haberman, J., Schilles, T., Kalchgruber, R., Wagner, G.A. (2000) Steps towards surface dating using luminescence, *Radiation Measurements*, 32, 847-851.

Leriche, P., Pidaev, C., Gelin, M., Abdoullaev, K. (2001) *La Bactriane au carrefour des routes et des civilisations de l'Asie Centrale. Termez et les villes de Bactriane-Tokharestan*, Actes du colloque de Termez de 1997, Maisonneuve et Larose, Paris, 422 p.

Roque, C., Guibert, P., Vartanian, E., Vieillevigne, E., Bechtel, F. (2004) Changes in luminescence properties induced by thermal treatments; a case study at Sipan and Trujillo Moche sites (Peru), *Radiation Measurements*, 38, 1, 119–126.

Sanderson, D.C.W., 1988, Fading of TL in feldspars: characteristics and corrections, *Nuclear Tracks and Radiation Measurements*, 14, 1/2, 155-161.

Vieillevigne, E., Guibert, P., Bechtel, F., Leriche, P. Thermoluminescence et chronologie du bâti médiéval : datation de briques de la citadelle de Termez en Ouzbékistan, *Revue d'Archéométrie*, *in press*.

Visocekas, R., Spooner, N.A., Zink, A., Blanc, P. (1994) Tunnel afterglow, fading and infrared emission in thermoluminescence of feldspars, *Radiation Measurements*, 23, 377-385.

Zimmerman, D.W., (1971) Thermoluminescence dating using fine grains from pottery, *Archaeometry*, 13, 1, 29-52.

Zink, A. (1996) *Thermoluminescence des feldspaths : émissions par effet tunnel et par thermoluminescence dans l'infra-rouge, incidences sur la datation des feldspaths*. PhD. Thesis, Universités de Paris VII et Bordeaux III, 275 p.

3. TECHNOLOGY AND PROVENANCE OF METALS

INDEX

METALLURGIC PROCESS USED IN THE "FARGA ROSELL"ANCIENT BLOOMERY FIRE (ANDORRA)

Aureli Álvarez
Facultat de Ciències. Dept. de Geología, Universitat Autònoma de Barcelona, 08193 Bellaterra, Spain

Antoni Vila, Josep M. Bosch, Olivier Codina
Àrea de Recerca Històrica del Govern d'Andorra, Andorra la Vella, Andorra

Xavier Clop
Servei d'Anàlisis Arqueològiques. Universitat Autònoma de Barcelona. 08193 Bellaterra, Spain

1. INTRODUCTION

The "Farga Rossell" (1842-1876) was the last active iron producing factory using the direct system in Andorra (figure 1) (Olivier Codina, 2001, p. 148).

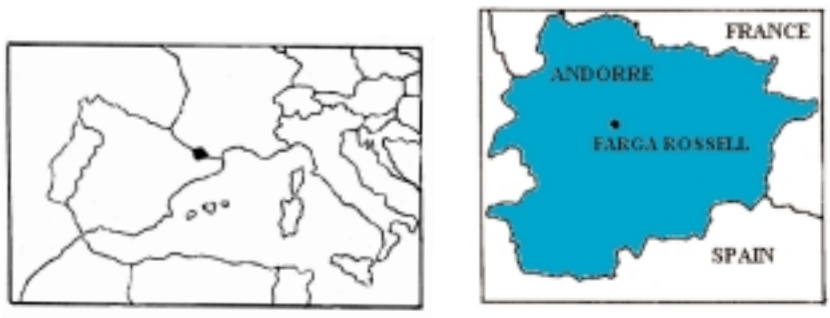

Figure 1. Geographyc location of Farga Rosell.

The Historical Research Service of the Government of Andorra started, in collaboration with the Archaeological Analysis Service of the UAB, a study project to characterize the different slag types obtained during the successive phases of ore reduction occurring in this ancient metallurgical process. During the first stage of this work a mineralogical study of the intermediate and final products has been carried out. The metallographyc study will be presented in a next paper.

2. ARCHAEOLOGICAL SETTING AND SAMPLING

The Farga Rossell factory (figures 2 and 3) has not been reused after its closure in 1876. For this reason, the excavation of this site provided a large amount of data about the structure of the furnace and a useful collection of slag. The main interest of the remains lays on the fact that the slag samples preserve their original location in the furnace.

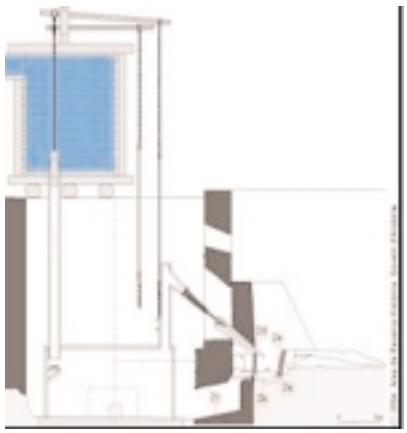

Figure 2. The Farga Rosell is a relatively modern factory. The iron metallurgy process used was the system known as "farga catalana" (bloomery fire).

Figure 3. A present day photographic view of the Farga Rossell furnace. Scale bar: 50 cm

The absence of a slagheap is a particularity of this type of factory during the last technological phase of bloomery fire in Andorra. This fact determined the methodology used in the present study differing from most of the published works about this metallurgical process as the latter are only based on data obtained from historical and related references. (Jean CANTELAUBE, 2001, p. 9).

The excavation process was specifically designed to collect the largest amount of slag in each of the different areas of the factory. Each area is associated with a specific process within the operative chain to obtain the wrought iron. The slag samples were selected after washing and cleaning and several cross- sections were performed in order to study the internal composition of slag. Finally, the most representative samples were chosen for analysis and further examination.

3. METALLURGICAL PROCESS

The bloomery fire system, known as "farga catalana", is a not totally controlled process. The obtained product may have a variable quality, and a similar final result can occur through diverse paths (MOLERA 1983). It is therefore difficult to recognise all the metallurgical processes, from mineral extraction to iron production. Determining the iron reduction degree in each slag sample permits to know their position and role within the global metallurgical process (figure 4). The ore minerals used in the Farga Rosell were hematite (Fe_2O_3), limonite ($Fe_2O_3.nH_2O$) and goethite (FeO.OH). These minerals were roasted in a special furnace previously to the introduction into the main kiln.

4. ANALYTICAL PROCEDURES AND RESULTS

Fourteen thin and polished sections of silicate and metallic phases were studied using transmitted and reflected light polarizing microscopy,

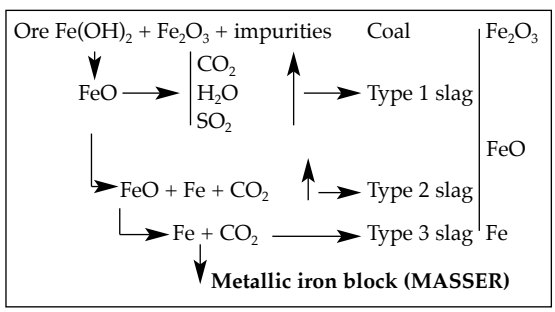

Figure 4. Metallurgical process.

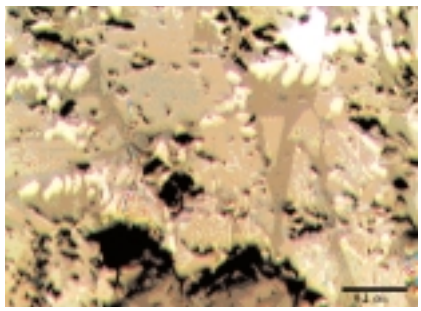

Figure 5. Sample 53 from the "Farga Rosell" observed under reflected light. Bright white: metallic Fe; dendritic forms: wüstite; light grey knebellite and dark grey: calcium silicate Scale bar: 0.1 cm.

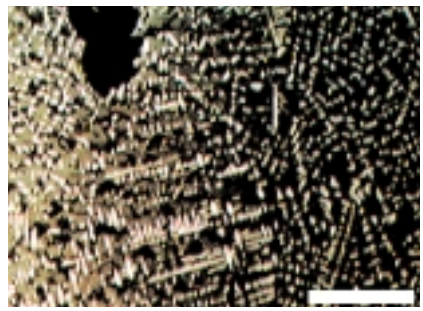

Figure 6. Sample 65 from the "Farga Rosell" observed under reflected light. Bright white: metallic Fe dendrites. Scale bar: 0.1 cm.

respectively. These methods allowed to observe the texture and distribution of the diverse mineral phases simultaneously (figures 5, 6). Mineral phases were also identified by X-Ray diffraction (XRD).

Semiquantitative elemental analysis of the different metallic phases were performed using Scanning Electronic Microscopy (SEM) (SIMON 1992). The distribution map of Fe and Mn helped to identify the knebellite crystals ($(Fe,Mn)_2SiO_4$), (figures 7 and 8).

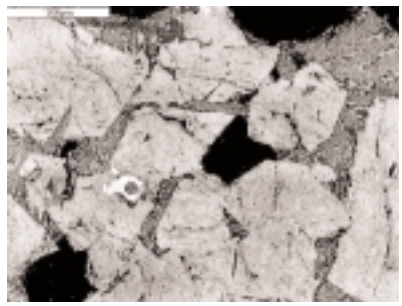

Figure 7. SEM image of sample 65. Components are knebellite (light grey) and wüstite (dark grey). Scale bar 200 μm.

Reflected light microscopy allowed to recognise the presence of two metallic phases with dendritic forms but different reflectivity (metallic iron and wüstite; see below). Dendritic textures are typical of fast crystal growth processes. In the present case, the physico-chemical reactions (wüstite and metallic iron formation) took place in the solid state. However, local melting processes have been observed (presence of small rounded metallic particles,

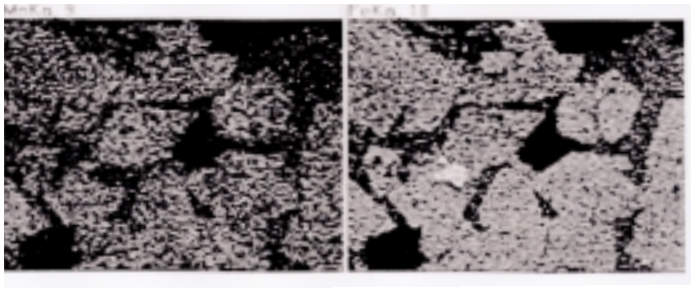

Figure 8. SEM image of sample 65- The matching distribution of Fe and Mn allowed the identification of knebellite crystals (see figure 7). Scale as in figure 7.

disseminated in the slag). It is interesting to note that, in some cases, metallic iron growths replacing, from the border to the core, wüstite grains (figure 9), showing that the reduction process was a gradual transformation of the previously formed wüstite.

Thin section study under transmitted light showed the presence of several silicate phases in the slag. The most abundant is knebelite, sink for most of the Mn from the ores. Knebelite grain size seems to be controlled by the temperature attained by the slag. Therefore, the larger crystals are found in slag from the bottom of the furnace, where the highest temperatures are reached. At lower temperatures knebelite crystals are smaller and developed a different texture (figures 10 and 11).

Feldspar and a Ca-bearing silicate vitreous phase are also present in slag. The vitreous phase is only found around the walls of the furnace and is produced from melting involving quartz, feldspar and carbonates, probably used as additives.

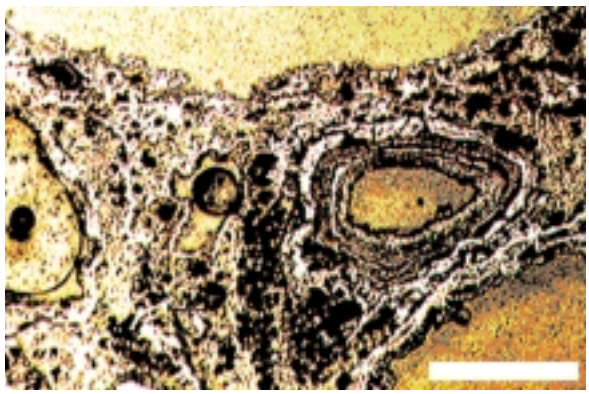

Figure 9. Sample 53 from the "Farga Rosell" observed under reflected light. Metallic iron (white) is coating ore mineral and wüstite. Scale bar: 0.1cm.

The different silicate phases in the slag, observed by transmitted light microscopy, were characterised by XRD. The presence of wüstite (FeO) and metallic iron was confirmed by SEM-EDS. Moreover, this technique allowed to know the chemical composition of knebelite ($(Fe,Mn)_2SiO_4$), as well as the presence of two amorphous phases: the Ca-bearing silicate glass and silica glass.

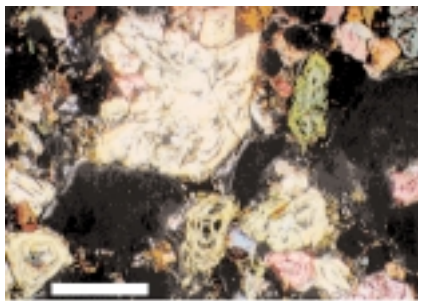

Figure 10. Crystallized knebellite. Crystals have a large size, indicating a high temperature in the furnace. Sample 65. Transmitted light. Scale bar: 0.1cm.

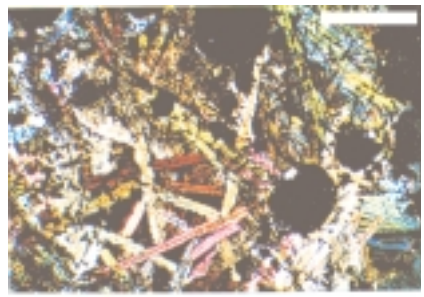

Figure 11. Sample 57. Transmited light. Knebellite crystals have a smaller size and different texture compared to fig. 10. Scale bar: 0.1cm.

5. DISCUSSION

The analysis and characterisation of slag samples from the Farga Rosell (Andorra), allowed to recognise three different reduction degrees of the iron ore in the metallurgical process. During the first stage, the iron ore (hematites, goethite and limonite) was partially reduced to wüstite and minor metallic iron (Fe). The slag produced (Type 1) was composed by iron ore, wüstite, Fe, silica glass and Ca-bearing silicate glass.

In the second stage, slag was mainly composed by wüstite, knebelite, silica glass and minor metallic iron (Type 2). Knebelite crystals were small in size and developed prismatic and acicular forms. In the third stage, slag usually showed spongy textures and was made up of wüstite, knebelite, metallic iron, and glass (silica and Ca-bearing silicate). Knebelite tended to develop rounded and larger crystals compared to Type 2 slag.

Mineralogical and textural study of slag allowed to recognise that reduction of the iron ore proceeded progressively with wüstite as intermediate phase. Replacement of wüstite by metallic iron increased proportionally with the temperature of the furnace. The presence of dendritic textures in metallic Fe, are also related to temperature allowing to locate the sampled slag within the metallurgic device. Our results also show that the combination of mineralogical, textural and analytical data is a useful methodology to investigate arqueometallurgical problems.

ACKNOWLEDGMENTS

The authors wish to thank Esteve Cardellach (UAB) for the critical revision and useful ideas that helped to improve the manuscript.

REFERENCES

Cantelaube, Jean (2001). De la forge à bras à la forge à la catalane: evolution du bas fourneau de réduction directe du minerai de fer dans les Pyrénées ariégeoises. *"Actes del 6è curs d'Arqueologia d'Andorra 2000"*. P 9-34.

Codina, Olivier (2001). Forn, rendiments i massers perduts a la farga Rossell. De la limitació tecnológica a la restricció dels costos. *"Actes del 6è curs d'Arqueologia d'Andorra 2000"*. P 148-160.

Codina, O., Bosch, J. M., Vila, A. (2000).- La Farga Rosell (1842-1876). El zenit de l'obtenció del ferro pel sistema directe. Ed. Govern d'Andorra. Andorra la Vella. D.A. (2001).

Molera, P., Barrueco C. (1983).- Llibre de la Farga. Ed. R. Dalmau. Barcelona.

Simon i Àrias, J. (1992).- La Farga Catalana. Ed. Societat Catalana de Tecnologia, Filial de l'Institut d'Estudis Catalans.

THE LEAD METAL FROM TWO HELLENISTIC TOWNS IN EAST CENTRAL GREECE

E. Asderaki
13th Ephorate of Prehistoric and Classical Antiquities, Athanassaki 1, 3822 Volos, Greece, elasder@hotmail.com

TH. Rehren
Institute of Archaeology, University College London, 31-34 Gordon Sq., London WC1H 0PY, UK, th.rehren@ucl.ac.uk

1. INTRODUCTION

Lead, a cheap and easily worked metal, was used widely in antiquity, but is not well studied scientifically. This paper focuses on two major cities which were economical, commercial and cultural centres, in east central Greece during the Hellenistic period; ancient Demetrias and ancient Pherai. Both cities belong geographically to what is today Magnesia, Greece, and are about 15 km apart from each other. In the framework of a wider study of the presence and use of lead in central Greece, initial analyses have been done in four objects from each site.

2. MAIN ASPECTS OF THE STUDY

The main aspects of the study are:

a) Identification and characterization of the metal,

b) Provenance of the metal, and

c) Significance of the data for the interpretation of the archaeological evidence.

3. ANALYTICAL TECHNIQUES

The main data we report here are from:

-*ICP-AES* for the analysis of trace elements indicating the degree of refining and desilvering, and to check for elements indicating possible

recycling, such as tin. The selection of elements included in ICP-AES analyses was based on the work done by Rehren and Prange (1998).

-*MC-ICP-MS* was done to determine the lead isotope ratios in order to geologically provenance the lead metal to known lead mines.

All analyses were done in the Dept of Earth Sciences of the University of Bristol.

3.1. Samples

All the Demetrias samples come from tombs in the northern cemetery of the town, excavated by the 13th Ephorate of Prehistoric and Classical Antiquities (E.P.C.A). They are from a lead sheet, 90 cm long, 10-25.5 cm wide and 2.4 mm thick, possibly part of a lead coffin and three lead trephines, parts of gilded wreaths (Asderaki & Rehren 2002), about 2 mm thick and 1.6 cm wide. Even though they are all extensively corroded to cerussite, hydrocerussite and litharge, as found by XRD analysis, both the lead coffin and the lead trephines preserve enough metal in their core for metallographic and chemical analysis.

Figure 1. Lead ingot 356.

Figure 2. Lead ingot 305.

The Pherai samples come from a suspected workshop area (Intzesiloglou, 1993), also excavated by the 13th E.P.C.A. They comprise two lead ingots (fig. 1, 2) and two lead sheets. The two ingots are bun shaped and similar in size to copper bun ingots. As far as we are aware, there are few known parallels for this type of ingot in lead, making them a particularly interesting group to study. Their dimensions are 8.7 cm and 7 cm in diameter, and they weight 540 g and 310 g, respectively. The two sheets (No 444a and 450) are 6.5 and 3.7 cm long and 5.1 and 2.5 cm wide respectively, and may represent off cuts from the workshop activity.

4. RESULTS AND DISCUSSION

4.1. Results from ICP-AES analyses

The results from ICP-AES analyses indicate (table 1) a very clean lead metal. The main trace elements found were copper at just below 0.1 wt% and iron with up to 0.03 wt%. The copper is about twice that of other published

values from ancient lead finds, while the elevated iron content in four of the samples may indicate a certain degree of corrosion of the lead metal (Rehren & Prange 1998). Antimony is rather low in the Pherai samples while it varies from 10-300 ppm in Demetrias samples. The low level of tin in most samples indicates that the metal probably was not recycled (Wyttenbach & Schubiger 1973); only the sheet from Demetrias has an elevated tin level which might indicate recycling. The metal was probably desilvered, an interpretation based on the silver content of around 45 ppm, a level found to be at the lower end for desilvered ancient lead. Bismuth scatters more closely around 40 ppm. Arsenic is also very low, with an average 20 ppm or less. This indicates a relatively 'clean' geological source for the galena, when compared e.g. to the LBA lead from Qantir (Rehren & Prange 1998), or some sort of refining.

The samples from Pherai have somewhat lower levels of antimony and arsenic, which might indicate the use of a slightly different ore. Rehren et al. 2002 have shown that within the Laurion ore field at least two different ore types occur, differentiated by their antimony and arsenic levels, among other parameters. The difference could alternatively be originated from a hotter or more oxidising cupellation procedure, resulting in an increased evaporation of the two metals.

	Nr	Date BC	Bi	Cu	Sb	Sn	Ag	Fe	Zn	As
DEMETRIAS	Treph 455	4th	40	800	285	11	30	190	4	22
	Treph 924	4th/3rd	45	895	10	14	30	190	1	3
	Treph. 140	3rd/2nd	40	835	45	7	40	275	1	3
	Sheet 876	4th/3rd	30	700	105	130	65	-	-	16
PHERAI	Ingot 356	2nd	40	755	4	-	110	10	1	1
	Ingot 305	2nd	35	700	11	18	36	70	1	3
	Sheet 444a	2nd	30	550	6	3	32	6	9	1
	Sheet 450	2nd	30	650	2	10	35	170	5	13

Table 1. ICP-AES analyses of selected lead objects from Demetrias and Pherai. The balance to 100 % is lead. Elements analyzed for but not found include selenium and tellurium. All analyses Dr Chung Choi, Dept of Earth Sciences, University of Bristol. (All values given in ppm).

4.2. Results from MC-ICP-MS analyses

The lead isotope ratios for the eight samples, determined by MC-ICP-MS, are given in table 2. Six of them fall well within the range known for lead metal from Laurion as most recently defined by Stos and co-workers (1996). The chemical composition and in particular the silver content are in agreement with their possible origin from Laurion (Konophagos 1980; Rehren *et al*. 2002). The other two samples, the sheet from Demetrias and ingot 356 from Pherai, have higher $^{207}Pb/^{206}Pb$ ratios than is usual for Laurion ores and

also lower $^{206}Pb/^{204}Pb$ ratios than the other samples. These two match both the Chalkidiki ore field and some as yet unpublished Laurion ore samples from near Agrileza (Stos pers.com. 2004).

	Nr	Date BC	$^{208}Pb/^{206}Pb$	$^{207}Pb/^{206}Pb$	$^{206}Pb/^{204}Pb$
DEMETRIAS	Trephine 455	end 4th	2.0562	0.83104	18.828
	Trephine 924	4th- 3rd	2.0548	0.83064	18.810
	Trephine 140	3rd-2nd	2.0587	0.83162	18.832
	Sheet 876	4th- 3rd	2.0677	0.83410	18.747
PHERAI	Ingot 356	2nd BC	2.0618	0.83259	18.786
	Ingot 305	2nd BC	2.0584	0.83171	18.809
	Sheet 444a	2nd BC	2.0564	0.83118	18.819
	Sheet 450	2nd BC	2.0568	0.83129	18.823

Table 2. MC-ICP-MS analyses of selected lead objects from Demetrias and Pherai. All analyses Dr Tim Elliott, Dept of Earth Sciences, University of Bristol.

5. CONCLUSION

Although only eight samples were analyzed from both sites, the present data demonstrate that some important information can be gained from the analysis of even these few lead objects. The first results indicate that fresh desilvered, and not recycled, lead was used in most cases. Small quantities of copper, antimony and arsenic, typical for ancient lead, are present throughout, and traces of some other elements at or just below the detection limits. There are some subtle differences in antimony and arsenic levels between the samples from Demetrias and Pherai. Tin in particular is an indicator for possible recycling of lead, as it does not normally occur geologically with lead deposits, but is frequently incorporated in scrap lead as pewter or solder. Wyttenbach and Schubiger (1973) found up to 10 ppm tin in Roman lead ingots, but several hundred to thousands of ppm in lead pipes. The values found here are thus in line with the use of fresh metal, as was already found to be the case for the copper in an earlier study (Asderaki & Rehren 2002). The lead sheet 876, though, which is also isotopically different, has nearly 200 ppm tin, and could well include a component of recycled lead metal.

The lead isotope signature of the metal, in all cases but two, is compatible with their origin from a single source, Laurion. Those samples with a higher ^{207}Pb / ^{206}Pb ratio may either indicate that the Laurion field is indeed more complex than previously thought, or that these samples come from a different source, such as the Chalkidiki (Stos pers.com 2004). This further underlines that the mining district of Laurion continued to be the dominant provider of metal even during the Hellenistic period, when we have little historical

evidence for ongoing mining there. The potentially more complex lead isotope signature of the Laurion region, and the overall pattern of lead provision and trade in Hellenistic central Greece, requires further work in order to confirm the above results and conclusions. The full evidence from a wider range of materials and archaeological features has to be considered, and we hope to make a contribution to the ongoing research in this area.

ACKNOWLEDGEMENTS

We would like to thank Dr Arg. Intzesiloglou, Director of the Archaeological Institute of Thessalian Studies, for giving us the material of Pherai, and Mrs E. Nikolaou, archaeologist of the 13th EPCA, for giving us the material of Demetrias.

Use of analytical facilities at the Department of Earth Sciences, University of Bristol by E. Asderaki was funded by the European Community Access to Research Infrastracture action of the Improving Human Potential Programme, contract HPRI-CT-1999-00008, awarded to Prof. J. Wood (EU Geochemical Facility, University of Bristol).

We particularly thank Dr Chung Choi from that department for his patience and dedication in running the ICP-AES lead analyses for us, as well as Dr Tim Elliott and Dr Chris Coath from the same department for running the MC-ICP-MS lead analyses. Mr Kevin Reeves of the Wolfson Archaeological Science Laboratories of the Institute of Archaeology UCL who helped us with the XRD analyses of the corroded lead.

Dr Sophie Stos, now at Exeter University, is thanked very much for her help in interpreting the lead isotope data measured for this project.

REFERENCES

Asderaki, E. & Rehren, Th. 2002, A study of Hellenistic gilding practice and manufacture of funerary wreaths. *iams* 22, 19-21.

Intzesiloglou A., 1993, Velestino (ancient Pherai): Pherai st., G. and Th. Apostolina, *Archaeologiko Deltio*, vol. 43 (1988) 1: Chronika 243-245 (in Greek).

Konophagos, K. 1980. *Le Laurium Antique*.

Rehren, Th. & Prange M. 1998, Lead metal and patina: a comparison. In: *Metallurgica Antiqua*, (=Der Anschnitt, Beiheft 8), eds. Th. Rehren, A. Hauptmann & J. Muhly, 183-196. Bochum: Deutsches Bergbau-Museum.

Rehren, Th., D. Vanhove & H. Mussche, 2002. Ores from the ore washeries in the Lavriotiki, *Metalla (Bochum)*, 9.1, 27-46.

Stos-Gale A.Z., Gale, H.N. & Annets, N. 1996, Lead isotope data from the isotrace laboratory, Oxford: Archaeometry data base 3, ores from the Aegean, part 1. *Archaeometry* 38, 381-390

Wyttenbach A. & Schubiger P., 1973, Trace element content of Roman lead by Neutron Activation Analysis. *Archaeometry* 15, 199-207

MANUFACTURED TECHNOLOGY AND MATERIALS OF AN EARLY HELLENISTIC FUNERARY BRONZE URN

E. Asderaki
13th Ephorate of Prehistoric and Classical Antiquities, Athanassaki 1, 38222 Volos, Greece, elasder@hotmail.com

K. Tsatsouli
Cardiff University, Department of History and Archaeology, tsatsoulik@cf.ac.uk

A. G. Karydas
Institute of Nuclear Physics, NCSR "Demokritos", 153 10 Aghia Paraskevi, Athens, Greece, karydas@inp.demokritos.gr

1. INTRODUCTION

During excavation works in 1995-96, carried out by the 13th Ephorate of Prehistorical and Classical Antiquities, in the northern cemetery of ancient Demetrias, tomb 389 revealed a bronze funerary urn (Nikolaou, 2000). It is dated in early Hellenistic period, first half of 4th century BC (fig. 1). Demetrias was the second capital of Macedonian Kingdom, one of the greatest economical centers of Thessaly and the base for military and political control of the cities in southern Greece.

1.1. Description of the urn

The urn was placed in a box-like case made of limestone (Varoufakis 1991; Nikolaou 2000). It is 41.5 cm high and 31 cm wide. The urn consists of the main body, the base, three handles, a decorative pattern and its lid which was attached to the body with a chain. The remains of a deceased man, existed inside the urn, were covered with two different types of textile, as it was identified from this study. Copper corrosion resulted into the preservation of the textiles through mineralization, thus enabling their study and the acquisition of valuable information.

2. MAIN ASPECTS OF THE STUDY

Our interest is focused on: a) the manufacturing techniques of the urn, b) the type of the alloy used for the manufacture of the various pieces of the urn,

Figure 1. The urn of Demetrias, dated to the first half of 4th century BC.

c) the welding techniques used to join the various pieces to the main body and
d) the technology of the mineralized textile found inside the body of the urn.

3. METHODS OF INVESTIGATIONS

a) A portable Energy Dispersive X-rays Fluorescence (EDXRF) developed at the Institute NCSR "Demokritos" and a Total Reflection XRF (TXRF) set-up, were used as the main analytical techniques for elemental analyses, in order to determine the alloy used as well as the welding material.

b) Optical microscopy helped us to understand how the metal was worked. The analysis was done at the Institute NCSR "Demokritos".

c) X-ray analyses, showed how many metal sheets were used for the manufacturing of the urn, and

d) as far as it concerns the textile analysis, a Wild M3 low power stereomicroscope was used for the investigation of weave patterns and threads twist, while a Camscan Maxim 2040 Scanning Electron Microscope,

equipped with Oxford Instrument energy-dispersive analytical system and Maxim 4 imaging software, was used for fibre identification and threads diameter measurements. Textile investigations were performed in Cardiff University, School of History and Archaeology.

4. RESULTS-DISCUSSION

4.1. Urn

The urn consists of cast and forged parts. The body of the urn was shaped from only one bronze sheet. Neck was made separately and then joined to the main body. The cover (lid) is hammered and the decorative figure hand-made. The handles and the base are cast. The size and the spherical shape of the base exclude the use of the lathe. The handles are attached on the rosettes both metallurgically and mechanically. The metal sheet of the body was first cast and then hammered. The metallographic examination showed that the metal was worked hot. An annealed texture, with large annealing twins is obvious; there is not much post-annealing deformation, but enough to prompt the intra-granular corrosion. There is precipitation of pure copper in cracks, not unusual corrosion phenomenon in bronze. It is clear that the dendrites are homogenized; however, some of the delta phase has survived and this indicates a relatively high tin content in the alloy.

4.1.1. XRF results

Using the portable XRF spectrometers, 23 points of the urn were analyzed. Two samples taken from the base and left handle of the urn were used for destructive analysis by means of the TRXRF method. The analytical data obtained by means of in-situ XRF analyses on the urn surface treated carefully as corrosion of the surface could alter considerably the alloy composition. Therefore, towards a reliable validation of these measurements it has been chosen to present directly raw XRF data (table 1). The shaded areas correspond to the variation of the various experimental parameters presented, in order to be in accordance with the TXRF analyses. Apart from the raw Cu-K_α and Sn-K_α X-ray intensities, the values of a qualitative parameter are presented, that expresses the Sn-K_α/Sn-L_α intensity ratio. If there is a uniform distribution of tin, between the surface and the bulk of the alloy, it is expected that this intensity ratio would be varied inside the corresponding shaded area, even for Sn concentration up to 20%. However, this intensity ratio should be considered only as a qualitative criterion; it doesn't prove that the analysis spot is free from any corrosion product. Among the total 23 spots that were analyzed in-situ, the Sn-K_α/Sn-L_α ratio was in full agreement with the TXRF results for 13 analysis

spots that were also, at least by visual observation, free from any surface corrosion product. However, only six spots on the body of the urn and two spots on the cover (lid) provided similar quantitative data with the TXRF one, as shown also in table 1. At the other five spots from the left handle and the base, the quantitative results gave an overestimation of the Sn concentration with respect to the TXRF results, proving the qualitative character of the Sn-K_α/Sn-L_α ratio.

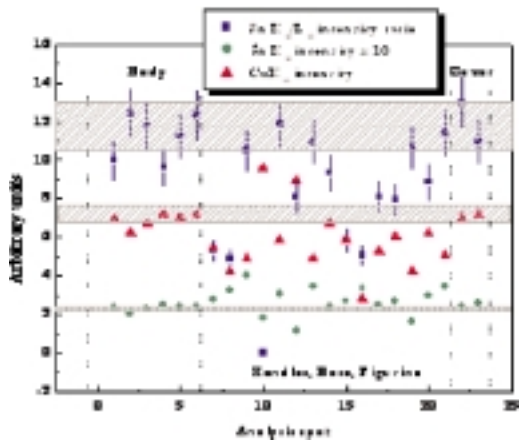

Table 1. Raw XRF data

The three handles, the base and the decorative figure were adhered on the body of the urn with a tin-lead soft solder, traces of which are still visible. The analyses for the soldering were performed with EDXRF. The analyses for the soldering were performed with EDXRF. The chemical analyses in the various parts of the urn as found with EDXRF and TXRF, in %, are given in table 2. Increased quantities of cuprite exist on the surface of the left handle due to the increased Cu signal with respect to the Sn one. Lead traces were identified on the surface of the lid but this is probably due to contamination of the lead sheet which is adhered on it. The yellowish appearance of the body is due to the high tin content.

No	Point	Method	Cu %	Sn %	Fe %	As ppm
1	Body of the urn (6 points)	In-situ XRF	88.2 ± 0.2	11.7 ± 0.2	0.12 ± 0.02	119 ± 53
2	Lid (2 points)	In-situ XRF	88.0 ± 0.4	11.9 ± 0.4	0.16 ± 0.08	-
3	Left handle	TXRF	89.0 ± 0.5	11.0 ± 0.5		-
4	Base	TXRF	89.0 ± 0.5	11.0 ± 0.5		-

Table 2. Results of the chemical analyses done both with EDXRF and TXRF in the various pieces of the urn

4.2. Textile

Textile investigations were performed on four mineralized samples. The results of the investigation are summarized in table 3.

	Type of Weave	Threads/cm	Thread Twist	Mean Thread Diameter in mm	Mean Fibre Diameter in µm	Fibre Type
Textile A	Plain	25 (System 1) 23 (System 2)	Low Z	0.25 (System 1) 0.19 (System 2)	11	Flax (?)
Textile B	Plain weft-faced	27 (Weft) 20 (Warp)	I (weft) High Z (warp)	0.35 (Weft) 0.19 (Warp)	20.5	Wool

Table 3. Summary of the investigation results on the textiles

Textile A was identified as a linen plain weave textile with a fairly open weave. Fibre identification possessed problems, since the sample had been previously consolidated with an unknown polymer. However, SEM made possible for certain fibre features (such as swelling along the fibre surface) to be visible (fig. 2). Furthermore, fibre diameter measurements, with the help of SEM, matched with those given for flax fibres (Ryder, 2000). Flax has a natural "S" twist, (Sheffer and Tidhar, 1991: 3; Ryder, 2001); however, analysts often encounter flax having a "Z"-twist (Walton, 1989: 347). **Textile B** was

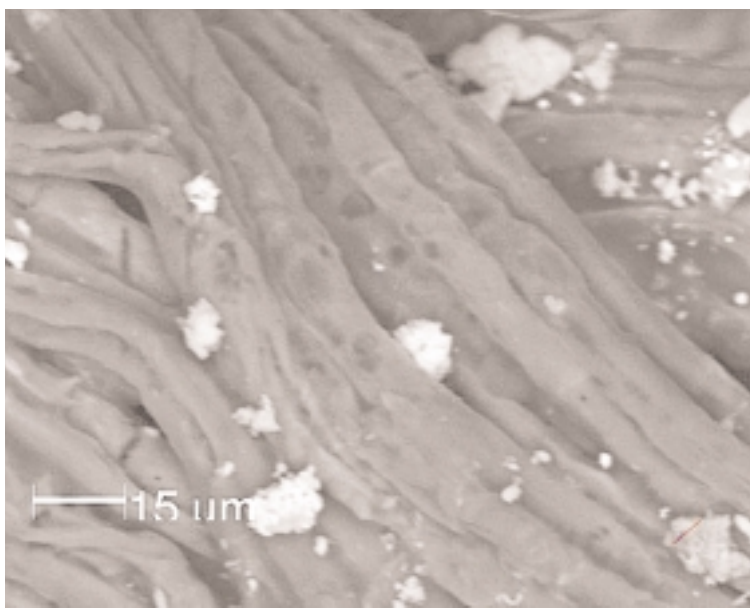

Figure 2. SEM photograph of fibres from sample 3 (X1000). The possible presence of swelling might indicate the presence of flax or hemp.

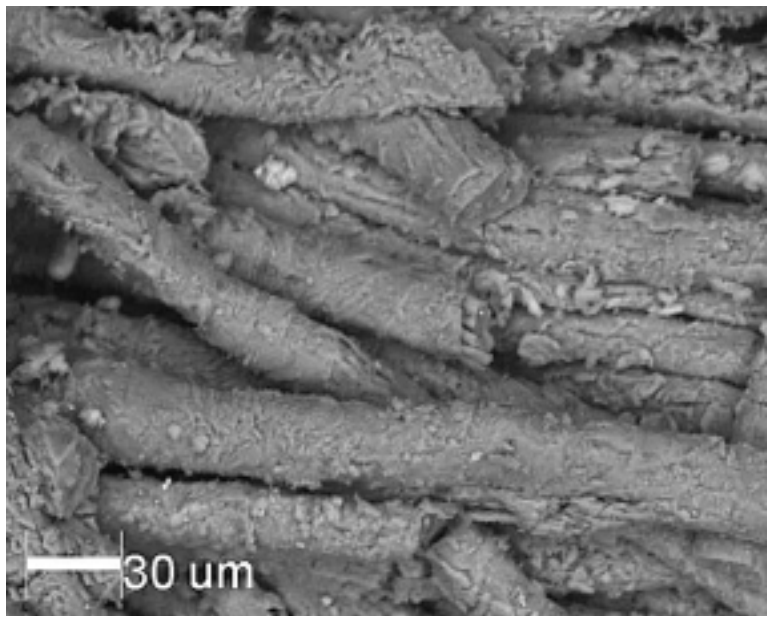

Figure 3. SEM photograph of the fibres of sample 4 (X500). The characteristic scale patterns indicate the presence of sheep wool.

identified as plain weft-faced wool (possibly sheep wool) made from a fine wool fleece (fig. 3). The accurate distance between the wrap threads, which ranged from 0.525 mm to 0.553 mm (fig. 4), show a highly developed textile manufacture industry in the area at that period.

5. CONCLUSION

Various analytical techniques were used in order to answer the questions which have been arisen concerning the manufacture of the urn and the identification of the mineralized textile which was found in its interior. EDXRF and TXRF were chosen to be the main analytical techniques for the elemental and quantitative analyses of the urn's metal. Compositional and manufacturing differences were observed between the various parts of the urn. Elemental analysis proved that the yellowish appearance of the body was due to the relatively high tin content in the alloy. Metallographic investigation showed that the body was first cast, then hammered and annealed, while a good quality of metal has been used for this purpose. X-ray examination showed that the urn was made of two sheets; one single bronze sheet up to the neck and a second one up to the rim. The decorative figure

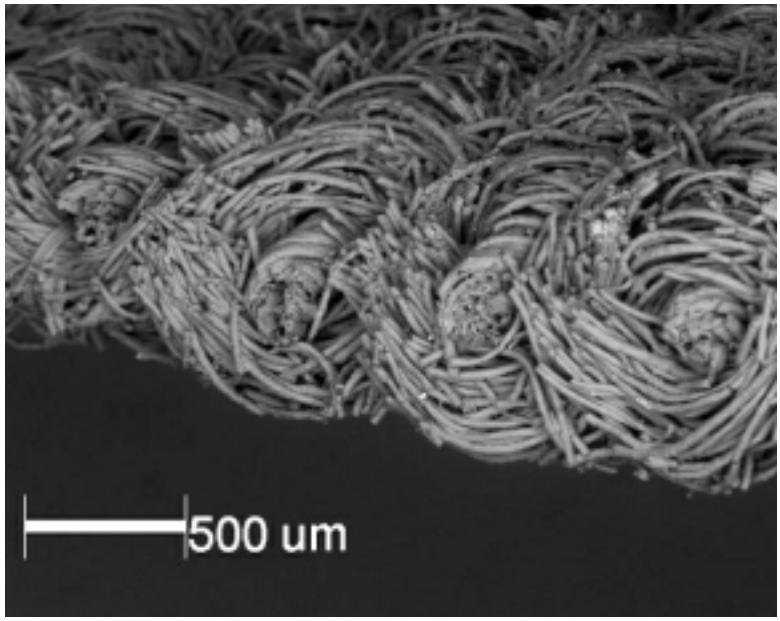

Figure 4. SEM photograph of cross section preserved by positive casting (x2000) of sample 4 showing the accurate distance between the warp threads (x50).

that ornaments the central part of the urn was hand-made. The base and the handles were cast. They were made of a slightly different alloy than the one used for the body. A tin-lead soft solder was used to adhere the three handles, the base and the decorative figure to the body of the urn. The question which could arise is why they used an alloy so difficult to shape? Did they intend to obtain just an attractive appearance, or it was to increase the corrosion resistance, since the urn could contain the remains of a specific person; or they had both aims?

Two different textiles were found to co-exist in the internal of the urn; wool and flax. For the weave and fibre investigations, the SEM has been proved to be the most useful technique, with two different types of weave and two different types of fibres being identified. The accurate distance between the wrap threads of the woollen textile might indicate as well the presence of a well established textile manufacture industry at the area at that certain period. Further investigation needs to be performed on the determination of the co-existing of the two different types of textile in the urn. The manufacturing of such highly standard products (both in the metals and textile industry) indicates the presence of a well organized community with well specialized craftsmen in Demetrias area.

ACKNOWLEDGEMENT

We would like to thank: E. Nikolaou, archaeologist of the 13th EPCA, for giving us the material. D. Watkinson, Dr. K. Anheuser and P. Parks from Cardiff University for their help and advice. Special thanks go to Dr. Y. Bassiakos, NCSR "Democritos", for allowing us to prepare the samples for metallographic examination, in his lab, as well as Prof. Th. Rehren, IoA, UCL for his continuous support and Th. Tselios, PhD student for his help in sample preparation

REFERENCES

Nikolaou E., 2000, Excavation of the north cemetery of ancient Demetrias. In: *Proceedings of the 1rst Scientific Meeting, The archaeological work done in the area of Thessaly (1990-1998)* Volos 2000, 309-314 (in greek).

Ryder, M.L., 2000, Issues in Conserving Archaeological Textiles. In: *Archaeological Textile Newsletter* 31. 2-7

Ryder, M.L., 2001, Fibres in Iron Age Textiles from the Dürrneberg, Austria. In: *Archaeological textiles Newsletter* 33. 2-5.

Sheffer, A. and Tidhar, A., 1991, Textiles and Basketry at Kuntillat 'Ajrud. In *'Atiqot'* 20, *Journal of the Israel Department of Antiquities*, 1-27.

Varoufakis G., 1991, "Metallurgical investigation of the bronze crater of Derveni", *Aspects of Early Metallurgy,* ed. W.A.Oddy, British Museum *Occasional Papers*, 17, 71-86.

Walton, P., 1989, Textiles, Cordage and Raw Fibre from 16-22 Coppergate. In: *Addyman, P. V.* (ed) The Archaeology of York, Vol. 17: The Small Finds. York Archaeological Trust.

ROMAN AND MEDIEVAL LITHARGE CAKES: STRUCTURE AND COMPOSITION

Justine Bayley
English Heritage Centre for Archaeology, Fort Cumberland, Fort Cumberland Road, Eastney, Portsmouth PO4 9LD, Great Britain.
Email: justine.bayley@english-heritage.org.uk

Kerstin Eckstein
Technical University Bergakademie Freiberg, Institute for Archaeometry, Gustav-Zeuner-Str 5,
D-09599 Freiberg, Germany. Email: kerstin.eckstein@am.tu-freiberg.de

1. INTRODUCTION

Many litharge cakes have been found in urban excavations in Britain. They were initially studied to identify the process that produced them – which confirmed them as by-products of silver refining. They are the porous lining of a hearth which absorbed litharge (lead oxide, PbO). The refining process is known as cupellation, and involved melting impure silver with lead metal. The melt was oxidised by blowing air across it, forming litharge which then both oxidised any base metals (such as copper) that were present and dissolved them, before being absorbed by the hearth lining. Although silver dissolves readily in lead metal it is insoluble in litharge. The pure silver was thus left behind on the surface of the hearth at the end of the process.

This paper aims to increase understanding of the process, show if any significant changes were made to silver-refining technology from Roman to medieval times and, compare archaeological finds with descriptions of cupellation in classical and medieval texts. The litharge cakes investigated range in date from the 1st to the 13th centuries AD. Note that litharge cakes which are found on rural silver-production sites normally contain no copper – they are not considered here.

2. THE PHYSICS AND CHEMISTRY OF CUPELLATION

Cupellation is a selective oxidation. Lead, the majority of the copper and most of the other impurities are oxidised while silver (and any gold)

remain unaltered. The diffusion of oxygen through a layer of molten litharge is very slow; for this reason the litharge must be removed from the surface of the melt. This can be done by skimming but usually a porous hearth lining is used. The molten metal oxides are removed by capillary attraction into the pores of the lining while the metal, having a higher surface tension, remains on top where it is further exposed to oxidation. The process finishes when all the lead is oxidised, leaving a pool of pure silver on the surface of the hearth.

The temperature required for cupellation initially depends on the degree of debasement of the silver (the Cu-Ag eutectic is 779°C at 71.5wt% Ag) (Brandes 1983, 11-13). As silver dissolves in lead but copper and lead are mutually insoluble, adding an equal amount of lead produces a melt that can be approximated by a Pb-Ag binary system with a melting point of around 650°C (Brandes 1983, 11-19). Oxidation produces litharge, which reacts with the copper, giving a melt with a eutectic of 680°C at just under 20wt% Cu_2O (Levin et al 1964, fig 163). Relatively low temperatures produce complete oxidation of impurities and keep volatisation losses of lead and silver to a minimum. As lead and copper are oxidised, the proportion of silver in the melt increases so the process temperature increases towards 960°C, the melting point of pure silver. Temperatures this high are only needed towards the end of the process.

In cupellation the oxides of arsenic and antimony are volatile and are carried off with the fumes at the beginning of the process. Tin oxide separates early on, but the eutectic of 850 °C corresponds to only 2.5% SnO_2 so larger proportions of tin require much higher temperatures (Levin et al 1964, fig 285) or the addition of a flux (like the glass Theophilus mentions – Hawthorne and Smith 1979, 97), as do quantities of zinc.

Litharge readily forms low-melting phases with any silicates, so silicate refractory linings begin to break down; copper-rich litharge is extremely aggressive. If the hearth lining is to have a lasting porosity so it can continue to absorb litharge, it should be made of a low-silica, basic material; from the end of the first millennium BC the preference has been for bone ash. This is powdered bone, with the organic matter, carbonate and water removed by calcination, leaving just the extremely stable calcium phosphate. Other materials were also used, especially when working on larger scales. Any material rich in calcium and/or magnesium will do, and mixtures of shell, lime, dolomite, clay and plant ashes have probably all been used.

3. HISTORICAL DESCRIPTIONS OF CUPELLATION

Theophilus, writing in the 12th century AD, has the earliest good description of cupellation: 'Sift some ashes … and take a fire-tested

earthenware dish … Put ashes in it, thinly in the middle and thickly around the rim … When it is dry … put the dish … beneath the [tuyère] hole, so that the blast from the bellows will blow onto it … place coals on top, and blow until the dish is red-hot. Then put the silver into it, add a little lead on top, heap charcoal over it, and melt it. You should have at hand a stick … with which you should carefully uncover the silver and clean away whatever impurity you see on it. Then put on it … a stick burnt in the fire, and blow gently, using a long stroke [of the bellows]. When you have removed the lead by this blowing, if you see that the silver is not yet pure, again add lead, place charcoal on it, and do as you did before. However, if you see the silver boiling and jumping out, know that tin or brass is mixed with it, and finely crush a small piece of glass and throw it on the silver. Then add lead, put charcoal on, and blow vigorously. Then inspect it as before, take away the impurities of glass and lead with the stick … Keep on doing this until it is pure' (Hawthorne and Smith 1979, 96-7).

He also describes what sort of ashes to use: 'Take the bones of any kind of animal that you may have found in the street and burn them; when they are cold, grind them very fine and mix with them a third part of beechwood ashes and make dishes, as we described above …' (ibid, 146).

Figure 1 comes from a 16th-century treatise (ibid, fig 12) and shows the refining of silver by cupellation. The right hand side shows the ash-lined hearth (B) just below the tuyère, through which air enters from the bellows (D). On the left the process is in progress with a fire (C) burning and the craftsman holding a tool (F) with which he manipulates the fire and scrapes the litharge off the molten silver.

Figure 1. Refining silver in a cupellation hearth (from Ercker 1574).

For the Roman period Pliny, writing in the 1st century AD, has a less clear and detailed description of cupellation: 'The method of refining [silver]

… is heating with lead … but the silver floats on top like oil on water' (Bailey 1929, 111). Lead and silver are mutually soluble so separation is only achieved by oxidising the lead to litharge. This is less dense than silver, so for silver to 'float on top' the litharge must have been absorbed by the hearth lining.

4. INVESTIGATION AND ANALYSIS

Samples removed from litharge cakes from six different sites were examined by optical microscopy and in a scanning electron microscope (SEM). SEM-based energy dispersive X-ray analysis was used to determine their bulk composition and to identify the individual phases present. All the data is calculated as conventional oxides and normalised, though in some cases the elements are present in other oxidation states (eg, copper is present as Cu and Cu^{+} as well as some Cu^{2+}). In general the composition of each litharge cake is fairly consistent, though the zones near the top and bottom surfaces are often atypical. Fig. 2 shows the average composition of the six litharge cakes.

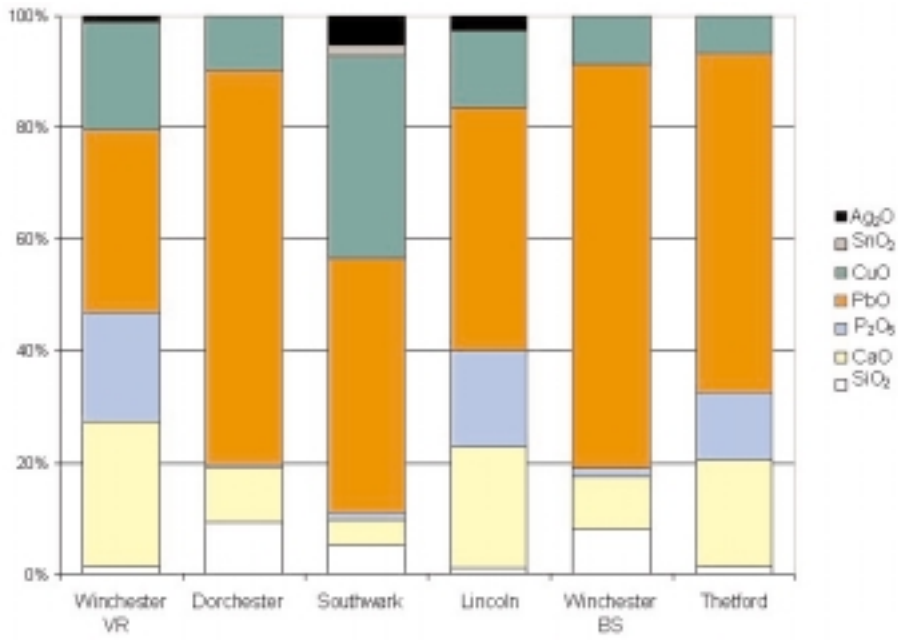

Figure 2. Average composition of analysed litharge cakes.

Site	Date	Composition of litharge cake	Pb:Cu	Silver in litharge	Reference
Winchester, Victoria Road	Roman	bone ash *	low	yes	unpublished
Dorchester, Colliton Park	Roman (1-2nd C)	clay marl	high	no	McDonnell 1993
Southwark	Roman	mixed *	low	yes	unpublished
Lincoln, Flaxengate	Anglo-Saxon (4-9th C)	bone ash *	medium	yes	unpublished
Winchester, Brook Street	medieval (11-12th C)	mixed	high	no	Bayley and Barclay 1990, 181
Thetford, Guildhall	medieval (12-13th C)	bone ash *	high	no	Bayley 1999

* = bone ash particles visible

Table 1. Samples investigated (see Section 5 for discussion of data in columns 3-5).

4.1. Litharge cake from Thetford

A segment of a litharge cake (fig. 3) was investigated. It is one fragment from a group weighing a total of 20 kg. The hearth lining was originally bone

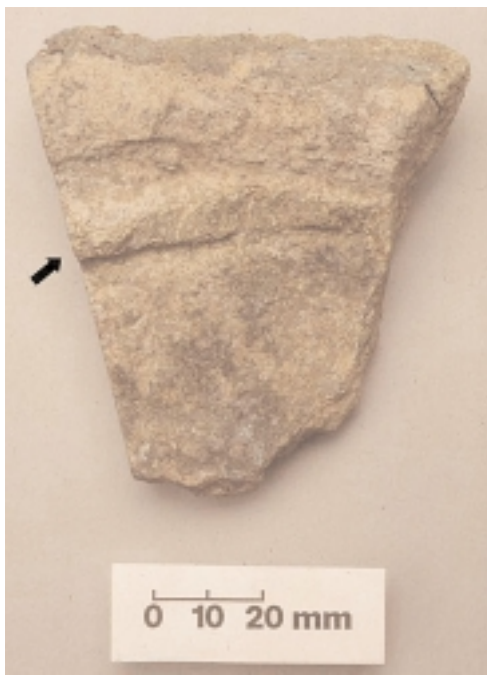

Figure 3. Fragment of litharge cake from Thetford. (Arrow show sfeature mentioned in text).

ash and can be reconstructed as a shallow dish about 200 mm across, like those shown in figure 1. The silver-rich litharge that solidified round the edge of the pool of silver (arrowed in fig. 3) was chipped off so it could be cupelled again to increase recovery of the silver. Figure 4 shows its internal structure.

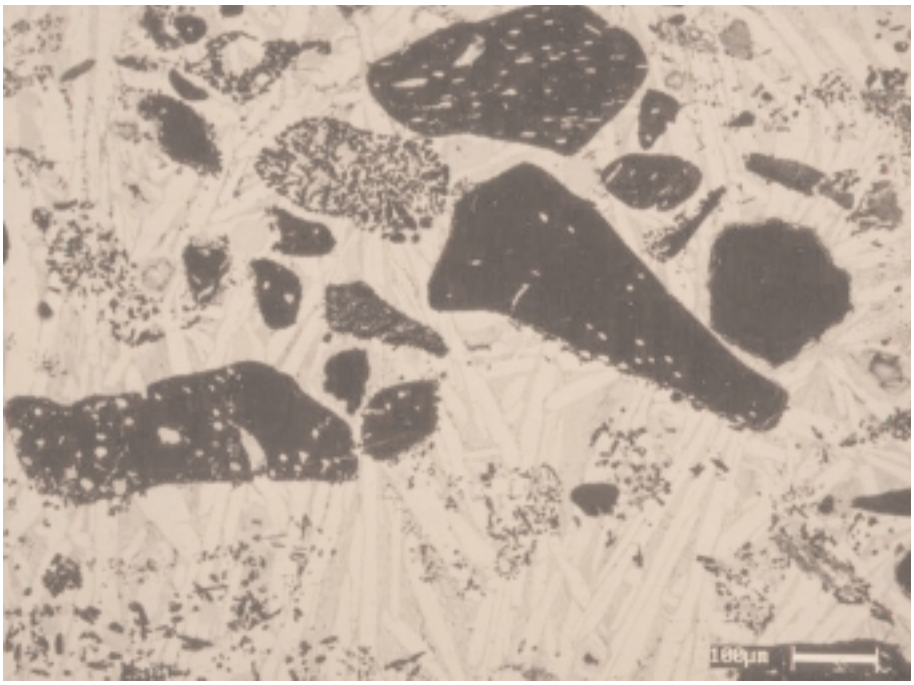

Figure 4. Backscattered SEM image of litharge cake from Thetford. The bone ash particles (black) are partly destroyed, forming newly-crystallised Ca-Si-phosphates. The matrix is a eutectic mixture of PbO (pale grey) and PbO + $PbO.Cu_2O$ (mid grey).

4.2. Litharge cake from Southwark

The degree of destruction of the hearth lining is more extreme than in the other bone ash litharge cakes, and suggests the upper part of the lining may have been partly molten. This may explain the why large silver droplets are trapped at the surface (fig. 5); they are typically 93wt% Ag and contain inclusions of copper and lead oxides. Figure 6 shows the copper-rich internal structure.

4.3. Litharge cake from Dorchester

This hearth lining was made of a lime-rich clay mixture. No bone particles or primary phosphorus-rich phases are present (fig. 7), and their absence is demonstrated by the high $CaO:P_2O_5$ ratio (fig. 2).

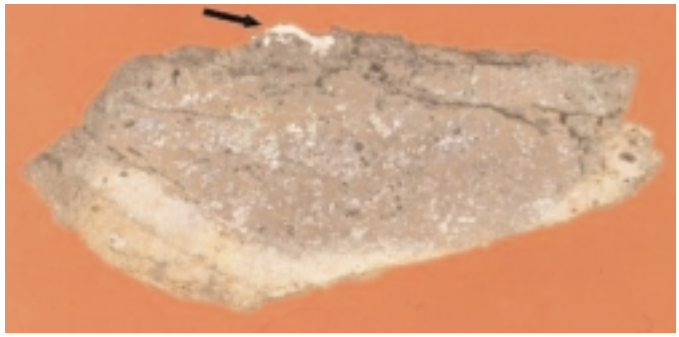

Figure 5. Section through litharge cake from Southwark, showing mechanically-trapped silver (arrowed) on the upper surface (sample is 78 mm across).

5. DISCUSSION AND CONCLUSIONS

SEM images of the litharge cakes show a range of different microstructures, and considerable variations in bulk composition were also noted (fig 2). These differences are due to the varying composition of the hearth lining, and to the proportions of metals present. Table 1 shows that in some cases the hearth had been lined with bone ash, while in other cases the results suggest a mixture (including bone ash and probably plant ash)

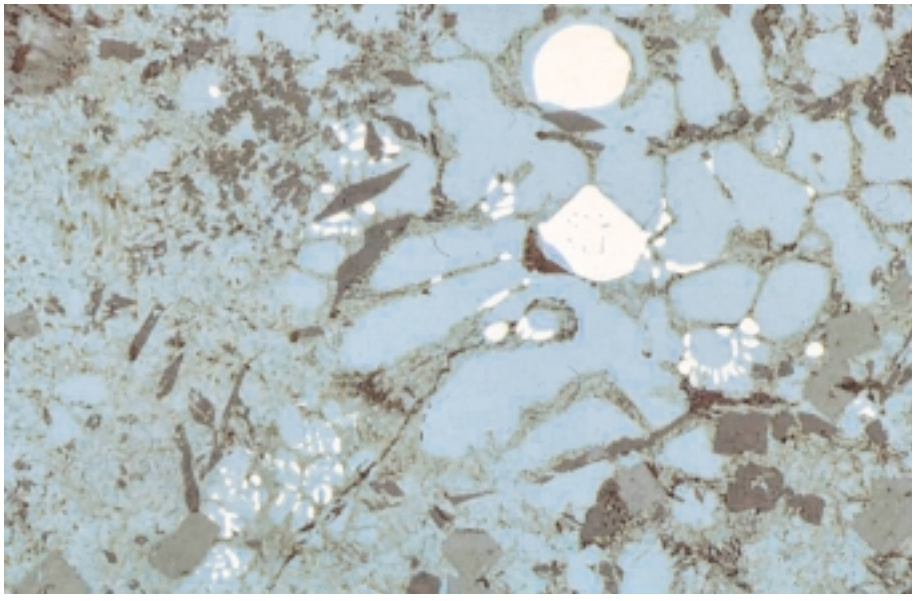

Figure 6. Thick section from core of litharge cake from Southwark showing silver (white) precipitated from cuprite (pale blue). Image width 660 μm.

or clay marl (lime-rich clay) was used. All are low in free silica so the formation of lead silicates is minimised, which leads to good absorption of the litharge by the hearth lining and thus effective separation of base metals from the silver.

The phase composition within the litharge cakes is also variable and seems to provide an indication of the efficiency of the cupellation process, which can be assessed on the basis of the amount of silver present. Table 1 shows that silver is only detected where the Pb:Cu ratio is low. When insufficient lead was added to the hearth, the oxidised copper was present as Cu_2O rather than $PbO.Cu_2O$. Up to 44% silver dissolves in Cu_2O (but is hardly soluble in $PbO.Cu_2O$) so significant amounts of silver are carried down into the litharge cakes, and separate on cooling, when free Cu_2O is present (see fig 6). This silver is lost, unlike silver physically trapped on the surface (fig 5).

There is no correlation between the composition of the hearth lining and the effectiveness of the cupellation process; all the linings used were adequate for their purpose. It is also clear that in three cases significant amounts of silver were lost into the hearth linings because insufficient lead was added. The Pb:Cu ratios are low, partly because the lead contents of the

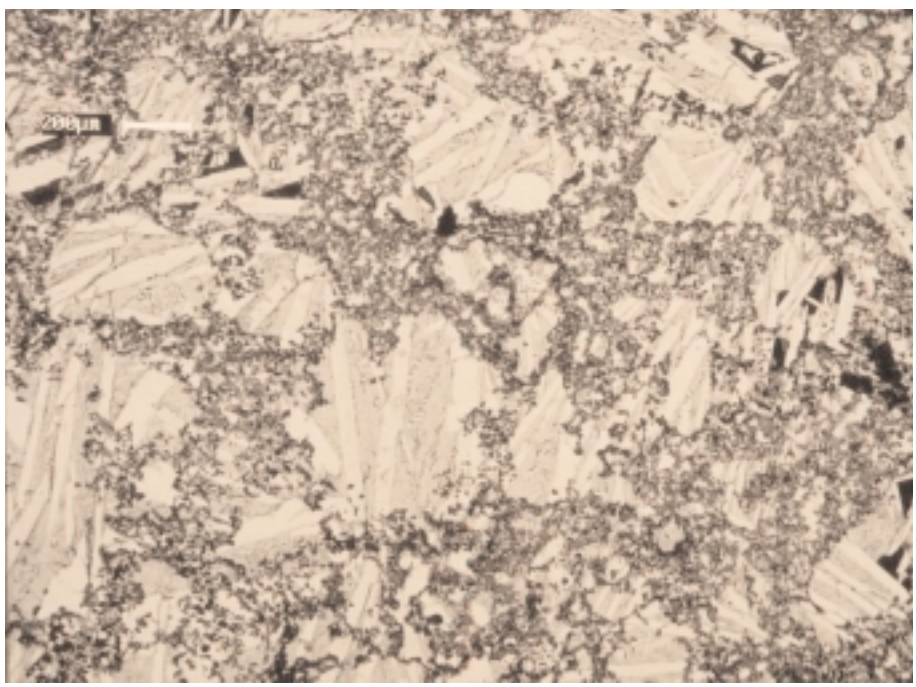

Figure 7. Backscattered SEM image showing the original clay-lime hearth lining from Dorchester is completely recrystallised and now consists of Pb-Ca-Mg-silicates and K-Al-silicates. The striped areas are a mixture of PbO and $PbO.Cu_2O$, as in Fig 4.

litharge cakes are low, but also because the copper contents are high. Two of the three cases are Roman in date (Southwark and Winchester, Victoria Road), and the other one (Lincoln) came from an Anglo-Saxon context but may be residual Roman material. The high copper values suggest that most of the Roman silver being refined was considerably less pure than later medieval silver. The higher lead contents of medieval litharge cakes may demonstrate the craftsmen had a better understanding of the process than their Roman predecessors did.

The reconstruction of the cupellation process from archaeological finds is very similar to that described in the historic texts. Unlike their descriptions of some other processes, those of cupellation mention only materials that are necessary. It thus appears that Roman and medieval craftsmen did understand, in an empirical if not a scientific way, what they were doing when they were refining silver.

REFERENCES

Bailey, K C (1929) The elder Pliny's chapters on chemical subjects, Part I. London: Edward Arnold.

Bayley, J (1999) 'Metalworking evidence', in P Andrews and K Penn, Excavations in Thetford, north of the river, 1989-90. Gressenhall: Norfolk Museums Service, 6-7.

Bayley, J and K Barclay (1990) 'The crucibles, heating trays, parting sherds, and related material', in M Biddle (ed), Object and economy in medieval Winchester. Oxford: OUP, 175-197.

Hawthorne, J G and Smith, C S (1979) Theophilus: On divers arts. New York: Dover.

McDonnell, J G (1993) 'The litharge cake', in R J C Smith, Excavations at County Hall, Colliton Park, Dorchester, Dorset, 1988. Salisbury: Wessex Archaeology, 35.

Brandes, E A (ed) (1983) Smithell's metals reference book 6th edn. London: Butterworth.

Levin, E M, Robbins, C R and McMurdie, H F (1964) Phase diagrams for ceramists Vol I. Columbus, Ohio: American Ceramic Society.

STRONTIUM ISOTOPES PROVENANCE ANCIENT IRON ARTIFACTS

P. Degryse*, P. Muchez
Fysico-chemische Geologie, K.U.Leuven, Celestijnenlaan 200C, B-3001 Leuven, Belgium, patrick.degryse@geo.kuleuven.ac.be

J. Schneider, M. Brauns, U. Haack
Institut für Geowissenschaften und Lithosphärenforschung, Justus-Liebig Universität, Senckenbergstrasse 3, D-35390 Giessen, Germany

N. Kellens, M. Waelkens
*Sagalassos Archaeological Research Project, K.U.Leuven, M. Theresiastraat 21, B-3000 Leuven, Belgium

1. INTRODUCTION

In the study of ancient ores, it remains notoriously difficult to establish the origin of a metal object from its composition (Gale and Stos-Gale, 1982). However, the lead isotopic composition of an artifact is identical, within analytical errors, to the signature of its ore (Brill and Wampler, 1965). Provenance determination of metals through lead isotope ratios is therefore a well-established method (Gale and Stos-Gale, 1982). A problem in the isotopic analysis of metal and ore, is the large variation in chemical composition of the ore itself. Lead isotope signatures may be 'broad' and fields may coincide (Brill and Wampler, 1965; Gale and Stos-Gale, 1982). Because of this and analytical difficulties, lead isotope ratios have hardly been employed for iron provenance determination (Gale et al., 1990).

Like lead, strontium isotopes are not fractionated by natural reactions or kinetic effects (Faure, 1998). Thus, the strontium isotopic composition of an artifact is inherited from its raw material and strontium isotopes should be suitable for tracing the origin of artifacts. The technique is unprecedented for provenance studies of ancient metals in general, and iron in particular.

The frequent occurrence of slag in the excavations, proves that iron was worked at Sagalassos. The territory of the ancient city offered a variety of mineral resources, including iron ore (Degryse et al., 2003). In early Roman excavation contexts, hematite ore was found in association with metallurgical waste, raw iron and many artifacts. In late Roman and Byzantine excavation

contexts, large amounts of slag and iron artifacts were identified, alongside a Byzantine iron workshop. However, no signs of the ore were found. Apart from the iron working in the city, in Byzantine times smelting sites were also active on the territory, where a magnetite sand was used as ore (Degryse et al., 2003).

2. METHODOLOGY

Iron ores and artifacts from Roman to Byzantine Sagalassos (SW Turkey), have been characterized on the basis of their lead and strontium isotopic composition. In this way, the strontium technique can be evaluated as a new means of ore provenance determination in archaeology.

Precleaned pieces of uncorroded iron artifacts were completely dissolved in aqua regia and split into two aliquots for separate determination of $^{87}Sr/^{86}Sr$ and Pb isotope ratios and Sr-Pb concentrations by isotopic dilution using mixed ^{206}Pb-^{84}Sr tracers. Pb contents in the iron objects were typically 200 to 500 ppb, Sr contents were typically around 1 to 2 ppm.

Strontium and lead were chemically separated with 3 N HNO_3 using EICHROM Sr resin on 250 μl Teflon columns, following the methods of Horwitz et al. (1991 a and b). Sr was stripped from the columns with 5 ml of H_2O. Subsequently, Pb was eluted from the same column with 5 ml of HCl 6 N. The Pb cut was further processed through a 250 μl column containing EICHROM Pre Filter Resin. After evaporation to dryness, the entire procedure was repeated using 50 μl columns to further purify both the Sr and Pb eluates.

For mass spectrometry, Sr was loaded with $TaCl_5$-HF-H_3PO_4 solution (Birck, 1986) onto W single filaments, and Pb loaded onto single Re filaments using silica gel-H_3PO_4 bedding. All Sr and Pb isotopic measurements were performed on a six-collector FINNIGAN MAT 261 solid-source mass spectrometer running in static multicollection mode. Sr isotopic ratios were normalized to $^{88}Sr/^{86}Sr = 0.1194$. Repeated static measurements of the NBS 987 standard over the duration of this study yielded an average $^{87}Sr/^{86}Sr$ ratio of 0.71025 ± 4 (2s mean, n = 22). Pb isotopic ratios were corrected for mass fractionation using a mean discrimination factor of 0.123 ± 0.029 (2s) %/[amu], based on replicate measurements of the NBS SRM 981 common lead (n=84) standard. Errors and error correlations were calculated after Ludwig (1980), the 2s uncertainties for the corrected $^{206}Pb/^{204}Pb$, $^{207}Pb/^{204}Pb$, $^{208}Pb/^{204}Pb$, $^{207}Pb/^{206}Pb$ and $^{208}Pb/^{206}Pb$ ratios are better than 0.3%. Individual a priori uncertainties (2s) are given for the Sr and Pb elemental concentrations. All Sr and Pb isotope data were corrected for maximum total procedure blanks (n=6) of 30 pg for both Sr and Pb.

3. RESULTS

Isotopic analysis data are given in table 1 and figure 1. It is clear that for the early Roman ore and iron artifacts, the Sr isotopic data are even better than those of Pb in providing similar signatures for ore and iron. Also, the magnetite sand and Byzantine raw iron from the territory, show an excellent correspondence for the strontium isotopic signature. As in both cases, ore and iron were found in a single production location, alongside smelting hearths (Degryse et al., 2003), their relation is certain. The data prove the validity of strontium isotope data in ore provenance determination. Remarkably, an iron object (03NK78) from the Byzantine excavation contexts at Sagalassos proper, shows an excellent correspondence to the isotopic field defined by the ore and raw iron from the territory. It is most probable that this object was manufactured from the magnetite sands.

All late Roman iron from the city proper shows a homogenous isotopic composition. The strontium signature, however, is far more reliable than the

Sample	Date - Location	$^{206}Pb/^{204}Pb$	$^{207}Pb/^{204}Pb$	$^{208}Pb/^{204}Pb$	$^{87}Sr/^{86}Sr$
Iron Ores					
02PDC11 - hematite	early Roman - Sagalassos	18.301	15.623	38.367	0.71149
03PDS7 - magnetite	early Byzantine - territory	19.363	15.709	39.257	0.70379
03PDS5 - magnetite	early Byzantine - territory	19.365	15.717	39.269	0.70373
03PDS8 - magnetite	early Byzantine - territory	19.375	15.730	39.327	0.70372
03PDS4 - magnetite	early Byzantine – territory	19.375	15.714	39.281	0.70375
Raw iron					
91N352	early Roman – Sagalassos	18.169	15.656	38.176	0.71097
00CS70	early Byzantine – Sagalassos	18.814	15.707	38.818	0.70534
03PDC33 (flake)	early Byzantine – Sagalassos	18.637	15.704	38.720	0.70535
02PDS1	early Byzantine – territory	19.011	15.674	38.971	0.70375
02PDS25	early Byzantine – territory	19.454	15.685	39.254	0.70375
Iron objects					
00LL4 - nail	early Roman – Sagalassos	18.139	15.641	38.191	0.71124
03NK145 A - arrow	late Roman – Sagalassos	18.777	15.667	38.846	0.70631
03NK145 B - arrow	late Roman – Sagalassos	18.782	15.672	38.883	0.70631
00LL5 - nail	late Roman – Sagalassos	18.648	15.702	38.835	0.70637
03NK78 - scissors	early Byzantine – Sagalassos	18.782	15.723	38.959	0.70379
03NK72 I - spatula	early Byzantine – Sagalassos	18.873	15.687	38.883	0.70535
03NK95 I - hammer	early Byzantine – Sagalassos	18.423	15.625	38.432	0.70587
03NK147 - pliers	early Byzantine – Sagalassos	18.773	15.692	38.892	0.70514
03NK79 - sickle	early Byzantine – Sagalassos	18.733	15.675	38.822	0.70484
03NK146 - axe	early Byzantine – Sagalassos	18.756	15.684	38.871	0.70469

Table 1. Lead and strontium isotope data of ores and iron from Sagalassos.

lead signature. Both differ from those of the earlier discussed local ores. A different ore was used for the manufacture of iron in late Roman times at Sagalassos.

In view of the large spread and weak correspondence in both the strontium and lead isotopic composition of the early Byzantine iron at Sagalassos, it is obvious that many different ore sources were used. It is unlikely that all these were imported and smelted locally. It can be assumed that iron was only worked locally, besides the import of finished objects.

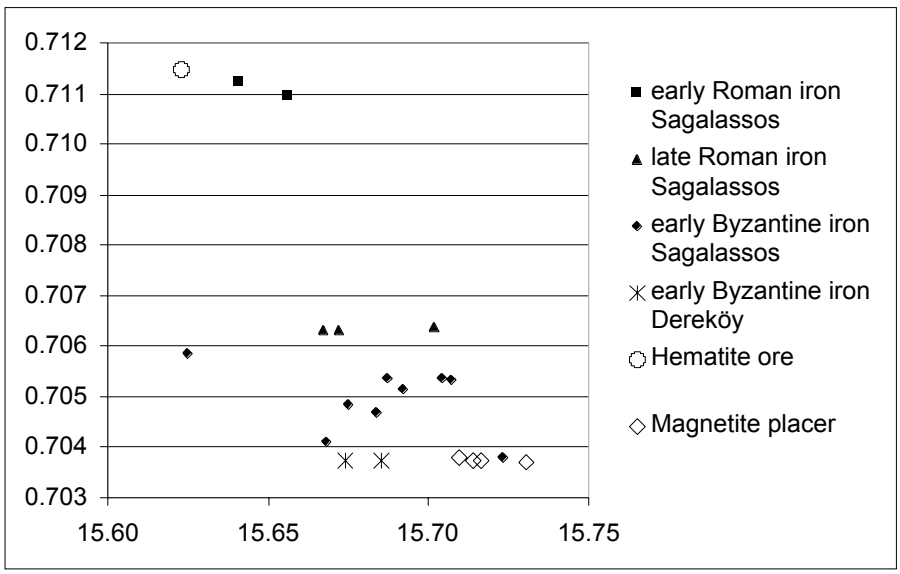

Figure 1. $^{207}Pb/^{204}Pb$ versus $^{87}Sr/^{86}Sr$ for all ores and iron analysed.

4. CONCLUSION

This work shows the advantages of strontium isotopic analysis in establishing the provenance of iron artifacts. While lead isotopic fields may be broad due to the often highly variable chemistry of the ore, the $^{87}Sr/^{86}Sr$ ratio permits distinction between overlapping lead isotope fields. It is therefore a more straightforward way of discarding or corroborating ore sources.

REFERENCES

Birck, J. L., 1986, Precision K-Rb-Sr isotopic analysis: Application to Rb-Sr chronology, Chemical Geology, 56, 73-83.

Brill, R. H., and Wampler, J. M., 1965, Isotope studies of ancient lead, American Journal of Archaeology, 71, 63-77.

Degryse, P., Muchez, Ph., Naud, J., and Waelkens, M., 2003, Geochemical prospection for iron-mineralisations (SW Turkey) and their use during Roman-Byzantine times, in: Mineral Exploration and Sustainable Development, (eds. G. Eliopoulos et al.), 969-972, Millpress, Rotterdam.

Faure, G., 1998, Principles and applications of geochemistry, 2nd edition, Prentice Hall, New Jersey.

Gale, N. H., and Stos-Gale, Z., 1982, Bronze Age Copper Sources in the Mediterranean: a New Approach, Science, 216, 11-19.

Gale, N. H., Bachmann, H. G., Rothenberg, B., Stos-Gale, Z. A., and Tylecote, R. F., 1990, in: Researches in the Arbah 1959-1985, (eds. B. Rothenberg, H. G. Bachmann), University College, London.

Horwitz, E. P., Dietz, M. L., and Fischer, D. E., 1991a, SREX: a new process for the extraction and recovery of strontium from acidic nuclear waste streams, Solv. Extr. Ion Exch., 9, 1–25.

Horwitz, E. P., Dietz, M. L., and Fischer, D. E., 1991b, Separation and preconcentration of Sr from biological, environmental and nuclear waste samples by extraction chromatography using a crown ether, Analytical Chemistry, 63, 522–525.

Ludwig, K. R., 1980, Calculation of uncertainties of U-Pb isotope data, Earth and Planetary Science Letters, 46, 212-220.

ANALYSIS OF Cu-BASED ALLOYS AND THEIR CORROSION PRODUCTS FROM THE BILBILIS ARACHAEOLOGICAL CONTEXT BY SEM-EDS

M. Gener, A. Martín Costea, V. López, E. Otero, M. Morcillo
Centro Nacional de Investigaciones Metalúrgicas (CENIM-CSIC) Av. Gregorio del Amo, 8 – 28040 Madrid. Tfn. 915 538 900, FAX 915 347 425.
e-mail: mcgener@cenim.csic.es

ABSTRACT

The analysis of the archaeological artefacts described here is part of the ongoing INCO-MED project EFESTUS (Contract No. ICA3-CT-2002-10030). Its objective is the study of the corrosion processes of well-defined groups of Cu-based artefacts from the Mediterranean Countries. These processes are to be related to the specific conditions of the archaeological context and to the chemical composition and structure of the objects. This knowledge will be used to develop tailored strategies for conservation of Cu-based alloy artefacts exhibited or deposited in Museums.

The Spanish archaeological context of choice has been the site of the ancient city of Augusta Bilbilis. At this stage of the project, characterization of the Cu-based alloys, the soil in which they were found and the resultant corrosion products is being undertaken. With this purpose, eight small Cu-based objects of quotidian use, from the 1^{st}-2^{nd} c. AC, in as-excavated condition, have been selected. Samples have been taken and prepared for metallographical analysis using Optical Microscopy, Scanning Electron Microscopy (SEM) and Energy-Dispersive Spectroscopy (EDS). Also was sampled the soil strata where the artefacts came from. The chemical and microstructural composition of the Cu-based alloy artefacts has been determined as well as the nature of their corrosion products and processes. The soil sample was subjected to analysis, and its humidity, resistivity, pH, as well as Cl^- and SO_4^{2-} contents have been determined, among other parameters.

1. INTRODUCTION

EFESTUS is an acronym for the European INCO-MED project *"Tailored strategies for the conservation and restoration of archaeological value Cu-based artefacts from Mediterranean Countries"* (Contract No. ICA3-CT-2002-10030). The general

objective of the EFESTUS project is to identify the degradation causes of well-defined groups of Cu-based artefacts from the Mediterranean Countries, selected as a function of the archaeological context and of their chemical composition and structure. After accomplishing this, Cu-based reference alloys with a microchemical structure similar to that of the studied ancient alloys are to be produced in order to test traditional and innovative restoration and conservation methods. The purpose is to develop and validate tailored approaches to deal with the degradation processes of archaeological bronze artefacts in order to prevent any further damage when in Museum show boxes and storehouses.

The five specific scientific and technological objectives of the EFESTUS project are:

—Selection of archaeological contexts and bronze artefacts representative of different buried conditions and materials.

—Production of Cu-based reference alloys characterised by a composition and a microstructure similar to that of the ancient alloys.

—Identification of the electrochemical degradation mechanism [Ingo *et. al.*: 2004].

—Design and production of tailored innovative removable conservation and restoration materials and procedures to be used for each specific degradation phenomenon [Favre-Quattropani *et. al.*:2000]

—Development of an integrated information system allowing communication, control and exchange of information as well as the production of an Atlas with detailed physical-chemical information on the selected Cu-based artefacts related to the burial conditions, degradation mechanism and conservation methods.

The Partner institutions for this project are from Italy, Spain, Greece, Turkey, Jordan, Tunisia, Algeria and Egypt.

2. EXPERIMENTAL PROCEDURES

At the moment, the project is in the stage of having analysed some selected bronze artefacts and actually carrying on some tests to establish the degree of corrosion-promoting elements present in the atmosphere in different environments of some selected museums. In order to produce an appropriate supply of suitable samples to perform comparative tests for conservation procedures, there is also currently going on some accelerated corrosion tests on Cu-based reference alloys produced following the results of preliminary analysis of some of the ancient artefacts [Constantinides *et. al.*: 2002].

Archaeological artefacts suitable for destructive analysis, essentially fragments of quotidian objects, have been kindly provided from the following contexts: Municipium Augusta Bilbilis, Corduba, Lancia, La Cabañeta and Contrebia Belaisca. Preliminary work is now completed for the Municipium Augusta Bilbilis context.

Bilbilis is a Celtiberian-Roman city located in three hills at the outskirts of present Calatayud, province of Zaragoza (Spain). Its preservation status is not good, as it was used as a source of construction materials since the Middle Age. Nonetheless, it is rich in all kind of archaeological materials. Nowadays, it is unknown if the Celtiberian population would have been settled on the main roman piece of land or on its surroundings, since the native discoveries were limited in inferior levels. Quoted by classical authors like Strabo, Pliny, Ptholemy, etc., it was also the birthplace of the famous poet Martial, well known for his *Epigrams*.

The metallurgical samples were prepared by cutting a suitable fragment off the artefacts, embedding it in resin and polishing with different grit sandpaper and diamond paste up to 1 μm. The samples were then studied via optical microscopy using a OLYMPUS PME 3 inverted metallurgical microscope. Furthermore, they were analysed using a JEOL JXA-840 Scanning Electron Microscope (SEM) with EDS.

A sample representative of the soil where the artefacts were buried was also taken and analysed. The sampled soil corresponds, chronologically, to the second half of the 1st century and first years of the 2nd century AC. It is composed of infillings of what appears to be a construction set-up belonging to the chronological moment quoted. It is a dark ochre soil with uniform coloration containing high amounts of sand and little stones with a small granulometry. It also contains, in a low proportion and in small sizes, some white nucleus (which seem to correspond to a lime and sand mortar or to a plaster), some small fragments of charcoal, and some bits of brick or other construction material. The fraction smaller then 2 mm was sieved and sent to the Laboratoire Eau et Environnement, Institut National de Recherche Scientifique et Technique (LEE-INRST) in Tunisia to be analysed.

The reference alloys selected for the experiments of buried, atmospheric and accelerated corrosion tests have the following composition: Cu: 92.3%; Sn: 7.5%; Pb: 0.2%. / Cu: 88.0%; Sn: 4.0%; Pb: 8.0%. / Cu: 82.3%; Zn: 14.0%; Sn: 3.0%; Pb: 0.5%. They have been produced at CNR-ISMN (Rome), and their composition duplicates that of some ancient bronzes and brasses. Also, a small amount of copper and copper + iron sulphides inclusions have been added to these alloys in order to better simulate the ancient chemical and microstructural features.

For the determination of corrosion-promoting factors in museum atmosphere, three significant institutions, representing different types of general environment, have been selected: the *Museo Arqueológico Nacional* in

Madrid (severe urban environment), the *Museo Nacional de Arte Romano* in Mérida (mild urban environment), and the *Museo Nacional de Arqueología Marítima* in Cartagena (marine environment). In order to monitor the atmospheric conditions and its effect on the selected materials, Control Stations (CS) have been set up in significant places in the museum. Each control station is composed by the following elements:

— A set of reference probes (10 mm diameter disks) of cu-based alloys to be exposed to the atmosphere. There is 3 disks of each material.

— A High Sensitivity Pure Cooper Atmospheric Corrosion Probe (RCS 610-TF50).

— A digital data logger that measures and registers environmental temperature and humidity (SEFRAM-LOG 1520).

The Stations have been placed at three different places in each museum: in a significant exposition hall, inside and outside an expositor, and in the Museum's storage room. After regular periods of time, one set of samples is retired to be analysed, and the data from the probe and the data-logger is collected. Right now, the first set is already retired ant being analysed.

In order to perform accelerated corrosion tests in the Cu-based alloys, some samples have been buried in the same soil where the selected archaeological artefacts were found. Then, the soil is soaked in distilled water to favour the corrosion conditions. In some cases, the concentrations of corrosion-promoting elements found after the soil's analysis are increased to further accelerate the degradation process.

Additionally, electrochemical monitoring of the corrosion rate of two of the alloys is being undertaken. An electrochemical cell has been set up with two alloy samples, with the sides not facing the counter-electrode protected, buried in the same soil.

3. RESULTS AND DISCUSSION

The sampled soil, representative of the terrain where the artefacts where found in, has been analysed and the results are shown in table 1:

(a) Fraction	**< 0.2 mm (%)** 31.53		**0.2 - 1 mm (%)** 47.4		**1 - 2 mm (%)** 20.16	**> 2 mm (%)** 0.67
(b) Properties	**Conductivity (µs/cm) [at 25.5°C]** 0.702		**Density in C_2H_6O** 2.27		**pH** 8.08	**HCO^-_3 (mg/g)** 0.15
(c) Composition	**Organic carbon (mg/g)** 1.035	**Nitrogen Total (Kjeldahl) (mg/g)** 0.420	**Sulfates (mg/g)** 0.052	**Chlorides (mg/g)** 0.07	**Sodium (mg/g)** 0.37	**Potassium (mg/g)** 0.23

Table 1. Results for the granulometric fraction, from an initial sample ≥ 2 mm (a), physical and chemical properties (b), and amounts of relevant elements (c).

The results of the analysis show us a soil slightly alkaline. The high amount of organic carbon is due to the fact that the strata is formed by debris and construction infillings.

The little concentration of chlorides and sulphates are indicative of a hardly corrosive environment. The relatively good (given their age) preservation state of the metallic archaeological remains found buried there, supports this results.

The analysis of the artefacts via SEM-EDS has yield the following results. In fig. 1a can be seen a macrography (x3) displaying a relatively thin external layer of generalised corrosion, a feature that is found, in continuous or discontinuous form, in all the eight archaeological items studied [Robbiola *et. al.*:1998].

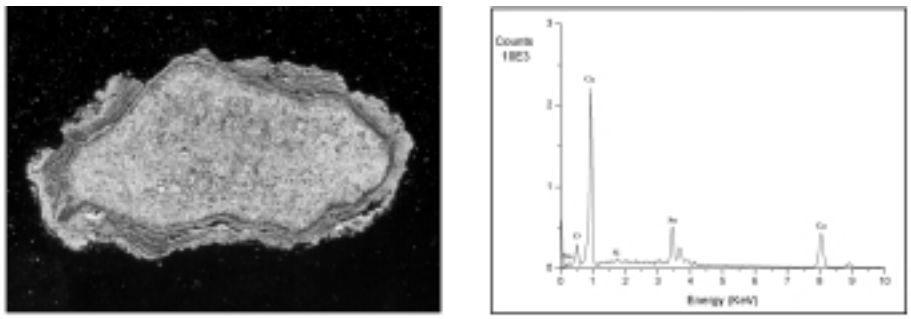

Figure 1. Macrography (x3) of the transversal cut of a sample **(a).** EDS analysis of the external layer of corrosion products **(b).**

The EDX analysis of the external corrosion layer (fig. 1b), shows an oxide of copper and tin, which are the components of this sample (Cu: 95.2%, Sn: 4.8%).

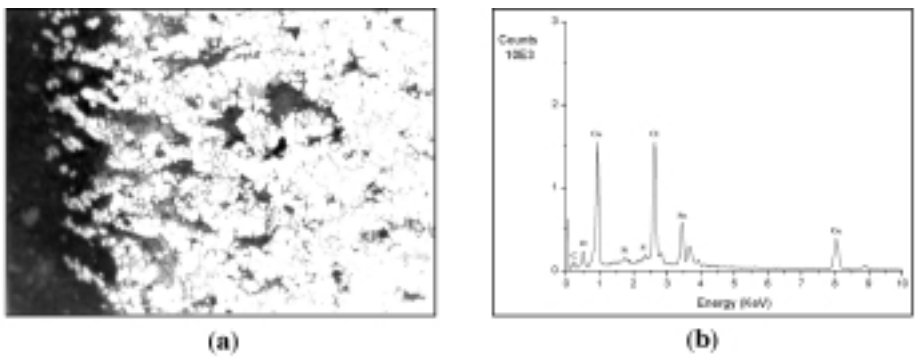

Figure 2. Macrography showing the selective attack of the tin-rich phase **(a).** EDS analysis of the selective attack corrosion products **(b).**

When a second phase is present, selective corrosion appears. In fig. 2a can be seen an example of the preferential attack to the tin rich phase of a bronze, that makes corrosion to penetrate deeply.

The EDX analysis of the selective attack corrosion products (fig. 2b) shows a tin and copper chloride.

In fig. 3a, the preferential attack to interdendritically segregated lead can be observed.

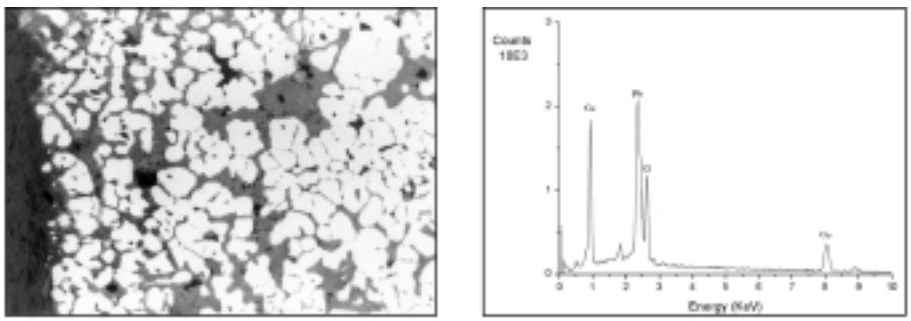

Figure 3. Macrography showing the preferential attack to segregated lead **(a).** EDS analysis of the preferential attack corrosion products **(b).**

The EDX analysis (fig. 3b) of the selective attack corrosion products shows now a lead chloride.

3. CONCLUSIONS

In concordance with the low corrosivity of the terrain, the penetration of the generalised corrosion is small.

Nonetheless, in presence of second phases (Pb, Sn), a selective attack develops. This can penetrate up to the nucleus of the artefacts, contributing to the general degradation state of the piece, and making extremely difficult the extraction of corrosion-promoting agents (mainly chlorides) during conservation interventions.

ACKNOWLEDGMENTS

The authors want to express their sincere gratitude to the people in charge of the excavation sites of Bilbilis, La Cabañeta, Lancia, Contrebia Belaisca and Corduba for their kindness and help in providing us with the necessary archaeological items to carry out this project.

They also want to thank specially Dr. Manuel Martín Bueno for his priceless collaboration.

This work it has been possible thanks to the support of the European Commission, through an INCO-MED contract (No. ICA3-CT-2002-10030)

REFERENCES

Constantinides, I.; Adriaens, A.; Adams, F. "Surface characterization of artificial corrosion layers on copper alloy reference materials", *Applied Surface Science*, (2002); **189**: 90-101.

Favre-Quattropani, L.; Groening, P.; Ramseyer, D., Schlapbach, L., "The protection of metallic archaeological objects using plasma polymer coatings", *Surface and Coatings Technology*, (2000), **125**: 377-382.

Ingo, G. M.; Angelini, E.; De Caro, T.; Bultrini, G.; Mezzi, A., "Combined use of XPS and SEM + EDS for the study of surface microchemical structure of archaeological bronze Roman mirrors", *Surf. Interface Anal.* (2004); **36**: 871–875.

Robbiola, L.; Blengino J. -M.; Fiaud, C., "Morphology and mechanisms of formation of natural patinas on archaeological Cu–Sn alloys", *Corrosion Science*, (1998), **40**: 2083-2111.

EARLY CYCLADIC METALLURGY IN A STTLEMENT CONTEXT: EXAMINATION OF METALLURGICAL REMAINS FROM DASKALEIO-KAVOS, KEROS (CYCLADES, GREECE)

Myrto Georgakopoulou
Institute of Archaeology, University College London

1. INTRODUCTION

Research into Early Bronze Age (EBA: third millennium BC) Cycladic metallurgy has to-date centred on the relatively large slag heaps of the western islands (e.g. Gale *et al*. 1985; Hadjianastasiou 1998; Wagner and Weisgerber 1985), while metallurgical remains found within settlement sites

Figure 1. Map ob the Cyclades showing the location of Daskaleio-Kavos.

have been largely neglected. This study is the first comprehensive analytical examination of such finds from an Early Cycladic settlement: Daskaleio-Kavos on Keros island (see Broodbank 2000a for a recent discussion of the site and a full list of relevant references). The material in this study was recovered during intensive surface survey, which covered part of the site and was carried out within a collaborative fieldwork project organised by the Universities of Ioannina, Athens, and Cambridge, and the Cycladic Ephorate in 1987 (Annual Reports 1986-7 32-4; Whitelaw 2003). The collection includes small numbers of slag, metallurgical ceramics, copper and lead metal fragments, iron mineral samples and a single litharge specimen.

The analyses aimed to clarify the types of metals processed at Daskaleio-Kavos and the nature (i.e. smelting or melting) and process parameters of these activities. The results provide interesting comparative material to the larger metal production sites of the western Cyclades.

A full presentation and discussion of the analytical results is currently under preparation and will be published in the forthcoming volume on the 1987 project on Daskaleio-Kavos (eds. Renfrew *et al*.). This paper presents a brief outline of some of the main results and conclusions.

2. LABORATORY METHODOLOGY

Polished mounted sections were studied using an optical microscope and a scanning electron microscope (SEM-EDS) for phase identification.

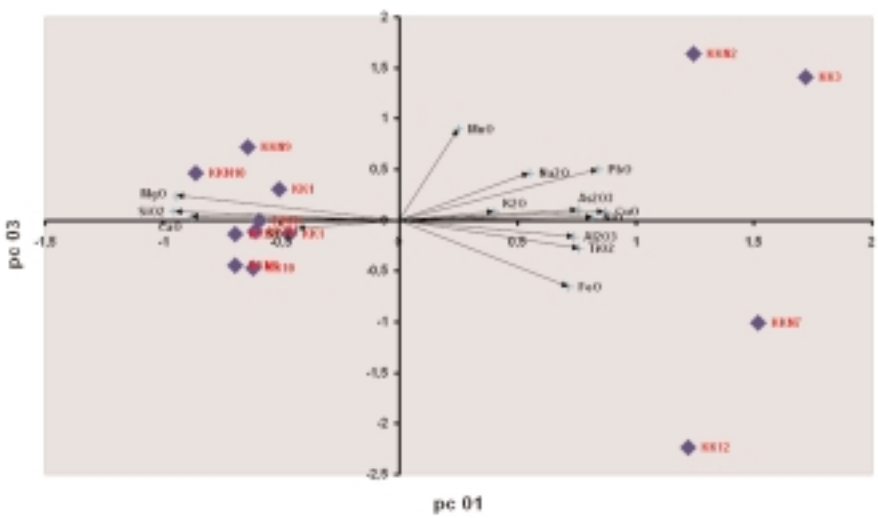

Figure 2. Scattergram of principal components for bulk measurement data (WDA-EPMA) of the slags. The tight group on the left of the y axis is Group 1, while the more dispersed points on the right are the Group 2 samples (larger variation in the bulk compositions of Group 2 samples is largely due to intense heterogeneity in their microstructure).

Metal prills were further analysed on the electron microprobe (EPMA-WDS) searching for S, Cl, Fe, Co, Ni, Cu, Zn, As, Ag, Sn, Sb, Pb, Au, Bi. Bulk analyses presented are averages of 10-15 area measurements (c. 160x120μm each) on the electron microprobe (searching for the oxides of Na, Mg, Al, Si, P, S, K, Ca, Ti, Mn, Fe, Co, Ni, Cu, As, Sn, Sb, Pb, Bi, and Cl).

3. RESULTS: THE SLAGS

A total of fourteen slag samples were examined. The specimens are all very small only a few cm in length. The majority of slags were divided into two distinct groups, which showed differences in their external characteristics, their bulk composition, their microstructure, and the composition of the prills entrapped within them. The main characteristics for each group are summarised in table 1.

	Group 1 (9 samples)	**Group 2 (4 samples)**
External characteristics	-little or no green staining -only slightly magnetic	-intense green and brown-orange staining and external green prills -very magnetic
Bulk composition (Figure 2)	-iron oxide/silica ratio c. 1 -copper oxide content 0.4-0.8% -no other base metals were identified in concentrations above the detection limit of the method used (c. 0.5%)	-iron oxide/silica ratio c. 2 -copper oxide content 2.7-10% -a number of other base metals were identified, the most important being arsenic (As_2O_3: 0.1-7.5%), lead (PbO: 0.8-10%), and nickel (NiO: 0-0.5%)
Microstructure	-mainly fayalite in glass -magnetite in smaller concentrations or absent -remains of partially reacted starting materials are very rare	-mainly magnetite in glass -fayalite present in only two samples -inclusions of unreacted or partially reacted starting materials (quartz and magnetite aggregates)
Composition of entrapped prills	-mainly matte (mixed copper and iron sulphides) free from other base metals	-mainly arsenical copper metal with smaller amounts of iron, nickel, antimony and distinct lead inclusions

Table 1. Summary of the main characteristics of Group 1 and Group 2 slags.

The composition and microstructure of the slags indicates that both groups are the by-products of copper smelting rather than secondary metalworking activities. The two groups appear to correspond to two

Figure 3. Examples of the metallurgical ceramic fragments.

separate processes rather than to consecutive steps of a multistage procedure. It is clear that different types of ore were used in the two cases resulting in the production of unalloyed copper for Group 1 slags and arsenical copper with small quantities of other base metals for Group 2.

4. RESULTS: THE METALLURGICAL CERAMICS

The metallurgical ceramic fragments are very small and shapeless. Fragments of refractory rocks such as schist and quartz are noted in the clay, together with imprints of burnt-out organic materials. A reconstruction of the size and shape of the original vessel cannot be made at this stage. The majority of these samples bear a slag layer in their inner surface.

Bulk analyses on the electron microprobe were carried out separately on the ceramic and slag layers. The two layers show compositional differences, consistent with a smelting origin for these specimens. More specifically, the silica to alumina ratio changes from approximately 3:1 in the ceramic layer to 4:1 in the slag layer, while calcium, iron, copper, and other base metal contents are significantly increased in the slag. The composition of the slag layer shows strong similarities with the Group 2 slags, suggesting a connection between the two types of material and strengthening the proposal that the Group 2 slags are smelting by-products.

5. RESULTS: THE LITHARGE

A single litharge fragment was identified in the collection. Significant quantities of CaO (c. 40%) were detected during preliminary X-ray fluorescence analysis of a mounted section and following examination under the optical microscope it was concluded that the sample actually corresponds to litharge-impregnated hearth lining (i.e. the calcium-rich lining that would have absorbed the forming litharge during cupellation).

This find raises the possibility that lead/ silver metallurgy was also carried out on Kavos. The sample is, however, unique in the collection and given the potential re-uses of litharge, it may be that the specimen was brought to the site for another purpose.

6. CONCLUSIONS

• Analyses of the metallurgical remains from Daskaleio-Kavos have provided strong evidence that copper production was taking place on the site, challenging previous suggestions that metal production was restricted to the western 'metal-rich' islands and only secondary metalworking activities were carried out within settlements (Barber 1987: 112; Broodbank 2000b: 293-7).

Figure 4. Litharge impregnated hearth lining fragment from Daskaleio-Kavos.

• The results showed a surprising variability in the metallurgical activities providing evidence for two copper smelting processes as well as possibly lead/silver metallurgy.

• This study offers a different perspective to the emerging picture of the overall organisation of Early Cycladic metallurgy and highlights the importance of careful individual examination of metallurgical remains from settlement sites, despite their often fragmentary nature and small quantity.

ACKNOWLEDGEMENTS

I thank the directors of the 1987 fieldwork project on Daskaleio-Kavos, Professors C. Doumas, L. Marangou, C. Renfrew, and Ms P. Zapheiropoulou, for permission to study this material. I am indebted to the following people for their valuable contribution to this study: Dr T. Whitelaw, Professor Th. Rehren, Dr C. Broodbank, Dr Y. Bassiakos, Mr K. Reeves, Mr S. Groom, and Mr M. Charlton. This research is funded by the Onassis Foundation, the Arts and Humanities Research Board (AHRB) and the Institute of Archaeometallurgical Studies (IAMS). Expenses for attending the archaeometry symposium were covered by grants from the Institute of Archaeology (UCL) and the Graduate School (UCL).

REFERENCES

Annual Report of the Managing Committee of the British School at Athens, 1986-7.

Barber, R. L. N., 1987. *The Cyclades in the Bronze Age*. London: Duckworth.

Broodbank, C., 2000a. Perspectives on an Early Bronze Age island centre: an analysis of pottery from Daskaleio-Kavos (Keros) in the Cyclades, *Oxford Journal of Archaeology*, **19**, 323-342.

Broodbank, C., 2000b. *An Island Archaeology of the Early Cyclades*. Cambridge: Cambridge University Press.

Gale, N. H., Papastamataki, A., Stos-Gale, Z. A., and Leonis, K., 1985. Copper sources and copper metallurgy in the Aegean Bronze Age, in P. T. Craddock and M. J. Hughes (eds.), *Furnaces and Smelting Technology in Antiquity*, 81-101. London: The British Museum.

Hadjianastasiou, O., 1998. Simeioseis apo tin Kythno, in L. G. Mendoni and A. J. Mazarakis Ainian (eds.), *Kea-Kythnos: History and Archaeology*, 259-273. Athens: Research Centre for Greek and Roman Antiquity.

Wagner, G. A. and Weisgerber, G., 1985. *Silber, Blei und Gold auf Sifnos*, Bochum: Deutsches Bergbau-Museum.

Whitelaw, T., 2003. Investigating site diversity in the Early Bronze Age Aegean, *Archaeology International 2002/2003, Annual Publication of the Institute of Archaeology, University College London*, 29-32.

ARCHEOMETALLURGICAL STUDIES WITH A MOVABLE EDXRF SPECTROMETER ON MESSENIAN GOLD

THE METHODOLOGICAL APPROACH

George STYL KORRES
Department of Archaeology, University of Athens, Greece

Giovanni E. GIGANTE, Stefano RIDOLFI
Department of Physics, University of Rome "La Sapienza", Italy

1. INTRODUCTION

With the permission of the Archaeological society of Athens and on the behalf of the European project XRF-ART, that developed a new x-ray spectrometer system devoted to archaeometric analysis, in the last few years, three Archaeometric campaigns were performed on gold artefacts excavated in the Messenia region.

These archaeometallurgical campaigns are part of a project leaded by G. Styl Korres, in collaboration with a group of the University of Rome "La Sapienza", which aim is to increase the knowledge, as far as archaeometallurgical aspects are concerned, on materials dig-up in the early '50 and '60 from the Messenian area.

These campaigns were mainly dedicated to the gold artefacts present at the museums of Athens (see fig.1), Olimpia, Kalamata, Chora and Pylos. Our main goal was to obtain a statistical significant set of data making a large number of measurement either on the same artefact (when large enough) as on many artefacts as well. More then 400 artefacts were studied.

The analysis were achieved with a non destructive movable system; non destructive means that the artefacts are not damaged at all, and movable means that the analysing instrument was taken to the precious artefacts rather than the opposite. This last characteristic is due to the significant improvement, occurred in the last years, of the scientific instruments involved in such a movable system. In this paper are shown the methodological aspects that are necessary to follow when analysing a big amount

Figure 1. Dagger (8340) from the Archaeological Museum of Athens.

of abject in a short time and especially for the golden objects of the XRF-ART research.

2. MATERIALS AND METHODS

All analysed samples were in the lot of that originally excavated by C.W. Blegen and S. Marinatos in the period 1939-1964. They are mainly tools, jewels, and decorative material. As a special group stands out the collection of gold found in the Peristeria tombs and chronologically dated as of the first Messenian period. The main elements of this treasure are the three gold vases and the big diadem nowadays shown at the museum of Xora. Apart these we can even find decorative forms such as birds, owls, bees and many golden sheets for which we are not able to determine the use. Very important are the finds of the Nestor Palace in Englianos. Among the gold finds the most beautiful is surely the helmet head. From the Archaeological Museum of Athens we would like to remember the daggers finely enriched with gold drawings, stamps and necklaces. From the museum of Kalamatta very important are the stamps.

The large number of samples we needed to analyse to obtain statistically significant results and their historical preciousness lead us to use a non destructive methodology as the EDXRF (Energy Dispersive X Ray Fluorescence).

A typical EDXRF-system is composed of three parts (see fig. 2):
an X-ray tube;
an X-ray detector with electronics;
an acquisition system with a multichannel analyser.

X-ray tube.

A dedicated X-ray tube, of reduced dimensions, easily transportable, air cooled and intrinsically stable has been adopted. It works at high-voltages, up to about 30 kV, and produces X-rays of energy large enough for exciting K-X-rays of elements up to silver. The maximum current is <1 mA. The advantage of using an X-ray tube is the possibility of collimating the beam on

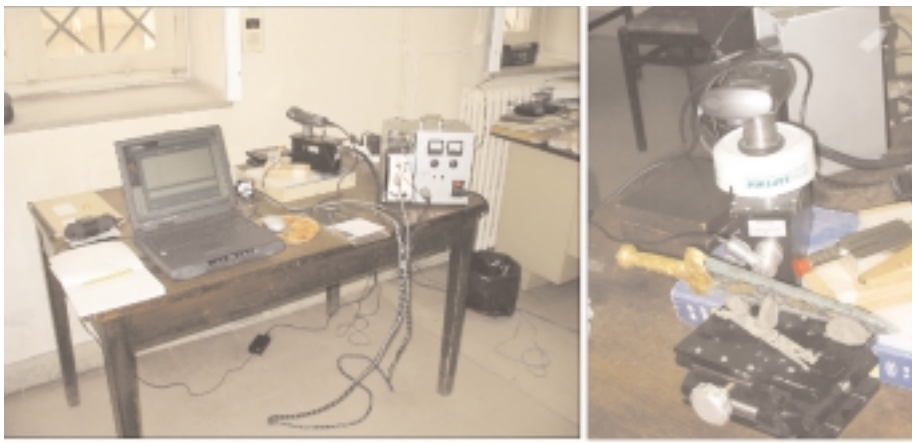

Figure 2. The instrumentation set-up during the measurement of the Dagger 8340.

a small area. In fact, the large amount of photons emitted by the tube allows the selection of a small solid angle of the source maintaining a sufficient number of photons.

X-ray detector.

The typical, high-resolution X-ray detectors were traditionally nitrogen-cooled Si(Li) or HPGe semiconductor detectors, with an energy resolution of about 140-180 eV at 5.9 keV. In the last few years, small-size thermoelectrically cooled detectors have become available, such as HgI2 ,Si-PIN and SDD. These detectors are cooled to about –10°C by means of a Peltier circuit, and they are contained in small size boxes which include a high quality preamplifier and the Peltier circuit.

For the measures here presented, the detector has been a Si-PIN with a thickness of 300 mm, and an energy resolution of 160-200 eV at 5.9 keV.

Acquisition system.

A compact multichannel (Amptek MCA 8000) connected to a portable computer has been adopted. The acquisition procedure is driven by the computer employing a simple user graphical interface that helps either in the choice of acquisition parameters and following in the processing of the spectrum.

The apparatus has been used in situ, placing it on a movable small wheelbarrow or a camera easel, and the analysed point was identified through the red light of a laser pointer indicating the position in which the exciting beam impinge on the golden surface.

With the graphical interface specifically engineered by us it is possible simultaneously to control all the phases of a EDXRF measure, and mostly to control the functionality of the measurement system.

3. SAMPLING AND DOCUMENTATION

A very important aspect of a non destructive analysis on ancient artefacts is the short time interval in which it is possible to analyse them. It comes up the problem to compact as much as possible the analysing time. In other words, we face the problem of taking and storing large amount of data, produced in a short amount of time, and afterwards we face the necessity of organising and presenting this amount of data in such a way that all the available information, this means historical, archaeological, iconographical and analytical, are presented in a suitable way to allow an overall comprehension.

Among all the aspects of data collection the iconographical one is very important. A suitable image of the analysed artefact is needed in order to firmly recognise the artefact in the following and to establish precisely the point in which the measurement was taken. This last point is very important

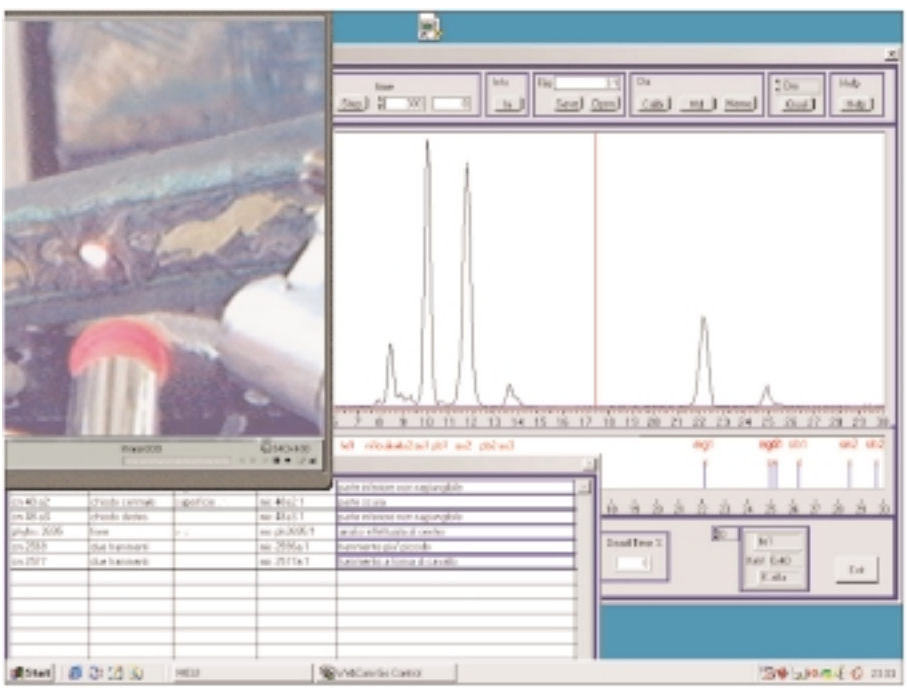

Figure 3. Software interface for the acquisition, at the same time, of the EDXRF spectrum, the spot of analysis and text information of the Dagger 8340.

because in a scientific language, a measure, to be adequate, has to be reproducible, and in an archaeometallurgical language, every point of an artefact can be different from others, e.g. body, soldering etc. and every different point can reveal new information about the artefact.

To speed up the data collection we have developed a graphical interface (see fig. 3) that correlates the result of a measurement (in our case a spectrum) with the image of the analysed spot and an image of the whole analysed artefact, together with the description of the artefact itself (catalogue number, typology etc.)

4. STATISTICAL EVALUATION

The statistical analysis of data started with the calculation of the most common statistical parameters and the use of 2D or 3D representations, with which it is possible to find classifications and grouping of artifacts with similar composition (see fig. 4).

The sampling of the objects plays a very significance role in the statistical analysis. Unfortunately it is practically impossible to find in a single archaeological collection an equal number of pieces for each subgroup. Anyway, the high amount of objects in the collections we analysed helps the sampling procedure with some limits due to the conservation conditions of many artifacts that cannot be recognized with a high degree of certainty (for example the many gold leafs). All of the work of classification is based on the multivariate analysis. Further on it is possible to use chemiometric techniques such as cluster analysis, principal component analysis and factor analysis.

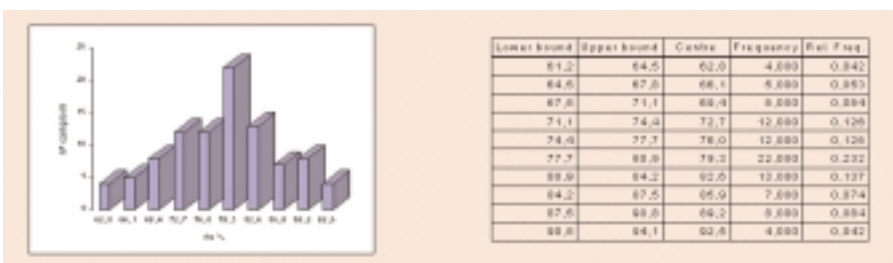

Lower bound	Upper bound	Centre	Frequency	Rel. Freq.
61,2	64,5	62,9	4.000	0,042
64,5	67,8	66,1	5.000	0,053
67,8	71,1	69,4	8.000	0,084
71,1	74,4	72,7	12.000	0,126
74,4	77,7	76,0	12.000	0,126
77,7	81,0	79,3	22.000	0,232
81,0	84,2	82,6	13.000	0,137
84,2	87,5	85,9	7.000	0,074
87,5	90,8	89,2	8.000	0,084
90,8	94,1	92,5	4.000	0,042

Figure 4. Example of a simple statistic descriptive table and graph.

5. CONCLUSIONS

The use of a non destructive technique such as EDXRF combined with the necessity of studying a large amount of ancient artefacts makes the researcher face all a new deal of problems. Very briefly these are: the control

of the instrument, the sampling, the storage of documentation, the statistical approach to the quantitative results. In this paper we have described the methodology we developed during the study of the Messinian collection of golden artefacts excavated by Blegen and Marinatos in Greece. This methodology was developed and improved in the three campaigns in Greece and can obviously be used for any other similar research.

REFERENCES

Gigante G.E., Cesareo R., 1998. "Non destructive analysis of ancient metal alloys by in situ EDXRF transportable equipment" Radiation Physics and Chemistry, 51,4, 689-700.

Gigante G.E., Guida G., Visco G., Ridolfi S.,2003 "Appraisal of the new approach to the archaeometric study of ancient metal artifacts by the use of movable EDXRF equipments", Proceedings of the conference: "Archaeometallurgy in Europe", Milano.

NON-DESTRUCTIVE* Pb ISOTOPE ANALYSIS OF HARAPPAN LEAD ARTIFACTS USING ETHYLENEDIAMINETETRAACETIC ACID AND ICP-MS. (**PRACTICALLY*)

Randall W. Law and James H. Burton
Department of Anthropology, University of Wisconsin-Madison

1. INTRODUCTION-LEAD ARTIFACTS AT HARAPPA

Raw ores, residues, and various other lead artifacts (figure 1) have been recovered during excavations at the Indus Civilization (ca. 2600 to 1700 BC) site of Harappa, located in present-day Pakistan. Determining the geologic sources of these artifacts can provide useful information about the long-distance trade networks that the ancient residents of Harappa were involved in. Lead isotopes (^{208}Pb, ^{207}Pb, ^{206}Pb, ^{204}Pb) are commonly used to determine the geologic provenance of archaeological metals (see Budd et al. 1995 for a discussion) but analysis requires that a small amount of material be removed from the artifact being assayed. For this study, lead was non-destructively extracted from 25 Harappan artifacts (18 galena fragments and 7 finished lead artifacts or residues) using ethylenediaminetetraacetic acid (EDTA) and analyzed by means of inductively coupled plasma mass spectrometry (ICP-MS).

2. EDTA SAMPLING OF LEAD ARTIFACTS AND ANALYSIS USING ICP-MS

EDTA is a hexadentate chelating agent that forms coordinate bonds with metals such as lead. The sampling solution used in this study to extract lead

Figure 1. Lead artifacts from Harappa.

from artifacts consisted of ultra-pure water and 0.05% dissolved EDTA. Lead artifacts that had previously been cleaned in purified water were placed into a disposable plastic sampling tray (figure 2a). Approximately 50 ml of the sampling solution was poured into the tray, immersing the artifact (an inscribed lead bar from Harappa is pictured in figure 2b). A sample was allowed to remain in the solution for two minutes while the tray was lightly agitated at 20 second intervals. This short immersion time in the saturated EDTA solution was sufficient to extract lead concentrations in the range of 100 ppb to as much as 100 ppm – orders of magnitude more than minimally required. The now lead-enriched solution was poured into a sample vial (figure 2c). Artifacts were rinsed in ultra-pure water and dried. While this sampling method is technically destructive (Pb molecules form 1:1 bonds with the EDTA and are removed from a sample), the short immersion time in the sampling solution did not result in any macroscopic alteration of the artifacts whatsoever.

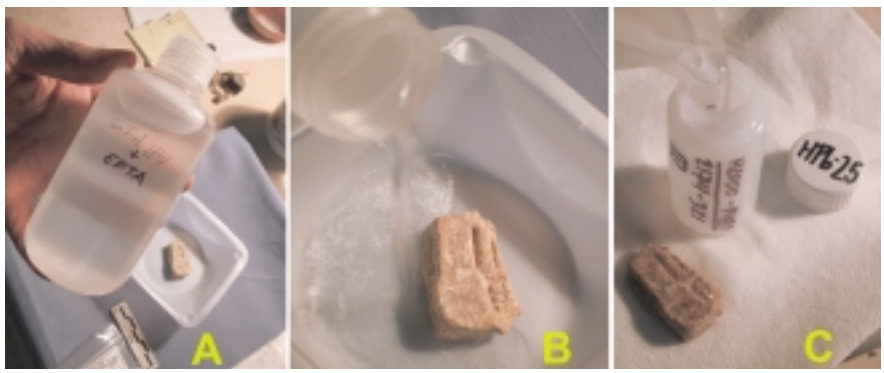

Figure 2. Sampling an inscribed lead bar at Harappa using the EDTA solution.

EDTA sampled solutions were analyzed at the Laboratory for Archaeological Chemistry, University of Wisconsin-Madison on a Finnegan MAT Element I high resolution, magnetic sector ICP-MS. For accurate counting statistics we required 10^7 counts per second (approx. 10 ppb) against a background of approximately 10^4 counts per second. The NIST Common Lead Isotopic Standard (SRM 981) was used to measure precision of this method. For all Pb isotopes except ^{204}Pb the precision was under 0.17% (table 1). In order to gage the accuracy this technique, one galena sample each from the isotopically well-characterized Zawar and Rajpura-Dariba lead deposits of southern Rajasthan was analyzed using our EDTA/ICP-MS method. The data were compared to the published thermal ionization mass spectroscopy (TIMS) derived isotopic values from those ore fields (Deb et al 1989). In both cases (left) the EDTA/ICP-MS derived isotopes values for the geologic test samples closely matched those of the highly accurate TIMS method (figure 3).

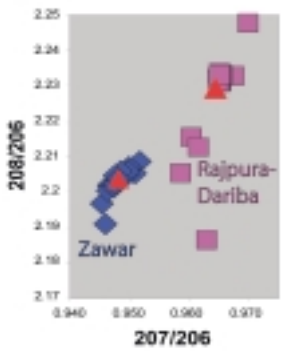

Figure 3. Accuracy.

	206/207	207/208	206/208
NIST Common Lead Isotopic Standard (SRM 981)	0.46122	0.42201	1.0929
Measured (n=5)	0.46088	0.42144	1.0935
+/-	0.00078	0.00052	0.0019

Table 1. Precision.

3. RESULTS

While the number of isotopic assays that have been done for lead deposits in the greater Indus Valley region does not approach the numbers done in other parts of the world (e.g. North America or Europe), there exists today a fair amount of published data regarding the lead isotope characteristics of many of the deposits that would have been directly accessible to Harappans (figure 4). The isotopic data from those deposits and that of the 25 archaeological samples are plotted in figure 5 as ratios of $^{208/206}$Pb to $^{208/207}$Pb. It is evident that lead ores and artifacts found at Harappa were obtained from four different source regions: deposits located in the Jammu and Kashmir region, the Amba Kala area of Himachal Pradesh, the Khara Mawal area of southern Rajasthan, and the Khanrach-Khuzdhar ore fields of southern Baluchistan.

4. CONCLUSIONS

There are many advantages to using a combination of EDTA sampling and ICP-MS for the analysis of lead artifacts. Sampling using this technique is, for all practical purposes, non-destructive. No fragment, no matter how small, need be removed from an artifact for digestion in acid (as with TIMS). While EDTA sampling is 'destructive' in the sense that some Pb ions are physically removed from the surface of the sample, this only takes place at an atomic level. Macroscopic alteration of artifacts is in no way evident. Ease, speed, and cost of sample preparation and analysis are other advantages. Preparing lead samples for TIMS is an extended and laborious process that results in such analyses being quite expensive and time consuming. The EDTA/ICP-MS method is considerably less difficult and comparatively less expensive. No hazardous acids or purification columns need be used. The simple and short sample preparation process and the ease of ICP-MS (as

Figure 4. Indus Civilization cities and lead deposits of northwestern South Asia.

compared to TIMS) help keep the cost of isotopic analysis using this method reasonably low. A final advantage is that artifacts sampled for Pb isotopes in this way need not be removed from location at which they are stored. A small kit containing purified water (for artifact cleaning before and after sampling), the EDTA solution, disposable containers (for artifact immersion in the solution), and vials (for holding the sampled solution) can be taken to a site or museum collection and lead artifacts quickly sampled on site.

The EDTA/ICP-MS method described in this paper allowed 25 lead artifacts from Harappa to be isotopically assayed accurately, non-destructively, and without having to remove them from the facility in Pakistan at which they are stored. We now have evidence that Harappans acquired raw ore from deposits in at least four different regions surrounding the Indus Valley. This knowledge improves our understanding of the extent of Indus Civilization trade networks during the third millennium BC.

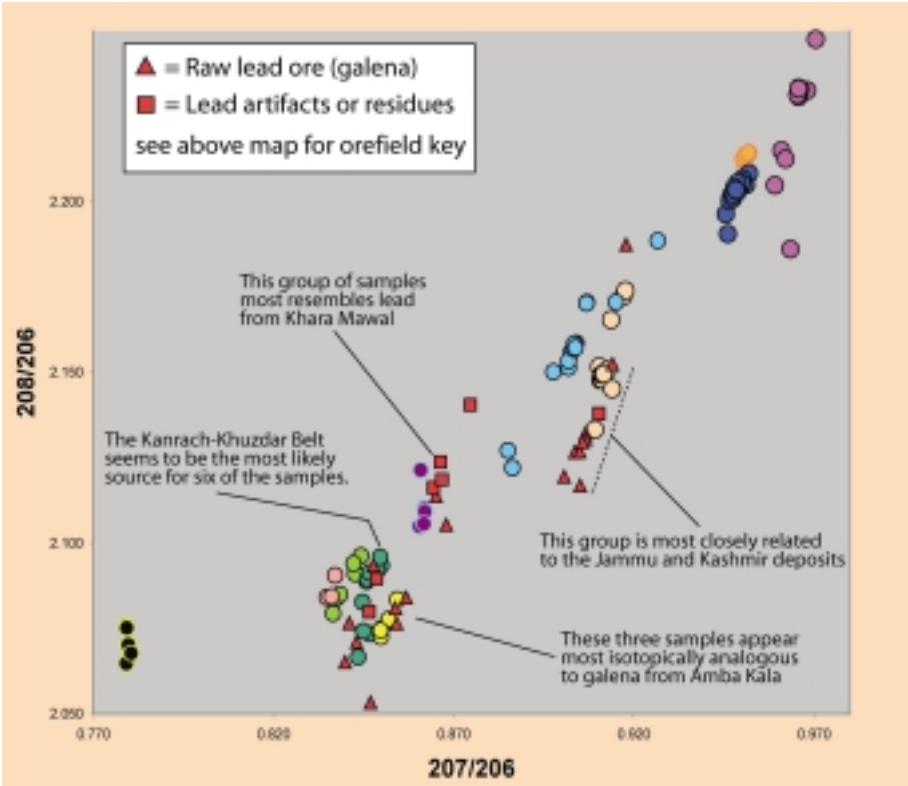

Figure 5. Isotope plot of Indus region lead deposits and lead artifacts from Harappa.

ACKNOWLEDGEMENTS

Thanks to the Mark Kenoyer and Richard Meadow, Directors of the Harappa Archaeological Research Project and to the Director-General, Department of Archaeology and Museums - Government of Pakistan for their support and for providing access to archaeological samples. Special thanks to T. Douglas Price, Director of the Laboratory of Archaeological Chemistry, University of Wisconsin-Madison. Funding for this study was provided by a grant from the National Science Foundation (BCS-0327246).

REFERENCES

Budd, P., R. Haggerty, A. M. Pollard, B. Scaife and R. G. Thomas (1995). New Heavy Isotope Studies in Archaeology. Israel Journal of Chemistry 35:125-130.

Deb, M., R. I. Thorpe, G. L. Cumming and P. A. Wagner (1989). Age, Source and Stratagraphic Implications of Pb Isotope Data for Comfortable, Sediment-hosted, Base Metal Deposits in the Proterozoic Aravalli-Delhi Orogenic Belt, Northwestern India. Precambrian Research 43:1-22.

INVESTIGATION OF A PRE-COLUMBIAN VICUS NOSE FILIGREE

Laura Limata, Aaron Shugar*, Mike Notis
Archaeometallurgy Laboratory, Lehigh University, Bethlehem, PA 18015 USA
*Smithsonian Center for Materials Research and Education, Suitland, MD 20746

Dale Newbury
NIST, Gaithersburg, MD 20899 USA

1. INTRODUCTION & PROCEDURE

The ancient Vicus culture (100 BC to 600 AD) of Pre-Columbian Peru produced some exceptional, technologically advanced, metal objects. The timeline in figure 1 shows the various cultures of the Pre-Columbian period.

The objects produced indicate that they had significant control of: alloy composition, sheet making, granulation, and advanced solder technology. These techniques are all clearly visible in the Vicus nose filigree presented here. Our investigation of this object focused specifically on the granulation technique and the simulated wire braiding methods employed in the construction of the filigree shown in figure 2.

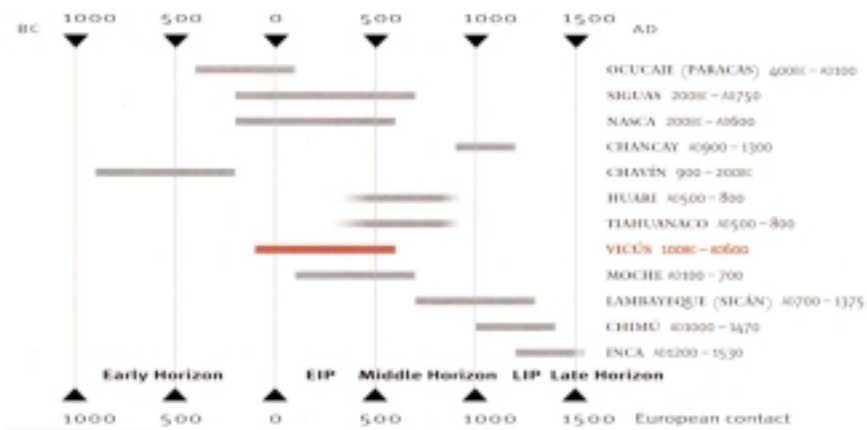

Figure 1. Timeline showing the relationship between the various cultures of Pre-Columbian people.

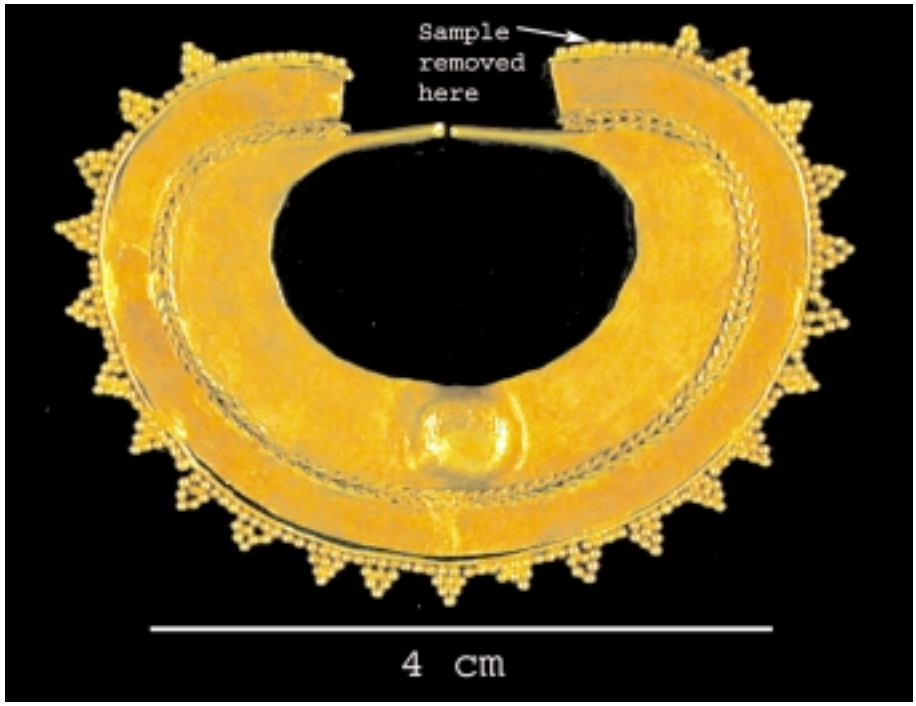

Figure 2. Pre-Columbian Vicus Filigree sampled for study. Sample was taken from upper right where noted.

Advanced light optical microscopy (LOM) with digital image capturing and Scanning Electron Microscopy (SEM) were used to photograph the granulation and wire braiding on the sample. Initial compositional analysis was performed using Energy Dispersion Spectrometry (EDS), followed by advanced quantitative mapping with and Electron Microprobe (EPMA), and advanced LISPIX.

2. OBSERVATIONS & DISCUSSION

Optical microscopy and SEM imaging revealed that the decorative "braiding" is actually two metal strips which have been flattened and twisted in opposite directions. This can be seen in figures 3 and 4. The twisted strips were then soldered to the filigree to simulate braiding, visible in figure 4. This is consistent with the known technology of the region, as there is no evidence that round wire drawn through dies, as is made today, was produced by the Pre-Columbian metal smiths.

Figures 5 and 6 show an example of granulation similar to that at the joint studied here. Figure 7 shows a metallographically prepared cross section of the joint studied.

Figure 3. Photograph, in unpolarized light, of the simulated wire braiding on the filigree. The edges display that this is twisted flat strip.

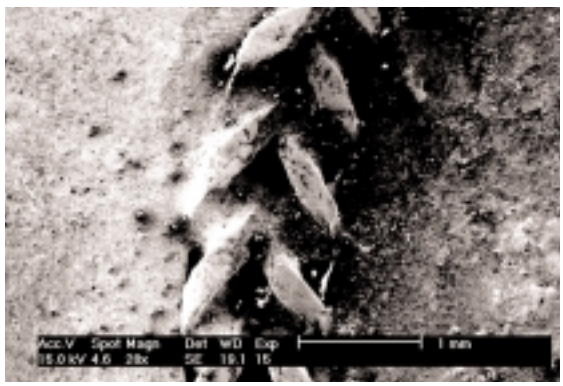

Figure 4. Secondary electron SEM micrograph of the twisted strip making the soldered joint visible on the sides of the sample. It is clear that the braiding is formed from a flat strip.

There were three granulation techniques believed to be used by the Vicus culture: solder, copper salts, and unaided fusion (McEwan, 2000: 229). EDS provided an initial observation that the composition of the joints was slightly copper rich, suggesting that it was likely that copper salts were used. LISPIX compositional maps indicated higher concentrations of copper at the joint, confirming the initial EDS spectra (Bright, 1987: 51-87). The results shown here in figures 8 and 9 indicate that the granulation on the filigree

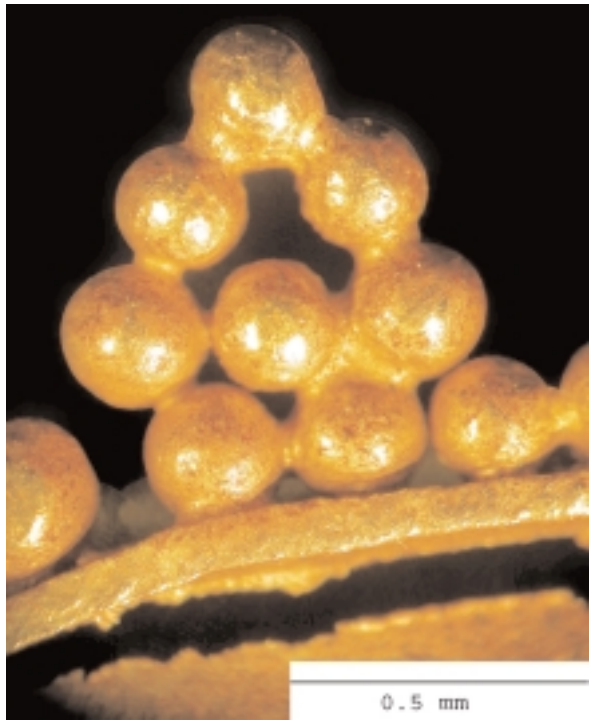

Figure 5. Photograph, in unpolarized light, displaying granulation similar to the samples studied but still attached to the filigree.

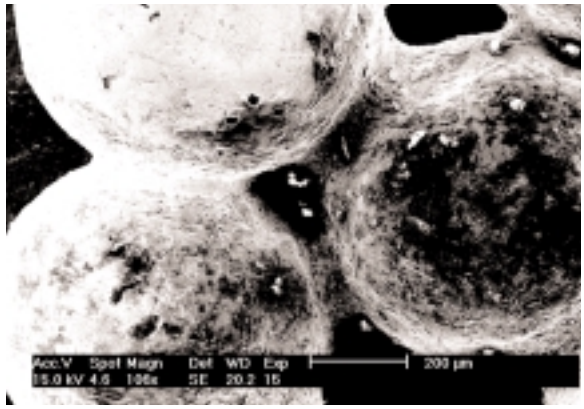

Figure 6. Secondary electron SEM micrograph of a granulatio joint similar to the one studied.

Figure 7. LOM micrograph showing the joint analyzed with LISPIX. Etched with Aqua Regia, unpolarized light.

was produced with copper salts. LISPIX revealed almost 10% copper at the joint, which corresponds to a low point in the melting temperature of copper-gold alloys.

In this technique, copper salts were mixed with an organic glue. This glue was then used to bind the spheres together before melting them together. The presence of the copper salts allowed for a lower melting temperature isolated at the joint. The phase diagram for the copper gold system predicts this drop in melting temperature and can be seen in figure 10. The depressed melting temperature due to localized composition difference, would have allowed for enough local melting for fusion and soldering, without liquefying the entire piece.

3. CONCLUSIONS

Vicus metal smiths had enough skill to be able to produce the ornate detailing on this piece. The meticulously hammered strips used for the braiding require large amounts of time and effort, and well simulate conventional drawn and braided wire. In addition, they were able to produce fine scale granulation by fusing the spheres together without melting the whole piece. Mineral salts allowed for the local depression

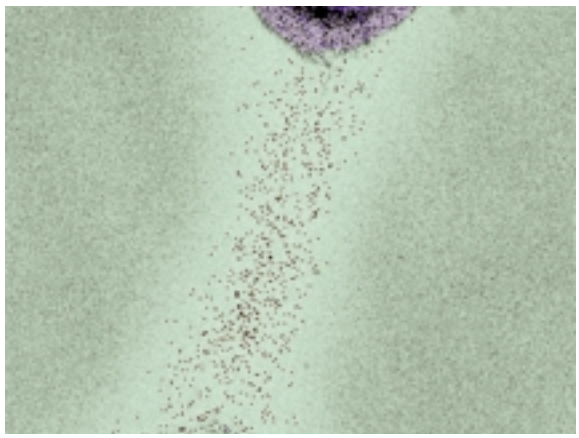

Figure 8. LISPIX compositional map showing almost 10% Cu at the granulation joint.

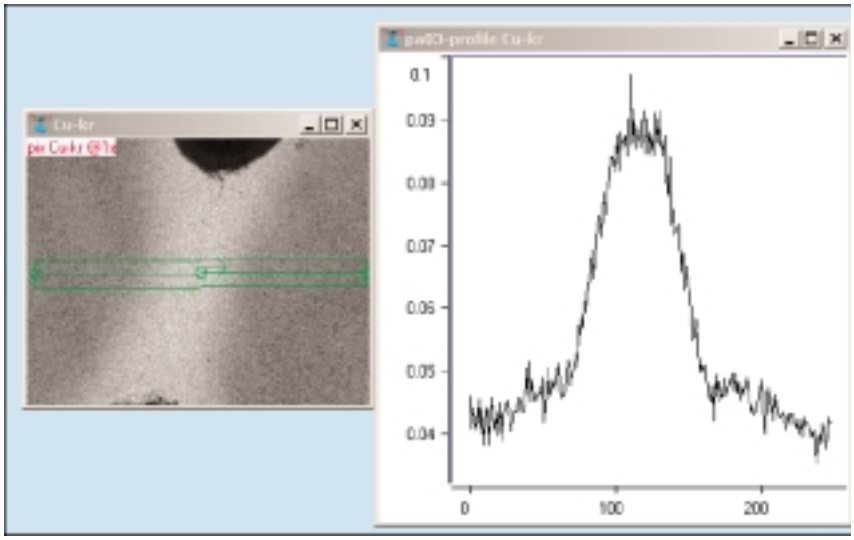

Figure 9. EDS line scan across the joint showing an increase to 10 % Cu in the vicinity of the joint, values ona log scale. SEM photo taken with LISPIX.

of the melting temperature. LISPIX compositional mapping allows scientists to clearly map, small localized concentration differences such as the one here, proving its strength as an analytical tool. The detailed investigation and analysis of this spectacular artifact exemplifies the technological skill and knowledge employed by these ancient metal smiths.

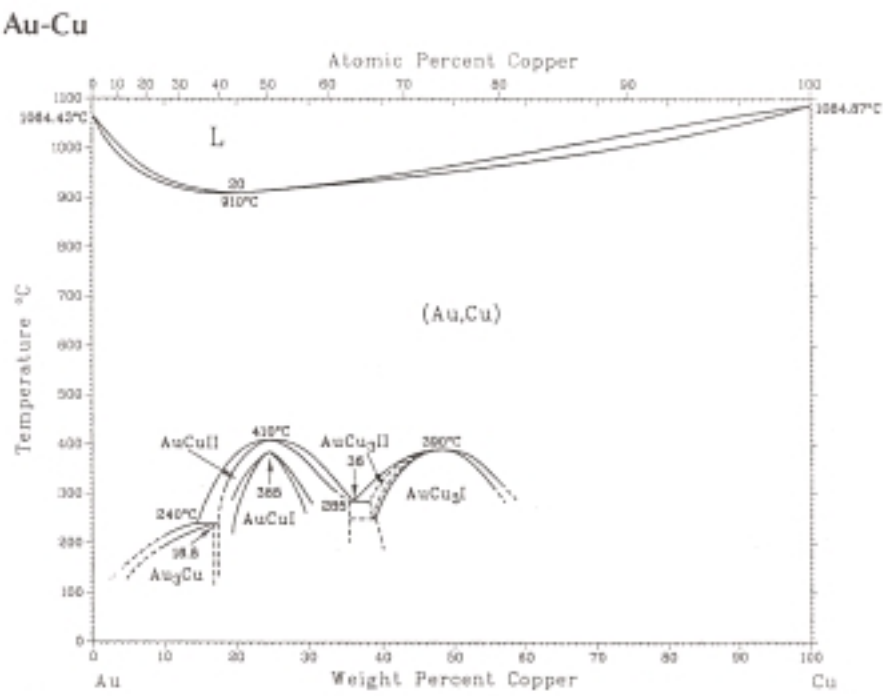

Figure 10. Au-Cu binary phase diagram showing a depressed melting point at around 10% Cu.

REFERENCES

Bright, D.S. "A LISP-based image analysis system with applications to microscopy." Journal of Microscopy. Vol. 148, (Oct. 1987) pg.51-87.

McEwan, Colin. ed. Pre-Columbian Gold: Technology, Style and Iconography. Fitzroy Dearborn Publishers: Chicago, (2000) pg. 229.

ARCHAEOMETRY AND THE INTERNATIONAL EVOLUTION OF STUDIES ON METALLURGY: A BIBLIOMETRICAL PERSPECTIVE

Elías López-Romero González de la Aleja and **Ignacio Montero-Ruiz**
Dpto de Prehistoria, IH, CSIC
C/Serrano 13, 28001-Madrid (SPAIN)
elopez@ih.csic.es imontero@ih.csic.es

1. INTRODUCTION

Analytical studies on prehistoric metals have their origins in the 19th century. Pernicka (1998) divided the history of archeometallurgy in three periods that we can labelled as: - formative (XIX century -1930), development (1930-1970) and expansion (1970-). The first one used wet chemistry, being the introduction of Optical emission spectroscopy (OES) in the 30ths the point of breaking-off. In this period the archaeometallurgical research mainly used OES developing projects of analytical corpuses aiming at solving questions of provenance and distribution networks of metals (Otto and Witter, 1952; Pittioni, 1959; Chernij, 1966; Junghans *et a*l., 1960, 1968). At the same time, studies on the History of Technology were being developed, using complementary techniques such as metallography or hardness test. In the 50ths and 60ths new analytical techniques were available, for example Alan Walsh develops atomic absorption spectroscopy in 1955 or Harry Bowman and colleagues publish in 1966 first energy-dispersive X-ray fluorescence (EDXRF) results (Ryon, 2001: 366), although some time passed until their general archaeological application. From the 70´s onwards a high diversity of multielemental techniques were in use and instrumentation improvements added to the introduction of digital control and standardisation of the computer platforms, software, portable equipments etc (Jenkins, 1999), let the archaeometallurgy research explore all capabilities looking for more sensitive and precise results.

We will focus on the third period, trying to define the kind of materials analysed (metals, alloys and production residues), the analytical techniques and their evolution as well as the chronological distribution of those materials, by the study of scientific periodicals and publications from 1975 to 2000.

2. SAMPLING

The database created for the global project of bibliometrical analyses consists on 1440 records; 245 of them refer to studies on metals and are the basis for the present paper.

Articles have been classified following a seven-type structure according to their main general purpose: 1)"analysis of archaeological materials", 2)"dating", 3)"analysis of soils & geology", 4)"statistics & computing", 5)"descriptive and general review papers", 6)"genetics", and 7)"other". Only types 1, 4 and 5 are represented in the current case of study.

Three have been the sources for our database collection: the journals *Archaeometry* (Oxford University) and *Revue d'Archéométrie* (CNRS), and the International Congresses on Archaeometry series, held every two years at different locations. Regarding to the latter, it must be said that they are unevenly published and they are not always easy to find; the first of those publications included in our database is the 16th International Congress on Archaeometry, held at Edinburgh in 1976, while the latest is the 30th Congress held at Urbana (Illinois) in 1996. However, only selected papers of all those presented were finally published in some Proceedings. Previous conferences remain unpublished or have not been available, but their absence in the current analysis is by no means essential for our basic aim was to show and identify the main trends in archaeometrical studies in the last 25 years; having this in mind, we considered setting the upper chronological limit in 2000.

As a general reference for the evolution of studies on metallurgy, we have also decided to analyse those papers presented to the 31st (Hungary) and 32nd (Mexico) ICA, though only abstracts of the sessions on metals have been available.

3. GENERAL TRENDS

Through the analysis of the previous data we can define some general trends and perspectives of research on metallurgy.

First of all, it comes out that the instrumental development of techniques is quickly applied to Archaeometallurgy, improving the capability and quality of analytical activities. Added to these improvements, a clear effort is being done to reduce the size of the analytical equipment, developing portable machines.

Several techniques are being complementarily applied for studying the archaeological material; we have documented up to six different physical and/or chemical techniques in the same paper. This is also a tendency in progress, and the multi-technique research will be probably increased in future in order to evaluate the accuracy of different techniques and to fulfil the definition of the metal objects and by-products.

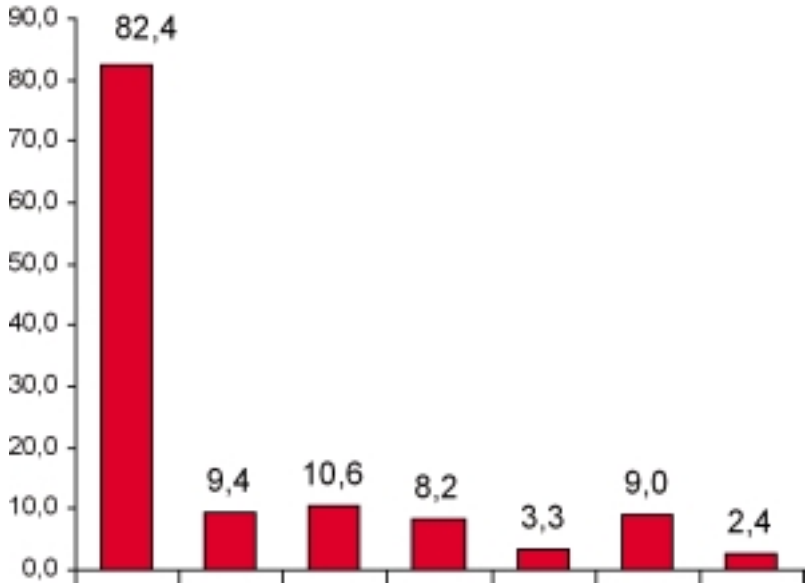

Figure 1. Type of analytical research.

In which respects to the techniques themselves (fig. 1), it is worth noting the prevalence of Elemental Analyses (82,4 % of papers include this type of data) as well as the increment -in the 90`s - of Lead Isotopes due to the creation and availability of new laboratories, linked to the interest in research on provenance analysis on metals.

Dealing with elemental analyses techniques (fig. 2) SEM was the most used (25,9 % of all registered techniques). It is from the second half of the 80`s when this dominance is apparent in concordance with the improvement of the equipments and its versatility for the interest of research. The chronological evolution of this and other main techniques can be seen in fig. 3, with the progressive decrease of NAA (including its instrumental implementation: INAA) in archaeometallurgy as another relevant trend, something that is not to apply to the general archaeometric research.

Papers dealing with the study of coins have shown the specificity of this field in the general context of Archaeometallurgy; techniques such as Proton Activation Analysis are almost exclusively used in the analysis of coins. Coins are, generally speaking, subject of less aggressive analyses; use of SEM has been nearly avoided until recent times. The historical, chronological and self-economical relevance of this kind of archaeological remain can be in the origins of such a behaviour.

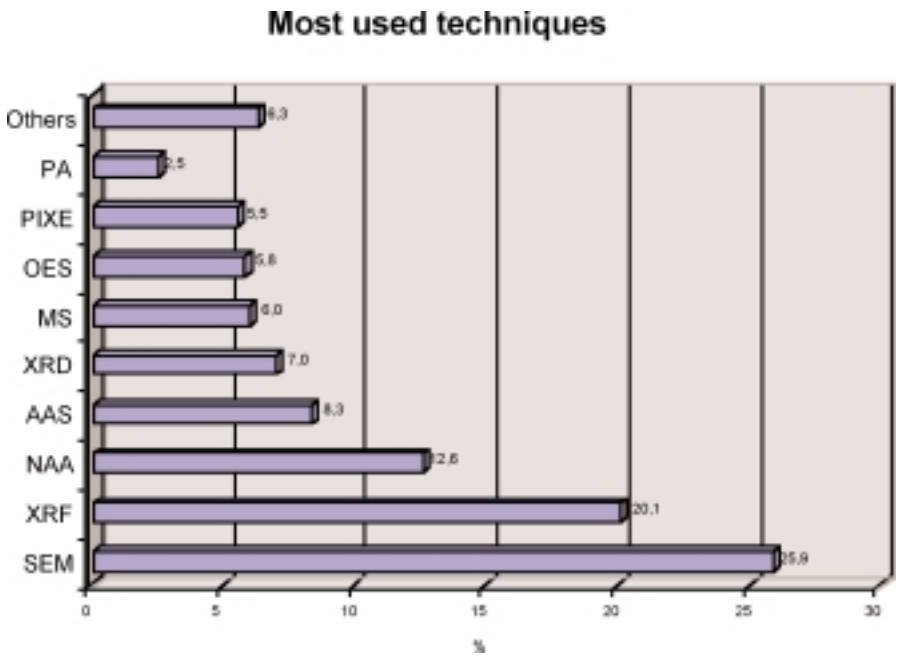

Figure 2. Elemental Analysis Techniques (percentages are based on the total number of techniques documented, not on the number of papers).

Among the different types of metals (fig. 4), copper-based items are studied in near the half of the papers, while surprisingly iron is one of the least commonly studied; though the situation is once more changing in the last years, as we can note from the original program of the 34th Conference itself. We could define some reasons why this has been the dominating trend in the last 25 years,

There is a difficulty in the chemical characterisation of iron and its by-products

Iron gets easily corroded, and the state of preservation of iron-made objects is not always appropriate for undertaking analytical procedures

Third, but not least, iron-made objects refer most often to day-by-day activities (nails, etc.) and used to be at the eyes of researchers less attractive.

Finally, we can highlight the increasing concern on experimentation and study of ores, slags and smelting debris as reflection of the interest in the knowledge of production technology as a whole.

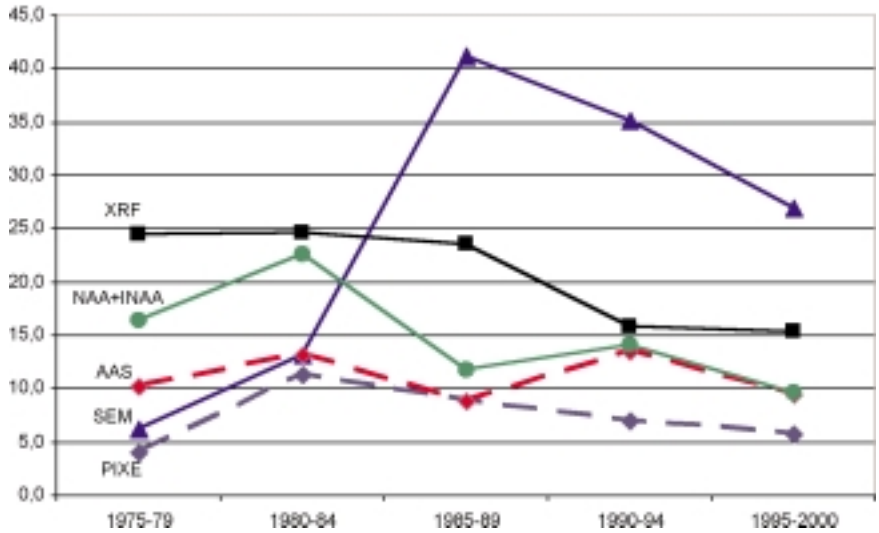

Figure 3. Chronological evolution of most used analytical techniques.

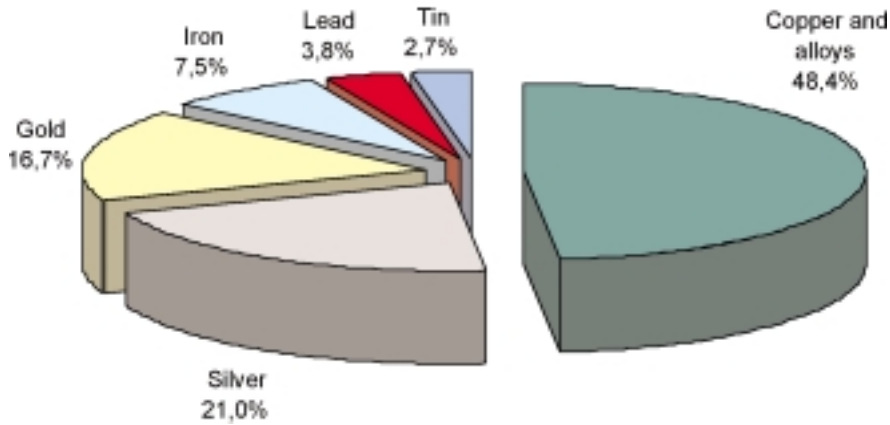

Figure 4. Percentage of metals studied in the papers sampled.

ACKNOWLEDGEMENTS

We are grateful to Duncan Hook (British Museum) for facilitating access to the research library of the British Museum; thanks are also due to the University of Reading and University of Oxford libraries (UK) and to

Catherine Le Gall of the Centre de Documentation - UMR6566 of the CNRS (Rennes, France). S. Rovira (MAN, Madrid) helped us with his comments on analyses and techniques and with his continuous support.

REFERENCES

Chernij, E. 1966: Istorija *drevnejsej metallurgii Vostocnoj Evropy*. Moskau: Akad. Nauk SSSR.

Jenkings, R. 1999: *X-Ray Fluorescence Spectrometry*. Chemical Analysis: A Series of Monographs on Analytical Chemistry and Its Applications 152. New York, Wiley-Interscience.

Junghans, S., Sangmeister, E. & Schröder, M. 1960: *Metalla-nalysen Kuperzeitlicher und frühbonze-zeitlicher Bodenfun-de aus Europe*. S.A.M., I.

Junghans, S., Sangmeister, E. & Schröder, M. 1968: *Kupfer u. Bronze in der frühen Metallzeit Europas. Katalog der Analysen 985-10040*. S.A.M. 2. Berlín.

Junghans, S., Sangmeister, E. & Schröder, M. 1974: *Kupfer u. Bronze in der frühen Metallzeit Europas. Katalog der Analysen Nr.10041-22000*. Berlín.

López-Romero, E. & Montero, I. (2003): "Arqueometría: tendencias y cambios en la investigación internacional (1975-2000)", *Libro de resúmenes de Actas del V Congreso Ibérico de Arqueometría*, Puerto de Santa María (Cádiz), 30 de septiembre a 3 de octubre de 2003, pp. 173-174.

Otto, H. & Witter, W. 1952: *Handbuch der ältesten vorgeschichtlichen metallurgie in mittleeuropa*. Barth Verlag. Leipzig.

Pernicka, E. 1998: "Whiter metal analysis in Archaeology". In C. Mordant, M. Pernot & V. Rychner (eds.): *L´atelier du bronzier en Europe*. Vol. I: Les Analyses de composition du metal : leur apport à l´arcéologie de l´Âge du Bronze. Paris. Comité des travaux historiques et scientifiques: 259-267.

Pittioni, 1959: "Zweck und ziel spektralanalytischer untersuchungen für die uegeschichte des kupferbergwesens". *Archaeologia Austriaca*, 26: 67-95.

Ryon, R.W. 2001: "The transistor and energy-dispersive x-ray spectrometry: roots and milestones in x-ray analysis". *X-ray spectrometry*, 30: 361-372.

LABORATORY INVESTIGATION OF INLAYS AND SURFACE TREATMENTS FOR THE DECORATION OF COPPER-BASE ALLOY OBJECTS FROM THE IMPERIAL ROMAN PERIOD

François Mathis*, **Dominique Robcis**, **Thierry Borel**, **Marc Aucouturier**
Centre de Recherche et de Restauration des Musées de France, (CNRS UMR 171), Paris, France
*Commissariat à l'Energie Atomique, SRMP, Saclay, France

Sophie Descamps
Conservateur en Chef, AGER, Musée du Louvre, Paris, France

1. INTRODUCTION

Metal polychromy has been widely used for the decoration of metallic artworks from the far antiquity. In the Hellenistic and Roman periods, the famous Corinthian bronzes (*Corinthium aes*) are a typical example of the skill of metallurgical craftsmen working in their aim to obtain coloured surfaces on copper-based alloys [Craddock 1993].

The present paper summarises a full characterisation study of three metallic objects from the Imperial Roman period kept in the Department of Greek, Etruscan and Roman Antiquities of the Louvre Museum: an inkpot, a strigil, and a bistoury handle. This investigation is aimed to a re-evaluation of the techniques of metal polychromy at the Imperial Roman period, as a part of a general study concerning the identification and understanding of the technical history of artificial surface treatments (patination) and inlaying on copper-base archaeological pieces of art.

The objects and their inlays and surface treatments have been studied by optical microscopy, X-ray radiography, elemental analysis by ICP-AES (Inductively Coupled Plasma Atomic Emission Spectroscopy) and PIXE (Particle Induced X-ray Emission), X-ray diffraction, RBS (Rutherford Backscattering Spectrometry), micro-Raman spectroscopy. All the results are discussed with reference to the scarce existing texts which describe the techniques of metal colour modifying in the antique Roma.

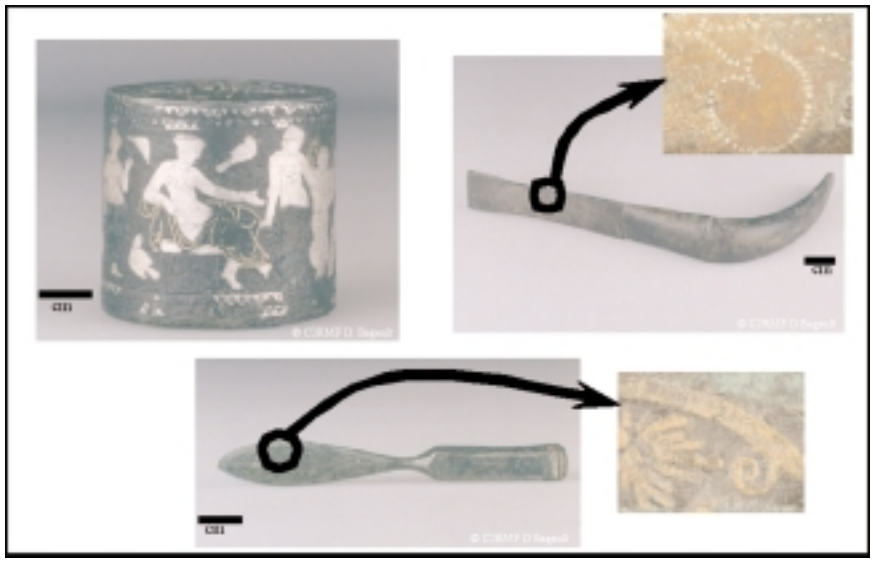

Figure 1. Objects from the Department of Greek, Roman and Etruscan Antiquities, Louvre Museum (1st – 2nd century AD). © C2RMF, D. Bagault.

2. THE OBJECTS

The three Roman Empire objects (fig. 1) are all dated from the Ist or IInd century AD:

— An inkpot (inv. Bj 1950), inlaid with various metals on a corroded background;

— A bistoury handle (inv. Br 2516), decorated with black and red inlays on a corroded background;

— A strigil (inv. Br 1582), decorated on a corroded background.

The inkpot is known since 1876 without any precise date and context of discovery; it was acquired by the Louvre museum in 1883 [Héron de Villefosse 1878]. The scene represents the goddess Venus with her entourage: Psyche, Adonis, a servant and several Eros. This kind of inkpot, functional and precious, decorated with figures, is very rare; apart from this one, only three complete are known: one in the museum of Alger (found in a tomb at Lambèse) and two in the British Museum; some inkpot covers are also known such as those from Mainz, Cologne or Volubilis.

The origin of the bistoury handle is uncertain. The iron blade has disappeared.

The strigil was found in the necropolis of Sicca Veneria, nowadays Le Kef in Tunisia, and given to the Louvre museum in 1895 [Denis 1894]. Part of the

handle decoration is punctured: on one side, the figure of a wrestler running to the right, on the other side, stalk and ivy leaves. These designs appear in-between chessboard-like patterns.

All artefacts show metallic inlays and/or patinated regions: the inkpot and bistoury handle are inlaid with black inlays (Venus and Adonis himations on the inkpot, the symmetrical decoration on the bistoury handle); the strigil exhibits regions (fig. 1) with a different colour and surface state than the neighbouring areas.

3. INSTRUMENTATION

After optical microscope observation, X-ray radiographs were done (100 kV, 4 mA, Pb screen); to obtain a lisible radiograph of the inkpot body, a special procedure had to be developed to avoid superposition [Borel 2004]. Bulk metal analysis of each object was performed on metal chips obtained by micro drilling with a 1mm drill; the sorted metallic chips are digested in acid to be analysed by ICP-AES [Bourgarit 2003].

The surface analyses had to be entirely non-destructive. Ion beam analyses were performed by using the external beam of the particle accelerator AGLAE, a 4 MV tandem accelerator delivering a proton or alpha particle beam of high energy, extracted to free atmosphere through a 100 nm thick Si_3N_4 window [Dran 2000]. The analysed spot is of 50 mm diameter. X-ray emission under 3 MeV protons or 6 MeV alpha particles allows PIXE quantitative analysis [Dran 2000]. Backscattered particles under 3 MeV protons or 3 or 6 MeV $^4He^{++}$ particles are used for RBS analysis, which allows in-depth profiling of the elemental concentrations over a few µm [Ioannidou 2000]. The RBS spectra are interpreted thanks to the SIMNRA code [Mayer 1997-98].

The surface crystalline compounds were identified by diffraction in an X-ray diffractometer equipped with a Co Kα tube (40 kV, 40 mA) and focusing mirrors.

The surface compounds were investigated by micro-Raman spectrometry (Jobin-Yvon Infinity equipped with CCD detector, notch filters and a

Figure 2. X-ray radiographs of the inkpot. Left: top; right: unrolled body
© C2RMF, T. Borel.

horizontal issue); the incident beam is a (Nd:Yag) laser (532 nm, 12 to 5 μW); spatial resolution is down to 2 mm.

4. RESULTS AND DISCUSSION

4.1. Radiography of the inkpot

The inkpot X-ray radiographs (fig. 2) reveal its fabrication by casting in three parts: the body, the top and the bottom, soldered afterwards. They evidence the sophisticated inlaying work. On the top, holes are managed to receive the butt hinge and the closing pin of the small cover presently missing.

4.2. Bulk metal analyses (table 1)

The inkpot body and the strigil are yellow brasses, whereas the inkpot top is a leaded bronze (red), and the bistoury handle is a quaternary alloy (reddish bronze colour).

Objects	Cu	Sn	Zn	Pb
Inkpot body	86	-	14	-
Inkpot top	69	6	-	25
Strigil	81	-	19	-
Bistoury handle	87	4	6	3

Table 1. Composition (wt % by ICP-AES) of the bulk metals.

4.3. Metallic inlays of the inkpot

The metallic uncorroded inlays are in gold or silver. The analyses (table 2) show that 2 different golds and 4 different silvers have been used. The reason of such diversity is partly based on mechanic constraints; but, as evidenced by the use of two different silvers for the friezes, these differences are an indication that the body and the top might have been elaborated independently. The radiographs and a peer examination of the objects showed furthermore that corroded inlays, not visible at the first sight, are present on several locations: the servant and Psyche himations, two boxes (one in the hand of Adonis, one behind the same figure), and butterfly wing figures attached to Adonis and Psyche figures. These corroded inlays show to be in pure copper (red original colour).

	Cu	Ag	Au	Pb
Venus himation gold inlay	0.40	0.12	98.61	-
Top gold inlay	0.21	1.87	95.35	-
Venus silver body	0.60	98.85	0.10	0.22
Servant silver body	0.56	98.87	0.09	0.23
Body silver frieze	4.72	93.57	0.91	0.56
Top silver frieze	3.14	95.44	0.60	0.67
Pelta-shaped base foot (silver)	2.53	95.60	0.75	0.86
Corroded inlays	> 99	-	-	< 1

Table 2. Analyses (wt % by PIXE, 6 MeV α particles) of the inkpot metallic inlays.

4.4. Patinated inlays of the inkpot

The Venus and Adonis himations are of black colour, as well as the wings of the Eros figures (fig. 3). The PIXE analysis shows that these inlays are made of a Cu-Ag-Au-As alloy (about 4 wt % Ag, 1 wt % Au, 4 wt % As, 1 wt % Pb), which could be considered to belong to the category of the "Corinthian bronze" (*Corinthium Aes*) described in the work of P. Craddock and A. Giumlia-Mair [Craddock 1993]. It is the result of the chemical attack of copper base alloys containing small amounts of gold and silver. This technique may be compared to the Japanese technique of *Shakudo* [Murakami 1993].

Figure 3. Black patinated inlays of the inkpot.

X-ray diffraction, micro-Raman spectroscopy and RBS profiling under 3 MeV protons and 6 MeV alpha particles proved that the patina is indeed cuprite Cu_2O enriched with gold and silver, as usually observed for this type

of patina. It is however much thicker (more than 20 μm) than the *Shakudo* patina [Murakami 1993].

4.5. Bistoury handle inlays

Different from the bulk metal alloy (reported in table 1), the inlay alloy (fig. 1) is low alloyed copper containing (in wt %) about 0.4 % Sn, 0.3 % Pb, 0.5 % As, 0.5 % Fe and 0.3 % Ag. X-ray diffraction, PIXE analysis and RBS profiling show that the black patina is cuprite enriched with silver.

One cannot qualify these inlays as being *Corinthium aes*, because they do not contain any gold addition. This is the first observation, to our knowledge, of black patina containing silver and no gold.

4.6. The strigil patination

The strigil handle exhibits intentional red-orange coloration (inside the ivy leaves, inside the wrestler body, on the strikes of the chessboard decoration at both ends of the handle). The patina layer is constituted of cuprite and is 4.5 μm thick. It is obviously another recipe, not reported yet in the literature. This peculiar surface treatment will be discussed in a forthcoming publication [Mathis 2004].

5. CONCLUSION

These objects are new examples of the desire of roman artisans to create metallic polychrome objects as is shown in the reconstitution of the inkpot, proposed in figure 4.

The study has confirmed the roman use of "black bronze" in the pursuit of polychromy, and brought the proof of the existence of several recipes for patination: at least two kinds of alloys have been patinated in black, one containing no gold; in that case, what is the mechanism of coloration of the cuprite?

On the strigil, an artificial red patina, of red-orange colour, also made on a base of cuprite, has been discovered. It has not been reported yet in the literature.

ACKNOWLEDGMENTS

David Bourgarit and Benoît Mille for micro-sampling and ICP-AES, Joseph Salomon for IBA, Dominique Bagault for photography, Catherine Bastien for the reconstitution.

Figure 4. Modern reconstitution of the inkpot colours based on analytical results
© Louvre, AGER, Catherine Bastien.

REFERENCES

Borel T., to be published.

Bougarit D., Mille B., "The elemental analysis of ancient copper-based artefacts by ICP-AES: an optimised methodology reveals some secrets of the Vix crater", *Meas. Sci. and Technol.*, **14** (2003), 1538-1555.

Craddok P., Giumla-Mair A., "*Hsmn-Km*, Corinthian bronze, *Shakudo*: black-patinated bronze in the ancient world", in: *Metal plating and patination*, ed. La Niece S., Craddok P., Butterworth, London (1993), pp. 101-127.

Denis Ch., "Fouilles d'une nécropole romaine au Kef (Tunisie)", *Bulletin archéologique du Comité des travaux historiques et scientifiques*, 1894, p. 376.

Dran J-C., Calligaro T., Salomon J., "Particle-induced X-ray emission", in: *Modern Analytical Methods in Art and Archaeology*, ed. Ciliberto E., Spoto G., John Wiley, Chichester (2000), p. 135.

A. Héron de Villefosse, "La pyxis de Vaison", *Gazette archéologique*, IV, 1878, p. 110-117, pl. 19.

Ioannidou E., Bourgarit D., Calligaro T., Dran J-C., Dubus M., Salomon J., Walter P., "RBS and NRA with external beams for archaeometric applications", *Nuclear Intruments and Methods in Physics Research B*, **161-163** (2000), 730-736.

Mathis F., Descamps S., Robcis D., Aucouturier M., "An original surface treatment of copper alloy in ancient Roman Empire: chemical patination on a Roman strigil", *18th Internat. Conf. on Surface Modification Technologies (SMT 18)*, Dijon, France, November 2004, to be published.

Mayer M., SIMNRA © Max-Planck-Institut für Metallphysik, www.rzg.mpg.de/~mam/, (1997-1998).

Murakami R., "Japanese traditional alloys", in: *Metal plating and patination*, ed. La Niece S., Craddok P., Butterworth, London (1993), pp. 85-94.

Willer F., "Fragen sur intentionellen Schwarzpatina an den Madhiabronzen", Exhibition Catalogue *Das Wrack, der antike Schiffsfund von Mahdia, Bonn 1994*, Rheinland-Verlag Gmbh, Köln.

THE QUESTION OF EARLY COPPER PRODUCTION AT ALMIZARAQUE, SE SPAIN

Roland Mueller, Thilo Rehren
Institute of Archaeology, London

Salvador Rovira Llorens
Museo Arqueológico Nacional, Madrid

1. ARCHAEOLOGICAL SETTING AND AIMS OF RESEARCH

The Chalcolithic settlement *Almizaraque* lies in the estuary of the *Rio de Almanzora* (Almería, Spain), about three kilometres from the Mediterranean. Discovered by Luis Siret at the beginning of the 20th century, Almizaraque still today bears the controversy of being one of the few completely excavated sites, but also one of the most disputed ones; interpretations range from understanding the settlement as a central place to a minor village (Delibes et al. 1996). Next to geological and archaeobotanical data, especially the comparatively numerous remnants of copper metallurgy have been the focal point in this scientific controversy, centring on the key questions: 1. What metallurgical processes were undertaken at Chalcolithic Almizaraque? 2. Was copper metallurgy a central, decisively society shaping technology? and 3. Can one speak of craft specialisation, or even a settlement specialised in copper production? In this paper we focus on the first question and more precisely on: 1. Do the crucible fragments, slags and copper prill samples of Almizaraque represent smelting or melting operations? and 2. Were the ores found at the site part of the same metallurgical processes? There is a desideratum of expanding previous investigations on these questions – which range from the first considerations of crucibles as copper melting and copper smelting devices by L. Siret to the scientific arguments on early copper metallurgy developed by the *Proyecto de Arqueometallurgia* in the 1980s and 90s – by more detailed chemical and mineralogical analyses of archaeometallurgical finds (Siret 1948; Delibes et al. 1996 and references there).

2. ANALYTICAL METHODS AND FRAMEWORK

We had access to 27 samples, i.e. crucible fragments, slags, ores and prills, originating from different occupation layers of Chalcolithic

Almizaraque. Working with such a sample assumes that there is no significant temporal development in copper technology at Almizaraque (Müller et al. 2004 and references there). The artefacts derived from the excavations in the early 1980s and were provided by Salvador Rovira. For chemical analysis we used a combination of scanning electron microscopy (SEM), electron probe microanalysis (EPMA), and X-ray fluorescence (XRF) analysis; for phase identification optical microscopy and SEM. The analyses were conducted at the Wolfson Archaeological Science Laboratory, Institute of Archaeology London and at the Servicio Interdepartamental de Investigación, Universidad Autónoma de Madrid.

3. DISCUSSION OF RESULTS

Phase analysis of slags and crucible slags – The isolated fragments of slag and those adhering to ceramic ('crucible slags') are very heterogeneous. They are dominated by magnetite, delafossite, cuprite and malachite in a glassy matrix (fig 1). Ferrous arsenical copper and sometimes speiss were detected too (fig 2; tab 1). This microstructure indicates a gas atmosphere during slag formation, which was fairly oxidic, but temporarily and spatially reducing enough to produce metallic copper. Silica occurs as residual quartz, in silicates and in silica-rich glasses, whilst fayalite was not detected at all (see fig 1). The absence of the latter phase together with the comparatively high amounts of trapped copper prills suggests that the slags must have been very viscous. Larger copper prills were probably separated from the slag by crushing. Further evidence for interpreting these remains as smelting ones is the presence of ore remnants, like barite inclusions, and residual quartz (Müller et al. 2004).

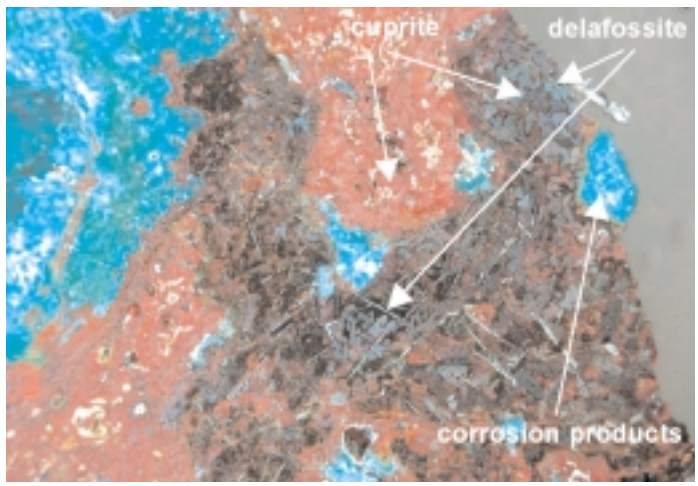

Figure 1. Slag B12; crossed polarized light (XPL); width of image is 1.8 mm.

Sample	Device	Phase	Fe	Cu	Sb	S	Ag	Pb	As	Co	MT
B9a-8	EPMA	speiss	32.7	19.5	0	0.08	0	0.13	40.0	6.50	97.5
B13-24	EPMA	Cu prill	2.05	87.0	0.05	0.06	0.05	0	10.6	0.01	95.6
B14-29	EPMA	speiss	4.46	72.3	0.25	0.1	0.05	0.02	22.7	0.04	97.3

Table 1. Major elements of normalised composition of copper and speiss inclusions detected in slag B9a and crucible slags B13 and B14 (wt%); MT – originally "measured total"

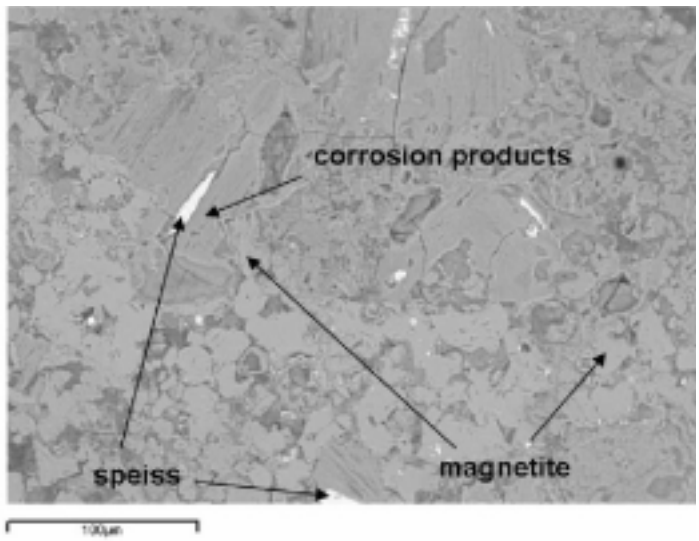

Figure 2. Slag B9a; SEM – backscattered electron image (SEM-BSE); width of image is 370 µm.

The slag-crucible interface of the crucible pieces indicates that the slags and crucible slags from Almizaraque are not merely a vitrification of crucible ceramic and copper metal/oxides as produced by melting operations. Sample B12 (fig 5) in particular has a lower, more homogenous layer of vitrified ceramic containing some cuprite, and an upper, more heterogeneous one dominated by delafossite, magnetite and corrosion products. This crucible was possibly used twice, firstly during a melting operation and secondly for extractive metallurgy (A. Shugar pers. communication).

Chemical analyses of slags and crucible slags – SEM area analyses were done to compare the chemical composition of the slags, the crucible slags and the crucible ceramic. Table 2 shows the chemical data normalised for potential gangue and ceramic oxides, in order to have a better comparability (these slags and crucible slags contain between 13 and 49 wt% copper oxide and up to 14 wt% arsenic oxides). The crucible slags can clearly be distinguished

from the crucible ceramic, in particular regarding the high iron oxide values. Iron oxides do occur in melting slags, but these high amounts rather suggest a smelting origin, especially considering the Chalcolithic context of the finds (see discussion in Müller et al. 2004). A further conclusive observation is that the magnesia content increases in the crucible slags compared to the respective ceramic pastes. This might be explained by the influence of fuel ash, containing considerable amounts of magnesia, next to the main components lime and potash. Yet, the latter two oxides rise only moderately or even fall, indicating that, next to the fuel ash, there was a further element influencing the ratio of these slag forming oxides, namely the gangue of processed ores. The individual slags fit very well into this picture: they have high amounts of iron oxides and similar amounts of magnesia, except for the last two samples.

Relating the slag results to ores and prills found at Almizaraque – The argumentation for crucible smelting correlates well with arsenic-rich copper ores discovered at the site. They are mainly oxidic, but in this study, we also identified two pieces of fahlore (fig. 3). These primary sulphidic ores were probably co-smelted unconsciously together with the oxidic ore. Isolated loose arsenic-rich copper prills complete the picture of copper extraction at Almizaraque. Sample B11c even contained a slag inclusion, demonstrating that they represent unrefined copper (Müller et al. 2004).

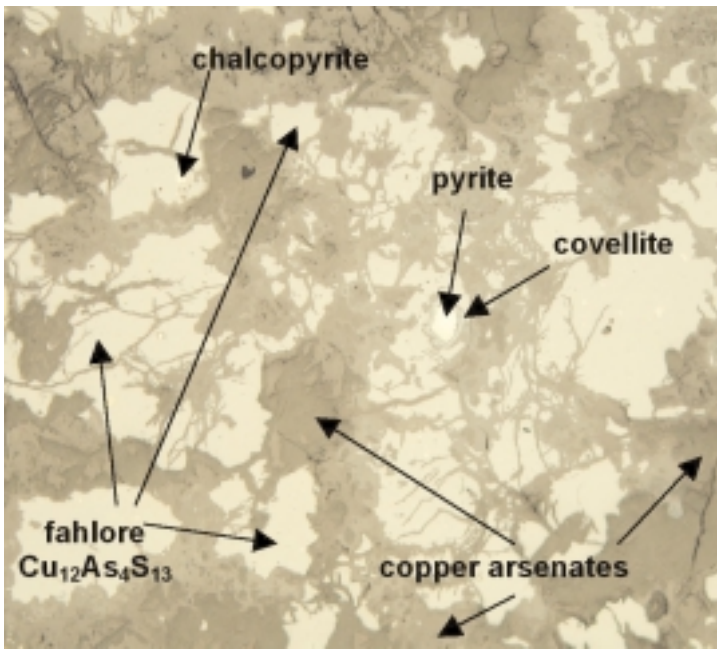

Figure 3. Ore B1; plane polarised light; width of image is 3 mm.

Sample	Area	SiO_2	TiO_2	Al_2O_3	FeO	CaO	MgO	K_2O
B12	crucible slag	15	0	3	70	6	6	1
	vitrified ceramic	42	1	13	21	19	3	2
	main ceramic body	50	2	16	16	12	2	3
B13	crucible slag	46	2	3	35	9	3	2
	main ceramic body	57	1	18	13	5	1	5
B14	crucible slag	33	1	10	42	8	3	2
	main ceramic body	48	1	14	16	17	2	3
B6b	slag	14	0	3	71	5	5	1
B8a	slag	35	1	7	34	15	6	3
B9a	slag	17	0	5	62	9	6	2
B10	slag	29	1	5	47	8	9	3
B11a	slag	39	1	6	25	17	7	5
B11b	slag	5	0	1	87	2	6	1
Almiz-03-1	slag	4	0	7	83	2	3	1
Almiz-18-1/6	slag	11	0	11	73	4	0	1
Almiz-31-1/5	slag	6	0	9	81	4	0	1

Table 2. Composition of crucible slags (B12 – B14) and slags (B6b – Almiz-31-1/5); SEM area analyses; data in wt% normalised for gangue and ceramic oxides to facilitate comparison.

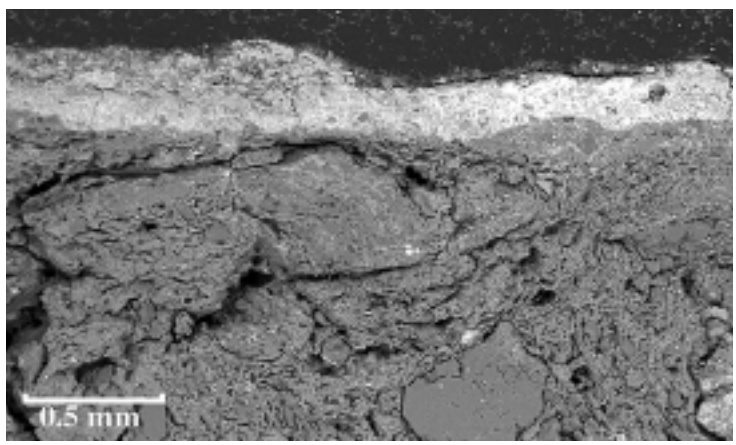

Figure 4. Crucible fragment Alm-32-13; SEM-BSE.

A further argument: contrasting smelting and melting remains – A further argument for substantiating the deduction of crucible smelting at Chalcolithic Almizaraque would be to contrast the proposed smelting slags and crucible fragments with melting crucible fragments or even dross. One should be able to find them at Almizaraque, due to the presence of the end-product of the metallurgical chain – the copper artefacts. One hypothesis already put forward by the Siret brothers is to distinguish melting from smelting crucibles by the

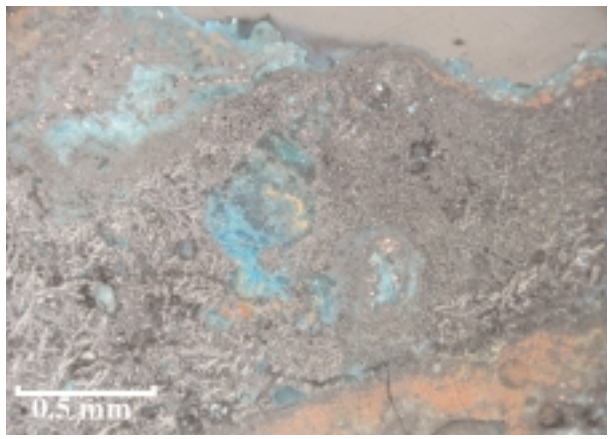

Figure 5. Crucible fragment B12; XPL.

thickness of the walls and the inner volume of the vessels (Siret 1948 and references there). We examined the entire Almizaraque assemblage again and did not find a typological clearly different vessel. Yet, we did discover a piece of a crucible that appears to be a bit thicker than the other sherds; which only bears a very thin green slag layer; and whose ceramic body does not seem to have been as affected by a high temperature process as the previously analysed ones. The scanty thickness of the slag layer of this crucible fragment – sample Alm-32-13 – is underlined by comparing it with the ones of the proposed smelting crucible fragments, exemplified here with crucible slag B12 (fig 4 & fig 5). Analyses of the crucible slag Alm-32-13 revealed that it contains about 50 wt% copper oxides and 10 wt% arsenic oxides. Normalising the results just for the gangue oxides as argued above, this crucible slag contains about 10 wt% iron oxides, which is much less than the iron oxide values measured in the proposed smelting slags and crucible slags (tab 2 & 3). These amounts would agree much better with a melting process. Lime, magnesia and potash increase proportionately, most likely due to the incorporation of fuel ash.

Sample	Area	SiO_2	TiO_2	Al_2O_3	FeO	CaO	MgO	K_2O
Alm-32-13	crucible slag	33	0	22	10	22	8	6
	main ceramic body	68	0	21	7	0	2	3

Table 3. Composition of crucible slag and crucible ceramic of sample Alm-32-13; SEM area analyses; data in wt%, normalised for gangue and ceramic oxides

4. CONCLUSIONS

The evidence strongly indicates that crucible smelting for the production of arsenical copper took place at Almizaraque. Slag was formed during this process, although relatively little compared to later periods. The extraction process took place under varying, only partially reducing conditions, yet spatially and temporarily reducing enough to form ferrous arsenical copper and sometimes speiss. The arsenic-rich, mainly oxidic ores, as well as the unrefined arsenical copper prills found at the site fit very well into this picture of copper production. A piece of a possible melting crucible contrasting the smelting ones was identified. Yet, differentiating between melting and smelting remains continues to be puzzling and more investigation to underline or discard the arguments proposed here is necessary, combining macroscopic functional-typological arguments, phase analyses and chemical analyses.

REFERENCES

Delibes, G., Diaz-Andreu, M., Fernández-Posse, M. D., Martín, C., Montero Ruiz, I., Muñoz, I. K. and Ruiz, A. 1996, Poblamiento y desarollo cultural en la Cuenca de Vera durante la Prehistoria Reciente, *Complutum Extra*, 6(1), 153-170.

Müller, R., Rehren, Th. and Rovira, S. 2004, Almizaraque and the early copper metallurgy of southeast Spain: new data, *Madrider Mitteilungen,* 46, 33-56.

Siret, L. 1948, El tell de Almizaraque y sus problemas, *Cuadernos de Historia Primitiva*, 3, 117-124.

"FREE SILICA TYPE" SLAGS OF SILVER PRODUCTION IN THE IBERIAN PENINSULA

Salvador ROVIRA
Museo Arqueológico Nacional, Madrid

Mark A. HUNT
Dep. Prehistoria, CSIC, Madrid

1. INTRODUCTION

In a first approach, "free silica type" slags are characterised by abundant non reacted silica grains entrapped in a matrix of what seems to be melted material. These slags connected with silver production only have been found in large amounts in southern Iberia, being unknown in other areas of the Mediterranean. They are described in literature since the 1960's and have been recorded in more than 20 sites of the western provinces of Andalusia, namely Huelva and Seville. The most of these sites are dated through the chronological frame of 8th-7th century BC, lasting a few of them up to the beginning of the 6th century BC, always in association with Phoenician material (Hunt 2003).

2. MATERIALS AND METHODS

Samples from 12 archaeological sites surveyed by one of us (M.H.) have been analysed in the laboratory. The complete analytical program includes phase and chemical composition determined by SEM-EDX analysis, PIXE analysis and lead isotope analysis. However this short paper has been focused on the results of SEM determinations.

Each sample has been packed in a cilynder of resin measuring 20 mm in diametre, polished as for metallography and slightly coated with gold to make the surface electricity conductor.

From the methodological point of view, analyses have been performed to the melted material, as we consider that free silica does not take part of the equilibrium system. So, bulk analyses we manage are referred to the micro-domains in which more or less complete reactions have occurred. It is important to be taken into account this procedure when comparing our

results with the few analyses performed by other colleagues because they usually measure the total silica content.

3. MICROSTRUCTURE AND BULK COMPOSITION OF THE SLAGS

The microstructures are very varied, frequently in the same sample, depending on the reaction products formed in each point. Despite this, two main groups of slags can be established:

A) Slags where fayalite is predominant. A complex glassy matrix containing aluminium, iron, calcium, barium and lead silicates or pyroxene-like material is filling the interstices between fayalite crystals when barium content is low. If barium content is about 3-4%, hyalophane crystals are formed. When barium is higher, feldspar celsian type, andremeyerite (a barium-iron silicate) and hyalophane-wollastonite use to be formed in the interstices between fayalite crystals.

B) Slags where wollastonite-hyalophane is predominant. The material is a more or less continuum wollastonite-hyalophane matrix, in which hyalophane sticks are interspersed.

Table 1 summarises the results. As can be seen, fayalite is the more frequent and dominant phase except for two samples, in which wollastonite-hyalophane predominates. As minor components we found pyroxene, andremeyerite, celsian and hyalophane. Few amounts of magnetite are present in almost all the samples.

SAMPLE	DOMINANT PHASE	OTHER PHASES
3A-1	Wollastonite-hyalophane	Hyalophane, magnetite
AZ-23	Fayalite	Celsian, magnetite
C2	Fayalite	Hyalophane, magnetite
CARA-1	Fayalite	Pyroxene, andremeyerite
CGE	Fayalite	Celsian, andremeyerite
CJF	Fayalite	Glass, magnetite
CMA	Fayalite	Pyroxene, magnetite
HD	Wollastonite-hyalophane	Hyalophane, magnetite
HU-6	Fayalite	Pyroxene, Fe-pyroxene, magnetite
SBA	Fayalite	Andremeyerite, wollastonite-hyalophane
TDV-2	Fayalite	Glass, magnetite
TJ-5	Fayalite	Glass, magnetite

Table 1. Crystallographic phases in the slags (identified by SEM-EDX analysis).

Table 2 shows the bulk composition of the slags. There must be remarked the medium to high barium content of almost all the samples and the too high silica and slightly low iron content if compared with typical fayalite tapped slags. The lead lost is estimated in the range of 0.7 to 3.3%, mainly as metallic lead.

SAMPLE	MgO	Al_2O_3	SiO_2	P_2O_5	Na_2O	K_2O	CaO	FeO	BaO	PbO	SO
3A-1/10	0	3.87	36.5	2.05	0	0.89	6.21	44.1	5.57	0.83	0
AZ-23/8	1.39	6.55	29.7	0	0	1.13	3.81	48.8	7.16	0.87	0.64
C2/6	1.51	6.41	37.5	0	0	0.95	4.47	42.7	3.19	3.29	0
CARA-1/6	0	6.59	37.0	0	0	1.05	4.62	37.9	10.4	1.45	0.98
CGE/6	0.8	10.1	28.6	0	0	0.77	4.41	41.2	11.7	2.37	0
CJF-1/6	0	12.4	34.1	0	2.56	0.62	5.38	42.0	1.98	0.69	0.36
CMA/8	0	5.90	42.0	0	0	0.80	5.17	40.9	3.29	1.94	0
HD-1/4	0.99	6.39	35.5	0	0.62	0.90	5.53	44.7	0	1.13	0
HU-6/11	0.88	6.86	39.1	0	0	0.88	5.06	41.2	4.04	0.81	0.52
SBA-4/8	0	7.25	31.9	0	0	0.79	4.04	44.1	8.73	1.88	0.53
TDV-2/6	0	6.22	38.9	0	0	0.42	3.77	46.1	1.59	3.02	0
TJ-5/4	0.78	4.18	42.4	0	0	0.72	3.76	42.3	4.18	1.68	0

Table 2. Bulk composition of the slags (SEM-EDX analysis).

When plotted on the equilibrium ternary diagram after re-calculation following the Bachmann's indications, all the samples are quite well grouped into or near the wollastonite region, with theoretical free-running temperatures in the range of 1,100-1,250º C (fig. 1).

The best set of analysis to compare is the one from the site Monte Romero, published by Kassianidou et al. (1995). There are remarkable differences, but they are related more to the analytical procedure than to real divergences. As has been said before, we only have analysed the melted material excluding free silica, as we estimate that free silica does not take part of the equilibrium system. Instead of this, Kassianidou et al. (1995) analysed the whole sample, including free silica. As a consequence, many dots from Monte Romero fall in the region of very high silica percentages (see fig. 1). Despite this, the description of phase components in the slags from Monte Romero (feldspar and olivine), too much elementary in the mentioned paper, allows to suppose compositions not very different than in the set we present here.

4. SILVER IN THE SLAGS

Another important aspect of lead-silver slags research is to confirm the presence of silver and where the silver is located, a matter this last that had not been accurately tackled before. Silver uses to be in lead prills, but not all

the lead prills entrap silver. Then, it is necessary to be patient and search the lead inclusions one by one, with the SEM, to characterise which ones have silver traces.

Table 3 shows elemental analyses performed to lead prills in some samples. What must be remarked is the complexity and polymetallic nature of the inclusions. This is in agreement with the smelting of a polymetallic ore typical of the south west of Spain called jarosite, as it is well-known.

SAMPLE	PHASE	S	Cl	Fe	Cu	As	Ag	Sn	Sb	Pb
3A-1/01	Grey area in Pb prill	0	0.57	13.0	1.62	19.9	1.29	0	0.99	59.6
3A-1/02	White area in Pb prill	0	0	0.71	0	0	0	0	0	99.3
3A-1/03	Dark grey area in Pb prill	0	0	1.92	36.1	30.8	0	0	0	0
3A-1/04	Ag prill		0 0	1.11	1.00	2.17	85.4	9.81	0	0
3A-1/05	Grey area en Pb prill	0	0	1.93	0	0.66	12.6	0.4	0	81.6
AZ-23/1	White area in metal prill	2.30	0	8.64	22.3	8.26	0.85	11.0	9.75	32.8
AZ-23/2	Grey area in metal prill	2.11	0	50.9	6.17	37.9	0	2.1	0	0
AZ-23/4	Grey prill	1.64	0	49.0	6.44	40.4	0	0	1.6	0
AZ-23/5	Grey prill	1.80	0	49.5	5.65	39.2	0	0	1.75	1.47
AZ-23/7	Pb prill	0	0	3.2	1.67	0	15.8	3.85	1.87	70.8
C2/1	Light grey area in Pb prill	0	0	2.42	47.8	0	0	2.49	46.1	0
C2/2	Light grey crystal in Pb prill	0	0	0.81	1.93	0	71.0	11.6	8.46	0
C2/3	Dark grey crystal in Pb prill	0	0	2.79	46.4	0	0	2.44	46.0	1.67
C2/3A	Pb prill (sound metal)	0	0	0	0	0	0	0	0	100
CARA-1/1	Pb prill	0	0	1.86	0	0	1.34	0	2.53	94.3
CGE/1	Pb prill	0	0	2.21	0	0	0	0	0	97.8
CJF-1/1	White area in Pb prill	0	1.56	2.19	0	14.1	0	0	6.04	70.8
CJF-1/2	Dark grey area in Pb prill	0	0.34	1.16	12.7	22.5	1.22	0	2.21	53.3
CJF-1/3	Light grey area in Pb prill	9.76	0	0	0	0	89.6	0	0	0
CMA/2	Grey area in Pb prill	0	0	0	29.1	0	3.6	25.5	21.2	17.5
CMA/3	White area in Pb prill	0	0	0	0	0	0	0	0	94.5
CMA/4	Light grey area in Pb prill	0	0	2	48.3	0	0.9	3.4	43.7	1.1
CMA/5	Dark grey area in Pb prill	0	0	42.8	10	47.3	0	0	1.2	3.8
CMA/6	White area in Pb prill	0	0	1.1	0	0	0	0	2.5	94.3

Table 3. Metallic inclusions in the slags (SEM-EDX analysis).

5. DISCUSSION

After this short excursion inside the "free silica" slags, it is time to start an also necessarily short discussion. What has been said about these slags? Before discussion it is important to remark that the smelting practice, no

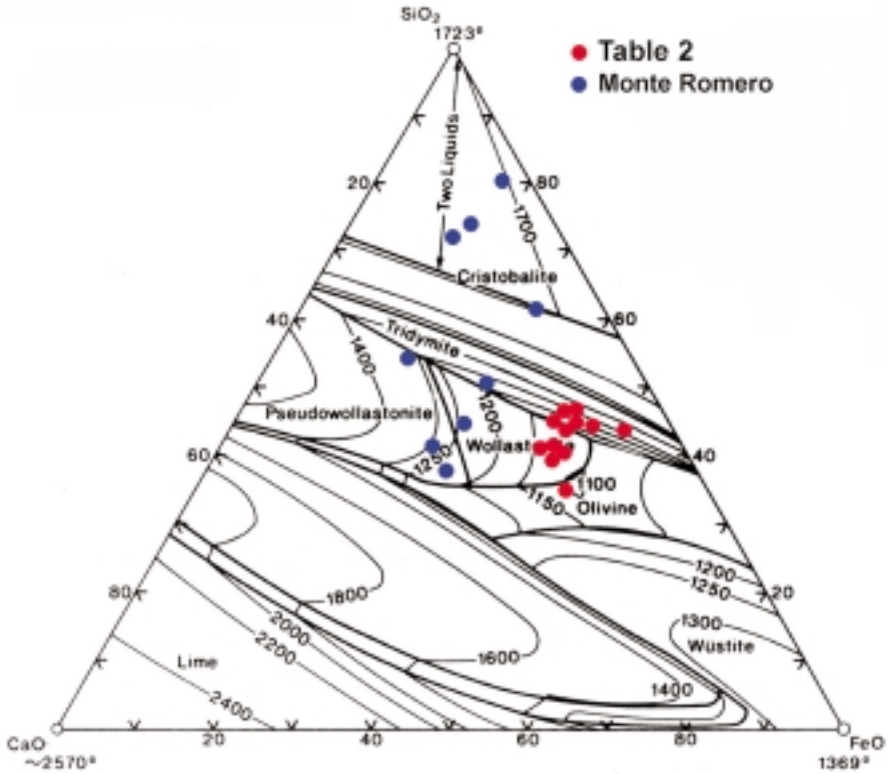

Figure 1. Bulk analyses of "free silica type" slags plotted on the equilibrium ternary diagram.

matter which was, included the addition of metallic lead or lead oxide to the furnace charge to act as collector for silver. Therefore, the end product should be a mass of lead containing silver and other metals entrapped or alloyed during the smelting process.

The first finds of these slags were interpreted as the result of lack of control, of a bad smelting practice. Later, when the finds were repeated and the analyses provided data, new interpretations were given, such as: make the slags more fragile to facilitate the extraction of the metallic globules they contained (Blanco and Rothenberg 1981); facilitate the separation by gravity of the metal through the slag (Rothenberg et al.1986); separation of the slag from the metallic mass (Hunt 1987); thickening of the slag to take it out like a sponge from the water (Tylecote 1987).

All these authors (and others) accepted that "free silica" slags were the result of an intentional process but only Kassianidou et al. (1995) have drawn a flow diagram, based on the evidences from Monte Romero, in which these slags take their place in the "chaîne opératoire". Following these authors, the

"free silica" slags would be the result of a first step in the smelting process and should be smelted again to extract the remnant lead-silver bullion, obtaining tap slags as final by-product. It is necessary to say that these two kinds of slags have been found at Monte Romero. Our question is: why a two steps process if it can be performed in only one step when fluxes are correctly dosed?

On the other hand, Bachmann (1999) stated that, in oxidizing conditions in the furnace, silica segregation can be formed when divalent iron is oxidised to trivalent iron in large amounts, blocking fayalite formation. So, a malfunction of the furnace can be responsible for non reacted, new crystallised silica forming in the slag. Well, that is true, but it is not the case of our samples: magnetite present in the slags is too low to justify such a segregation process. The slags, indeed, show quite clearly, we believe, that the abundant silica fragments are broken natural rocks, not re-crystallised silica.

Which is our position on the topic? Slags containing large amounts of non reacted silica are a real fact. Are they formed in the upper part of the furnace while tap slags occur simultaneously in the lower part? May be. In that case, they would be merely immature material which did not reach the reaction chamber and would remain into the furnace after tapping the slag and leaving the furnace to stop. This is probably the more appropriate explanation. They could be crushed and used in a new charge (as suggest Kassianidou et al. 1995) or not. The fact that many slag fragments are commonly found in the surveyed sites is an indication that not all the "free silica" slags were systematically profitable for re-cycling and perhaps they were actually rejected by the smelters.

More research must be done in future both in the laboratory and on the field to determine the relative amounts of coeval "free silica" and tapped slags.

REFERENCES

Bachmann, H.G. (1999) A note on "free silica slags". *IAMS Newsletter*, 20: 18.

Blanco, A. and Rothenberg, B. (1981) *Exploración Arqueometalúrgica de Huelva*. Labor. Madrid.

Hunt, M.A. (1987) *Silver Metallurgy in the South-West Iberian Peninsula, with special reference to Rio Tinto, Huelva*. M.Sc. Thesis. Institute of Archaeology. London.

Hunt, M.A. (2003) *Prehistoric Mining and Metallurgy in the South West Iberian Peninsula*. BAR International Series 2288. Oxford.

Kassianidou, V., Rothenberg, B. and Andrews, P. (1995) Silver production in the Tartessian Period. The evidence from Monte Romero. *Arx*, 1(1): 17-34.

Rothenberg, B., Andrews, P. and Keesmann, I. (1986) Monte Romero September 1986. The discovery of a unique Phoenician silver smelting workshop in south-west Spain. *IAMS Newsletter*, 9: 1-4.

Tylecote, R.F. (1987) *The Early History of Metallurgy in Europe*. Longman. London.

PROVENANCE OF IRON ARTEFACTS FROM THE CELTIC OPPIDUM OF MANCHING (BAVARIA)

R. Schwab, B. Höppner, E. Pernicka
Institute of Archaeometry, TU Freiberg, 09596 Freiberg, Germany

1. INTRODUCTION

The oppidum of Manching is one of the largest settlements of the la Tène period in central Europe. It is located in southern Bavaria on the banks of the river Danube, right on the bank of the small river Paar and surrounded by swamp areas. In the Celtic period one branch of the Danube was still open and functioned as harbour. Today the site is some distance away from the river. The basic supply was probably guaranteed by local crafts and agriculture, but Mediterranean goods like amphorae and other imported pottery and stone implements provide evidence for a well developed regional and long-distance trading system (Sievers 2002).

Traditionally it was thought that iron or iron products were the major trading goods of the site, because of abundant finds. Indeed, the local iron ores were considered as a major reason for the location and the size of the settlement. However, in the last years excavations uncovered areas where metal scrap was accumulated during the last decades before the settlement was abandoned at about 40/30 BC, which would suggest scarcity of iron rather than an abundant production. In order to clarify the long standing hypothesis of iron production from local ores, a number of iron objects from the oppidum and various regional iron ores were examined to study the iron technology at Manching and the provenance of the metal.

2. ARCHAEOLOGICAL AND GEOLOGICAL BACKGROUND

There is no doubt that inside the oppidum intensive ironworking was carried out and the craft of the blacksmith was obviously important for the production and repair of utilitarian tools. But there is no evidence for bloomery ironwork inside or outside the walls. Local and regional open cast mining, slag occurrences and remains of furnaces were traditionally associated with Celtic iron production (see Pleiner 2000, 40 and 94). However,

there are very few sites in the whole region that were systematically excavated and reliably dated to the la Tène period (Wischenbarth et al. 2001, 36-42).

Different iron bars (currency and bi-pointed bars) excavated inside the settlement, suggest trade of iron. Nevertheless, since the oppidum of Manching is one of the most famous excavation sites in Germany of the Iron Age, the provenance of the iron was always discussed and various iron ore deposits were proposed as sources for Manching by different scholars. These include bog ores from flood plains or swamp areas in the surrounding of Manching and iron ores from the Franconian Mountains. They consist of *Bohnerz* (bean ore), iron crusts and iron-sandstone. Iron-sandstone can virtually be excluded from the possible sources, because there is no indication for their use and for technical reasons it is unlikely that they were used before medieval times. Bog ores were associated with ^{14}C dated (400 - 100 BC) bloomery furnaces in the Rothtal, some 80 km away from Manching (Wischenbarth et al. 2001, 123-136), while *Bohnerz* was probably used in early la Tène times in southwest Germany (Gassmann 2002, 71).

The main iron bearing component of all these ores is the iron hydroxide goethite, but they differ in minor and trace element concentrations due to different formation conditions and ages (Borchert 1959/60, 262-270).

3. ANALYTICAL METHODS

To investigate the iron technology at Manching, in particular the question of piling and recycling, 70 different tools and weapons were examined with various methods (radiography, optical microscopy, SEM and TEM analysis with EMPA and ED). While most of the banding structures seem to be consequences of segregation due to the refining of raw materials, it is possible to show that several objects are made by folded and welded sheet metal (fig. 1). The cross sections reveal structures of folded sheet metal, occurring in scrap metal deriving from cauldrons and scabbards (Schwab 2002; 11-13; Schwab et al. 2003, 12-13).

Concerning the provenance of the iron several different approaches, such as metallographic features or chemical analysis, have been suggested, but the evidence thus obtained is still in dispute. Mostly instrumental analytical methods or methods with high lateral resolution were used to determine minor and trace elements in metal and non-metallic inclusions; lead isotopic ratios were also applied (see Schwab et al. 2003, 14). But in our case only a combination of different methods appeared to be promising.

Samples were taken from various ores from the Franconian Mountains and the fluvial plain of the Danube. They were analysed by WD-XRF, ICP-AES and AAS. Bulk concentration of iron artefacts were determined by ICP-

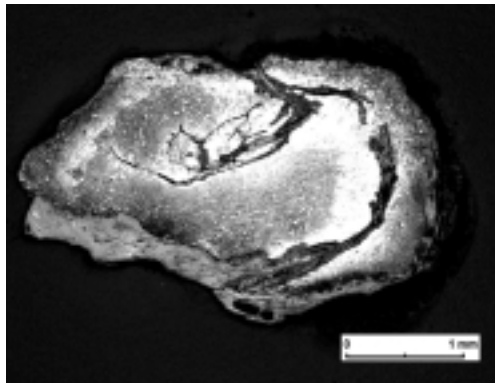

Figure 1. Cross section of a chisel made of scrap. Welded seams are visible due to the formation of scale (Oberhoffer etched).

AES and AAS, while slag inclusions were studied with SEM /EDX and with an electron microprobe. After separation on an ion exchange column lead isotope ratios of ores and artefacts were measured with a double focusing multiple-collector ICP-MS (Schwab et al. 2003, 14). Lead isotope ratios of iron ores from la Tène smelting sites in the Rothtal and from the Swabian Mountains were measured and included in the investigation.

Surveys of different iron ores, which were investigated in the course of the archaeometallurgy program funded by the "Volkswagen Foundation" during the last ten years formed a statistically relevant basis for the present analysis (see Yalçin and Hauptmann 1995, Ganzelewski 2000, Heimann et al. 2001).

4. RESULTS AND DISCUSSION

The major element composition of slag inclusions (iron, silicon, aluminium) are strongly correlated with the surrounding metal phases dependent on furnace conditions. Possible contributions of flux materials, furnace lining or charcoal are intensively discussed (Kronz 2003), but hold that these can be neglected, if one considers only elements which are not present in charcoal ashes. The contribution of furnace lining may have been exaggerated, since Celtic furnaces have large combustion chambers (see Pleiner 2000, 145-172, Gassmann 2002, 74).

Comparing the ratios of the major elements in slag inclusions within one object, it comes apparent that they are more or less similar. With an increase of glassy components in low iron slag, as can be found within pearlite structures or high phosphorous ferrite, the ratios become more variable. This probably indicates higher smelting temperatures and therefore the melting of

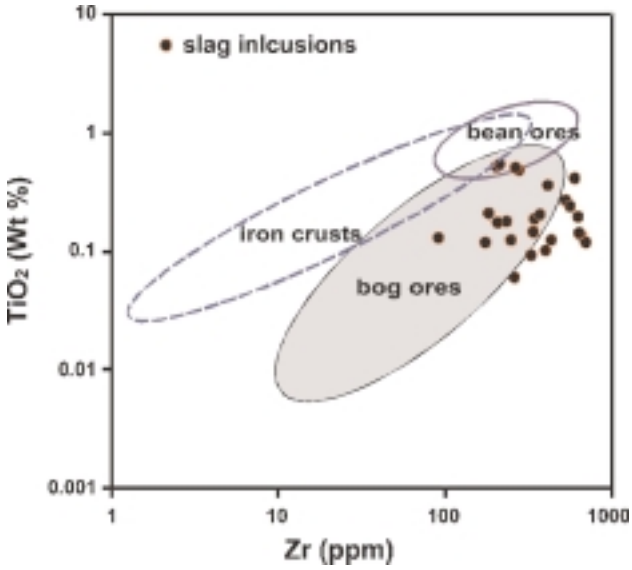

Figure 2. Titanium and zirconium ratios in ores (WDXRF) and in slag inclusions (WDX-EMPA). Bog ores from the "Feilenmoos", eastern and northern Germany (Ganzelewski 2000, Heimann et al. 2001). Iron crusts and bean ores from the Suebian Mountains (Yalçin, Hauptmann 1995) and from the Franconian Mountains.

furnace lining or even the addition of flux. Based on concentrations of several minor and trace elements it is possible to distinguish slag inclusions based on ores from different genetic environments (fig. 2). These suggest that the slag inclusions suggest bog ores as principal ore source for the iron objects of Manching, but a positive assignment to a specific deposit is impossible.

The results of lead isotope ratios confirm these impressions and consequently it seems to be possible to exclude *Bohnerz* (bean ore) as ore sources for the iron supply of Manching (fig. 3).

Iron crusts can also be excluded to a large extent from the compositions of slag inclusions. The lead isotope ratios are as yet inconsistent since not enough samples have so far been measured. Of the investigated ore deposits there remain one bog ore sample from a local swamp area ("Feilenmoos") and two regional bog ores from the Rothtal, whose lead isotope ratios match the iron objects (fig. 4). However, it has to be considered that the bog ore deposits show a wide spread in the usual three isotope plots $^{208}Pb/^{206}Pb$ versus $^{208}Pb/^{206}Pb$ (fig. 4). In addition, the ores and artefacts are also inhomogeneous at the micro-scale, because the lead contents of the bog ores and in consequence of the iron samples is very low and inhomogeneously

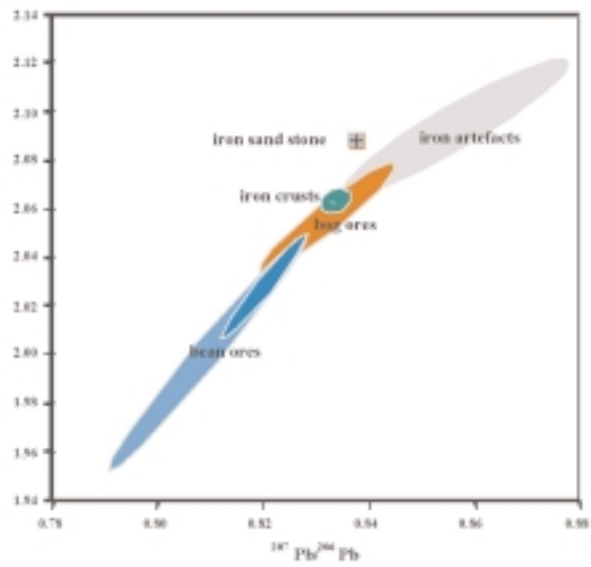

Figure 3. Lead isotope ratios of different iron ores from Southern Germany and archaeological iron objects.

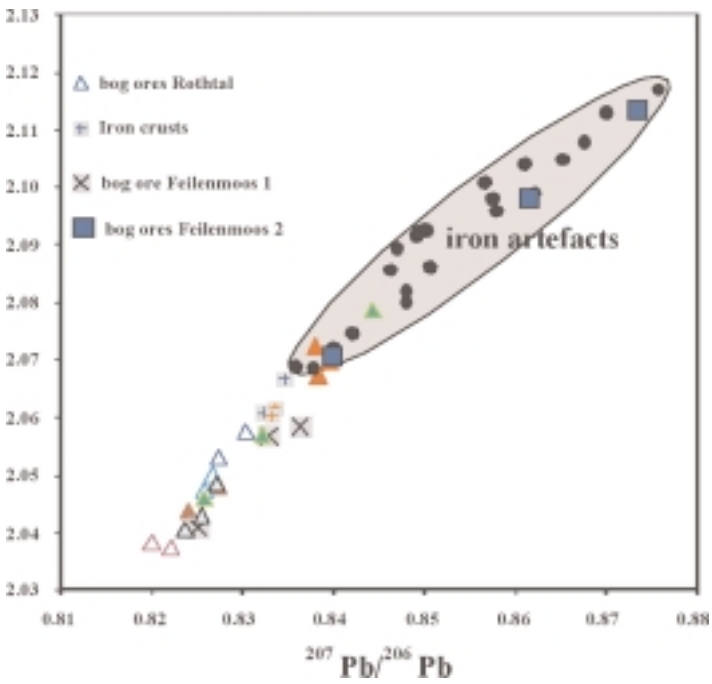

Figure 4. Detail of figure 3 without bean ores and iron sand stone. The standard error is smaller than the size of the symbols.

distributed. Since the iron was not molten, the inhomogeneity remains even in the artefacts. For the purpose of provenance determination the large spread within artefacts and deposits makes it difficult to discuss possible relationships of the ores to artefacts.

Siderophile trace elements like cobalt, nickel, copper or arsenic are concentrated in the metal, while lithophile elements and a considerable part of the iron enter the slag. Thus the concentrations of siderophile elements cannot be compared directly with the iron ores. However, analyses of trace elements in iron ores before and metal after smelting experiments show an enrichment of siderophile elements by about one order of magnitude (Senn et al. 2001, 86). Applying this enrichment factor to our samples, it becomes clear that only a few ores match the iron artefacts excavated in the oppidum of Manching (fig. 5).

In summary, we conclude that in general bog ores were most likely the source for iron working in Manching while only one of the examined ore samples from a local swamp could actually have been used. Since we have found evidence for the recycling of scrap metal, the diminishing iron production can only be explained by a change in the economic structures of the settlement due to the political situation of the Celtic world at the end of the la Tène period.

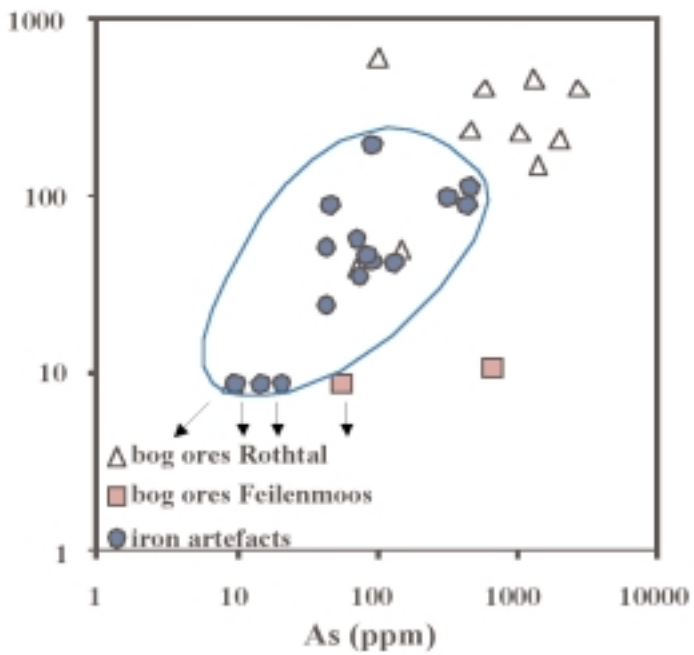

Figure 5. ICP-AES and AAS analyses of artefacts, local and regional bog ores. Ores from the Rothtal after Wischenbarth et al. (2001). Arrows indicate detection limits.

Assessing the applied methods, each provided valuable information but is limited in some area (e.g. detection limits of EMPA). More experimental work seems desirable on the behaviour of trace elements during smelting and more data are needed to assess the potential of isotope ratios of various iron ores. Thus, the provenance determination of early iron is still at its beginning and needs further attention and research.

REFERENCES

Borchert, H., 1959/60, Genesis of Marine Sedimentary Iron Ores, *Transactions of the Institution of Mining and Metallurgy*, **69**, 261-279.

Ganzelewski, M., 2000, Archäometallurgische Untersuchungen zur Verhüttung von Raseneisenerzen am Kammberg bei Joldelund, Kreis Nordfriesland, *Universitätsforschungen zur prähistorischen Archäologie*, **59**, 3-100.

Gassmann, G., 2002, Recent discoveries and excavations of 6th -2nd century BC furnaces in SW Germany, *Historical Metallurgy*, **36** (2), 71-76.

Heimann, R. B., Kreher, U., Spazier, I., and Wetzel, G., 2001, Mineralogical and chemical investigations of bloomery slags from prehistoric (8th Century BC to 4th Century AD) iron production sites in Upper and Lower Lusatia, Germany, *Archaeometry*, **43 (2)**, 227-252.

Kronz, A., 2003, Ancient iron production compared to medieval techniques in Germany: Fayalitic slag and element balances, *Archaeometallurgy in Europe,* Vol. **1**, Milan, 555-564.

Pleiner, R., 2000, *Iron in Archaeology: The European Bloomery Smelters*, Prague.

Schwab, R., 2002, Evidence for carburized steel and quench-hardening in the 'Celtic' oppidum of Manching, *Historical Metallurgy,* **36** (1), London, 6-16.

Schwab, R., Höppner, B., and Pernicka, E., 2003, Studies in Technology and Provenance of Iron Artefacts from the Celtic oppidum of Manching (Bavaria), *Archaeometallurgy in Europe,* Vol. **1**, Milan, 11-16.

Senn, M., Lienemann, P., Bührer, T., 2001, Archäologische Eisenverhüttung im Experiment, *Zeitschrift für Schweizerische Archäologie und Kunstgeschichte,* **58** (1), 81-88.

Sievers, S., 2002, Manching revisited, *Antiquity*, **76**, 943-944.

Wischenbarth, P., Ambs, R., and Gassmann, G., 2001, *Keltische Stahl- und Eisenproduktion im Rothtal (Bayerisch-Schwaben), Berichte zur Archäologie im Landkreis Neu-Ulm und in den angrenzenden Gebieten*, **2,** Neu-Ulm.

Yalçin, Ü., and Hauptmann, A., 1995, Archäometallurgie des Eisens auf der Schwäbischen Alb, *Forschungen und Berichte zur Vor- und Frühgeschichte in Baden-Württemberg*, **55**, 269-309.

TRACKING CHRONOLOGICAL DEVELOPMENTS IN CHALCOLITHIC METALLURGY: AN ASSESSMENT OF POSSIBLE CORRELATIONS BETWEEN RADIOCARBON DATA AND COMPOSITIONAL ANALYSES

Aaron N. Shugar*
Smithsonian Center of Materials Research and Education
*Lehigh University Archaeometallurgy Laboratory

Christopher J. Gohm
Near and Middle Eastern Civilizations, University of Toronto

1. RESEARCH OBJECTIVES

The Late Chalcolithic or 'Ghassulian' period of the Levant (*ca.* 4500-3600 BCE) is characterized by the earliest evidence of major copper production in the region, and it has received considerable scholarly attention since the discovery of the famous Nahal Mishmar hoard in 1961 (Bar-Adon 1980). Nearly 600 copper and alloyed-copper artifacts have been published from 'Ghassulian' sites (table 1). Numerous archaeometallurgical studies carried out over the past two decades have demonstrated that the ancient metallurgists produced two classes of artifacts, including relatively pure copper 'utilitarian' tools and alloyed copper 'prestige' items containing arsenic and antimony (Levy and Shalev 1989; Shalev and Northover 1993). Additionally, evidence of a two-stage process model of metallurgical production has emerged from Abu Matar, including initial furnace smelting followed by crucible remelting (Shugar 2000). While the compositional dichotomy between 'utilitarian' and 'prestige' items has been repeatedly upheld by analyses of artifacts from the southern Levant (*i.e.* the Beer-Sheba region), recent investigations of finds from more northern sites, including Peqi'in, Ketef Jericho and Givat Oranim, have cast doubt on its wholesale applicability (Segal and Kamenski, pers. comm.; Namdar 2002). Due to the significantly homogenous nature of the period's ceramic assemblage (Garfinkel 1999), it has been difficult to tease out any chronological or developmental patterns relating to the emergence of these two classes of artifacts. However, the past decade has witnessed an incredible increase in

the number of studies making use of radiocarbon dating methods, and the number of new determinations is growing every year (for e.g., see Burton and Levy 2001; Blackham 2002). Thanks to these new determinations, coupled with advances and refinements in the field of radiocarbon research in general, Chalcolithic scholarship has reached a point were it has become feasible to attempt to provide a relative chronological framework for changing metallurgical technology. The purpose of this study is to correlate radiocarbon dates from northern and southern sites at which copper artifacts have been unearthed to the stratigraphic contexts best associated with the finds, in order to approximate their relative chronological relationships. A second objective of this research in to present new archaeometallurgical data obtained from the analyses of an axe from the southern Chalcolithic site of Neve Noy, an eastern extension of Bir es-Safadi excavated as part of a salvage operation in 1983 (Eldar and Baumgarten 1985).

2. METHODS

In order for such a correlation to have any meaning in terms of reconstructing Chalcolithic technology, a well defined and consistently followed methodology is a prerequisite. Recently, many radiocarbon samples have been processed and published from Levantine sites, yet all do not belong to the occupational or depositional phases associated with copper-based artifacts. 'Relevant' dates, defined here as those obtained from samples originating from stratigraphic contexts best associated with such finds, are used exclusively for the purposes of this study. In the case of sites where the original stratigraphic interpretations have been questioned (*e.g.* Abu Matar, Bir es-Safadi/Neve Noy and Horvat Beter; Gilead 1994), or where artifacts have been found in secondary contexts (*e.g.* Gilat), all of the radiocarbon determinations have been included. These dates have been recalibrated using CALIB v4.4.2 software (Stuiver and Reimer 1991) with the INTCAL98 dataset (Stuiver *et al.* 1998). In order to obtain a realistic picture of the possible dates for each radiocarbon sample, both 1- and 2-sigma ranges are taken into consideration for the interpretation of each site. However, as many of the calibrated dates cover an exceptionally wide range of radiocarbon years, especially those taken early in the history of the technique, a 'trimmed' date range for each stratigraphically related assemblage in presented for each site. This range is generated from the upper and lower extremes of the 1-sigma date ranges from each site, discounting imprecise samples with over 150 years of standard deviation and those previously discredited as erroneous (see figure 1). For the purpose of the overall interpretation, these ranges are considered representative (at 68% confidence) of the most likely date range from which each artifactual assemblage was deposited.

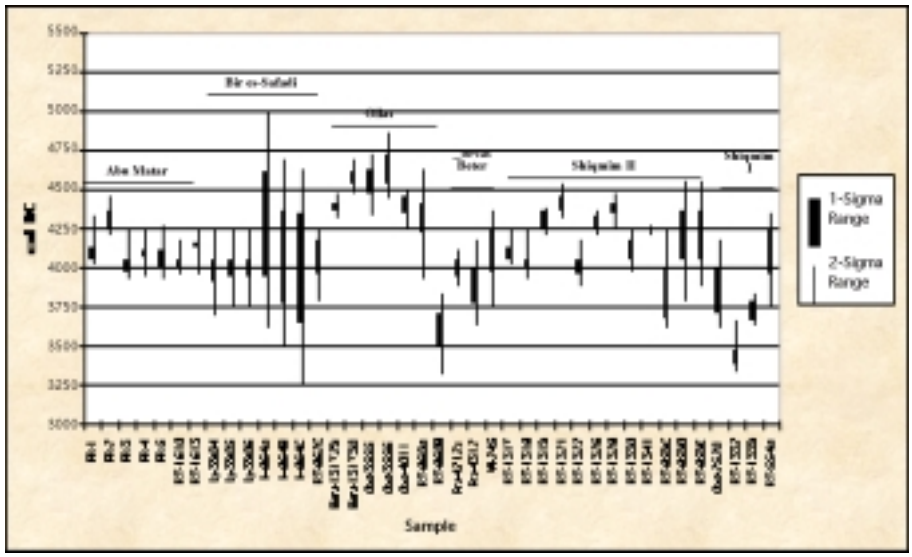

Figure 1. Relevant Radiocarbon Determinations from Southern Chalcolithic Sites.

3. DISCUSSION

Due to the imprecision of many of the early radiocarbon determinations and the relative scarcity of samples obtained directly from contexts associated with deposited copper-based artifacts, this attempted correlation between radiocarbon dates and specific finds yielded no conclusive results regarding changes in artifact compositions over time. Judging from the data generated by this study, it appears as if both 'prestige' and 'utilitarian' items were deposited contemporaneously between the 45th and 37th centuries cal BCE, as both are found side-by-side in identical contexts at sites such as Abu Matar, Shiqmim, and even Peqi'in. As a result of the radiometric correlations, this study has provided evidence suggesting that the earliest full-scale processing took place at Abu Matar and Bir es-Safadi/Neve Noy, and that roughly contemporaneous crucible remelting took place at Shiqmim. Also of interest is the emerging pattern of a change from the use of pure copper for prestige objects early in the period, evident at the northern site of Peqi'in, to the use of alloyed copper for prestige objects later in the period, well known at Nahal Mishmar and Shiqmim I. The practice of producing prestige objects from relatively pure copper appears to continue into the 38th century cal BCE in the north, judging from the recent analyses of finds from Ketef Jericho (Segal and Kamenski, pers. comm.). Analysis of axe 82-1190 from the southern site of Neve Noy as part of this research project resulted in the discovery that is was produced from pure copper, which lends further support to previously identified dichotomy of simple (pure) vs. complex (alloyed) (see figure 2).

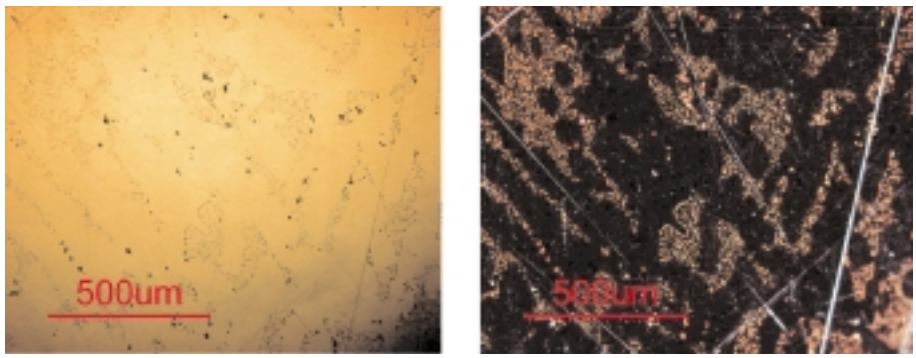

Figure 2. The collection of copper-based artifacts from Neve Noy is currently being studied to determine their chemical composition and method of manufacture. Artifact 82-1190 is a flat axe that has been investigated by optical microscopy and SEM. Images 1 and 2 show the cross section of the sample under normal and cross-polarized light, and the inclusions (bright red in Image 2) are oxides. This observation is confirmed using LISPIX and suggests that the axe was cast in an open-air mould, allowing for the oxidization of the metal.

4. CONCLUSION

The radiometric correlations identified by this preliminary investigation have yielded strong evidence that simple tools and complex artifacts were deposited contemporaneously in the archaeological record, and therefore one form did not develop prior to the other. The styles of artifacts produced by ancient metallurgists, including mace-heads, axes, chisels, awls and standards, appear to have emerged as a complete unit, each of which were elaborated upon later in the 'Ghassulian' period, judging from the finds from Nahal Mishmar. One interesting trend that requires further study is the apparent change from pure copper prestige objects early in the period to alloyed prestige goods later in the period, perhaps relating to technological developments or changes in political economics, such as the improvement of resource acquisition over time. This study is part of an ongoing research project geared towards addressing these issues, and further analyses of artifacts from the Chalcolithic period will be forthcoming.

ACKNOWLEDGMENTS

We would like to acknowledge the financial support provided by the Social Sciences and Humanities Research Council of Canada for this ongoing research project , as well as the Israel Museum for allowing archaeometallurgical sampling of artifacts from the Neve Noy assemblage.

REFERENCES

Bar-Adon, P., 1980, *The Cave of the Treasure*. Jerusalem: Israel Exploration Society.

Blackham, M., 2002, *Modeling Time and Transition in Prehistory: The Jordan Valley Chalcolithic (5500-3500 BC)*. BAR International Series 1027. Oxford: Archaeopress.

Burton, M. and T. E. Levy, 2001, "The Chalcolithic Radiocarbon Record and its Use in Southern Levantine Archaeology." *Radiocarbon* 43/3:1223-1246.

Eldar, I. and Y. Baumgarten, 1985, "Neve Noy: A Chalcolithic Site of the Beer-Sheba Culture." *Biblical Archaeologist* 48:134-39.

Garfinkel, Y., 1999, *Neolithic and Chalcolithic Pottery of the Southern Levant*. Qedem 39. Jerusalem, Institute of Archaeology.

Gilead, I., 1994, "The History of the Chalcolithic Settlement in the Nahal Beer Sheva Area: The Radiocarbon Aspect." *Bulletin of the American Schools of Oriental Research* 296:1-13.

Levy, T. E. and S. Shalev, 1989, "Prehistoric Metalworking in the Southern Levant: Archaeometallurgical and Social Perspectives." *World Archaeology* 20/3:352-72

Namdar, D., 2002, The Copper Industry in the Chalcolithic Period in Israel: The Findings from the Site of Give'at Ha'Oranim. *Department of Archaeology and Ancient Near Eastern Civilizations*. Tel-Aviv University.

Shalev, S. and J. P. Northover, 1993 ,"The Metallurgy of the Nahal Mishmar Hoard Reconsidered." *Archaeometry* 35:35-47.

Shugar, A. N., 2000, Archaeometallurgical Investigations of the Chalcolithic Site of Abu Matar, Israel: A Reassessment of Technology and its Implications for the Ghassulian Culture. *Institute of Archaeology*. London: University College London.

Stuiver, M. and P. J. Reimer, "Extended ^{14}C Data Base and Revised CALIB 3.0 ^{14}C Age Calibration Program." *Radiocarbon* 35/1:215-230.

Stuiver, M., P. J. Reimer, E. Bard, J. W. Beck, G. S. Burr, K. A. Hughen, B. Kromer, F. G. McCormac, J. van der Plicht and M. Spurk, 1998, "INTCAL98 Radiocarbon Age Calibration, 24,000-0 cal BP." *Radiocarbon* 40/3:1041-1083.

EARLY CHINESE SCISSORS AND SHEARS: CATEGORY, DESIGN AND SHAPE: A METALLURGICAL STUDY

Aaron Shugar*, Mike Notis, Laura Limata, DongNing Wong, Parsaoran Hutapea
Archaeometallurgy Laboratory, Lehigh University, Bethlehem, PA 18015 USA
*Smithsonian Center for Materials Research and Education, Suitland, MD 20746 USA

Han Rubin
Beijing University of Iron and Steel Technology, China

1. INTRODUCTION

The earliest scissors or shears known in China come from the early Han dynasty and are comparable in chronology to the earliest Roman shears. These utilitarian objects are typically made of iron and their designs and shapes differ chronologically and by geographic region.

We have previously reported on a number of shears found in Roman context identifying unique aspects of material control and ergonomic design choices (Notis, 2003:109-118). For this present study, we have been able to investigate and perform metallographic studies on a total of nine scissors or shears from ancient China (7 from the Beijing University of Iron and Steel Technology and 2 from the Royal Ontario Museum).

Iron from China is known to derive from a two main processing methods. One is the production of bloomery iron, a solid state process. The other is to decarburize molten cast iron to steel.

2. RESULTS

A summary of all results and observations is presented in table 1. This study has produced examples of both types of iron production illustrated in the microstructures of figures 1 and 2. figure 1 displays object 706, one of the samples on loan from Beijing University. The absence of slag is a strong indication of the use of decarburization of a cast iron to produce these objects (Wagner, 1993: 472). Also note the fine ferrite grains interspersed with pearlite of large interlamellar spacing. Figure 2 displays the shears from the Royal

Ontario Museum. In this sample, the presence of slag indicates the use of bloomery wrought iron for its manufacture. The pearlite fraction is much smaller indicating a lower overall carbon content.

Sample #	Provenance	Observations	References and Notes about the sample
706	Zhengzhou, Henan, DongShiMa city **Dong [east] Han** (25-220AD)	• partially corroded ferrite • grain boundary corrosion • Very uniform pearlite • **NO SLAG**	• This is the only piece with some microstructure published in ZhongYuanWenWu, 1983 special volume on research thesis of Henan archaeology institution, P239~241
967.246.3	Later Han - 3 Kingdoms (400 AD)	Blade • Cracking Along prior Austenite grain boundaries • cold work lines • Martensite • Single phase silicate Slag Back • Two Phase Slag, silicates • Ferrite and Pearlite • Edges had a higher fraction of pearlite than center • Pearlite is coarser at edges than center	• 13" long • [ROM]
925.25.4	Later Han - 3 Kingdoms (400 AD)	• Remnant pearlite in a ferrite matrix	• 13-5/8 long • [ROM]
122	Louyang, HeNan **Sui Daye JiuNian** (613 AD)	• ferrite grains • Two phase silicate slag inclusions • deformed grains • cold working lines • dual phase morphology with pockets of martensite and pearlite	• From Louyang Longmen Tiguanzhan tomb M1:22 • Two phase silicate slag inclusions • deformed grains • cold working lines • dual phase morphology with pockets of martensite and pearlite
2086	Shanxi, **Tang** (618-907 AD)	Corroded Round Sample • remnant metal – pearlite structure Corroded Rectangular Sample • One phase silicate slag • remnant metal • pearlite • corroded Widmanstatten ferrite	• The museum of Shanxi offered these broken iron scissor pieces for analysis. • No further related field report. • No publication on this piece.
2087	Shanxi, **Tang** (618-907 AD)	• corroded fyalite/silicate slag inclusions • Fully corroded sample with remnant metal	• The sample came from the same source as the one above, 2086. • No more details on the piece.
118	Louyang, **Tang XingYuan YuanNian** (784 AD)	• Grain Boundary Corrosion • Uniform Corrosion • Elongated two phase silicate slag • Ferrite • Martensite • Neuman Bands • Pearlite • Similar to 122, dual phase morphology with pockets of martensite and pearlite	• The sample was from excavated tomb M76:15 at 162 sites in Louyang, Henan Province. • The mounted piece was taken from the sharp tip of the scissors • The lab analysis was reported in Wang Ke's Master Thesis. • WenWuCanKaoZiLiao 1956 (Vol. 5) p. 41~44
220	Liaoning, **Bei [north] Song** (960-1127AD)	• Corrosion layer contains remnant metal • Two phase silicate slag	• Excavated from M7 tomb at Faku Yemaotai. • Taken from the sharp blade tip. • The scissors was severely corroded and was not in good shape to take more photos • No further related field report referring to this object.

Sample #	Provenance	Observations	References and Notes about the sample
231	Henlongjiang, A-cheng[city] Zhaodongbalicheng, district **Jin** (1115-1234 AD)	• Wrought single phase silicate slag • ferrite in center • pearlite at edge • martensite at edges • very non uniform structure • grain size variation • Two Phase Slag	• Published field report In KaoGu 1960 Vol 2 p. 36~41 • No details about the scissors other than listing

Table 1. Compiled results of the collection of scissors and shears studied. Objects are listed in chronological order from the earliest to the latest.

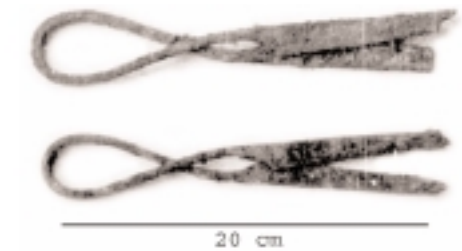

1(A)

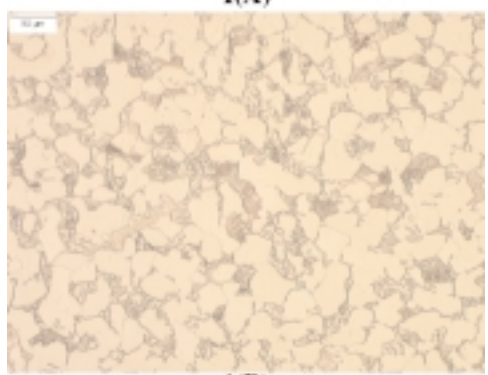

1(B)

Figure 1. A) Sample 706 was taken from one of the two shears above, both excavated together [2]. **B)** LOM micrograph of the microstructure from sample 706. Note the absence of slag and the large pearlite lamellar spacing indicative of a decarburized cast iron. Etched 4% Picral, unpolarized light.

3. DISCUSSION

Both the Chinese and the Roman smiths made a conscious decision to use iron rather than bronze in the blades. This was an understandable

2(A)

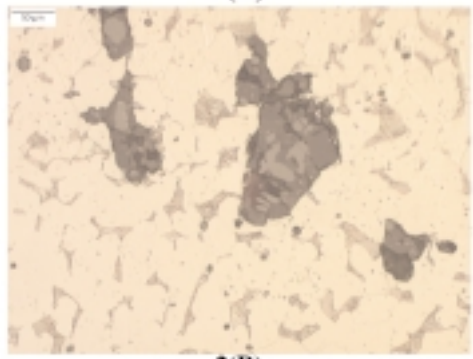

2(B)

Figure 2. A) Photo of shears from the ROM (photo copyright of the ROM). **B)** LOM micrograph of the microstructure of the sample taken from the back of the shears. Note the large slag inclusions characteristic of a wrought iron. Etched 4% Picral, unpolarized light.

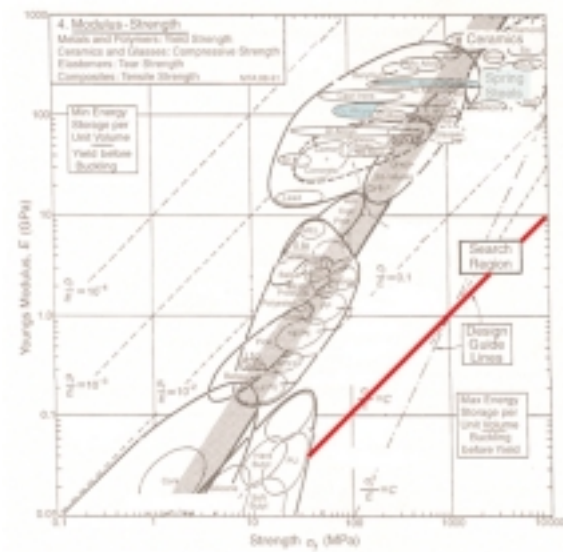

Figure 3. Material selection plot for springs. The selection criteria line is shown in red, both materials are shown in blue. It is clear that steels are an order of magnitude better than copper alloys using the selection index s/E.

choice based on the material selection plot in figure 3. Steels and irons have almost an order of magnitude better flexibility vs. strength based on the selection index for spring design (σ/E).

However, a major difference is seen in the design shape chosen for the Chinese and Roman shears. Figures 4 and 5 are finite element analysis (FEA) maps showing the differences in stress distribution between the Roman and Chinese designs. The Roman smiths chose a design that resulted in tension at the highest stress locations (figure 4a, b). Although the maximum stress is on the inside of the bend in the Chinese design, it also resulted in tension (figure 5 a, b). The Chinese design may be based on the superior quality of iron being used in production.

Early Chinese scissors and shears were designed from a single piece on metal, while early Roman scissors and shears were formed from separate pieces of metal either riveted or forge welded together (Notis, 2003:109-118). There was no evidence for weld or forge lines, or of intentional hardening in the samples studied.

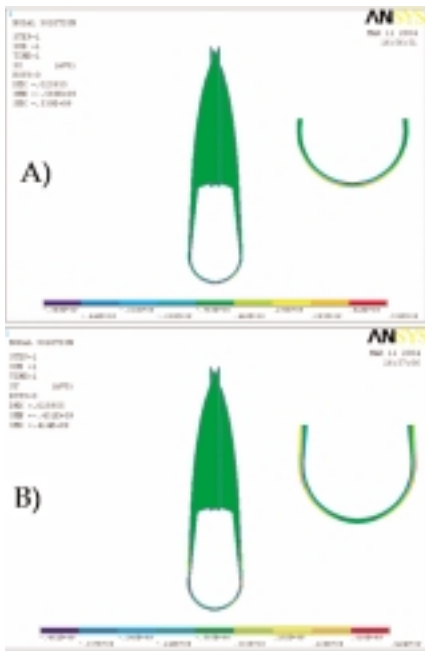

Figure 4. Finite element analysis stress maps for Roman shear design. Stresses for x component are shown in A) and stresses for y component are shown in B).

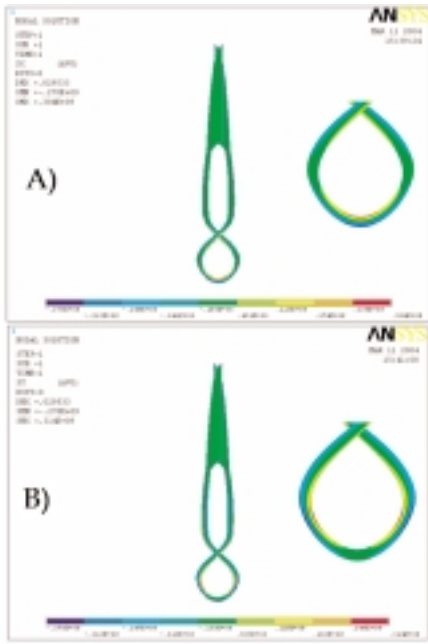

Figure 5. Finite element analysis stress maps for Chinese shear design. Stresses for x component are shown in A) and stresses for y component are shown in B).

Based on this research, Chinese scissors and shears were manufactured in the following manner; First, the iron was produced with of the two ways mentioned above; either the iron was cast as thin rods and decarburized, or the wrought iron was shaped into rods. Second, the rod would be bent into shape and the blade would be flattened and sharpened. This technique is different than the observed early Roman technique of manufacturing two different types of steel, a softer and more ductile ferrite for the spring, and a harder, more wear resistant martensite for the blade (Notis, 2003:109-118). Whereas the Roman design has a harder, sharper blade, the Chinese design is unique because it's inherent resistance to fracture under stress.

4. CONCLUSIONS

Chinese iron smiths used a very different iron production process than Roman smiths. The decarburization of iron resulted in a slag free and higher quality material. Because the materials were inherently different, the designs are also different. This study highlights how basic metallography can be used to recreate an ancient smith's process.

REFERENCES

Notis, Mike R. and Aaron N. Shugar. "Roman shears: metallography, composition and a historical approach to investigation." International conference Archaeometallurgy in Europe, 24-26 Sept 2003, Milan, Italy: Proceedings Vol. 1, Associazione Italiana di Metallurgia (2003) Pg 109-118.

Wagner, Donald. *Iron and Steel in Ancient China*. (1993), p. 472 (Translation 6.14).

IRON SMELTING SLAG FORMATION AT TELL HAMMEH (AZ-ZARQA), JORDAN

Xander Veldhuijzen and Thilo Rehren

Institute of Archaeology, University College London, United Kingdom

1. ARCHAEOLOGICAL BACKGROUND

At Tell Hammeh (az-Zarqa), Jordan, a wide range of metallurgical debris from an early iron smelting operation (ca. 930 CalBC) was excavated (van der Steen 1997; van der Steen 1997; van der Steen 2001; van der Steen 2001; van der Steen 2001; van der Steen 2003; van der Steen 2003; van der Steen 2003; Veldhuijzen 1998; Veldhuijzen 1998; Veldhuijzen 1998; Veldhuijzen 2000; Veldhuijzen and van der Steen 1999; Veldhuijzen and van der Steen 1999; Veldhuijzen and van der Steen 2000). Tell Hammeh is a relatively small site in northern Jordan, located where the Zarqa river valley opens into the Jordan Valley. It is close to several of the larger tells in this part of the Jordan Valley as well as the main iron ore deposit of the wider region at Mugharet al-Warda (Abu-Ajamieh *et al.* 1988; Bender 1968).

Several periods have been attested at the site, starting with Chalcolithic (ca. 4500-3000 BC) and Early Bronze Age (ca. 3000-2000 BC) material, followed by more substantial layers of Late Bronze Age (ca. 1600-1150 BC) material, to Iron Age I (ca. 1150-1000/900 BC) and Iron Age II (ca. 1000/900-586 BC) (van der Steen 2003).

It is at the transition of Iron Age I and Iron Age II that metallurgical activity took place at the site. As iron production finds predating the Roman period are very rare in the Near East, Hammeh allows a unique insight into the earliest developments of iron smelting technology in this region.

2. THE IRON PRODUCTION PHASE

The large deposit of iron production debris at Hammeh forms a stratigraphically well defined phase. It has a complex internal layering, possibly indicating seasonal activity over an extended period of time.

Based on elevation levels of the remaining tell, half or more of the original production area may have been lost due to bulldozer activity. Less

than 7% of the projected production area has been excavated, yielding roughly 500 kg of slag. The excavated area reveals no indication of domestic or non-metallurgical use of the site, nor of any distinct activity areas, except possible furnace structures.

Radiocarbon analysis of two charcoal samples (identified by Eleni Asouti as olive wood (*Olea europaea*), pers. comm.), provides a date at 930/910 Cal BC (±40 years; 1 sigma ranges of 1000-900 and 940-850 Cal BC; AMS Analysis with C13-C12 correction). With due caution (see: "van Strydonck *et al.* 1999), these dates place Hammeh among the earliest known finds of iron smelting in the Near East (Pleiner 2000; Pleiner 2000; Pleiner 2000; Snodgrass 1980 p.338; Waldbaum 1999). Taking these dates as a *terminus post quem*, production at Hammeh may cover a period from around 910 BC to ca. 800 BC.

3. CLASSIFICATION

Initial classification of the finds took place during excavation, based on macroscopic features that can be observed in the field such as colour, shape, presence or absence of rust, flow patterns, and surface inclusions (Bachmann 1982 p. 2-6; pers. comm.; Sperl 1980; Sperl 1980). This was examined further using various laboratory techniques (Veldhuijzen and Rehren 2005).

Several types of material were identified, the bulk consisting of slag and tuyère fragments. The slag types range from black/grey, free flowing slag (tap slag; ca. 50%), through less dense glassy slag (possible ceramic origin) and plano/concavo-convex slag-cakes (furnace bottom and possible primary smithing) to rusty lumps (bloomery furnace mess; ca. 45%). The non-slag material ranges from tuyère fragments (approx. 350) to charcoal and possible furnace structures. The tuyère fragments are characterised by a vitrified nozzle and a 5 x 5 cm square section with a 1 cm bore (Veldhuijzen in press).

4. SLAG FORMATION

AAnalyses of the main type of slag demonstrate that clay is a major contributor to the slag formation in the Hammeh iron smelting process (Veldhuijzen 2003; See also: Serneels and Crew 1997; Crew 2000).

Mass balance calculations, based on a haematite ore sample from Warda and smelting tap slag from Hammeh (see table 1), indicate that 100 kg of ore contain theoretically enough wüstite (FeO) to enable the production of ca. 48 kg metallic iron, while retaining 38 kg of slag of an iron oxide level comparable to the Hammeh slag. Other oxide components in this theoretical slag, however, do not match the actual slag composition, particularly in their lime content, which is too high, and alumina levels, which are too low. The addition of a further ca. 20 kg of local and tuyère clay to the system,

simulating the absorption of furnace wall and tuyère material, balances the theoretical and archaeological slag composition much more closely.

	SiO_2	Al_2O_3	FeO	TiO_2	MnO	CaO	MgO	K_2O	P_2O_5	S
Mugharet al-Warda Ore	8.50	0.38	82.32	0.07	0.05	8.29	0.15	0.03	0.21	0.00
Local Clay/Tuyère average (3 samples)	58.76	12.13	5.05	1.05	0.05	17.04	2.54	2.82	0.32	0.24
Hammeh Tap Slag average (6 samples)	24.05	5.47	52.80	0.31	1.32	11.26	2.30	0.74	1.42	0.33
Hypothetical slag ceramic-free	22.98	1.03	52.20	0.18	0.15	22.39	0.41	0.09	0.56	0.00
Hypothetical slag with ca 20 kg ceramic	26.31	3.65	52.37	0.36	0.08	15.19	0.86	0.77	0.35	0.06

Table 1. Main components of Hammeh slag formation related materials (Warda ore, local clay and tuyère ceramic), actual Hammeh slag, hypothetical ceramic-free slag and hypothetical slag with ca. 20 kg of ceramic contribution. Results are expressed in weight % and normalised to 100%. Samples were measured by (P)ED-XRF on Spectro XLab Pro 2000 with "Slag_fun" calibration method (Veldhuijzen 2003). See text for details on hypothetical slag composition.

This addition though reduces the iron metal yield to ca. 33 kg, i.e. less than 2/3 of the amount calculated without the addition of ceramic. While there is little doubt that a major ceramic contribution did in fact occur during the smelting operation, one wonders why the design in particular of the tuyères was done in such a way as to actually promote the absorption of ceramic material, which reduces the iron yield.

5. DISCUSSION

One possible explanation for this seemingly counter-productive feature may be found in the relevant phase diagram CaO-FeO-SiO_2 (see figure 1), and in particular in the morphology of the liquidus surface of this system.

The hypothetical ceramic-free slag has been calculated to about 20 wt% SiO_2, 50 wt% FeO and 20 wt% CaO; alumina being a major contributor to the remaining 10 wt%, but not exceeding 2 wt% on its own. Reducing such a slag to its three main components (or rather six, adding Al_2O_3 to SiO_2, MnO to FeO and MgO to CaO) and plotting it into the phase diagram indicates a melting temperature in excess of 1250 °C, probably beyond the thermal ability of an early furnace and the thermal refractority of the local clay.

The addition of clay/ceramic to the system, in quantities of ca. 1/5 of the ore weight, lowers the estimated liquidus temperature to around 1120 °C if not less, much more in line with the assumed performance characteristics of

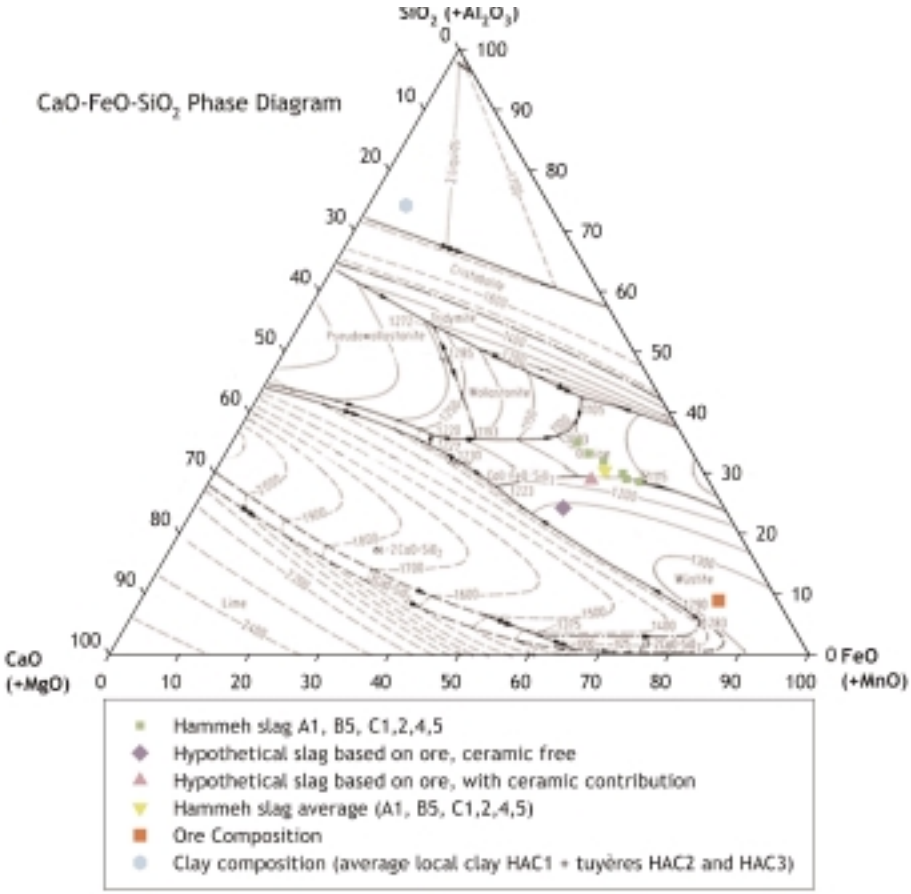

Figure 1. CaO-FeO-SiO2 Phase diagram. Plotted are six Hammeh tap slag (in green) and their average composition (yellow), the local ore (red) and average local clay/ceramic composition (light blue), the hypothetical, ceramic free slag (dark blue) and the hypothetical slag when ca. 20 kg of local ceramic is added to the system (purple) (for numerical values see table 1); values are plotted with MgO added to CaO, MnO added to FeO and Al_2O_3 added to SiO_2.

an early furnace. This difference of ca. 100 °C makes the difference between thermal survival of the technical ceramic and fuel consumption and sufficient fluidity to allow the metal/slag separation to occur.

ACKNOWLEDGEMENTS

Excavations at Tell Hammeh (az-Zarqa) are part of the *Deir ᶜAlla Regional Project*, a joint undertaking of Leiden University (the Netherlands) and Yarmouk University (Jordan) in conjunction with the Department of Antiquities of Jordan.

Study of the material is part of ongoing PhD research, carried out at the Wolfson Archaeological Science Laboratories, Institute of Archaeology, UCL. It is sponsored by BHP Billiton through the Institute for Archaeo-Metallurgical Studies (IAMS).

REFERENCES

Abu-Ajamieh, M.M., Bender, F.K. and Eicher, R.N. 1988. Natural Resources in Jordan, Inventory-Evaluation-Development Program. Amman: Natural Resources Authority .

Bachmann, H.-G. 1982. The Identification of Slags from Archaeological Sites. Occasional Publication 6 London: Institute of Archaeology Occasional Publication 6.

Crew, P. 2000. The influence of clay and charcoal ash on bloomery slags. in Tizzoni, C.C. and Tizzoni, M., (Eds). 38-48.

Pigott, V.C. (1999) The archaeometallurgy of the Asian Old World. Ephrata, Pennsylvania: University Museum, University of Pennsylvania.

Pleiner, R. 2000. Iron In Archaeology. The European Bloomery Smelters. Praque: Archeologick_ Ústav Av Cr.

Serneels, V. and Crew, P. 1997. Ore-slag relationships from experimentally smelted bog-iron ore. in Crew, P. and Crew, S., (Eds). 78-82. Maentwrog: Plas Tan y Bwlch Occasional Paper 3.

Tizzoni, C.C. and Tizzoni, M. (2000) Il ferro nelle alpi. Giacimenti, miniere e metallurgia dall' antichità al XVI secolo. Atti del convegno/Iron in the alps. Deposits, mines and metallurgy from antiquity to the XVI century. Proceedings of the conference. Bienno: Commune di Bienno.

van der Steen, E.J. 2001. Excavations at Tell el-Hammeh. Studies in the History and Archaeology of Jordan VII, 229-232.

van der Steen, E.J. 2003. Tribes and Territories in Transition: the central East Jordan Valley and surrounding regions in the Late Bronze and Early Iron Ages: a study of the sources. Groningen: Rijksuniversiteit Groningen.

van Strydonck, M., Nelson, D.E., Crombé, P., Bronk Ramsey, C., Scott, E.M., van der Plicht, J. and Hedges, R.E.M. 1999. What's in a 14C Date. Rapport du Groupe de travail : Les limites de méthode du carbone 14 appliquée à l'archéologie, 433-440. Rennes: Mémoires de la Société Préhistorique Française, XXVI, 1999 et Supplément 1999 de la Revue d'Archéométrie.

Veldhuijzen, H.A. 1998. Early Iron Smelting. Analysis and Interpretation of Late Iron Age Iron Smelting Remains from Tell Hammeh az-Zarqa, Jordan. Leiden: Leiden University, Faculty of Archaeology, unpublished M.A. Thesis.

Veldhuijzen, H.A. 2003. 'Slag_Fun' - A New Tool for Archaeometallurgy: Development of an Analytical (P)ED-XRF Method for Iron-Rich Materials. PIA (Papers from the Institute of Archaeology) 14, 102-118.

Veldhuijzen, H.A. 2004 (in press). Technical Ceramics in Early Iron Smelting. The Role of Ceramics in the Early First Millennium BC Iron Production at Tell Hammeh

(az-Zarqa), Jordan. In Proceedings of EMAC '03, (Ed.). Série Monográfica, Instituto Português de Arqueologia (IPA).

Veldhuijzen, H.A. and Rehren, Th. 2005 (submitted). Early Evidence for Iron Smelting in Jordan; how classification in the field relates to analyses in the laboratory. IAMS Journal 25. London: Institute for Archaeo-Metallurgical Studies.

Veldhuijzen, H.A. and van der Steen, E.J. 1999. Iron Production Center Found in the Jordan Valley. Near Eastern Archaeology 62 (3), 195-199.

Waldbaum, J.C. 1999. The Coming of Iron in the Eastern Mediterranean. Thirty years of Archaeological and Technological Research. in Pigott, V.C., (Ed.). 16, 27-57. Philadelphia: MASCA, University Museum, University of Pennsylvania.

4. TECHNOLOGY AND PROVENANCE OF STONE, PIGMENTS AND PLASTERS

INDEX

SCIENTIFIC STUDY OF GRÆCO-ROMAN WALL PLASTERS & PIGMENTS IN ALEXANDRIA, EGYPT

Dr. Safaa Abd El Salam
University of Alexandria, Faculty of Fine Arts, Department of Painting,
Mural Painting Section

1. RESEARCH OBJECTIVES

Samples of wall plasters were collected from the remains of a painted tomb, dated to the second century BC, uncovered in the region of the western cemetery of the ancient city in 1960 (Venit 1988: 71-91). The paintings are installed in the Græco-Roman museum in Alexandria, where all but one is currently on view (photographs 1 & 2). Some other samples from the Græco-Roman museum have been collected from the temple of El-Tamsah, dated to the late Greek period and other samples from the fragment of El-Gabbary (photograph 3) and from Kom El Sokafa, dated to Roman times (photograph 4). The scheme of decoration and the colours used for painting were executed on a thin, or sometimes, thick layer of plaster and on layers of *stucco* applied to the stone, in the *fresco* technique (Brown 1957 & Hassen 1963). The colours used were; blue, black and brown, also red brown tending to violet or red violet and yellow.

2. THE METHODOLOGY USED TO IDENTIFY THE PLASTERS & PIGMENTS

The methods used to identify the plasters and pigments were:

— Examination using microscopy (10X) and cross-section.

— Micro-chemical analysis; water-soluble salt to identify sulphate, chloride, carbonate, nitrite and nitrate and measurement of calcium carbonate.

— Scanning electron microscope and energy dispersive spectroscopy (SEM & EDS).

— Inductively coupled plasma optical emission spectrometry (ICP-OES).

— X-ray diffraction to identify the mineralogical compound of the pigments used.

— Polarized light microscope (PLM).

1

2

3

4

Photograph 1 shows the remains of El Wardian Necropolis, No 27029. The measurements of the paintings are: 1 about 137 X 187 cm, 2 " 58 X 187 cm, 3 " 46 X 187 cm. 2, shows different fragment from the same El Wardian Necropolis, the size is 75 X 117 cm, No 27031. No 3, fragment from Gabbary, the size is; 90 X 183 cm, No 3772. No 4, fragment from Kom El Sokafa, the size is; 75 X 117 cm, No 372. Graeco-Roman Museum, Alexandria, Egypt.

3. RESULTS & SIGNIFICANCE OF THE STUDY FOR ARCHAEOLOGICAL SCIENCE

The results showed that the plasters/mortars used were a lime plaster/mortar, a mixture of lime/chalk/marble (identified by spot test) containing fossil shell, with very fine grain size quartz and some other minerals. The painted layer was covered with a very thin layer of calcite film, indicating *boun fresco* techniques and/or *fresco secco*. The plaster/mortar was calcareous.

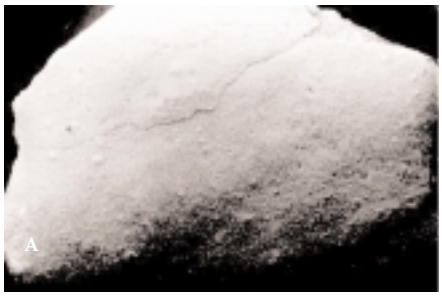

15 KV X 0.9.6 Bar is1.04 μm.

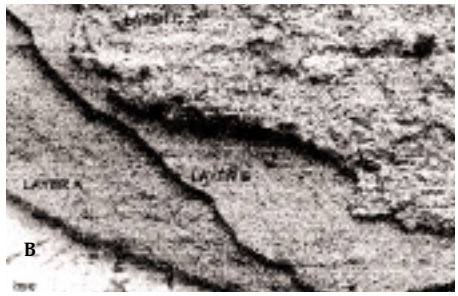

15 KV X 032 Bar is 313 μm.

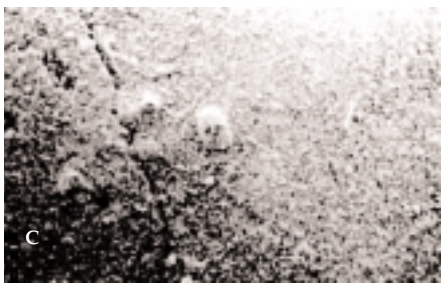

15 KV X 032 Bar is 0288 μm.

15 KV X 104 Bar is 96.2 μm.

Photographs 4 A-C show the plaster (S. 6). A shows the surface structure, notice the micro-crack, B shows the stratigraphy of the plaster, which consisted of three layers. C is a detail of A, the clear patch in the middle, the elements shown on the surface are; P, S, Ca, Si & Au. D shows a detail of C.

3.1. The Results of Analysis of Water-Soluble Salts

The weight of the samples used was 2 g. The results of analyses indicated that the most significant salts were found in S. TTAL/L were chlorides and nitrates (as illustrated in table 1), due to the weathering decay, as the temple is displayed in the museum garden.

Samples No	Sulphates	Chlorides	Nitrates	% Dissolved
S. 27029/M	+-	+	+-	2.78
S.3772/M	+-	+-	+	1.46
TT Al/L	+-	++	++	2.88

+-= Traces + = Present ++= Notably present L= Limestone M=Mortar

Table 1.

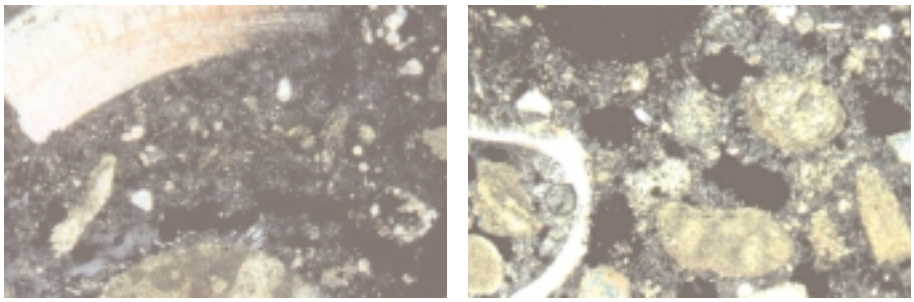

A (2.6) No 3726 B

Photographs 5 A & B (S.6) of fragments from Kom El Sokafa; show the internal structure of the plaster. A shows a shell fragment on top left & intraclasts. B shows calcareous algae, superficial oolitic & shell fragment. Magnification 40 X.

Chlorides, seawater contains small amounts of sulphates, especially of magnesium. Sea spray can deposit sulphates on a surface. The presence of nitrites suggested an old burial or recent formation, which may originate from the contamination source. It can be assumed that the presence of nitrates is a result of the oxidation of nitrites. Chlorides, sulphates and nitrates are commonly found coming from different sources. Another possibility is that the materials used in the preparation of mortars and plasters can contain small quantities of sulphates as impurities e.g. sand, which can dissolve in water as efflorescence, leading to the presence of sulphates. Nitrates could result from the decomposition of extraneous organic materials or from old burials. However, nitrites are not found frequently in wall painting (Teutonico 1988: 60)

3.2. The Results of the Measurement of Calcium Carbonate ($CaCO_3$)

As the plaster/mortar was totally calcareous, the samples dissolved completely in HCl.

3.3. The Results of Inductively Coupled Plasma Spectroscopy

The results from the powdered samples show very high amounts of metal ions in S. TTAL/P. The most significant results were obtained where I found high amounts of ions, in particular sodium (Na) and iron (Fe). It is possible to compare the result of both powdered and dissolved samples as illustrated in Graph 1, to see which ions have dissolved, as a result of extraction calcium (Ca), sodium (Na), potassium (K) and in some instances magnesium (Mg), and iron (Fe) were the most important elements present in

powdered samples. However, the solution results have indicated that the highest ions were mainly Ca and Na. In addition to K and Mg in S. TTAL/S.

3.4. SEM & EDS Results

The results of the polished cross sections show variation of the elemental structure, carried out on three samples from the fragments; No 27031 (S. 7), (S. 6) No 3726 & (S. 4 & S. 5) No 3772. It was interesting to find a difference between the samples. Broken and polished sections show the composition and structure of samples from the fragment No 27031. Broken section did not provided any more information compared with a polished one, which was quite interesting, showing high element counts on the polished section of: - S, Ca, P & Si, also shown on all polished samples. Analysis has shown a smooth area on the back of S. 7, No 27031 indicating a white lump. The highest counts of Ca, P, Si, S and also Fe & Al on some areas. The most important sample was S. 6, No 3726, as the structure of the plaster contained three layers (photographs 4 A-C), analysis being carried out on both sides. Notice the micro cracks on this sample.

From the results of EDS which was carried out on different areas and measurements of the soluble ions, it can be conclude that the most important ions in the composition structures of the samples, given by EDS, are Ca, S, Si, K, Cl, with little exchange between Ca, S, Si on the surfaces analysed, but both Ca and S are the most common. Energy dispersive spectroscopy (EDS) gives a measure of the leaching of the soluble ions.

3.5. The Result of Polarized Light Microscope (PLM)

The identification of the samples from the Graeco-Roman museum has shown that the structures of the plasters/mortars in S. 6 (No 3726) contained calcareous algal, intraclasts, quartz grain, foraminifera, shell fragment, and superficial oolitic limestone as shown on Photographs 5. However, the sample of limestone from El-Temsah S. TTAL, contained foraminifera, shell fragments, little algae, fine grain quartz, charinpers (which live on surface on the water). The presence of microfossils and shell fragments were visible, but with variation of the organism types found due to the geological source, which were found in samples from Alexandrian sites in a previous study by the author (Abd El Salam 1999 & 2001).

3.6. XRD Identification

Samples showed the presence of calcium carbonate $CaCO_3$ (calcite) from the plaster, which indicated to the *fresco* technique. It was very difficult to

distinguish whether if it was *buon fresco* or *fresco secco*, more research would be required to see if any organic materials were used in terms of *secco* painting, as it seems to be used especially on the fragment in photograph 2 No 27031. The pigments were those traditionally used in ancient as well as classical times (Profi & *et al* 1974, Filippakis & *et al* 1997, Járó 1997, Segal & Porat 1997, Calamiotou & *et al*. 1983). The differences found may be related to the impurities as well as the geological sources of the pigments used, natural or artificially produced, compared with those related to the Alexandrian sites (Abd El Salam 2001).

ACKNOWLEDGMENT

My sincerest thanks to Dr. Ahmed Abd El Fatiah, who was the Director of the Alexandria Museum and to Mrs. America Abu Baker, who was the Head of the Conservation Department in the Alexandria Museum (when I had the sample in 1997). Thanks to Dr. Graham Morgan at the University of Leicester for X-RD analysis and Ms Emma Mansely for ICP analyses. I also thank Mr. George McTurk of the University of Leicester for SEM & EDS analyses.

REFERENCES

Abd El Salam, S. 1999. Analytical techniques used in the examination of materials of wall paintings from the Ancient sites of Mustafa Pasha and Anfushi in Alexandria. In C. Parisi, S. Galiardi, G. M. Parisi and G. Torcinaro (eds), *6th international conference on Non-Destructive Testing and Microanalysis for the Diagnostic and Conservation of the Cultural and Environmental Heritage,* Vol. 1: 449-46, Rome: I.C.R. and AIPnD.

Abd El Salam, S. 2001. Egyptian & Græco-Roman Wall Plasters/Mortars: A Comparative Scientific Study University of Leicester, School of Archaeological Studies, Ph.D. Thesis.

Brown, R. B. 1957. *Ptolemaic Painting and Mosaics and the Alexandrian Style*, U.S.A, Cambridge Archaeological Institute of America.

Calamiotou, M.; Siganidou, M., and Filippakis, S. E. 1983. X-Ray analysis of pigments from Pella, Greece, *Studies in Conservation*, Vol. 28, No. 3: 117-121.

Filippakis, S. E.; Perdikatsis, B., and Assimenos, K. 1979. X-Ray analysis of pigments from Vergina, Greece (second tomb), *Studies in Conservation*, Vol. 24, No. 2: 54-58.

Hassen, M. A. 1963. *History of Alexandria and Its Civilization since Old Centuries*, Egypt: Alexandria's Council (In Arabic).

Járó, M. 1997. Comparison of the painting materials used for wall painting in four sites of the Roman Province Pannonia. In Béarat. H. , Fuchs M. , Maggetti M. , and Paunier D. (eds), *Roman Wall Painting: Materials, Techniques, Analysis and Conservation*: 75-84, Proceedings of the International Workshops, Fribourg: Institute of Mineralogy and Petrography.

Profi, S.; Weier, L., and Filippakis, S. E. 1974. X-Ray analysis of Greek Bronze age pigments from Mycenae, *Studies in Conservation*, Vol. 19, No. 2: 105-112.

Segal, I., and Porat, N. 1997. Composition of pigments from the Hellenistic wall in Acre. In Béarat. H., Fuchs M., Maggetti M., and Paunier D. (eds), *Roman Wall Painting: Materials, Techniques, Analysis and Conservation*: 93-104, Proceedings of the International Workshops, Fribourg: Institute of Mineralogy and Petrography.

Teutonico, J. M. 1988. *A Laboratory Manual for Architectural Conservators*, Rome: ICCROM.

Venit, Marjorie Susan. 1988. The painted tomb from Wardian and the Decoration of Alexandrian tombs: *Journal of the American research centre in Egypt*, Vol. XXV, 71-91.

NON-DESTRUCTIVE RAMAN CHARACTERISATION OF PIGMENT ON BYZANTINE FRESCOES IN SOME CAVE CHURCHES OF SALENTO (PUGLIA, ITALY)

G. E. De Benedetto, R. Vatinno
Dipartimento dei Beni delle Arti e della Storia, Università di Lecce, viale San Nicola, I - 73100 Lecce

1. INTRODUCTION

Lecce Province (Puglia, Italy) has a wealth of extraordinary cave churches [1]. These churches, most of which have been dated to the X-XII centuries, are Byzantine and deserve a permanent interest as relevant to one of the greatest artistic periods in south Puglia.

The wall paintings, the substrates and the masonry of the ecclesiastical structures raise several problems for conservators and scientists, since pollution, micro-organisms, temperature and humidity have disastrous effects on the stability and integrity of the artworks. More subtle changes arising from the presence of human beings, e.g. soot and hydrocarbons from smoking lamps and candles, reactivity of body vapours and perspiration and the instability of the pigments or pigment mixtures with time, also produce dramatic deterioration in wall paintings. Moreover most of these churches are under the road level and these problems are often greater. Conservation of mediaeval wall paintings is subject to the same basic principles as other branches of conservation: preservation is the prime objective. However, it is of primary importance to determine both the chemical and physical nature of the materials employed and the substrate in the planning of a satisfactory conservation strategy. The relevant knowledge should be preferably gathered by non-destructive techniques, which leave the sample intact for further analyses. Among the non-destructive techniques, Raman spectroscopy has found in the last decades many applications in the field of cultural heritage [2] and frescoes are among the different analyzed artefacts [3].

Main features of the micro-Raman technique are high spatial resolution and low penetration depth for non-transparent samples, both in the micron range; in pigment analysis, the microscope objective focuses the laser beam

on the sample in order to exclude signals from the medium matrix surrounding the pigment grain. The technique does not usually require any sample pre-treatment, and it can be considered non-invasive for small or flat objects (such as book pages), which can be put directly on the stage under the objective of a conventional microscope without previous sampling; however, when sampling is necessary, the amount of sample required is limited and the technique can just be considered micro-destructive. To avoid sampling at all, instruments for Raman microscopy based on fibre optics technology have been recently developed: they can be used for in situ analysis and do not suffer from any limitation about the size of the analysed object. Such characteristics in a transportable instrument can constitute a major advantage in the non-invasive analysis of pigments used in wall paintings. This poster reports on the use of a mobile micro-Raman equipment for non-destructive in situ identification of the pigments used in the execution of a cycle of frescoes. A series of preliminary diagnostic investigations has been planned as the first step before paintings restoration; non-invasive techniques, among which Raman microscopy plays an essential role in this respect.

2. DESCRIPTION OF THE PAINTINGS

The surviving Byzantine wall-paintings taken into consideration in this paper are located in five different sites: St. Salvatore in Giurdignano, the crypt of St. Stefani in Vaste, St. Solomo (or St. Elena: the dedication is doubtful, figure 1 A) in Uggiano la Chiesa, St. Marina (figure 1 B) in Muro Leccese and the fragments in a chapel in the Acaya castle, near Lecce.

Figure 1. Images of two frescoes found in two different cave churches, whose analyses are herein reported.

The few frescoes still preserved in St. Salvatore are located in the central apse and in the niches along the south and north walls. In apse there are the Virgin and the Child, flanked by two archangels; in the lower part, the

fragments of four nimbi decorated with pearls. Along the walls there are other remains of painted layer: vegetal decoration, and some figures, none of them entirely preserved. They probably dated from the 13th century onwards. To the first fresco layer of the decoration of St. Stefani belong two archaic, monumental and high-quality figures of the apostles Andrew and Philip, painted on the pillars surface (10th century). The 11th-century decorative phase includes the scene in the right apse: Christ flanked by two angels in proskynesis; in the left apse, three saints, stylistically similar to the figures on the right. Other fragments are dated to the 13th and 14th centuries. Very few fragments of the original decoration of the church of St. Solomo remain, but two scenes entirely preserved on the iconostasis, on the naos-side: a 14th-century (1365-66) Virgin with the Child depicted between the right and central aisles; St. Solomo on the opposite side; a later-dated archangel represented on one of the pillars. The building of S. Marina received its decoration in two important moments: in the 10th century (S. Barbara and the scene of the Ascension). To the 11th century belong the saints in the intrados of the arches, a Virgin with the Child, and one of the most ancient hagiographic cycle of the Life of St. Nicholas. Eight fragmentary and highly expressive figures of bishops are in the apse: the style and the brilliant and still well-preserved colours of the paintings, indicate a dating around the end of the 11th, or, most probably, to the beginning of the 12th. Few years ago a chapel with fragmentary frescoes was discovered in the Acaya castle, still unpublished, with a 14th-century Koimesis.

3. EXPERIMENTAL

The spectrum collection was carried out with two transportable Renishaw RA 100 micro-Raman instruments, one equipped with a 785 nm diode laser, the other with an Ar 514 nm laser. Both were connected with the measuring probe by means of a fibre-optic cable. To avoid any possible damage, the laser power at the painted surface was kept as low as 1.0 mW. Two long working distance microscope objectives, 20× and 10×, were used to focus the laser beam on the painted surface and to collect the backscattered Raman signals. Exposure time and accumulations were chosen in order to get defined spectra. A silicon standard was used to calibrate the wavelength scale.

The figure 2 shows some spectra of coloured pigments found in different areas of the samples.

4. RESULTS AND DISCUSSION

The colours which were widely employed by the artist were red, yellow, green, blue and black; here, Raman bands were obtained from red

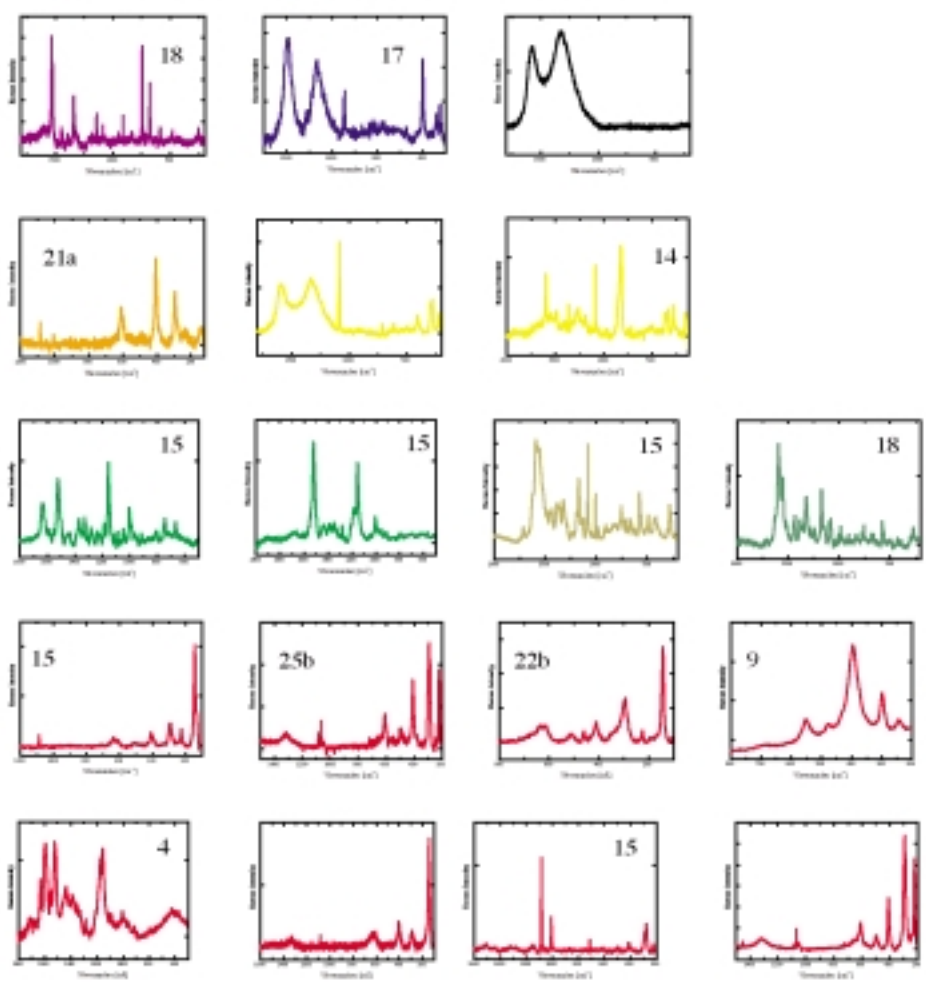

Figure 2. Spectra of coloured pigments in the samples.

areas at 295, 410 and 609 cm^{-1}, matching those of haematite (Fe_2O_3, anhydrous iron oxide) and at 301 and 391 cm^{-1} from yellow areas, matching bands of goethite (FeO(OH), iron oxyhydroxide): these iron compounds are the main colouring agents in red and yellow ochres, respectively. Black has been identified as carbon black by the presence of two broad bands at about 1320 and 1600 cm^{-1}. It may be interesting to observe that carbon black is found again in some other colours, like blue, and it is the only black pigment surely identified in the frescoes; ochres, on the other hand, are usually replaced by, or appear together with, other red and yellow pigments. As to white lead, it was also identified in white areas as the sole pigment present. In green areas, the yellow pigment

might have been mixed with a blue or even a green one. Actually the green pigments which have been identified have not been identified in any of the spots analysed, while bands from azurite (basic copper carbonate, $2CuCO_3 \cdot Cu(OH)_2$) at 248 and 402 cm^{-1} are clearly recognisable in spectra recorded on blue areas, such as the sky in the background of some scenes or some details in minor characters' clothing. No evidence has been obtained for the presence of blue pigments other than azurite but the synthetic phtalocianine blue used in the restoration of St. Stefani: it seems then that an alternative blue pigment, such as the more expensive lapis lazuli, has been deliberately avoided by the artist, perhaps on grounds of cost and availability.

A yellow and a grey area and two red ones gave spectra characterised by two bands at 289 and 545 cm^{-1}, which is possible to ascribe to yellow massicot (orthorhombic PbO) and red lead (Pb_3O_4), respectively. Raman bands from either red lead or massicot alone have never been obtained in the church and this may support the hypothesis that only one of these compounds was the pigment knowingly employed by the painter, while the other could be present as an impurity. An alternative explanation may be that lead mono- and tetroxide formed as byproducts of the light stimulated degradation of lead dioxide (plattnerite, PbO_2). Raman spectra indicate that white lead was used. Raman spectra could therefore indicate the presence of the first intermediate (Pb_3O_4) and the final product (orthorombic PbO) of plattnerite degradation under the laser action. Some Raman bands obtained from areas of different colours can be related to the presence of organic compounds, like the binders. Raman analysis gave also evidence that calcium carbonate sulphation occurred in many areas of the frescoes, as testified by the frequent presence of the main band of calcium sulphate dihydrate (1005 cm^{-1}). Calcium oxalate, carotenoids or chlorophyll are other compounds associated with degradation processes, whose bands have been very often encountered in spectra from different areas of the frescoes.

5. CONCLUSIONS

The use of a transportable micro-Raman equipment enabled the in situ identification of many pigments used in the fresco decoration, without taking any sample from the painted surfaces both originally used by the artists and later on by the restaurateurs. The collected Raman spectra also enabled the identification of some decay products, such as calcium sulphate and oxalate, lichens and their relevant metabolic products.

The research has been carried out with the financial support from CUIS (Consorzio Universitario Interprovinciale Salentino).

REFERENCES

Falla Castelfranchi, M., *Pittura monumentale bizantina in Puglia*, Milano 1991.

Coupry, C.; Brissaud, D., in: G. Turrell, J. Corset (Eds.), *Raman Microscopy, Development and Applications*, Academic Press, London, 1996, 421.

Edwards,H.G.M.; Gwyer, E.R., Tait, J.K.F., *J. Raman Spectrosc*. 28 (1997) 677.

CARPATHIAN OBSIDIANS: MYTH AND REALITY[1]

T. Biró, Katalin
Hungarian National Museum, H-1088 Budapest, Múzeum krt. 14-16.
E-mail: tbk@ace.hu

ABSTRACT

This paper is intended to give a review on the study of Carpathian obsidian. The name implies the only source region in Central Europe, for long, the only source of archaeological obsidian in Continental Europe. Their archaeological, as well as geological research started in the sixties of the 19th century by the activity of pioneering personalities of Hungarian archaeology, geology and archaeometry. By the late 70-ies, separation of Carpathian obsidian sources from other sources of European and other Mediterranean sources could be achieved (investigations of Warren and Williams), and intensive studies continued in the past decades. In spite of several publications devoted to the subject, there are still a lot of clearly erroneous views lingering in technical literature concerning the location of the sources and allocation of archaeological specimens.

The first review of the author on the Carpathian obsidian was published in 1981: in the meantime, several research groups performed smaller or bigger research series on related finds, using various methods of analysis (NAA, EDS, XRF, FTD, PIXE-PIGE and recently, PGAA). Collection of obsidian distribution was completed using reference data as well as analysis of various assemblages dating from Middle Palaeolithic to Iron Age. Distribution maps were compiled for specific periods using percentage values. Access strategies, political implications could be claimed on the basis of changes in distribution areas.

The present study contains a review of recent achievements, prepared for the project IGCP-442 (Raw Materials of Neolithic Artefacts) as well as in the frames of the project "Raw material atlas Non-metallic prehistoric raw materials on the territory of Hungary and adjacent regions" (OTKA- T 025086).

1. INTRODUCTION

Over the glass mountains… This is a regular introduction to a lot of tales in Hungary. Perhaps it is not too much intrusion to the field of ethnography

1. This paper contains the extended version of the lecture presented on the 34th ISA Meeting at Zaragoza, Spain (Biró 2004).

to say that this clause dates back to prehistoric times, notably to the time of rare and distant, legendary obsidian sources.

Obsidian is a spectacular raw material attracting attention both in modern as well as prehistoric times. Archaeological and archaeometrical technical literature as well as hearsay and gossip abounds in references based more on legends than reality. This is the reason why the author decided to summarise again our current knowledge on one of the most important element of prehistoric mineral resources. The name, 'Carpathian obsidian' is misleading in itself as it implies origin from the Carpathes (which is no source for obsidian, being mainly composed of Mesozoic sedimentary rocks and Palaeozoic constituents) or, for a more specific geological (but false) implication, the Carpathian obsidians are not related to the Middle Miocene Carpathian Stage; they were formed in the Late Miocene Sarmatian period and all of the known and archaeologically important occurrences can be found in the Tokaj-Prešov Mountains, in NE Hungary and SE Slovakia, respectively. The term Carpathian obsidian was given by the English scientists performing the first successful fingerprinting studies and became known in international archaeometrical literature; it would no point and useless to fight against this name.

It is, however, necessary to know the raw material exactly and separate from other materials and legendary claims. Some basic facts on obsidian may help in the correct identification.

Obsidian is not a mineral but a rock. It is quenched volcanic rock, natural glass, without specific mineral composition, crystal structure or stoechiometrical formula and exact chemical composition. In course of long time, obsidian will turn to a felsitic volcanic rock with acidic composition (rhyolite) with high SiO_2 content. Typically, obsidian can be found associated with geologically very young volcanic activity, because rock glass is not very stable under surface conditions, will get crystallised or weathered in course of time. At the same time, not all the volcanic glasses can be considered obsidian and even less could be suitable for making stone tools. Not all of the sources referred to as 'obsidian' in geological technical literature yielded workable obsidian. The problem is further complicated by the fact that some of the sources have been exploited or became inaccessible till our days. Claims on non-existing sources, at the same time, can lead to not adequately founded historical conclusions and render the results of the archaeometrical fingerprinting questionable.

2. OBSIDIAN SOURCES WORLD-WIDE

Due to the specific conditions of its formation, obsidian occurs at limited regions. The last synthetical summary based on bibliographical entries by

Hans-Otto Pollmann (Pollmann 1999) resulted in mapping the potential sources all over the World (fig. 1). The source regions are visibly confined to island arches with strong volcanic activity on the contact zone of continents and oceans. Though Hungary is centred in continental Europe, it is well known that similar conditions used to exist here in the Tertiary period. Obsidian was formed here by the end of the Tertiary period.

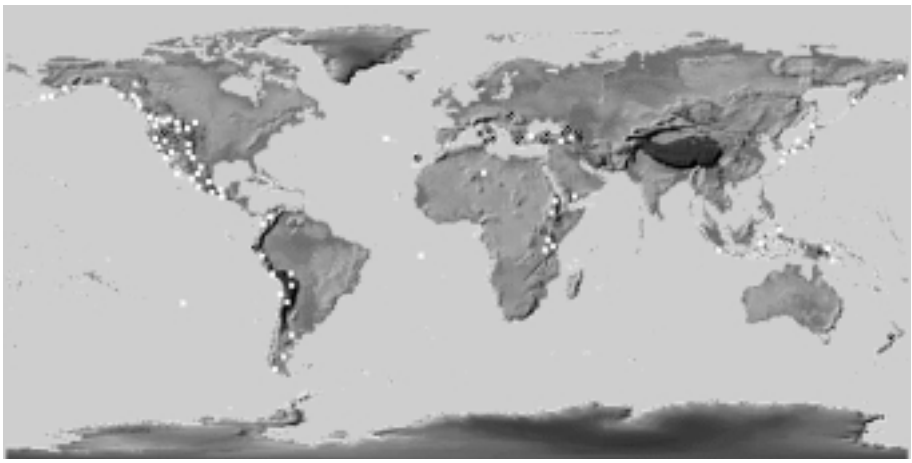

Figure 1. Obsidian geological sources worldwide after H. Pollman. Sources represented in the Lithotheca Collection of the Hungarian National Museum are marked by black dots, other sources with white squares.

Data collection by Pollmann naturally could not aim at a critical review of all cited work, thus the resulting comprehensive map contains a number of 'dots' existing perhaps only in the (modern) legends. These and constant references to non-existing sources compelled the author to collect existing evidence again, separating certain from uncertain and false.

In the comparative raw material collection of the Hungarian National Museum we are making all efforts to collect evidences from existing lithic raw materials sources (Lithotheca-Collection: Biró & Dobosi 1990, Biró & al. 2000a); look after all claims, collect and document the wealth of prehistoric potential raw material sources and try to characterise them in a manner to be recognised in the archaeological lithic industries. Naturally, we are mainly interested in Hungarian raw materials and resources available to the prehistoric population that used to live here. Obsidian is one of the raw materials preferentially collected from all over the world. All of the known European sources are represented in the Collection with abundant samples from the Near East (Anatolia) as well. On fig. 2. the obsidian raw material sources of the so-called Mediterranean region are presented, based on Pollmann's data and hand specimens in the Lithotheca.

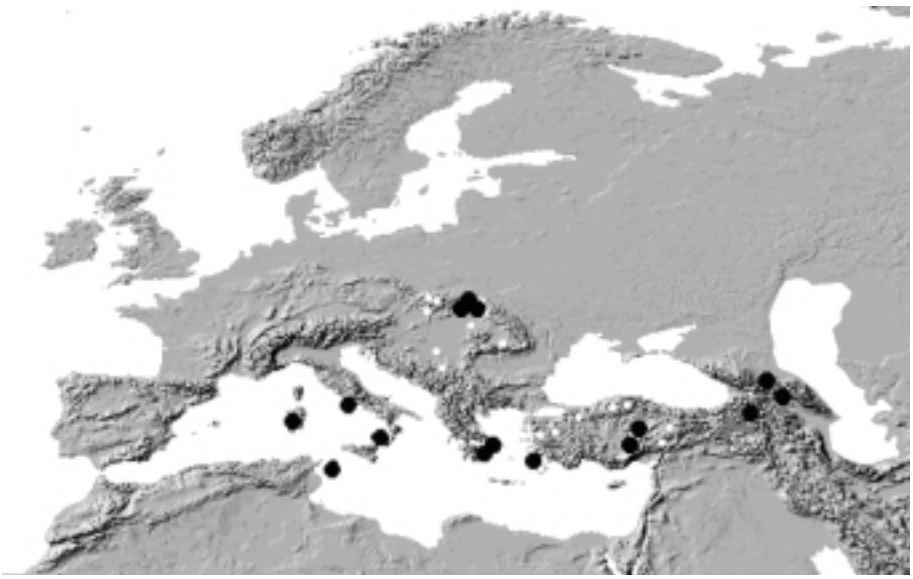

Figure 2. Obsidian geological sources of the Mediterranean region after H. Pollman and hand specimens in the Lithotheca. Sources represented in the Lithotheca Collection of the Hungarian National Museum are marked by black dots, other sources (?) with white dots.

3. THE SCIENTIFIC INVESTIGATION OF THE CARPATHIAN OBSIDIANS

Archaeological and geological study of the Carpathian obsidians started in the second half of the 19th century by pioneering Hungarian personalities of both disciplines (Rómer 1867, 1876, Szabó 1867, 1876). The Carpathian sources were, at the same time, the oldest known sources of archaeological obsidian in Europe, with the exception of Georgian and Armenian sources at the eastern fringes of the continent. The first studies on archaeological distribution made still in the 19th century were followed by a range of data collections concerning special areas or time periods e.g., those of M. Roska and S. Janšák (Roska 1934, Janšák 1935). Another wave of interest was observable just prior to modern archaeometrical studies in the fifties and sixties. In the first publication of the author on archaeological distribution of the Carpathian obsidians (Biró 1981) these archaeological data collections were summarised and completed, and the results presented on a comprehensive map. By the end of the seventies, modern analytical studies created the possibility for separating Carpathian sources from other sources in Europe and also distinguish groups of different sources within the Carpathian Basin (Warren & al. 1977, Williams & al. 1984). Ever since, several series of analytical studies by different methods (OES, NAA, EDS, XRF, FTD, PIXE-PIGE and most recently, PGAA) and different groups of scientists have

been performed and published. Archaeological distribution of the Carpathian obsidians can be followed by the help of macroscopical studies and instrumental analyses from the Middle Palaeolithic period till Iron Age.

4. RAW MATERIAL SOURCES

All the known sources of Carpathian obsidian are located in the Tokaj-Prešov Mountains, partly on the southern part close to Tokaj (Mád-Erdőbénye-Olaszliszka environs, C2E group), partly around Tolcsva and Erdőbénye-Abaujszántó, located at the middle of the Tokaj Mts. (C2T group), both of them in Hungary. The best quality and seemingly most popular raw material sources, however, are already located outside the present borders of Hungary in Slovakia; geological sources of obsidian occur in the environs of Viničky (Szőllőske) and Mala Bara (Kisbár) even today (Kaminska & Duda 1985), the chemical composition of which is closest to those occurring most frequently in archaeological context. Probably they were not the only and most productive sources-a group of sources can be supposed to the North of them, impossible to locate by now, the evidences of which are found on the Late Palaeolithic and Neolithic workshop sites of Kašov and Cejkov (Bánesz 1967, 1991). We suppose that these highest quality sources were exploited by the Late Neolithic. All of the obsidian sources in the Carpathian region are secondary: primary sources with obsidian lava flows or tuff layers including workable nodules are not known. Small nodules below the workable dimensions do occur in rhyolite tuff around Tolcsva. It is possible that the primary sources of workable nodules have been eroded but it is also possible that they will crop out sooner or later.

Rock glass similar to obsidian, mainly perlite occurs at several locations within the Carpathian Basin and these are justly mentioned among potential sources of obsidian; however, they did not yield so far archaeologically serviceable obsidian. Such localities include Hliník (Szabova-skála) in Central Slovakia, the territory of Avas (Oaş) in Romania, as well as the environs of Hust in the Ukraine.

Beside these potential sources several claims of non-existing obsidian sources were made, partly as simple mistakes ("Bükk obsidian", Tompa 1929), rumours ("Börzsöny obsidian" Bárta, J. & Petrovský-Švichmann, A. 1962), "Mecsek obsidian" (hearsay but persistent), based probably on the frequent occurrence of obsidian on prehistoric sites which served more or less as trade centres controlling larger areas. In other instances other rocks and substances resembling obsidian in their macroscopic appearance but essentially different in formation and composition including artificial materials have been erroneously identified (even described) as obsidian. One of the well-known cases is the case of black opals in the Hargita Mts., a mistake corrected by J. Nandris (Nandris 1975). Recently we have come across several specimens considered to be obsidian, the chemical composition

of which exclude their identification as natural rock glass corresponding best to modern industrial slag (Oláhlápos (Lapus)).

The above mentioned potential raw material sources and mistakes more or less coincide with the data points presented by Pollmann; with some remaining unidentified dots, e.g. on the territory of Serbia where I was not able to locate even the basis of the legend as yet.

5. CHARACTERISATION

The identification of Carpathian obsidians is a comfortably settled problem, within the known European sources as well as the local varieties. Inside the Carpathian Basin, even macroscopic identification will give adequate results, at least good guesses can be made. The Slovakian (C1) obsidian is typically transparent-translucent, often clear, having a vivid glassy lustre and a dissected cortex. Hungarian obsidians are typically non-transparent, only slightly translucent on edges, their characteristic colour is dark graphite grey (C2E), black and sometimes mahogany red (C2T), typically with fine striped patterns.

Under the petrographical microscope the obsidians will be transparent with some crystallites, the perfect extinction of the isotropic glass in crossed polarised light can be observed well. Slovakian obsidian tend to have many trichites, while in the case of the Hungarian obsidians we can observe more crystallites of definite shape and opaque grains arranged in linear patterns.

Obsidian source characterisation is mainly done on the basis of chemical composition. Namely, the chemical composition of the high silica content magma the obsidian originated from would change from volcano to volcano. The differences are apparent both in the main element composition and the trace elements, equally suitable for the characterisation of the source.

In the first, classical studies of obsidian characterisation the basis of identification was the determination of trace elements using OES. This method was not sensitive enough to reveal inter-group differences within the Carpathian obsidians, but even the first trials were adequate to separate Carpathian obsidian from the other obsidian sources of the Mediterranean region (Cann & Renfrew 1964). A more exact separation including the separation of Carpathian I-II types was achieved using NAA by the end of the seventies (Warren & al. 1977). The publication of the series of analyses comprised unfortunately only a summary of the results (Williams & al 1984). In the meantime, the measurements were started in Hungary as well; in the beginning, using AAS for main components and OES for semi-quantitative analysis of trace elements (Biró 1981), later on, using EDS and XRF on several series of archaeological and geological samples (Biró & Pozsgai 1984, Biró & al. 1986, 1988). In Romania, also X-ray spectroscopical methods were used for

the identification of archaeological obsidian (Salagean & al. 1988, Daraban & al. 2002). More recently, ion beam analytical techniques were used successfully for source characterisation of obsidian in the Nuclear Research Institute of the HAS in Debrecen, using PIXE and PIGE (Elekes & al. 2000a-b). Currently we are using PGAA for the characterisation of several lithic resources including obsidian (see the paper by Kasztovszky & Biró in the same volume). This is very favourable for the analysis of obsidian, being sensitive enough for the purpose and completely non-destructive.

Source characterisation of obsidian can be also successfully achieved using the formation age of the rock determined by FTD, independently and also in association with chemical composition data. In case of the Carpathian obsidians, the basic data were collected and published by G. Bigazzi (Biró & al. 2000b).

Characterisation studies within the Carpathian Basin yielded so far only one item that could not be fit into the Carpathian I-II categories (Biró & al. 1986:). Outside the territory of the Carpathian Basin the possibility of interacting sources increase: the confines of distribution of the Carpathian obsidian have been demonstrated so far till Istria (Williams & al 1984) and Thessaly (Bassiakos & al. 1993).

6. ARCHAEOLOGICAL DISTRIBUTION

Archaeological distribution of obsidian was mapped already in the 19th century. The first systematical collection of data was published by Flóris Rómer (Rómer 1876), followed by a number of efforts in respect of a certain territory, period or cultural unit. The data published in technical literature prior to 1980 were collected and presented on a comprehensive map, without aiming at a critical review, by K. Biró (Biró 1981). Apart from the data obtained from references, Hungarian Palaeolithic obsidian finds from the collection of the Hungarian National Museum and the Herman Ottó Museum, Miskolc were published based on personal investigations, separating the categories Carpathian I-II on the basis of macroscopical observations (Biró 1984). Later on, by the application of analytical methods and general petroarchaeological surveys, distribution data from a great number of archaeological sites have been collected and organised into a database. This approach allowed to register the changes of utilisation and circulation in a quantitative manner on a series of maps (Biró 1992, 1998).

A new impetus for distribution studies was given by the project "Raw material atlas Non-metallic prehistoric raw materials on the territory of Hungary and adjacent regions", supported by the Hungarian National Scientific Fund (OTKA)) between 1998 and 2002 (OTKA T- 025086), aiming at a regular collection of distribution data on raw materials identified on

Figure 3. Distribution data on Carpathian obsidians: a, geocoded references from technical literature; b. Carpathian 1 (Slovakian) obsidian identified by macroscopic analysis; c. Carpathian 1 (Slovakian) obsidian identified by instrumental analytical methods. Obsidian on archaeological sites are marked with squares, the location of main geological sources are indicated with empty dots.

Hungarian prehistoric sites. Collection of data was extended to references in technical literature as well as our own analytical work and observations. The work has been continued after the official closing of the projects as well. One of our specific aims is to study and characterise specimens of obsidian occurring relatively far from the source regions, and the non-destructive analytical technique applied offers a good possibility for this.

The results are plotted on geocoded series of maps (fig. 3). Compared to previous maps we are loosing many data points because not all the localities mentioned in old descriptions could be identified, but the existing data become more reliable and can serve as a basis for further synthesis.

7. CONCLUSIONS

Carpathian obsidians used to serve as important element of the raw material stock utilised by prehistoric peoples in the central parts of Europe. Their investigation offers a rare chance for unfolding the system of long-distance prehistoric trade and regular supply of raw materials. Our purpose is to support the research of both raw material resources and distribution studies with reliable, controllable objective data and study this legendary raw material in the realm of facts.

REFERENCES

Bánesz 1967: Bánesz, L., Die altsteinzeitlichen Funde der Ostslovakei. Quartär 18 (1967) 81-98.

Bánesz 1991: Bánesz, L., Neolitická dielna na vyrobu obsidiánovej industrie v Kašove. Vychodoslovensky Pravek 1991 39-68.

Bárta, J. & Petrovský-Šichmann, A. 1962: Bárta, J. & Petrovský-Šichmann, A., Paleolitické nálezy z Ipel'skej kotliny - Archeologické Rozhledy 14/3 (1962) 297-308.

Bassiakos & al. 1993: Bassiakos, Y. - Kilikoglou, V. - Souvatzis, K. - Grimanis, A.P, Provenance Studies of Obsidian from Mandalo in Macedonia, Greece. Abstracts of Asmosia 1993, Third Int.Conf. Athens 17-23 May Demokritos, Athens NCSR Demokritos 1993.

Bassiakos & al. 1998: Bassiakos, Y. - Biró, K. - Kilikoglou, V., Obsidian trade - the South-Eastern connection. Poster presented at 31st ISA Symposium, Budapest. In: Biró K.-Horváth T. (eds.), 31st International Symposium on Archaeometry. Program and Abstracts Budapest 1998 p. 22.

Biró 1981: T. Biró K., A Kárpát medencei obszidiánok vizsgálata (Investigation of obsidian from the Carpathian Basin). Archaeologiai Értesítő, Budapest 108 (1981) 196-205.

Biró 1984: T. Biró K., Distribution of obsidian from the Carpathian Sources on Central European Palaeolithic and Mesolithic sites. Acta Archaeologica Carpathica (Kraków) Kraków 23 (1984) p. 5-42.

Biró 1998: T. Biró Katalin Lithic implements and the circulation of raw materials in the Great Hungarian Plain during the Late Neolithic Period Budapest Hungarian National Museum 1998 1-350.

Biró & Pozsgai 1984: Biró Katalin - Pozsgai Imre Obszidián minták vizsgálata elektronsugaras mikroanalizissel (Investigation of obsidian samples by electron beam microanalysis) - Iparrégészet / Industrial Archaeology 2 (1984) 25-38.

Biró & Dobosi 1990: Biró, K. T.—Dobosi, V., LITOTHECA - The Comparative Raw Material Collection of the Hungarian National Museum. Catalogue. (1991) Budapest 1-268.

Biró & al. 1986: T. Biró K. - Pozsgai I. - Vladár A., Electron beam microanalyses of obsidian samples from geological and archaeological sites. ActaArchHung 38 (1986) 257-278.

Biró & al. 1988: Biró K. - Pozsgai I.- Vladár A., Central European obsidian studies. State of affairs in 1987. Archaeometrical Studies in Hungary 1 (1988) Budapest KMI 119-130.

Biró & al. 2000a: Biró, K.T., Dobosi, V., Schléder, Zs., LITOTHECA II. - The Comparative Raw Material Collection of the Hungarian National Museum. Catalogue Vol. II. (2000) Budapest 1-320.

Biró & al. 2000b: Biró, K. T., Bigazzi, G., Oddone, M., Instrumental analysis I. The Carpathian sources of raw material for obsidian tool-making. In: Dobosi ed. 2000 Bodrogkeresztúr-Henye. (NE-Hungary) Upper Palaeolithic site. Budapest, Magyar Nemzeti Múzeum 221-240.

Cann & Renfrew 1964: Cann, J.R. — Renfrew, Colin, The characterization of obsidian and its application to the Mediterranean region.. Proceedings of the Prehistoric Society 30 (1964) 111-130.

Daraban et al. 2002: Daraban, L., Cosma, C., Cozar, O., Simon, V., Znamirovschi, V., Ghiurca, I., Salagean, M. & Pantelica, A., Obsidian provenance studies. In: Jerem, Erzsébet, Biró, Katalin T., eds., Archaeometry 98. Proceedings of the 31st Symposium, Budapest, April 26-May 3. Vol. II BAR British Archaeological Reports International Series Oxford Archaeopress 2002 1043 /II 705-707.

Elekes & al. 2000a: Elekes Z., Uzonyi I., Gratuze B., Rózsa P., Kiss Á. Z. 1, Szöőr Gy. Contribution of PIGE technique to the study of obsidian glasses. NIM/BSCI Nuclear Instruments and Methods in Physics Research Section B: Beam Interactions with Materials and Atoms 2000 161 836.-841.

Elekes & al. 2000b: Elekes, Z.-Biró, K.T.-Rajta, I.-Uzonyi, I.-Gratuze, B.-Kiss Á.Z. Analyses of Obsidian and Radiolarite Samples by Ion Beam Techniques. - Paper presented at 32th ISA Conference, Mexico City.

Janšák 1935: Janšák, Stefan, Praveké sidliska s obsidianovou industriou na Vychodnom Slovensku. - Bratislava 1935 1 - 193.

Kaminska & Duda 1985: Kaminska, Lubomira & Duda, R. K., Otázke vyznamu obsidiánovej suroviny v paleolite Slovenska. - Archeologiczke Rozhledy 37 (1985) 121-129.

Nandris 1975: Nandris, John. A re-consideration of the South-East European Sources of archaeological obsidian. - Univ. of London Bull. of the Inst. of Archaeology 12 (1975) 71-94.

Otkat- 025086: Raw material atlas Non-metallic prehistoricraw materials on the territory of Hungary and adjacent regions. Project funded by the Hungarian National Scientific Fund http://www.ace.hu/atlas/index.html

Pollmann 1999: Pollmann, Hans-Otto, Obsidian-Bibliographie. Artefakt und Provenienz - Bochum Verlag des Deutschen Bergbau-Museums 1999 1-151.

Rómer 1867: Rómer Flóris, Első obsidian-eszközök Magyarországon (First obsidian implements in Hungary). - Archaeológiai Közlemények 7 (1867) 161-166.

Rómer 1876: Rómer Flóris, Les silex taillés et les obsidiennes en Hongrie. Congr. Int. d'Anthr. et d'Arch. Prehist. VIII. Compte-Rendu 2 Budapest 1876 6-17.

Roska 1934: Roska M., Adatok Erdély őskori kereskedelmi, művelődési és népvándorlási útjaihoz (Data on the trade, cultural and migrational routes of prehistoric Transsylvania). Archaeológiai Értesítő 47 (1934) 149-158.

Salagean & al. 1988: Salagean, M., Pantelica, A., Daraban & L., Fiat, T, Provenance studies of obsidian from the neolithic settlement of Partza in South-Western Romania. Ist Conference on the Application of Physics Methods in Archaeology, Bucharest 1988 73-86.

Szabó 1867: Szabó József, A Tokaj-Hegyalja obsidiánjai (Obsidians of the Tokaj mts). - A Magyarhoni Földtani Társulat Munkálatai Pest3 (1867) 147-172.

Szabó 1876: Szabó József, L'obsidienne prehistorique en Hongrie et en Grece. - Congr.Int. d. Anthr. et d. Arch. Prehist., Compte-Rendu II Budapest 1876 96-100.

Tompa 1929: Tompa Ferenc, A szalagdiszes agyagmüvesség kultúrája / Die Bandkeramik in Ungarn Magyarországon - Archaeologia Hungarica 5-6 (1929).

Warren & al. 1977: Warren, Stanley - Williams, Olwen - Nandris, John The sources and distribution of obsidian in Central Europe. - Int. Symp. on Archaeometry and Archaeological Prospection Pennsylvania 1977.

Williams & al. 1984: Williams-Thorpe, O.—Warren, S. E.—Nandris, J., The distribution and provenance of archaeological obsidian in Central and Eastern Europe. Journal of Archaeological Science 11 (1984) p. 183-212.

RAW MATERIALS CHARACTERISTICS AND DURABILITY OF SOME MEDIEVAL PAINTED PLASTERS IN ANATOLIA

Evin Caner
Archaeometry Program, Middle East Technical University, 06531 Ankara, Turkey;
e-mail: evin29caner@yahoo.com

Şahinde Demirci
Archaeometry Program and Department of Chemistry, Middle East Technical University, 06531 Ankara, Turkey; e-mail: sahinde@metu.edu.tr

Emine N. Caner-Saltik
Conservation Laboratory, Archaeometry Program, Restoration Program, Department of Architecture, Middle East Technical University, 06531 Ankara, Turkey;
e-mail: canersal@arch.metu.edu.tr

1. INTRODUCTION

Seljuk culture have affected a large part of Anatolia, especially in Medieval period. In spite of several studies on this culture such as the architectural and stylistic features of its buildings, few studies had been done on the characteristics of the building materials such as plasters, mortars and the decorative materials (tiles, frescoes, etc.) (Özçilingir-Akgün, 1997; Akkuzugil, 1997; Tunçoku, 2001; Caner, 2003).

In this study 12th-13th century Seljuk painted plasters from some historic structures in the archaeological sites namely Alanya Castle, Selinus Archaeological Site (Sekerhane Kösk), Hasbahçe and Asphendos Amphitheatre were examined.

The plasters were used on either interior (fig. 1) or exterior (fig. 2) surfaces of the walls, mostly with red zigzag patterns on a white background. Those plasters with red zigzag patterns are archaeologicaly important especially in two aspects; firstly, their presence being an indication of royal administrative or residential buildings of Seljuk Culture (Redfort, 2002), secondly their durability that is the resistance to environmental conditions for centuries (Caner, 2003).

Their characteristics will help to the description of durable and compatible plasters during repair and conservation works.

Figure 1. A view of red zigzag painted Plasters in a room of Alanya Castle Palace (ALP2).

Figure 2. A view of red zigzag painted Plasters on H Building of Hasbahçe (HKP1).

2. DESCRIPTION OF THE PLASTERS

Some of painted plasters studied are as follow:

ALP2: Alanya Castle Palace, a room of palace, interior lime plasters, red and white zigzag patterned fine plaster layer with a thickness of 1.49 cm.

ALP4: Alanya Castle, Byzantine tower with frescoes, southern wall of a room, interior lime plaster, red painted fine plaster layer with a thickness of 0.58 cm.

ALP7: Alanya Castle, Byzantine Church, southern wall, interior lime plaster, red painted fine plaster layer with a thickness of 1.03 cm

SYDP1: Syedra Archaeological Site, street with colums, S10 place, exterior lime plaster, red painted fine and rough plaster layers with a thickness of 0.58 cm.

SYDP5: Syedra Archaeological Site, street with colums, S10 place, exterior lime plaster, red painted fine and rough plaster layers with a thickness of 1.07 cm.

ASP1: Aspendos Amphitheatre, exterior lime plaster, red-white zigzag patterned fine plaster layer with a thickness of 0.55 cm.

SKP1: Selinus Archaeological Site in Gazipasa-Alanya, Byzantine Masonry, which is used in Seljuk Period as a Kösk (Sekerhane Kösk), red-white zigzag patterned fine layered plaster with a thickness of 0.47 cm.

HKP1: Hasbahçe Kösk in Alanya, exterior lime plaster, red-white zigzag patterned, fine plaster layer with a thickness of 0.51 cm.

HKP2: Hasbahçe Kösk in Alanya, exterior lime plaster, red-white zigzag patterned, fine plaster layer with a thickness of 0.77 cm.

3. EXPERIMENTAL STUDIES

Analysis of the red-white zigzag patterned plasters of five different locations involved determination of basic physical and mechanical properties, raw material composition and minerological properties of them.

The basic physical properties of the plasters were studied by the measurements of bulk density and total porosity using RILEM standard test methods (RILEM 1980). Water vapour permeability, Modulus of Elasticity (Emod) (obtained from ultrasonic pulse velocity measurements and bulk density values) were also obtained.

Raw Material Properties were examined doing several experiments which are given as follow:

- binder and aggregate ratio by acid treatment
- determination of calcium ion in the binder by volumetric method,
- particle size distribution of aggregates by sieve analysis,

- determination of amount of water soluble salts by measurement of electrical conductivity
- determination of types of soluble salts by spot tests of anions,
- determination of pozzolanic activity of fine aggregates by electrical conductivity measurements and volumetric method,
- analysis of pozzolanic reaction products by recrystallization
- determination of mineralogical properties using XRD, TGA, FTIR and SEM-EDX analyses.

4. RESULTS AND DISCUSSION

The results of basic physical properties indicated that zigzag painted plasters had low density, high porosity (fig. 3) and appreciable amount of water vapour permeability (fig. 4) (RILEM,1980; ASTM, 96-90; TS 7847).

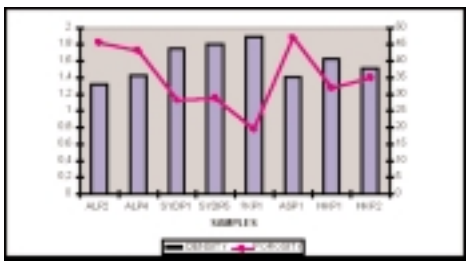

Figure 3. Bulk density and porosity values of plasters.

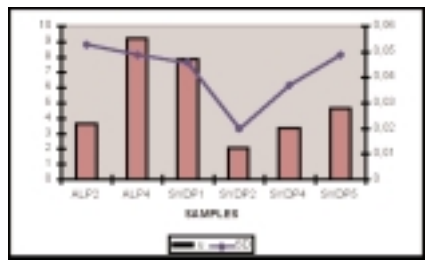

Figure 4. Water vapor resistance difussion coefficient (μ) and SD values of plasters.

Emod of the plasters studied being in the range of 1.0 to 3.0 GPa (fig. 5) showed that they had sufficient mechanical strength comparable to some historic mortars and bricks presented in other studies (Tunçoku, 2001).

All plasters studied were found to be high lime plasters, the amount of $CaCO_3$ being in the range of 60.0-90.0% by weight (fig.6). The binder in all plasters was found to be fat lime which was fully carbonated into micritic calcite. Micritic calcite crystals were together with very fine siliceous grains with the size less than 5 μ. Those siliceous particles were identified as opal-A of high pozzolanicity. They had produced considerable amount of pozzolanic products in the binder matrix. In addition, they must have taken important role in the carbonation process (Martinez-Ramirez et al.,1995; Güney, 2003).

Pozzolanic reaction products should be important in the development of physical and mechanical properties of the plasters (Tunçoku, 2001).

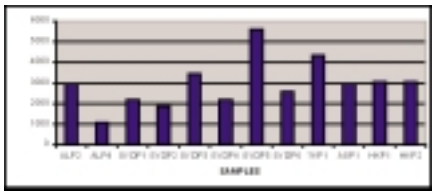

Figure 5. Modulus of Elasticity values of plasters.

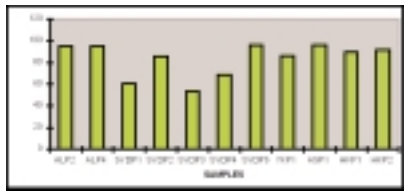

Figure 6. Binder content (%) of plasters.

Decorations of all plasters were prepared by using fresco technique. Haematite was found to be the mineral of red color. Characteristics of haematite can be described by its fine particle size and the minerals, which accompany it such as quartz, opal-A and dolomite. Haematite peaks of XRD were not so sharp indicating its not well crystallized feature (Bearat and Pradell, 1997). Accompanying minerals quartz, opal-A and dolomite may indicate the source of haematite mineral in nature. It is also probable that opal-A was added to haematite pigment to increase the formation of pozzolanic reactions and durability of the pigment layers.

The white pigment layer which formed the base of the red zigzag decorations was found to be calcite together with quartz, opal-A and dolomite. The presence of opal-A both in red pigment haematite and white pigment calcite increases the possibility of its use as additive to promote pozzolanic reactions and increase durability of pigment layers.

Well carbonated structure of binder lime and its microtexture, aggregate composition with highly pozzolanic components such as opal-A that had provided the formation of considerable amount of C-S-H in the matrix of the plasters and in the pigment layers must have powerfully increased durability of plasters and pigments. Recrystallization experiment of CSH on finest aggregates proved their high pozzolanicity (Shi, 1998; Luxan et al., 1989; Caner, 2003; Baronio and Binda, 1997) .

The physical properties of the plasters such as low bulk density, high porosity and good breathing property expressed as water vapor permeability and their compatibility with the wall that carries the plasters should be the additional factors affecting durability.

REFERENCES

Akkuzugil, A., 1997, A Study on Historical Plasters, Unpublished MSc. Thesis, Middle East Technical University, Ankara p. 109.

ASTM E 96-90, Standard Test Methods for Water Vapour Transmission of Materials.

Baronio, G., and Binda, L., 1997, Study of the Pozzolanicity of Some Bricks and Clays, Construction and Building Materials, Vol.11, No.1, pp. 41-46.

Bearat, H., and Pradell, T., 1997, Contribution of Mossbauer Spectroscopy to the Study of Ancient Pigments and Paintings, in: Roman Wall Painting, Materials, Techniques, Analysis and Conservation, Eds: H. Bearat, M. Fuchs, M. Maggetti, D. Paunier, Institute of Mineralogy and Petrography, University of Fribourg, Fribourg, pp. 239-256.

Caner, E., 2003, Archaeometrical Investigation of Some Seljuk Plasters, M.Sc. Thesis, Middle East Technical University, Ankara, 113 p.

Drees, R. L.; Wilding, L. P.; Smeck, N. E., and Senkayi, A.L., 1989, Silica in Soils: Quartz and Disordered Silica Polymorphs, in; Minerals in Soil Environments, SSSA Book Series: 1, Co-Eds; Dixon J. B. and Weed S. B., Soil Society of America, Madison, Wisconsin, U.S.A., pp. 913-975.

Güney, B. A., 2003, Investigation of the Effects of Some Additives on the Carbonation of Calcium Hydroxide, M.Sc. Thesis, Middle East Technical University, Ankara, 44 p.

Luxan, M. P.; Madruga, F., and Saavedra, J. 1989, Rapid evaluation of pozzolanic activity of natural products by electrical conductivity measurement, *Cement and Concrete Research*, Vol. 19, pp. 63-68.

Martinez-Ramirez, S.; Puertas, F., Varela, B. M. T., 1995, Carbonation Process and Process and Properties of New Lime Mortar with Added Sepiolite, Cement and Concrete Research, Vol.25, pp. 39-50.

Özçilingir-Akgün, S., 1997, Study of the Glazed Building Materials on Some Seljuk Period Buildings, Unpublished MSc. Thesis, Department of Archaeometry, in Middle East Technical University, 92 p.

Redford, S., 2001, Selçuklu Anadolu'sunda Adalet ve Peyzaj, Proceedings of I.International Seljuk Culture and Civilization Congress, Konya, pp. 213-224.

RILEM , 1980, Tentative Recommendations, Comission-25-PEM, Recommended Test to Measure the Deterioration of Stone and to Assess the Effectivenes of Treatment Methods, Materiaux and Construction, Vol.13, No.73, pp. 173-253.

Shi, C., 1998, Pozzolanic Reaction and Microstructure of Chemical Activated Lime-Fly Ash Pastes, ACI Materials Journal, pp. 537-545.

TS, 1990, TS 7847 Siva Yapim Kurallari.

Tunçoku, S. S., 2001, Characterization of Masonry Mortars Used in Some Anatolian Seljuk Monuments in Konya, Beyşehir and Akşehir, Ph.D Thesis in Middle East Technical University, Ankara, p. 128.

DIRECT DETERMINATION OF CHROME YELLOW BY A HARMLESS ELECTROANALYTICAL TECHNIQUE

Cepriá, G., Campos, M. T., Pérez-Arantegui, J.
Analytical Chemistry department, Faculty of Sciences, University of Zaragoza
C/ Pedro Cerbuna 12, 50009 Zaragoza (SPAIN)

1. INTRODUCTION

Sometimes the characterization of a sample makes impossible its transport to a laboratory due to its size or its high economical or cultural value. In this case it is necessary to approach the lab to the sample and only some analytical techniques can be used with an added low cost and friendly use.

But not all the electroanalytical techniques are suitable for this purpose, a reagentless, no-sample-treatment procedure is required to avoid any harm to the sample. This is accomplish by Voltammetry of Immobilized Microparticles, a technique developed by F. Scholz in the 90's (Scholz, 1998).

Some microparticles of the sample are physically attached to the electrode surface by gently rubbing it on the selected area or spot of the sample. Then a potential scan is applied to the electrode in a three-electrodes electrochemical cell and the current intensity is recorded. Whenever an adequate potential for the reduction or oxidation of a compound of the sample is attained an increase of the current is observed and a peak is registered at this potential. The peak potential is the fingerprint of the electroactive component in the solution in which the experiment is performed.

2. INSTRUMENTATION AND PROCEDURE

An AUTOLAB Eco-Chemie potentiostate was used to obtain all the voltammograms. The reference electrode was a Ag|AgCl|KCl sat, a platinum wire was used as counter electrode and a paraffin impregnated graphite electrode (PIGE) served as working electrode.

A spectroscopic- grade graphite bar was soaked in paraffin and one of its bases was smoothed by rubbing on a filter paper placed on a flat tileplane till a shiny surface was observed. The powdered pigment was extended on a white paper with the help of a plastic spatula and a 2 cm long line was dragged by softly pressing with the PIGE. Then it was transferred to the electrochemical cell filled with 10 ml of the selected electrolyte (fig. 1).

The working electrode was carefully smoothed after each voltammogram to clean it. All voltammograms were obtained with freshly prepared surfaces.

The potential scan was performed from -1.0 V to 1.0 V using square wave voltammetry. Scan speed was 60 mV/s.

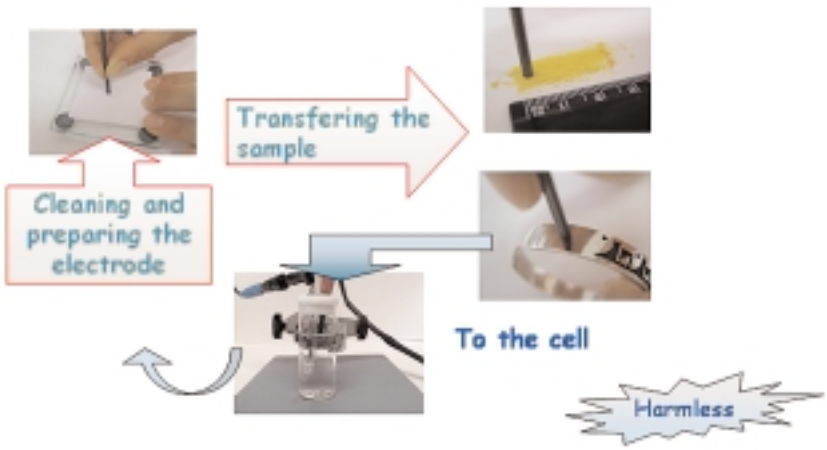

Figure 1. Scheme of the procedure for sample transfer to the electrochemical cell.

3. RESULTS AND CONCLUSIONS

Only one component is electroactive in a chromium yellow pigment: lead. Chromate exhibits a very slow electrode reactions showing no peak at all in a voltammogram. Lead can be involved in the following electrode process:

$$Pb(II) + 2e^- \Leftrightarrow Pb^o$$

at a potential related to the physicochemical form of lead and the supporting electrolyte. Several electrolytes were investigated but only HCl and NaOH offered clear and well shaped peaks that could be used for identification.

In HCl we observed two peaks, one around -0.40 V and another one around -0.50 V. The former is related to the electrode process:

$$PbCl_3^- + 2e^- \Leftrightarrow Pb^o + 3\ Cl^-$$

and the later:

$$PbCl_2 + 2e^- \Leftrightarrow Pb^o + 2\ Cl^-$$

But the standard potential of these processes does not correspond to the peak potential of them, because the physicochemical surrounding of the Pb(II) is different depending on the original substance attached to the electrode. In the case of $PbCrO_4$, the first peak appears at -0.39 V to -0.46 V depending on the concentration of the HCl and the second one at -0.52 V. But usually $PbCrO_4$ is mixed with $PbSO_4$ to adjust the hue, and for this compound the peak potentials are -0.42 V to -0.46 V and -0.49 to -0.51 V for the two electrode processes above depicted (see fig. 2A).

In NaOH the electrochemistry of the microparticles is much more complex because it involves the formation of several hidroxy species on the surface of the microparticles affecting clearly the peak position clearly. Lead cChromate showed two peaks, one at -0.80 V to -0.71 V and the second at 0.67 V to 0.65 V, depending on the concentration of the supporting electrolyte. The first peak is due to the electrode process:

$$Pb(OH)_2 + 2e^- \Leftrightarrow Pb^o + 2\ OH^-$$

and the second one:

$$PbO_2 + H_2O + 2e^- \Leftrightarrow PbO + 2OH^-$$

For $PbSO_4$ also two peaks are obtained. The first one correspond to the same electrode process as in the case of lead chromate. The second one is related to the reduction of some hydroxy salts:

$$Pb(OH)_2 + 2e^- \Leftrightarrow Pb^o + 2\ OH^-$$

$$Pb(OH)_2.PbSO_4 + 4e^- \Leftrightarrow 2Pb^o + SO_4^{2-} + 2\ OH^-$$

The first peak potential is -0.69 V to -0.76 V depending on increasing concentration of NaOH and the second one at -0.58 V, but it disappears at concentrations of NaOH higher than 0.8 M due to the chemical dissolution of the whole microparticle as PbO_2^{2-} (fig. 2B).

Due to these differences it is possible to distinguish the presence of $PbSO_4$ in a chrome yellow pigment.

When $PbCrO_4$ and $PbSO_4$ are mixed, the first peak is clearly influenced by the mixture composition and a linear relationship was found between its potential and the $PbCrO_4$ percentage, of $PbCrO_4$ in a binary mixture of both components. This linear relationship was:

$Ep = - 0.488 - 0.00032\ [\%PbCrO_4]$, $r^2 = 0.990$ in 1.0 M HCl and

$Ep = - 0.707 + 0.00038\ [\%PbCrO_4]$, $r^2 = 0.992$ in 0.4 M NaOH

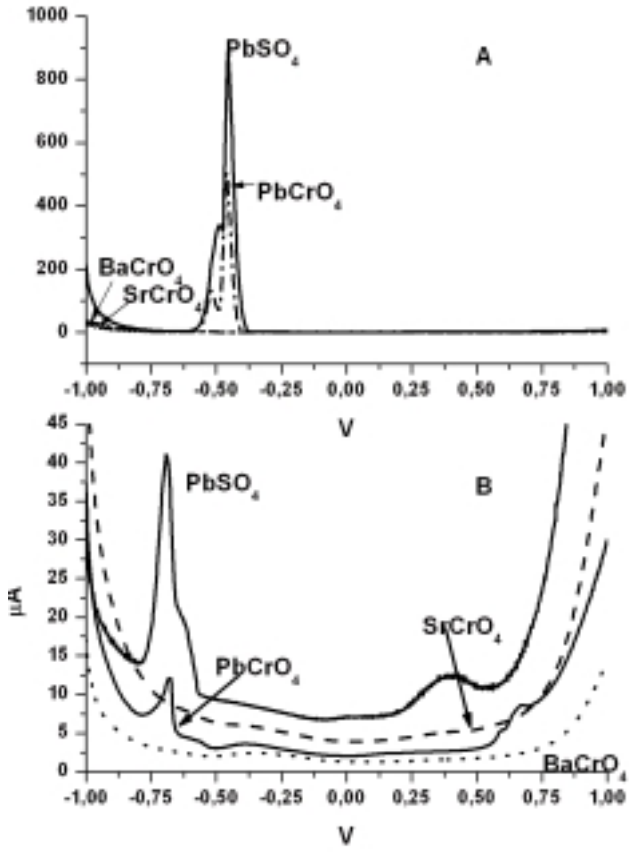

Figure 2. Voltammograms of $PbCrO_4$ and $PbSO_4$ in 1.0 M HCl (A), and in 0.4 M NaOH (B).

Several current yellow paints, watercolours and cosmetics were investigated to detect the presence of chrome yellow but it was not found. A more widespread yellow pigment, goethite, was found in some of them, specially in cosmetics.

REFERENCES

Sholz F., Meyer, B., 1998, Voltammetry of solid microparticles immobilized on electrode surfaces, in *Electroanalytical Chemistry* (A. J. Bard, I. Rubisntein, Eds.) vol 20, Marcel Dekker, Inc, New York, pp. 1-85.

USE OF GRANITOID STONES FROM CALABRIA (SOUTHERN ITALY) IN ANTIQUITY: PETROGRAPHIC AND GEOCHEMICAL CHARACTERIZATION OF ANCIENT QUARRIES OF ROMAN AGE

Cirrincione, R., Crisci, G. M., De Vuono, E.
Dipartimento di Scienze della Terra, Università della Calabria, Italy

Pezzino, A., Punturo, R.
Dipartimento di Scienze Geologiche, Università di Catania, Italy

1. INTRODUCTION

As it is known, the granitoid rocks were widely employed as worthy building materials during the Roman times; the Romans, who called the granite

Figure 1. Abandoned pillars in the quarry near Parghelia town.

Marmor (i.e. marble), quarried it all over the Mediterranean basin and used in the most important centres of the Empire. As far as Italy is concerned, the main extraction sites at that time were located at Giglio, Elba (this also known as "Vecchio Granitello") and Sardinia islands. The two formers were diffused only in central Italy and in Rome meanwhile the latter was diffused in the whole Italian peninsula (Galetti et al., 1992).

The aim of this work is the geochemical and petrographic characterization of the granitoids of Calabria (southern Italy), which were used and traded during the Roman Age (see e.g. Solano, 2003). In particular, we focused on the granitoids from two different extraction sites located in the surroundings of Vibo Valentia (near Parghelia and Nicotera Marina towns, respectively), whose occurrence of huge remnants of abandoned pillars (fig. 1) supports evidence about the employment of such materials for both ornamental and structural purposes.

2. THE ANCIENT QUARRIES

The two extraction sites investigated are located nearby the western coast of Calabria as parts of larger masses of bodies which are exposed over an area of 1,250 Km^2 which are Late Carboniferous to Early Permian in age (fig. 2). Two different groups of granitoids have been distinguished, related in time and partly also in space: a) a calc-alkaline suite, biotite dominated and b) a strongly peraluminous type, which is two micas and Al-silicates bearing granitoid. Even though these granitoids have been the subject of petrologic studies (i.e. Rottura et al., 1991 and therein references; Caggianelli et al., 1991), they only recently have been dealt as worthy building materials for archaeometric aims (Cirrincione et al., 2004).

Figure 2. Geological sketch of the study area.

The two extraction sites are far away a few kilometres in distance: this means the availability to exploit two different types of *Marmor*, of both the grey and the pinkish variety, within a very restricted area. Moreover, very little evidence of weathering and/or occurrence of extended fractures were recognised as affecting

the materials in the quarries: these good characteristics allowed the extraction of large and fresh blocks, which were in situ manufactured and hence transported by boats .

3. EXPERIMENTAL RESULTS

The specimens studied include the two different litho-types collected from the plutonites where the quarries are located. Particular care was taken in sampling fresh and representative rocks, also due to the large grains of the peraluminous granitoids.

Subsequently, samples were analysed by means of XRF at the Department of Geological Sciences, University of Catania, on powder pellets with a $Li_2B_4O_7$. Loss on Ignition (L.O.I.) was determined by gravimetric method. The results have been compared with international reference samples of granitoid rocks. Analytical data are presented on Table 1.

		SiO2	TiO2	Al2O3	Fe2O3	MnO	MgO	CaO	Na2O	K2O	P2O5	L.O.I.	V	Ni	Zn	Rb	Ba	Nb	Sr
PA	Mean	68.83	0.47	16.07	3.16	0.04	1.04	2.74	3.19	3.56	0.11	0.81	33	8	68	85	1554	7	395
	STD	1.11	0.09	0.37	0.58	0.01	0.21	0.16	0.15	0.61	0.05	0.57	8	2	24	7	387	1	13
NM	Mean	63.42	0.70	16.19	5.47	0.09	3.21	5.28	2.67	1.97	0.18	0.83	129	16	81	60	660	4	307
	STD	0.69	0.06	0.21	0.27	0.01	0.25	0.27	0.08	0.22	0.01	0.40	13	1	9	10	69	2	10

Table 1. Chemical data of the granitoids from the two quarries (average and standard deviation values). PA= two micas granites from Parghelia (10 samples); NM=granodiorites and tonalites from Nicotera Marina (14 samples).

All samples were investigated in thin section under a polarising microscope, also equipped with a point-counter for the modal composition estimate. The most important petrographic characteristics of the granitoids are set out on table 2.

The modal estimates have been used for the classification of granitoid rocks according to the AQP modal diagram shown on fig. 3.

As it may be seen, litho-types from the quarry of Nicotera Marina consist of grey in colour and medium grained granodiorites and minor tonalites. Biotite is the main femic mineral phase (20-25 vol%); nevertheless amphibole (green Ho) is ubiquitous in the specimens examined (1-3 vol%). Epidote is the most abundant accessory phase; it occurs either as individual crystals or aggregate assemblages with the varieties of allanite and epidote s.s. Other accessories are opaques, zircon, rutile and apatite.

As far as the granitoids from Parghelia are concerned, the litho-types localised nearby the quarry constitute a sub-facies, characterised by heterogranular pseudo-porphyritic texture with large K-feldspar megacrysts,

Locality name of granitoids	Quartz	K-feldspar	Plagioclase	Biotite	Amphibole	Muscovite	Accesory and secondary phases	Textural Characters
Nicotera Marina Quarry (NM)	Interstitial, weak ondulose extiction; sometimes with rutile *("capel venere")* and zircon inclusions	Few individuals; often altered into clay products	Idiomorphous, Ab and Ab/C twinning, sometimes zoned; Some with biotite, epidote and opaque oxides inclusions	α = yellow β≈γ = brown euhedral to sub-hedral crystals; some parts altered into chlorite; som. ragged outlines	α = yellow β = light green γ = apple green; some crystal sshow a skeletal microstructure	*absent*	Epidote (allanite; epidote s.s.), zircon, apatite, rutile, opaque minerals, chlorite, clay minerals	Holocrystalline, Hypidiomorphic and homogranular textured. Medium grained
Parghelia Quarry (PA)	Interstitial; weak ondulose extiction; sometimes with rutile and zircon inclusions	Large individuals; some Carlsbad twinned; Orthoclase and Microcline, both micropertitic; some altered into clay products; microcrystalline inclusions of muscovite, plagioclase, opaque oxides, apatite	Idiomorphous, Ab and Ab/C twinning, Some with biotite, epidote and opaque oxides inclusions	α = yellow β≈γ = brown euhedral to sub-hedral crystals; some parts altered into chlorite and with ragged outlines	*absent*	Some in late magmatic patches; Some individuals enclosed as thin flakes on plagioclase, quartz and K-feldspar; others grown over biotite crystals; Some weakly deformed	Opaque minerals; zircon; apatite; rutile; epidote; chlorite, clay minerals	Holocrystalline, Hypidiomorphic and heterogranular textured; porphyrite

Table 2. Petrography of NM and PA granitoids.

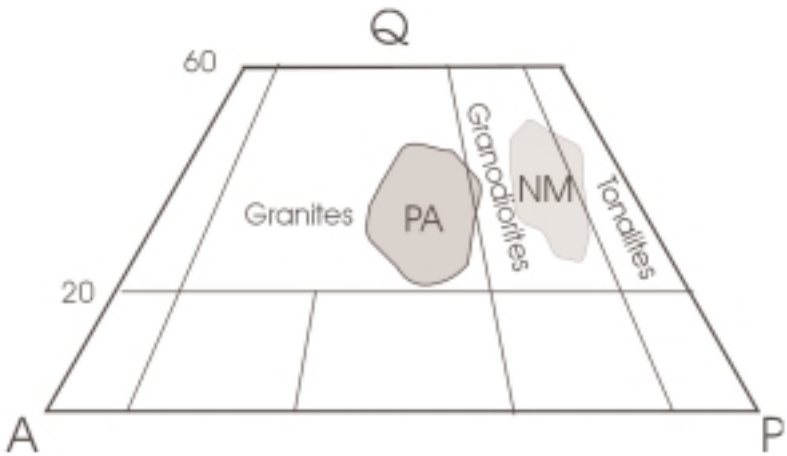

Figure 3. Plot of the NM and PA samples studied in the QAP classification diagram.

which plots within the muscovite-biotite granites field (Ms 2-4 vol%; Bt 6-10 vol%). The accessory assemblage is given by opaque minerals, zircon, apatite, rutile and epidote.

The two groups of litho-types display well preserved magmatic textures and very minor evidence of secondary alteration occurrences, given only by a few flakes of sericite in plagioclase as well as rare chloriticizations of the biotite individuals.

Selected major and minor elements plotted on the Harker binary diagrams of fig. 4 put into evidence the different geochemical characteristics of the two groups studied. In particular, the "NM" granitoids show calc-alkaline affinity; they are from metaluminous from very weakly peraluminous, with Aluminum Saturation Index ASI≈1 and Na+K< molecular Al. They are characterised by low TiO_2 (<1wt%), high Al_2O_3 (≈ 16wt%), $FeO_{tot}/(FeO_{tot}+MgO)$ in a restricted range (0.62-0.65) and Na_2O+K_2O-CaO (Modified Alkali-Lime Index = MALI) ranging from –0.96 to 0.21. Moreover, they exhibit low Rb (~60ppm) and Nb (~4ppm) contents, for a very restricted range in silica composition (62.7-65wt%).

The "PA" peraluminous granites (ASI >1) are characterised by a restricted silica interval (67-70 wt%); very low TiO_2 (0.40-0.65) and MgO (~1wt%) contents; $FeO_{tot}/(FeO_{tot} + MgO)$ ranges from 0.74 to 0.77, Ba contents are variable (1211-2300ppm), and relatively high Rb and Nb average values. On the contrary, Ni (~ 8ppm) and V (~33 ppm) contents are sensibly lower. The MALI index ranges from 3.2 to 5.1.

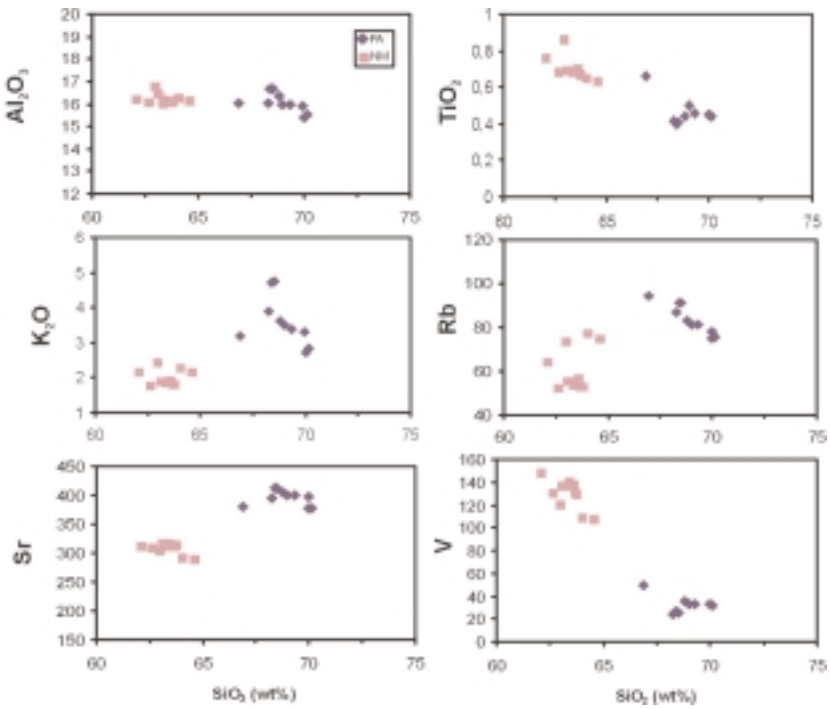

Figure 4. Harker diagrams for a selection of major (wt%) and minor (ppm) elements.

5. FINAL COMMENTS

The preliminary study which was carried out put into evidence that, within the granitoid suites which outcrop in the surroundings of Vibo Valentia (southern Calabria, Italy), the petrographic and geochemical characteristics of the granitoids from the ancient quarries are peculiar and therefore permit to distinguish them from the other similar granitoids of the area, previously studied for petrological aims (e.g. Rottura et al., 1991)

In fact, within each quarry, both the granitoids (granodiorites and tonalites) from the calc-alkaline suite as well as the two-micas peraluminous granites exhibit a restricted compositional range and some petrographic characteristics (e.g. the occurrence of K-feldspar megacrysts in the granites from Parghelia) which make them unique in terms of archaeometric purposes. This fact may give important constraints about the studies concerning the provenance of granitoid-type rocks employed in some monuments of archaeological importance in southern Italy.

REFERENCES

Caggianelli, A.; Del Moro, A.; Paglionico A.; Piccarreta G.; Pinarelli L., Rottura, A. (1991). Eur. J. Mineral., 3, 159-180.

Cirrincione R.; Crisci G. M.; De Vuono, E.; Pezzino, A., Punturo, R. (2004). AIAr, GNAA National Congress, Bressanone (Italy), 11th-12th February 2004.

Galetti, G.; Lazzarini, L., Maggetti, M. (1992). Acta Archaelogica Lovanienesia; Monographiae 4, 167-178.

Rottura, A; Del Moro, A.; Pinarelli, L.; Petrini, R.; Peccerillo, A.; Caggianelli, A; Bargossi G. M., Piccarreta G. (1991). Chem. Geol., 92, 153-176.

Solano, A. (2003): AIAr, National Congress, Ravello (Italy), February 2003.

EXAMINATION OF BURNT MUD BRICK AND PLASTER FROM ŞAPINUWA- HITTITE CITY FOR THE CHARACTERIZATION OF THEIR TECHNOLOGICAL PROPERTIES

Gülnur GÜDÜCÜ
Graduate Program of Archaeometry, METU, 06531, Ankara, Turkey,
e-mail: glnurgdc@yahoo.com

Emine N. CANER-SALTIK
Materials Conservation Laboratory, Graduate Program in Restoration,
Dept. of Architecture & Graduate Program of Archaeometry, METU, 06531, Ankara,
Turkey, e-mail: canersal@arch.metu.edu.tr

Şahinde DEMIRCI
Graduate Program of Archaeometry & Dept. of Chemistry, METU, 06531, Ankara,
Turkey, e-mail: sahinde@metu.edu.tr

1.INTRODUCTION

The Şapinuwa Hittite city is situated in central Anatolia, near Çorum (fig. 1). The peak period of the archaeological site was dated to about 1500 B.C. The site is being excavated since 1990 (Süel, 2000). The unearthed buildings were mostly half-timber buildings having timber structural elements with mud brick infill, coated with mud plasters. The site had witnessed a fire in ancient times and all timber elements were lost and mud bricks were burnt.

The aim of the study was to investigate the mud brick technology of Hittites with respect to earth walling techniques and raw materials characteristics which included type of binder, type and size distribution of aggregates, the presence of organic and /or inorganic additives. It is known that those aspects are of main importance on the performance of mud bricks (Brown and Clifton, 1978; Brown et al, 1979; Sickels, 1981; Houben and Guilloud, 1994).

2. EXPERIMENTAL STUDIES

Visual examinations have revealed the earth walling technique as the use of molded mud brick units of about 24 x 48 x 10 cm sizes for the construction of mud brick walls which were about 110 cm. wide and covered by mud plasters of about 3.5-4.0 cm thickness.

Figure 1. Archaelogical Hittite Site, Şapinuwa, Çorum, Turkey.

About twenty samples were taken from four half timber buildings that had different functions; A, an administrative building, B, a store, C and D not yet identified.

In a series of analyses, physical, mechanical and compositional properties were examined. The bulk density, total porosity, water absorption by capillarity and water vapour permeability were obtained by RILEM standard tests (RILEM 1980).

The mechanical properties were expressed by the modulus of elasticity that was calculated from ultrasonic pulse velocity measurements and bulk density values (RILEM 1980; Topal, 1995).

Petrographic and mineralogical properties were determined by optical microscopy, XRD, TGA and SEM coupled with EDX analyses. Elemental analyses were also supported by XRF analyses. In addition, degree of pozzolanic activity in powdered samples was determined by TS EN 196, 2002.

3. RESULTS AND DISCUSSION

The results showed that the burnt building materials had low bulk density (mud bricks: ~1.35g/cm^3, mud plasters: ~1.20g/cm^3), high porosity (mud bricks: ~40%, mud plasters: ~50%), and high water vapour permeability (fig. 2).

The calculated E_{mod} values were in the range of 0.60-1.50 GPa that indicated somehow sufficient mechanical strength of mud brick and mud plaster pieces comparable to some historic mortars and bricks (fig. 2) (Moropoulou et al., 2000; Tunçoku, 2001).

The petrographic and mineralogical analyses of burnt materials indicated a mud brick composition of 50-55% sand with an average particle size of about 0.8 mm., medium sized sand. Quartz was the most abundant

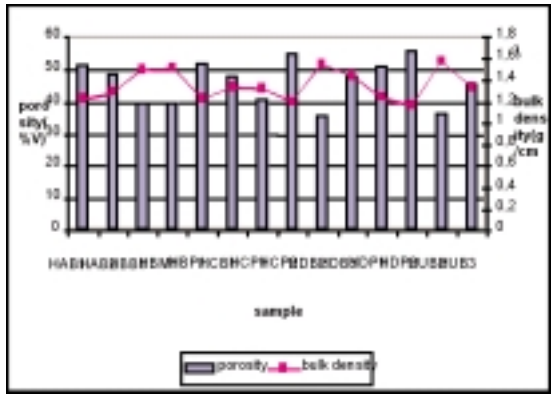

Figure 2. Bulk density and porosity values of samples studied.

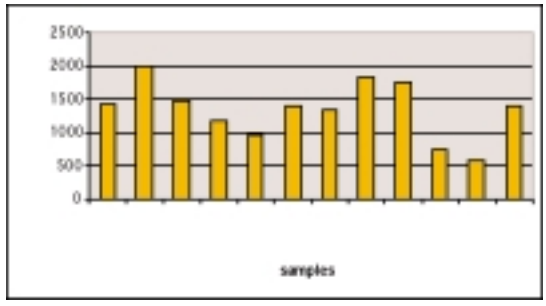

Figure 3. Modulus of elasticity values of samples studied.

aggregate, followed by quartzite, feldspars, biotite and opaque minerals. Mud plasters had fine sized sand.

All mud brick and mud plaster samples showed high pozzolanic activity. It is known that kaolinite produces products of high pozzolanicity upon heating to about 700°C -800°C (Benharbit, 1994). Combined results of XRD, XRF, EDX, pozzolanic activity measurements as well as petrographical and mineralogical analyses indicated that the binder clay was mainly kaolinite with some illite together with high amount of micritic calcite (~ 20%) homogeneously distributed in the matrix both for mud bricks and mud plasters (table 1, figs. 3-4). Such high lime content is expected to improve the mechanical strength and water resistance of mud brick (Brown and Clifton, 1978; Houben and Guilloud, 1994). In fact, it is supposed to be the best way of mud brick stabilization (Ngowi, 1997).

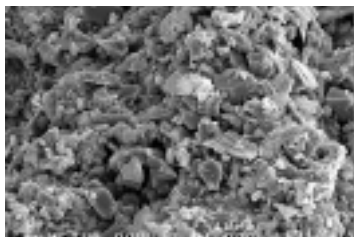

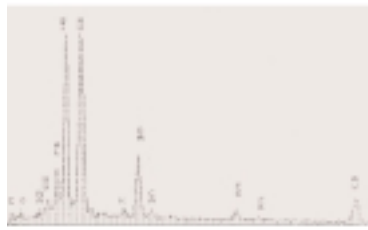

%SiO_2:	57.0
%CaO:	18.0
%Al_2O_3:	14.3
%Fe_2O_3:	6.3
%MgO:	2.3
%K_2O:	1.7
%Na_2O:	0.9

Figure 4. SEM wiew and EDX analysis of a mud mortar in building B (HBM1).

Traces of plant fibres, of about 2-3 mm thicknesses possibly of wheat straw were identified in burnt materials. Fibres were more abundant in plasters. The temperature during the fire was estimated to be around 700°C or a bit higher by the combined interpretation of XRD, TGA, XRF, low or no vitrification observed by SEM images and high pozzolanic activity values.

%	HBPU	HPP1L	HBP2	HAB2
SIO_2	47.5	49.5	49.5	56.5
CaO	14.5	18	18	12.5
Al_2O_3	13	10.8	11.8	12
Fe_2O_3	7.5	5.5	6.8	7
MgO	3.5	2.7	3	2.5
K_2O	2.8	1.9	1.7	1.8
Na_2O	0.8	0.7	0.9	0.9
TiO_2	0.8	0.6	0.7	0.8
P_2O_5	0.2	0.1	0.1	0.1
MnO	0.1	0.1	0.1	0.1
Cr_2O_3	0.02	0.02	0.02	0.02
SO_3	0.09	0.06	0.1	
CI	0.04	0.04		
SrO	0.03	0.03		

Table 1. XRF results of the burnt mud brick of building A (HAB2) and burnt mud plaster layers of building B (HBP1U, HBP1L, HBP2L).

REFERENCES

Benharbit, M., 1994, Interface Piérre-Mortier, Mechanismes de Transfert et d'alteration, Procédé Passivation, Thése de Doctorat, Université Monpellier II, 196 p.

Brown, P. W and Clifton, J. R., 1978, Adobe I: The Properties of Adobe, Studies in Conservation, V. 23, Num 4, pp. 139-146.

Brown, P.W., Robbins, C. R., Clifton, J.R., 1979, Adobe II. Factors Affecting the Durability of Adobe Structures, Studies in Conservation. Vol.24, Num.1 , pp. 23-39.

Houben, H., and Guillaud, H., 1994, Earth Construction, Intermediate Technology Publications, London, 362 p.

Moropoulo, A.; Çakmak, A. S., Lohvyn, N., 2000, Earthquake Resistant Construction Techniques and Materials on Byzantine Monuments in Kiew, Soil Dynamics and Earthquake Engineering, 19, pp. 603-615.

Ngowi, A. B., 1997, Improving the Traditional Earth Construction: A Case Study of Botswana, Construction and Building Materials, V.11, No. 1, pp. 1-7.

RILEM, 1980, Tentative Recommendations, Comission-25-PEM, Recommended Tests to Measure the Deterioration of Stone and to Assess the Effectiveness of Treatment Methods**,** Materiaux et Construction, Vol. 13, No. 73, pp. 173-253

Sickels, L. B., 1981, Organics vs. Synthetics: Their Use as Additives in Mortars, in: Prooceedings of the Symposium on Mortars, Cements and Grouts Used in the Conservation of Historic Buildings, Rome, pp. 25-52.

Süel, M., 2000, Studien zu den Boghazköi-Texten (StBoT) 45.

Topal, T., 1995, Formation and Deterioration of Fairy Chimneys of the Kavak Tuff in Ürgüp-Göreme Area (Nevşehir-Turkey), Ph.D. Thesis, Department of Geological Engineering, Middle East Technical University, Ankara, pp. 61-67.

TS EN 196, 2002, methods of testing cement-Part 5: Pozzolanicity test for pozzolanic cements, TSE, Ankara.

Tunçoku, S.S., 2001, Characterization of Masonry Mortars used in Some Anatolian Seljuk Monuments in Konya, Beyşehir and Akşehir, Ph.D Thesis in Restoration, METU, Ankara, 128 p.

FINGERPRINTING CARPATHIAN OBSIDIANS BY PGAA: FIRST RESULTS ON GEOLOGICAL AND ARCHAEOLOGICAL SPECIMENS

Zsolt KASZTOVSZKY
Institute of Isotopes, Chemical Research Centre, H-1525 Budapest, PO.Box 77.
E-mail: kzsolt@alpha0.iki.kfki.hu

Katalin T. BIRÓ
Hungarian National Museum, H-1088 Budapest, Múzeum krt. 14-16.
E-mail: tbk@ace.hu

1. INTRODUCTION

Obsidian is one of the classical subjects of archaeometrical analyses. Major and trace-element data can provide indispensable information on the provenance of valuable archaeological objects. Most analytical methods however will require destruction or preparation of the samples equal to destruction. Therefore most of the choice pieces are not to be analysed by these methods. Prompt Gamma Activation Analysis (PGAA) is in principle suitable for analysing various kinds of pieces without destruction and without any residual radioactivity (Anderson-Kasztovszky in press). The method is based on the detection of γ-photons originated in (n, γ) reaction.

The question is how distinctly we can separate different source regions according to the detected components, and how effectively we can allocate the archaeological pieces into the resulting data sets. We had previous experience on provenancing various chipped stone raw materials, like Szeletian felsitic porphyry and various kinds of grey silex (radiolarite, flint, hornstone). PGAA proved to be effective for the former (Markó et al. 2003) while with silex, we have to refine our method (Kasztovszky et al. in press).

2. EXPERIMENTALS

The measurements were performed at the PGAA facility of the Institute of Isotopes, which is planted on the cold neutron beam of the Budapest Research Reactor.

Figure 1. Map of the obsidian samples analysed.

The pieces were placed into a horizontal cold neutron beam of 5 x 10^7 $cm^{-2}s^{-1}$ flux. An area of 2 x 2 cm^2 of each object was irradiated without any special preparation, intact and naturally, without any destruction or sampling. Since neutrons penetrate the whole sample, the information we get reflects the bulk composition of the material, which is very advantageous for the glassy, homogeneous volcanic glass (obsidian).

The irradiation times were between 1000 and 50.000 s, and were chosen to achive sufficiently low statistical error in the spectra. For spectrum evaluation 'Hypermet PC' software was used.

In these experimental conditions we were able to detect major components (H, Na, Al, Si, K, Ca, Ti, Mn and Fe) accessory and trace elements (B, S, Cl, Cr, Sm and Gd) in the chosen obsidian samples. The distinction between the raw material sources was made using series of bivariate plots and Principal Component Analysis (PCA). As it is usual in geochemistry, the major components' concentrations are expressed as oxides.

Our results of two measurement series seem promising; however we are working on extending our database of PGAA measurements concerning archaeological, as well as geological obsidian samples.

3. SAMPLES ANALYSED

Geological samples from all the important known obsidian sources of the Mediterranean region were measured with special regard to Central European (Carpathian I, II) sources, as well as archaeological sources mainly from Hungary (fig. 1).

Two analytical series comprising 45 items (20 archaeological obsidian, 16 comparative samples of known obsidian sources, one modern glassy slag and 8 other pieces claimed to be obsidian-like on macroscopic basis were analysed, see table 1).

4. DISCUSSION

Based on PGAA measurements, PCA was used to distinguish obsidian (glass of rhyolitic composition) from the rest (fig. 2). On one hand, silex (hornstone, radiolarite) samples separate well by PGAA; erroneous classification could be corrected for one piece described in archaeological technical literature from Ságvár as obsidian (Gábori 1964, Biró 1984). On the other hand, low silica content (probably artificial) glass was separated with claims to be obsidian from Oláhlápos (Romania) and Zeitlarn (Germany). They compare best to modern industrial slag from iron-smelting obtained from Kup. We have to make further analyses to prove the artificial character of these low-silica melts, however they clearly fall outside the range of obsidian.

Glassy andesite from Korolevo (raw material of the well-known Palaeolithic site) was also analysed and found clearly different from all obsidians, however much closer to the composition of rhyolitic glass. Rhyolitic glass from Transcarpathian Ukraine (Rokosovo) was also included in our series of measurements. The composition allows us to call it obsidian; however its composition is clearly different from Carpathian obsidians known so far. No archaeological pieces known so far had similar composition.

	Locality	Inv. Nr.	Archaeological Age	LabNr	Obs. type
Geological obsidian	Auvergne, France (1)	L 89/150	-	AUVERGNE?	
	Sardinia, Italy (2)	L 86/244	-	SARD (1)	
	Sardinia, Italy (2)	L 86/244	-	SARD (2)	
	Lipari, Italy (3)	L 86/240	-	LIPARI (1)	
	Lipari, Italy (3)	L 89/152	-	LIPARI (2)	
	Lake Sevan, Armenia (4)	L 86/268	-	SEVAN (1)	
	Lake Sevan, Armenia (4)	L 89/153.	-	SEVAN (2)	
	Melos, Greece (5)	L 87/51	-	MELOS (1)	
	Melos, Greece (5)	L 89/151	-	MELOS (2)	
	Rokosovi, Ukraine (6)	L 92/129	-	ROKOSOVI	
	Mád-Kakashegy, Hungary (7)	L 86/124	-	MÁD	C2E
	Tolcsva-Rányi dűlő, Hungary (8)	L 86/170	-	TOLCSVA	C2T
	Vinicky, Slovakia (9)	L 86/191	-	VINICKY (1)	C1
	Vinicky, Slovakia (9)	L 86/152	-	VINICKY (2)	C1
	Cejkov, Slovakia (10)	L 86/186	Upper Palaeolithic workshop-on-outcrop	CEJKOV	C1
	Kasov, Slovakia (11)	L 86/188	Upper Palaeolithic workshop-on-outcrop	KASOV	C1
Archaeological obsidian	Arka - Herzsarét (12)	HNM-Pb. 63/949	Upper Palaeolithic (Gravettian)	ARKA	C2Tr
	Balatonszemes-Bagódomb (13)	17/21, not inventorised	Early-Middle Neolithic, Earliest LBC	BSZEMES	C1
	Dömös (14)	HNM-Pb. 73/111	Upper Palaeolithic (Gravettian)	DÖMÖS	C1
	Érd-Érdliget (15)	HNM Ő.1960.40.4.	Copper Age	ÉRD	C2E?
	Galgagyörk - Csonkás-hegy (16)	HNM, not inventorised	Palaeolithic	GALGAGY	C2T
	Hidasnémeti-Köteles (17)	HOM, Miskolc not inventorised	Middle Neolithic, Bükk Culture	HIDAS	C1
	Hont - Molnárhegy (18)	HNM-Pb. 99/234	Upper Palaeolithic	HONT	C2E?
	Kálló-Puszta-hegy 4. (19)	HNM, not inventorised	Upper Palaeolithic (Gravettian)	KALLO	C2Tr
	Legénd Káldy tanya (20)	HNM, not inventorised	Palaeolithic	LEGÉND1	C1

	Locality	Inv. Nr.	Archaeological Age	LabNr	Obs. type
	Legénd Káldy tanya (20)	HNM, not inventorised	Palaeolithic	LEGÉND2	C2T
	Legénd Káldy tanya (20)	HNM, not inventorised	Palaeolithic	LEGÉND3	C2E
	Mikola (Mikula), Romania (21)	private collection, not inventorised	Prehistory	MIKO1	C1
	Mogyorósbánya - Újfalusi-dombok (22)	HNM-Pb. 2000/735	Upper Palaeolithic (Gravettian)	MOGYOR	C1
	Nagykálló (23)	HNMŐ. 1961.3.204	Bronze Age	NAGYK	C1
	Pilismarót - Bitóc (24)	HNM-Pb. 91/129	Upper Palaeolithic (Gravettian)	PILISM	C1
	Pilisszántó II rock shelter (25)	HNM-Pb. 51/110	Palaeolithic	PILISSZ	C1
	Püspökhatvan - Viszoki-hegy (26)	HNM, not inventorised	Palaeolithic	PÜSPÖK	C2T?
	Ságvár - Lyukas-domb (27)	HNM-Pb 51/159.12	Upper Palaeolithic (Gravettian)	SAGVAR	C1
	Szigetcsép-Tangazdaság (28)	HNMŐ. 1977.7.408.	Copper Age, Baden culture	SZIGET	C2T
	Tahitótfalu-Szülő-domb (29)	HNMŐ. 1965.15.8.	Copper Age, Boleráz culture	TAHI	C1
Others	Zeitlarn, Germany (30)	Naturkunde Museum, Regensburg	-	ZEITLARN	slag?
	Kup (31)			KUP	slag
	Oláhlápos, Romania (32)			OLÁH1	slag?
	Oláhlápos, Romania (32)			OLÁH2	slag?
	Mikola (Mikula), Romania (21)	private collection, not inventorised	prehistory	MIKO2	flint
	Mikola (Mikula), Romania (21)	private collection, not inventorised	prehistory	MIKO3	lqu
	Ságvár - Lyukas-domb (27)	61/1950/29	Upper Palaeolithic (Gravettian)	SÁGVÁR	rad
	Zeitlarn, Germany (30)	Naturkunde Museum, Regensburg		ZEIT1	silex
	Korolevo (28)	Kiev Kor 75.4286	Korolevo	andesite	

Table 1. Obsidian samples from archaeological and geological sites analysed by PGAA. Numbers in brackets at column **Locality** stand for reference nr. on fig. 1.

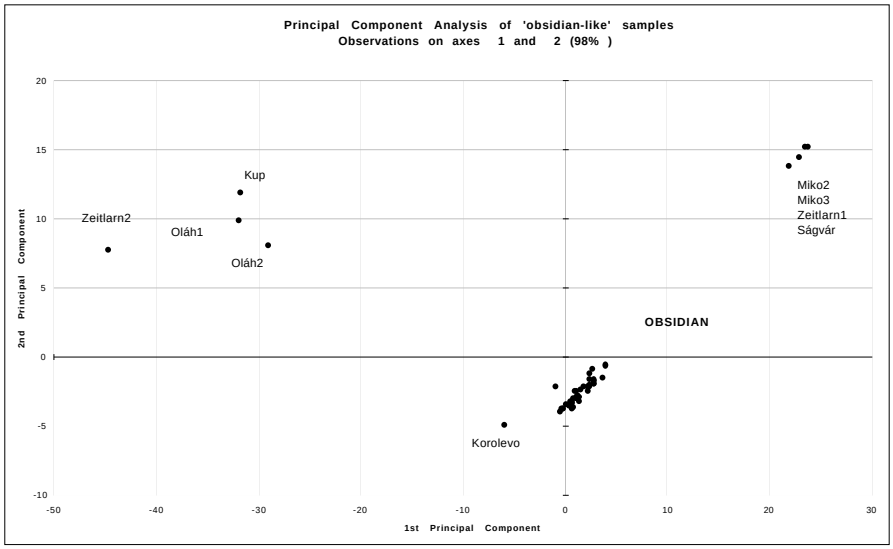

Figure 2. Separation of obsidian/non obsidian by PCA.

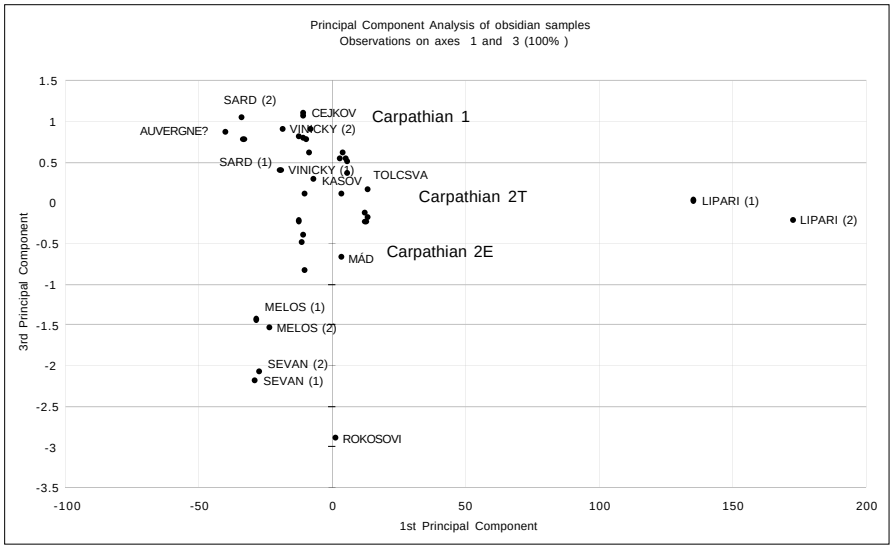

Figure 3. Clusters of obsidian from different (archaeological and geological) location obtained by PCA.

The rest of the samples were accepted as genuine obsidian (either archaeological or geological) and compared within the two analytical series by PCA and bivariate plots (fig. 3 and 4). Some elements, or combination of

elements seem to distinguish one source; low potassium for Melos, high B and Cl for Lipari. The differences observed in main components using EDS and EDS-XRF (Biró et al. 1986, 1988) can be ascertained also by PGAA. The Carpathian obsidians form two main groups, Carpathian I (Slovakian) and Carpathian II (Hungarian) obsidian. There is further differentiation within these groups as described by Williams et al. 1984 - C2T, C2E and probably also among the C1 samples (Bassiakos et al. 1998).

"Red" (mahogany) obsidian was overrepresented in our series of analysis (C2Tr). This type of obsidian occurs very rarely in Hungary both in the archaeological and geological material. The chemical composition as well as field experience connects the occurrence of these pieces to the Tolcsva sources.

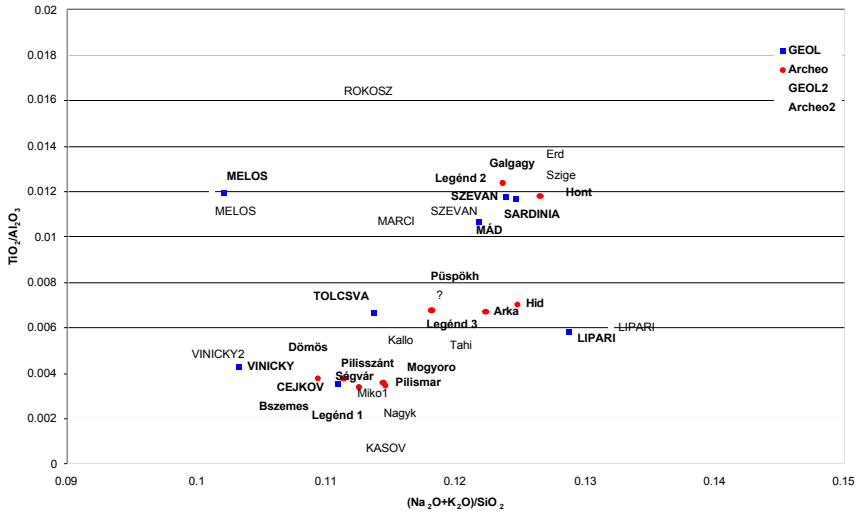

Figure 4. Separation of different obsidian samples based on TiO_2/Al_2O_3 vs. $(Na_2O+K_2O)/SiO_2$ ratios.

6. CONCLUSION

PGAA seems to be an adequate, fast and non-destructive method to analyse obsidian. So far, the results are in good agreement with the previous observation (chemical composition of reference material) and macroscopic observation made on the archaeological specimens. In addition, PGAA results were in accordance with NAA and supported by other analytical techniques (EDS-XRF, PIGE-PIXE) as well (Elekes et al. 2000a, b).

The analytical series as well as the reference material has to be extended in the future, with an eye on long distance imports as well as more source-collected reference materials.

REFERENCES

Anderson-Kasztovszky, 2004: Anderson, D. L. – Kasztovszky, Zs., Applications of PGAA with beams, in: *Handbook of PGAA with Neutron Beams*, Ed. G.L. Molnár, Kluwer Academic Publishers, Dordrecht / Boston / London, *in press.*

Bassiakos et al. 1998: Bassiakos, Y. - Biró, K. - Kilikoglou, V., Obsidian trade - the South-Eastern connection. Poster presented at 31st ISA Symposium, Budapest. In: Biró K.-Horváth T. (eds.), 31st International Symposium on Archaeometry. Program and Abstracts Budapest 1998 p. 22.

Biró 1984: T. Biró K., Distribution of obsidian from the Carpathian Sources on Central European Palaeolithic and Mesolithic sites. Acta Archaeologica Carpathica (Kraków) Kraków ***23***(1984) p. 5-42.

Biró - Pozsgai - Vladár 1986: T. Biró, K. – Pozsgai, I. – Vladár, A., Electron beam microanalyses of obsidian samples from geological and archaeological sites. ActaArchHung ***38***(1986) 257-278.

Biró - Pozsgai - Vladár 1988: Biró, K. - Pozsgai, I.- Vladár, A., Central European obsidian studies. State of affairs in 1987. Archaeometrical Studies in Hungary ***1***(1988) Budapest KMI 119-130.

Elekes et al. 2000a: Elekes, Z.-Biró, K.T.-Rajta, I.-Uzonyi, I.-Gratuze, B.,—Kiss Á.Z. Analyses of Obsidian and Radiolarite Samples by Ion Beam Techniques. - Paper presented at 32th ISA Conference, Mexico City.

Elekes et al. 2000b: Elekes Z. , Uzonyi I., Gratuze B., Rózsa P., Kiss Á. Z. 1, Szöőr Gy. Contribution of PIGE technique to the study of obsidian glasses. NIM/B SCI Nuclear Instruments and Methods in Physics Research Section B: Beam Interactions with Materials and Atoms 161 (2000) p. 836.-841.

Gábori 1964: Gábori M., A késői paleolitikum Magyarországon [The Late Palaeolithic period in Hungary] Régészeti Tanulmányok (Budapest) Budapest ***3***(1964) 1-83.

Kasztovszky et al. in press: Kasztovszky, Zs., Biró K. T., Dobosi V., Investigation of gray flint samples with Prompt Gamma Activation Analysis. In press for the Proceedings of the 33rd ISA Symposium, Amsterdam.

Markó et al. 2003: Markó, A. — Biró, K. T. — Kasztovszky, Zs., Szeletian Felsitic Porphyry: Non-Destructive Analysis of a Classical Palaeolithic Raw Material Acta Archaeologica Hungarica, Budapest ***54*** (2003) p. 297-314.

Williams et al. 1984: Williams-Thorpe, O.—Warren, S. E.—Nandris, J., The distribution and provenance of archaeological obsidian in Central and Eastern Europe. Journal of Archaeological Science ***11*** (1984) p. 183-212.

A TECHNIQUE FOR DETERMINING THE PROVENANCE OF HARAPPAN BANDED LIMESTONE "RINGSTONES" USING ICP-AES

Randall W. Law and James H. Burton
Department of Anthropology, University of Wisconsin-Madison

1. INTRODUCTION - BANDED LIMESTONE ARTIFACTS AT HARAPPA

Among the largest artifacts recovered at Indus Civilization (ca. 2600 to 1700 BC) cities in Pakistan and northwestern India (figure 1) are limestone "ringstones". Two ringstones found at the northernmost Indus city of Harappa are composed of a distinctive yellow-brown sandy textured

Figure 1. Indus Civilization cities and banded limestone sources.

limestone with reddish-brown bands and patches (figure 2). Several dozen flakes and fragments of this particular variety of banded limestone have also been recovered. For this study, 29 banded limestone artifacts (including the two ringstones) from Harappa were compared with two potential sources of that material using elemental data obtained through partial digestion of powdered samples and analysis using an inductively-coupled plasma atomic emission spectrometer (ICP-AES).

Figure 2. Banded limestone ringstones from Harappa. Scale = 0.5 meter.

2. POTENTIAL SOURCES OF BANDED LIMESTONE IN THE INDUS REGION

While limestone is found in abundance in each of the major geologic provinces surrounding the Indus Basin, there are few formations where material having the distinctive banding and sandy texture occurs. The most well-known source is in the vicinity of Jaiselmer in western Rajasthan, India, 450 km south-southwest of Harappa (figure 1). The limestone deposits of Jurassic age that occur here have long been exploited as a source decorative building stone (Agrawal et al. 1999) and past excavators at Harappa used the term 'Jaisalmer stone' to describe various artifacts found at those sites (Vats 1940: 358). Twenty five samples from three locations - Mool Sagar Khan, Jethway, and Habur, in the Jaiselmer Formation were analyzed for this study. Another possible source of the banded limestone artifacts from Harappa has recently come to light nearly 800 km to the south-southwest in the Kutch region of Gujarat, India. Here the Pachchham limestone formation of Jurassic age is found on several islands located within the intermittent inland sea known at the Great Rann of Kutch (Merh 1995). The southernmost Indus city

of Dholavira is located on one of these islands called Khadir (Bisht 1990). Twenty nine samples were collected for analysis from an ancient limestone quarry located 3 km north of Dholavira.

3. GEOCHEMICAL ANALYSIS OF BANDED LIMESTONE ARTIFACTS AND SOURCES USING ICP-AES

Banded limestone samples were analyzed using the ICP-AES facilities at the Laboratory of Archaeological Chemistry, University of Wisconsin-Madison. Preparation of geologic samples involved the removal of one gram of material from a freshly broken surface using a tungsten carbide drill. Depending on the size and condition of each archaeological sample, either the same procedure was used or a small chip (size > 1 g) of the material was powdered by hand in an agate mortar. The one gram sample was crushed to provide a homogeneous, representative sample from which a smaller sample could be taken for analysis. For all samples exactly 0.004 g of homogenized powder was weighed out and placed in a polyethylene analysis vial. One milliliter of nitric acid was placed in each vial and the samples were left to dissolve for 24 hours. After that time they were filtered of any remaining mineral particulates and 19 ml of purified water was added. This solution could then be passed through the ICP-AES, which is capable of quantifying a wide range of elements at parts-per-million levels. All samples were analyzed during a single session and data was acquired for the elements Ca, Ba, Sr, Mg, and Fe. Because there was a large component of quartz in these sandy limestones we were uncertain of precisely how much calcium carbonate was dissolved from sample to sample. We therefore divided each element by measured Ca to normalize for variable carbonate content, expressing the results as Ba/Ca, Sr/Ca, Mg/Ca and Fe/Ca. The resulting data were converted to log 10 values and subjected to exploratory canonical discriminant analysis (Baxter 1994) using SPSS 10.1 to evaluate the extent to which the two sources could be distinguished from one another and the degree to which archaeological samples resembled either source.

4. RESULTS

Figure 3 shows all samples plotted using discriminant functions derived from measured concentrations Sr Ba Mg Fe (each divided by Ca and log normalized). Geologic samples from the Jaisalmer formation were split into two groups: samples from Jethway and nearby Mool Sagar Khan (MSK) were combined as one group while the Habur samples are another. These were compared to the group of Pachchham limestone samples from the prehistoric quarry Khadir Island. While there is a degree of overlap between the outliers of the Jaiselmer and Pachchham formations, good separation overall between

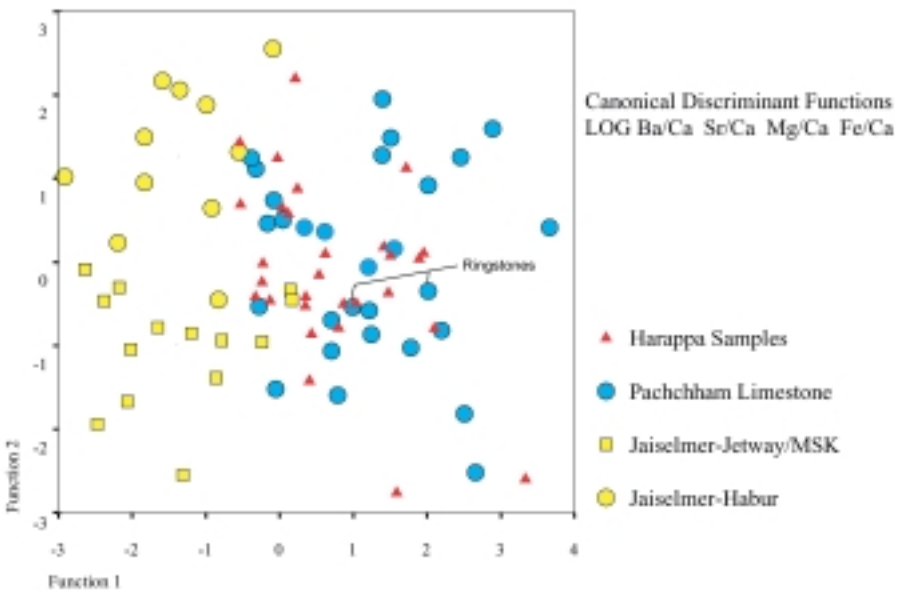

Figure 3. ICP-AES Analysis of Banded Limestone Sources and Artifacts.

the three groups was achieved with nearly 77% of cross-validated cases correctly classifying. When the archaeological samples are superimposed over the sources as ungrouped cases it is evident that they very much tend to cluster with the Pachchham formation samples. Some of the archaeological fragments (red triangles) fall within the overlapping margins of the two formations and, because they are closer to the center of one of the Jaiselmer groups, are classified as belonging to them. However, they may in fact be similar to outliers of the Pachchham formation, which themselves are misclassified as belonging to one of the Jaiselmer groups. Samples taken from the two ringstones (noted on figure 3), however, fall unambiguously in the center of the Pachchham group cluster.

In order to more clearly present the data as a comparison between the two source formations, all of geologic samples from the Jaiselmer formation were compared as single group to the Khadir Island quarry samples using canonical discriminant analysis. The resulting discriminant scores were used generate the box plots of the two formations and plot the archaeological samples (figure 4). Good separation between the two source formations was again achieved even though there is still a small degree of overlap evident. When the archaeological samples are plotted it is strikingly clear that they cluster within the range of Pachchham formation. In this plot even those archaeological samples that could potentially be outliers of the Jaiselmer formation fall closer to the center of the Pachchham cluster. The ringstone samples (noted on figure 4) are once again aligned with the center Khadir Island quarry source.

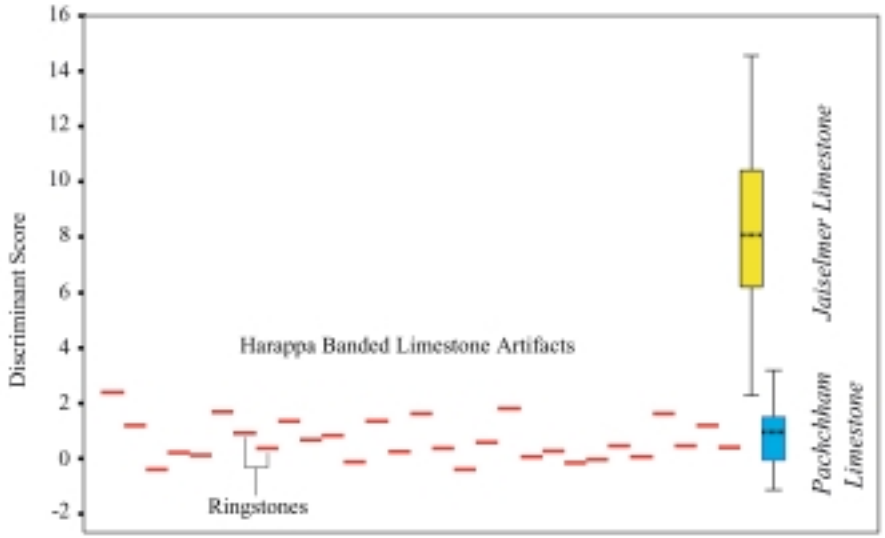

Figure 4. ICP-AES Analysis of Banded Limestone Sources and Artifacts (BOX PLOTS).

5. CONCLUSION

This study is ongoing. Additional geologic samples are to be analyzed that will help to generate a clearer picture of geochemical variability in the potential source formations and to provide a larger data set for more statistically secure provenance appraisals. Other potential sources of banded limestone elsewhere in the Indus region may come to light and that will have to be evaluated also. At this time, however, the evidence strongly suggests that, of the two potential sources examined, the banded limestone ringstones and fragments excavated at Harappa most likely derived from the Pachchham formation of northern Kutch, perhaps from the ancient quarry near Dholavira itself.

ACKNOWLEDGEMENTS

Many thanks to Mark Kenoyer and Richard Meadow, Directors of the Harappa Archaeological Research Project; Fazal Dad Kakar, Director-General, Department of Archaeology and Museums-Government of Pakistan; RS. Bisht, Joint Director-General, Archaeological Survey of India; and T. Douglas Price, Director of the Laboratory of Archaeological Chemistry, University of Wisconsin-Madison.

REFERENCES

Agrawal, S. C., P. Bhatnagar and N. Khabya (1999). Limestone Deposits of Rajasthan. Udaipur, Department of Geology and Mines.

Baxter, M. J. (1994). Exploratory multivariate analysis in archaeology. Edinburgh, Edinburgh University Press.

Bisht, R. S. (1990). "Dholavira: New Horizons of the Indus Civilization." Puratattva 20: 71-82.

Merh, S. S. (1995). Geology of Gujarat. Bangalore, Geological Society of India.

Vats, M. S. (1940). Excavations at Harappa. Delhi, Government of India Press.

NON-DESTRUCTIVE CHARACTERISATION OF PIGMENTS BY MEANS OF THE COMPLEMENTARY USE OF PIXE-ALPHA AND XRD PORTABLE SYSTEMS

Lighea Pappalardo, Giuseppe Pappalardo, Francesco Paolo Romano
Laboratori Nazionali del Sud, INFN, Via S. Sofia 44, 95123 Catania, Italy
Sezione di Catania dell'Istituto per i Beni Archeologici e Monumentali, CNR, Via A. di Sangiuliano 262, 95100 Catania, Italy

Francesca Amorini, Ermelinda Scafiri
Dipartimento di Fisica e Astronomia dell'Università di Catania, Viale Andrea Doria 6, 95123 Catania, Italy

Maria Grazia Branciforti, Agata Taormina
Servizio Archeologico, Soprintendenza per i BBCCAA di Catania, Via L. Sturzo 62, 95100 Catania, Italy

ABSTRACT

The portable PIXE-alpha system realised by INFN-CNR has been employed for the analysis of pigments present in some Roman frescoes.

The PIXE data have been used to select between the possible mineralogical phases of interest present in the XRD spectrum of a portable diffractometer.

It is shown, in a typical case, that, by taking into account both the XRD and PIXE data, a quantitative determination of concentration of the various components is possible.

1. INTRODUCTION

The non-destructive characterization of the pigments present in the wall paintings is one of the objectives of the modern Archaeometry (Uda et al., 1999, Damiani et al., 2003). Also, since the artifacts cannot be moved from their place, non destructive analyses must be carried out with portable systems.

Among the most known n. d. techniques, the PIXE (Particle Induced X-Ray Emission) is one of the most appropriate: in fact the charged particles allow to confine the analysis only to the surface of the sample without

interference from the substratum (Malmqvist 1995; Lucarelli & Mandò, 1996). However by using the PIXE technique it is possible only to perform elemental analysis. In several cases the knowledge of the chemical elements present in the surface is not sufficient to perform a complete characterization and other n.d. techniques are requested to be used. The Micro-Raman technique (Damiani et al., 2003) is very useful for the identification of the pigments. Also portable XRD analysis is interesting because allows a simultaneous information on all the present mineralogical phases. However, the portable diffractometers display in general a limited angle - resolution and some ambiguity can arise in the determination of the mineral components. The complementary use of PIXE and XRD can overcome the above difficulties as it has been shown (Uda et al., 1999). However the above authors make use of the PIXE technique from the accelerator which is, obviously, a non-portable system.

In the Laboratori Nazionali del Sud a portable PIXE system has been developed. The present paper constitutes a preliminary communication concerning a wide program of in-situ characterization of Roman frescoes carried out in collaboration to the Soprintendenza ai Beni Culturali e Monumentali of Catania (Italy). The frescoes concern artefacts from the excavations at the Convento dei Benedettini, the Roman theatre and via Crociferi in Catania (Italy). We present a typical case to illustrate the general method used in order to obtain quantitative analysis making use of both portable PIXE and XRD systems.

2. THE LNS PIXE-ALPHA PORTABLE SYSTEM

The system has been described in several papers (L. Pappalardo et al., 2003). The charged particles are produced by using an annular radioactive

Figure 1. Fragment of a Roman fresco from the excavations of via Crociferi in Catania.

37 MBq ^{210}Po source; the outgoing energy is 5.1 MeV. The detector is a 10mm^2 diameter Si-drift (145 eV resolution at 5.9 MeV). A He flux ensures the detection of elements as light as Na.

Fig. 1 shows a fragment from the excavation of a Roman villa in via Crociferi. The surface is well preserved. The colour is reddish-brown. The main dimension is 7.5 cm length.

The PIXE-alpha energy spectrum taken on the painted surface of the Roman fresco fragment on fig. 1 is shown in fig. 2. Si, Ca, Fe lines are clearly

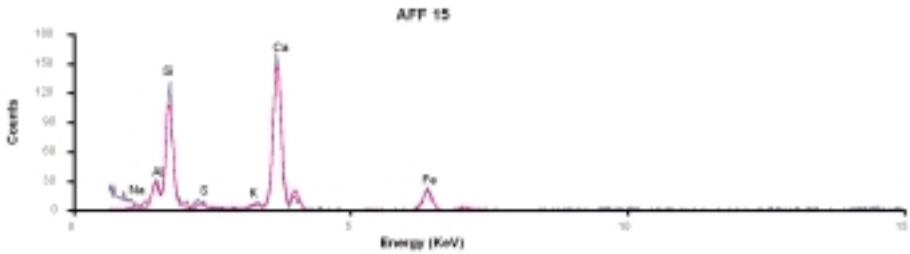

Figure 2. PIXE - alpha energy spectrum of the surface of the fresco sample displayed in fig.1. Si, Ca, Fe are the most visible elements.

present. The iron peak indicates the possible presence of a red hearth pigment like ocra. However it must be pointed out that the pigment is diluted on the plaster that generally contains calcite and in some case quartz. To obtain further and quantitative information XRD analysis has been performed with a portable diffractometer.

3. THE XRD PORTABLE SYSTEM

The system is a commercial one (ASX-DUST, Assing SpA, Rome). An iron anode x-ray tube is used to produce x-rays. An energy-dispersive XR100-CR Si PIN (AMPTEK inc.) detector generates XRF spectra and is used to select the Fe Kα line devoted to produce diffraction. The angle -resolution was about 0.3 degrees which corresponds to about 1.6 % resolution on reticular distance at small angles.

The angular step and the acquisition time for each step can be previously presetted. Both the detector and the tube rotate in a goniometric circle. The typical beam current was 250 μA and the tube voltage was 30 kV. The system is operating by means of a dedicated software control. The X-ray diffraction pattern taken on the same sample of fig. 1 is shown in fig. 3.

Peak at various angles are present.

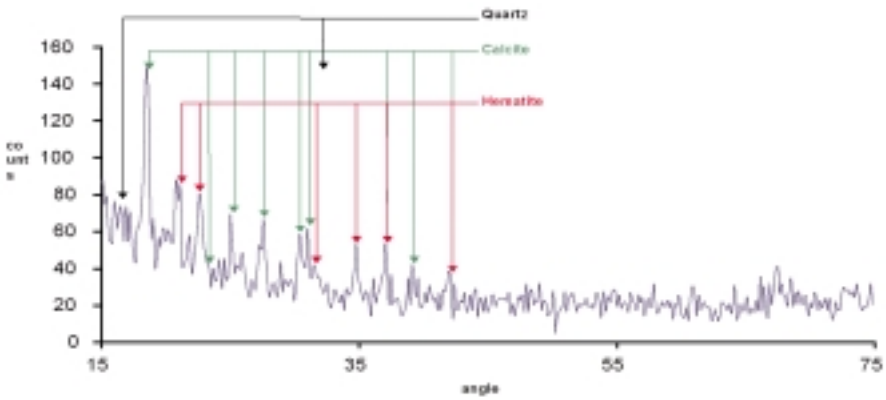

Figure 3. Mineralogical pattern of XRD data on the fragment of fig1. Calcite and hematite are the most important components. Quartz is suggested.

4. QUANTITATIVE ANALYSIS OF THE DATA

The moderate angular resolution of the XRD instrument can originate some ambiguity in the individuation of the various mineral components. However the PIXE qualitative data from the spectrum of fig. 2 strongly reduces the possible minerals to be taken into account. In our case, by combining the PIXE data with the XRD data, we unambiguously assign to calcite ($CaCO_3$), hematite (Fe_2O_3) and quartz (Si_2O) the data of the diffraction pattern. To obtain the absolute value of the concentration and to check the correctness of our procedure we used the qualitative composition found by the XRD to perform quantitative PIXE data. So, we introduced in the GUPIX CODE (Maxwell et al., 1995; Hopman et al., 2002) the stoichiometric compositional data of XRD to estimate the concentration. First, we carefully calibrate the PIXE – alpha system by using suitable petrologic standards to deduce the H constant. With the above H value we calculated the final concentrations assuming the stoichiometric composition given by the XRD data. The quantitative data are displayed in table 1. It must be emphasized that the sum of the calculated values would be 100%, without applying any normalization, if the compositions have been correctly considered.

Mineralogical phases	$CaCO_3$	Fe_2O_3	SiO_2	Others (Na, Mg, Al, P, S, CI, K, O)	Total
Concentration (%)	53.3 ± 1.6	28.3 ± 10	11.7 ± 0.6	7.7 ± 5	**101 ± 5**

Table 1. Quantitative results obtained from analysis of PIXE data on the basis of the XRD stoichiometric indications. The code GUPIX has been used in the "Matrix Calculation" option.

5. CONCLUSIONS

The complementary use of portable PIXE and XRD systems has given the possibility to obtain a complete quantitative characterization of a Roman fresco fragment surface.

REFERENCES

Damiani, D.; Gliozzo, E.; Memmi Turbanti, I., Spangenberg, J. E., 2003, Pigments and plasters discovered in the house of Diana (*Cosa,* Grosseto, Italy): An integrated study between Art history, Archaeology and Scientific Analyses. *Archaeometry* 48, 2 (2003), pp. 341-354.

Hopman, T. L.; Nejedly, Z.; Maxwell, J. A., Campbell, J. L., 2002, Extension of GUPIX to ^{2}He, ^{3}He and ^{4}He excitation, *Nuclear Instruments and Methods in Physics Research B,* 189, 138.142.

Lucarelli, F., Mandò, P.A., 1996, Recent application to the study of ancient inks with the Florence external-PIXE facility, *Nuclear Instruments and Methods in Physics Research B*, vol. 109/110, pp. 644-652.

Malmqvist, K. G., 1995, Particle induced X-Ray Emission Spectrometry, *Chemical Analysis*, vol. 133, John Wiley and Sons.

Maxwell, J. A.; Teesdale, W .J., Campbell, W. J., 1995, The Guelph PIXE software package II, *Nuclear Instruments and Methods in Physics Research B,* vol. 95, pp. 407-421.

Pappalardo, L.; Romano, F.P.; Garraffo, S.; De Sanoit, J.; Marchetta, C.; Pappalardo, G., 2003, The improved LNS PIXE-alpha portable system: archaeometric applications, *Archaeometry 45,* 2, pp. 333-339.

Uda, M.; Sassa, S.; Yoshioka, T.; Taniguchi, K.; Nomura, S.; Yoshimura, S.; Kondo; Nakamura; M., Iskandar N.; Zagholul B., 1999, X.Ray analysis of pigments on ancient Egyptian monuments, *International Journal of PIXE,* Vol. 9, Nos. 3&4, pp. 441-451.

e-VISARCH: AN ON-LINE RAMAN SPECTRA DATABASE OF ARCHAEOLOGICAL MATERIALS ON STONE AND PLASTER SUPPORTS

M. Pérez Alonso, K. Castro, M. A. Olazabal, and J. M. Madariaga
Dept. of Analytical Chemistry, University of The Basque Country, B.º Sarriena, s/n, 48940 Leioa (Bizkaia), Spain. e-mail: qabpealm@lg.ehu.es

1. INTRODUCTION

In last years the interest in archaeological materials has grown tremendously since the need of sustainability has reached to the Archaeology and Fine Arts fields. Some of the traditional techniques employed in the laboratories applied to the field of Archaeometry, eg. X-Ray Fluorescence Spectroscopy (XRF), Scanning Electron Microscopy (SEM) and energy-dispersive X-ray analysis (EDX), X-ray diffraction (XRD), X-ray fluorescence (XRF), ICP, IR spectroscopy, are destructive, and/or necessitate sampling, affecting the integrity of the art object under analysis. The new research trends plead for the use of non-destructive analytical tools as artwork and archaeological materials are unique and irreplaceable.

Among these non-destructive techniques Raman spectroscopy is arising as one with the most promising future. The important development on detector construction in last decade is really remarkable and has provided new perspectives on its application. As FTIR spectroscopy, Raman spectroscopy is a very reliable, sensitive and specific analytical technique that can provide molecular and structural information either of organic or inorganic materials, with the main advantage that can be applied "in situ" (Vandenabeele 2001). In the bibliography there are some references to Raman databases principally in the application of pigment and mineral determination (Bouchard 2003, Wangm 1994) but no one is focused on the study of archaeological materials. However if you wish to make an electronically based compound identification, the access to electronic format of the spectra is necessary in order to include them in the software package and to get good analyses (Castro 2003).

The proposal of this work is to present our e-VISARCH Raman spectra database of materials with archaeological interest. The database in electronic format is available free of charge at the web site: http://www.ehu.es/database/

database.html (login: spectra, password: database). The database will be continuously updated as soon as new substances susceptible of being found in archaeological artefacts and materials will be processed.

2. INSTRUMENTATION

The standard spectra of the pigments and materials were collected on two different spectrometers. In both cases no sample preparation was required to perform the analysis of the specimens.

2.1. Fourier Transform Raman Spectroscopy (FT-Raman)

A Nicolet FT-Raman 950 spectrometer equipped with a 1064 nm Nd:YAG Laser and a InGaAs detector was used. The analyses were performed using low laser powers (between 12 and 17 mW) to avoid thermal decomposition of the specimens. Whenever it was necessary, a neutral density filter with an optical throughput of 10 % was employed. The spectra were recorded with a resolution of 4 cm^{-1} and with 500-2000 scans depending on the scattering of each sample.

2.2. Raman fibre optics micro-probe (Raman dispersive)

Raman dispersive spectra of standards were carried out using a portable Renishaw Raman Analyzer RA 100 system coupled to a Raman fibre optics micro-probe (with a 785 nm diode laser and a CCD detector). In this case, the laser power used was in the range 5-50mW. When necessary neutral density filters with optical throughputs of 1% or 10% were used. The spectra were recorded with integration times between 100-300s, and with 1-5 scans per spectrum accumulated. In both cases, no sample preparation was performed to analyse the specimens.

3. DATABASE CONTENTS

The web page was home-made developed using HTML 4.0, CSS 2.0, PHP 4.0 and Java Script programming languages. The current database has 168 Raman spectra collected with the Raman system from Renishaw (785 nm), and 80 spectra recorded with the FT-Raman system from Nicolet (1064 nm). However, the database does not provides only the spectra, but also information about the names of the specimens in different languages and well-known synonyms, the identification number, origin, composition, chemical composition, compatibility and permanence, use and applications, and some adulterations.

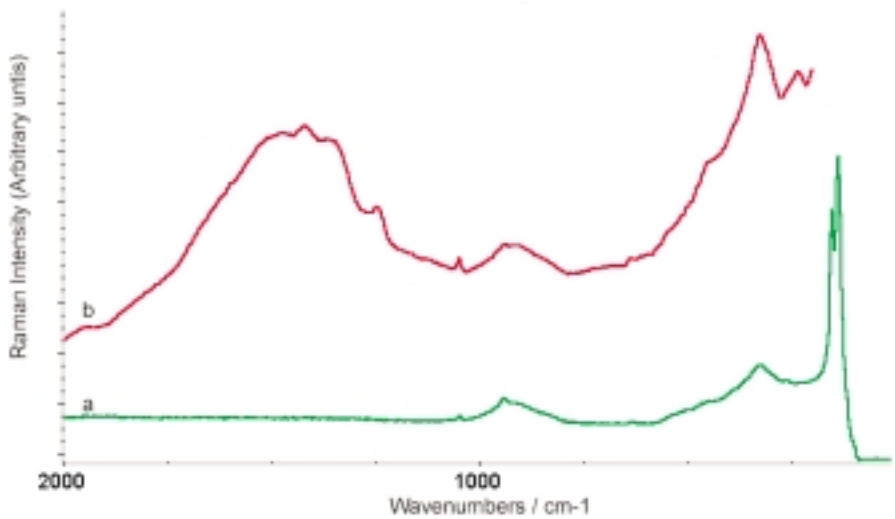

Figure 1. Raman spectra of Lead Tin Yellow Type II ($PbSnSiO_7$) a) FT-Raman spectrum with 1064 nm excitation wavelength, b) Raman spectrum with 785 nm excitation wavelength.

Whenever it has been possible different spectra for the same compound provided by different dealers are included in the database. In this way some adulterations have been detected in some supposedly pure specimens, assigning to the specimen only those Raman signals belonging to the pure compound (Pérez 2002). This is especially important to analyse unknown samples.

Raman theory states that the Raman signals for each compound appear at the same wavenumber position independently of the wavelength we use to excite the sample. However, the employment of different configurations on the analytical equipments can provide spectra with no identical Raman response refering to fluorescence processes or range studied. Figure 1 shows two Raman spectra of the same sample recorded by both analytical techniques. It is easily observed in figure 1 how the Raman system from Renishaw does not work properly under 200 cm^{-1}, and depending on the nature of the specimens, the analytical response may show a higher fluorescence that the one provided by the FT-Raman equipment. On the contrary we have stated that the Nicolet FT-Raman spectrometer with the 1064 nm excitation wavelenght is not the appropiate technique to analyse several blue pigments due to the low response of the InGaAs detector employed.

In general, when comparing the spectra obtained by the use of the two different excitation lasers, three phenomena can be observed: the magnification or attenuation of the intensities for some bands, the difference

in band intensities (e.g. calcite, azurite) or the identical spectra recorded (e.g. minium, anhydride plaster, alabaster).

All the information contained in the e-VISARCH database has been organised in 5 different categories according to the nature and use of the materials:

— Bulk components in stones and building materials (calcite, dolomite, silicates...).
— Pigments usually employed in wall paintings and/or decoration of buildings (from antiquity to XVth century).
— Decaying products produced by physical, chemical or biological weathering (gypsum, whewellite, scytonemin...).
— Binders (piscis glue, gum arabic, colophony...).
— Materials used in restoration and conservation (methylcellulose, paraloids...).

4. APPLICATION TO REAL SAMPLES

The e-VISARCH database has been employed until now with great results in the study of different kinds of samples, such as round tombstones (funerary stone based artefacts from the IIth till the XVth centuries), marbles from a graveyard near the sea, a Romanesque church in a non-polluted area (Pérez-Alonso 2004(a)), and some wall paintings from the Church of Santa María de Hermo (Asturias) (Pérez-Alonso 2004(b)). The analyses have been focused on the determination of the composition of the samples as well as in

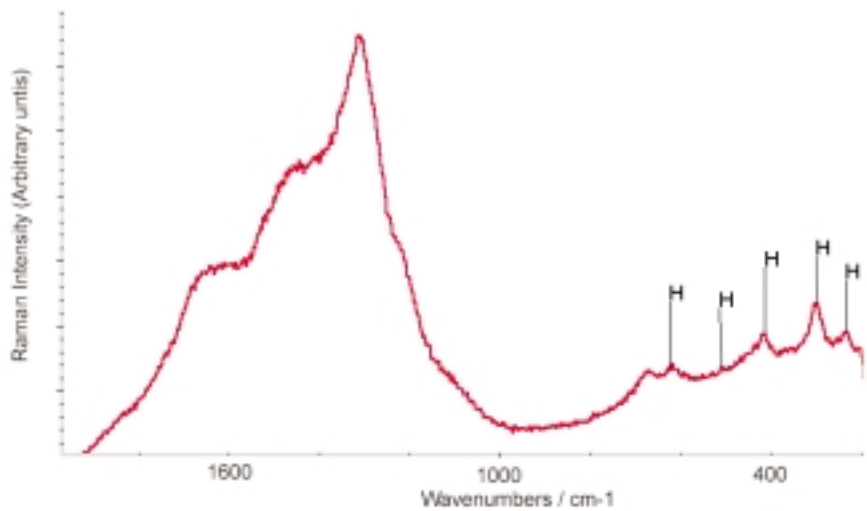

Figure 2. Raman spectum of the Greek Pottery analysed showing the characteristic bands of haematite.

the understanding of the decaying processes that take part due to the environment surrounding each sample.

The identification of decaying products is also important to design an adequate conservation action. In this way it has been possible to state the outcome of acid attack in old carbonaceous stone at open air in non-polluted areas or in modern stone artefacts by direct exposition to atmospheric gases in sites affected by oil refineries or power generation plants (high levels of SO_2 and CO_2). Also biodeterioration phenomena have been detected as well as the detachment of pigment grains in frescoes by chemical reaction between $CaCO_3$ and ammonium nitrate salts (Pérez-Alonso 2004(b)).

Although the e-VISARCH database was initially created to analyse archaeological materials on stone and plaster supports, it is supposed to be gradually updated with other specimens characteristic of other archaeological artefectas, such as ceramics, glasses or metals. In this case we have analysed a Greek pottery found in Magna Graecia, Locri, Italy. No pigment was determined in the white areas of the pottery, but a mixture of haematite (Fe_2O_3) and magnetite (Fe_3O_4) were found in the red and brown polychromed areas.

ACKNOWLEDGMENTS

This work has been financially supported by the project UPV UE02-A06. M. Pérez-Alonso acknowledges her predoctoral fellowship from the Basque Government.

REFERENCES

Bouchard, M., Smith, D. C., Spectrochim. Acta, 2003, 59A, 2247-2266.

Castro, K.; Pérez, M.;Rodríguez-Laso, M. D.; Madariaga; J. M, Anal. Chem., 2003, 75, 214A-221A.

Pérez, M.; Castro, K.; Rodriguez-Laso, M. D.; Olazabal, M. A., Madariaga, J. M., Proceedings of Art 2002, the 7th international Conference on Non-Destructive Testing ad Microanalyisis for the Diagnostic and Conservation of the Cultural and Environmental Heritage (Univ. of Antwerp, Belgium, Antwer-Wilrijk), 2002, 173-182.

Pérez-Alonso, M.; Castro, K., Martinez-Arkarazo, I., Angulo M; Olazabal, M. A., Madariaga J. M:, Anal. and Bioanal. Chem., 2004, 379, 42-50.

Pérez-Alonso, M., Castro, K., Álvarez, M.; Madariaga, J. M., Anal. Chim. Acta, 2004, 524, 379-389.

Vandenabeele, P., Verpoort, F.; Moens, L., J. Raman Spectrosc., 2001, 32, 263-269.

Wangm, A.; Han, J., Guo, L., Yu, J., Applied Spectrosc., 1994, 48, 959-958.

NON-DESTRUCTIVE ANALYSIS OF PAINTINGS LAYERS BASED ON REFLECTANCE SPECTROSCOPY AND ENERGY DISPERSIVE XRF

Gianluca Poldi, Letizia Bonizzoni, Nicola Ludwig, Ilaria Mascheroni, Mario Milazzo
Istituto di Fisica Generale Applicata, Università degli Studi di Milano, via Celoria, 16 20133 Milano (Italy); e-mail: g.poldi@tiscali.it

Key words: paintings; pigments detection; pigment layers sequence; non destructive techniques; visible-NIR reflectance spectroscopy; XRF analysis, infrared reflectography; portable instruments

1. THE METHOD

The importance of using non-destructive techniques (n.d.t.) in studying a painting is well known. Despite of it, some information on the painting materials can be obtained only through micro-samples and microscopic (optical and SEM) and chemical analyses. In this work we discuss the possibility of using a n.d. method in painting examinations suitable for pigment identification, giving at the same time a hint on the layer sequence without resorting to micro-sampling and stratigraphic analysis. Basically, the method consists in comparing the results of two different analyses: visible and near infrared reflectance spectroscopy (vis-NIR RS) and Energy Dispersive XRF analysis (EDXRF) both achieved by portable instruments. In principle, XRF analyses detect pigment elements of the layer sequence down to the ground level, while the reflectance spectra in the visible is characteristic only of the most external layer, and NIR (up to 1 micron) can give data related up to tens microns of thickness (Bruni, 2002). After the identification of pigment of the most external layer from the reflectance spectrum, to infer the composition of the underlying layers is then possible. A valid help to choose the zones to be investigated by our method is obtained from infrared reflectography (between 0.8 and 1.1 micron), which in most cases allows to recognize whether original or restored areas, also giving some additional information on the painting materials.

EDXRF is the most used among the n.d. non-imaging analytical methods applied to paintings (Mantler, 2000), while vis-NIR RS (Bacci, 1999) is

normally not employed for identification of pigments, but is more widely used in restoration works to obtain colorimetric data in order to evaluate cleaning process effects (Bacci, 2001) or to study ageing phenomena on surfaces (Kirby, 2004; Saunders, 2004).

2. LABORATORY RESULTS AND DATABASE OF THE PIGMENTS

In order to test our method we achieved a set of paint layers (more than 50 multilayers and more than 100 single layers) of different composition. Namely we prepared *single layers of pure pigment*, someones mixed with lead white; *single layers of mixed pigments*; *multiple layers of pure pigments*, someones mixed with lead white; *multiple layers of mixed pigments*. The choice of pigments was made according to tradition following treatises and essays on painting, from 13th century to the beginning of 20th century, and looking at the stratigraphic data published by various research institutes in the last 30 years. Particular attention was payed to reproduce typical 15th century pictorial multilayers (Mantegna, Giovanni Bellini, Raphael, Memling), and, in particular, *thin* superficial layers (from Italian: "velature").

Effects of different media in reflectance spectra were evaluated for most pigments by making mixtures with egg tempera, linseed oil and, in a few cases, arabic gum. All pigments were also studied in powder form. The layers have been applied to wood panels prepared with a "gesso" ground. In some instances, still according to tradition, a lead white priming was added. Some layers were directly painted on commercial canvases prepared with titanium white.

Concerning reflectance spectra, pigments can be classified according to the main behaviour of spectra in the vis-NIR region. The first class (typically blue and green pigments) have one or more peaks. The second class shows S-shaped spectra with no peak at all (typically non-iron oxides yellow, orange, red, brown pigments) or a small one (iron oxides: earths and ochres). Possibility of identification for each pigment relies on peculiar characteristics: maxima, minima, and changes of slope (rising points, shoulders, plateau) of the related reflectance curve occurring at specific wavelength values. Examples of our results are given in table 1. The obtained spectra have been compared to those published by IFAC, Florence (see http://fors.ifac.cnr.it).

The main modifications of the reflectance spectra induced by different media consist generally in an overall bias in reflectance level (usually lower for oil medium) and a minor wavelength shift of the peak (e.g.: 15 nm longer for azurite and natural ultramarine in oil).

Pigment	Reflectance spectrum characteristics (360-1000 nm)
Azurite	max 470; rises from 900
Natural ultramarine	max between 470 and 485; min at 590; rises from 650-680; small shoulder at 750
Smalt blue	max between 450 and 470, relative max 560; rises from 650-680 like
	ultramarine; small shoulder at 730
Indigo	max 430; rises from 600 nm
Malachite	max 540; min at 750, then flat
Verdigris	max 515-525; min at 700 ; very small rise, or none
Copper resinate	max 520; min < 670; th en rises
Green earth	max 540; then almost flat
Yellow ochres	rises from 500-550; shoulder at 590; max 770; plateau min 900
Lead yellows	rises from 430; shoulder at 600; max at 840
Orpiment	rises from 450; shoulder at 620; max at 840
Vermilion	plateau min < 500; rises from 580; shoulder at 640; max 840-850
Red ochre	plateau min ; rises from 550; small shoulder at 600-610; max 760-780
Haematite	similar to red ochre, darker; max at 785
Cochineal lake	small max at 450; min a 520-560; rises from 580-600; shoulder at 670; max 850
Brazil wood lake	almost flat up to 570-650 nm, where rises
Madder lake (Robbia)	small rise up to 450, then small plateau; rises from 550
Siena raw (natural)	small shoulder at 450 and 600 (more evident), max 770

Table 1. Characteristics of reflectance spectra of some pure pigments in linseed oil or egg tempera (max=reflectance peak; min=minimum). The values, representing wavelengths in nanometers, are mean values of the ones obtained varying experimental conditions: medium, pigment variety, surface roughness.

Pigments containing only light elements, like natural ultramarine and lakes, can be recognized only by RS but not by EDXRF, since X-rays emitted by elements with atomic number lower than 13 (Al) are absorbed in the paint layer or in the detector window. A synthesis of the results obtained for pigments typical of European art between 14th and 16th century is reported in table 2.

Our results show that the combined use of vis-NIR RS and EDXRF allows the identification of pigment sequence, provided that no more than two painting layers are involved. Moreover, these pigments may possibly be mixed with white. It is a valuable improvement of the usual reliable pigment detection in pictorial layers.

For the history of art overpaintings of ultramarine over azurite, typical of Venetian and Flemish schools in the early Renaissance, are particularly interesting and are clearly revealed in a wholly non-destructive way, by our method. Similarly, we can detect overpaintings of ultramarine over smalt

blue, or over a mixture of smalt blue and azurite, or overpaintings of various red lakes over vermilion, used to create shadows in red garments.

Pigment	Chemical elements detectable through EDXRF	Certainly identifiable through EDXRF	Certainly identifiable through vis-NIR RS
Lead white (biacca)	Pb	Yes, in respect to other whites	No
Whitewash	Ca	No, cfd. with white chalk or bone white	No
Bone white	P, Ca	Yes, when P is detected	No
Gesso (white chalk)	S, Ca	Yes, when S is detected	Not always
White earth (caolino)	(Al), (Si)	Yes, when Al is detected	?
Azurite	Cu	Yes	Yes
Natural ultramarine	(Al), (Si), tracks of Fe	Not always	Yes
Smalt blue	K, Co	Yes	Yes
Indigo	-	No	Yes
Malachite	Cu	No, cfd. with verdigris and copper resinate	Sometimes
Verdigris	Cu	No, cfd. with malachite and copper resinate	Sometimes
Copper resinate	Cu	No, cfd. with malachite and verdigris	Sometimes
Green earth	(Al), (Si), (Mg), (K), Fe	Yes	Yes
Green lakes	(Al)	No	Sometimes
Yellow ochre	(Al), (Si), Fe	Yes	Yes
Lead yellows	Pb, in some cases also Sn or Sb	Yes, if only Pb they are undistinguishable from litharge	Sometimes, cfd. with orpiment
Orpiment (yellow) and realgar (orange-red)	S, As	Yes, but undistinguishable one from the other	Sometimes, cfd. with lead yellows
Yellow lakes	-	No	Sometimes
Red ochre	Fe	Cfd. with haematite	Cfd. with haematite
Haematite	Fe	Cfd. with red ochre	Cfd. with red ochre
Venetian red	Fe	Cfd. with red ochre	Sometimes
Vermilion	S, Hg	Yes	Yes
Red bole	(Al), (Si), Fe	Yes, when Al is detected	?
Minium	Pb	Yes	Sometimes
Red lakes	-	No	Yes, and usually distinguishable cochineal lake, madder lake, Brazil wood
Earths (brown earths)	Fe, Mn	Yes, but undistinguishable the different types (Siena raw, burnt umber …)	Some of them
Brown lakes	-	No	Yes, in respect to earths

Table 2. Possibility of identification through EDXRF and vis-NIR RS of typical 14th and 16th century pigments (pure single layer or mixed with lead white). Elements in tracks in parentheses; cfd.= may be confused.

2.1. Limitations of the method

Evidently, we do not know previously how many layers of different pigments have been used in the painting, and experimentally we can only distinguish the upper layer from the underlying ones. We know, however, that the 15th century Venetian and Flemish schools rarely used more than one or two layers of pigment over the preparatory ground or priming. In addition, some elements are almost always linked to the underlayers: e.g. the detection of Ca and S means in almost every case the existence of "gesso" ground. But S can be found also in vermilion (from cinnabar or artificial), this time associated with Hg. Specific limitations of RS, and in less extent also of XRF, are related to the difficulty of detecting mixed pigments (Poldi 2004).

3. IN SITU RESULTS

More than 40 paintings of different periods belonging to Italian museums have been studied by our method. In particular, the results for masterpieces of Cima da Conegliano, Bartolomeo Montagna, Hans Memling, van Dyck, Tiepolo, have been published in the first two volumes of the general catalogue of the Civic Gallery of Vicenza (Poldi 2003). Of particular interest we consider the discovery of smalt blue (cobalt) in a 1333 Paolo Veneziano's painting (first attestation), and the diffuse presence of zinc (not to be ascribed to restorations) in 14th century Italian paintings.

4. CONCLUSIONS AND FURTHER DEVELOPEMENTS

The reliability of the proposed n.d. method has been tested on a large set of pigment samples. If coupled with micro-sampling, this method should allow the extension of the results of stratigraphic examinations to other zones without additional sampling.

Further foreseen developements in reflectance spectrometry are the study of the influence of whites when mixed with coloured pigments, the influence of surface roughness, pigment grain size, varnish and of ageing. The extension of RS wavelength range up to 2 microns and the combined use of portable Raman spectroscopy are also in program.

REFERENCES

Bacci, M.; Casini, A.; Lotti, F; Picollo, M., and Porcinai, S., 1999. *Non-invasive spectroscopic methods for the characterisation of painted surfaces*, in *Proceedings of the 6th International Conference on NDT and Microanalysis for the Diagnostics and Conservation of the Cultural and Environmental Heritage*, Rome, 5-13.

Bacci, M.; Picollo, M.; Radicati, B., 2001. *Study of colour variation in the paint layers through reflectance spectroscopy*, in *Giotto. The Crucifix in S. M. Novella*, M. Ciatti and M. Seidel editors, Edifir, Firenze, 381-386.

Bruni, S.; Cariati, F; Consolandi, L.; Galli, A.; Guglielmi, V.; Ludwig, N.; Milazzo, M., 2002. *Field and laboratory spectroscopic methods for the identification of pigments in a Northern Italian eleventh century fresco cycle*, in *Applied Spectroscopy*, Volume 56, Number 7, 827-833.

Kirby, J.; Saunders, D., 2004. *Fading and Colour Change of Prussian Blue: Methods of Manifacture and the Influence of Extenders*, in *National Gallery Technical Bullettin*, Volume 25, London, 73-99.

Mantler, M.; Schreiner, M., 2000. *X-Ray Fluorescence Spectrometry in Art and Archaeology*, in *X-Ray Spectrometry*, 29, 3-17.

Poldi, G.; Villa, G. C. F., 2003. *Schede scientifiche*, in *Pinacoteca Civica di Vicenza. Dipinti dal XIV al XVI secolo*, M. E. Avagnina, M. Binotto & G. C. F. Villa editors, Silvana Editore, Cinisello Balsamo (Milano), 501-567.

Poldi, G.; Bonizzoni, L.; Ludwig, N.; Milazzo, M., 2004. *Stratigrafie senza prelievi mediante XRF e spettrometria in riflettanza*, in the proceedings of the *Terzo Congresso Nazionale Aiar*, Brixen, february 2004 (in print).

Saunders, D.; Kirby, J., 2004. *The effect of Relative Humidity on Artists' Pigments*, in *National Gallery Technical Bullettin*, Volume 25, London, 62-72.

NON-DESTRUCTIVE INVESTIGATIONS OF INDIAN MINIATURES BY A COMBINED SPECTROSCOPIC APPROACH: PIXE, 3D-μXRF AND UV-VIS SPECTROSCOPY

Ina Reiche
UMR 171 CNRS – Centre for research and restauration of the French Museums (C2RMF), Palais du Louvre, 14 quai F. Mitterrand, 75001 Paris, France, ina.reiche@culture.gouv.fr

Raffael Dedo Gadebusch
Museum for Indian Art (MIK), State Museums of Berlin, Takustr. 40, 14195 Berlin, Germany, r.gadebusch@smb.spk-berlin.de

Oliver Hahn, Uwe Reinholz
Laboratory IV.22 & Divison Nuclear Analysis, Federal Institute for Materials Research and Testing (BAM), Unter den Eichen 87, 12205 Berlin, Germany, {oliver.hahn/uwe.reinholz}@bam.de

Birgit Kanngießer, Wolfgang Malzer
Institute for Atom physics , Technical University Berlin, Hardenbergstr. 36, 10623 Berlin, Germany, {bk/wolf}@atom.physik.tu-berlin.de

1. INTRODUCTION

In India, there is a long-lasting tradition of miniature painting. This artistic technique is at its cumulating point during the Mughal period. Genre scenes or typical depictions of sovereigns and other important personalities are represented in these paintings. They were produced in particular workshops in Northern India from the 16th to the 19th century. The painting technique was characteristic and remained unchanged during this period of time. So it can be assumed that a typical pigment palette could be established by analysing the painting materials of a sufficiently large number of stylistically coherent and dated Mughal miniatures (fig. 1).

Thanks to literary sources, the painting technique can be summarised as follows: a water colour technique was used for painting on paper with gum Arabic as binding medium. The detailed fabrication process involved the preparation of paper sheets by sticking several sheets of rag paper together probably using animal glue to obtain a thin cartoon (*wasli*) which was

Figure 1. Portrait of a Princess. Mughal-Style, Jaipur, 18th Century. I 5670. Museum of Indian Art, State Museums of Berlin.

intensively polished. A first sketch with ochre or graphite was applied on this cartoon. It follows a white preparation layer which is still transparent for the preparation sketch. Successive paint layers were applied. Every paint layer was polished using generally an ivory support and an agate stone. The polishing confers a particular gloss and delicacy to the paintings. The painting was finished by the application of details like contours, shadows or glance, light modelling, gold and silver with fine animal hair brushes. In later decades, miniatures were mounted as sheets of an album with exquisite frames (Goswamy and Fischer, 1987, Ohri, 2001). There was an important production of miniatures copying masterpieces from the "classical" period from the 18th century onwards because of their success.

The aim of this work was to obtain new clues on the painting technology and to find out which kind of criterion can be used to distinguish later copies from originals by characterising the pigment palette and the layered paint structure of a large number of Indian miniatures from the Mughal period kept in the Museum of Indian Art (MIK), State Museums of Berlin (Gadebusch, 2000b, Gadebusch, 2000a).

2. METHODS

A combined spectroscopic approach was used for the completely non-destructive investigation of painting materials as well as of the paint layers of these miniatures. External beam Proton-Induced X-ray Emission analyses (EB-PIXE) in air at the tandem ion accelerator of the BAM with 2 MeV protons, a current of about 0.3 nA and a beam diameter of about 500 μm (Reiche et al., in press) and investigations using a new 3D μ-X-ray-fluorescence analysis method at the Synchrotron source BESSY, Berlin (3D μ-XRF) (Kanngießer et al., 2003, Kanngießer et al., submitted) were complemented with VIS reflectance spectroscopy (Hahn et al., 2004) and observation under UV light. This methodology permits the identification of mineral and organic pigments as well as dyes and also insights into the paint layer structure of these miniatures.

3. REFERENCE MATERIALS AND ANALYSED MINIATURES KEPT IN THE MIK

38 Indian paintings from the MIK collection executed in the Mughal style and dated between the 16th and the 19th century (Album n° I 5004, folios n° I 5005(1), I 5005(14), I 5169, I 5202, I 5404, I 5615, I 5666 and I 5670) were analysed by EB-PIXE. Prior to the investigation of originals, beam conditions were tested using known reference pigments mixed with dextrin applied on cotton paper. EB-PIXE enabled the determination of characteristic chemical elements detected in each pigment. This reference base was used for the identification of the unknown minerals of the miniatures. Not all pigments can be identified unambiguously using EB-PIXE. Especially it is difficult to detect light elements in air. Therefore, some pigments as lapis lazuli or organic dyes that are mainly composed of light elements cannot be revealed this way. For this reason, it is important to combine EB-PIXE with VIS reflectance spectroscopy and observation under UV light. In particular, Indian yellow shows a characteristic fluorescence when stimulated under UV light (Baer et al., 1986). UV observation was systematically performed whereas VIS spectroscopy was applied on 15 miniatures which showed undetermined pigments or dyes in the visible range between 400 and 800 nm with a spot size of Ø 3 to 10 mm. Comparison of the sample spectrum (including first derivation) with a data base permitted the identification of the pigments and dyes. Furthermore, some pigment identification has to remain ambiguous because of

the paint layer structure. Several layers contribute to the PIXE spectrum and it is not always obvious to which layer the detected elements belong (Reiche et al., in press). Thus, paint layer analyses were performed on 4 paintings; the performance of this newly developed 3D μ-XRF set-up being tested on imitated paint layers of chrysocolla applied on lead white where the paint layers. The layer thickness were verified on cross sections under the stereomicroscope. The paint layer investigation also enables the discovering of the assumed painting technique (Kanngießer et al., submitted).

4. RESULTS

4.1. EB-PIXE analyses

Analyses using EB-PIXE enabled to define typical mineral pigments belonging to a large palette of different colours used for painting. Blue, green, red and white mineral pigments as well as precious metals could be identified and are listed in table 1. An example of a pigment spectrum evidences the major presence of Sn and Zn in a white pigment is shown in fig. 2.

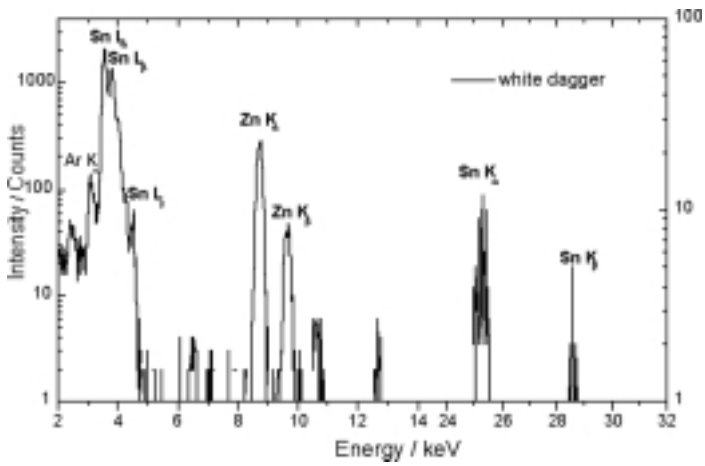

Figure 2. EB-PIXE spectrum of the white dagger on the folio n° 10 of the album I 5004.

4.2. Observation with VIS reflectance spectroscopy

VIS reflectance spectroscopy confirmed the pigment identification based on the EB-PIXE analyses and revealed unambiguously further pigments and dyes in the miniatures (table 1). In addition, VIS permitted to reveal the presence of organic pigments like Indian yellow and indigo, mineral pigments like Prussian Blue and lapis lazuli as well as organic dyes like red kermes, madder lake, carmine and lac dye (fig. 3).

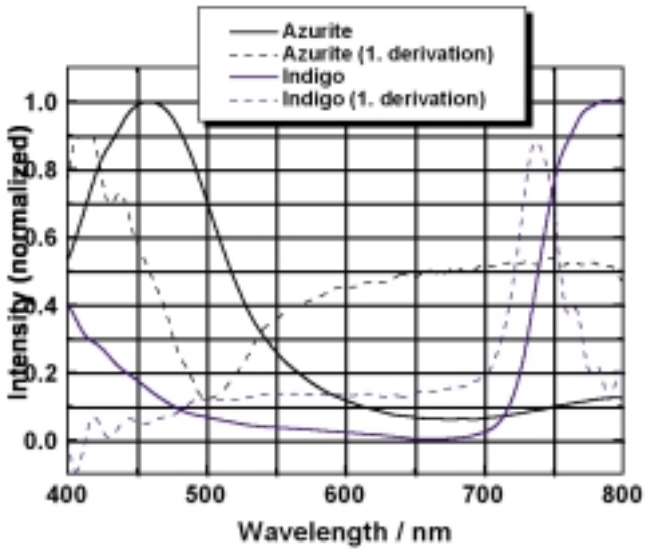

Figure 3. VIS spectra of azurite and indigo and first derivatives.

4.3. Analyses using the new 3D-micro-XRF set-up at the synchrotron BESSY

The layered structure of the miniature paintings could be revealed thanks to depth profiles measured without any sampling on well selected areas of four paintings (Kanngießer et al., 2003). In order to illustrate this new analytical capability with a large archaeometric potential, we represent here one example of non-destructive depth profile measured on the red fence of the folio n° 19 of the album I 5004 (fig. 4).

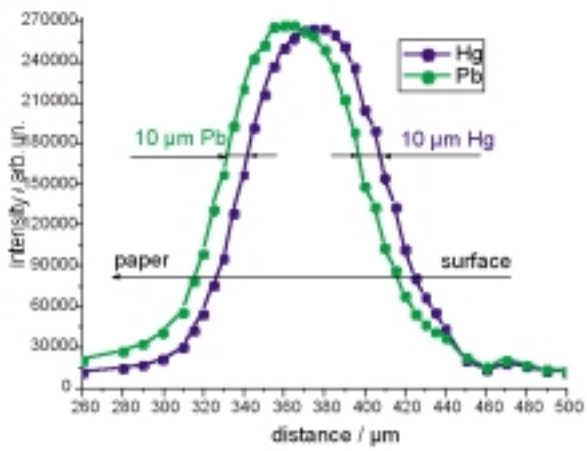

Figure 4. Depth profile showing two successive layers of cinnabar and lead white with 10 μm thickness each.

colour	identified through particular elements with EB-PIXE	determined with VIS
blue (sky – dark)	azurite (Cu) (I 5404), Prussian blue (K, Fe) (I 5666)	azurite (I 5404), indigo (I 5004(3)), lapis (ultramarine) (I 5004(19)), Prussian blue (I 5666)
green (turquoise-olive)	Cu green pigments (malachite, atacamite) (I 5004 (10), green earth (Fe, Si, Ca, K) (I 5202 olive green)	Cu green pigments (I 5004 (10), indigo + Indian yellow (I 5202 light green background)
yellow	ochre (Fe, Si, Ca) (I 5004(17))	Indian yellow (I 5169,…)
skin colour	? (Pb) (I 5666)	undetermined
orange /	minium (Pb) (I 5004(10))	minium (I 5004(10))
red (pink-dark)	cinnabar (Hg) (I 5004(10)), ochre (Fe, Si, Ca) (I 5004(24))	cinnabar (I 5004(10)), ochre (I 5202), minium (I 5666), carmin (I 5169), kermes (I 5404), lac dye, (I 5004(5)), madder (I 5004(18))
brown	ochre (Si, Ti, K, Fe) (I 5004(4))	ochre
t purple and viole	? (Pb, Ca, Fe, (Cu))	carmin+indigo (I 5615), kermes+indigo (I 5004(17)), kermes (I 5005)
black	? (Fe)(I 5169)	undetermined
white	lead white (Pb) (I 5202), tin and zinc white (Sn, Zn, traces of Pb)	–
grey, silver	relatively pure silver (Ag)	–
gold	gold (Au, (Cu))	–

Table 1. Main pigments determined using EB-PIXE on 38 and VIS reflectance spectroscopy on 15 miniatures (exhaustive list in (Reiche et al., forthcoming)).

5. DISCUSSION AND CONCLUSIONS

Particularly interesting is the evidence of the use of Sn and Zn containing pigments in the Mughal miniatures. According to our knowledge, there was no evidence of this until now. However, this paintings should not be considered as a later copy because tin white was used in manuscripts until the 17th c. (Harley, 1982) and it is known from archaeometallurgical analyses that Zn has already been mined very early in Northwestern India, especially in the Zawar mine, next to Udaipur in the Aravalli Hills of Rajasthan (Craddock, 1987). The detection of Prussian blue is also unattended but consistent with miniatures of the middle of the 18th. A more detailed presentation and discussion of the results can be found in a forthcoming publication (Reiche et al., forthcoming). This work also illustrates the importance of crossing different analytical methods. Particularly, it highlights the potential of 3D μ-XRF spectroscopy to get non-destructively insights into painting techniques.

ACKNOWLEDGEMENTS

We gratefully acknowledge the help and support of T. Gabsch and M. Yaldiz, MIK, as well as R.-R. Pausewein and J. Riederer, Rathgen research laboratory, State Museums of Berlin. We also thank H.-P. Weise, G. Bukalis, R. Britzke, J. Fessel, M. Radtke, H. Riesemeier, BAM.

REFERENCES

Baer, N. S.; Joel, A.; Feller, R. L., and Indictor, N. (1986). In *Artists' Pigments A Handbook of their History and Characteristics*, Vol. 1 (Ed, Feller, R. L.) Cambridge University Press, Cambridge, pp. 17-36.

Craddock, P. T. (1987). *Endeavour, New Series,* 11, pp. 183-191.

Gadebusch, R. D. (2000a). *Orientations,* 31 (9), pp. 69-74.

Gadebusch, R. D. (2000b). *Magische Götterwelten - Werke aus dem Museum für Indische Kunst, Berlin*, Potsdam.

Goswamy, B. N., and Fischer, E. (1987). *Wunder einer Goldenen Zeit Malerei am Hof der Moghul-Kaiser Indische Kunst des 16. und 17. Jahrhunderts aus Schweizer Sammlungen,* Museum Rietberg, Zürich.

Hahn, O.; Oltrogge, D., and Bevers, H. (2004). *Archaeometry,* 46 (2), pp. 273-282.

Harley, R. D. (1982). *Artists' Pigments c. 1600-1835,* Butterworth Scientific, London.

Kanngießer, B.; Malzer, W., and Reiche, I. (2003). *Nuclear Instruments and Methods in Physics Research B,* 211, pp. 259-264.

Kanngießer, B.; Malzer, W.; Rodriguez, A. F., and Reiche, I. (submitted). *Spectrochimica Acta Part B*.

Ohri, V. C. (2001). In *The Technique of Pahari Painting An inquiry into aspects of materials, methods and history,* Aryan Books International, New Dehli, pp. 20-50.

Reiche, I.; Britzke, R.; Bukalis, G.; Reinholz, U.; Weise, H.-P., and Gadebusch, R. D. (in press) *X-Ray Spectrometry*.

Reiche, I.; Kanngießer, B.; Malzer, W.; Hahn, O.; Gadebusch, R.; Gabsch, T., and Reinholz, U. (forthcoming).

DISCOVERING OF THE EGYPTIAN BLUE EMPLOYMENT FOR THE DECORATION IN A 10th CENTURY MANUSCRIPT, CHARACTERISED BY ABSORPTION IN DIFFUSE REFLECTANCE SPECTROMETRY

P. Roger, J. N. Barrandon
Centre Ernest-Babelon, CNRS, Orleans

A. Bos
Orleans Public Library

1. INTRODUCTION

A lot of articles on medieval manuscripts' decoration has been produced, but if we focus on European studies on analysis of painting matter manuscripts, the number will be smaller (Clarke M., 2001). In particular, few studies using non-destructive methods *in situ* have been published (Guineau B., 2002; Villela-Petit I., 2003). The interest of measurements on place of conservation of ancient manuscripts, is that the decoration of the document is entirely considered and taken in the context, what is impossible with analysis from samples. This paper relates a colour matter's study on a *corpus* of French manuscripts dated between the VIIIth and the XIIth century, conserved at Orleans public library and issued from Fleury abbey. Only one part of the results is related here because of the discovering of the Egyptian blue. This matter is especially known as color material for mural paintings, but no occurrence exists for medieval text decoration.

2. MATERIALS

The study concerns fourteen decorated or illuminated manuscripts coming from Fleury abbey. Situated close to Orleans on the right bank of the Loire river (actually St Benoît-sur-Loire), it was founded in the VIIth century. The activity of the *scriptorium* is known from the VIIIth century on and will let a rich production. The best product period starts from the IXth to the beginning of the XIth century, under abbot Abbon, which took the directory of the monastic center at the Xth century. He gave it a so intellectual development that the reputation of the abbey will go out of the kingdom and further in England at Winchcombe and Ramsey. Fleury will receive many times artists

coming from other countries. Few manuscripts provide evidence about that. Inside our *corpus*, one manuscript, BMO 127, has been prepared in England in the Xth century and was brought to the abbey's library (Davril A., 1995).

3. METHODS

The analyses on decoration in French libraries' manuscripts, need to preserve these precious documents, so it is absolutely necessary to use non-destructive analysis methods, portable on conservation places. Three spectrometric analyse systems have been developed in the Ernest-Babelon center, CNRS Orleans, to answer to these criterions. Two permits measurements by absorption in diffuse reflectance in near ultraviolet, visible and very near infra-red (fig. 1) to characterize paint layers. Systems are composed with light source covering the useful wavelengths domain, optic fibers and detector. The other one is a spectrometric fluorescence X system with X generator, which completes precedent measures notably for metal atoms' detection.

Figure 1. View of the spectrophotometric system for measurements *in situ*.

4. RESULTS

The analyses show the use of woad and lapis lazuli for the all manuscripts. For one of them, BMO 127, the artist who was responsible for the decoration employed Egyptian blue. The characterisation of these different pigments is rapid and comfortable with absorption in diffuse reflectance systems. We can appreciate the spectral differences with their characteristic absorptions on the following curves (fig. 2, 3, 4) in the 400-1000nm. Each of these blue pigment or colorant shows specifics areas of absorption due to the electronic transitions produced in the molecular form present in the colorant or in the pigment; the indigo curve shows maximum around 660nm due to the *indican* contained in the original plant from where

this colorant was extracted (*indigofera* species from India, China, Japon…); another plant cultivated in Europe, notably in France in the Middle Ages, the woad (*isatis tinctoria L.*) contains a part of this colorant and has probably been used. The lapis lazuli curve shows maximum around 600 nm due to the electronic transitions of S^{3-} contained in omplex sulfur sodium aluminium silicate. The third Egyptian blue curve shows three characteristic peaks attributed to Cu^{2+}, localized around 530-540nm, 630 and 795 nm.

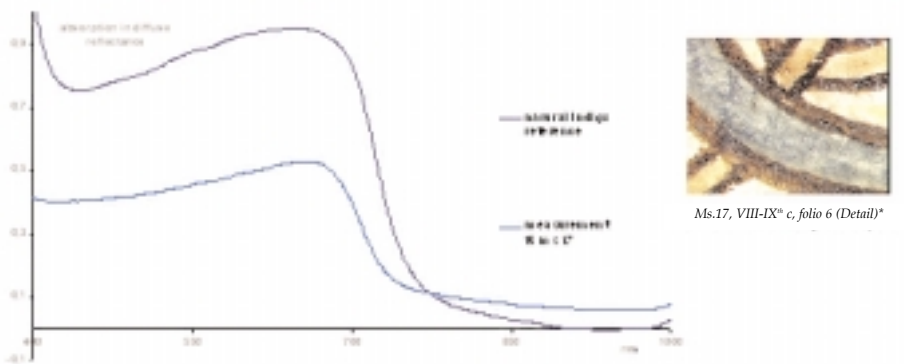

*Ms.17, VIII-IX^th c, folio 6 (Detail)**

Figure 2. Curve in absorption in diffuse reflectance of natural indigo and measurement on folio 6, BMO 17.

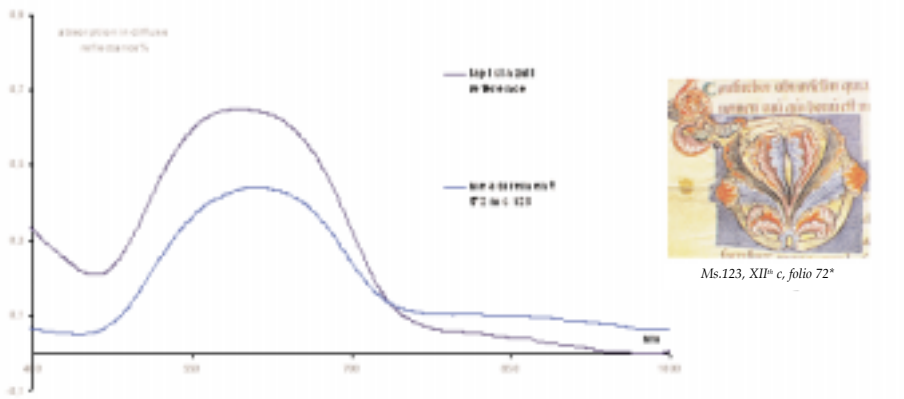

*Ms.123, XII^th c, folio 72**

Figure 3. Curve in absorption in diffuse reflectance of lapis lazuli and measurement on folio 72, BMO 123.

The color of Egyptian Blue is given by the cuprorivaite ($CaCuSi_4O_{10}$), "so scarce in the nature that it could not be collected in large enough quantities to be used as a pigment" (Riederer J., 1997, p.32). Numerous analysis of several samples coming from different origins have been done and various compositions have been found of this synthetic pigment: 50.5-88.7 percent of silicon dioxyde

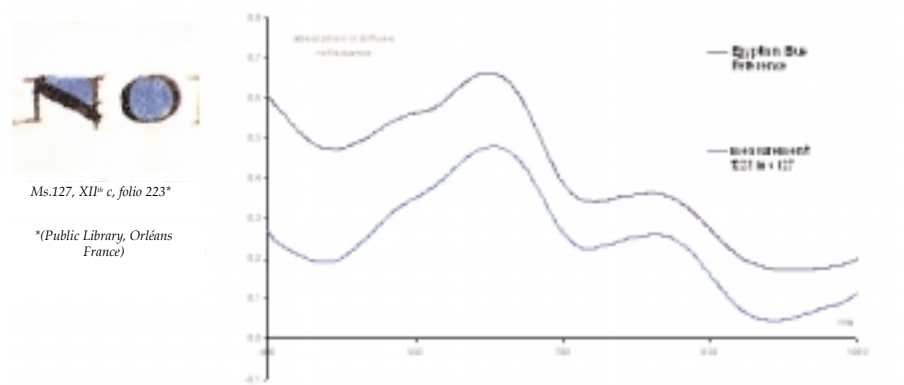

*Ms.127, XII^th c, folio 223**

**(Public Library, Orléans France)*

Figure 4. Curve in absorption in diffuse reflectance of Egyptian blue and measurement on folio 223, BMO 127.

(SiO_2), 4.9-16.8 percent of calcium oxyde (CaO), 2.1-21.4 percent of copper oxyde (CuO) and other oxides (Na, K, Mg, Al, Fe, Sn) in more little proportion (Riederer, 1997). In the case of BMO 127, principal components (Cu, Ca, Si (with a little peak because of weak response of the detector in this part of space)) are visible on fluorescence X spectra but no more information can be found. Twenty three measurements of absorption in diffuse reflectance have been realised on the blue letters onto the 362 pages of the BMO 127. From page 9, all obtained spectra present the characteristics of Egyptian blue. The colorimetric coordinates obtained from experimental spectra are visible on the following graph constructed in the CIElab system and C*L* plane (illuminate C, observator 10°, 380-780nm, L* is the clearness, C* is the chroma related to a* and b* coordinates by relation $C^*=(a^{*2}+b^{*2})^{1/2}$) (fig. 5). This graph shows the homogeneity of the observed blue colour. Points are distributed as an ellipse along a typical line, representing a common tint more or less dark, the coordinates corresponding to lapis and indigo are out of it. Considering the age of the manuscript, we can suppose that the used matter was relatively homogenous and of good quality.

5. CONCLUSION

The aim of our color study is to show, throughout the identification of the colour materials, a practical and a particular style of Fleury *scriptorium*. At that time, one of the important point revealed is the use of Egyptian blue in only one of the manuscripts. This discovery is surprising because the Egyptian blue is principally known for mural painting, from Antiquity to IX^th century. A recent study indicates occurrences in association with lapis lazuli for Middle Ages on church walls (Santamaria U., 2004). That discovery in the decoration of a X^th century manuscript constitutes a new information. The use of Egyptian blue is very interesting to understand the presumed origin of BMO 127.

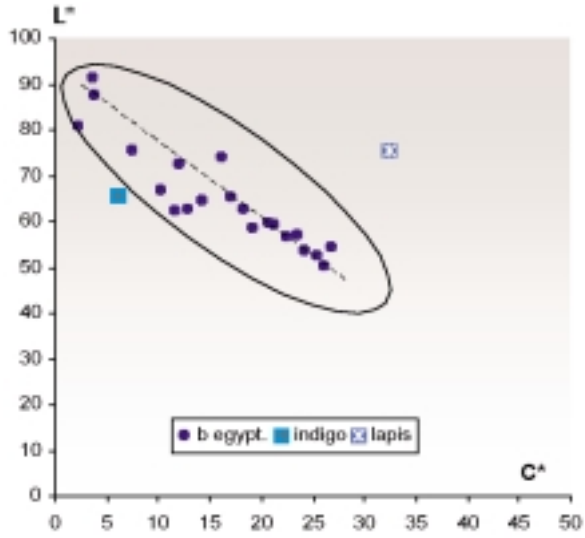

Figure 5. Colorimetric graph in C*L* coordinates of measurements on blue letters of BMO 127 (Egyptian blue) compared to lapis and indigo.

Indeed, the history of this manuscript is amazing: historians think that it could have been written in Winchcombe (or in Ramsey by a monk of Winchcombe), then it has been carried to the Mont Saint Michel near Avranches and brought only at the beginning of the XIth century to Fleury. The use of this specific pigment may confirm the attribution to English *scriptoria*, because Egyptian blue has not been found by analysis in manuscripts definitely realised in Fleury *scriptorium*. We would like to know if this use is peculiar to Winchcombe, or if another English manuscripts are decorated so with it. Our research must be continued in this way, to answer that new question.

REFERENCES

Clarke, M., "The Analysis of Medieval European Manuscripts", *Reviews in Conservation*, 2, 2001, 3-17.

Davril, A., *The Winchcombe Sacramentary*, London, 1995.

Guineau, B., et Villela-Petit, I., 'Couleurs et technique picturale du Maître de Boucicaut', *Revue de l'Art*, 135, 2002, 23-42.

Rieder, J.,"*Egyptian Blue*", Artist's Pigments, 3, West Fitzhugh ed., 1997, pp. 23-45.

Santamaria, U., Seccaroni, C., "The use of Egyptian blue and lapis lazuli in the Middle Ages: the wall paintings of the san Saba church in Rome", *Studies in conservation*, 49, 1, 2004, pp. 13-21.

Villela-Petit, I., Roger, P., *Le Brévaire de Châteauroux. Couleur, une étude des pigments*, Somogy ed., 2003, 119- 136.

STONE MATERIALS OF THE BAROQUE TOWN OF NOTO (ITALY): PETROGRAPHIC AND GEOCHEMICAL FEATURES AND THEIR BEHAVIOUR IN DECAY

L. G. Russo, P. Mazzoleni, A. Pezzino
Università di Catania
Dipartimento di Scienze Geologiche, Corso Italia 55, 95129 Catania (Italy)

1. INTRODUCTION

The problem of conserving the stonework in historical cities is of paramount importance, for much of the history of mankind is preserved in it. The decay of calcarenite in the town of the Noto is one example, among many, that has alarmed the civilized world regarding the limits to the lifespan of the natural stone. The aim of this paper is the study of the characteristics of the calcarenite of Noto with relevance to conservation and restoration. These are: petrographical and geochemical composition of total sample, mineralogical assembly of insoluble residue, physical properties and behaviour in ageing tests.

2. THE CITY AND ITS STONE MATERIALS

The town of Noto, recently added to the UNESCO World Heritage List ("Late Baroque Towns of the Val di Noto"), was rebuilt after the terrible earthquake of 11th January 1693. The rebuilding started in a new location, 7 kilometres from the ancient site (Ancient Noto). The stone materials employed in the constructions of the city was Miocene calcarenite of the Palazzolo Formation, quarried in the surrounding area and called "Pietra of Noto". This calcarenite presents two different lithotypes: a) a pale cream calcarenite; b) a yellowish calcarenite. The first, called locally "pietra 'ntagnu", was used in the production of the ornamental architectural elements, while the second, called locally "pietra tufo", was used as building stone; this variety contains sedimentary tubular structures called "skolithos", originating from by endobenthic animals. These structures are often subject to a type of stone decay called alveolization which, together with differential erosion, is a typical decay pattern distinctive of the "Pietra di Noto".

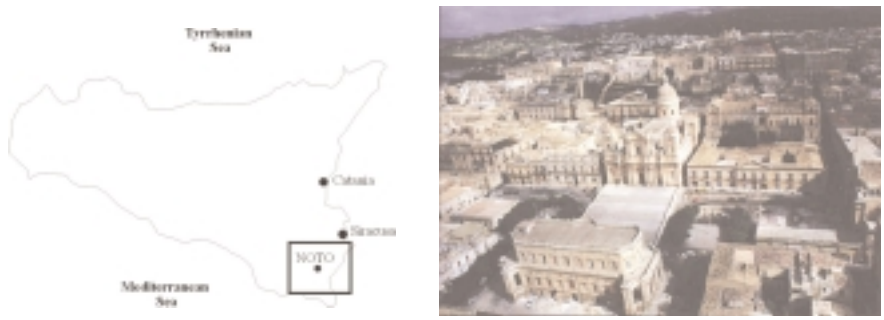

Figure 1. a) Geographic location of Noto town. b) A view of the city.

3. EXPERIMENTAL

The lithological types (pale cream and yellowish calcarenites) used for construction in Noto were sampled from a typical section of Palazzolo Formation (Di Grande *et al.*, 1982). The laboratory testing programme included: a) Petrographical observations and modal composition estimate by polarizing microscopy. b) Geochemical analyses of major element by XRF spectrometry (Philips PW 2404) and minor elements ICP-MS SF-ICP-MS (Element2, FinniganMAT) after acid dissolution. c) Mineralogical investigation on the insoluble residue in two phases: 1) the dissolution of selected samples using a sodium acetate-acetic acid buffer at pH 5 and determination of granulometric fractions (sand & silt and clay fractions); 2) qualitative and quantitative mineralogical determination, using X-ray diffraction. d) Water absorption by capillarity (EN 1925). e) Salt crystallisation tests (EN12370). f) Tests to determine resistance to ageing by SO_2 action in presence of humidity (prEN13919).

4. THE STONE MATERIALS

4.1. Mineralogy and texture

Four microfacies types were evidenced by: particle types, fossils, groundmass, depositional and texture, and other microfacies features (Flugel, 1982). The mineralogical and textural features of the calcarenites are set on table 1.

4.2. Insoluble residue analysis

The results of the analysis of insoluble residue evidence that the percentage of insoluble residue is higher in pale cream calcarenite (14%) than in yellowish calcarenite (4%). Furthermore, the quantitative analyses showed that for both calcarenites the clay fraction consists mainly of swelling clay minerals of the smectite group: illite-smectite (80% and 66% respectively), illite (13% and 33% respectively) and kaolinite (7% and 1% respectively). The sand and silt fractions present: feldspars (17% and 26% respectively) and quartz (83% and 74% respectively).

Lythotype	Microfacies Type	Mineralogical and textural features
Pale cream calcarenite	Marly bioclastic wackestone with microsparite matrix	The grains are dominantly planktonic (Globigerinides) and benthonic foraminifers. The clastic grains are dominantly quartz with minor feldspar. The intergranular space is filled by microsparite. The textures is mud supported.
	Marly bioclastic wackestone with micrite matrix	The grains are mainly planktonic and benthonic. The clastic grains are dominantly quartz with minor feldspar. The micrite matrix is rarely neomorphized to microsparite. The texture is mud supported.
Yellowish calcarenite	Bioclastic wackestone with micrite matrix	The skeletal grains range from 10 to 20%. The grains are dominantly planktonic (Globigerinides) and benthonic. The intergranular space is filled by micrite. The texture is mud supported.
	Bioclastic wackestone with microsparite matrix	Principal grains are dominantly planktonic (Globigerinides) and benthonic. The clastic grains are very rare. The groundmass consists of micrite, rarely neomorphized to microsparite. The texture is mud supported.

Table 1. Mineralogical and textural features of microfacies types.

4.3. Geochemical features

The two groups of rocks (yellowish and pale cream calcarenites) showed distinctive chemical characteristics for both elements related to the terrigenous fraction (i.e. Ti, Al, Si) and to the carbonate fraction (i.e. Ca, Sr, Mg).

As far as the elements related to the terrigenous fraction, the pale cream calcarenites are characterised by higher values of Ti, Al, Si, Rb and IR (insoluble residue) than the yellowish calcarenites.

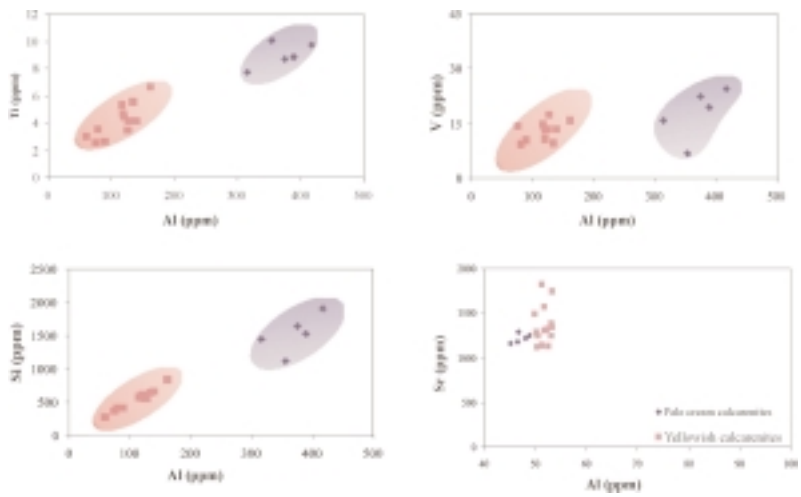

Figure 2. Selected variation diagrams for elements related to the terrigenous and carbonate fractions.

4.4. Analysis of decay

In order to characterise the stone material in terms resistance to more common causes of limestone weathering, such as the crystallisation of salts and deposition of SO_2 on rock surface, we carried out the following tests: water absorption by capillarity (EN 1925), salt (Na_2SO_4) crystallisation (EN 12370), and, finally, determination of resistance to ageing by SO_2 action in presence of humidity (prEN 13919). Table 2 summarises the results of the laboratory testing.

Lithofacies	**Crystallisation of salts* Weight loss (Δm)**	**Resistance of ageing by SO_2 action****	**Coefficient of water adsorption by capillarity*** C** *(g/m².s$^{0.5}$)*
Pale cream calcarenite	36.18%	A white crust, largely composed of gypsum and calcite forms on the surface of the rock.	292.93
Yellowish calcarenite	Broken at the 10th cycle		286.58

Table 2. Physical properties and results of ageing tests.

The results of the tests evidence that, from the first cycle, the specimens of yellowish calcarenites show a loss of material round the "skolithos", and break at the start of the 10th cycle, separating the "skolithos" from the stone (fig. 3a). At the end of test (15th cycle), the sharp edges of the pale cream calcarenite specimen are rounded and about 36.18% of its initial dry weight is lost (fig. 3b). Combined with the value of coefficient of water absorption by capillarity and the results of resistance to ageing by SO_2 action in presence of humidity (fig. 3c), this data clearly demonstrates that the stones under examination are more vulnerable to the crystallisation of salts than to SO_2 action. Furthermore, the behaviour of the yellowish calcarenites in the salt crystallisation tests shows that the alveolization of the stone of Noto is due, in the early stages at least, to the crystallisation of salts around the "skolithos". These observations suggest that the boundary between the "skolithos" and the stone is a preferential path for water evaporation and consequently for salt crystallisation (Alessandrini et ali, 1992).

a) b) c)

Figure 3. a) Yellowish calcarenite after 10 cycles of salt crystallisation test;
b) Pale cream calcarenite at the end of salt crystallisation test (15th cycle);
c) Pale cream calcarenite at the end of resistance to ageing by SO_2 action in presence of humidity.

REFERENCES

Alessandrini, G.; Bocci, A.; Bugini, R.; Emmi, D.; Peruzzi, R.; Realini, M. (1992). *Stone material of Noto (Siracusa) and their decay* – In "Proceeding 7th Int. Congr. On Deterioration and Conservation of Stone" Lisbon, June 15-18 1992, pp. 11-20.

Di Grande, A.; Romeo, M.; Raimondo W. (1982). *Il membro di Gaetanì ed il membro di Buscemi della formazione Palazzolo: facies, distribuzione ed età*. Boll. Soc. Geol. It., 101, pp. 343-372

Flugel, E (1982). *Microfacies analysis of limestone*, Springer- Verlag

Moore D. M.; Reynolds, J. R. R. C. (1989). *X-ray diffraction and the identification and analysis*. Oxford University Press, pp. 332.

UNI EN 1925 (1999). *Determination of coefficient of adsorption of water for capillarity*, 9 p.

UNI EN 12370 (1999). Determination of resistance to crystallization of salts, 6 p.

prEN 13919 (2001). *Determination of resistance to ageing by SO_2 action in presence of humidity.*, 7 p.

WHERE DOES LAPIS LAZULI COME FROM? NON-DESTRUCTIVE PROVENANCE ANALYSIS BY PGAA

J. Zöldföldi*
State Office of Historical Monuments, Baden-Württemberg,
Berliner Strasse 12, D-73728 Esslingen a.N., Germany,
E-mail: judit.zoeldfoeldi@uni-tuebingen.de

S. Richter
*Department of Geochemistry, Institute of Geoscience, University of Tübingen
Wilhelmsrt. 56, D-72074 Tübingen, Germany

Zs. Kasztovszky
Institute of Isotopes, Chemical Research Centre of the Hungarian Academy of Sciences;
H-1525 Budapest, PO. Box 77, Hungary, E-mail: kzsolt@alpha0.iki.kfki.hu

J. Mihály
Chemical Research Centre of the Hungarian Academy of Sciences
H-1525 Budapest, PO. Box 77, Hungary, E-mail: mihaly@alpha0.iki.kfki.hu

ABSTRACT

Lapis lazuli is one of the oldest of all precious stones, with a history going back as high as 7000 years or more in the past. Lapis lazuli has been highly valued for thousands of years. Archaeological objects made of lapis lazuli are widely distributed in the ancient East and some date back as early as the second half of the fourth millennium B.C. in Central Asia.

Although considerable attention has been previously paid to the mineralogy of lapis lazuli, the new non-destructive analytical techniques offer wider perspectives to the archaeometry research. Knowledge of the elemental composition, including major and trace elements may provide clues concerning the provenance and raw materials. In this project we succeeded to collect lapis lazuli samples from the most relevant quarries in the world. Rock samples from Afghanistan, from Lake Baikal, from Chile and from Ural Mountains have been investigated. With PGAA we were able to detect the major components, H, Na, Ca, Al, Si, S, Cl, K, and the accessory elements Mg, Fe, Mn. In addition, the trace elements of B, Sc, Cr, Co, Sm and Gd were also identified. According to some characteristic element ratios the samples from Afghanistan and Baikal are more or less overlapping, while the samples from Ural and Chile are definitely different from the others. This paper also attempts to determine the origin of the natural ultramarine, based on provenance analysis on lapis lazuli by PGAA and complementary FTIR Spectroscopy.

1. INTRODUCTION

Lapis lazuli is one of the oldest precious stones, which was considered to be the most valuable one. The history of lapis lazuli started as early as 7000 years ago. It was favourable jewellery thanks to its dynamic blue colour. It was frequently used for production of amulets, gemmas and vases, which were assigned to have magic force. Lapis lazuli archaeological finds has been found on different sites of the ancient East, some middle-eastern pieces were dated to the second half of the 4th millenium B.C.

Lapis lazuli was an important raw material not only for jewellery, but also for dye (pigment) production. The so-called "natural ultramarine" is made of grinded lapis lazuli.

2. MINERALOGY AND GEOLOGY

Lapis lazuli is an opaque semi-precious stone consisting mainly of a blue mineral, lazurite, and an alumina-silicate of the complex feldspathoid sodalite group. Other minerals of the sodalite group are sodalite, nosean and haüyne. The chemical formula for lazurite can be written as $(NaCa)_4(AlSiO_4)_3(SO_4SCl)$, but with considerable variation in the amounts of SO_4, S and Cl (Dana and Hurlbut 1954).

Additionally, pyrites and calcite together with relatively small amount of accessory minerals can be found in the stone lapis lazuli. The colour of lapis lazuli can vary from intense marine blue to violet blue, but lighter blue and green varieties also occur, depending on the shifting chemical composition.

The main geological sources of lapis lazuli are the following.

The most important sources can be found in contact metamorphic zones of limestone/dolomite and sienite (Blaise and Cesbron 1966; Schreyer and Abraham 1976; Grew 1988; Faryad 1999). Yurgenson and Sukharev (1984) describe sources which arise during Na-metasomathosis of high pirit-containing marbles. According to Kulke (1976), Hogarth and Griffin (1978) and Schreyer (1977) lapis lazuli can be produced during metamorphosis of evaporites and clay.

The low probability of the co-occurrence of these geological conditions implies that only 13 sources of lapis lazuli exist all over the world (see fig. 1).

These are: 1. Badakhshan, Afghanistan (Herrmann 1968; Schreyer and Abraham 1976; Faryad 1999); 2. Pamír Mts. (Goldstein 1981; Herrmann 1968; Webster 1975); 3. Lake Baikal and surrounding (Korzinskij 1947); 4. Burma (Rosen 1988); 5. Baffin Island, Canada (Hogarth and Griffin 1978; Kulke 1976); 6. Edwards, N.Y. State, USA (Jensen 1969); 7. Wyoming-Colorado-Utah, USA

Figure 1. Map of the lapis lazuli sources all over the World.

(Webster 1975; Hogarth and Griffin 1980); 8. California, USA (Webster 1975); 9. Chile (Webster 1975); 10. Angola (Webster 1975); 11. Atlas Mts. (Kulke 1976); 12. Latium, Italy (Rosen 1988); 13. Ural Mts., Russia.

3. CHEMICAL ANALYSIS

Although great attention has previously been paid to mineralogical and chemical analysis of lapis lazuli, the only archaeometrical provenance study was published by Herrmann in 1968. Since lapis lazuli finds represent high archaeological values, there is a very limited possibility to perform destructive investigations on them. The new non-destructive methods offer a greater potential for archaeometry. In most cases, the chemical (elemental) composition provides information on the provenance and the raw material sources.

One of the most up to date nuclear analytical tools is the Prompt Gamma Activation Analysis (PGAA) which satisfies most of the requirements in archaeometry, most of all the requirement of non-destructivity. PGAA is based on the detection of prompt γ-photons which originate following the capture of thermal or cold neutrons into the atomic nuclei. Qualitative and quantitative analysis is done by precise identification of the characteristic γ-lines in the spectra. The PGAA apparatus and the method are described by Révay et al. in 2004.

4. EXPERIMENTAL

We performed PGAA measurements of around 50 lapis lazuli samples at the Institute of Isotopes, Chemical Research Centre, Budapest. We have chosen 37 representative samples from the most important quarries in the World (Ural Mts., Afghanistan, Lake Baikal and Chile). In addition, 9 artificial and natural pigments and two archaeological objects were investigated.

The samples – in rock or in powder form – were placed into a horizontal cold neutron beam of $5 \cdot 10^7$ $cm^{-2}s^{-1}$ neutron flux. 2 x 2 cm^2 areas of the samples were irradiated. Since the neutrons can reach the deeper layers of the sample, the results give the "bulk" composition of the investigated volume. The irradiation times last for 1000 to 50000 seconds, in order to achieve acceptable statistics of the spectra. The spectra were evaluated with 'Hypermet PC' software.

In order to identify some pigments, Fourier Transform Infrared Spectroscopy was applied. Samples were diluted in KBr pellets. The spectra were recorded as an average of 64 scans, using a Bio-Rad 175C spectrometer equipped with MCT detector of typical 4 cm^{-1} resolution.

5. RESULTS AND DISCUSSION

Under the above mentioned conditions we were able to detect all the major components (H, Na, Al, Si, K, Ca, Mn, Fe, Cu and Zn), some accessory

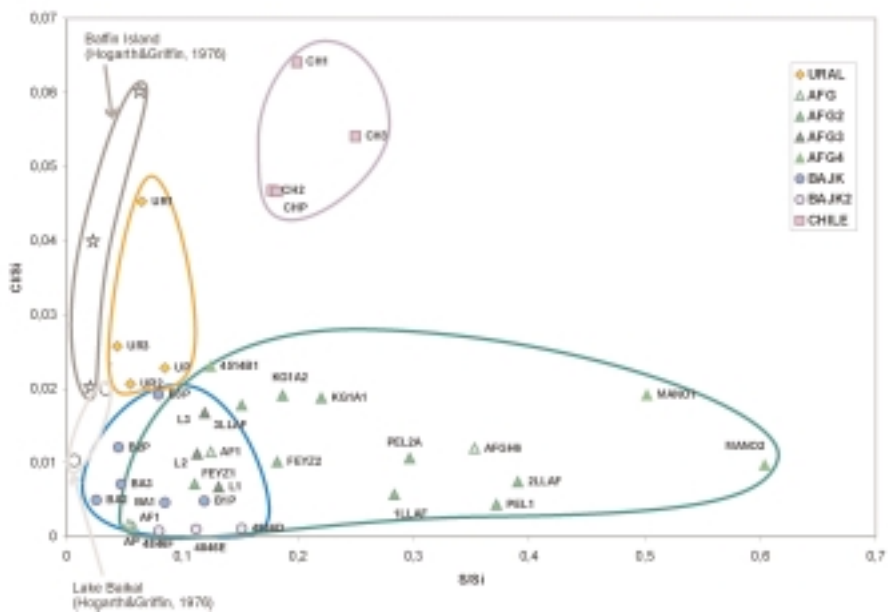

Figure. 2. Discrimination of the investigated lapis lazuli samples according their Cl/Si. vs. S/Si ratios.

and trace elements (B, S, Cl, Sm and Gd) in the samples. In order to distinguish between the geological sources, bivariate plots were constructed and Principal Component Analysis (PCA) was applied.

Based on mineralogical considerations, Cl and S were chosen as discriminative elements in provenance study. According to fig. 2, the samples from Afghanistan and Lake Baikal show low Cl/Si ratio (0.001-0.02), while the samples from Chile and Ural show higher. On the other hand, samples from Afghanistan show higher S/Si ratio (0.05-0.4) and those from Lake Baikal show lower (0.02-0.12). These two groups, however more or less overlap. Samples from Ural and Chile are significantly different from the first two groups. These results are reinforced by PCA too (see fig. 3).

Fourier Transform Infrared Spectroscopy is a convenient tool for preliminary investigation of pigments. With the help of FTIR it can be judged if the blue pigment is "natural ultramarine" (i.e. made of lapis lazuli). On fig. 4. FTIR spectra of a 'commercial', a 'natural' and a self-prepared ultramarine are compared. The first one turned to be a pure azurite.

6. CONCLUSIONS

Prompt Gamma Activation Analysis proved to be an easy and effective non-destructive method for investigation of lapis lazuli objects. Based on the results raw materials from the Ural Mts. and Chile can be distinguished from those of Afghanistan and Lake Baikal. Another additional method is Fourier

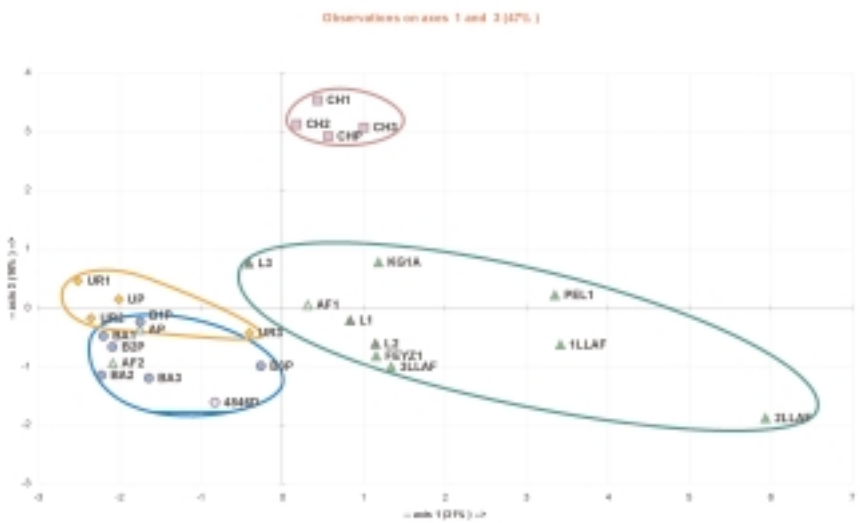

Figure. 3. Principal Component Analysis of the investigated objects.

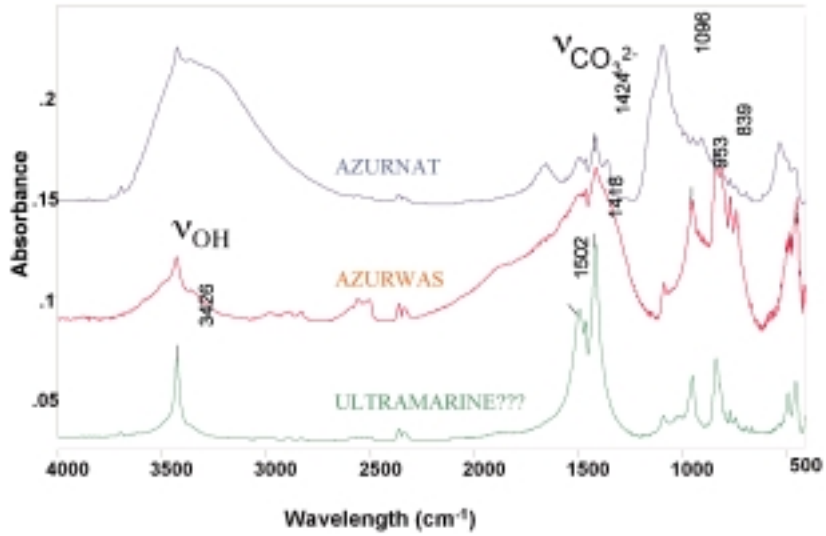

Figure. 4. FTIR spectra of a natural, a commercial and a self-prepared ultramarine.

Transform Infrared Spectroscopy for identification of pigments. Based on the first results we plan to extend the study towards the investigation of valuable archaeological objects.

ACKNOWLEDGEMENT

The PGAA measurements were realized within the EU 5th Framework HPRI-1999-CT-00099 contract at the Budapest Neutron Centre.

REFERENCES

Blaise, J., and Cesbron, F., 1966, "Données minéraliques et pétrograhiques sur ke gisement de lapis-lazuli de Sar-e-Sang, Hindou-Kouch, Afghanistan", *Bulletin de la Société Francaise de Minéralogie et de Cristallographie* 89, pp. 333-343.

Faryad, S. W., 1999, "Metamorphic evolution of the Precambrian South Badakhshan block, based on mineral reactions in metapelites and metabasites with whiteschists from Sare Sang (Western Hindu Kush, Afghanistan)", *Precambrian Research* 98, pp. 223-241.

Goldstein, A. D., 1981, "The Gemstones of Russia, Pamir and Baikal", *Jewellery Making Gems and Minerals*, 528.

Grew, E. S., 1988, "Kornerupine at the Sare Sang, Afghanistan, whiteschist locality: implications for tourmaline-kornerupine distribution in metamorphic rocks." American Mineralogist 73, pp. 345-357.

Herrmann, G., 1968, "Lapis lazuli: The early Phases of its trade". *Iraq* 30.

Hogarth, D. D., and Griffin, W. L., 1978, "Lapis Lazuli from Baffin Island. A Pre-Cambrian Meta-Evaporite", *Lithos*, 11, pp. 39-54.

Jensen, D. E., 1976, "Lapis lazuli from Edwards, New York", *Rocks and Minerals* 51, pp.

Korzinskij, D. S., 1947, "Bimetasomaticeskie flogopitovye i lazuritovye mestorozdenije archeja pribaikalja". *Akademija Nauk. SSSR. Trudy Instituta Geologiceskich Nauk,* 29, *Petrograficeskaja Serija* 10.

Kulke, H. G., 1976, Metamorphism of evaporate carbonate rocks (NW Africa and Afghanistan) and the formation of lapis lazuli, *International Geological Congress, Sydney*, Section 3B, Abstract 25.

Révay, Zs.; Belgya, T.; Kasztovszky, Zs.; Weil, J. L., and Molnár, G.L., 2004, "Cold neutron PGAA facility at Budapest." *Nuclear Instruments & Methods in Physics Research Section B- Beam Interactions with Materials and Atoms,* 213, pp. 385-388.

Rosen, L. von, 1988, *Lapis lazuli in geological and in ancient written sources.*

Schreyer, W., 1977, "Whiteschists: their compositions and pressure-temperature regimes based on experimental, fluid, and petrographic evidence", *Tectonophysics* 43, pp. 127-144.

Schreyer, W., and Abraham, K., 1976, "Three stage metamorphic history of whiteschist from Sare Sang, Afghanistan, as part of a former evaporate deposit", *Contributions to Mineralogy and Petrology* 59, pp. 111-130.

Webster, R., 1975, *Gems, their Sources, Description and Identification*. London.

Yurgenson, G. A., and Sukharev, B. P., 1984, "Localization of lapis lazuli bodies and their mineral zonation in Badakhshan", *Zapiski Vsesoyuznogo Mineralogicheskogo Obshchestva* 113, pp. 498-505.

		H	B	Na	Mg	Al	Si	P
URAL	UR1	0.05	0.0044	5.70	12.3	8.22	37.5	0.00
	UR2	0.10	0.0064	7.38	12.9	10.78	38.7	0.00
	UR3	0.12	0.0130	6.56	12.9	8.75	39.3	0.00
	UP	0.15	0.0050	9.08	12.0	11.29	38.0	0.00
AFGHANISTAN	AF1	0.11	0.0072	10.73	11.5	11.95	38.7	0.00
	AF2	0.42	0.0007	5.16	13.5	8.95	42.2	0.00
	AFGH6	0.30	0.0076	11.96	11.2	13.88	29.4	2.51
	AP	0.54	0.0010	5.61	14.2	9.61	40.7	0.00
	FEYZ1	0.12	0.0097	10.27	9.6	12.89	40.3	0.00
	FEYZ2	0.05	0.0087	6.50	11.3	8.02	39.8	0.00
	KG1A1	0.24	0.0084	12.43	9.6	14.99	33.3	0.00
	KG1A2	0.25	0.0081	11.92	11.6	15.04	34.0	0.00
	PEL1	0.27	0.0082	4.79	9.0	6.46	34.7	0.00
	PEL2A	0.18	0.0292	8.26	22.8	12.92	30.0	0.00
	1LLAF	0.42	0.0100	4.72	14.5	7.23	34.9	0.00
	2LLAF	0.18	0.0255	4.10	26.9	6.35	24.2	0.00
	3LLAF	0.25	0.0079	11.08	12.9	13.64	32.5	0.00
	4514B1	0.30	0.0010	11.90	10.2	13.85	36.0	1.00
	4514B2	0.18	0.0009	9.10	10.1	10.81	30.4	3.93
	MANO1	0.13	0.0086	4.81	11.3	6.86	28.5	0.00
	MANO2	0.13	0.0091	2.51	13.3	4.17	28.7	0.00
LAKE BAIKAL	L1	0.12	0.0083	11.76	10.8	13.02	38.7	0.00
	L2	0.26	0.0110	8.45	13.8	9.93	38.5	0.00
	L3	0.13	0.0105	5.44	14.9	6.34	41.3	0.00
	BA1	0.12	0.0026	7.94	13.2	9.51	38.2	0.00
	BA2	0.13	0.0082	4.41	16.2	7.11	43.4	0.00
	BA3	0.12	0.0091	5.95	14.0	9.45	41.9	0.00
	B1P	0.12	0.0024	8.96	12.2	9.69	37.6	0.00
	B2P	0.16	0.0081	5.98	14.6	8.30	41.7	0.00
	B3P	0.17	0.0096	8.21	11.6	12.27	39.9	0.00
	4846D	0.44	0.0008	8.01	12.0	14.08	30.6	0.00
	4846E	0.26	0.0008	6.45	10.8	8.59	30.2	1.27
	4846F	0.26	0.0007	5.29	12.7	6.87	33.1	1.42
CHILE	CH1	0.25	0.0085	7.58	10.8	9.94	37.6	0.00
	CH2	0.17	0.0088	7.97	10.9	10.14	38.9	0.00
	CH3	0.23	0.0078	7.11	11.1	8.59	35.9	0.00
	CHP	0.22	0.0092	7.63	12.8	9.20	38.0	0.00
PIGMENTS	ZJ23	0.76	0.0263	22.75	0.0	21.27	31.7	0.00
	ZJ14	0.63	0.0184	20.21	0.0	16.02	37.1	0.00
	ZJ19	0.78	0.0031	24.73	0.0	20.69	31.5	0.00
	ZJ26	0.64	0.0063	14.29	0.0	29.69	40.0	0.00
	ZJ28	0.64	0.0064	13.88	0.0	30.60	40.6	0.00
	UMZO	2.14	0.0204	5.13	18.2	1.83	41.5	0.00
	ZJ10	1.12	0.0001	0.00	0.0	1.52	10.9	0.00
	ZJ09	1.13	0.0018	0.00	0.0	0.00	4.5	0.00
	ULTRA	1.10	0.0007	0.00	0.0	0.00	4.4	0.00
ARCHAEO	UULL	0.23	0.0109	3.50	18.4	6.81	31.4	0.00
	A830	1.14	0.0045	0.65	0.0		1.9	0.00

Table 1. Composition of the investigated samples in m% units.

		S	Cl	K	Ca	Fe	Mn	Cu	Zn	Sm	Gd
URAL	UR1	2.43	1.70	8.33	31.8	0.77	0.021	0.0	0.00	0.00005	0.00006
	UR2	2.13	0.80	8.35	26.6	0.14	0.023	0.0	0.00	0.00002	0.00005
	UR3	1.71	1.01	1.06	29.2	0.29	0.035	0.0	0.00	0.00022	0.00040
	UP	3.22	0.87	8.32	24.9	0.16	0.021	0.0	0.00	0.00007	0.00006
AFGHANISTAN	AF1	4.82	0.44	2.07	17.4	2.12	0.029	0.0	0.00	0.00020	0.00026
	AF2	2.43	0.06	2.55	23.4	1.21	0.033	0.0	0.00	0.00006	0.00008
	AFGH6	10.37	0.35	5.85	11.1	2.72	0.000	0.0	0.00	0.00029	0.00036
	AP	2.18	0.07	3.76	22.3	1.15	0.069	0.0	0.00	0.00007	0.00007
	FEYZ1	4.45	0.29	4.31	16.6	0.59	0.032	0.0	0.00	0.00034	0.00044
	FEYZ2	7.23	0.40	21.36	0.3	4.99	0.037	0.0	0.00	0.00008	0.00018
	KG1A1	7.34	0.65	4.26	15.3	3.47	0.000	0.0	0.00	0.00014	0.00021
	KG1A3	6.34	0.65	4.00	13.3	3.52	0.056	0.0	0.00	0.00015	0.00022
	PEL1	12.90	0.15	0.85	21.2	5.54	0.000	0.0	0.00	0.00029	0.00035
	PEL2A	8.89	0.32	5.81	3.6	6.65	0.034	0.0	0.00	0.00004	0.00008
	1LLAF	9.88	0.20	2.00	19.4	6.63	0.017	0.0	0.00	0.00035	0.00043
	3LLAF	9.43	0.18	3.67	17.8	7.34	0.037	0.0	0.00	0.00027	0.00034
	3LLAF	4.92	0.58	3.84	18.3	1.57	0.020	0.0	0.00	0.00026	0.00034
	4614B1	4.48	0.85	8.87	19.7	0.89	0.024	0.0	0.00	0.00008	0.00012
	4614B2	4.34	1.81	1.73	26.8	1.63	0.000	0.0	0.00	0.00025	0.00032
	MANG1	14.32	0.85	1.33	20.1	11.85	0.066	0.0	0.00	0.00018	0.00022
	MANG2	17.36	0.29	1.13	17.3	16.99	0.034	0.0	0.00	0.00009	0.00013
	L1	5.88	0.26	1.14	19.8	1.07	0.024	0.0	0.00	0.00035	0.00037
	L2	4.34	0.43	2.06	20.1	2.11	0.031	0.0	0.00	0.00030	0.00037
	L3	4.93	0.69	8.81	22.7	3.65	0.056	0.0	0.00	0.00010	0.00013
LAKE BAIKAL	BA1	3.33	0.18	8.46	26.5	0.67	0.028	0.0	0.00	0.00004	0.00006
	BA2	1.18	0.22	1.86	25.8	0.28	0.032	0.0	0.00	0.00002	0.00004
	BA3	1.96	0.30	3.39	22.6	0.24	0.029	0.0	0.00	0.00002	0.00005
	B1P	4.47	0.18	8.24	25.3	1.14	0.024	0.0	0.00	0.00008	0.00006
	B3P	1.85	0.50	1.86	25.8	0.31	0.030	0.0	0.00	0.00003	0.00007
	B3P	3.16	0.77	4.82	18.9	0.15	0.023	0.0	0.00	0.00005	0.00014
	4646D	4.63	0.03	3.18	25.7	1.04	0.017	0.0	0.00	0.00011	0.00013
	4646E	3.38	0.03	8.61	37.3	0.98	0.039	0.0	0.00	0.00021	0.00028
	4646F	2.63	0.03	8.49	36.5	0.69	0.040	0.0	0.00	0.00019	0.00024
CHILE	CH1	7.48	3.41	8.65	18.8	8.21	0.058	0.0	0.00	0.00010	0.00013
	CH2	6.91	1.82	8.77	18.1	4.17	0.069	0.0	0.00	0.00011	0.00014
	CH3	8.96	1.96	8.61	19.2	6.23	0.054	0.0	0.00	0.00011	0.00016
	CHP	6.96	1.77	8.68	17.5	5.22	0.065	0.0	0.00	0.00010	0.00014
PIGMENTS	ZJ23	19.79	0.28	1.86	1.1	0.39	0.000	0.0	0.00	0.00063	0.00080
	ZJ14	17.39	0.10	1.24	0.8	0.16	0.000	0.0	7.13	0.00050	0.00063
	ZJ19	20.56	0.33	8.69	0.8	0.41	0.000	0.0	0.00	0.00079	0.00070
	ZJ26	12.12	0.24	1.43	0.3	0.59	0.000	0.0	0.00	0.00088	0.00065
	ZJ28	11.93	0.28	1.06	0.8	0.47	0.000	0.0	0.00	0.00087	0.00065
	UNZO	4.95	0.17	3.63	19.5	3.42	0.073	0.0	0.00	0.00027	0.00040
	ZJ10	0.88	0.00	8.00	0.8	0.66	0.155	85.6	0.00	0.00027	0.00057
	ZJ09	0.88	0.01	8.00	0.8	0.00	0.000	94.3	0.00	0.00021	0.00034
	ULTRA	0.88	0.00	8.47	0.8	0.00	0.000	94.8	0.00	0.00022	0.00032
ARCHAEO	UULL	7.28	0.23	3.46	22.6	5.69	0.023	0.0	0.00	0.00017	0.00000
	A838	0.31	0.03	1.25	0.6	0.62	0.109	0.0	0.00	0.00000	0.00000

Table 1 *(Cont.)*

5. TECHNOLOGY AND PROVENANCE OF CERAMICS AND GLASSES

INDEX

SGRAFFITO CERAMICS FROM FLORENTINE AREA (XVIth CENTURY): ARCHAEOMETRIC CHARACTERIZATION OF PASTE AND COATING

Francesca AMATO, Bruno FABBRI, Sabrina GUALTIERI, Andrea RUFFINI
CNR, Institute of Science and Technology for Ceramics, Faenza

Anna VALERI MOORE
Archaeologist and Art Historian, Florence

1. INTRODUCTION

This research moves from a recent renovated interest for sgraffito ceramics coming from Tuscany. Although they appear in archaeological contexts only in the second part of XVth century, in delay compared to the production of Northern Italy, sgraffito ceramics are documented everywhere in florentine area. They were manufactured by a large amount of workshops situated all around the region, while, on the contrary, majolica was produced only in a few places with industrial organization.

This work is focused on artefacts attributed to Cafaggiolo (Florence), Borgo San Lorenzo (Florence) and Castelfiorentino (Empoli), dating from the second part of 15th to the 17th century, through stylistic methods. Materials of the first two places come from the same excavation of Villa Valle, a little village in the north of Florence (Baragatti *et al.* 2002), while pottery from Castelfiorentino were found in six different archaeological excavations carried out in the historical part of the town, nearby the ancient kilns (Amato *et al.* 2004).

The research deals with the study of pastes and coatings of sgraffito ceramics of the three sites in exam, in order to characterize the technological features proper to each production, pointing out similarities or differencies.

2. MATERIALS AND ANALYTICAL METHODS

Thirty samples were analyzed: 9 from Cafaggiolo, 4 from Borgo San Lorenzo and 17 from Castelfiorentino. This selection of fragments represents

objects of open shapes (plates, cups and bowls) coated by a white slip and a transparent glaze, at least on the recto side. Some kiln wastes among samples of Castelfiorentino present only the slip layer. A few artefacts are monochrome, but in most cases the slip is engraved and enriched with yellow, blue and green pigments. Finds from Castelfiorentino differ from the others due to a more elaborated style, characterized by counter-relief surfaces forming vegetal and geometric motifs (figure 1).

Figure 1. Artefacts from Cafaggiolo (on the left), Borgo San Lorenzo (in the middle and Castelfiorentino (on the right).

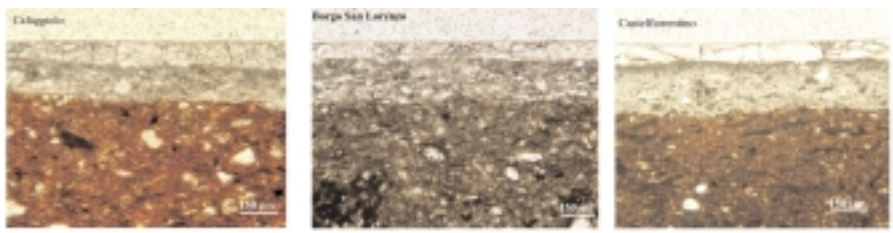

Figure 2. Thin sections of ceramic bodies and coatings.

Chosen samples were subjected to microstructural observations, carried out by optical microscopy in thin section. Mineralogical analysis of pastes was carried out by means of X-ray diffraction (XRD). Chemical composition of bodies were determined through an X-ray spectrometer (XRF), after removing the slip and glaze layers using a lancet, while scanning electron microscopy combined with energy dispersion spectroscopy (SEM-EDS) was used for the chemical analysis of coatings.

3. RESULTS AND COMMENTS

3.1. Investigation on pastes

The bodies have a yellowish-red colour and a fine structure quite similar for all the samples (figure 2). They consist of an anisotropic, fine-grained

paste with fairly abundant quartz and variable content of plagioclase and K-feldspar. Calcite, probably of secondary origin, is present inside pores or as encrustation on external surface. The yellowish-red colour is in agreement with the low Fe_2O_3/CaO ratio, generally less than 0.9 (Fabbri, Dondi 1995).

The crystalline phase composition is constant in almost all samples, being characterized by quartz, feldspar and newly-phormed calcium compounds, in particular pyroxene (more abundant) and gehlenite. This mineralogical composition underlines that the maximum firing temperature is around 950°C.

The results obtained by XRF analysis are reported in table 1; the data are normalized excluding phosphorus, that reaches 0.5-0.7% in some pastes from Villa Valle excavation, as a result of post-depositional pollution from soil solutions. Chemical analyses indicate that all the three productions have bodies characterized by a content of silicon oxide around 56-58% and amount of iron oxide around 6%, while some differencies can be evidenced for alumina, magnesium and calcium contents. Castelfiorentino has a higher alumina percentage (21.6% Al_2O_3 vs. about 17% of Cafaggiolo and Borgo San Lorenzo) and lower magnesium content (3% MgO vs. 4% of the finds from Villa Valle). Borgo San Lorenzo shows a higher calcium content (about 12% CaO vs. 7-9% in Castelfiorentino and Cafaggiolo). Because these differencies could be useful in order to distinguish the three productions from each other, it would be worth increasing the number of analysed samples, especially in the case of Borgo San Lorenzo and Cafaggiolo.

3.2. Investigation on coatings

Coatings consist of a very fine permeable slip and a transparent glaze (figure 2), except for a few slipped kiln wastes from Castelfiorentino. All sgraffito ceramic samples attributed to Cafaggiolo differ from the others because they are glazed both inside and outside.

Sites		SiO_2	Al_2O_3	TiO_2	$Fe_2O_3^{tot}$	MnO	MgO	CaO	Na_2O	K_2O
Cafaggiolo	*average*	58.53	17.72	0.76	6.20	0.14	3.92	8.71	1.06	3.04
	st.dev	1.96	0.64	0.06	0.60	0.05	0.67	2.00	0.12	0.38
Borgo San Lorenzo	*average*	55.88	16.88	0.77	6.07	0.12	4.48	11.77	1.02	2.98
	st.dev.	1.18	0.43	0.02	0.21	0.02	0.43	1.47	0.04	0.17
Castelfiorentino	*average*	57.46	21.57	0.72	6.28	0.08	3.12	6.99	0.62	3.16
	st.dev.	0.88	1.36	0.02	0.19	0.01	0.25	0.87	0.22	0.20

Table 1. Average chemical composition (wt%) and standard deviation of the ceramic bodies.

The samples attributed to Cafaggiolo and Borgo San Lorenzo present similar thickness of the slip layer (~150 μm), but the thickness of the glaze layer is different, measuring ~100 μm in Cafaggiolo artefacts and ~60 μm in Borgo San Lorenzo ones. The coating thickness in Castelfiorentino samples is variable in the range 80-180 μm for the slip, and 60-110 μm for the glaze. The variations depend on the fact that both unglazed and glazed fragments were taken into account. In fact the slip thickness is higher in the unglazed pieces, probably because the application of the glaze results in a compacting of the corresponding slip layer. In addition it was observed that the ratio between slip and glaze thickness is different depending on the archaeological excavation where the finds come from. In this way it is possible to individuate two groups of artefacts, which probably correspond to two different workshops in Castelfiorentino.

Several undissolved crystals and bubbles of variable dimensions, together with fine cracks, can be observed in the glaze layer of all samples.

Chemical analyses performed by SEM-EDS are reported in table 2. As it regards the slip, the data were recalculated to 100, excluding lead (0,8-1% PbO), attributed to infiltration of vapours from the glaze during firing. Slip is characterized by a high potassium content (K_2O ~8% for Cafaggiolo, ~6.5% for Borgo San Lorenzo and Castelfiorentino) and a low $Fe_2O_3^{tot}$ amount (less than 2%) as required by the function of the slip, which is to provide a light coloured base to the glaze. Samples of Castelfiorentino show lower values of magnesium (5.6% MgO instead of 7-8% MgO); on the contrary, the amounts of alumina are higher (26.2% Al_2O_3) than the others (21-23% Al_2O_3). In conclusion, it deals with three quite different slip compositions, probably depending on the supplying area. In any case, these compositions are different from that of the famous "Vicenza kaolin", which is magnesium poor. We hypothesize that the slip of the examined sgraffito samples comes from at least two different areas in Tuscany, probably not far from the two production centres.

The results of chemical analyses for transparent glaze show very similar compositions for the three productions, indicating a very standardized processing technology. They were prepared mixing only two raw components: lead (around 50% PbO) and quartz sand with some impurities like alumina (5% Al_2O_3).

4. CONCLUSIONS

Investigations indicate that all the studied samples of sgraffito ceramics have a red and fine paste, obtained with intermadiate calcium containing clays. Vessels from Castelfiorentino constitute a good chemical reference group, different from the finds of Villa Valle, mainly due to its higher amount

of alumina. Compositions of Cafaggiolo and Borgo San Lorenzo are very similar and the observed differences in calcium amount, more abundant in pastes of Borgo San Lorenzo, possibly reflect normal variations of this element within a single deposit.

	Cafaggiolo	Borgo		San Lorenzo		Castelfiorentino	
SLIP	SiO_2	57.32	1.09	57.45	2.73	57.18	2.77
	Al_2O_3	22.97	1.54	21.29	2.07	26.25	3.65
	TiO_2	0.90	0.26	0.88	0.11	0.89	0.20
	$Fe_2O_3^{tot}$	0.95	0.34	1.06	0.45	0.95	0.38
	MgO	7.35	1.06	7.91	0.99	5.64	1.86
	CaO	1.54	0.58	3.62	1.74	1.57	1.29
	Na_2O	0.97	0.11	1.00	0.12	1.14	0.23
	K_2O	8.00	0.37	6.79	0.81	6.37	1.08
GLAZE	SiO_2	39.56	2.92	39.77	2.55	41.45	5.22
	Al_2O_3	4.02	1.13	5.08	1.22	5.18	1.35
	TiO_2	0.29	0.13	0.26	0.07	0.20	0.07
	$Fe_2O_3^{tot}$	0.78	0.63	0.58	0.13	0.49	0.15
	MgO	0.82	0.67	1.14	0.45	1.29	0.73
	CaO	1.15	0.65	0.99	0.27	0.87	0.23
	Na_2O	0.41	0.16	0.47	0.04	0.43	0.16
	K_2O	1.21	0.38	1.32	0.65	1.45	0.67
	PbO	51.55	5.54	50.26	4.69	48.25	7.68
	SnO_2	0.19	0.17	0.12	0.16	0.40	0.56
		average	*st.dev.*	*average*	*st.dev.*	*average*	*st.dev.*

Table 2. Chemical composition of slip and glaze (wt%).

So a different provenance of raw clays should be taken into account for Castelfiorentino, on one hand, and Borgo San Lorenzo and Cafaggiolo on the other. The same can be said with reference to the chemical composition of the slip, according to the higher alumina content in Castelfiorentino ceramics.

From a technological point of view, the mineralogical composition indicates that the temperature reached during firing always is around 950 °C. Concerning coatings, the main difference is that sgraffito ceramics attributed to Cafaggiolo are glazed on both inside and outside surfaces. In addition the ratio between slip and glaze thickness let us subdivide the potsherds from Castelfiorentino into two groups, possibly correspondent to two workshops contemporaneously operating in the town. Concerning glaze layer, it seems not possible to underline any difference in composition. In fact in all cases it is a lead glaze, prepared by mixing only two components: around 50% of PbO and 50% of a quartz sand with impurities (predominantly Al_2O_3).

In conclusion the archaeometric investigation of sgraffito ceramics from Tuscany seems to give important instruments for supporting the archaelogical attribution of new finds. In this perspective, it would be useful to define better the characteristics of each reference group by increasing the analysed samples.

REFERENCES

Amato F., Fabbri B., Gualtieri S., 2004, *Studio archeometrico* in "Ceramiche Rinascimentali di Castelfiorentino. L'ingobbiata e graffita in Toscana" a cura di A.Valeri Moore, Edizioni Polistampa, Firenze, pp. 77-80 .

Baragatti B., Moore Valeri A., Marini M., 2002, *Ceramiche Postmedievali nel Mugello: il ritrovamento di Villa Valle (Borgo San Lorenzo, Fi)*, in "Archeologia Postmedievale", n. 6, pp. 1-27.

Fabbri B., Dondi M., 1995, *Caratteristiche e difetti del laterizio*, Gruppo Editoriale Faenza Editrice, Faenza.

EARLY BRONZE AGE FAIENCE FROM NORTH ITALY AND SLOVAKIA: A COMPARATIVE ARCHAEOMETRIC STUDY

Ivana Angelini, Gilberto Artioli, Angela Polla
Dip. di Scienze della Terra, Università di Milano, Via Botticelli 23,
I-20133 Milano, Italy

Raffaele C. de Marinis
Dip. di Scienze dell'Antichità, Università di Milano, Via Festa del Perdono 3 ,
I-20122 Milano, Italy

ABSTRACT

Early Bronze Age faience beads from Italy (Lavagnone) and Slovakia (Mýtna Nová Ves and Nižná Myšľa) were analysed by SEM-EDS, computerised 2-D image analysis, EPMA, and XRPD. The glass phase in the faience is present in different amount and invariably shows a mixed alkali composition, with the exception of two Carpathian samples showing an unusually Cu-rich glassy matrix. The chemical and mineralogical results seem to indicate a local production based on very similar glass-making technology, and the use of different starting materials.

1. INTRODUCTION

Faiences were known in the Near East and Egypt since the 4th millennium BC (Aspinall *et al.* 1972, 27; Tite *et al.* 2002, 585), and in Europe since the Early Bronze Age (EBA, end of the 3rd – first half of the 2nd millennium BC) (de Marinis 1999, 25-38). The European faience beads are essentially of simple typology (annular, stellate, segmented, cylindrical, and biconical), although several local variation or specialised form are present (Harding 1971). In spite of the importance and diffusion of this material during the protohistory, only a few analyses of Central European faiences are available in the literature (Aspinall *et al.* 1972, Harding and Warren 1973, Henderson 1993). No Italian EBA faiences have been analysed to date, with the exception of one biconical bead from the Gaban rock shelter (Trentino, Angelini *et al.* 2004b, in press), which is unfortunately strongly weathered.

In the present work EBA faience beads from three important sites, two cemeteries located in the Carpathian area (Slovakia) and one settlement located North Italy, have been selected for a comparative analytical study, in view of the similarity of the coeval objects. The research aims to characterise the nature of faience material and to interpret the probable production techniques.

2. SAMPLES AND EXPERIMENTAL METHODS

The Italian samples come from the pile-dwelling village of Lavagnone, an infra-morainic basin near Desenzano del Garda (Brescia), a few km from the South shore of the Garda Lake. The site was inhabited from the end of the 3rd millennium BC (Polada culture) to the Recent Bronze Age (after the Italian terminology: cfr. de Marinis 1999, fig. 1 and 44, about 1300-1200 BC). Analysed faience beads from Lavagnone are dated to the EBA IC (1900-1800 BC) and are of the following typologies: biconical (6 samples), cylindrical (1 sample) and segmented (1 sample) (fig. 1). They are all of blue-green colour, except one biconical beads that is brown (de Marinis ed., *Studi sul Lavagnone*, in press).

The Slovakian faience beads analysed come from two cemeteries: Mýtna Nová Ves (Topol'čany region), of the Nitra culture (Slovakian EBA, 2100–1800 BC); and Nižná Myšl'a (Košice region), of the Otomany Culture (1800–1600 BC) (Bátora 1995). Eight blue-green coloured beads (2 flattened biconical, 2 cylindrical and 4 segmented) from eight different graves of Mýtna Nová Ves and 7 cylindrical beads of a faience-decorated apron and skirt pieces (a set of 2187 beads) discovered in a woman grave of the Nižná Myšl'a cemetery have been analysed (fig. 1).

The archaeometric characterisation of the samples were carried out by Scanning Electron Microscopy with Energy Dispersive Spectroscopy (SEM-EDS), Electron Probe Microanalysis (EPMA), and X-ray Powder Diffraction (XRPD); fabric and texture were studied with a computerized 2-D image analysis applied to SEM backscattered electron images. Specifications about the instrumentation and the analytical methodologies, optimized for vitreous materials micro-samples, may be found in: Angelini *et al.* 2002, 2004a, and 2004b.

3. RESULTS AND DISCUSSION

EBA faience finds are quite rare, especially in Italy, therefore in most cases only surface microsampling was possible. Complete sections of the body have been cut only for 5 Slovakian and 1 Italian beads. As expected, several surface samples are completely altered and no "original" glass phase

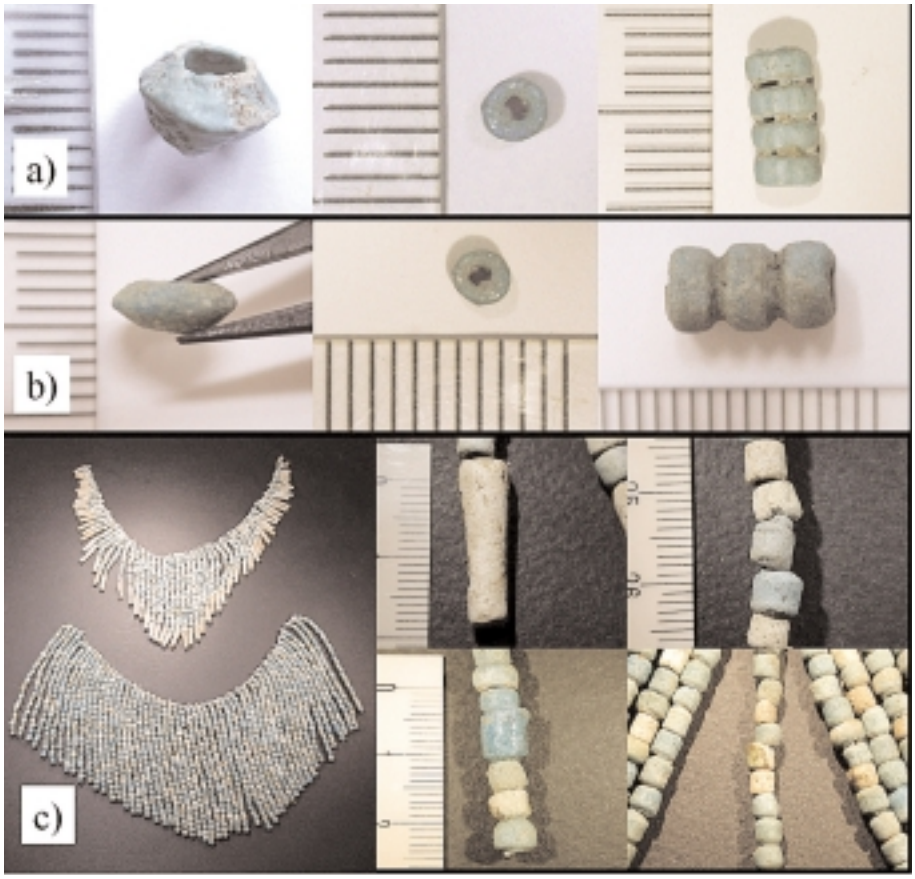

Figure 1. Selected faience beads from: a) Lavagnone, Italy; b) Mýtna Nová Ves, Slovakia, and c) Nižná Myšľa, Slovakia.

remains (Tab.1). In table 1 the major elements chemistry of the glass phase is reported (values are expressed as oxide wt%, calculated as the mean values of 5 spot analyses), together with the sample typology and origin.

All but two of the faience glass phase show a mixed alkali recipe with a very low amount of Mg (0.3<MgO<1.6 wt%). The total amount of alkali and the Mg content of these glass phases are comparable to those observed in the *low magnesium high potassium* (LMHK) glasses of the Final Bronze Age (Angelini *et al.* 2002, 2004a, Henderson 1993) and to the Italian Middle Bronze Age conical buttons made of glassy faience (Angelini *et al.* 2004b). The amount of alkali (Na_2O+K_2O) of the faiences is consistently higher, by about 4-7 wt%, with respect to the available data in the literature concerning Central Europan faiences, relative to three samples from Hauterive-Champréveyres,

Sample	Locality	Typology	Colour	Note	Na_2O	MgO	Al_2O_3	SiO_2	Cl	K_2O	CaO	FeO	CuO	totale
T27-9V *	Nižná Myšľa (Košice region, Slovakia)	Cylindrical bead	Pale green		0.00	0.25	1.96	39.67	0.08	0.09	1.68	0.57	32.45	76.76
G15-6V *		Cylindrical bead	Pale green		0.02	0.23	2.35	41.06	0.12	0.22	1.99	1.01	31.02	78.03
G46-13VA *		Cylindrical bead	Pale blue-green		6.77	1.18	3.43	67.61	0.46	5.97	3.88	1.06	7.13	97.49
G49-4a *		Cylindrical bead	Pale blue		9.03	0.41	2.76	70.16	1.33	5.57	2.78	0.77	6.88	99.71
T30-14A *		Cylindrical bead	Pale blue		8.50	0.32	3.54	70.13	1.06	5.02	2.37	0.93	7.25	99.12
T20-1B *		Elongated cylindrical bead	Opaque white	1 2	6.38 5.80	1.57 1.16	3.76 1.31	73.56 69.84	0.56 0.52	8.29 8.18	3.28 2.39	1.77 10.27	0.03 0.02	99.21 99.49
T59-1B *		Elongated cylindrical bead	Opaque white	1 2	3.90 2.71	1.51 0.54	4.71 11.40	73.79 71.83	0.96 0.37	10.29 9.75	2.68 2.23	1.64 0.82	0.04 0.09	99.53 99.74
MNV61/1 *	Nižná Myšľa Ves (Topoľčany region, Slovakia)	Segmentated bead	Pale blue		11.60	0.86	3.75	72.61	1.78	2.16	2.25	1.34	4.22	100.58
MNV129/1 *		Segmentated bead	Blue		10.13	0.64	1.98	68.05	2.08	2.99	2.39	0.91	10.99	100.18
MNV-198-2 *		Cylindrical bead	Pale blue		3.79	0.27	1.38	72.18	0.84	10.71	1.69	0.44	8.72	100.04
MNV-453 *		Biconical bead	Pale blue		5.79	0.49	2.14002	77.33	0.16	7.25	1.50	0.79	5.04	100.49
MNV509/2 *		Biconical bead	Pale blue		5.96	0.60	2.45	70.24	0.54	8.08	1.97	1.27	8.28	99.38
MNV535 *		Segmentated bead	Blue		4.87	0.26	1.79	72.94	0.10	11.13	1.22	0.66	6.20	99.17
MNV548 *		Anular bead	Blue		8.89	0.91	4.03	74.91	1.75	0.99	2.23	1.54	3.69	98.94
LAV-B3r *	Lavagnone (Brescia, Italy)	Biconical bead	Pale blue-green		4.50	0.64	2.47	80.63	0.64	6.41	1.27	0.60	3.12	100.28
LAV-BR-M #		Biconical bead	Beige-brown		6.75	1.34	13.37	64.01	0.50	6.93	2.52	1.31	1.05	97.78
LAV-B1 #		Biconical bead	Pale blue-green		1.21	0.00	1.61	56.95	0.23	0.16	1.54	0.25	0.32	62.26
LAV-B2 #		Biconical bead	Pale blue-green		1.51	0.18	1.09	75.44	1.04	0.00	2.59	0.13	3.50	85.49
LAV-B4R #		Biconical bead	Pale blue-green		1.45	0.19	0.51	78.06	0.54	0.00	3.11	0.18	1.98	86.03
LAV-DE-B1 #		Biconical bead	Pale blue-green		2.59	0.25	1.81	91.25	0.85	0.04	2.63	0.28	3.19	102.90
LAV-DE-B2 #		Biconical bead	Pale blue-green		1.63	0.09	0.58	77.48	0.90	0.00	0.67	0.12	4.95	86.43
LAV-DE-CIL #		Cylindrical bead	Pale blue-green		1.45	0.20	0.51	80.22	0.64	0.06	2.17	0.21	3.13	88.57
LAV-DE-SEG #		Segmentated bead	Pale blue-green		1.71	0.10	0.29	79.58	0.98	0.00	1.76	0.10	4.71	89.22

Table 1. List of analysed samples, original localities, typology, and mean EPMA (*) or SEM-EDS (#) chemical analyses of the glass phase (in oxide wt %).

Switzerland (Henderson 1993, 114-116). The data reported in the works of Aspinall *et al.* 1972, and Harding and Warren 1973, are not directly comparable because they were carried out with Neutron Activation Analysis, and they do not distinguish between glass phase and crystalline inclusions.

Two faiences from Nižná Myšl'a (T27-9V and G15-6V) have no alkali in the glass phase and they show an unusually high level of metal: CuO = 31.0-32.4 wt%. Even if the analyses are of poor quality because of the size and nature of these samples, they are clearly a distinct class of materials. To our knowledge only one comparable composition is available, it pertains to a conical button glassy faience of the Italian Middle Bronze Age from Grotta dello Sventatoio, Lazio (our unpublished data).

The two white faiences from Nižná Myšl'a (T20-1B and T59-1B) show a chemically rather heterogeneous glass phase, with point analyses clustering around two distinct compositions (1 and 2 in Tab.1). The compositions n. 2 of samples T20-1B and T59-1B, rich in Fe and Al respectively, are quite unusual for a glass phase.

The Lavagnone samples are strongly weathered, only in the section of sample LAV-B3r the unaltered LMHK glass phase can be identified. The brown faience LAV-BR-M also shows a small fraction of glass matrix around the quartz grains, and it appears to be very rich in Al (Tab.1). The Lavagnone samples systematically have a lower content of Fe, Al and Cu in the glass phase with respect to the Carpathian faiences. Since these elements are hardly subject to leaching, these differences are thought to be characteristics of the material. Concerning the minor elements that were detected by EPMA (P, S, Ti, Mn, Co, Ni, Sn, Sb and Pb), Sn is present in significant amount in the faiences from Nižná Myšl'a (SnO = 0.4-1.2 wt%) and Sb and Ni are often present in correlated amount in the beads from Mýtna Nová Ves (Sb_2O_3 = 0.0-0.4 wt%; NiO = 0.0-0.2 wt%).

SEM-EDS and XRPD analyses helped identifying the nature of the crystalline inclusions in the faiences. Quartz is consistently the main silica mineral phase. Interestingly, the presence of a well preserved diatom in a Mýtna Nová Ves sample (fig. 2) suggests that very reactive continental sands (fossil flour) were also used as the source of silica.

Minor crystalline phases seems to be related to the area of provenance, and they may be used as indicators of the raw materials employed. Carpathian faiences have a significant quantity of metallic inclusions, especially Fe or Fe-rich metal inclusions. Specifically, a Nižná Myšl'a sample shows the occurrence of tin oxide particles (irregular habit), that may represent a possible link with the metallurgical process. The Lavagnone faiences show a number of feldspar and apatite grains. In one sample (LAV-B4R) cristobalite is present.

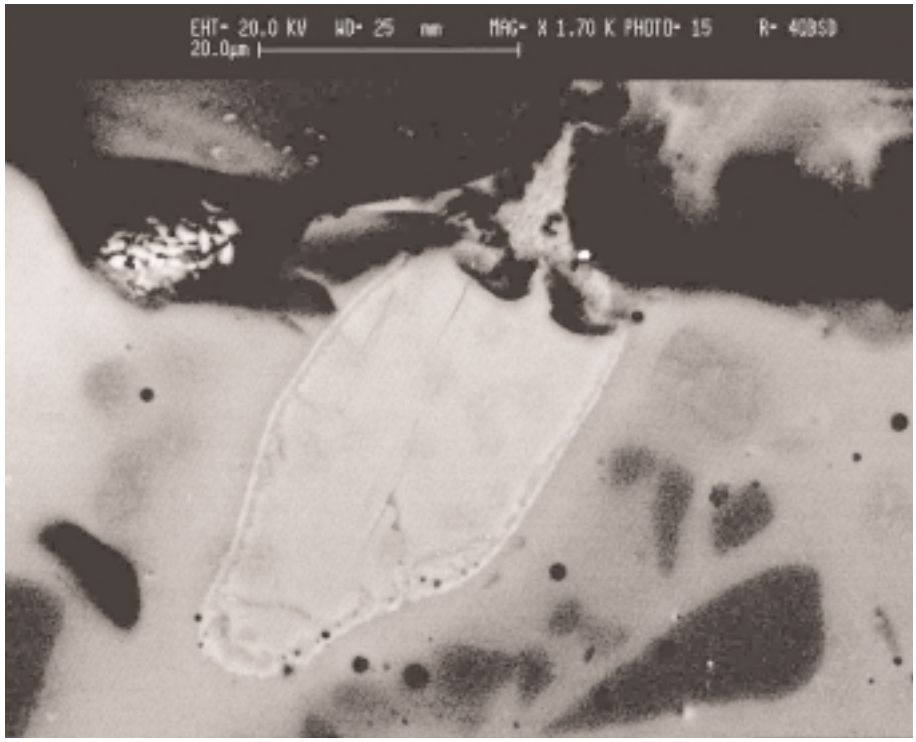

Figure 2. SEM backscattered electron image of diatom inclusion in the bead MNV 453.

Computerised 2-D image analysis applied to SEM backscattered electron images of the beads section allow to measure: the thickness of the surface glaze and of the glaze-core interaction layer, the mean size of the mineral grains, and the χ_M parameter describing the relative proportion of the glass phase (Angelini *et al*. 2002, 585-586; Angelini *et al* 2004, 1176-1177) in the rim and in the core. These parameters help defining the nature of the faience and the production technique. Two bead sections from Mýtna Nová Ves (fig. 3a) show no surface glaze, a thick glaze-core interaction layer, and almost no glass phase in the core. The same is observed in the bead section from Lavagnone (fig. 3b), which however shows a very thin layer of glaze at the surface. These beads were likely produced by the direct application technique. The bead MNV 453/1 (fig. 3c) was probably made by the efflorescence method because the glass phase is extensively present in the core (Tite 1987, 24-28; Tite *et al.* 2002, 587-589, Nicholson 1993). Two Carpathian samples show a rather unusual texture (fig. 3d) with the total absence of glass phase and a very thin layer (10-15 µm) of sintered quartz grains at the surface. At this stage the manufacturing process is not clear.

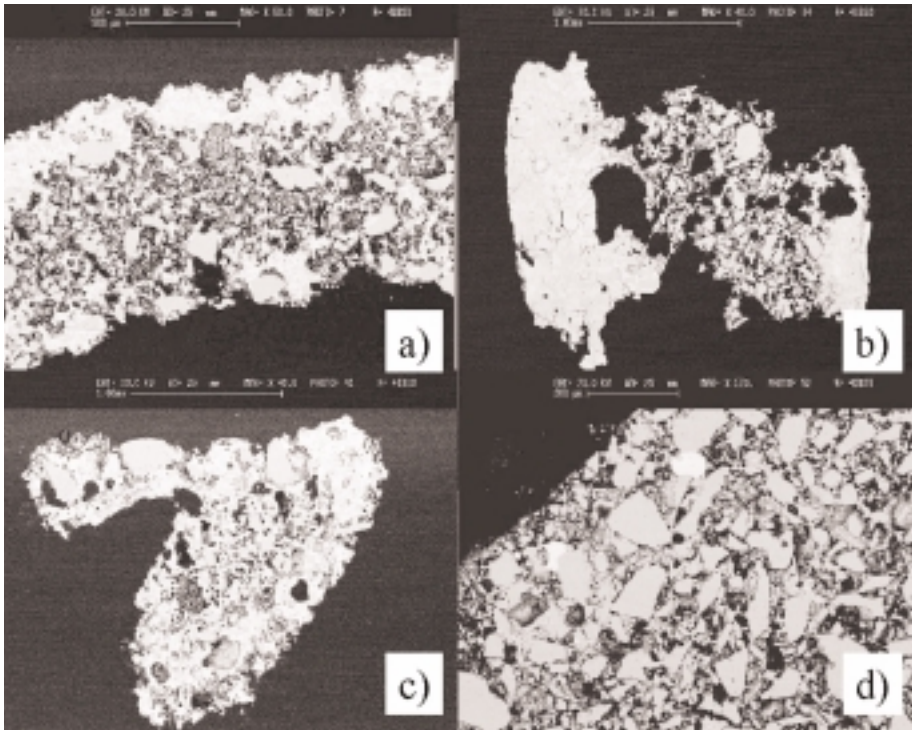

Figure 3. SEM backscattered electron images of the samples: a) MNV 198-2; b) LAV-B3r; c) MNV 453/1 and d) MNV 149-1. The sample MNV 149-1 is a segmented bead from Mýtna Nová Ves that is not listed in Tab. 1 because no glass phase is present for the chemical analysis.

4. CONCLUSIONS

The chemical analyses of the faience glass matrix of the EBA North Italian and Carpathian beads show a comparable main elements chemistry: all but two of the glass phases have a LMHK composition. The distinction between the faience production in the two areas is possible on the basis of the low levels of Al, Fe and Cu in the Lavagnone beads and of the different mineral inclusions. The minor elements composition, especially Sn, Sb, and Ni may also help distinguish the faience beads of the two Slovakian sites. The two samples from Nižná Myšl'a showing a remarkably high level of Cu and no alkali represent an unknown "class" of metal-rich materials, distinct from normal faiences. The presence of Sb in the Mýtna Nová Ves faiences and of Sn in the Nižná Myšl'a samples represents a link with the coeval metallurgical process and materials.

Based on the present data it is likely that faience was locally produced at each site using a set of similar recipes but different starting materials.

ACKNOWLEDGEMENTS

The authors are grateful to Prof. V. Furmánek, Prof. J. Bátora (Archeologický Ústav Slovenskoj Akadémie, Slovakia), and Dott. G. Belluzzo (Museo Civico di Legnago, Italy) who provided archaeological data and materials for the analyses. The CNR Istituto per la Dinamica dei Processi Ambientali, Milano, provided the SEM-EDS facilities and A. Rizzi helped with the analyses. Mr. R. Carampin (Università di Padova, Dip. Scienze della Terra, Italy) is thanked for help with the EPMA analyses.

REFERENCES

Angelini, I., Artioli, G., Bellintani, P., Diella, V., Polla, A., and Residori, G., 2002. 'Project "Glass materials in the protohistory of North Italy": a first summary, *Atti del Secondo Congresso Nazionale AIAr, Bologna 29 Gennaio-1 Febbraio 2002* (ed. C. D'Amico), Pàtron Editor, Bologna, 581-595.

Angelini, I., Artioli, G., Bellintani, P., Diella, V., Gemmi, M., Polla, A., and Rossi, A., 2004a.'Chemical analyses of Bronze Age glasses from Frattesina di Rovigo, Northern Italy', *Journal of Archaeological Science*, **31**, 1175-1184.

Angelini, I., Artioli, G., Bellintani, P., and Polla A., 2004b. 'Protohistoric vitreous materials of Italy: from early faience to Final Bronze Age glasses.' *AIHV 2003, 16e Congrès de l'Association Internationale pour l'Histoire du Verre, 7-13 September 2003, London*, UK, in press.

Aspinall, A., Warren, S. E., Crummett, J. G., Newton, R. G., 1972. 'Neutron activation analysid of the faience beads'. *Archaeometry* **14**, 27-40.

Bátora, J., 1995. 'Fayence und Bernstein im nördlichen Karpatenraum während der Frühbronzezeit', *Handel, Tausch und Verkehr im Bronze- und Früheisenzeitlichen Südosteuropa*, (ed. *B. Hänsel),* PAS 11, München-Berlin.

de Marinis, R.C., 1999. 'Toward a Relative and Absolute Chronology of the Bronze Age in Northern Italy', *Notizie Archeologiche Bergomensi* 7, 23-100 (Museo archeologico di Bergamo).

de Marinis ed., *Studi sul Lavagnone*, Bergamo, in press.

Harding, A., 1971. 'The earliest glass in Europe', A*rcheologickè Rozhledy,* **23**, 188-200.

Harding, A., and Warren, S. E., 1971. 'Early ronze Age faience beads from Central Europe', *Antiquity,* **47**, 64-66.

Henderson, J., 1993. 'Chemical analysis of the glass and faience from Hauterive-Champréveyeres, Switzerland'. *Hauterive-Champréveyeres, 9: Mètal et Parure au Bronze Final,* (ed. A.-M. Rychner-Faraggi). Neuchatel, Musèe Cantonal d'Archèologie, 111-117.

Nicholson, P. T., 1993. *Egyptian Faience and Glass*. Shire Publications, Aylesbury.

Tite, M. S., 1987. 'Characterization of early vitreous materials'. *Archaeometry* **29**, 21-34.

Tite, M. S., Shortland, A. and Paynter, 2002. 'The beginning of vitreous materials in the Near East and Egypt'. *Acc. Chem. Res.*, **35**, 585-593.

INDEX

ARCHAEOMETRICAL INVESTIGATIONS ON CERAMICS OF THE LATE-MIDDLE AGE IN CALABRIA (SOUTH-ITALY)

S. Aragona, F. A. Cuteri, L. Mavilia
Dipartimento PAU, Università "Mediterranea" di Reggio Calabria, Via Melissari , I-89124 Reggio Calabria

M. Rotili
Dipartimento di studio delle componenti culturali del territorio, Seconda Università di Napoli, Via G. Paolo I, I- 81055 S. Maria Capua Vetere, CE

R. Ponterio, S. Trusso, C. Vasi
CNR- Istituto per i Processi Chimico-Fisici, Via La Farina 237, I -98100 Messina

ABSTRACT

Fragments of glaze, recovered during the archaeological excavations performed in the period 2000-2003 at castle of Amendolea, Condofuri (RC, Italy), have been submitted to accurate laboratory investigations in order to find differences or analogies on both raw material compositions (major ingredients, minor active and passive constituents etc.) and production technologies (i.e., techniques of moulding, firing temperature, oven atmosphere). The employed techniques have been the following: OM (optical microscopy), micro-Raman, micro-FTIR (Fourier Transformed Infrared), LIBS (Laser Induced Breakdown Spectroscopy), SEM-EDS (Scanning Electron Microscopy + Energy Dispersion Spectroscopy) with or without BSE (Back Scattered Electron and XRD (X-Ray Diffraction). Raman, FTIR and LBIS analyses together with SEM-EDS observations given detailed information on the qualitative composition of different coatings and pigments. Observations in OM supported also by an accurate digital images elaborations allowed the elucidation of both the number and the thickness of the various external layers allowing to classify and gather the ceramics in various subgroups.

1. INTRODUCTION

In the Calabria region there is a need for investigating medieval pottery in order to acquire by means of a rational-systematic research detailed knowledge on raw materials selection, production techniques applied

mainly firing technology and glazing modality (Capelli et al.,1999). Further study on the identification, classification, and composition of various coating layers (engobe, pigments and glaze) are also important findings, as results may represent a useful supplementary instrument to differentiate production units and origin sites CCapelli et al.,1998). The main interest for the close examination of this theme is linked to strengthen the hypothesis that glazes represent a very meaningful part of archaeological finds in the castle of Amendolea. Vice versa, ceramics with a tin based enamel are scarce as in the rest of the Calabria region. So the production of glazes and particularly that painted constitutes, relatively to the centuries XII-XV, a very important chapter of our regional material civilization and in general that of the entire southern Italy. For studying these covering layers, besides the usual techniques of optical microscopy on a thin section, Raman and LIBS have been also employed (F. Colao, 2002 and F. Magistero, 2001). The analyses were carried out on sixteen samples of fragments accurately selected among those recovered during the excavation in Amendolea, a castle of Norman foundation inhabited till the XVII century (M. Rotili et al. 2001).

2. MATERIALS AND METHODS

The selected specimens are considered to be enough representative of above mentioned ceramic typologies. Five of them (labelled as AMD3, 4, 5, 6, 7) are indicative of different composition mixes, while the other eleven (labelled as AMD1, 2, 3, 4, 6 1.1, 1.2, 1.3, 1.4. 1.5, 1.6, 1.7, 1.8, 1.9) represent various decorations and coatings. This paper refers on preliminary results about the more representative ssamples. The analysis of the mixtures has been performed to verify the existence of a local production and to put in evidence chromatic, compositional and manufacturing differences if any. X-ray analysis was always performed on pre-powdered specimens. SEM-EDS on polished sections of AMD3 and AMD4 specimens and on small pieces of original fragments pre-coated with carbon for all the remaining investigated samples. LIBS and Raman measurements were carried out as described elsewhere (R. Ponterio et. al., 2004).

3. RESULTS AND DISCUSSIONS

3.1. Ceramic body

A first analytical investigation of samples was preformed by OM. Differences observed on both the mineralogical genesis and the microstructure allowed to subdivide the fragments into three main subgroups by using a mineralogical-petrographical classification named

Metamorphic-Acid (MA) (Capelli-Mannoni, 1998b). The MA1 subgroup (AMD3 and AMD4), is characterized by the presence by a pure clay with small grains (0.008-0.023 mm) constituted a major fraction of quartz-feldspar and a minor fraction of micas and muscovite. Rare crystals of biotite and lithic fragments (e.g. siltstones with a medium size 0.05 mm) were also observed (look forward figure 3D). The porosity is low with the presence of sub-spherical vacuoles that, in AMD3, show heterogeneous dimensions and moderate orientation while, in AMD4, the same appear elongated with homogenous dimensions and a more marked orientation.

In figure 1, are shown the SEM-EDS spectra of AMD3 and AMD4 with reference to a transversal section of the ceramic body. By a first inspection the two samples show two superimposed bands of different colours, in fact AMD3 appears red-orange to the center and beige to the sides, while AMD4 appears beige to the center and bright red to the sides.

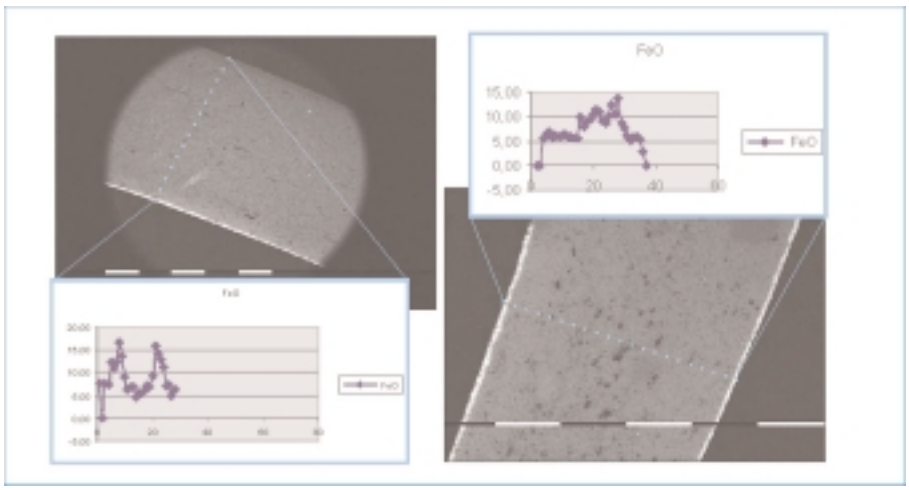

Figure 1. Analytical lines related to iron on AMD3 and AMD4 specimens.

An EDS micro-analytical crossbar examination on a 325.5 μm^2 "windows analysis" allow us to suppose that the different colour of the band could be correlated to the use of original mixtures with different content of iron. It might be also derived by a process operated by artisans by applying different decantation time (Capelli, 2001). The subgroup MA2 (fire achromatic ceramics), is represented by AMD5 and AMD7. These show a homogeneous aspect and a high micro-porosity with pores of irregular aspect and spherical symmetry extended to an orthogonal direction to the thickness, as in AMD7 (look forward figure 3C). The mineralogical phases found in AMD5 are

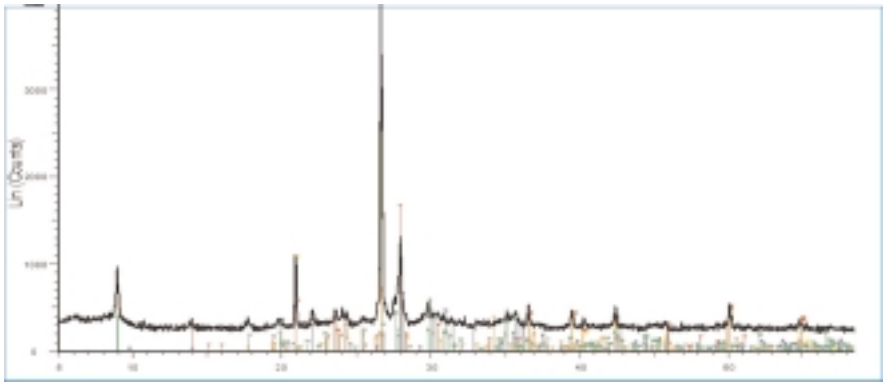

Figure 2. X-ray powder diffraction spectra of AMD5 specimen.

anorthite, quartz, labradorite, biotite, augite, enstatite, sericite e cristobalite as shown in figure 2. These last two phases are characterized by a peak only, that decreases in a zone of the spectrum where there are not superimpositions with other phases compatible with the found mineralogical paragenesis, so that some doubts regarding their contemporaneous presence remain unsolved. Mineral phases found in AMD7 are quartz, anorthite, labradorite, hornblende, enstatite, hematite, biotite and fragments of chamotte with dimensions varying from 0.035 to 0.080 mm. The above-mentioned phases allow us to obtain a high thermal insulation. The subgroup MA3, made up of only AMD6, presents a well depurated red-orange coloured clay with brown areas, grains of varying dimensions between 0.03-0.015 mm made up of quartz, poly and mono-crystalline, microcline, plagioclase, biotite, muscovite and the rare pyroxenes, zircon and titanite (as additional minerals). It has also been observed some small lithic fragments of orthogneiss (meta-granitoids?) as well as the occasional appearance of carbonated microfossils-foramnifers (globigerinas) and, slightly more siliceous fragments of chamotte (look forward in the figure 3B).

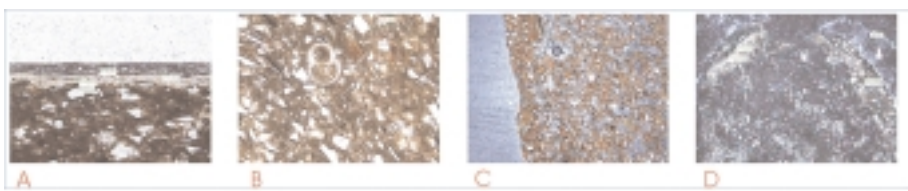

Figure 3. Images of thin sections observed by OM: (A) AMD6 glazed layer (10x, Nicols //); (B) AMD6 mixes (10x, Nicols //); (C) AMD5 mixes (4x, Nicols +); (D) AMD3 glazed layers (4x, Nicols //).

3.2. Coatings

They have been ascertained a great variety of coatings, from the single glazes on ceramic body as in AMD1.4, AMD1.5, AMD1.6 specimens, up to four different coating layers as in the AMD6 one (figure 3A).

The latter and the remaining others exhibiting chromatic effects, alternation of pigments, opacity agents and glazes (figure 4), result remarkably complicated (AMD2) requiring therefore to be identified with the aid of a great knowledge of raw materials and of the productive techniques.

The use of different micro-analytical techniques on such specimens allowed to identify the following groups: i) glazes based on silicon and lead found common to all the samples except those under listed; ii) glazes based on silicon and lead with the addition of tin and phosphorus (AMD4); iii) glazes based on silicon with low percentage of lead as fluxing agents (AMD1.2); iv) glazes based on silicon and lead with low percentage of fluxing agents (AMD1.5); v) glazes with phosphorus (AMD1; AMD1.1; AMD2) as showed in figure 4. In figure 5 the LIBS spectra obtained on the red layer of the sample AMD2 concerning the LIBS measurements are reported. To such end several laser pulses were released at the same sample surface position in order to investigate the stratified structure of the specimen. Independently from the position and the number of laser pulses emission from Ca, Al and Si species were always observed. In correspondence of the red pigment emission from Fe and Mn were identified. In figure 6 there has been report the Raman spectrum obtained on the red area that clearly revealed the presence of hematite (Fe_2O_3).

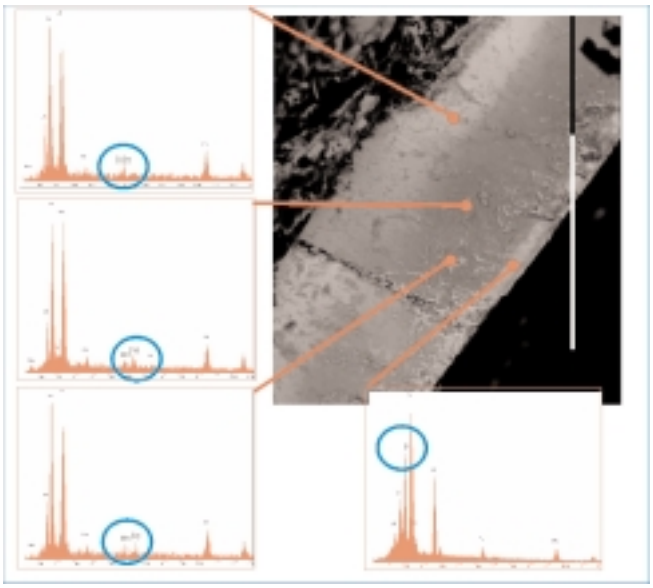

Figure 4. SEM-EDS on AMD2 specimen.

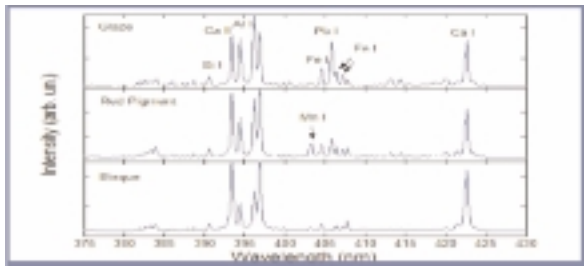

Figure 5. LIBS spectra on AMD2 speciem.

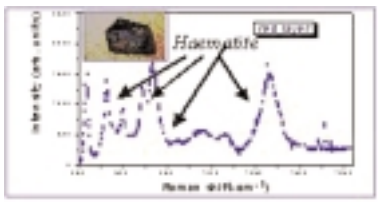

Figure 6. Raman spectra on a red area.

4. CONCLUSIONS

The micro-Raman, micro-FTIR, SEM-EDS and LIBS analysis given enough information to discover the coatings and consequently to gather them in various groups. As regards raw mixes and productive technologies it has been ascertained the chromatic differences on AMD3 and AMD4 they are nor correlated to different firing condition but to different pre-treated raw materials. Comparison the origin with the aid of a geologic paper and with other known regional productions there are some evidences that do not allow to exclude a local production, in particular the subgroup MA1, resulting the less characterized specimen could have been presumably produced in Calabria and Sicily north-oriental. The subgroup MA2 indeed is compatible with the geology of the Calabria (mainly that of the Costa Tirrenica) as also the subgroup MA3 both, on archaeological on archaeological basis underline good analogies with other held productions, so that for both ceramic groups we hold probable a production in local sites.

ACKNOWLEDGMENTS

The authors wish greatly to thank Dr. E. Andronico (Soprintendenza Archeologica della Calabria). This work has been carried out on behalf of

prof. Simonetta Valtieri (head of the M.A.R.E. laboratory) and prof. Enzo Bentivoglio (head of the PAU Department).

REFERENCES

Capelli-Lebole 1999, in Atti del XXX Convegno Internazionale della Ceramica, Albisola 1997, pp. 67- 68.

Capelli C., Mannoni, T. 1998a, in Atti del XXIX Convegno Internazionale della Ceramica, Albisola 1996, pp 229-233.

Colao, F.; Fantoni, R.; Lazic, V., Spizzichino, V., Spectr. Chim. Acta, 2002. Vol. B 57, 1219-1234.

Magistro, F.; Majolino, D.; Migliardo, P.; Ponterio, R. and Rodriquez, M.T., Journal of Cultural Heritage, 2001 Vol. 2, Iss.3.

Rotili, M.; Cuteri, F. A.; Fusaro, F.; Calabria, A., in Quaderni PAU, 2001, Vol. 19/20, pp. 5-59.

Ponterio, R.; Trusso, S.; Vasi, C.; Aragona, S., Mavilia, L., 2004, in Plasma production by laser ablation., PPLA 2003., Edited by S. Gammino, A.M. Mezzasalma. F. Neri, L. Torrisi, World Scientific (Singapore) in press.

Capelli C., Mannoni, T. 1998b, in Le scienze della Terra e l'Archeometria, Atti del convegno, Napoli 1997, pp.123-125.

Capelli C. 2001, in Atti del XXXII Convegno internazionale della ceramica, Albisola 8-29-maggio, 1999, pp 43-48.

CHARACTERIZATION OF BRICKS AND TILES FROM 17th-CENTURY MARYLAND

Ruth Ann Armitage
Department of Chemistry, Eastern Michigan University, Ypsilanti, MI 48197 USA

Leah Minc
OSU Radiation Center, Oregon State University, Corvallis, OR 97331-5903 USA

David V. Hill
Anthropology Department, University of Texas, Austin, TX 78712 USA

Silas D. Hurry
Archaeology Research Laboratory, Historic St. Mary's City, P.O. Box 39,
St. Mary's City, MD 20686 USA

1. INTRODUCTION

St. Mary's City was founded in 1634 as the capital of the Maryland Colony. While the "city" began as a shared Native American site, it quickly progressed into an Italian-Baroque style designed town. By the 1670's, several brick structures existed at the site, including the State House and Prison (1674), and residences like St. Peter's (1679). None of these buildings is extant; when the capital of the colony was moved to Annapolis, St. Mary's City was abandoned and the bricks were scavenged for use at other subsequent sites.

The most impressive brick structure at St. Mary's City was arguably the Chapel, built around 1667. While no records exist of it's construction, archaeological investigations in 1938 and again in the 1980's revealed it to have been a massive cruciform structure, with foundations nearly 1 meter thick and reaching nearly 1.5 meters into the ground. The Chapel is currently being reconstructed on top of the original foundations, with bricks manufactured from a local clay source.

While there were several brick structures within the city, only a few archaeological locations of brickmaking have been discovered and none have been systematically studied. The volume of bricks used at St. Mary's City strongly suggests local manufacture. Bricks from the Chapel have a unique appearance, with many dark inclusions, often with vitrified margins. As these are not common to bricks from other buildings, the question has arisen as to whether

the Chapel bricks specifically were made using locally available materials. To determine this, we have used geological and chemical methods to compare bricks from the Chapel foundation with other bricks, tiles, and local clays.

2. METHODS AND MATERIALS

Brick and tile samples were selected from various sites within St. Mary's City and from other nearby 17th-century Tidewater sites (table 1). To remove surface contamination, all samples were abraded using a rotary tool, rinsed with deionized water and left to dry overnight at room temperature. Portions of the abraded and rinsed materials were selected for petrographic analysis or crushed for INAA. Nineteen samples were examined petrographically: tiles made in the laboratory from three local clays, five Chapel bricks and the Chapel tile, and 10 bricks and tiles from other historical sites. A total of 60 samples were used for neutron activation analysis.

Location	Number of samples
St. Mary's City (SMC), MD	16 bricks and 1 flat tile from Chapel 7 bricks from domestic and government buildings
Jamestown, VA	2 flat tiles, one *in-situ* in kiln 2 pantiles
Flower Dew Hundred, VA	1 flat tile
VA pottery kilns	2 kiln wasters
18th-c. England (spanished)	2 bricks
SMC clays and reproduction bricks	27 samples
Total:	**60 samples**

Table 1. Location and number of samples studied.

2.1. Petrographic Analysis

Thin sections of brick and fired clay samples were analyzed using a Nikon Optiphot-2 petrographic microscope. Inclusion size is described in terms of the Wentworth Scale, a standard method of characterizing particle sizes in sedimentology, and derived by measuring a series of ten grains using a graduated reticule built into one of the microscopes optics. The percentages of inclusions observed in the samples of clay and brick were estimated using standard comparative charts.

2.2. Instrumental Neutron Activation Analysis (INAA)

Approximately 200 mg of crushed brick was encapsulated and submitted for INAA at the University of Michigan's Ford Nuclear Reactor. The samples

were exposed to two separate irradiations: a 1-minute p-tube irradiation (at 2.1 x 10^{12} n/cm^2/s thermal) for elements with short half-life isotopes, and a 10-H core-face irradiation (with an average thermal neutron flux of 4.2 x 10^{12} n/cm^2/s) for elements with intermediate and long half-life isotopes; each was followed by two separate counts of gamma activity. Element concentrations were determined for 30 elements (Al, Ca, Ti, V, K, Mn, Na; As, Ba, La, Lu , Sm, U, Yb, Ce, Co, Cr, Cs, Eu, Fe, Hf, Nd, Rb, Sc, Sr, Ta, Tb, Th, Zn, Zr) based on comparison with three replicates of the SRM NIST1633A (coal fly ash), except for Ca, which was based on NIST688 (basalt rock).

2.3. SEM-EDS

Two thin sections from petrographic analysis were diamond polished, coated with carbon, and examined using the Hitachi S3200 SEM-EDS at the Electron Microprobe Analysis Laboratory at the University of Michigan.

3. RESULTS AND DISCUSSION

3.1. Petrography

The local clays (n=3) which were prepared as tiles were examined petrographically and displayed a strong bimodal distribution in the sand fraction, with approximately 25% silt-to-very-fine-sand rounded grains and 15% medium-coarse angular grains present. The mineral inclusions were mainly quartz and alkali feldspar with traces of biotite and quartzite. The Chapel bricks (n=6) were quite different, having instead a strong unimodal distribution in very-fine-sand to fine-sand fraction. Mineralogically, the inclusions were primarily subangular quartz grains and pedorelicts, described as redeposited indurated nodules of an older soil material. Voids within the Chapel bricks often displayed vitrified margins.

Ten other historic bricks and tiles were examined petrographically. All of the samples contained inclusions which were mainly quartz sand, often with traces of biotite. A brick sample from the Priest's House displayed the bimodal distribution of sands characteristic of the local clays. The St. Peter's brick sample contained pedorelicts, similar to the Chapel bricks. The Virginia tile and kiln waster samples were small, but most did display pedorelicts and very fine rounded sand grains. Two 18th-century bricks from England were examined because they were manufactured using the "Spanishing" technique, whereby debris and coal ash were added to the clay mixture before firing. These samples were included to compare known "Spanish" to the vitrified inclusions in the Chapel bricks. Not only were the inclusions quite different, but the London bricks contained significant quantities of sedimentary inclusions such as shale. This strongly indicates that the Chapel bricks were neither imports from London nor the result of the "Spanishing" process.

3.2. INAA

Petrography determined that the local clays contained large amounts of sand. Sand temper added to clay causes a dilution effect in the elemental concentrations measured by INAA. To determine the effect, bivariate plots of different element concentrations were made against aluminum as a proxy for clay content. For the local clays, most elements covaried with Al. The Chapel bricks, however, lacked the medium and coarse sand fractions and thus had higher overall concentrations of most elements. Significantly, a few key elements including Hf, Zr, and Ti in the Chapel bricks did not covary with Al (figure 1). As these elements are characteristic of heavy mineral sands (where Hf substitutes for Zr in zircons and Ti represents rutile), the negative correlation indicates that the Chapel bricks contain sands which are quite different from those that naturally occur in the local clays. This is indicative of a separate source for any added sand, or of a different clay source.

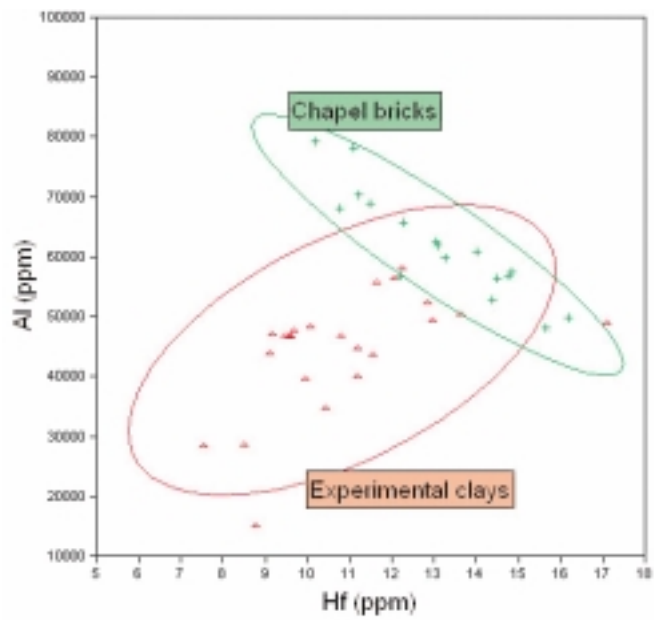

Figure 1. Bivariate plot showing that while Hf covaries with Al in the local St. Mary's clays, the Chapel bricks display a negative correlation between these elements.

Principal component analysis (PCA) illustrates overall trace elemental compositions between the Chapel bricks, local clays, and other historic brick samples (figure 2). Bricks from the Priest's House clearly fall into the local experimental clay grouping. The St. Peter's brick which was similar in

appearance and mineralogy to the Chapel bricks also groups with the Chapel based on chemical composition. The Virginia materials are quite diverse, as they represent flat tiles, pantiles, and pottery kiln wasters from different sites. This heterogeneity precludes making them a distinct group.

The Chapel bricks form a distinct population from the sampled local clays, with those from the State House and St. John's falling between compositionally. Based on the similarities in chemical and mineralogical composition, the Chapel bricks most closely resemble the comparative materials from Virginia. Importation from Jamestown could account for these similarities. However, trade between Maryland, a proprietary colony that was predominantly Catholic, and Virginia, a royal colony of Protestants, was expensive because of high tariffs and duties and unfriendly because of ideological differences. Nonetheless, chemical and geological similarities exist between the Chapel and Virginia building materials.

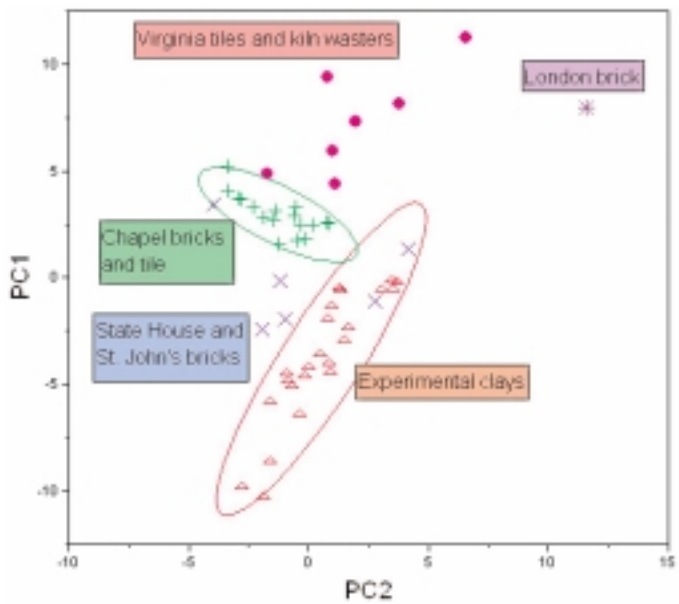

Figure 2. Principal component analysis showing relationships between chemical compositions of different brick, tile, and clay sources.

All of the clays sampled were from one geologic formation, the Quaternary Lowland deposit. These samples were selected based on archaeological evidence of brickmaking activity. As there are two other formations that are clay-bearing in the St. Mary's City area, and quite near the locations sampled, it is possible that the Chapel bricks and those from other St. Mary's City buildings were made from one of these other clay bodies or

some mixture. If the body from which the Chapel bricks were made is geologically of the same deposit as that used in Virginia, this could explain the similarities. This could also explain why the State House and St. John's bricks span the Chapel and local groups, if the clays from two bodies were combined either intentionally or inadvertently during excavation.

3.3. SEM-EDS

Two thin sections were examined using SEM-EDS to determine if the localized chemistry of the inclusions in the Chapel bricks would lead to major differences in the bulk composition. Brick #5 from the Chapel contained a soil pedorelict. The major difference in composition from brick matrix to pedorelict was in Fe, which increased markedly in the inclusion. The inclusions in Brick #13 were mostly black vitrified areas surrounding voids. The black vitrified margins were chemically similar to the bulk, but with a slightly higher concentration of Mg. Backscattered electron images showed small crystals of high-Z elements clustering at the void edge; these crystals were predominantly Fe and Al. These crystals probably formed through the action of a localized flux, such as K, Mg, or Na, during firing of the bricks.

4. CONCLUSIONS

Some of the bricks used at St. Mary's City, such as those used in the Priest's House, were clearly made using the local materials tested. However, the Chapel bricks do not resemble the tested locally available clays at St. Mary's City either chemically or mineralogically. Compared to 18th-century English bricks which were manufactured using the "Spanishing" process, the Chapel bricks do not appear to have been prepared in the same manner. The inclusions instead appear to be naturally occurring and similar in composition to the brick matrix. The chemical composition of the London brick is distinct from that of the Chapel bricks, indicating that they are highly unlikely to be bricks manufactured in England using the "Spanishing" process. The Chapel bricks were manufactured from a clay source either in Virginia or one in St. Mary's City that is geologically similar to one in Virginia but as yet untested.

ACKNOWLEDGEMENTS

Research funding was provided by DOE University Reactor Sharing Program and the Seller's Research Fund. Thanks to: T.P. Smith and I. Betts, Museum of London Specialist Services; F. Skomurski, E. Essene, and C. Henderson, Geosciences, and J. Halloran, Materials Science and Engineering, all University of Michigan; and geologists J. Reger (MD Geological Survey) and I. Armitage (Environmental Management, Inc.) for their input, advice, and samples.

AN INVESTIGATION OF THE CERAMIC TECHNOLOGY OF A LATE IZNIK CERAMIC PRODUCTION (XVIITH CENTURY AD)

Ayed Ben Amara, Max Schvoerer, Maïa Cuin
Centre de Recherche en Physique Appliquée à l'Archéologie, Université de Bordeaux 3/ CNRS (IRAMAT, UMR5060), Maison de l'Archéologie, 33607 - Pessac Cedex, France

Mohamed Baji Ben Mami
Institut National du Patrimoine, 4, Place du Château, Tunis, Tunisie.
Corresponding author: BEN AMARA A. (E-mail: ayed1@caramail.com)

1. AIMS OF THE RESEARCH

This paper describes the results of a physical study on a late Iznik ceramic production in order to investigate the ceramic technology of the 17th century Ottoman workshops. More particularly it will help to determine the specificity of a "red Iznik colour" dating from this time (Ben Amara, 2002). This colour made the originality of the Iznik ceramic workshops from the second half of the 16th century to the end of the 17th century. The first known examples of the "red Iznik colour" appeared around 1550 on the *mihrab* of Suleymanie mosque in Istanbul (Soustiel, 1985; Süslü, 1995; Altun, 1997).

Our main objective is the characterisation of the nature and composition of the different parts of the ceramic architectural ornaments. These quantitative data will help us to find technological processes used to produce these ceramics. Secondly, we will compare our data with bibliographical data relative to the first production (Tite, 1989).

2. MATERIALS

We have worked on four fragments of tiles presenting polychrome decoration (red, blue, green and black). These samples are of a late Iznik glazed production and decorate the walls of the Sidi Mehrez Mosque in Tunis, built by M'Hammed Bey in 1692. Bibliographical data (Daoulatli, 1979; Ben Mami, 2000) tell us these tiles were an ottoman production and were imported from Iznik workshops. Actually, Tunisia was an Ottoman province as early as 1574. Iznik (ancient Nicaea) is a town located on the main trade

routes linking Middle East to Balkans through Anatolia since the 4th century AD. Its name is synonymous with the brilliant period of ceramic production during the Ottoman era.

3. METHODOLOGIES

The description of the texture was carried out with scanning electron microscopy (SEM). Observations under scanning electron microscopy (JEOL JSM 820) were carried out on a thick blade detached by sawing, perpendicularly to the surface of the sample.

The elementary composition of the various layers was determined by energy-dispersive X-ray spectrometry with the system Link AN10000, coupled with the SEM. The analysis was made on five distinct zones of about 1.08 µm x 0.88 µm for the ceramic support and of 108 µm x 88 µm for the glazes and decoration. In accordance with the use, contents are expressed in percentage of weight of oxides.

Crystalline phases were identified by X-rays diffraction. We used a powder diffractometer (Siemens, Krystalloflex D500 with copper anticathode); the explored angular range was between 5° and 60° (for 2σ) and the lines of the diffractograms obtained were allotted by comparison with the A.S.T.M. (American Society for Testing and Materials) reference card.

Raman spectrometry analysis was used for a more precise characterisation of the "red Iznik colour", with the help of Dr. Pham V Huong (Laboratory of Molecular Physicochemistry, CNRS-University of Bordeaux 1). The spectra were determined by micro-Raman spectrometry (Dilor, model LABRAM) using 514.5 nm and 632.8 nm laser emission. The energy of the laser was always maintained very weak (lower than 10mW) to avoid any deterioration of the dyes. The spectra resolution was about 1nm.

4. EXPERIMENTAL DATA AND RESULTS

4.1. Texture and elementary composition

The ceramic material is made up of various layers: a pink-beige ceramic body on which is applied a white slip, used as a background for the decoration, and recovered by a transparent glaze. A SEM photomicrograph (fig. 1) of a section through a red-painted region shows (from top to bottom) the different parts of this complex material:

1. The transparent glaze, which thickness varies between 200 and 250 µm, covers the entire surface. It is a lead glaze (46.2 - 53.5% PbO). The sodium and potassium contents are relatively weak: 3.6 to 4.5 % Na_2O and lower than 0.6 % K_2O. This glaze is slightly coloured in green with copper Cu^{2+} (about 0.3 % CuO).

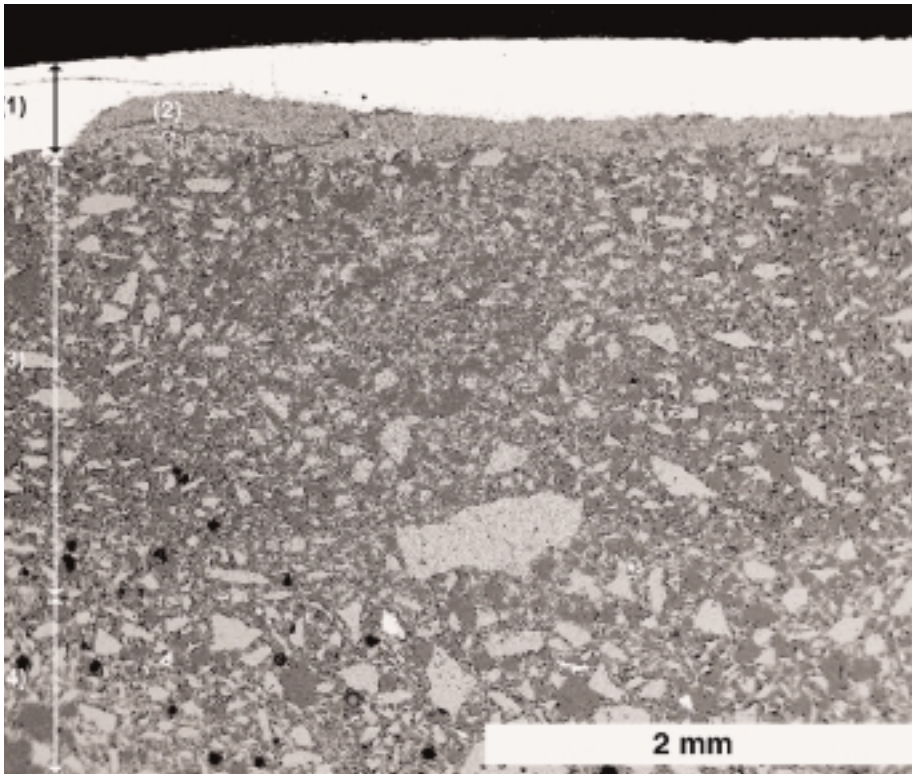

Figure 1. A SEM photomicrograph (BSE image) of a section through a red-painted region, showing (from top to bottom), the transparent glaze (1), the "red Iznik colour" (2), the white slip (3) and the ceramic body (4).

2. The "red Iznik colour" is very rich in silicon (71.3 – 81.4% SiO_2) and also contains iron (5.6 - 8.1% Fe_2O_3). We have detected also aluminium (3.9 - 5.3% Al_2O_3), lead (1.6 - 5.7% PbO), sodium (2.5 - 2.9% Na_2O) and calcium (1.8 - 2.9% in CaO). The presence of these elements could be due to the penetration of the glaze in "red Iznik colour". Analysis by X-ray diffraction shows the presence of quartz (SiO_2) and hematite (Fe_2O_3).

3. The white slip is very rich in silicon (89.5 - 92.7% SiO_2) and the analysis by X-ray diffraction only reveals the presence of quartz. Other elements are present in small quantity, mainly calcium (1.9 - 2.8% CaO), aluminium (1.6 - 1.7% Al_2O_3), iron (0.7 - 1.4% Fe_2O_3), sodium (0.7 - 1.1% Na_2O) and magnesium (0.8 - 0.9 % MgO).

4. The elementary composition of the ceramic body is relatively close to that of the slip: 96.5 - 93.2 % SiO_2, 1.7 - 1.3% Al_2O_3, 0.6% Fe_2O_3 and 1.0 - 0.9 % MgO.

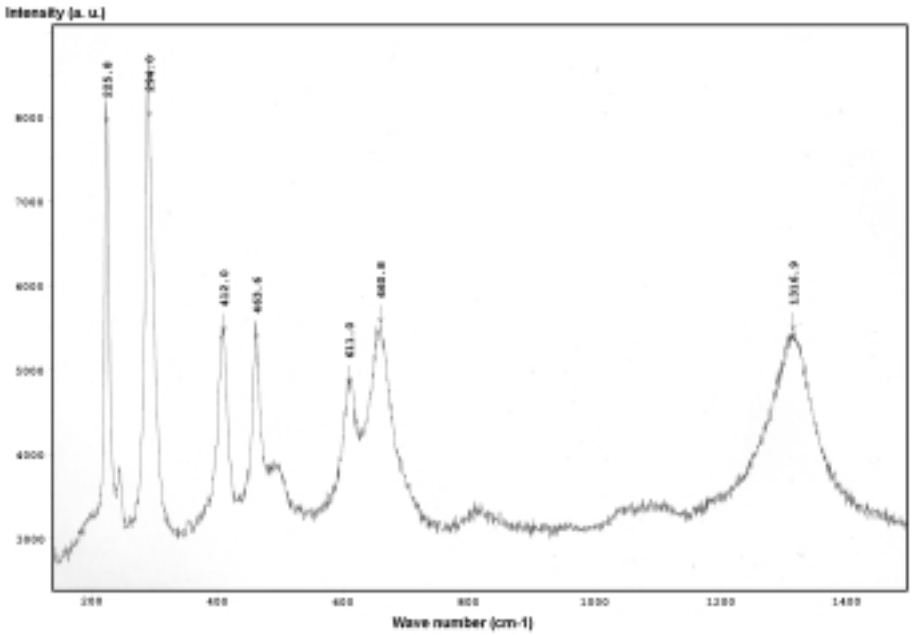

Figure 2. Raman spectrum of red grain present in the red decoration. The line at 463.6 cm^{-1} is specific of quartz. The others lines correspond to hematite (Fe_2O_3).

We note that the red decoration is different from the first Iznik production. Actually, it tends to be brown-red coloured. This colour is composed of differently coloured grains (red, black and orange). The analysis carried out on red grains gave a Raman spectrum (fig. 2) which one could assign to hematite (Edwards and Tait, 1998). Among the identified Raman lines, it is necessary to note the presence of another line at 463.6 cm^{-1}, independent of the hematite, which we identified as being quartz. The relative intensity of this line is variable and seems to be correlated to the colour of the analyzed grain. When the red grain is clearer, the line of quartz is more intense. This makes us consider the use of ferruginous sand. The presence of small black grains in the red colour, identified by Raman spectrometry as amorphous carbon (fig. 3), contributes to darken the colour of the red decoration.

The other colours of decoration are:

Blue: The elementary composition of the blue-painted region is close to that of the transparent glaze. The blue decoration is obtained with a cobalt dye.

Green: The elementary composition of the green-painted area is also close to that of the transparent glaze. One notices the presence of copper (Cu^{2+}) in greater proportion in this region (2.1 - 0.7% CuO) compared to the transparent glaze (about 0.3% CuO).

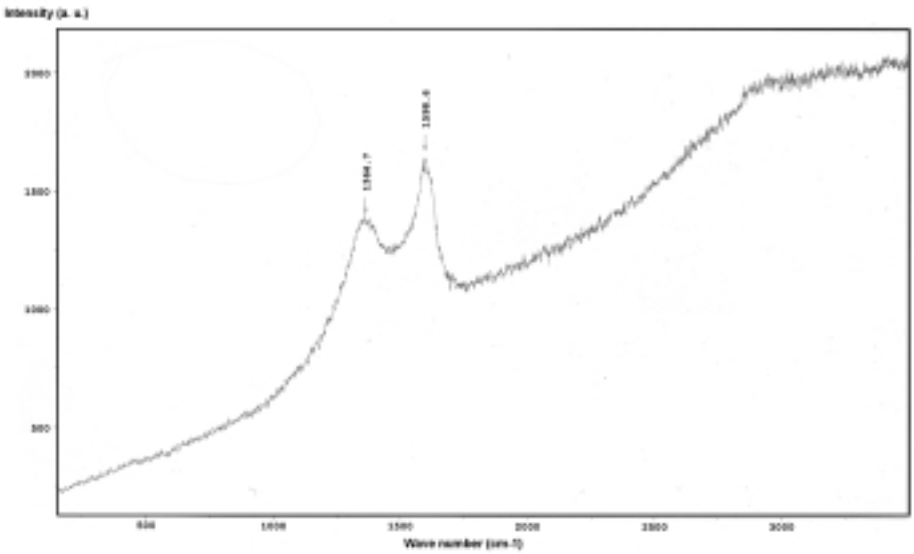

Figure 3. Raman spectrum of black grain present in the red decoration. We note two wide lines at 1364.7 and 1598.6 cm^{-1} characteristic of amorphous carbon (David *et al.*, 2001).

Black: It was carried out using a material made up of quartz and chromites. Copper is not a component of chromites [$(Fe, Mg)(Cr, Al, Fe)_2O_4$]. Its presence in the crystals would be due to the aptitude of chromites for capturing copper present in the transparent glaze (Tite, 1989).

4.2. Comparison with the first Iznik production

The comparison of these results with bibliographical data relative to the first productions (Tite, 1989) shows some differences which could be at the origin of the decline of this ceramics:

— The transparent glaze is a lead glaze whereas it was lead-soda glaze in the first productions (20 - 40% PbO).

— The amount of clay and soda-lead frit is more important in the first production.

— Concerning the "red Iznik colour", the first production was made of iron-rich quartz-frit mixture whereas the late Iznik production was made with ferruginous sand.

5. CONCLUSION

The physical-chemical properties of the various parts of this complex material were determined.

The Raman spectrometry analysis proves that the studied "red Iznik colour" is composed of ferruginous sand and amorphous carbon. This is completely different from the famous red Iznik colour of the first production.

The comparison of our results with the first Iznik production shows many differences which can explain the "technological decline" of the late production. The main difference is the nature of the glaze. That "choice" supposes the change of firing conditions, glaze viscosity and preparation mode of the glazing mixture.

REFERENCES

Altun, A. (1997) *The story of ottoman tiles and ceramics*, Istanbul Stock Exchange.

Ben Amara, A. (2002) *Céramiques glaçurées de l'espace méditerranéen (IX^e – XVII^e siècles): matériaux, techniques et altération* (in Fr.), Ph.D Physic Thesis in archaeomaterials, Université de Bordeaux 3, 121-144.

Ben Mami, M.B. (2000) La Mosquée M'Hammed Bey - Un exemple de la présence architecturale et artistique ottomane dans la médina de Tunis, *Africa*, 12, 1-22.

David, A.R., Edwards, H.G.M., Farwell, D.W., De Faria, D.L.A. (2001) Raman spectroscopic analysis of ancient Egyptian pigments, *Archaeometry*, 43, 4, 461-473.

Edwards, H.G.M., Tait, J.F.K. (1998) FT-Raman spectroscopic study of decorated stained glass, *Applied Spectroscopy*, 52, 5, 679-682.

Soustiel, J. (1985) *La céramique islamique*, Office du livre, Fribourg, 309-344.

Süslü, Ö. (1995) The first examples of red coloured underglazed ottoman ceramics of the XVI^th century, *Ceramics in Architecture*, 395-402.

Tite, M.S. (1989) Iznik pottery: an investigation of the methods of production, *Archaeometry*, 31, 2, 115-132.

INTERACTION BETWEEN LEADS GLAZES AND BODIES: RESEARCH ON THE MODE OF APPLICATION OF THE GLAZING MIXTURE

Ayed Ben Amara, Max Schvoerer
Centre de Recherche en Physique Appliquée à l'Archéologie (CRPAA), Université de Bordeaux 3/CNRS (IRAMAT, UMR5060), Maison de l'Archéologie, 33607 - Pessac Cedex, France.
Corresponding author: BEN AMARA A. (E-mail: ayed1@caramail.com)

1. INTRODUCTION

Concerning the techniques of manufacture of glazed ceramics, historians of the techniques and archaeologists often wonder about number of firing:

— The use of a double firing (application of the glazing mixture on fired body).

— The use of a single firing (application of the glazing mixture on unfired body).

In order to find an answer to that question, we carried out experiments of replication of high-lead glazes on unfired or fired bodies. Our objective is to find analytical criteria relative to the glaze-body interaction to distinguish the different mode of application of glazing mixtures.

In Bordeaux, the interest of the laboratory of CRPAA in the glaze-body interaction started at the end of the 1970's. In 1977, the study of medieval ornemental tiles of Aquitaine (France) by cathodoluminescence revealed the presence of a blue luminescence at the glaze-body interface. In 1987, finer observation associating cathodoluminescence with scanning electron microscopy showed that the blue luminescence was due to small crystals (Müller, 1988). Later, studies by X-ray fluorescence and X-ray diffraction specified that these crystals were K-Pb feldspar crystallites (Schvoerer *et al.*, 1991). Other teams (Barcelona, Oxford…) had done many works about this subject. Molera *et al.* (2001) note that the glaze-body interaction consists of a *digestion/diffusion process* which involves:

— The decomposition of the phases forming the clay body.

— The chemical diffusion of elements between the lead glaze and the clay body.

— The formation of a layer (interface between the glaze and the body) of small K-Pb feldspar crystallites.

We also know that the interaction depends on many parameters: the clay composition, the glaze mixture composition, the use of a single or a double firing, the firing conditions (thermal path, T° max…) (Tite *et al*., 1998).

2. MATERIALS AND METHODS

The study of the interface glaze/body was carried out with the binocular magnifying glass, by cathodoluminescence and scanning electron microscopy (JEOL JSM 820). In order to determine the importance of the elements diffusion between glaze and clay bodies, chemical profiles were done on cross sections. More than 100 points of EDXS analysis (Link AN10000 system) every 5 μm were plotted from the glaze to the body.

For the preparation of glazed ceramic, we chose different parameters:

— We used two different glazing mixtures: a high lead glaze with sodium (60% PbO, 25% SiO_2, 5% Al_2O_3 and 10% Na_2O) and one without sodium (70% PbO, 25% SiO_2 and 5% Al_2O_3) to evaluate the sodium effect on high-lead-content glaze.

— We used two different clay bodies: an illitic-kaolinitic noncalcareous clay (1.5 % CaO) and the same clay mixed with 25% of calcium carbonate powder ($CaCO_3$). In this paper the results relative to calcareous bodies only are presented (for the other case, see Ben Amara, 2002).

— We used two different thermal paths (electric kiln): a thermal path with one firing stage (heating and cooling rates: 100°C/h, temp. of plateau: 950°C, cooling time: 9.25 h) and one with three firing stages (heating and cooling rates: 100°C/h, temp. of plateau: 950, 850 and 750°C, cooling time: 11.25 h). The cooling time was more important in the second case.

Glazes were prepared in the laboratory by mixing pure analytical powders (PbS, SiO_2, Al_2O_3 and Na_2CO_3). They were applied in a water suspension on ceramic body by brushing.

3. EXPERIMENTAL DATA AND RESULTS

3.1. Study of the texture of the glaze-body interface by SEM and cathodoluminescence

In all cases, we note the presence of crystals in the glaze-body interface. They were identified as K-Pb feldspar crystallites (with low content of calcium) or wollastonite crystals ($CaSiO_3$). We observed that glaze-body interface did not only correspond to the lower part of the glaze (rich in

crystals) but also to the higher part of fired body in which we also found crystals. The evaluation by scanning electron microscopy of the size of the interaction area in the body is difficult by BSE image but easier by X-ray mapping. This study shows that cathodoluminescence is a quick method to determine the thickness of the glaze-body interface. Actually, at the interface, the luminescence area corresponds to the interface thickness (the lower part of the glaze and higher part of fired body).

With the exception of two samples, which present a weak glaze-body interaction, table 1 shows that the thickness of the glaze-body interface is more important when:

— The glazing mixture is applied on unfired body.

— The glazing mixture contains sodium.

— The thermal path has three firing stages (low cooling).

		Thermal path with one firing stage	Thermal path with three firing stages
glazing mixture with sodium	Unfired body	120 μm	450 μm
	Fired body	80 μm	300 μm
glazing mixture without sodium	Unfired body	20 μm	40 μm
	Fired body	20 μm	20 μm

Table 1. The thickness of the glaze-body interface in the case of calcareous bodies.

3.2. Chemical diffusion between lead and clay bodies

The chemical profiles of lead diffusion (fig. 1) also permit an easy determination of interface thickness. In this area the lead content is very variable because of the presence of K-Pb feldspar crystallites. We noted that the

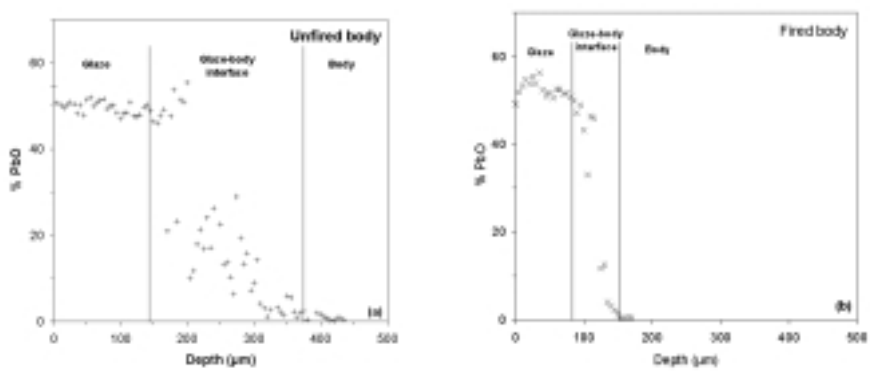

Figure 1. Chemical profiles of lead diffusion plotted from the glaze to the body for two unfired (a) and fired body (b). The other parameters are glazing mixture with sodium and thermal path with three firing stages.

interface thickness is more important when the glazing mixture is applied on unfired body. The diffusion profiles of silicon (fig. 2a) and aluminium (fig. 2b) correspond only to the glaze area. As a result of the diffusion of Si and Al from body into glaze, these elements contents are higher than in the initial glazing mixture composition (70% PbO, 25% SiO_2 and 5% Al_2O_3). Near the interface, we noted that the elements diffusion is more important in the case of unfired body. However, near the surface of the glaze, elements contents are very similar.

Lead diffuses differently from aluminium and silicon (fig. 2c). Lead diffuses from the "glaze" into the body. The lead-glaze-content (between 50 and 63% PbO) is lower compared to the initial glazing mixture (70% PbO). Near the interface, in the case of unfired body, the lead content is lower so its diffusion into the body is more important. We showed a higher body decomposition that

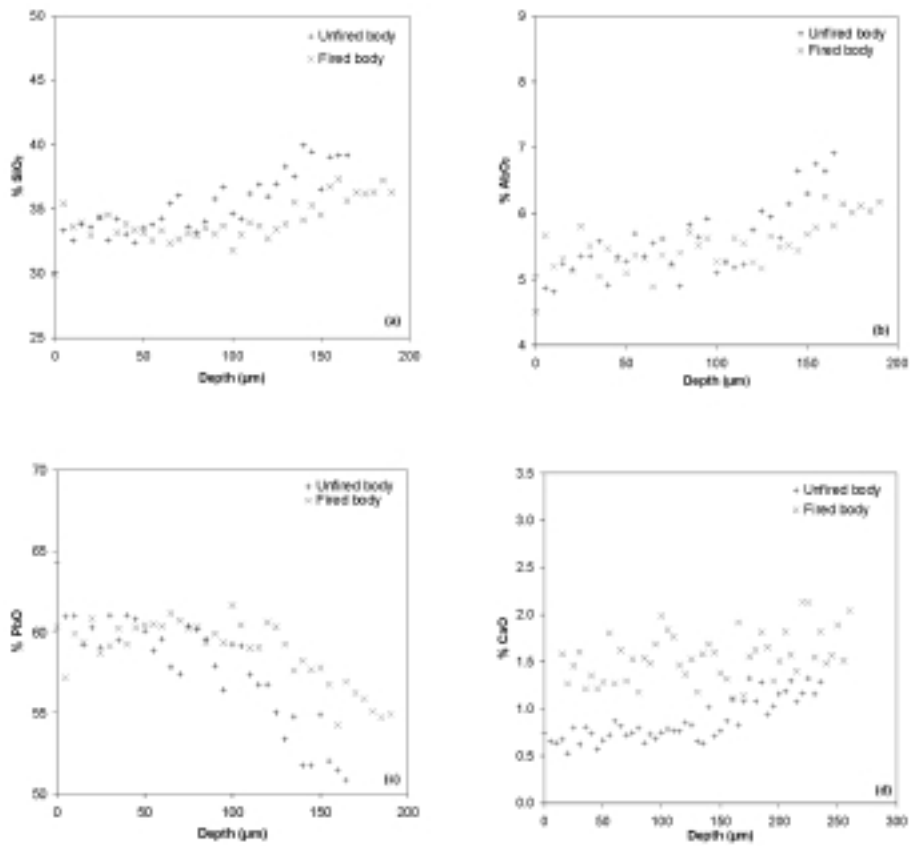

Figure. 2. Diffusion profiles of silicon (a), aluminium (b), lead (c) and calcium (d) only in the glaze area (from the glaze surface to the interface. For these samples, glazing mixture composition is: 60% Pb0, 25% SiO_2, 5% Al_2O_3 and 10% Na_2O and the glazes were fired with a thermal path with three firing stages.

explains the increase of interface thickness. the addition of sodium in glazing mixture increases the calcium diffusion from the body into the glaze, the calcium profiles are plotted only in the case of application of glazing mixture with sodium (fig. 2d). In the other case, the calcium content is too low (<0.3 %). The calcium content is less important in the case of unfired body. In fact calcium is involved essentially in the formation of wollastonite crystals at the interface.

5. CONCLUSION

Observations carried out at the glaze-body interface by cathodoluminescence and scanning electron microscopy did not allow us to determine with no doubt if the glazing mixture was applied on fired or unfired bodies. Nevertheless, we noted that the interaction is often increased by unfired bodies. Thus, the presence of an important interface zone may indicate the application of the glazing mixture on an unfired body. It was shown that a slower cooling or modification of the glazing mixture could generate an important interface zone. It was shown that some crystals are always present at the interface, independently from the nature of the bodies (fired or unfired).

In addition, this study highlights the following points:

— The cathodoluminescence allows to observe and especially to evaluate the interface thickness.

— The addition of sodium, in the carbonate form, in a lead glazing mixture increases the process of decomposition/diffusion between glaze and body and so the thickness of the glaze-body interface. A slower cooling also increases this thickness.

— The glaze composition is influenced by the elements diffusion between the glaze and its support, particularly lead and silicon. Nevertheless, the elements diffusion is not always more important in the case of unfired bodies.

REFERENCES

Ben Amara, A. (2002) *Céramiques glaçurées de l'espace méditerranéen (IX^e – XVII^e siècles): matériaux, techniques et altération* (in Fr.), Ph.D Physic Thesis in archaeomaterials, Université de Bordeaux 3, 121-144.

Molera, J., Pradell, T., Salvadó, N., Vendrell-Saz, M. (2001) Interactions between clay bodies and lead glazes, *J. Am. Ceram. Soc.*, 84, 5, 1120-28.

Müller, P. (1988) *Luminescence thermostimulée de verres silicatés. Application aux verres nucléaires et archéologiques* (in Fr.), Ph.D Thesis, Université de Bordeaux 3.

Schvoerer, M., Raffaillac-Desfosse, C., Bechtel, F., Ney, C., Chapoulie, R. (1991) Détection grâce à leur luminescence, de cristaux de dévitrification dans des

glaçures médiévales: implications technologiques, *European Workshop*, Université de Roma - La Sapienza, 10-12 oct. 1991, 323-342.

Tite, M.S., Freestone, I., Mason, R., Molera, J., Vendrell-Saz, M., Wood, N. (1998) Lead glazes in antiquity - Methods of production and reasons for use, *Archaeometry*, 40, 2, 241-260.

TRADE PATTERNS IN PHILISTINE POTTERY

David Ben-Shlomo
The Institute of Archaeology, The Hebrew University, Jerusalem
davben@h2.hum.huji.ac.il

1. INTRODUCTION

Philistine pottery is one of the main components of the new material culture brought to the southern coastal region of Israel (Philistia) by immigrants from the Aegean region and Cyprus. This pottery is most common in the main philistine cities: Ashdod, Ashkelon, Ekron and Gath, appears to a lesser extent in other regional sites and rare in sites outside Philistia (Dothan 1982; Dothan and Zukerman 2004). The Philistine pottery shows three major development stages: the earliest is the Monochrome style, then comes the Bichrome style (both appear in the Iron Age I, 12th –11th centuries BCE) and the third stage, during the Iron Age II, is of red-slipped late Philistine pottery. The early stages of this pottery show high resemblance in form, decoration and technology to contemporary Mycenaean wares from the Aegean and Cyprus. During the subsequent period, the 10th-9th centuries BCE, there is a decline in the Aegean character of the Philistine material culture, but a distinct type of decorated pottery in Philistia, defined as 'Late Philistine Decorated Ware' (also termed 'Ashdod Ware'), still appears (Ben-Shlomo et al. 2004).

Previous NAA and petrographic studies showed the Iron I Philistine pottery to be locally made in Philistia (Gunneweg et al. 1986; Killebrew 1998). Moreover, several of the wares indicated specified technological aspects of clay selection and treatment. Killebrew especially showed this in her petrographic and stylistic study of Monochrome pottery from Ekron (1999). Hence, it was clear that the Philistine pottery represents, at least in the early stages, pottery made in Philistia by potters with some Aegean technological skills. The main aim of this research was to try and find regional patterns in the manufacture and trade of this pottery by comparing Philistine pottery from all four excavated Philistine cities; the question was whether more specified production centers of this pottery could be identified. Moreover, the later Iron II Philistine pottery was to be similarly studied in order to compare it with the earlier wares.

2. METHOD

This study employed a combination of several disciplines and methods: the archaeological data and distribution of pottery as well as the archaeological remains of Iron Age pottery production in Philistia were examined. An archaeometric study of the pottery included new chemical and petrographic analysis together with the examination of all earlier studies.

The archaeometric analyses included 315 vessels analyzed by thin section petrography of these 225 samples chemically analyzed by ICP-AES and ICP-MS. The samples came from 25 different sites, although the majority are from the Philistine cities (Ashdod, Ekron, Gath and Ashkelon). About 30% of the samples are considered as reference material including clay samples, vessels from kilns at Ekron (Iron I), Ashdod (Iron II) and a site near Gath (Iron II); coarse ware and undecorated common types were also included.

The chemical analysis, ICP-MS and ICP-AES, was undertaken at the Earth Sciences Department of the University of Bristol, and was made possible by the European Commission Program for Access to Research Infrastructures (Contract No. HPRI-1999-CT-00008). The samples were dissolved in acid and composition of up to 40 elements was obtained: the major and minor elements were obtained by ICP-AES, while trace and rare earth elements were obtained by ICP-MS. The output was calibrated by international rock standards and synthetic standards for some of the elements in the ICP-MS runs. The main grouping procedure included values of 26 well acquired elements, which were free of contamination and dilution effects. The log transformed data were treated by hierarchical cluster analysis using Euclidean distance; in a second stage outliers were excluded. Principal Component and discriminant analyses were conducted as well with the same data set.

3. RESULTS AND DISCUSSION

As a result of the examination of Philistine pottery from all excavated sites a distinct sub-ware was defined as *fine* Monochrome with a much lighter colored and highly levigated clay. This sub-ware was most common at Ekron, rarer at Ashdod and absent at Ashkelon. The Bichrome pottery was more homogenous in its appearance and had a wider geographical distribution; the Late Philistine pottery was less common in the relevant assemblages, abundant only at Ashdod and Gath.

The region under investigation is relatively small, and most distances between sites are less than 20 km. The geology of this region illustrates several aspects: the coastal strip of about 10-15 km is relatively homogenous and covered with alluvial brown soil, sand dunes and kurkar ridges. The southern part of this coast yields more *loess* type soil, containing wind-blown

sand and sediments coming from the southeastern Mediterranean together with alluvial brown soil. The eastern part of Philistia is termed as the inner plains. Its western part lies still on the same alluvial soil but its eastern part shows a change in the geological formation exposing carbonatic Eocene formations with chalk and limestone. Several rivers, some adjacent to the Philistine sites, carry clays from the inner plains to the coastal area making the situation more complicated, though the coastal soils should still be characterized by beach sand and less calcareous inclusions.

The vast majority of the samples were represented by five petrographic groups with several subgroups therein. All of these fabrics represent clay which could be found in the region of Philistia. The largest group was of a fabric representing a porous alluvial, optically inactive clay matrix with a high quantity of quartz inclusions and hardly anything else. This group could be further subdivided into two subgroups, mostly according to the texture of the quartz inclusions and the frequency of various calcite inclusions (limestone and chalk): A. A bimodal texture of quartz with rounded sand sized and angular silt sized inclusions and hardly any calcareous inclusions, tentatively assigned to a coastal origin (Group A1, fig. 1). B. No bimodal texture and quite more calcareous inclusions, identified as having an inland provenance. Another petrographic group represents clay made of *loess* soil, identified by its silty carbonatic matrix; this soil is present in southern coastal Israel though appearing in more inland locations as well. The bimodal quartz, however, suggests a coastal origin.

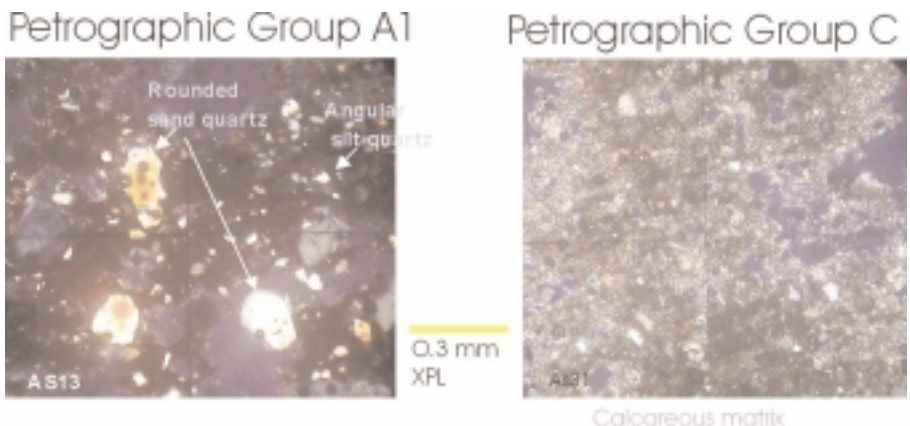

Figure 1. Thin sections of pottery sherds from Petrographic Groups A1 and C.

A clearly different petrographic group contains a silty calcareous matrix and a high proportion of chalk and limestone inclusions (Group C, fig. 1). A subgroup has a large component of rounded foraminifferous inclusions representing worn chalk. This fabric represents a well levigated clay possibly

originating from the Eocene Maresha and/or Adulam formations which have outcrops less that two km from both Ekron and Gath. The fabric is similar to Killebrew's Miqne-A1 fabric (Killebrew 1999:199-202), though the exact clay source was not identified.

The initial chemical grouping yielded four general groups: 1. A major group of 138 samples including most of the reference material from Philistia; this group had a spread (CV) of around 15% from the mean value in most elements; 2. A high Calcium group (43 samples, Groups 4A+4B); 3. A group with a slightly different composition than the main group, probably representing other clay profiles from southern Israel (26 samples); 4. Eighteen outliers that did not fall in the main groups. Thus, in the preliminary grouping most Philistine pottery made in Philistine cities was grouped together, which is not surprising given the small region and geological homogeneity. The high calcium group (Chemical Group 4A+4B) included mostly the fine Philistine Monochrome vessels as well as reference samples from Ekron. It also virtually overlapped petrographic Group C. Therefore, it is implied that the fine Philistine Monochrome pottery had distinct technological features, was manufactured at Ekron and was exported to other Philistine cities (especially to Ashdod). Furthermore, this clay recipe was hardly used later on in the Iron II period. It seems that this clay had a natural high calcite value, and to a lesser extent illustrated intentional tempering of calcite inclusions. Tracing this profile to Ekron conforms to the archaeological data well.

In order to refine the grouping further sub-grouping was made within the major Chemical Group A. This yielded four subgroups (termed here Chemical Groups 1, 2, 3, and 5; see table 1 and fig. 2); these groups were more compact in their composition, and most elements had a spread (CV%) of 5-10% of the mean values. According to the reference material and the

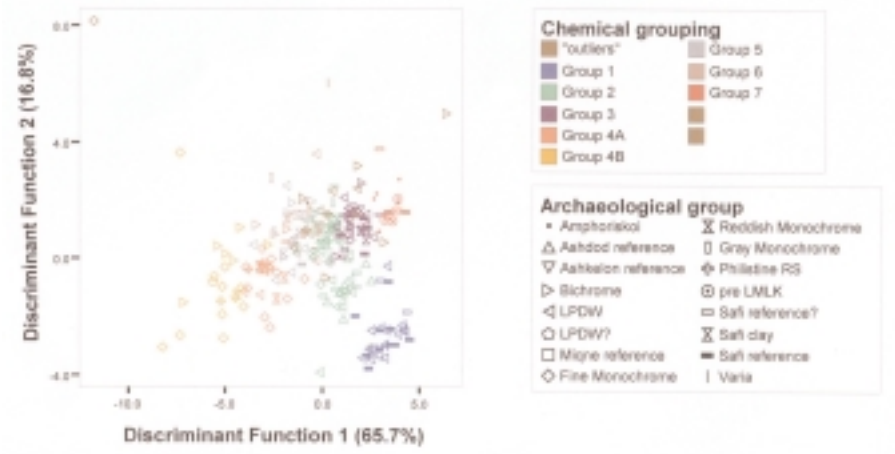

Figure 2. Scatter plot of two major discriminant functions of ICP data set according to chemical grouping and archaeological groups.

petrographic features of the respective samples, two groups were tentatively assigned to the coastal region of Philistia: Groups 2 and 5; Group 2 represents Ashdod and Group 5 possibly represents Ashkelon. Two other groups, 1 and 3 were assigned to the inner plains of Philistia, probably originating from the region of Gath. The high calcium group was also sub divided into Groups 4A and 4B, the latter with a higher calcium value reaching a mean of above 18%. Two other chemical subgroups, 6 and 7, possibly represent clay from southern Israel though not enough reference material from the sites was analyzed to achieve better provenancing. Several of the outliers group together; these are mostly vessels from northern Israel; the petrographic analysis shows these vessels to be produced in the north as well. Other outliers may represent various clay recipes not fitting any group but still local to Philistia, or imported vessels.

	Group 1		Group 2		Group 3		Group 5		Group 4A		Group 4B	
Element (ppm)	Mean (27 samples)	CV%	Mean (59)	CV%	Mean (32)	CV%	Mean (20)	CV%	Mean (23)	CV%	Mean (20)	CV%
Al(%)	6.01	5.8	5.50	5.5	5.85	5.8	5.06	9.4	4.12	6.2	3.33	10.0
Fe(%)	4.55	7.2	3.91	7.4	4.18	7.5	3.55	11.6	2.86	7.0	2.25	9.3
Ca(%)	5.17	43.4	5.87	39.1	5.93	30.1	4.44	37.1	13.09	29.5	18.08	27.9
Ti(%)	0.64	8.0	0.60	8.8	0.65	10.8	0.59	12.0	0.43	9.9	0.34	14.4
K(%)	1.14	16.5	1.29	16.3	1.37	21.3	1.40	21.9	1.33	22.2	1.37	20.5
Na(%)	0.65	18.4	0.61	11.4	0.68	24.9	0.59	14.3	0.45	20.1	0.35	24.7
Co	18.36	8.2	18.39	11.6	20.77	10.2	17.87	12.3	12.32	12.5	9.30	21.7
Cr	90.21	8.3	89.33	12.9	99.80	8.7	86.50	14.4	76.17	7.8	67.93	14.1
Mn	741	8.7	729	15.6	814	10.4	662	10.8	507	13.4	401	23.5
Sr	318.6	19.3	296.8	24.9	314.1	18.8	272.4	17.3	412.2	20.0	434.8	27.6
V	118.6	10.1	103.3	20.3	101.5	8.5	85.6	10.9	70.6	11.8	63.9	14.7
La	30.6	5.9	27.9	6.7	31.0	6.9	24.1	8.1	24.4	7.5	21.2	8.2
Ce	63.7	4.9	57.8	5.5	64.0	6.7	52.6	7.1	46.4	7.5	39.2	7.5
Pr	7.28	6.1	6.77	4.9	7.54	5.0	6.03	7.7	5.55	6.8	4.89	6.9
Nd	29.35	6.1	26.80	4.5	29.66	4.3	23.16	8.3	21.69	6.1	19.10	7.5
Eu	1.44	5.8	1.33	6.1	1.46	6.2	1.12	10.3	1.13	9.01	0.94	9.55
Sm	6.27	5.8	5.57	5.4	6.11	5.1	4.78	8.5	4.58	6.87	3.97	9.38
Tb	0.78	7.7	0.70	5.8	0.76	6.1	0.58	9.9	0.58	6.79	0.51	9.14
Gd	5.14	6.5	4.75	5.1	5.24	5.1	3.97	9.7	3.97	4.87	3.47	8.81
Dy	4.36	8.1	3.98	5.6	4.42	4.9	3.31	9.6	3.46	5.75	3.01	8.54
Ho	0.85	8.5	0.75	5.3	0.83	6.2	0.63	9.3	0.63	7.49	0.57	9.28
Er	2.34	10.0	2.08	5.7	2.29	6.8	1.72	8.4	1.80	6.98	1.61	9.43
Tm	0.33	8.5	0.31	7.8	0.36	11.5	0.29	12.0	0.27	10.00	0.26	10.41
Yb	2.10	9.9	1.90	5.1	2.13	7.7	1.64	8.1	1.71	7.04	1.52	9.51
Lu	0.31	9.1	0.28	6.9	0.31	9.7	0.24	8.5	0.24	7.99	0.22	10.38
Y	20.74	14.9	21.03	13.9	24.81	10.3	18.52	7.5	21.50	8.10	19.12	12.04
Hf	4.64	8.8	2.85	15.1	2.88	8.8	2.41	15.5	2.21	8.82	1.70	15.40
Ta	1.85	11.4	1.16	11.1	1.34	10.1	1.04	26.3	0.84	13.66	0.63	21.99

Table 1. Means and standard deviation, as percentage of mean, of Chemical Groups 1-5.

Although compositional differences in many elements between the subgroups were not large, one can see distinct differences in more specific elements; for example: in Samarium and Tantalum between Groups 1, 2, 3 and 5. Discriminant analysis shows Groups 1 and 2 to be especially well defined (fig. 2). It should be stressed, however, that the sub-grouping is tentative, and used as a starting point for further research and analysis. Moreover, it is more difficult to distinguish either petrographically or chemically between the coastal or inland cities themselves: that is between Ashdod and Ashkelon or between Ekron and Gath, which are only nine km apart. If the petrographic conclusions are plotted against chemical ones about 90% of decisively designated samples have agreeing results (fig. 3), possibly substantiating the suggested provenancing.

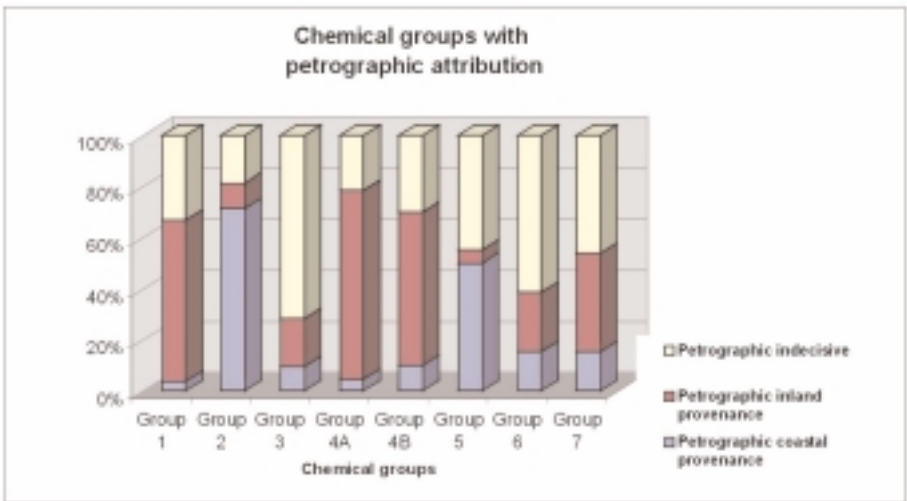

Figure 3. Comparison between the chemical groups and the proposed provenance according to petrography.

The conclusions from the tentative provenancing could have implications both on typological aspects and the trade patterns of the pottery studied. The Late Philistine pottery, studied in detail for the first time with up to 106 samples analyzed, seemed to have been produced in Philistia with possibly two production centers: Chemical Group 2 of an Ashdod provenance and Groups 1 and 3 from an inland provenance of Gath and/or Ekron. Generally, this pottery is made of silty alluvial soil with rather consistent composition.

4. TRADE PATTERNS

During the Iron I a distinct sub type of Philistine Monochrome pottery, defined here as fine ware, was produced in Ekron. It seems that the workshop

at Ekron specialized in this sub ware, which has the highest resemblance to Mycenaean pottery, and exported it to the other Philistine sites, especially to Ashdod. Other sub wares of Philistine Monochrome pottery were produced locally by each of the Philistine cities. Philistine Bichrome pottery was also usually supplied by local workshops though some cases of trade between the coastal and inland cities do occur. Pottery similar to Philistine pottery in northern Israel was not imported from Philistia in most cases, although more research is needed on this issue. During the Iron II there seems to be a somewhat opposite trend in the trade of Philistine pottery (fig. 4). There are no imports of Late Philistine pottery made in inland Philistia at the coastal Philistines cities. On the other hand several Late Philistine vessels from Gath and quite a few from Ekron are seemingly imported from the coast. Nevertheless, each Philistine city produced this pottery locally as well. Sites

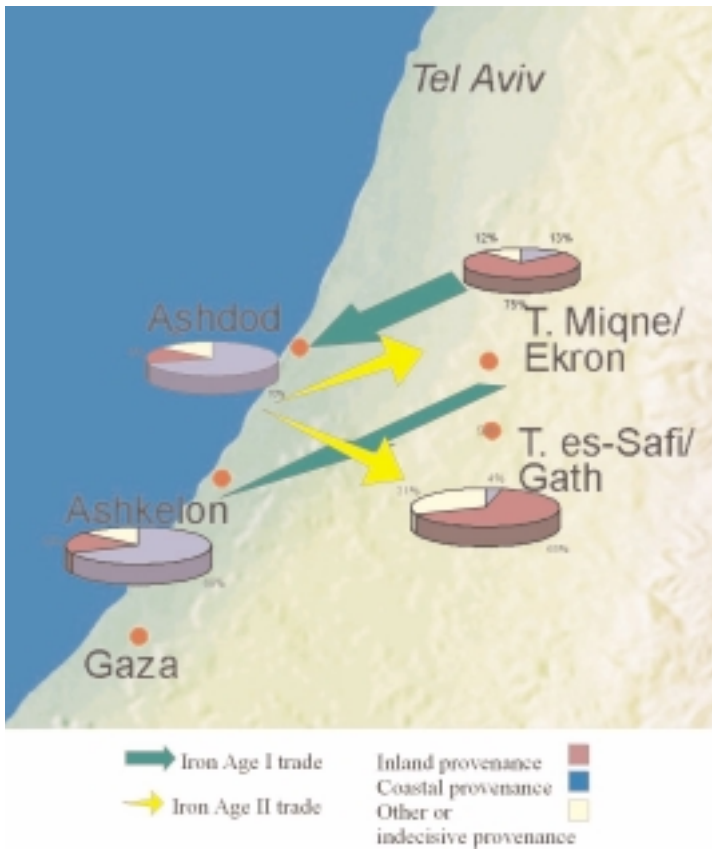

Figure 4. Proposed trade patterns of Philistine pottery between the Philistine cities during the Iron Age.

other than the four Philistine cities often imported this pottery from either coastal or inner Philistia production centers.

These intra-regional trade patterns of Philistine pottery should be seen in the perspective of other archaeological and historical evidence we have on the Philistine cities during the Iron Age. During the Iron IA Ekron is the most rapidly growing city illustrating the strongest characteristics of an Aegean-Philistine culture. Later, during the Iron IB and Iron IIA Ashdod and Gath become stronger; a process reaching its peak in the 9th and 8th centuries BC; meanwhile Ekron is reduced to a small city. During the close of the Iron Age, the 7th century BC, Gath is destroyed and Ashdod is significantly reduced; meanwhile Ekron becomes again a large and strong city. If we see the Philistine pottery, both early and late, as an important ethnical marker of the material culture, and I think we should see it as such, the differences in the direction of trade between the Iron I and Iron II in Philistia conforms well to the archaeological and historical picture.

REFERENCES

Ben-Shlomo, D., Shai, I. and Maeir, A.M. 2004. Late Philistine Decorated Ware ("Ashdod Ware"): Typology, Chronology and Production Centers. *Bulletin of the American Schools of Oriental Research 335:1-36.*

Dothan, T. 1982. The Philistines and Their Material Culture. Jerusalem: Israel Exploration Society.

Dothan, T. and Zukerman, A. 2004. A Preliminary Study of the Mycenaean IIIC:1.

Pottery Assemblage from Tel Miqne-Ekron and Ashdod. *Bulletin of the American Schools of Oriental Research* 333:1-54.

Gunneweg J., Perlman I., Dothan T., and Gitin S. 1986. On the Origin of Pottery from Tel Miqne-Ekron. *Bulletin of the American Schools of Oriental Research* 264:3-16.

Killebrew, A.E. 1998. Ceramic Typology and Technology of Late Bronze II and Iron I Assemblages from Tel Miqne-Ekron: The Transition from Canaanite to Philistine Culture. In S. Gitin, A. Mazar and E. Stern (eds.) *Mediterranean Peoples in Transition. Thirteenth to Early Tenth Centuries BCE*. Jerusalem: Israel Exploration Society. Pp. 379-405.

Killebrew, A.E. 1999. *Ceramic Craft and Technology During the Late Bronze and Iron I Ages: The Relationship Between Pottery Technology, Style and Cultural Diversity*. Unpublished Ph.D. Dissertation, Hebrew University, Jerusalem.

PETROGRAPHIC ANALYSIS OF ROMAN-BYZANTINE ROOF TILES: PRELIMINARY RESULTS

David Ben-Shlomo
The Institute of Archaeology, The Hebrew University, Jerusalem
davben@h2.hum.huji.ac.il

1. INTRODUCTION

Architectural ceramic elements in general and roof tiles in particular are a rather common find in Roman and Byzantine sites (e.g., McWhirr 1979), though they are not often analyzed in depth. In the site of Caesarea, Israel (the Israel Antiquities Authority and Haifa University excavations; see, e.g., Patrich 1996) a large assemblage of roof tiles was recovered in excavations, most are fragmentarty. These objects come from late Roman to Byzantine contexts (first to sixth centuries AD). The roof tiles include *tegulae* (lower flat tiles) and *imbrices* (upper rounded tiles). Several typological groups of tiles were defined by the excavators according their morphology and fabric. Nevertheless, it should be noted that roof tiles are often difficult to date as they are continuously reused for very long periods.

From the onset it was evident that the roof tiles from Caesarea were somewhat different in their appearance than roof tiles common in Israel during the Roman period. A center for tile production was excavated in the vicinity of Jerusalem (Bnianei Ha'uma) and is affiliated with the 10th Roman Legion dating to the 1st and 2nd centuries AD (Arubas and Goldfus 1995; Goldfus and Arubas 2002). This site included kilns containing roof tiles and other ceramic building material together with regular pottery, and supplied roof tiles for various Roman building activities in the Jerusalem region. Nevertheless, not much is known about late Roman and Byzantine tile production in Israel. These late roof tiles often bear only geometrical imprints, while the 10th Legion tiles bear imprints naming the legion. The tiles from Caesarea lack any imprints and are also somewhat different and more versatile in their shapes.

Consequently, several questions arise concerning the production and distribution of building material, roof tiles in particular, in this period. Were

roof tiles locally produced? If so was it at a central factory. Other possibilities are of a regional production center of building materials (such as at Jerusalem) sustained by a military or municipal establishment. Another option is of importation of building materials from distant regions. This was suggested for tiles found in Tell Keisan (Glass 1980:87-88). Such a phenomenon is known for stone and wood, but is hardly known for ceramic building materials, which are used in large quantities and can be made from local raw materials. For these reasons further analysis was called for in order to examine whether these building material were produced locally or imported from other regions.

2. METHOD

Thin-section petrographic analysis (TSPA) was employed in order to attempt solving these questions. In addition to the identification of the clay source TSPA can illuminate technological aspects of the production. In the preliminary stage of the study a group of ten roof tiles from Caesarea was selected as a pilot study for this research. The samples represent several morphological and fabric types of tiles. In addition regular common pottery from Caesarea and tiles from Jerusalem were analyzed by TSPA for comparison.

3. RESULTS AND DISCUSSION

According to TSPA the fabric of the roof tiles from Caesarea was relatively vesatile. Generally, two groups were defined: a fine silte fabric and a coarser one. This division accords to a ceratin degree with the typological categories defined by the excavators. The fabrics have a micaceous matrix with large ferruginous regions (figs. 1-3). The clay is rich with fine to medium sand biotite inclusions, some showing metamorphic characteristics (possibly mica schist; fig. 3). Also present are large basalt fragments, mostly worn, various types of bioclasts (fig. 1) and occasional inclusions of plagiclase (fig. 2). The clay is relatively poor in quartz inclusions, although there are inclusions of ferruginous fine sand quartz (figs. 1-2). Grog fragments appearing in several of the samples possibly indicate the use of old tiles in the production. Firing temperature is probably above 800°C according to the absence of crystalline calcite.

All of the roof tiles were of fabrics very different from what is known in the vicinity of the site. The clays in this region include large quantities of beach sand, calcite and a calacareous silty matrix. In addition most of the samples are also different from Roman and Byzantine roof tiles from Jerusalem. Those were made of various types of a marly clay from the Motza Clay Formation (Goren 1996:51-52). This clay is characterized by a fine silty

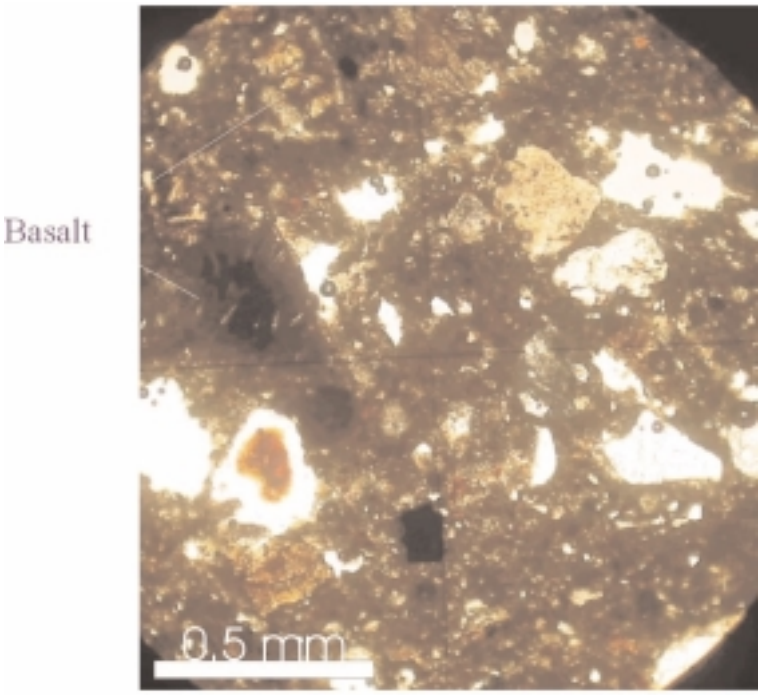

Figure 1. A thin section of a *tegula* roof tile from Caesarea showing a micaceous fabric and basalt (PL; QeS6).

calcareous matrix containing fossilized mollusk and occasionaly dolomitic sand. A similar fabric is evident in a roof tile from the Jewish Quarter, Jerusalem (see fig. 4).

Moreover, it seems that the fabrics of the tiles from Caesarea are most probably foreign to Israel. The micaceous fabric, worn basalt and possible mica schist inclusions may point to the Aegean region although other regions, further to the west, may also be suggested as well. Some of the tiles have a fabric somewhat similar to fabrics of Corinthian and Samian amphorae (Whitbread 1995:123-128, 271; Pl. 5.8). However, there are not enough similarities with any published fabric from the Mediterranean region to clearly identify the clay source.

The preliminary results of this study show that apparently roof tiles were imported to Roman-Byzantine Caesarea from distant regions. This result is not completely unexpected. Using roof tiles as building material is alien to Near Eastern building traditions until recent days. During the Roman period the Roman legions sustained several workshops producing building materials, which would cater to the Roman building activities.

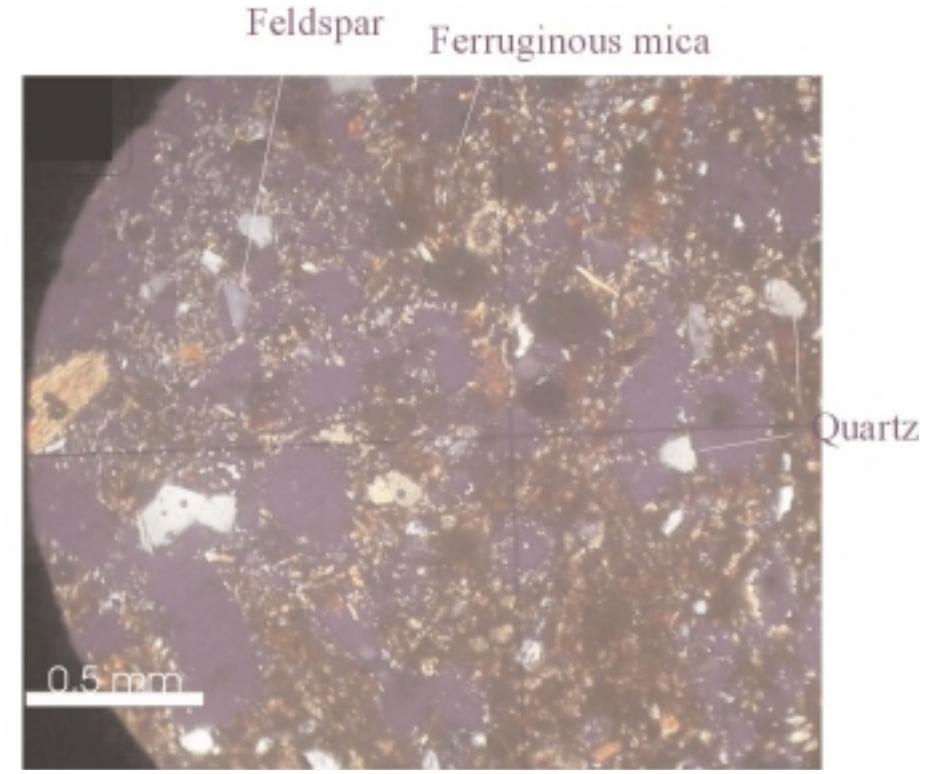

Figure 2. A thin section of a *tegula* roof tile from Caesarea showing micaceous fabric with angular quartz (XPL; QeS7).

Later on, during the Late Roman and Byzantine periods, these military factories possibly ceased to exist and, therefore, it is conceivable that when large quantities of roof tiles were needed they were imported from the west. It seems it was cheaper to import new tiles or reuse old ones than to produce them locally. Even if roof tiles were produced inland it might have been easier to transport them by sea to the port of Caesarea than to carry them overland on account of their heaviness. Roof tiles could have been carried as ballast on ships, carrying goods from the east, after they were emptied. The tiles would be eventually unloaded when the ships returned to the east. An example for long distance shipping of roof tiles in the Late Roman period are Corinthian-Style roof tiles found on Cypriote outbound ship wrecks (Green 1973:153, 161-164); similar tiles were analyzed by TSPA and NAA and were found to by of a Cypriote provenance (Rautman et al. 1999:378-382, 389).

The origin of the imported roof tiles from Caesarea is not yet known. It should be probably sought in the eastern Mediterranean region (maybe at

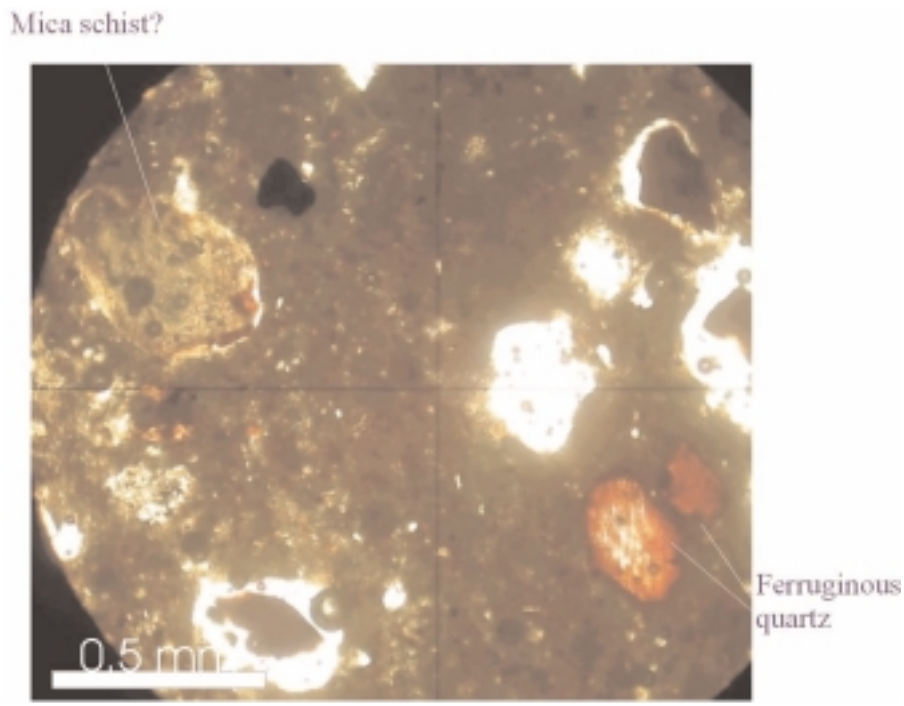

Figure 3. Thin section of a *tegula* tile from Caesarea showing possible mica schist and ferruginous quartz (PL; QeS8).

western Turkey or the Aegean Islands). Archaeological and historical records of contemporary tile production in this region need also be searched for. Further research will attempt to localize more specifically the provenance of the Caesarea roof tiles and to examine tiles from other contemporary sites as well.

ACKNOWLEDGEMENTS

I wish to thank Prof. J. Patrich and U. Davidovitch for for their assistance and for allowing me to sample roof tiles from Caesarea and H. Geva for allowing me to sample roof tiles from the Jewish Quarter.

REFERENCES

Arubas, B. and Goldfus, H. 1995. The Kilnworks of the Tenth legion Fretensis. In *The Roman and Byzantine Near East: Some Recent Archaeological Research* (Journal of Roman Archaeology Suppl .# 14). Ann Arbor, MI. Pp. 95-107, 273.

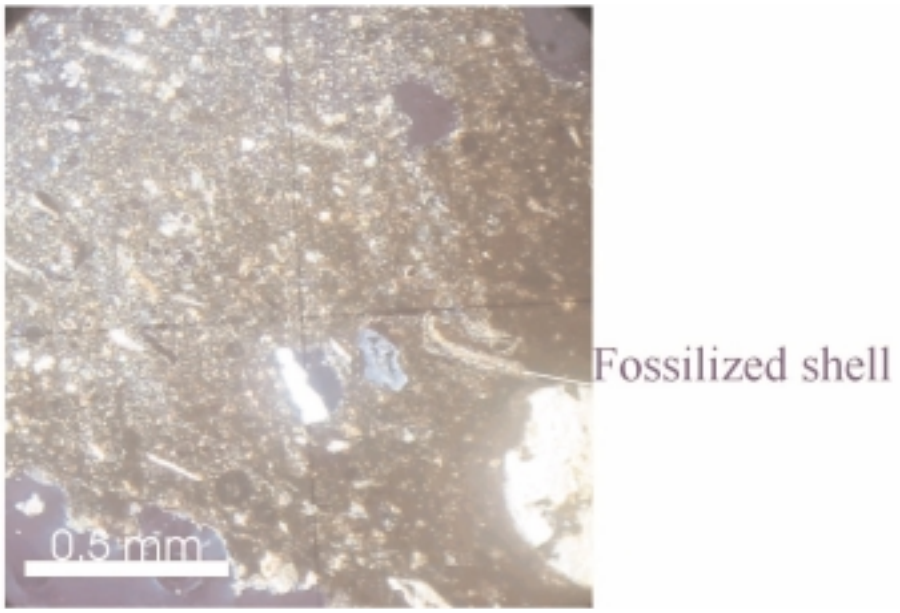

Figure 4. Thin section of a stamped roof tile from Jerusalem (XPL; JQ1).

Glass, J. 1980. Petrological Analysis of A Type A Tegula. In J. Briend and J-B. Humbert, *Tell Keisan (1971-1976). Une cité phénicienne en Galilée*. Paris: Gabalda. Pp. 87-88.

Goldfus, H. and Arubas, B. 2002. The Kilnworks of the Tenth Legion at the Jerusalem Convention Center. *Qadmoniot* 122/2:111-119 (in Hebrew).

Goren, Y. 1996. The Southern Levant in the Early Bronze Age IV: The Petrographic Perspective. *Bulletin of the American Schools of Oriental Research* 303:33-72.

Green, N.J. 1973. An Underwater Survey of Cape Andreas, Cyprus, 1969-1970. A Preliminary Report. In D.J. Blackman (ed.) *Marine Archaeology*. London: Colston Paters 23. Pp. 141-180.

McWhirr, A. (ed.). 1979. *Roman Brick and Tile.* Oxford: British Archaeological Researches Series No. 68.

Patrich, J. 1996. Warehouses and Graneries in Caesarea Maritima. In A. Raban and K. G. Holum (eds.), *Caesarea Maritima - Retrospective After two Millennia*, Leiden. Pp. 146-76.

Rautman, M.L., Neff, H., Gomez, B., Vaughan, S. and Glascock, M.D. 1999. Amphoras and roof-tiles from Late Roman Cyprus: a compositional study of calcareous ceramics from Kalavasos-Kopetra *Journal of Roman Archaeology* 12:377-391.

Whitbread, I.K. 1995. *Greek Transport Amphorae. A Petrological and Archaeological Study.* Exeter: The British School at Athens. Fitch Laboratory Occasional Paper 4.

‘POTTING HISTORIES’ CERAMIC PRODUCTION AND CONSUMPTION IN ALMOHAD SEVILLE

Rebecca Bridgman
Archaeology, University of Southampton, Southampton, UK.
E-mail: rmb399@soton.ac.uk.

1. INTRODUCTION

This paper will provide a summary of an on-going research project, which examines the production and consumption of pottery dating to the Almohad period (AD 1147-1248) in Seville, Spain. Ceramic assemblages comprising predominantly common vessel types from archaeological excavations in and around the city have been examined. Pottery selected for this study has been recovered from both a kiln complex and occupation sites, in order to identify ‘local’ and ‘non-local’ ceramics used in urban occupation contexts in Seville during the Almohad period. Hand specimen and petrological examination of fabrics has been carried out and it is anticipated that further analyses will include an assessment using X-ray fluorescence spectrometry.

2. BACKGROUND

During the Almohad period Seville became the capital of al-Andalus or the Muslim ruled areas of the Iberian Peninsula. Despite the size and relative importance of the city at this time (Valor Piechotta 2002: 45-58), our understanding of the economy of Seville and associated consumption patters of the urban populace is limited. Knowledge of these issues is predominantly derived from documentary sources, which are frequently limited to a description of the day to day functioning of the urban market place (Guichard 2000: 181). In terms of studies of material culture, art-historical analysis and more recently archaeometry has been employed most notably in the field of ceramics. Scientific analysis of the pastes and glazes of pottery vessels has primarily facilitated the identification production locations of highly decorated forms and their techniques of their manufacture (for example Molera, Pradell et al. 1997).

Only limited scientific analysis of non-decorated or common ceramic vessels dating to the period of Islamic rule has been pursued. However, plainer vessel types predominate in the archaeological record, where their presence probably reflects the consumption patterns of the general populace. Analysis of these ceramics is particularly vital in south-west al-Andalus, due to a recognised typological standardisation of common pottery forms in this area during the Almohad period (Lafuente Ibáñez 1999: 208). The problem of standardisation limits current typological research, by hampering identification of any possible movement or exchange of ceramics in this region during the 12th or 13th centuries.

This study differs from previous research as it attempts to assess a range of common pottery types recovered from archaeological sites in or around Seville. It is anticipated that this research may provide an indication of the extent to which Seville was self-reliant in basic manufactured items, such as ceramics during the Almohad period.

3. METHODOLOGY

Initially, ceramic samples were selected from waster sherds, excavated from the Almohad kiln site of 'La Cartuja', located immediately outside the city walls (Amores Carredano 1995). Petrology was then employed in the analysis of these clay fabrics, thus characterising what could be classed as 'local' products of Seville. At present, any fabrics dissimilar to these kiln products but recovered on occupation sites within the city have been categorised as possible 'non-local' items.

Subsequently, samples of pottery were taken from a variety of urban occupation sites located within the city walls, where sealed contexts of Almohad date had been excavated. Initially, all fabrics were classified by hand specimen analysis and ceramic assemblages were quantified. Samples for archaeometric analyses were then selected, to include examples of the form and fabric types present in each assemblage.

4. PRELIMINARY RESULTS

Petrology has indicated the presence of 11 distinct fabric groups, within the 87 sherds already tested from both production and occupation sites (see table 1). Of these fabrics, 5 are considered to represent products of the kiln site at 'La Cartuja' as they are identical or very similar to those observed in waster sherds. These 'local' fabrics occur in both red and white firing pastes, which are most likely to represent clays, extracted from the River Guadalquivir, located immediately to the west of the Almohad city. Waster sherd clays contain a heterogeneous mix of geological elements probably washed down from the Sierra Morena mountain range to the north. Red fabrics appear

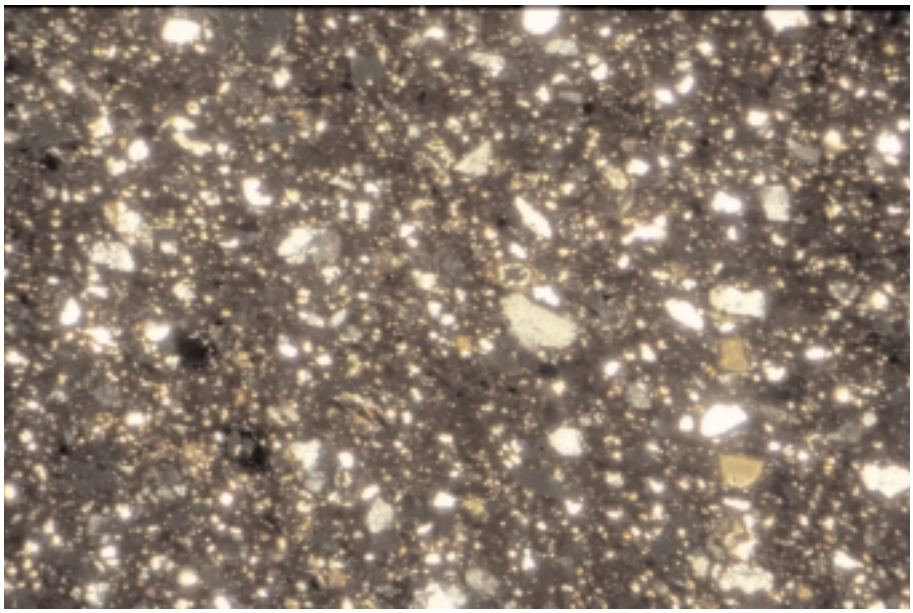

Figure 1. Fabric I (x40).

limited to cooking or tableware vessels, which may have come into contact with heat or flames (see fig. 1/Fabric I). In contrast to the more rounded inclusions, usually encountered in riverine clays, this red fabric contains angular grains of quartz, probably added by the potter to improve the thermal shock properties of this product. White firing fabrics can be divided into 2 types: a coarse version associated with storage vessels (see fig. 2/Fabric II) and a finer type generally analogous with tableware jars (see fig. 3/Fabric III).

Six fabrics characterised by this study do not appear similar to those identified from waster products of the kiln site at 'La Cartuja'. At present, these have been tentatively identified as possible 'non-local' items. The geological elements identified in these fabrics are similar to those in waster sherds from 'La Cartuja'. However, the relative quantities of these elements and their distribution in the clay matrix seem to indicate an alternative production centre, possibly located elsewhere along the River Guadalquivir. Unfortunately, there is not sufficient scope to describe all these fabrics in detail here. Instead, this article will focus briefly on the most interesting of these possible imports, represented by Fabric V. The vessels, made from this fine white clay are predominately table wares such as glazed bowls or jars, often classed as 'luxury' goods (Lafuente Ibáñez 1999: 215). Petrology has indicated that although this fabric appears homogeneous in hand specimen, it is two different fabrics (see table 1 and fig. 4). Currently, production source or sources

of these wares remains unknown; however the nearby town of Jerez de la Frontera could be one possibility. Evidence to support this tentative theory centres on the discovery of a kiln site in Jerez (Aguilar Moya 1999: 229-230), which probably produced luxury vessels, including lustre wares (Martín Patino, Garrote Martin et al. 1987-1988: 206). Further testing is needed, to confirm or refute this theory. Nevertheless, in other contexts ethnographic evidence has been drawn on to strengthen hypotheses of specialised production of ceramics in small, often rural settlements, whose products can then be exported to supply large cities, such as Seville (Peacock 1982: 38-43).

5. CONCLUSIONS

Preliminary results indicate that petrology has been successful in analysing a large group of diverse ceramic material. It has provided a basis for the differentiation of 'local' and 'non-local' ceramic products, recovered from sites in and around Almohad Seville. Clearly, further analysis needs to be carried out to confirm hypotheses suggested here. However, it does appear that a large city such as Seville may not have been capable in supplying all the ceramic needs of the urban populace during the period studied. The question of why this city may have been reliant on imported ceramic material remains uncertain, but we could suggest here that these vessels may represent luxury products. It is anticipated that future work, combining archaeometry with a contextual assessment and incorporating theoretical frameworks, may elucidate this subject further.

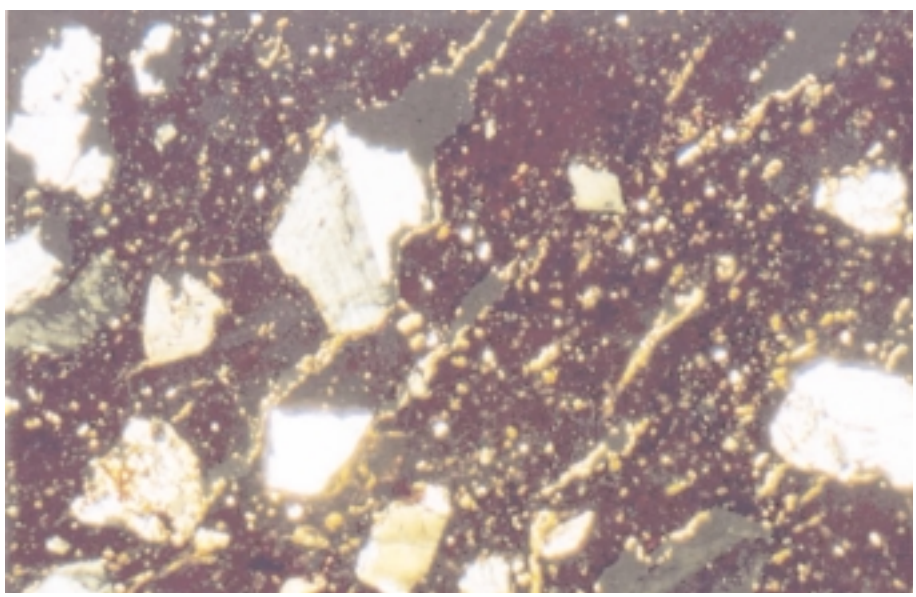

Figure 2. Fabric II (x40).

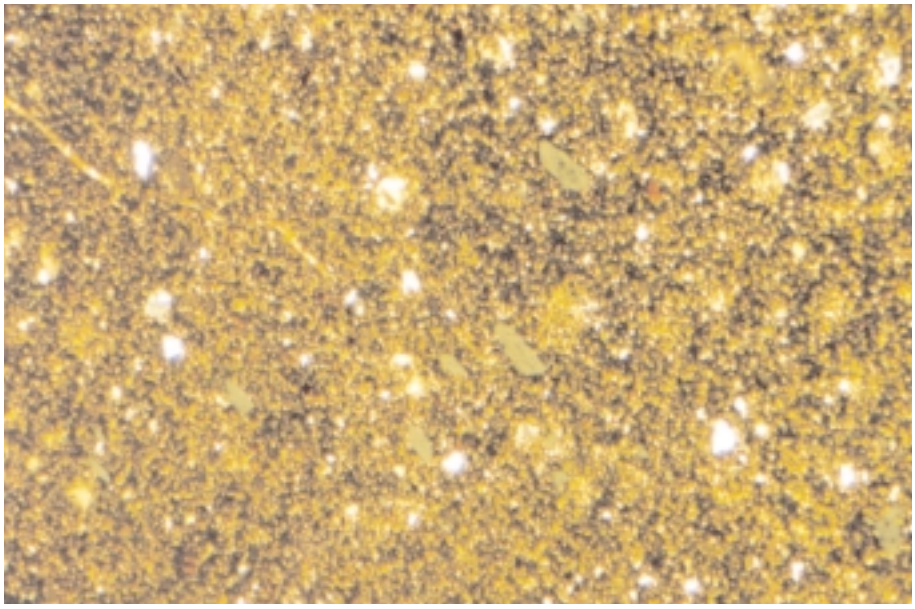

Figure 3. Fabric III (x40).

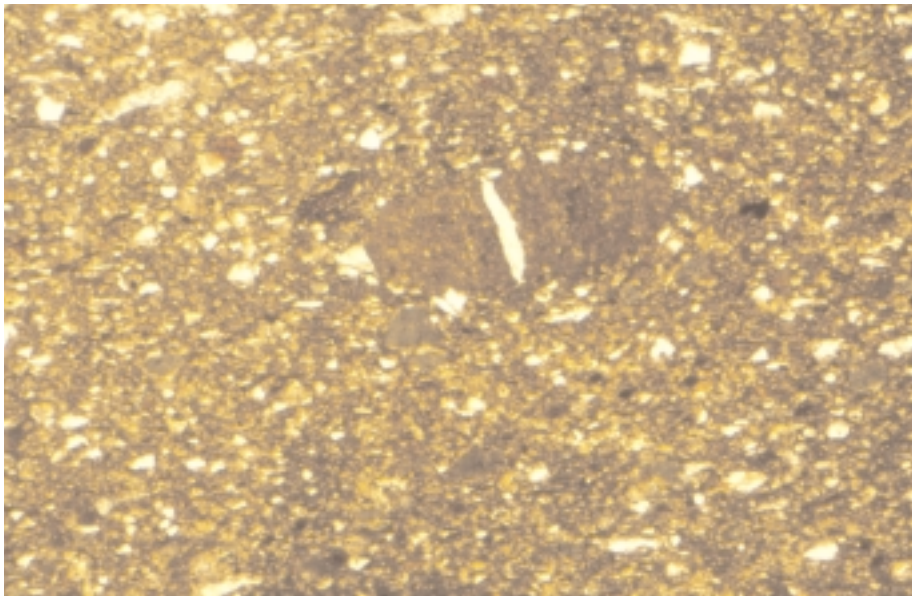

Figure 4. Fabric V (x40).

Fabric group	Summary description and principal inclusions	Vessel types (most common use)	Possible production centre
Fabric I	**Coarse red iron rich fabric. Quartz, s-a; 25%, Limestone 15%, Biotite Mica 5-7%, Iron rich pellets 5-7%, Feldspars 2-7%, Metamorphic rock (largely Phyllite 1-2%), degraded**	Cooking wares e.g. **Granite 1-2% .** 'olla' and table wares e.g. 'cazuela' and 'ataifor'.	**La Cartuja – local production.**
Fabric II	**Coarse buff coloured fabric. Quartz, s-r, 20%, Limestone 5-7%, Feldspar 2-7%, Biotite Mica 5-15%, Metamorphic rock (largely Phyllite 1-2%) Granite 1-2%, Iron rich pellets 5-7%.**	**Storage wares e.g. 'Tinaja', 'jarra', 'cantimplora'.**	**La Cartuja – local production.**
Fabric III	**Fine buff fabric. Quartz, s-r 15-20%, Limestone 5-10%, Biotite Mica 5-7%, Feldspar 1-2%, Calcite 3%, Iron rich pellets 2%.**	**Storage and table wares e.g. 'Jarrita/jarra'**	**La Cartuja – local production.**
Fabric IV	Highly fired coarse vesicular green/buff fabric. Quartz, s-r, 20%, Limestone 10%, Feldspar 1-2%.	Kiln furniture.	La Cartuja – local production, only found at production site.
Fabric V	**Fine, buff coloured fabric. Quartz, s-a 15-20%, Iron rich pellets 5-10%, Granite 1-2%, Metamorphic rock 1-2%. Two sub-sets in this type: first contains Limestone 3-7%, Biotite Mica 20%. Second contains Limestone 20%, Biotite Mica 7% (see fig. 4).**	**Most commonly table wares e.g. 'Jofaina' and 'ataifor'. Plus domestic wares such as 'arcaduz'.**	**Unknown – possible import. Likely 2 versions from different sources, one could be Jérez**
Fabric V1	Coarse red firing fabric. Quartz, s-r, 20-25%, Limestone 5-7%, Iron rich pellets 5-7%, Biotite Mica 15-20%, Metamorphic rock (largely Phyllite) 1-2%, Granite 1-2%.	Fire containers, particularly 'anafe'. Kiln furniture, cook and table wares e.g. 'olla', 'cuenco'.	Unknown source, possibly made in the administrative district or 'kora' of Seville.
Fabric VII	Coarse buff fabric with iron rich inclusions visible to naked eye. Quartz, s-r, 20%, Limestone 10-15%, Biotite Mica 10-20%, Feldspars 2-7%, Iron rich inclusions 10%, Metamorphic rock (Phyllite) 1-2%, Granite 1-2%.	Domestic wares 'lebrillo' and 'arcaduz'.	La Cartuja – probable local production, similar to Fabric II.
Fabric VIII	Fine, buff fabric with tiny red pellets visible to the naked eye. Quartz, s-a 12-25%, Limestone, 10%, Iron rich pellets 7-10%, Biotite Mica 5-10%, Calcite 5%, Feldspar 1-2%, Metamorphic and Igneous rocks 1-2%.	Predominantly glazed table wares e.g, 'jarra,' 'ataifor', 'cuenco'.	Unknown but possibly a coarser variant of Group III. Therefore could be locally produced.
Fabric IX	Orange sandy coarse fabric. Quartz, s-r, 20%, Biotite Mica 7-10%, Limestone 7-10%, Orthoclase Feldspars 7-10%, Granite 3%, Iron rich pellets, 10-15%.	Domestic and table wares – 'Lebrillo' and 'ataifor'.	Unknown – possible import.
Sgraffito	Fine, buff, micaceous fabric. Quartz, s-r, 20%, Muscovite Mica (20%), Limestone (7%), Iron rich pellets (5%), possible grain of Slate (1%) and remnant of shell fragment (1%).	Slipped jar (jarra) with incised decoration.	Likely eastern al-Andalus.

Table 1. Fabric descriptions, with most common types displayed in bold.

ACKNOWLEDGEMENTS

This project is supervised by Prof. S. Keay. Dr D.F. Williams is scientific advisor. Research could not be carried out without permission and advice of colleagues in Seville: Dr F. Amores Carrendano, Dr F. Fernández, Dr M.A. Tabales Rodríguez, Dr M. Valor Piechotta, Dr L. Aguilar Moya, Sr. Rodríguez Hidalgo, Pilar Lafuente Ibáñez, Rosario Huarte Cambra, Pina López Torres. Funding is provided by the Arts and Humanities Research Board, Southampton University and The Barakat Trust, Oxford.

REFERENCES

Aguilar Moya, L. (1999). Jerez Islámico. *Historia de Jerez de la Frontera*. 1999. Cádiz, Diputación de Cádiz**:** 189-249.

Amores Carredano, F. (1995). Las Alfarerías Almohades de la Cartuja. *El Último siglo de la Sevilla islámica (1147-1248)*. M. Valor Piechotta. Salamanca**:** 303-306.

Guichard, P. (2000). *De la Expansión Árabe a la Reconquista: Esplendor y Fragilidad de al-Andalus*. Granada, El Legado Andalusí.

Lafuente Ibáñez, P. (1999). La cerámica. *Sevilla Almohade*. M. V. Piechotta and A. Tahiri. Sevilla, Rabat**:** 207-223.

Martín Patino, T., I. Garrote Martin, et al. (1987-1988). Resultado de los análisis químico y mineralógico de las cerámicas almohades del yacimiento de la Encarnación (Jerez de la Frontera). *Estudios de Historia y Arqueología Medievales*. Cadiz, Servicio de Publicaciones, Universidad de Cadiz.

Molera, J., T. Pradell, et al. (1997). "La Tecnología de la Cerámica Islámica y Mudéjar." *Caesaraugusta* **73**: 15-41.

Peacock, D. P. S. (1982). *Pottery in the Roman world*. London, Longman.

Valor Piechotta, M. (2002). De Hispalis a Isbiliya. *Edades de Sevilla: Hispalis, Isbiliya, Sevilla*. M. Valor Piechotta. Sevilla, Ayuntamiento de Sevilla**:** 41-58.

METALLIC LUSTRE OF GLAZED CERAMICS: EVOLUTION OF DECORATIONS IN SEARCH FOR DISCRIMINATING ELEMENTS

D. Chabanne*, O. Bobin, M. Schvoerer, C. Ney
Centre de Recherche en Physique Appliquée à l'Archéologie, UMR 5060-IRAMAT,
Université de Bordeaux3 / CNRS , 33607 PESSAC Cedex, France

Ph. Sciau
CEMES-CNRS, 29 rue J. Marvig, 31055 TOULOUSE Cedex, France
*corresponding author: delhia.chabanne@caramail.com

1. INTRODUCTION

The metallic lustre of glazed ceramics is a very special type of decoration where metallic copper and silver colloids embedded in glaze compose lustre decoration (Bobin *et al*, in press; Perez Arantegui and Larrea, 2003; Borgia *et al*, 2004). It presents "red", "brown", "ochre yellow" or "green" colours in scattered light but shows, in specular reflection, coloured metallic shines (blue, golden yellow, orange, pink…) (Bobin *et al*, 2003).

The technique of lustre decoration applied to the glazed ceramics appears to the ninth century AD in Mesopotamia (Lane, 1947). Lusterware presented different decorations in scattered light ("red", "green", "ochre yellow" and "brown") with varied metallic shines. It spread to Persia, Syria, Egypt and Spain during medieval times (Caiger-Smith, 1985; Mason, 1994). From the thirteenth to the seventeenth centuries, lusterware, so called *dorado* in Spanish, was produced in Valencia (Spain) (Amigues and Mesquida, 1993). Nevertheless, coloured metallic shines are less varied and, for the end of the production, seems to be a surface metallization. Decoration stylistics can be used to discriminate the evolution over one thousand years but physical elements are necessary to understand aesthetic evolution.

The aim of this study is to compare the beginning of lusterware production (IXthAD) in Mesopotamia and the end of "archaeological" production in Spain (XVIIth AD). So we have analysed two samples of Suse (Mesopotamia) corresponding to first examples known for this technology (IXth AD) and two samples of Paterna (Valencia, Spain), of the end of Spanish production (XVIIth AD). Then, in order to compare with a contemporary

production in Spain (XXthAD) and the beginning of the area of Valence in Spain (XIIIth AD), two shards of the beginning of Spanish production in Paterna, Valencia (XIIIth AD) and a contemporary object (XXth AD) made by Arturo Mora, a ceramist of Manises (Valencia, Spain) have been studied.

2. EXPERIMENT

Analytical investigations were performed on seven shards. Spectroradiometry was used for a physical description of lustre colour in scattered light and specular reflection. Chemical compositions of the glaze and the lustre were determinated by energy-dispersive X-ray spectrometer (EDX) coupled to a scanning electron microscope (SEM). Distribution of nanoparticles in the glaze was also carried out on CM20 ST transmission electron microscope (TEM) equipped with a Gatan PEELS spectrometer with an energy resolution of 1.2 eV. For TEM studies, cross-sectional samples were thinned by mechanical grinding and ion-milling (using a PIPS system) to achieve the electron transparency.

3. RESULTS

3.1. Mesopotamia (IXth AD)

First shard decoration, *BDX 8192*, is "yellow" with orange yellow metallic shines. It is characterized by a majority of silver colloids embedded in alkaline glaze, without lead and tin. From TEM study, small silver and copper colloids (diameter: 5-20 nm) appear to be buried under a colloid-free glaze of 100 nm of thickness (fig. 1).

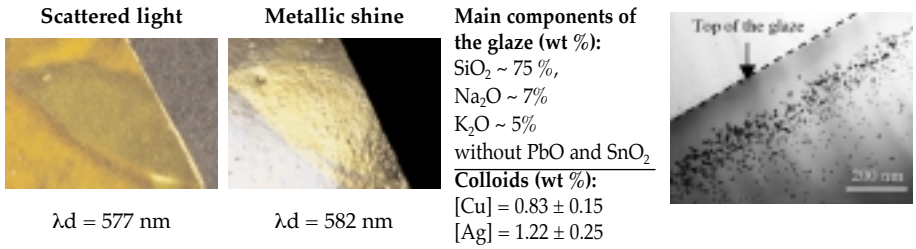

Figure 1. Mesopotamian sample (IXth AD), *BDX 8192*. Main components of the glaze; colours, components and microstructure of decoration.

Second sample, *BDX 8203*, shows a "red orange" decoration with greenish blue or yellow metallic shines according to the observed area. EDX measurements reveal a majority of copper ([Cu] / ([Cu] + [Ag]) ~ 98%) embedded in alkaline glaze, without lead and tin. TEM micrographs present

small colloids (diameter: 10-20 nm) buried under a colloid- free glaze of 100 to 150 nm of thickness. We observe a high density of colloids, and various layers deeper with larger colloids (diameter ~ 30-40 nm) (fig. 2).

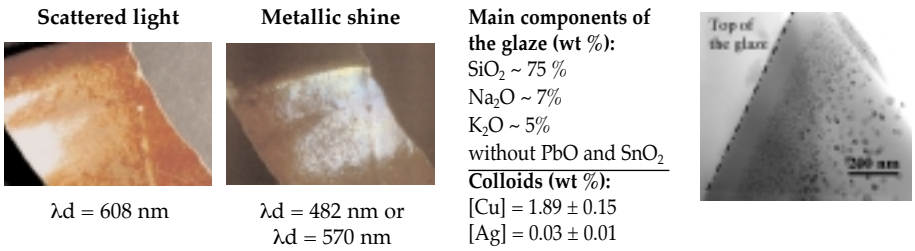

Figure 2. Mesopotamian sample (IXth AD), *BDX 8203*. Main components of the glaze ; colours, components and microstructure of decoration.

3.2. Spain (XIIIth AD)

Lustre decorations of two analysed shards, *BDX 8315* and *8316*, are slightly different in scattered light but present close colour metallic shines (blue, purple). We have observed different compositions with, on the one hand, an equivalent rates between copper and silver and on the other hand, a more important copper proportions. Finally, glazes are different to the ones of the IXth AD with presence of lead and opacifier, SnO_2. Finally, TEM observations show copper colloids (diameter: 10-40 nm) buried under a colloid-free glaze of 20 to 30 nm of thickness (fig. 3).

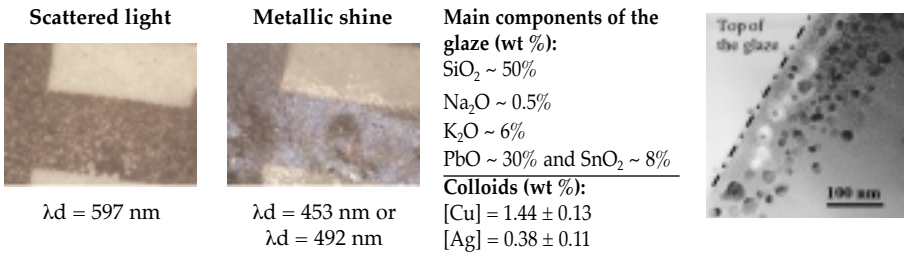

Figure 3. Spanish sample (XIIIth AD), *BDX 8316*. Main components of the glaze ; colours, components and microstructure of decoration.

III.3. Spain (XVIIth AD)

Both samples, *BDX 8389* and *8391*, present similarly colours in scattered light (orange) and in specular reflection (orange, orange yellow). Elementary composition of the decoration by EDX measurements show same proportions with a majority of copper colloids (Cu ~ 90%) in both samples suspended in mixed glazes (lead and alkaline) without tin. TEM study shows big copper

colloids (30-130 nm) slightly buried. Distances inter-colloids are very small (≤ 3 nm), it is similar to a metallic film. We note also the presence of smaller size colloids more profoundly buried (fig. 4).

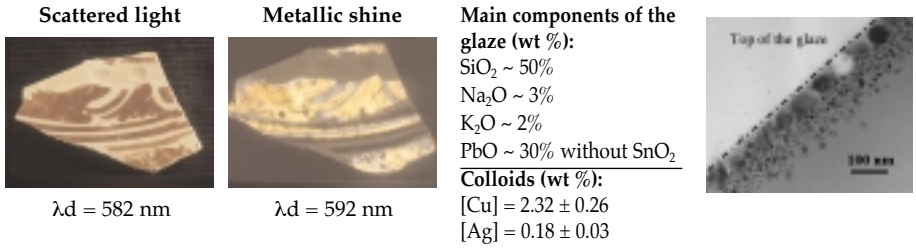

Figure 4. Spanish Sample (XVIIth AD), *BDX 8391*. Main components of the glaze ; colours, components and microstructure of decoration.

3.4. Spain (XXth AD)

This sample is very close to XVIIth AD shards. Same colours with similar copper and silver proportions are observed. Moreover alkali-lead glaze presents lead majority for melting but presents some part of tin unlike XVIIth AD samples, a more important concentration of sodium and less important one of potassium than XIIIth AD samples (fig. 5).

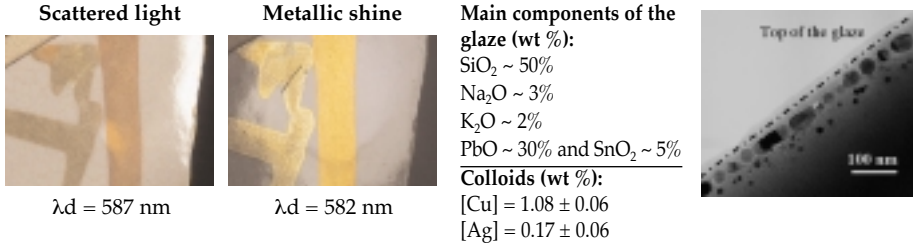

Figure 5. Spanish Sample (XXth AD), *Arturo Mora*. Main components of the glaze ; colours, components and microstructure of decoration.

4. DISCUSSION

In spite of different compositions decorations, IXth AD samples present similarity in microstructure with small copper and silver colloids of (5-20 nm of diameter buried in 100-150 nm). The microstructure of XVIIth AD samples is different with large copper colloids (30-130 nm of diameter), very close to each other, forming as a metallic film close to the top of the glaze.

Comparison with a contemporary object (XXth AD) shows a strong resemblance with XVIIth AD decorations for colorimetry and microstructure.

Colloids present equivalent dimensions and an inter-colloidal distance almost non existent.

Finally, a comparison with XIIIth AD samples indicates a microstructure very close to XVIIth AD and XXth AD shards and it, in spite of few differences to glaze components. It seems to indicate a very close know-how. However, we have revealed a drastic difference between inter colloidal distances. We are not any more in a configuration of metal film, and thus optical properties which are involved.

Differences between Mesopotamian samples (IXth AD) and Spanish samples (XIIth AD, XVIIth and XXth AD) are to be connected to glaze compositions. However, we will have to investigate the influence of other parameters like lustre recipes and firing process.

5. CONCLUSION

The results show a real evolution in the lustreware technology (size and distribution of the colloids). Lustreware of Mesopotamia (IXth AD) is composed by metallic silver and copper colloids with diameter from 10 to 20 nm buried under a glaze layer of 100-150 nm of thickness. Lustre decorations of the XVIIth and XXth AD in Spain are characterized by larger colloids (30-50 nm), close to the surface of the glaze ($\leq$ 30 nm), like a thin film. These characteristics involve a surface metallization appearance. The varied coloured metallic shines, observed in the IXth AD (Mesopotamia) and in the XIIIth AD (Spain) seem to be lost. Results can be connected to colours lusterware (scattered light and specular reflection).

ACKNOWLEDGEMENTS

This work has been done within the European Commission research programs (DG Recherche – ICA 3 CT 1999 00002). We are grateful to Mercedes Mesquida, manager of the "Museo Municipal de Ceramica" de Paterna, to Dr François Amigues and the manager of the Narbonne Museum who entrusted Abbassids lusterware and, finally, Josep Perez Camps, manager of the "Museo municipal de Manises" and Arturo Mora, ceramist. Thanks to Jacques Crestou for his assistant during samples preparation for the TEM.

REFERENCES

Amigues, F., Mesquida, M., 1993, *Les ateliers et la céramique de Paterna (XIII-XIV^{ème} siècle)*, Ed. Musée Saint-Jacques, Béziers.

Bobin, O.; Schvoerer, M.; Chabanne, D.; Ney, C., Sellier, E., Mise en évidence de la nanotexture des constituants des décors de lustre métallique de l'espace

méditerranéen, *Proceedings of «Glaçures et lustre métallique»*, CUEBC, CNRS, Ravello, 11-12 octobre 1998, *In Press*

Bobin, O.; Schvoerer, M.; Miane, J.L., Fabre, J.F., 2003, *Coloured metallic shines associated to lustre decoration of the glazed ceramics : a theoretical analysis of the optical properties,* Journal of Non –Crystalline Solids, 382, 28-34

Borgia, I.; Brunetti, B.; Giulvi, A.; Padovani, S.; Sgamelloti, A.; Shokouhi, F.; Oliaiy, P.; Rahighi, J.; Lamehi-Rachti, M.; Mellini, M., Viti, C., 2004, *Characterisation of decorations on Iranian (10-13th Century) lusterware*, Appl. Phys. A 79, 257-261.

Caiger-Smith, A., 1985, *Lustre pottery technics, tradition and innovation in islamic and western world*, Faber and Faber, London, 246 p.

Lane, A., 1947, *Early Islamic pottery : Mesopotamia, Egypte and Persia*, Faber and Faber, London, 2-16, 37-40.

Mason, R.B., 1994, *Islamic Glazed Pottery*, Thesis of de doctor of Philosophy, Oxford University, 298p.

Mesquida García, M., 2001, *La Cerámica Dorada, quinientos años de su producción en paterna,* Ayuntamiento de Paterna, Concejalía de Cultura.

Pérez-Arantegui, J., Larrea A., 2003, The secret of early nanomaterials is revealed, thanks to transmission electron microscopy, Trends in Analytical Chemistry, vol. 22, n° 5.

CATHODOLUMINESCENCE IN ARCHAEOMETRY THROUGH CASE STUDIES: CLASSIFICATION OF CHALCOLITHIC CERAMICS FROM SYRIA, ENGLISH GLASS STEMS (XVI-XVIIth C.AD), AND GLASS/PASTE INTERFACE OF GLAZED ISLAMIC CERAMICS (X-XIIth C. AD)

Rémy Chapoulie, Floréal Daniel
CRP2A (Physics in Archaeology), UMR 5060 CNRS, University Michel de Montaigne Bordeaux 3, Maison de l'Archéologie, 33607 Pessac, France
chapoulie@u-bordeaux3.fr, fdaniel@u-bordeaux3.fr

Cathodoluminescence (CL) is a method which presents some advantages when compared to other methods of examination and analysis of archaeomaterials. It can be useful when a classification of samples is needed or when observing microscopic areas inside a sample. The principle of luminescence produced by inorganic solids when submitted to high energy electrons, has been well-documented (Yacobi, 1990). Many fields are concerned by its applications such as geosciences and archaeology (Pagel *et al*, 2000 and references therein).

1. EXPERIMENTAL

The equipment used is that of our laboratory in Bordeaux which has been specializing in this method for years. Two types of sets are developed depending on the expected results. One concerns the CL imagery, while the other is about CL spectrometry.

1.1. CL imagery

The first apparatus that we used was from Nuclide. It is very convenient when large areas need to be analysed i.e. up to 340 mm^2. Small areas, down to 0.3 mm^2, are better investigated with a system made by OPEA; this system

also provides a very good reproducibility of the recordings thanks to a standard position of the electron beam. The dimensions of the archaeological samples and the need of reproducibility for the experiment have dictated the choice of our equipment. Both devices use a cold cathode to produce the beam, in a primary vacuum chamber. Images are registered via digital cameras and appropriate software is used in order to exploit these images. In table 1 the main parameters with their commonly used values are presented.

NUCLIDE	System	OPEA
51 mm	Diameter of top window	10 mm
3 – 18 kV (common:10kV)	Accelerating voltage	5 – 30 kV (common:10kV)
1 mA	Current intensity	100 – 300 μA
5 Pa	Chamber pressure	10 Pa
Wild Heerbrugg Binocular	Optics	Olympus microscope Bx51
16.2x20.8 – 8x10.2		
3.8x4.8 – 2x2.4	Areas (mm^2)	2.42x3.25 – 0.48x0.64
Leica D300FX	Digital camera	Olympus DP50
analySIS (Soft Imaging System)	Software	analySIS (Soft Imaging System)

Table 1. Main parameters of the two sets of CL equipments used.

1.2. CL spectrometry

CL spectra were obtained using a JEOL 820 SEM facility where light is collected with an ellipsoidal mirror (Oxford Instruments) guided to a silica optical fibre which is connected to a SPEX monochromator and iCCD detector (Princeton Instruments) with Peltier cooler enabling a signal between 300 and 850 nm to be recorded (for details, see Cazenave *et al*, 2003, and references therein).

2. CASE STUDIES

2.1. Chalcolithic ceramics from Syria

The excavations directed by M.G. Masetti-Rouault since 1996 at Tell Masaïkh (Syria), on the left bank of the Euphrates river (5 km north of Terqa) have produced a lot of ceramics from this mound of 9.5 ha. Differentiating them has always been a problem for archaeologists. Are there some specific features for Halafian (5800-5400 BC), HUT (Halafian Ubaidian Transitional) also called "Hybrid" (5400 BC) or Ubaidian (5400-4500 BC) ceramics? CL imagery was used on large surfaces which were cut from the samples and polished; no thin sections were required. As a comparison, pictures taken under white light (WL) and CL were registered. The main comments are reported in figure 1.

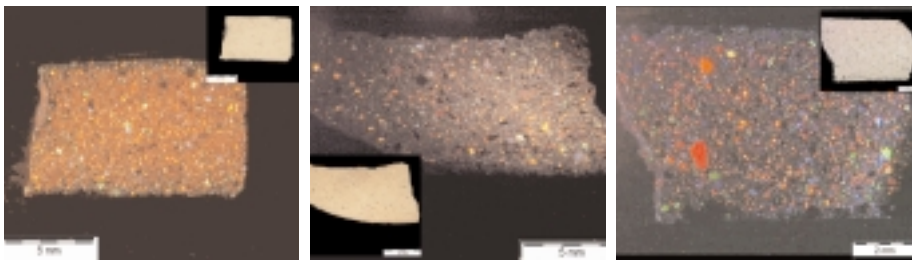

Figure 1: a) Halafian 5800-5400 BC. Paste: buff colour (White Light); intense red CL. Mineral inclusions: many grey, white and orange-red (WL); red, green, blue (CL). Grain size: 100-200μm, homogeneous scattering. **b**) HUT 5400 BC. Paste: orange (WL); purple CL. Mineral inclusions: many grey, white and orange grains (WL); red, blue, yellow, green and purple CL. Grain Size: 100-200 μm, homogeneous scattering. **c)** Ubaidian 5400-5000 BC. Paste: creamy-green (WL), dark purple CL. Mineral inclusions: many grey, white and orange (WL); red, green, blue and purple CL. Grain size: around 500 μm, homogeneous scattering.

Although the classical microscopic images (with WL) produced pertinent information (inserts in fig. 1), the three groups of pottery were only partially identified. They were totally identified with the help of additional specific features revealed by CL. Moreover, the existence of these three groups confirmed the existence of the transitional period so-called HUT, a period between Halaf (and more precisely Recent Halaf) and Ubaid (Robert *et al*, 2005).

2.2. English glass stems

A classification of excavated lion mask stems, from glasses dating from the 16th and 17th centuries (stored at the Museum of London under the responsibility of the curator Hazel Forsyth), was carried out by Hugh Willmott, a historical archaeologist at the University of Sheffield. The classification was based upon stylistic considerations; 26 samples were separated into 7 groups (Willmott, 1998). The purpose of the physico-chemical analyses was to determine the elementary compositions of glasses and to try to identify the elements likely to differentiate the samples.

SEM-EDX data (table 2) pointed out a similar chemical composition for all the samples and thus could not differentiate them. Note that Neutron Activation Analyses were carried out on one sample (courtesy of R. Hancock, Univ. Toronto and J.-F. Moreau, Univ. of Chicoutimi, Canada). For this sample, NAA data confirmed our EDX results for major and minor elements. As for trace elements, they did not show the presence of metals like cobalt, copper, tin, arsenic and antimony (under detection limits).

Element	O	Na	Mg	Al	Si	Cl	K	Ca	Ti	Mn	Fe	Pb
Mass % (sigma)	44.86 -	6.68 (0.56)	1.95 (0.35)	0.66 (0.31)	31.32 (0.13)	0.58 (0.27)	6.20 (0.52)	6.56 (0.55)	0.06 (0.05)	0.83 (0.43)	0.42 (0.40)	0.47 (0.31)

Table 2. EDX data (normalized to 100%, balance with O) of a representative sample (sample ref.: BDX 7072).

CL images were recorded. They showed a bright and homogeneous yellow-green colour for each sample, but pictures did not allow us to easily distinguish the samples. Thus spectrometry was carried out focusing on Mn^{2+} CL emissions (fig. 2).

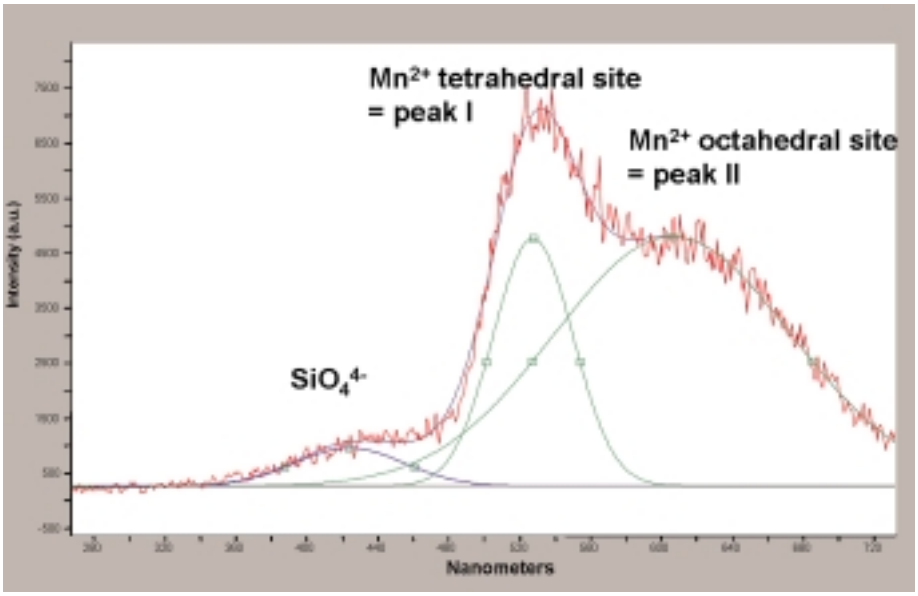

Figure 2. Representative CL spectrum of the samples analysed (sample ref.: BDX 7066). Identification of the CL emission bands.

CL quantitative measurements carried out on peak areas (I / I+II), could not really differentiate them. In this case the substantial uncertainty (±10%) due to current density variations (±3%) and to spectra treatments (±7%) may be an explanation. Another explanation concerns the archaeological aspect: this glass production might have been a homogeneous one across Northern Europe, so the glass recipes used in different places were the same or very similar. These suggestions are not in contradiction with H Willmott's proposals which only concerned a stylistic approach.

2.3. Glazed Islamic ceramics

Within a research programme developed with the universities of Toulouse (C. Déléry and P. Sciau), Zaragoza (J. Pérez Arantegui) and Barcelona (M. Vendrell-Saz), EDX and CL analyses were carried out on polished sections at the interface paste/glaze of Islamic *Cuerda Seca* glazed ceramic from *al-Andalus* (12th c. AD, Mértola, Portugal). Results concerning other features of these *cuerda seca* ceramics are forthcoming (Chapoulie *et al*, *in press*). Here, CL was used in parallel with EDX and SEM imagery focusing on the interface paste/glaze. The main data are reported in figure 3 for a selected area.

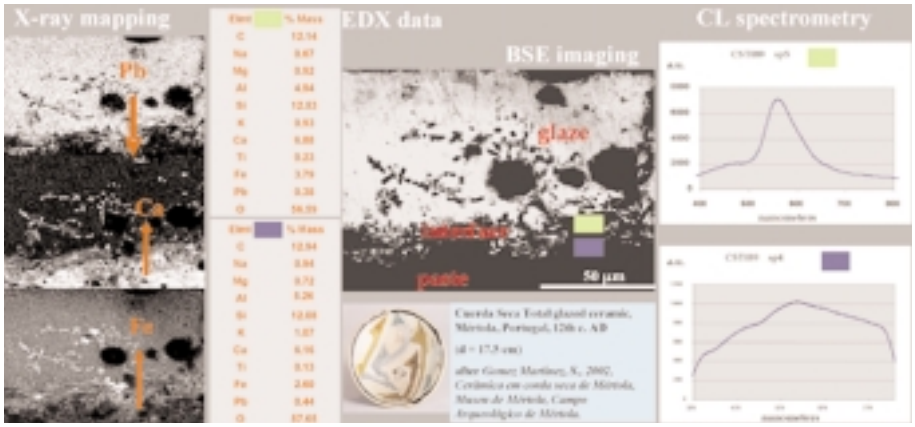

Figure 3. X-ray mapping, BSE imaging, EDX quantitative analysis and CL spectra at the interface paste/glaze of a glazed ceramic (cross-section of CST089 sample). An example of a piece of *Cuerda Seca Total* glazed ceramic is shown at the bottom.

X-ray mapping and EDX quantitative data corroborate to show the migration of ions such as Pb, Ca and Fe during firing which results from a digestion/diffusion process as described in Molera *et al* (2001). At the interface, the material can be amorphous with crystalline inclusions. CL enables us to show the relative concentration of crystals in these zones, which is linked to the crystallinity degree: the more intense and well-defined the spectrum, (sp5 in fig 3), the better the crystallinity degree. These observations enable us to better understand why the glaze sticks so well to the body of the ceramic.

3. CONCLUSIONS

Cathodoluminescence can help to solve problems in archaeology. The method is relatively simple to run when only examination is needed; sample

preparation is fast and easy (thick slices with rough polishing can be sufficient). CL enables us to obtain a quick view of a sample with specific features either on a macroscopic or a microscopic scale associated with the texture and the homogeneity of the surface. Taking advantage of SEM facilities, high resolution CL provides other data such as the presence of chemical impurities in low concentrations, physical defects in crystalline or amorphous structures, all being characteristic of the history of the material. Combining CL with other methods like optical microscopy and SEM-EDX has proved to be efficient in case studies and should be developed.

ACKNOWLEDGMENTS

Conseil Régional d'Aquitaine, University of Bordeaux 3, engineers of our laboratory: N. Gourdon-Platel and S. Dubernet, students: S. Desgouilles and N. Boukhetaia, and Pr. L. Lawrance (improvement of the English version) for valuable contributions.

REFERENCES

Cazenave, S., Chapoulie, R., Villeneuve, G. (2003) Cathodoluminescence of synthetic and natural calcite : the effects of manganese and iron on orange emission. *Mineralogy and Petrology*, 78, 243-253.

Chapoulie, R., Déléry, C., Daniel, F., Vendrell-Saz, M., *Cuerda Seca* ceramics from al-Andalus, Islamic Spain and Portugal (10th-12th c. AD). Investigation with SEM-EDX and Cathodoluminescence. *Archaeometry, in press.*

Molera, J., Pradell, T., Salvado, N., Vendrell-Saz, M. (2001) Interactions between clay bodies and lead glazes, *Journal of American Ceramic Society*, 84, 1120-1128.

Pagel, M., Barbin V., Blanc, P., Ohnenstetter, D. (eds) (2000) *Cathodoluminescence in geosciences*. Berlin Heidelberg New York Tokyo, Springer.

Robert, B., Blanc, C., Chapoulie, R., Masetti-Rouault, M.-G. (2005) Characterizing the Halaf-Ubaid Transitional period by studying ceramic from Tell Masaïkh, Syria. Archaeological data and archaeometry investigations. *Proceedings of 4th ICAANE International Congress on the Archaeology of the Ancient Near East, Berlin, 29 March – 3 April 2004, to be released.*

Willmott, H., (1998) The classification and mould grouping of lion mask stems from London. *Proceedings of the "14e Congrès de l'Association Internationale pour l'Histoire du Verre", Italy, Venice – Milan.*

Yacobi, B.G., Holt, D.B. (1990) *Cathodoluminescence microscopy of inorganic solids*. New York, Plenum Press.

STUDY AND CHARACTERIZATION OF ISLAMIC CERAMIC TILES FROM ONDA-CASTELLON (SPAIN)

L. Chiva, J.J. Gómez
Scientific Instrumentation Central Service (SCIC). University Jaume I. Castellon. Spain

V. Estall
Museo del Azulejo. Onda. "Manolo Safont". Onda. Castellon. Spain

I. Núñez, J.B. Carda
Dept. Inorganic and Organic Chemistry. University Jaume I. Castellon

1. INTRODUCTION

Onda is a city near Castellon, with a great history, mainly from the Islamic period, which left an important culture and patrimony as the 300 Towers Castle and the typical narrow streets in the center of the city.

Valencia was part of Al-Andalus during the Islamic period in the Iberian Peninsula. It was constituted by ten agricultural areas, five of them corresponded to the nowadays Castellon province, in the Northern of the Comunidad Valenciana. Onda was one of these Islamic areas, and the medina was the most important city in Northern Castellon. It was the administrative and religious center in this area. The Onda medina appears cited in Arabic texts in the 11st century, in fact, during this century the city was fortified and it became the most important area in Northern Valencia during the Islamic period, with important people in Science and Culture (1).

Nowadays, Onda is an important producer of ceramic tiles in Spain as a result of the important manufacturing in the 18th and the 19th centuries, which was highly developed and industrialized during the 20th century. The importance of ceramics in the area is reflected in the Museum of the city "Museo del Azulejo. Manolo Safont", which promotes ceramic patrimony and studies about origin and history of Onda.

In this context, an important archaeological research has been developed during last decade. In recent excavations in the city, there appeared medieval and post-medieval tiles. One of the most important discoveries is the Islamic

house from finally of the 12th century and the beginning of the 13th century, related to the Islamic group of plasterings which come from the same place (near San Cristobal square in Onda).

The ceramic tiles we study here belong to the Islamic Courtyard located in this architectural group. They were located in the water channel surrounding all the courtyard in the house (2). The tiles have a rectangular shape, their average dimensions are 38x18 cm and 2.53 cm of thickness, with irregular dimensions due to be handmade (fig. 1). The upper and the four lateral parts in tiles are covered by a very weathered green-turquoise glaze layer. The body presents yellowish colour with different tonalities.

We only have similar tiles in an Islamic fountain from Valencia, which is preserved in the National Ceramic Museum Gonzalez Martí from this city.

This work means the beginning of the collaboration between the Museum in Onda and the University Jaume I, with the aim of supporting and promoting tradition in ceramics in Castellon. The objective of this work is the study and characterization of the glaze and body of these tiles with the aim of determining approximately the technique used for their manufacturing in those days.

2. EXPERIMENTAL METHODOLOGY

A representative piece of these tiles was studied in the Scientific Instrumentation Central Service (SCIC) by optical microscopy (LEICA, Scanning electron microscopy with energy dispersive X-ray spectrometry (SEM/EDX) (LEO 440i, OXFORD), X-ray powder diffraction (XRD) (SIEMENS D5000), and X-ray fluorescence spectrometry (XRF) (SIEMENS SRS3000).

3. ANALYTICAL RESULTS

All these techniques have been applied to the study of the glaze and the body tile: microstructure, chemical composition and mineralogical analysis.

3.1. Study of the glaze

Study by SEM/EDX of the glaze surface shows different vitreous phases (fig. 2):

A. The original green-turquoise glaze, rich in Si, Pb, and presence of Na, K, and Cu, Sn.

B. The weathered glaze with the same elements but different composition, rich in Si. Less Pb and Al than **A** composition. Presence of Sn and Cu.

C. A layer rich in Si, Pb, Ca and P.

The study by SEM/EDX of the transversal section of the tile shows (fig. 3):

D. A layer above the glaze with **C** composition (Si, Pb, Ca and P).

E. Crystallizations rich in Sn.

F. Dark zone: Si, Al and K, without Pb.

•There are no quartz particles

Figure 1. Islamic tile from Onda.

The study by X-ray fluorescence spectrometry corroborates the results from SEM/EDX. In table 1 we can see the most important elements of the surface, including the surface layer rich in P and Ca.

SiO_2	Al_2O_3	Na_2O	MgO	K_2O	CaO	TiO_2
33.7	5.3	0.8	1.2	2.4	10.0	0.1
Fe_2O_3	CuO	SnO_2	P_2O_5	PbO	SO_3	Cl
0.6	1.7	4.7	10.6	26.8	1.1	1.0

Table 1. Glaze surface: Normalized semiquantitative chemical analysis by X-ray fluorescence spectrometry (%wt).

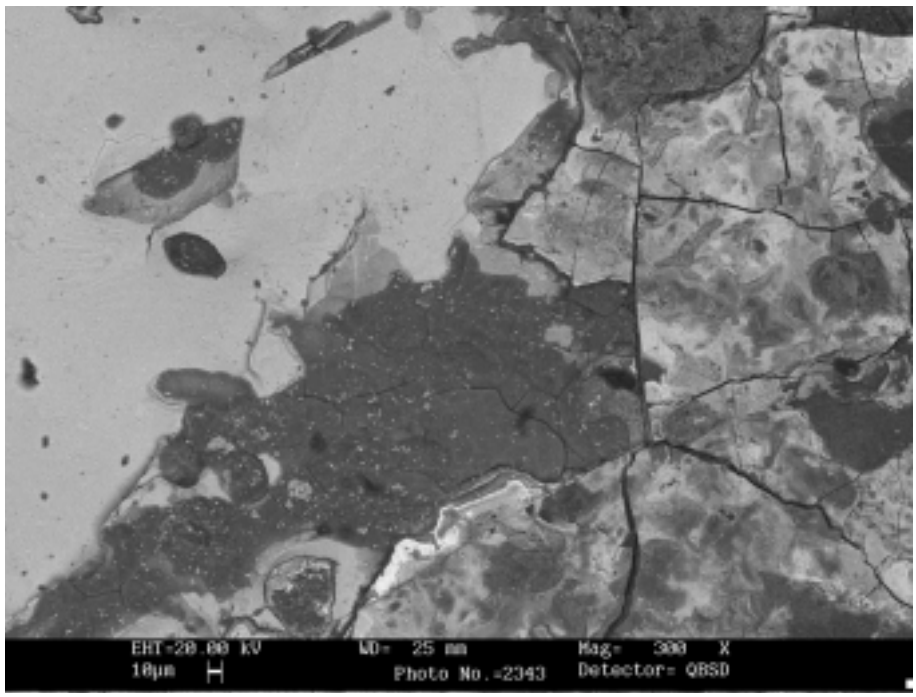

Figure 2. Glaze surface: SEM/EDX (Backscattered electron image).

Table 2 shows the recalculated composition without Ca, P and Cl, considering these elements only from the located upper layer. This could be the original composition. A glaze rich in Pb, Si, with Cu as colouring and Sn as opacificant.

SiO_2	Al_2O_3	Pb0	MgO	Na_2O	K_2O	TiO_2	CuO	SnO_2
40.1	6.0	40.1	1.3	0.9	3.0	0.1	1.9	6.6

Table 2. Glaze without Ca-P layer, the most important elements: Normalized semiquantitative chemical analysis by X-ray fluorescence spectrometry (%wt).

The X-ray powder diffraction detects the cassiterite, SnO_2 (41-1445 JCPD), and an important vitreous phase.

3.2. Study of the body tile

Optical microscopy of the body let to see two different zones: a yellowish zone and a reddish one. Chemical analysis is the same for both of them, so the difference is due to different heating speed during the drying or firing process.

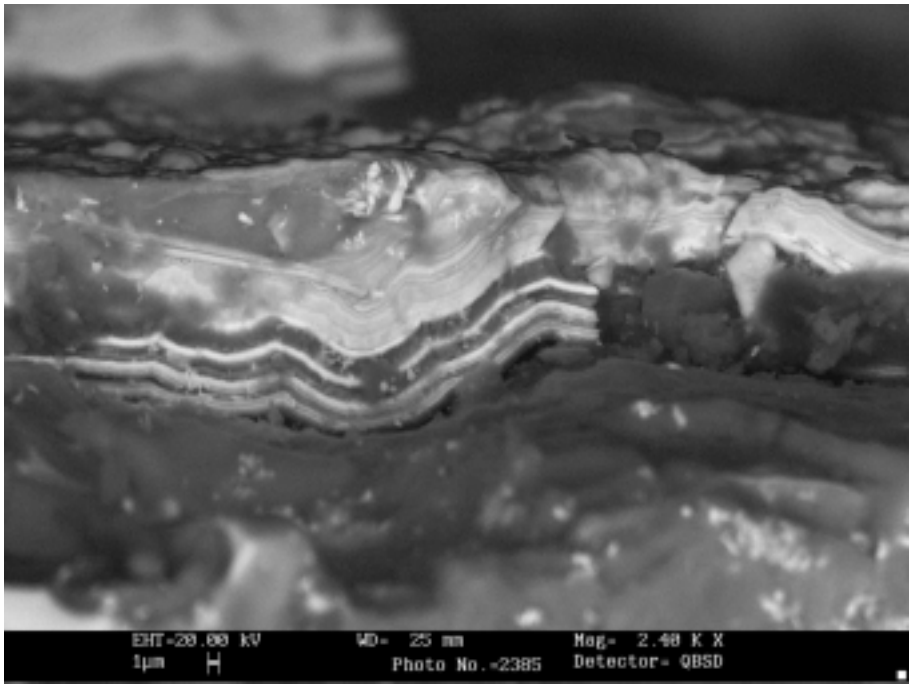

Figure 3. Glaze: study of transversal section by SEM/EDX (Backscattered electron image).

The SEM/EDX shows the zones (fig. 4):

G. Particle: mainly Ca, less Si and Al.

H. Aluminumsilicates, crystallizations of different composition: Si, Al, Ca, K, Fe.

I. Dark particle: Si. Probably Quartz.

SiO_2	Al_2O_3	Fe_2O_3	CaO	MgO	Na_2O	K_2O	TiO_2	L.O.I.
58.00	11.00	3.20	15.95	1.87	0.31	3.48	0.56	5.63

Table 3. Body tile: Quantitative chemical analysis by X-ray fluorescence spectrometry (%wt)

Quantitative chemical analysis shows a typical composition of a calcareous body, with a great amount of Ca. The percentage of iron oxide produces the reddish colour. The X-ray powder diffraction of the body shows different crystalline phases:

— Quartz, SiO_2 (33-1161 JCPD): the residual of the raw materials, corroborates the SEM/EDX.

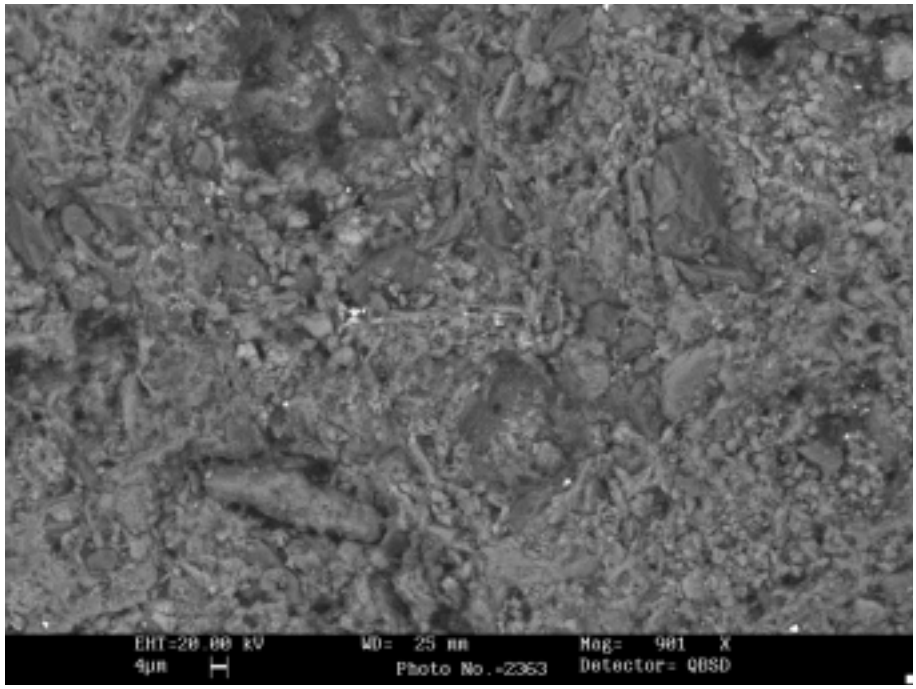

Figure 4. Body tile: SEM/EDX (Backscattered electron image).

— Calcite, $CaCO_3$ (24-0027 JCPD): the residual of the raw material which has not reacted.

— Ghelenite, $Ca_2Al_2SiO_7$ (20-0199 JCPD) and Diopside, $Ca(Mg,Al)(Si,Al)_2O_6$ (25-0154 JCPD): aluminumsilicates, they have formed by thermal modifications of raw materials.

—Hematite, Fe_2O_3 (24-0072 JCPD): the responsable of the reddish colour.

4. CONCLUSIONS

With the obtained results we can conclude:

— The glaze is composed by one layer, without a slip between the glaze and the body.

— The main components in glaze are SiO_2 and PbO (bisilicate of lead), using cassiterite as an opacificant and copper as colourant.

— There is a superficial layer coating part of the glaze, composed mainly by calcium and phosphorous , probably calcium phosphate formed by the canalised water and the soil deposited above the pieces during centuries.

— There are no residual big sized quartz particles in glaze, and tin appears as very small crystals of cassiterite very well distributed in the glaze. This one seems to indicate that, probably, glaze was first prepared as a frit of all components applied later on a previously fired body (3).

— These results allow us to determine the manufacturing process, similar to that used in other workshops in Eastern Spain, such as the Paterna and Denia ones in the 13th century. So these tiles would be very similar to those of the Islamic fountain in Valencia.

— The results in the study of the body show that the manufacture of the tile would have required high temperature conditions, ranging from 800 to 950ºC, as evidence by the loss of the crystal structure of the clay minerals, part decomposition of the calcite and the neoformation of aluminumsilicates as Ghelenite and Diopside (4).

— The body was conformed using calcareous clays, widely used in Eastern Spain during this time, tiles made with these material have a stable microstructure over the temperature range 850ºC – 1050ºC, and the control of firing temperature is not critical.

— Differences in the body colour are due to a gradient in drying or firing temperature, with Fe in a different crystalline phase.

— The results of these studies support the historical fact that Onda was an important point in the area during the Islamic and Middle Age period, and its tradition in ceramics has a remote origin.

ACKNOWLEDGEMENTS

Authors are grateful with all staff from SCIC and the Museum: Museo del Azulejo "Manolo Safont". Onda.

REFERENCES

(1) "Onda en el siglo XIII. (Notas para su estudio)", 1988, Vicente García Edo. Magnífico Ayuntamiento de Onda.

(2) "Arqueología del Pavimento Cerámico desde la Edad Media al siglo XIX", Asociación de Ceramología. Pavimentos Medievales y Post-Medievales de Onda. Pp. 133-143. 2003. V. Estall i Polés. Joaquín Alfonso Llorens.

(3) Chemical and Textural Characterization of Tin Glazes in Islamic ceramics from Eastern. Spain. J. Molera, M. Vendrell-Sanz, J. Pérez-Arantegui. Journal of Archaeological Science (2001) 28, 331-340.

(4) Characterization and Technology from Studies of Clay Bodies of Local Islamic Production in Zaragoza (Spain). P. Lapuente, J. Pérez-Arantegui. Journal of the European Ceramic Society (1999) 19, 1835-1846.

EXPERIMENTAL PETROLOGY OF THE FIRING PROCESS OF RENAISSANCE POTTERY FROM DERUTA (UMBRIA, ITALY)

Claudia CONTI
Istituto Superiore di Ricerca e Formazione sui Materiali Speciali per Tecnologie Avanzate - loc. Pentima Bassa, 21 - 05100 Terni (Italy)

Beatrice MORONI
Dipartimento di Scienze della Terra, Università di Perugia - Piazza Università - 06100 Perugia (Italy)

1. INTRODUCTION

Deruta is one of the most important centres for pottery production in Italy. Local archaeological excavations and numerous personal and public collections of Deruta ceramics show that this activity, whose most archaic forms date back to the beginning of human settlement, reached its maximum levels of elegance and technological refinement in the Renaissance period (Fiocco and Gherardi, 1986). This work is focused on the assessment of the firing technology of paste in Deruta in the Renaissance period. For this purpose, clay samples best representing the chemical composition of ceramic products from different workshops active in Deruta in the Renaissance period underwent laboratory experimental firing tests at different conditions following the procedure of firing applied in the XVIth century as reported in the ancient historical documents (Biringuccio, 1977; Piccolpasso, 1976). The products of firing were then compared with original shards from ancient workshops in order to assess the firing conditions applied in ancient times.

2. MATERIALS AND METHODS

Clay samples and pottery fragments coming from the excavation of workshops dating back to the XVIth century were characterized using different analytical techniques (Alunni, 2002; Conti, 2002): optical microscopy, image and phase analysis by scanning electron microscopy coupled with EDS microanalysis on thin sections, X-ray fluorescence spectroscopy, and X-ray powder diffraction with quantitative phase analysis by Rietveld method. Rietveld method (Rietveld, 1967, 1969) is a full-profile fitting, structure refinement method in which the observed profile is compared point by point

with a calculated pattern obtained by imposing a structural model for each phase in the mineralogical assemblage. The model parameters are adjusted by least-squares methods. Refinements were carried out using GSAS computer program by Larson and Von Dreele (1987), with starting models for the phases taken from literature.

Two clays best representing the chemical composition of the shards (fig. 1) underwent the firing tests at different firing conditions as reported in table 1. The firing products underwent textural, chemical and mineralogical characterization by the same analytical techniques applied in the characterization of clays and shards. In this paper, only the results of quantitative phase analysis by Rietveld method are reported and briefly discussed for safe of brevity.

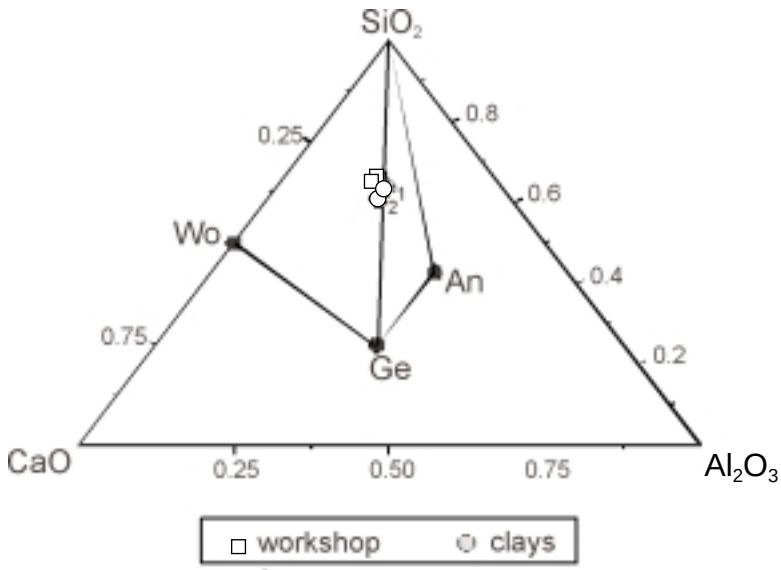

Figure 1. Chemical composition of shards and of representative clay samples reported on the ACS (Al_2O_3-CaO-SiO_2) diagram. The clay samples show different calcite amounts (25% in clay type 1 and 29% in clay type 2). In the graph the bulk composition of the shards and selected clay samples lay in the area of pertinence of typical calcareous illitic clays (after Heimann, 1989).

3. RESULTS

Increase of temperature at lower heating rate and longer time at peak temperature (samples 1A-1G; Tab. 2) gives no changes in the mineralogical composition until 750°C when calcite and illite drastically decrease. At 850°C calcite is out, a very low quantity of lime is still present whereas gehlenite and diopside appear. In the meanwhile, haematite is present and illite and amorphous phase drastically decrease. The ratio diopside/plagioclase

Sample	Clay type	Heating rate (°C/min)	Peak temperature (°C)	Time at peak temperature (h)
1A	1	1	450	4
1B	1	1	550	4
1C	1	1	650	4
1D	1	1	750	4
1E	1	1	850	4
1F	1	1	950	4
1G	1	1	1050	4
1H	1	8.7	850	4
1I	1	1	850	1
1L	1	8.7	850	1
2A	2	1	850	4
2B	2	1	850	1
2C	2	8.7	850	1

Table 1. Experimental firing conditions.

(Di/Pl) is about 1. At 950°C illite is out, diopside and plagioclase drastically increase whereas gehlenite is practically unchanged. Lime and amorphous phase are absent. At 1050°C gehlenite is out, diopside increases and plagioclase decreases so that Di/Pl comes 1.73. Haematite is almost unchanged whereas amorphous phase appears again.

At 850°C peak temperature, with variable clay type, heating rate and time at peak temperature (samples 1H-1L and samples 2A-2C; Tab. 2), the lime quantities always exceed those found in the former experiments, particularly at higher heating rates and lower time at peak temperature (samples 1L and 2C) when significant amount of illite are also found. Moreover, amorphous phase is always very high ranging from 24.3% to 56.8%. The ratio diopside/gehlenite is significantly higher in the clay with the higher calcite amount at the same heating rate and time at peak temperature (see samples 1E-2A and 1L-2C), whereas it does not seem to be significantly influenced by the heating rate and the time at peak temperature (see samples 1E-1I, 1E-1H, 1I-1L, 1H-1L).

The shard samples (samples A, B, PI1, PI3, and S5 in table 2) are all characterized by significant amounts of calcite. SEM observations revealed the presence of small isolated calcite grains within the paste, probably deriving from recarbonation of lime, and of large calcite precipitates in the cavities within the shards, clearly deriving from external deposition. In both cases calcite is of secondary origin and points to the remarkable presence of humidity in the environment at the burial conditions. Another important distinguishing feature of the shards is the presence of biotite in all of them, and the presence of illite in only one of them. Comparison between the shards and the firing products shows good affinities with the products obtained at 850-950°C at lower heating rate (samples 1F, 2A and 2B), except for sample S5 which shows best similarity with sample 1G fired at 1050 °C at lower heating rate.

4. CONCLUSION

Results of experimental tests show that any product of firing is the result of a complex mix of physical and chemical variables strictly interrelated one to each other. Above all, the heating rate, the time at peak temperature and the amount of calcite in the raw material are crucial driving forces in the kinetics of firing. Namely, increasing heating rate facilitates the breakdown of the original crystal structures leading to the formation of the oxide phases (lime, haematite). At the same time it tends to reduce the reactivity of the newly formed phases leading to a decrease in the rate of formation of the firing phases. The time at peak temperature facilitates the reaction between the oxide phases and, thus, leads to the stabilization of the firing phases at the expense of precursor phases (lime, haematite, illite). The calcite amount in the original clay promotes the formation of the firing phases at lower heating rate, but drastically reduces the amount of firing minerals at higher heating rate. After all, among the considered variables, heating rate is the main factor controlling the development of firing phases followed by time at peak temperature and calcite amount.

In the light of these points, comparison between shards and experimental samples show that the best pottery production was obtained using high-Ca illitic clays fired at temperatures of 900-1000°C. The persistence of phyllosilicates in the matrix at temperatures well exceeding those normally delimiting their fields of existence is clear evidence of kinetic control during firing. These results testify the high technological level attained by the pottery craftsmen in Deruta during the Renaissance period.

	1D	1E	1F	1G	1H	1I	1L	2A	2B	2C	A	B	PI1	PI3	S5
Quartz	26.9	39.7	7.6	16.0	24.7	22.3	23.1	20.8	25.3	27.7	17.2	22.5	18.3	20.4	12.4
K-Feldspar	3.3	4.6	2.7	6.2	2.2	1.9	0.9	2.5	1.4	2.8	5.4	1.9	1.8	3.8	-
Lime	-	0.4	-	-	1.4	0.6	6.5	1.8	0.8	16.3	-	0.3	1.0	1.0	-
Plagioclase	6.1	11.7	29.2	21.9	16.7	5.9	10.9	8.5	10.2	8.8	22	23.3	18.6	18.3	12.2
Illite	13.7	4.2	-	-	-	-	8.6	-	-	8.9	-	-	-	0.5	-
Diopside	-	11.3	24.9	37.9	9.3	6.6	10.1	18.3	12.8	2.9	22	15.8	22.4	20.5	27.8
Gehlenite	-	10.3	10.9	-	8.2	4.5	9.6	7.8	8.2	1.1	2.4	7.6	5.8	4.5	-
Haematite	-	2.0	4.3	3.4	0.7	0.8	5.0	-	-	3.7	2.8	1.5	2.6	1.1	-
Calcite	2.0	-	-	-	-	-	-	-	-	-	8.2	1.1	5.5	6.0	8.3
Biotite	-	-	-	-	-	-	-	-	-	-	0.2	0.5	0.4	0.5	0.2
Amorphous	48.9	15.3	-	13.8	35.9	56.8	24.3	39.8	41.1	27.6	19.4	25	22.5	23	38.3

Precision is better than 5% for the most abundant phases (amounts greater than 20%), and better than 10% for the rest of phases.

Table 2. Results (wt%) of Rietveld structure refinements of experimental firing products and of representative shard damples.

REFERENCES

Alunni, M., 2002, *Archeometria storica della ceramica di Deruta (Perugia): il pavimento della chiesa di San Francesco (XVI secolo)*, unpublished B. Sc. Thesis, University of Perugia.

Biringuccio, V., 1977, *De la pirotechnia libri X*, Il Polifilo, Milano, 168 pp.

Conti, C., 2002, *Petrologia sperimentale applicata a problematiche archeometriche: le ceramiche cinquecentesche di Deruta*, unpublished B. Sc. Thesis, University of Perugia.

Fiocco, C. and Gherardi, G., 1986, La produzione ceramica a Deruta dal secolo XV al XVII, in *Omaggio a Deruta* (ed. G. Busti), Il Torchio, Firenze, 37-46.

Heimann, R. B., 1989, Assessing the technology of ancient pottery: the use of ceramic phase diagrams, *Archeomaterials*, **3**(2), 123-148.

Larson, A. C. and Von Dreele, R. B., 1987, *GSAS, Generalized Crystal Structure Analysis System*, Report LAUR-86-748, Los Alamos National Laboratory, Los Alamos, MN, USA.

Piccolpasso, C., 1976, *Li tre libri dell'arte del vasaio*, All'insegna del Giglio, Firenze, 119 pp.

Rietveld, H. M., 1967, Line profile of neutron powder-diffraction peaks for structure refinement. *Acta Crystallographica*, **22**, 151-152.

Rietveld, H. M., 1969, A profile refinement method for nuclear and magnetic structures, *Journal of Applied Crystallography*, **2**, 65-71.

THE 'INVENTION' OF LEAD CRYSTAL GLASS

David Dungworth
English Heritage, Centre for Archaeology, UK

Colin Brain
Private Researcher, UK

1. INTRODUCTION

The invention of 'lead crystal' glass is traditionally attributed to George Ravenscroft who obtained a patent for "a perticuler sort of christalline glasse resembling rock christall" (Moody 1988). It is widely believed that this was a clear lead glass made using potash, lead oxide and crushed flint, however, the patent does not specify how the glass was made (and does not even mention lead). Ravenscroft's first attempts to produce a clear glass were not completely successful (despite the granting of a patent); the glass was unstable and quickly began to 'crizzle' (a fine network of surface cracks). By 1676, however, Ravenscroft was able to announce that the problems had been overcome (again it has been *assumed* that this was achieved by increasing the proportion of lead oxide) and was granted permission to use a raven's head seal to identify his successful products (Charleston 1984). In 1681 Ravenscroft's patent expired and other glasshouses quickly adopted the new glass. The lead glass was extremely successful and (with the coal-fired furnace) allowed England to take a leading role in glass manufacture. Despite the importance of the invention of lead crystal glass, there are almost no quantitative analyses of glasses of this period (Watts 1975).

2. SAMPLING AND ANALYTICAL TECHNIQUE

Fifty-two late 17th century drinking vessels have been examined and the chemical composition determined. Small samples of glass (1–3mm) were detached and mounted in epoxy resin. Mounted samples were ground and polished to a 1-micron finish and coated with carbon. The samples were examined using a scanning electron microscope. The back scattered electron detector allowed identification of corroded/crizzled surface layers and the assessment of the homogeneity of the uncorroded glass (figure 1). Chemical composition was determined using a germanium X-ray detector. The results

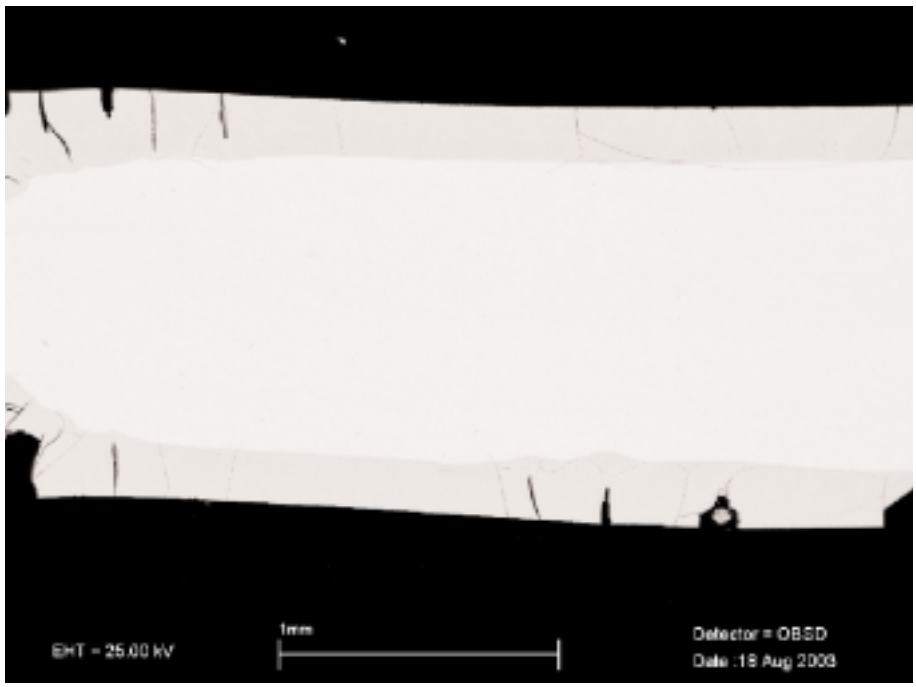

Figure 1. Cross-section through a piece of lead glass (scanning electron microscope, back scattered electron detector). The corroded/crizzled surface of the glass is clearly visible as the darker zone surrounding the uncorroded (light grey) glass.

were calibrated against standard reference materials (e.g. Corning standards). The detector used is not able to quantify the amount of boron present in the glass but the results for 95% of the samples show analysed totals between 98% and 101%. Therefore it is unlikely that boron is a significant addition to any of the glasses analysed. Several samples were analysed using a wave-dispersive detector which confirmed that boron was not present (<1wt%). Linescans were carried out to quantify the degree of homogeneity within the samples. The samples which (using the back scattered electron detector) appeared to be most heterogenous were selected. The linescans showed that the composition within a sample varied by approximately the same amount as the analytical precision (c.0.4wt%). In five cases two samples were taken from different areas of the same vessel (e.g. foot and bowl). The results for the two areas generally differed by no more than the analytical precision.

3. ALKALI GLASSES

Thirteen of the vessels sampled are made from alkali glasses: some of these are soda glasses with chemical compositions comparable with the finest

Venetian soda glasses while others are mixed alkali glasses. The alkali glasses have a fairly constant ratio of manganese oxide to iron oxide (c.1.7) showing that just enough manganese was added to counteract the green colour produced by iron. The alkali glasses also have a constant magnesia to lime ratio (c.0.3) which may indicate that a magnesian/dolomitic limestone was added to the glass. The alkali glasses with low levels of lime have generally suffered from crizzling. Some of the alkali glasses contain small amounts of lead oxide. In some cases these may have been made after the invention of lead crystal glass and the lead may have been accidentally incorporated due to the use of lead glass cullet. However, in some cases these glasses were made before 1674 and the 'invention' of lead crystal (cf. Dungworth & Cromwell forthcoming). Nevertheless, the amounts of lead oxide present in the alkali glasses is low and would not have had a significant effect on the properties of the glass.

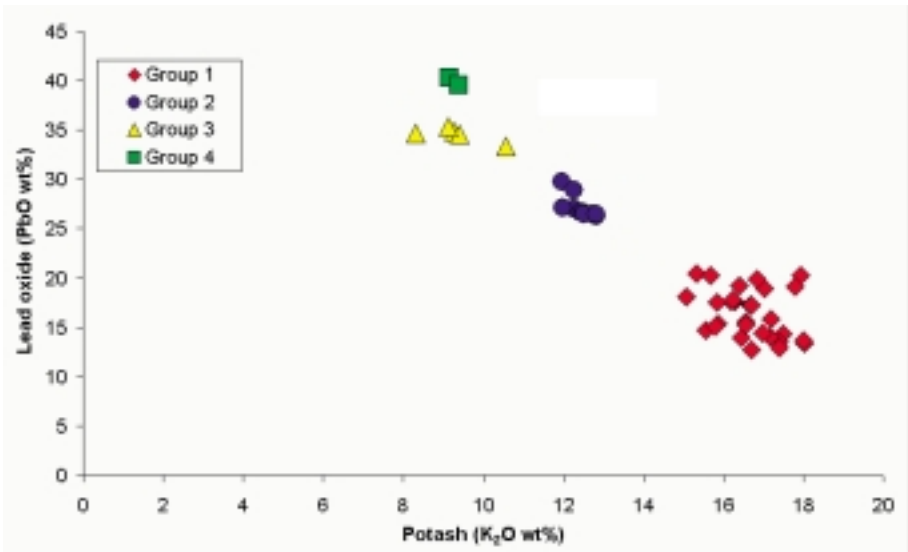

Figure 2. Potash and lead oxide content of lead glasses.

4. LEAD GLASSES

The remaining glass vessels were made from lead glasses which are chemically very different from the alkali glasses. These glasses are composed almost entirely of silica, lead oxide and potash: the oxides that are minor components in most alkali glasses, such as magnesia, phosphorus oxide, iron oxide, and lime, are absent or present at much lower levels. These glasses were made used crushed flint, potassium nitrate and lead oxide. These raw materials were significantly more pure than the traditional raw materials

used for alkali glasses (plant ash and sand) and so were truly colourless. There was usually no need to added decolourisers, such as manganese, to lead glasses.

Group	SiO_2	K_2O	PbO
1	65.3±2.4	16.6±0.8	16.4±2.4
2	58.8±1.2	12.4±0.3	27.2±1.2
3	55.4±0.5	9.3±0.8	34.5±0.7
4	49.5±0.4	9.3±0.2	39.9±0.6

Table 1. Average and standard deviations for major oxides in late 17th century lead crystal glass.

The lead glasses can be divided into four types based on the amounts of lead oxide and potash (figure 2, table 1). The available information on the date of the analysed vessels has been used to construct date ranges for each of the compositional groups (figure 3). Few vessels can be dated to a single year and most can be dated to a period, e.g. 1674-1681. Figure 3 has been constructed using the same principles used by those who compare the range of coins recovered from Romano-British settlements. For each compositional group, each vessel contributes a 'score' of 1 (divided by its date range) to each

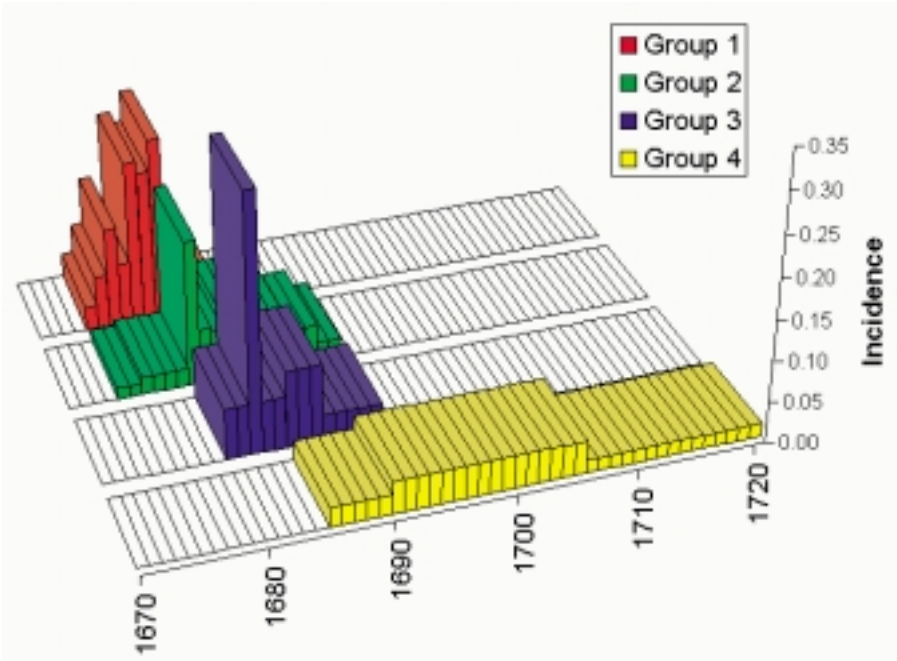

Figure 3. Date range for the four groups of lead glasses.

year of its date range. The scores for each year are summed and divided by the total number of vessels in the group. Figure 3 shows that group 1 is the earliest of the lead glasses and was probably produced between 1674 and 1681, and so was contemporary with the duration of Ravenscroft's patent. Group 2 glass could be dated to between 1674 and 1692 but were most common in the years between 1680 and 1686 and so are likely to post-date Ravenscroft. Group 3 glass was produced between 1680 and 1692 and group 4 glass was produced in the decade or two after 1690.

All of the group 1 glasses have suffered from crizzling but it is not certain when this occurred. It could have occurred in the 1670s or during the years since. The crizzling occurred because the amount of stabiliser (in this case PbO) was too low. The later groups of lead glass have more lead oxide and so are stable: they have not suffered from crizzling.

5. CONCLUSIONS

It can be seen that true lead glasses were not produced before 1674 and that the 'invention' can be associated with Ravenscroft. There is still some uncertainty over what was 'invented' and what measures were taken in 1676 to cure the problem of crizzling. Group 1 glass, which can be dated to the period of the Ravenscroft patent, has suffered from crizzling. However, some of these glasses have seals which should indicate that they were made with an improved recipe and would not crizzle. It is possible that the glass produced between 1674 and 1676 was so bad that it has not survived. A final answer will have to wait until the opportunity arises for the excavation of Ravenscroft's glasshouses.

REFERENCES

Charleston, R.J. 1984 *English Glass and the Glass used in England, circa 400–1940*. London: Allen & Unwin.

Dungworth, D.B. & Cromwell, T. forthcoming 'Glass and pottery manufacture at Silkstone , Yorkshire' *Post-Medieval Archaeology.*

Moody, B.E. 1988 'The life of George Ravenscroft' *Glass Technology* 29: 198–210.

Watts, D.C. 1975 'How did George Ravenscroft discover lead crystal?' *Glass Circle* 2: 71–84.

ANALYZING A MIRROR FROM THE MIRROR'S HALL AT LA GRANJA ROYAL PALACE, SEGOVIA, SPAIN. SOME PROBLEMS IN COMPOSITION, CONSERVATION AND HERITAGE MANAGEMENT

Angel Fuentes, Joaquín Barrio
Dep. Phª y Arqueología. UAM

Rosario García, Pilar Da Silva
Dep. Química Agrícola. UAM

Paloma Pastor
Conservadora Museo Del Vidrio FCNV. La Granja de San Ildefonso.

Victoria Muñoz
Conservadora Palacio de La Granja. Patrimonio Nacional

ABSTRACT

The accidental breaking of a mirror dated on the mid XVIII th from the so called Mirror's Hall at the Royal Palace of La Granja (Segovia, Spain) allowed us to make for the first time a detailed analysis of such exceptional glass from the neighbor La Granja workshop. Analyses included many items others than composition and physical evidence, so we try to compare with similar mirror productions in contemporary Europe. It has been the occasion to analyze the physical location related to specific problems in composition and deterioration. From these data we try to diagnose efficiently such problems in location and conservation and to offer solutions in order to improve the safekeeping of this exceptional glass patrimony. The paper has been carried out by a real interdisciplinary team that includes near all involved proffesionals, as a glass historian, an expert in conservation, a chemist, an archaeologist and a curator of the spanish National Heritage Trust.

1. THE HALL. THE FACTS

The so called 'Mirror's Hall' at the Royal Palace in La Granja, is really the 'Marbles and Mirrors Hall', and is among the oldest rooms in the building.

The hall yet existed in the original religious construction from the XV century, and when the monastery went in Royal Palace, was perhaps the royal couple's first sleeping rooms.

From the beginnings of the XVIII century, renamed as 'royal cabinet', the entire room was reconstructed and evidently embellished with the addiction of marbles and, by king's suggestion, '*some mirrors between walls to multiply the water of the neighbors fountains and to evoke a pleasant illusion'*.

At the end of 1749 the new hall was almost finished, and some bronze 'cornucopia', belonging to the queen, and some statues of roman emperors, personal belongings of the king, were added.

At 2000, during customary restauration works, one of the mirrors was accidentally broken and detached for reparation. So appeared two inscriptions stocked at the back of glasses. One in paper, perhaps the order bill, explaining that the total cost of glasses was 37.784 *reales*, and another made in pencil on the timber surface, stating that 'Juan de Uzeda put those mirrors, chief glassmaker of His Majesty. At June, the 27, of the year 1750, with the help of Antonio Alonso'.

This accident was too the occasion to improve a more extensive study of glass and conservation conditions in the Palace.

2. THE MIRRORS AND MAKING TECHNIQUES

As is recorded in archives, was the architect Subisati who makes the order of 6 mirror of about 2 m high by a bit more than 1 m wide to the Royal Glass Factory of La Granja de San Ildefonso, very close to the Palace and devoted to high standard productions nourishing the Court needs. Urged by time, stocked glasses from the testamentary of the queen Isabel de Farnesio were used .

These glasses were cast by glassmaker Ventura Sit, using the technique of pouring the hot glass mass on the surface of a hot bronze-made table. Once finished, the glass was polished in both sides and smoothed with sand powders and water. Due to big dimensions, this work should be performed without further machinery help.

The glasses then were carried until Madrid to be completed as mirrors at the atelier of the French masters Juan Bautista Marié and Diego Naygeon. The technique was called 'azogado' (from *azogue*, mercury) and basically includes a slight film of mercury between a film of tin and glass. The chemical alloy of mercury and tin, the 'amalgam' adherent to glass, makes this a mirror.

3. MIRRORS IN EUROPEAN PALACES

Mirrors entered the European palaces as soon as in the early XVII century, following the Venetian inspiration and fashion. Inmediately, French

Minister Colbert, launched a some kind of industrial spying to obtain the same products as Italians. Spanish Royal Glass Factory of La Granja joined the race too few years after, in order to avoid the very expensive imports for local palaces. In fact at 1735, 26 mirrors came from Paris to decorate another 'mirrors cabinet' now disappeared. Two years after started the local making at La Granja.

4. THE MACROSCOPIC ANALYSIS

Just watching to the new glass put on the place of broken, is patent the dramatic difference between both mirrors. New is substantially more enlighten, but old one is really better for architectural purposes, as could be sawn in photograph. Glass quality and thickness act more than to the only reflection of images. Mirror optically open a door to another space like hidden inside the glass, as the' illusion' suggested by the monarch.

The mirror is 5.8 mm thick in the section observed. It is possible to be different from one part to another of the mirror, due to the hand making. Under magnifying lenses 5x, 20x and 50x the glass shows the very quality of fabrication. Glass mass is near perfect in visual characteristics: homogeneity, grey colorless and transparent. The color is characteristic of rich leaded glass (crystal) of La Granja productions. No bubbles are observed in the pieces picked to study, although in other parts and in other mirrors (made at the same time and atelier, as we know), bubbles are scarcely present in small dimensions, less than 0.5 mm diameter. And appear, when did, organized in linear patterns. Under UV light excitation no gas intrusion could be sawn everywhere.

Surface is smooth and does not show any trace of desegregation or weatherization (dry conditions of the palace avoid it). The only thing we can see are undulating and concentric lines, suggesting the glass mass falling and extending on the table, and waves suggest the stretching phase after pouring the hot mass. Bubbles, always rounded when appear, indicate the same fact: glass was made on plane, not blown.

Although most could have been removed by smoothing works, some rests of cracking (from reheating and cooling) are visible somewhere, probing the enormous difficulties in working such a big and thick glass.

Broken rims shows conchoids and sharp edges, typical of the very quality of glass mass.

The backside of the mirror shows several scars and out breakings that have damaged severely the mirror. Apparently it seems that scares are lined in strips, following the wooden bars of the frame. But not always are coincident bars and pathology, in fact in some cases (external frames) wood was from pine tree, and scares are not very common. Inside bars, or 'ribs',

made in oak wood are more frequent and, we can suppose, perhaps 'pathogenic'. Accumulated dust between glass and bars, humidity and microorganism activity are responsible for such deterioration.

5. COMPOSITION AND MICROANALYSIS

One fragment of mirror of about 1 cm sq. was separated for analysis, as well as 5 small pieces of amalgam from different areas for the same purpose. The glass was no prepared in advance.

Samples were studied under a Stereoscopic Microscope up to 40x (LEICA WILD 3M) to recognize deterioration problems, specially the adherence of tin slip to glass, as well as its wealth.

The chosen NDT technique is SEM with EDAX (Electronic Microscopic Laboratory –SIDI- University Autonoma), once glass sample was previously make conductive with gold.

5.1. Composition

Using oxide quantification corrected by ZAF, the glass is characteristic sodium based, almost in eutectic amounts stated in most common standards; although has a very high amount of potassium, this one could cause some damage in stability of glass, mainly with high moisture conditions, as have occurred. Thus, the amalgam prevented from a bigger deterioration, avoiding glass hydrolization.

Specific gravity: 2.498; reflective index: 1.519.

5.2. Amalgam

The EDAX analysis show an amalgam made from a thin tin slip stacked to glass by an alloy with mercury. Even today a considerable amount of mercury is present (not sublimated). Small quantities of Si and Ca should come from smoothing or from the very close wall plaster.

The most prominent deterioration process noted here is the oxidation of tin slip, transformed in Stannosum Acid (SnO), which induces the opacity of back surface and impossibility of image reflection.

Amalgam deterioration is more evident in the surfaces close the oak wood ribs. This is caused by corrosion due to gas emissions, full of organics acids (VOA), up to ten times more corrosive than pine tree emissions (Blaskshaws/Daniels 1978; Mourey 1987).

Sulphur could come from several origins, the most probable are the tissues made in animal fibres and/or coloured fabrics, even from gypsum

mortar of the adjacent wall. A special collaboration is devoted to high HR levels (Fernández Navarro 2000). The wall behind the mirror shows a very important level of humidity climbing from the ground or perhaps filtered from anywhere. Moisture and dust hidden backside are responsible for that.

6. CONCLUSIONS

For the first time we have the occasion to deeply study a glass from an important historic place in Spain. We know a lot of details of fabrication, time, workers and art masters, techniques, and even origins of different techniques, and so we are able to compare to other productions from the contemporary Europe, from where most of techniques are introduced. As well as the diffusion of such advances in private works and buildings from royal possessions.

Specially interesting is to offer efficient and well based diagnoses for explicit or hidden problems in conservation of the various royal palaces dated in XVIII and XIX centuries. We are thinking in, at least, these preservations measures, as follows:

a) Eradicate humidity tested in wall as major cause of disease for mirrors.
b) Adequate covering of gypsum plaster.
c) Frequent dust cleaning from the rear.
d) Isolate the oak wooden ribs avoiding the corrosive gas emissions.
e) Prepare a complete testing program for other palaces with mirrors in similar conditions (Villegas 2000).

REFERENCES

Blackshaw, S.M.& Daniels, V.D. (1978) "Selecting safe materials for use in the display and storage of antiquities", *Proceedings ICC,* Zagreb.

Mourey, W. (1987) *La conservation des antiquités métalliques, de la fouille au musée,* LCRRA, Draguignan.

Fernández Navarro, J.Mª (2000) "Causas de deterioro físico y químico de los vidrios históricos", en Fernández Navarro, J.Mª. & Pastor Rey de Viñas, P. (eds.) *Jornadas Nacionales sobre Restauración y Conservación de Vidrios,* Fundación Centro Nacional del Vidrio, La Granja de San Ildefonso, 17-37. ***21-28.

Villegas, Mª.A. (2000) "Indicadores cromáticos de acidez ambiental", en en Fernández Navarro, J.Mª. & Pastor Rey de Viñas, P. (eds.) *Jornadas Nacionales sobre Restauración y Conservación de Vidrios,* Fundación Centro Nacional del Vidrio, La Granja de San Ildefonso, 145-159.

OIL LAMPS FROM TWO SPANISH ROMAN ARCHAEOLOGICAL SITES.

I. CHEMICAL CHARACTERIZATION AND MULTIVARIATE ANALYSIS

Rosario García Giménez, Raquel Vigil de la Villa
Departamento de Química Agrícola, Geología y Geoquímica. Facultad de Ciencias.
Universidad Autónoma de Madrid. E-28049 Madrid, Spain

María Dolores Petit Domínguez and María Isabel Rucandio Sáez
Departamento de Química Analítica y Análisis Instrumental. Facultad de Ciencias.
Universidad Autónoma de Madrid. E-28049 Madrid, Spain

ABSTRACT

Roman culture employed architectural terracotta made of baked clay as original material to manufacture ceramic pieces. A selection of them was collected in Roman quarries discovered in old cities from Roman age and studied. Flame Absorption and Emission Spectrometries were the main techniques used for the elemental analysis (major and minor elements). Results obtained from Multielemental Analysis and Multivariate Statistical Study by Principal Component Analysis (PCA) lead us to the following conclusions: minor elements allowed us to establish differences among manufacture processes as well as employed raw materials. Their concentrations were noticeable higher in samples found in Cordoba than those from Herrera de Pisuerga.

Keywords: Multivariate Analysis, FAAS, Archaeometry, Terracotta.

1. INTRODUCTION

Three different kinds of Roman oil lamps made of ceramic material were analysed in this study (García *et al.*, 1999 y Morillo, 1999). They were found in two Spanish archaeological sites: Cordoba and Herrera de Pisuerga (Palencia) (figure 1), a military settlement during the Roman occupation. Some of these lamps located in the latter were probably brought from Italy by the Roman legions together with their initial furniture household. The pottery oil lamps from Palencia (García Bellido *et al.*, 1962) were Dressel 4 type (figura 2) and dated from 10BC to 40AD (Hughes *et al.*, 1988). Those from Cordoba were

found together with *terra sigillata hispanica* pottery and consequently dated in the Julius-Claudius period (García *et al.*, 1999). All samples are Late Republicans.

Figure 1. Location map of the archaeological sites.

The purpose of this work was to compare the lamps from Herrera de Pisuerga (Palencia, Spain), those supposedly from Italy found at the same location and the lamps from Cordoba, sited in the South of Spain (Bernal & García, 1995). This study allows us to provide other proofs supporting the previously formulated hypothesis about the existence of a local production centre of pottery in Herrera de Pisuerga. These data also help us to establish relations between the composition of the ceramic paste of these oil lamps and the nature of the employed raw materials or the technological aspects of the manufacturing process.

2. EXPERIMENTAL

A chemical characterization of 54 fragments of oil lamps was made by Flame Atomic Absorption and Emission Spectrometry analysis (Jeffery & Hutchison, 1983). After dissolution of each sample, contents of Al_2O_3, CaO, MgO, K_2O, Na_2O, Fe_2O_3, MnO, TiO_2 were determined as major constituents, and SiO_2 was deduced by difference. Concentrations of Cu, Ni, Cr, Pb and Zn were also obtained as minor elements.

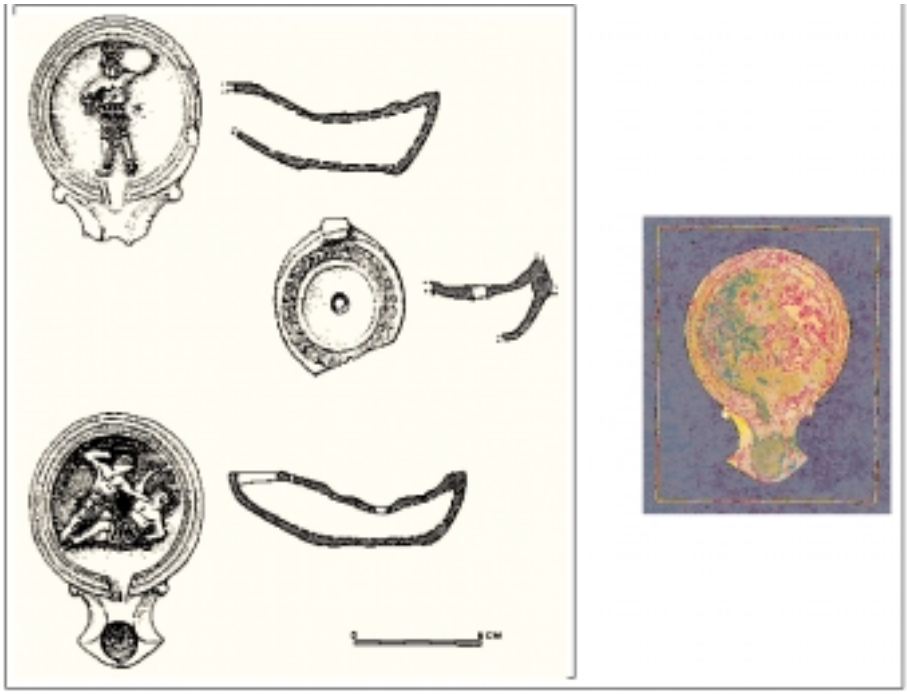

Figure 2. Front, cross section and total view of different oil lamps.

The analytical results were subjected to a statistical treatment by Principal Components Analysis (PCA) using the SPSS 11.5 program, trying to establish possible relations and differences among them. As an archaeometry approach, it is a very important method that enables us to reduce the space dimension of the variables, as well as the extraction of new variables called "factors".

3. RESULTS AND DISCUSSION

The results deduced for the different compounds were represented in two Box & Whisker diagrams (figure 3), showing the median, the interquartile range, the outliers and the extreme values. A great variability in CaO contents was observed mainly caused by lime mill treatments. The median and the standard deviation of the concentration of this compound were higher in Cordoba samples than in Palencia ones. K_2O and Na_2O had more dispersal values in samples found in Cordoba, but there were more outliers and extreme values in those from Palencia.

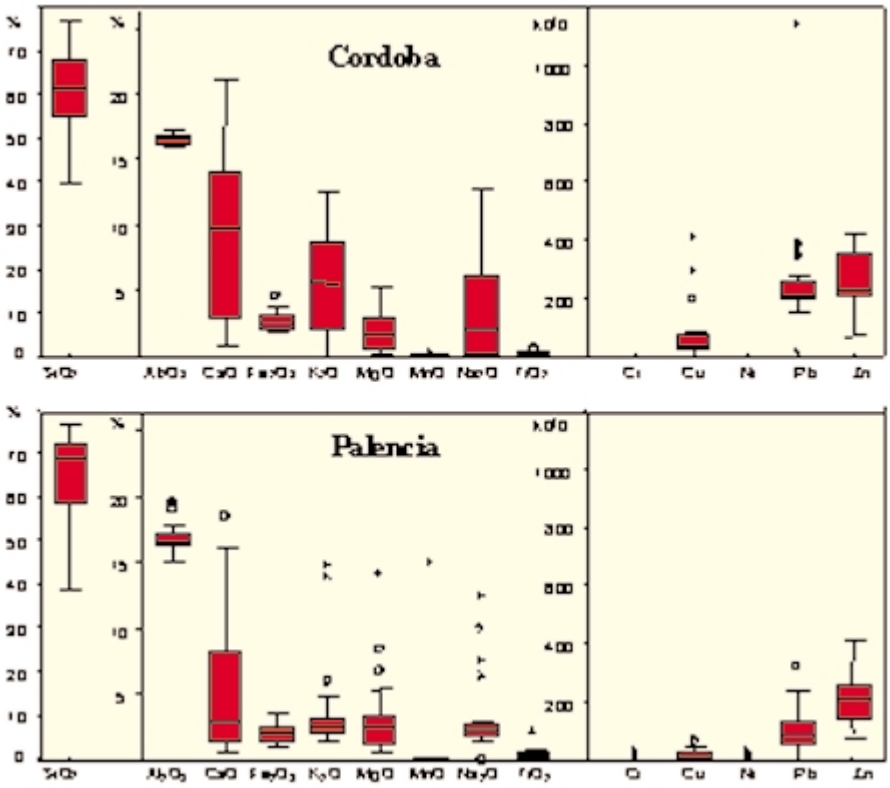

Figure 3. Box & whisker diagrams of the chemical components.

A group of minor elements were studied. They were selected as indicators of the raw materials as well as of the deliberated addition of certain substances to improve the properties of the ceramic paste. In this sense, concentration of Cu, Pb and Zn were higher in samples from Cordoba than those from Palencia, Cr and Ni were non-detected in all cases except in four isolated samples.

Multivariate statistical studies of the obtained data for 54 samples and 14 chemical variables were performed. Relations among lamps that shared a similar composition were established by PCA. The advantages of this multivariate study were demonstrated as applied to a large date-set, reducing the space dimension of the variables. Among other remarkable conclusions, some of the deduced factors allowed the gathering of oil lamp samples in groups as a function of their composition, showing distinctions in groups of elements among samples coming from different origins.

The compounds were gathered in five charge factors representing the 69% of the total variance. The figure is one of the most remarkable graphics among those deduced from the representation of these factors.

It is a representation of the F1 and F2 data. F1 (figure 4) gathers several parameters such as Si, in the negative part, and Ni, Cr, Na and K, in the positive one, as indicators of the raw materials and the deliberated addition of certain substances containing Cr and Ni during the manufacturing processes to improve the properties of the ceramic paste. This factor explains the maximum percentage of variance (22% of the total variance). F2 represents the Pb and Cu contents, both indicators of the manufacture process (Diamandopoulos *et al.*, 1994), and it explains the 16% of the variance. Samples from Cordoba could be distributed in two groups: the positive and the negative part of F1 axis. Among them, there were distributed all Palencia samples, except four samples that where displaced in another region well-differentiated. The different nature of these samples suggests another manufacture place. They could be imported from Italy through the commercial links by the Ebro Valley ports. In other representations the association of the Palencia samples in groups was also possible.

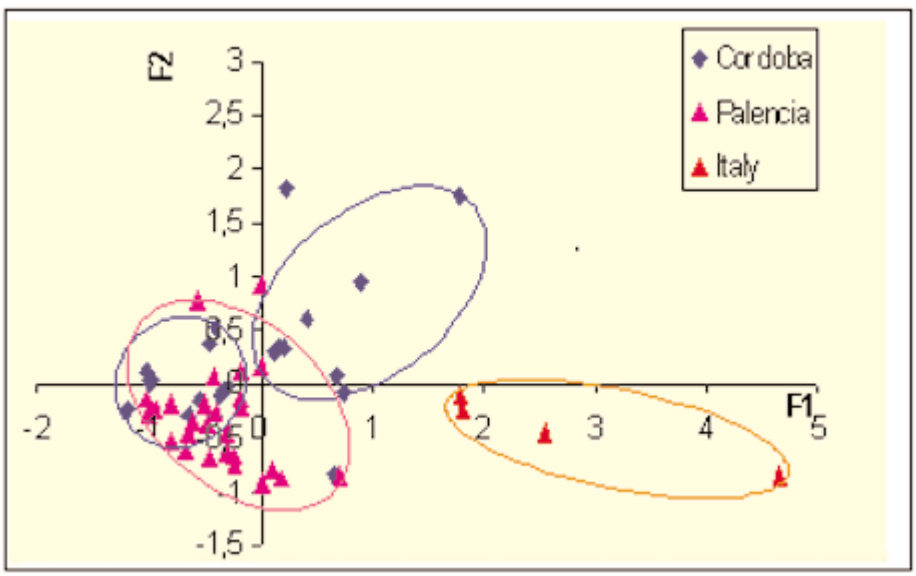

Figure 4. Projection of the oil lamps in a PCA plot.

4. CONCLUSIONS

Concentration of major compounds showed significant differences in relation to the variability of the results and their proportion, mainly CaO, K_2O and Na_2O.

Minor elements were selected as indicators of the manufacture process as well as the raw materials. Their concentrations were also substantially higher in samples found in Cordoba than those from Herrera de Pisuerga.

The "workshop" of Palencia reproduced the Italian models by use of clay found in the neighbourhood. The firing treatment helped us to distinguish the samples made in Italy from the Spanish ones, but the mineralogical and chemical analyses did not.

The chemical results studied by Principal Component Analysis have not allowed distinguishing between samples according to the settlement where they were found, but it is possible to classify samples in compositional groups. F1 established the segregation of four atypical samples that could be considered as a sign of their incursion coming from Italy.

REFERENCES

Bernal, D. & García, R. (1995). Talleres de lucernas en Colonia *Patricia Corduba* en época bajoimperial: evidencias arqueológicas y primeros resultados de la caracterización geoquímica de las pastas. Anales de Arqueología Cordobesa, 6, 175-216.

Diamandopoulos, A., Kolonas, L. & Grapsa-Kotrotson, M. (1994). Use of lead cosmetics in Bronze Age, Greece. Lancet, 344, 754-755.

García Bellido, A., Fernández de Avilés, M.A., Balil, A. & Vigil, A. (1962). Herrera de Pisuerga, 1ª. Campaña (Excavaciones Arqueológicas en España, 2), Madrid, 325 pp.

García Giménez, R., Bernal Casasola, D. & Morillo Cerdán, A. (1999). Consideraciones sobre los centros productores de lucernas tipo Andujar: análisis arqueométrico de materiales procedentes de los Villares de Andujar (Jaén) y de la submeseta norte. In J. Capel Martínez (Ed.), Arqueometría y Arqueología (pp.187-195). Granada, Universidad de Granada.

Hughes, M.J., Leese, M.N. & Smith, R.J. (1988). The analysis of pottery lamps mainly from western Anatolia, including Ephesus by neutron activation analysis. In D.M. Bailey (Ed.), A catalogue of the lamps in the British Museum, III: Roman provincial lamps (pp. 461-485), London.

Jeffery, P.G. & Hutchison, D. (1983) Chemical Methods of rocks Analysis, Pergamon Series on Analytical Chemistry, Pergamon Press, Oxford, England, 98 -101

Morillo, A. (1999). Lucernas romanas en la región septentrional de la Península Ibérica, Monographies instrumentum. Montagnac, Editions Monique Mergoil, 2 volumes, 1512 pp.

OIL LAMPS FROM TWO SPANISH ROMAN ARCHAEOLOGICAL SITES.

II. PHYSICAL CHARACTERIZATION AND MULTIVARIATE ANALYSIS

Rosario García Giménez, Raquel Vigil de la Villa
Departamento de Química Agrícola, Geología y Geoquímica. Facultad de Ciencias.
Universidad Autónoma de Madrid. E-28049 Madrid, Spain

María Dolores Petit Domínguez and María Isabel Rucandio Sáez
Departamento de Química Analítica y Análisis Instrumental. Facultad de Ciencias.
Universidad Autónoma de Madrid. E-28049 Madrid, Spain

ABSTRACT

Roman culture employed architectural terracotta made of baked clay as original material to manufacture ceramic pieces. A selection of them was collected in Roman quarries discovered in old cities from Roman age and studied. A physical characterization of the samples from Palencia, Cordoba and Italy was carried out by using XRD Spectrometry, Dilatometry, SEM and Polarizing Petrographic Microscopy for the observation of thin layers and mineral identification.

Keywords: Multivariate Analysis, SEM, XRD, Archaeometry, Terracotta, Heavy minerals.

1. INTRODUCTION

The aim of this work was to obtain a mineralogical, dilatometric and other physical characterization of the oil pottery lamps described in part I, that allowed us a better knowing of the manufacturing process and of the original employed materials, as well as to establish a statistical processing of the data in order to determine possible relations among physical parameters of the three types of oil lamps (Palencia, Cordoba and Italy).

A physical characterization of the samples was carried out by using the following analytical techniques: Dilatometry at constant rate heating (CRH) for the thermal behaviour, X-Ray Diffraction Spectrometry (XRD) for the mineralogical composition, and, in a group of selected samples, Scanning

Electron Microscopy (SEM) and Polarizing Petrographic Microscopy for the observation of thin layers and mineral identification. A separation of light and heavy minerals was carried out with bromoform.

Two statistical studies were individually developed with the mineralogical data obtained of both fractions in order to classify, in a rational way, groups of the samples sharing a similar composition.

2. EXPERIMENTAL

A physical characterization of 54 fragments of oil lamps was made by XRD, SEM and Polarizing Petrographic Microscopy. Thin sections of samples have been studied in order to identify the minerals. Observations of 1μm layers corresponding to some ceramic samples, polished with diamond, were made by (SEM). In addition, we were able to recognise light and heavy minerals. These minerals were separated by means of bromoform (2.89 specific gravity) and the grains identified through optical microscopy (Williams, 1977). The analytical results were subject of a statistical treatment by Principal Components Analysis (PCA) using the SPSS 11.5 program, trying to establish possible relations and differences among them.

3. RESULTS AND DISCUSSION

The mineralogical composition of the original samples was deduced by XRD. Samples supposedly made in Italy show the strongest peaks for quartz and clay mineral relics (peaks at 3.30Å and 2.85Å corresponding to calcite and gehlenite, respectively). The peaks for calcium aluminosilicate are displaced due to the solid solution of iron and magnesium on the gehlenite (Peters & Iberg, 1978). The peaks at 2.98Å and 2.94Å correspond to pseudowollastonite (effect of iron and magnesium on the concentration). Peaks at 3.27Å, 3.22Å

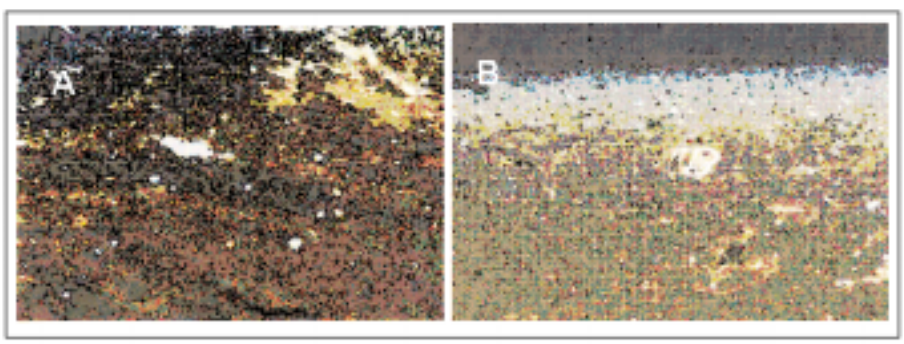

Figure 1. A) Microphotograph of oil lamp from Palencia with fine grains of quartz and feldspars (X120). B) Microphotograph of oil lamp from Cordoba with fossil in the ceramic microconglomerate (X120).

and 3.18Å show the formation of anorthite, with small size and low crystallisation degree. After CRH test the intensity of peaks for pseudowollastonite and anorthite increase due to carbonate extinction.

From the physical studies we could conclude that Italian lamps were manufactured at higher firing temperatures than the Spanish ones. In this sense, only the Italian lamps showed the presence of gehlenite and wollastonite as a consequence of a treatment at temperatures close to 900ºC or higher (Schneider, 1993). These samples also exhibited a defective synterization, high porosity and irregular distribution of porous size with a higher density in the outside area, easily detected by microscopy. These effects were a consequence of a short and heterogeneous heating that provides decarbonatation processes followed by the evaporation of CO_2, as well as the cracking of the ceramic material caused by the quick transformation of calcite in CaO (Tite & Maniatis, 1975, Maniatis *et al.*, 1981 and Sourie & Glasser, 1993).

The observations made by Polarization Microscopy using thin sections allow distinguishing different material types in relation to their texture and mineral composition and the classification of the ceramic paste as artificial micro-conglomerates. In all cases they contained clayish-carbonaceous tempers and cement. Three examples are shown in figures 1 and 2. The four supposed Italian lamps showed a defective synterization that can be seen by SEM (figure 2). These lamps are characterized by their high porosity, and an irregular distribution processes followed by evaporation of CO_2.

Quartz, phyllosilicates, feldspars, calcite and dolomite were the major

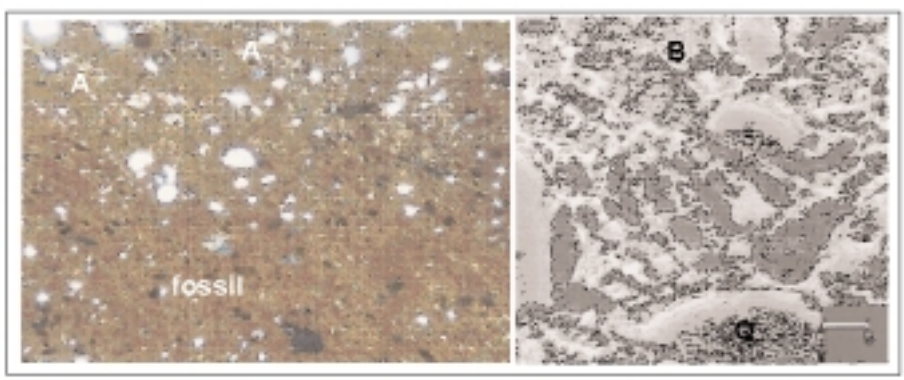

Figure 2. A) Microphotograph of an oil lamp made in Italy with quartz crystals and fragments metamorphic rocks (X120). B) SEM image with microstructure very heterogeneous composed by quartz grains(Q), gehlenite and various aluminosilicates.

minerals. In general, the samples found in Palencia showed lower contents of carbonates than those found in Cordoba. The distribution of the average of

minerals found in each fraction grouped by their origin is shown in the histograms (figure 3).

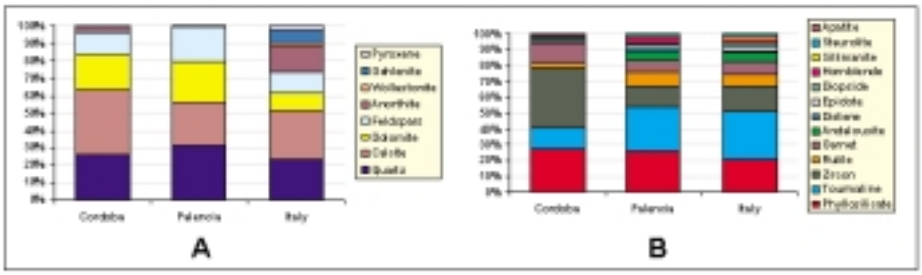

Figure 3. Mineralogical composition of light mineralogical fraction (A) and heavy mineralogical fraction (B).

One of the remarkable differences was that samples found in Cordoba showed a lower proportion of feldspars and quartz and they were enriched in calcite. Another noticeable difference in the heavy mineral fraction was the important amount of garnet in the Cordoba oil lamps and rutile and andalousite in the Palencia ones**.**

Two multivariate statistical studies of the obtained mineralogical data for 54 samples were performed, one of them for the light mineralogical fraction of crystalline minerals and the other for the heavy mineralogical fraction. A total of 17 mineralogical variables (calcite, quartz, dolomite, gehlenite, anorthite, phyllosilicates, tourmaline, zircon, piroxene, rutile, garnet, andalousite, distene, epidote, hornblende, sillimanite, staurolite) were considered, reducing the variables to 3 and 4 factors, respectively (figure 4A). As well as the chemical results, the light mineralogical fraction did not allow a clear grouping of oil lamps according to the place they were found, and in both cases, it is remarkable the different behaviour of the Italian lamps. However, the results of the heavy mineralogical fraction help us to a better distribution of samples from Cordoba and Palencia in different regions (figure 4B).

These studies lead us to a clear sample classification, corroborating the hypothesis of the existence of an own production centre in Herrera de Pisuerga (Palencia). On the other hand, lamps from Palencia showed an association of heavy minerals different from the Cordoba and Italian lamps.

4. CONCLUSIONS

Dilatometry and Microscopy analysis provide a clear distinction between oil lamps made in Palencia, Cordoba and Italy, due to their differences in their morphological and physical aspects.

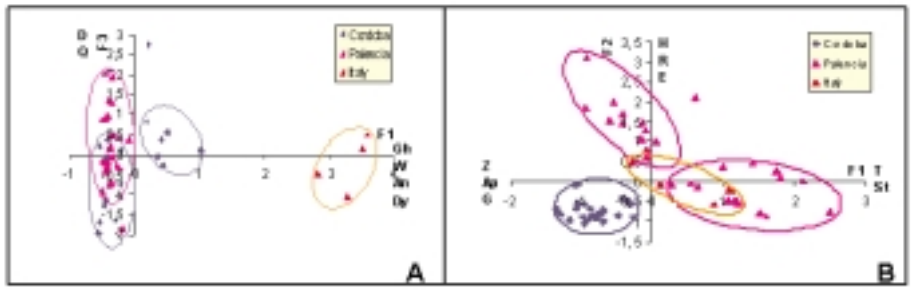

Figure 4. Projection of the oil lamps in a PCA plots. A) Light mineralogical fraction. B) Heavy mineralogical fraction.

Mineralogical and PCA statistical study allowed us to differentiate a group of samples with a noticeable behaviour in relation to the bulk of samples.

These analytical techniques provide evident proofs supporting the hypothesis about the existence of a local production centre of pottery in Herrera de Pisuerga (Palencia), and on the other hand, they support the idea of the penetration of certain oil lamps into this settlement from Italy through the Ebro Valley ports.

Heavy minerals found are very different in oil lamps made in Italy and in the manufactured in Spain (Palencia and Cordoba), where the materials used seem to be from the surroundings of workshop.

REFERENCES

Maniatis, Y., Simopoulos, A. & Kostikas, A. (1981). Mössbauer study of the effect of calcium content on iron oxide transformation in fire clays. Journal of the American Ceramic Society, 64, 263-269.

Peters, T. & Iberg, R. (1978). Mineralogical changes during firing of calcium-brick clays, Ceramics Bulletin, 57, 503-508.

Schneider, G. (1993). X-ray fluorescence analysis and the production and distribution of terra sigillata and Firmalampen. In W.V. Harris (Ed.), The inscribed economy. Production and distribution in the roman empire in the light of instrumentum domesticum (pp. 129-137). JRA, supplementary series, 6, Ann Arbor.

Sourie, A. & Glasser, F.P. (1993). Composition of melilites crystallised from CaO-Al_2O_3-Fe_2O_3–SiO_2 melts, British Ceramic Transactions, 92, 152-154.

Tite, M.S. & Maniatis, Y. (1975). Scanning electron microscopy of fired calcareous clays, Transaction British Ceramic Society, 74, 19-22.

Williams, D.F. (1977). The Romano-British Black Burnished industry: an Essay on characterization by heavy mineral Analyses. In D.P.S. Peacock (Ed.), Pottery and Early Commerce (pp. 163 - 220). London, Academic Press.

EXPERIMENTAL TESTS FOR RECOGNIZING APPLICATION TECHNOLOGY AND FIRING CONDITIONS OF ARCHAEOLOGICAL GLAZED CERAMICS

Sabrina GUALTIERI, Giampaolo ERCOLANI, Andrea RUFFINI, Idema VENTURI
CNR – Institute of Science and Technology for Ceramics
Via Granarolo 64, I-48018 Faenza (Italy)

1. INTRODUCTION

One of the most frequent problems encountered by archaeologists in the study of archaeological glazed ceramics is referred to the individuation of coating application techniques, in particular if the slip glaze was applied on dried body (single firing) or on already fired body (double firing). In fact to distinguish a single or a double-firing production represents an important step in the reconstruction of working technology of these types of artefacts.

The goal of this research is to individuate a useful and valid tool for recognizing the firing process (single or double firing) which ancient shards underwent and, in addition, by considering the thickness of the glaze layer on both sides, to verify the type of the application techniques used for the slip glaze.

In this way archaeological-historical-stylistic parameters and chemical-physical information could be used together to obtain a simpler attribution of the finds together with a better definition of the technological evolution.

We tried to measure the thickness of the interface layer in an objective way and to study the parameters that influence the interaction processes between body and glaze, like paste composition, pieces shape, glaze composition, and the glaze application technique.

2. MATERIALS AND INVESTIGATION METHODS

About 500 pieces of small majolica artefacts, representative of restricted (pot) and open (dish) vessels, were prepared by using two types of paste differing from calcium contents and white and red in colour after firing. Then

they were coated with lead opaque glaze by using two application techniques: full immersion into the slip glaze and by pouring in two times (figure 1). The choise of lead glaze was conditioned by its large use in the antiquity. Two different glazes were used, a commercial glaze and a glaze especially prepared in respect of the Piccolpasso recipe (sixteenth-century ceramic treatise) and by considering the results of the characterisation of archaeological majolica (Fabbri et al. 2000); in this case a few pieces were coated.

The two clays were characterised chemically and mineralogically, before and after firing, by using ICP-AES and XRD respectively; further porosimetric analyses (MIP) of unfired and fired products to verify the influence of the pore size and distribution on the adherence of glaze powder onto the ceramic support were performed. The lead glazes were also analysed by ICP-AES. Vessels and dishes were fired at 950°C both for single and double firing, with slow time of rising (8 hours) and a permanence of one hour at maximum temperature.

Representative samples of obtained products (realised in the two different shapes, with two types of clays and glazes, subjected to different glaze application techniques and firing processes) underwent observations by optical and electronic microscopy.

Figure 1. Examples of glaze application techniques a) full dipping and b) pouring.

3. RESULTS AND DISCUSSION

3.1. Experimental condition

The research has been developed in different steps. In the first one all the raw materials were characterised and the products were realised. In the second phase some products obtained with two clays were fired at 950°C, that is the firing temperature usually indicated for ancient majolica artefact, and the others were coated at dried state in the two ways (by full dipping and by

pouring) and then fired. In the third phase the already fired products were coated in the two ways and then re-fired. In the fourth phase all the products were characterised. The characterisation of the two raw materials (AgF and AgT) shows different calcium and iron contents; in AgF calcium is about 19% CaO and iron about 5.5% Fe_2O_3, while AgT shows about 13% CaO and 6% Fe_2O_3. These differences seem to influence the total open porosity (P) of the two pastes, but not the pores distribution. At dried state P of AgF samples is higher than AgT products (30% vs 24%), and after firing the difference between two pastes increases (47 vs 38%). The increasing of open porosity, of the average diameter and also of the pore size after firing are in agree with bibliographic references (Fabbri, Dondi 1995) that indicate a directly proportionality between porosity and carbonate contents. The glaze composition shows high values of lead oxide and silica (25% PbO and 45% SiO_2) and ~ 7% of tin oxide.

More important information could be obtained just at macroscopic scale; the two bodies show different behaviour after single and double firing. In particular, after firing, the glaze applied on AgT paste maintained its white colour able to mask the paste colour. The glaze on AgF bodies was very light in colour so the paste colour was visible.

3.2. Optical observation

The observation on thin section permits to explain the different behaviours of the two paste subjected at the same glazing and firing processes and the interaction between paste and glaze. AgF bodies showed a great interaction with underlying body after single and double firing. In double firing the thickness of the interaction zone varied from 15 (only in one sample) to 40μm, while after single firing, the interaction body/glaze was more marked and the interface thickness was comprised between 30 and 60μm. Generally two parts have been distinguished in the interface layer: the first inside the coating layer and the second one in the outer part of the body (figure 2a,b).

The first one is a little dark layer and the thickness is related to the firing conditions. When the glaze is applied over fired body the thickness is between 5 and 10μm, and over dried paste it varies from 10 to 15μm. As

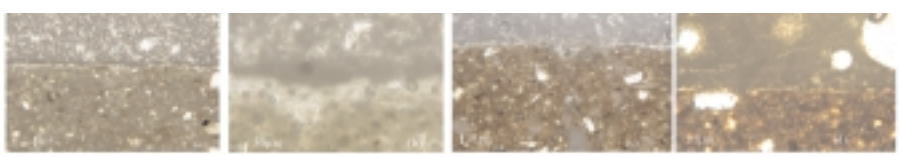

Figure 2. Micrographs of AgF products after single (a) and double firing (b), and of AgT products after single (c) and double firing (d).

regards the layer inside the body the value of the thickness is similar to the dark layer one according to the firing conditions.

The high reaction between body and glaze is also marked by the different thickness of the glaze layer of single- and double- fired products. In fact, the glaze thicknesses of single-fired artefacts are thinner than the ones measured for double fired pieces (100-200μm vs 400-800μm). During the firing process it seems that the glaze layer thickness recedes greatly, maybe due to a greater reactivity of unfired body and according to the values of open porosity and overall pore size of the paste before firing. In fact, the prevalence of pores with little diameter causes their immediate saturation and the water of the slip glaze is not completely absorbed, influencing the thickness of the glaze layer.

The behaviour of AgT paste favours a thin interaction zone between body and glaze (figura 2c,d). Precisely, the double fired products are characterised by a scarce development of the interface layer that measures about 5μm, in both glaze application techniques, and in particular, the little dark layer is never visible. The situation is different when the slip glaze is applied over dried paste; in this case, the thickness is 25-30μm.

As regarding the artefacts coated with the glaze prepared following the indication of Piccolpasso, thin section observations confirm that obtained for commercial glazes.

By comparing the thicknesses of glaze layer on the recto and verso sides of various artefacts, it was possible to verify that the glaze application by full dipping into slip glaze permits to obtain same thicknesses of glaze layer on both sides. The pouring application favours the formation of glaze layers different in thickness on the two sides.

3.3. SEM Observation

In order to discover what happens chemically and mineralogically, we analyzed the interaction zone by using SEM mapping technique because no microstructural variations between interface, body and glaze have been observed.

The maps of double fired pieces evidenced first that glaze application techniques do not influence the development of interface zone and then confirmed that AgF bodies are always more reactive with thicknesses of interface comparable with optical microscopy ones. The area of interaction is characterised by concentration of calcium and lead; in particular we noted a migration of calcium forward glaze layer and vice versa of lead from glaze to body (figure 3). On the contrary in AgT samples no exchange is evidenced; body and glaze are clearly separated.

For both AgF and AgT single fired products, the development of interaction area is always enriched in calcium and lead, with the addition of potassium in some samples.

AgF				AgT			
Double firing		Single firing		Double firing		Single firing	
Full dipping	pouring	Full dipping	pouring	Full dipping	pouring	Full dipping	pouring
25-30	**25-30**	**25-50**	**30-60**	**5-10**	**5-10**	**20-30**	**25-30**

Table 1. Thickness of the interface layer under optical observations on thin section (μm).

The analysis of the different zones by using EDS underlined the formation of new mineral phases, silicates of lead potassium and calcium, wollastonite and gehlenite. The chemical composition of the interface layer is the following: SiO_2 ~ 50% , Al_2O_3~ 15%, PbO ~ 4%, Na_2O ~ 3%, CaO ~ 14%, K_2O ~ 10%, MgO ~ 3%.

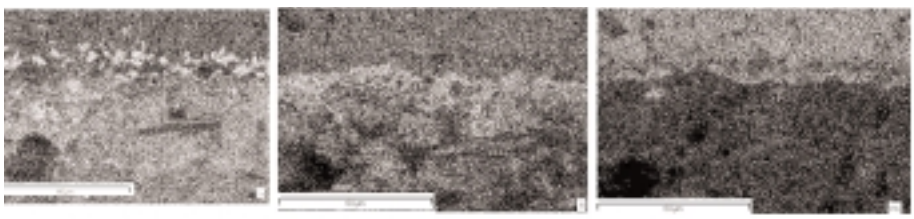

Figure 3. Elemental maps of AgF piece after pouring and double firing.

4. CONCLUSIVE POINTS

The influence of the body to obtain a perfect glazed surface is noticeable. The same glaze applied over different bodies has a different behaviour. Bodies characteristics seem to influence the development of the interface zone. More reactive calcareous bodies favoured a visible interface zone also in double-fired products. This is maybe due to its porosity at the moment of glaze application that influences the thickness of interface and also of glaze layer. In fact, by maintaining invariate the period of applying, the glaze layer thickness on dried body is less than that applied on fired body. The double firing favours a thin interface zone (from 0 to 25 microns), while in the single fired products the thickness varies from 30 up to 60 microns.

The glazing technique could be recognized by considering the thickness of the glaze layer on both sides of artefacts; similar thicknesses indicate full immersion technique while different thicknesses application in two times.

SEM observations showed lead (coming from glaze layer), calcium and secondly potassium (from body) enrichment in the permeation zone, confirming the relationship between this zone, the chemistry and the microstructure of the body.

ACKNOWLEDGEMENTS

The authors thank Bruno Fabbri for the discussion and Federica Fontana (Agenzia Polo Ceramico) for her help with the preparation of products.

This research has been realised with Agenzia 2000 funds.

REFERENCES

Fabbri B., Gualtieri S., Lega A.M., 2000, Application technology and composition of the glazes of the Renaissance "Italo-moresque and diluted zaffera" majolica manufactured in Faenza (Italy), Proc. of 32nd International Symposium Archaeometry, Mexico City 2000.

Fabbri B., Dondi M., 1995, *Caratteristiche e difetti del laterizio*. Gruppo editoriale Faenza editrice, Faenza.

EVIDENCE FOR THE PERIOD OF DISTRIBUTION OF EUROPEAN GLASS BEADS AT THE SPANISH MISSION OF TIPU IN BELIZE

R.G.V. Hancock
Department of Chemical Engineering and Applied Chemistry, University of Toronto, Toronto, Canada, M5S 3E5

E. Graham
Institute of Archaeology, University College London, 31-34 Gordon Square, London, WC1H 0PY, England

1. INTRODUCTION

A Spanish mission was established at the Maya town of Tipu in Belize in the mid-16th century. It was actively administered until the area was disrupted by a Maya rebellion in 1638-41 (Jones 1989). Several buildings comprising Tipu's historic central precinct have been excavated (Graham 1991; Graham and Bennett 1989; Graham *et al*. 1985, 1989). Among these was the mission church, from the nave and environs of which 585 burials were recovered (Cohen et al. 1989, 1994, 1997; Danforth *et al.* 1997; Jacobi 2000:86). Nineteen of these 585 burials contained European glass beads that formed parts of necklaces, bracelets or earrings (Smith *et al*. 1994:27-29).

European-made glass trade beads have been analysed and reported in the literature (Hancock *et al*. 1994, 1996, 1997; Sempowski *et al*.1999); therefore it is possible to compare data on glass beads from Tipu with published data to add to our knowledge of the chronology of the burials with bead accompaniments at Tipu.

2. EXPERIMENTAL

Eighty glass beads from Tipu, Belize were analyzed non-destructively using instrumental neutron activation analysis at the SLOWPOKE Reactor Facility of the University of Toronto. Beads of mass 5-10 mg were first cleaned ultrasonically, as required. They were stored individually in 1.2 ml polyethylene vials, were irradiated serially for 5 minutes at a neutron flux of 1.0×10^{12} neutrons.cm^{-2}.sec^{-1}. Five to 7 minutes after irradiation, the induced

radioactivity was counted for 5 minutes using a hyper-pure germanium detector-based gamma-ray spectrometer. This produced analytical concentration data for Co, Sn, Cu, Na, Al, Mn, Cl and Ca. The samples were recounted for 5 to 33 minutes the next day to measure the concentrations of the longer-lived radioisotopes of Na, As, Sb and K. The sodium measurements were used to link both counts. Elemental concentrations were calculated using the comparator method. Beads of larger masses were irradiated at suitably lower neutron fluxes to make enough radioactivity for reasonable chemical analyses.

3. RESULTS AND DISCUSSION

Specific glass bead-producing burials, along with bead colours and sizes, are presented in table 1. Included are 23 turquoise blue beads, 30 dark / royal blue beads, 19 white / ivory beads, and 8 purple beads. The beads came in different shapes (circular, round and tubular) and sizes (smallest glass fragment 5.1 mg; smallest seed bead 6.2 mg; largest tubular bead 1479 mg).

Burial	Green	Dark Blue	Turquoise	White	Purple	Ivory
75	-	-	1	-	-	-
95	-	-	2	-	-	-
139	-	2+4s	6s	1	8s	10s
247	1	-	-	-	-	-
361	-	-	1	-	-	-
362	-	-	-	1	-	-
363	-	-	1	2	-	-
379	-	1	-	-	-	-
397	-	-	-	2	-	-
427	3	10s	-	5s	-	-
533	8s	1+4s	5	-	-	-
nb	-	1	-	-	-	-

s = seed nb = non-burial

Table 1. Summary of bead burials, sizes and colours.

3.1. Turquoise blue beads

The turquoise blue beads were all made of soda-lime-silica glasses and were coloured with copper (0.3 % to 1.6 %). Pale variants were opacified with tin at levels of 1.4 % to 7.0 %. Of the twenty-three turquoise beads, four exhibited distinct chemistries; 6 beads formed 3 chemical pairs; the final 13 beads formed 2 chemical groupings.

Six of the turquoise beads have very high sodium contents (≈13 %), similar to beads found in Ontario, Canada, and associated with Bead Period II (≈1600-1620) (Hancock *et al*., 1994), as may be seen in table 2.

Element	BP I ≈1580-1600 33 beads	BPII ≈1600-1620 6 beads	BPIII ≈1620-1650 41 beads	Tipu Belize 6 beads
Al %	0.63±0.16	0.59±0.07	0.62±0.20	0.77±0.03
Ca %	1.8±0.7	3.3±0.6	3.4±1.0	3.1±0.1
Cl %	1.29±0.15	1.57±0.22	1.55±0.26	1.47±0.07
Cu %	1.23±0.23	0.80±0.20	0.97±0.28	1.46±0.37
Mn ppm	320±250	430±470	660±490	330±60
Na %	10.2±1.0	13.1±0.3	11.4±0.7	13.4±0.2

Table 2. Comparison of the soda-rich turquoise blue beads with 17th century literature data.

3.2. Royal blue beads

Of the dark / royal blue beads, only one was coloured with a combination of cobalt and copper. All of the rest were coloured with cobalt at levels ranging between 270 ppm and 2000 ppm, with the As varying between 990 ppm and 5700 ppm. The probable association of arsenic and cobalt has been observed previously in early 17th century royal blue beads excavated in north-eastern North America (Hancock *et al*. 2000). As with the turquoise blue beads, some of the royal blue beads were opacified with tin (0.5 % to 3.5 %). In the royal blue bead sampling, there were 7 singletons, 1 pair, and 3 groupings.

3.3. White beads

The 19 white beads represent 3 distinct manufacturing technologies / materials. There are 2 very high Ca (34 %) beads. Next come 6 lead-silica glass beads; 2 single beads and a grouping of 4 beads, all of which are opacified with Sn. Finally, there are 10 soda-lime-silica glass beads that form at least two chemical groupings, some of which are opacified with Sn. Tin opacification, with no hint of Sb opacification, implies that the opacified beads were made in Europe before about 1625-1650 CE (Hancock *et al*., 1997, 1999; Sempowski *et al*., 2000).

3.4. Purple beads

The 8 purple, manganese-rich beads form 2 chemical groupings. All of these beads came from the same burial (B139).

4. CONCLUSIONS

Some of the turquoise blue beads were similar chemically to beads found in Ontario, Canada from Bead Period II (≈1600-1620). Royal blue beads are consistent with beads made and traded to North America in the early 17th century. Beads opacified with tin were made in Europe before at least ≈1620-1650. All three findings are consistent with the proposal that most of the European goods were brought into Tipu during the active mission period that began in the mid-16th century and largely ended with the Belize Maya rebellion in 1638-1641.

REFERENCES

Cohen, M.N., Bennett, S., and Armstrong, C., 1989, *Final Report to the National Science Foundation on Grant BNS-85-06785, Health and Genetic Relationships in a Colonial Maya Populations,* Ms. on file at the Dept. of Anthropology, SUNY, Plattsburgh.

Cohen, M.N., O'Connor, K., Danforth, M., Jacobi, K., and Armstrong, C., 1994, Health and Death at Tipu, In *In the Wake of Contact,* (eds. .S. Larsen and G.R. Milner), Wiley-Liss, New York, 121-133.

Cohen, M.N., O'Connor, K., Danforth, M., Jacobi, K., and Armstrong, C., 1997, Archaeology and Osteology of the Tipu Site, In *Bones of the Maya: Studies of Ancient Skeletons,* ed. by S.L. Whittington and D.M. Reed, Smithsonian Institution Press, Whashington, D.C., 78-86.

Danforth, M.E., Jacobi, K.P., and Cohen, M.N., 1997, Gender and Health among the Colonial Maya of Tipu, Belize, *Ancient Mesoamerica,* 8(1), 13-22.

Graham, E., 1991, Archaeological Insights into Colonial Period Maya Life at Tipu, Belize, In *Columbian Consequences, Volume 3: The Spanish Borderlands in Pan-American Perspective,* (ed. D.H. Thomas), Smithsonian Institution Press, Washington, D.C., 319-335.

Graham, E. and Bennett, S., 1989, The 1986-1987 Excavations at Negroman-Tipu, Belize. *Mexicon,* 11(6), 114-117.

Graham, E., Jones, G.D., and Kautz, R.R., 1985, Archaeology and Ethnohistory on a Spanish Colonial Frontier: The Macal-Tipu Project in Western Belize. In *The Lowland Maya Postclassic,* (eds. A.F. Chase and P.M. Rice), University of Texas Press, Austin, 206-214.

Graham, E., Pendergast, D.M., and Jones, G.D., 1989, On the Fringes of Conquest: Maya-Spanish Contact in Early Belize, *Science,* 246, 1254-1259.

Hancock, R.G.V., Chafe, A. and Kenyon, I., 1994, Neutron activation analysis of sixteenth and seventeenth century European blue glass trade beads from the eastern Great Lakes Region of North America, *Archaeometry*, 36(2), 253-266.

Hancock, R.G.V., Aufreiter, S., and Kenyon, I., 1997, European white glass trade beads as chronological markers, in *Materials Issues in Art and Archaeology*, Materials Research Society, Pittsburg, U.S.A., 462, 181-191.

Hancock, R.G.V., Aufreiter, S., Kenyon, I. and Latta, M., 1999, White glass beads from the Auger Site, southern Ontario, Canada, *Journal of Archaeological Science*, 26, 907-912.

Hancock, R.G.V., Aufreiter, S., Moreau J.-F., and Kenyon, I., 1996, Chemical chronology of turquoise blue glass trade beads from the lac-saint-Jean region of Québec, in *Archaeological Chemistry: Organic, Inorganic and Biochemical Analysis* (ed. M.V. Orna), 23-36.

Hancock, R.G.V, McKechnie, J., Aufreiter, S., Karklins, K., Kapches, M., Sempowski, M., Moreau, J.-F., Kenyon, I, 2000, The non-destructive analysis of European cobalt blue glass trade beads, *Journal of Radioanalytical and Nuclear Chemistry*, 244(3), 567-573.

Jones, G.D., 1989, Maya Resistance to Spanish Rule: Time and History on a Colonial Frontier, University of New Mexico Press, Albuquerque.

Sempowski, M., Nohe, A.W., Moreau, J.-F., Kenyon, I., Karklins, K., Aufreiter, S., Hancock, R.G.V., 2000, On the transition from tin-rich to antimony-rich European white soda-glass trade beads in northeastern North America, *Journal of Radioanalytical and Nuclear Chemistry*, 244(3), 559-566.

Smith, M.T., Graham, E. and Pendergast, D.M., 1994. European Beads from Spanish Colonial Lamanai and Tipu, Belize. *Beads: Journal of the Society of Bead Researchers* 6, 27-49.

THE EARLY ISLAMIC GLAZED CERAMICS OF AKHSIKET, UZBEKISTAN

C. Henshaw, Th. Rehren
Institute of Archaeology, 31-34 Gordon Square, London WC1H 0PY

O. Papachristou
Haras 12. Neo Iraklio. 14121 Athens, Greece

A.A. Anarbaev
Institute of Archaeology, Samarkand, Uzbekistan

1. THE SITE

Poised on the edge of a plateau overlooking the Syr Darya river, the site of Akhsiket is preserved by abandonment – defensive walls and towers are now grassy mounds, the town with its market place, densely packed housing and industrial areas is now a gently undulating field, with a high citadel in the SW corner. Akhsiket is located in the Ferghana Valley of Uzbekistan, part of the growing Islamic Empire from 715 AD until the Mongol invasions of the early 12th century, and a regional capital from the 8th to 10th century AD according to the written sources and the archaeological evidence (Anarbaev & Rehren, unpub.).

2. THE PROJECT

Akhsiket has been excavated for many years, but until recently no scientific analysis had been undertaken on any of its finds. A joint project, begun in 1999 by the Institutes of Archaeology at UCL and Samarkand, focuses on the analysis of ceramic steel-making crucibles (Papakhristu & Rehren 2002). The glazed ware project is also conducted in conjunction with Samarkand, and it is their work on the typology and stratigraphy of the pottery that makes the project possible. The purpose of this paper is to introduce a research project focusing on the glazed fineware, which are found in large quantities in the medieval layers of the site. Incorporating optical, scanning electron and microprobe microscopy, typological analysis and petrography, the data retrieved will provide a framework for future studies.

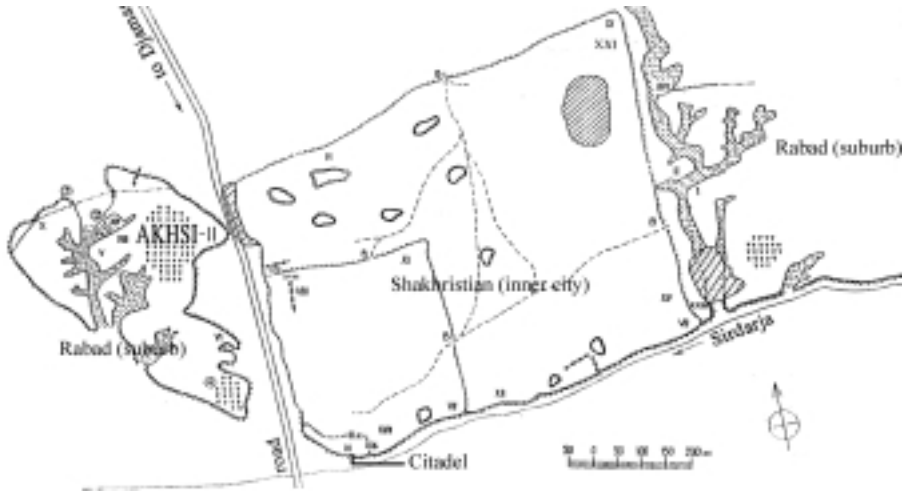

Figure 1. Map of Akhsiket.

These research issues will be addressed: What raw materials were used, and did technology change over time? Does the evidence support the working chronology that is already in use? Was there a glazed fineware industry at Akhsiket? What comparisons can be made to pottery from other sites? Is it possible to interpret the role of ceramics in the social and economic environment at Akhsiket using the data collected? With these questions in mind, samples have been taken from both common types and 'exotic' examples. This pilot sampling strategy is targeted to make available for study a range of wares, which will hopefully provide a basis for an informed sampling strategy in future research.

3. POLYCHROME SLIPWARE

The predominant glazed ware present on the site is polychrome underglaze, applied to simple bowl forms and lamps. This type of glazed decoration is an innovation of earlier traditions of high-lead glazes dating back to the Hellenistic period (Kleinmann 1986, 73). Black, brown, red, olive and occasionally yellow slips were painted onto a white engobe, then covered with a colourless lead glaze. Several design types are present, including geometrical and linear patterns, interlacing, floral 'bouquets' and 'rosettes', and pseudo-kufic epigraphical.

So far the colourless lead glazes on these polychrome wares show a high lead content, with 47-61%. In the 3 samples so far analysed with a black/brown decoration, each has a different technique. One is typical slip-paint

with MnO under a true colourless lead glaze (see table 1), another has a lead glaze of average composition applied directly to the engobe, but with a crystalline interface layer that has small amounts of MnO and is rich in Fe_2O_3, while the dark brown example is a lead glaze also applied directly to the engobe, but coloured with MnO and Fe_2O_3. More work must be done to determine whether these differences are significant.

The white slip engobe, which covers nearly the entire vessel, is based on crushed quartz mixed with clay, with a high alumina content and up to 13% PbO. The coloured slips have essentially the same composition as the engobe with the addition of colourants as follows: 16-18% PbO and 1% Fe_2O_3 for red and 5-10% Cr_2O_3 and 2-5% Fe_2O_3 for olive. Yellow and lighter brown slips have yet to be analysed. The presence of chromium oxide as a colorant in the olive slips is unusual, although not unheard-of for this time period – it could be that glaze makers discovered the use of chromium as a side effect of extracting iron from chromite, the location of which could shed light on provenance of the glaze.

4. ISHKOR

Another type of glazed pottery that is common throughout the time span of Akhsiket's medieval development is ishkor ware. Ishkor (as it is defined here) is similar to the ancient Mesopotamian glass of the Late Bronze Age, with a basic quartz + plant ash mixture (Kleinmann 1986, 79). An alkaline glaze, the colours are either turquoise blue of varying shades or lilac. Other alkaline glazes exist, such as matte black and green, but these are very different in their vessel form and design. Ishkor is applied directly onto the earthenware body, and is partially transparent. The ishkor designs are fairly simple with only two colours or shades present, and usually consist of blue strokes forming geometric or floral designs with a lilac or lighter blue 'background'.

The composition of ishkor glaze is silica-based with notable amounts of all the typical alkalies and alkaline earths, as can be seen in table 1. The colours are produced with MnO and CuO, with changes in hue caused by variations in the amount of copper oxide present. The example in table 1 shows compositions for the darker blues only. The lilac composition indicates that the reduction of CuO rather than an increase of MnO compared to the blues is responsible for the colour, plus the presence of nearly 10% TiO_2. The fact that copper rather than cobalt is used for the blue colours of ishkor glaze is consistent with the ancient alkaline glaze technique. Cobalt was not used in Central Asia at all, although it was popular in the Middle East (Keblow Bernsted 2003, 4-5). The grey wares, although tentatively grouped here with blue ishkor, may belong to a separate group considering the lack of copper oxide and the lower amounts of soda.

	Na2O	MgO	Al2O3	SiO2	K2O	CaO	TiO2	MnO	Fe2O3	PbO	CuO	Cr2O3
Glaze Colourless n=5	0.6		2.7	42	2.0	0.8		0.3	0.9	51.4		
D. Brown n=1	1.0		2.9	36	2.4	1.7		2.7	5.3	48		
Black n=1	0.9		11	48	3.3			0.7	12	20.4		
Blue/turquoise n=3	5.7	2.0	3.4	67	5.3	6.5		1.7	1.4		5.3	
Lilac n=1	5.7	4.7	3.9	67	0.6	3.4	9.7	1.6	2.2		1.2	
Grey n=1	2.6	1.7	3.0	66	7.9	9.4	0.5	2.7	1.9			
Slip White/ engobe n=5	0.8	1.6	16.6	60	5.8	4.2	0.6		0.7	9.8		
Black/ brown n=1		0.6	9.3	44	2.9	1.2	0.7	3.7	28	8.9		
Red n=2	0.3	1.2	15.0	57	5.2	1.4			3.0	18.4		
Olive n=2	0.4	2.6	10.3	61	3.7	2.2	0.5		3.5	7.1		9.0
Body –Glazed Average n=8	1.0	3.0	11.4	55	3.4	18	0.7		6.2	0.4		
St. Dev.	0.7	2.2	4.0	8.0	2.7	6.9	0.4		1.8	1.0		
Body -Unglazed Average n=13	1.5	3.6	12.7	58	3.0	15	0.5		5.4			
St. Dev.	0.2	0.3	1.0	4.0	0.2	0.8	0.01		0.4			

Table 1. Table of average compositions.

5. COMPARISON

There are many other fabrics and glaze designs that do not fall into these groups, and part of this project is to determine what range of variation there is in these 'exotic' sherds, and where they could have been produced. Comparative material that may shed light on these includes pottery from Kuva, which succeeded Akhsiket as regional capital in the 11th century (Shirinov, *et al*. 1998, 26), while Samarkand and Chach (Tashkent) are potential sources of imports. Regarding the wider influence of glazing techniques, comparison can be made to material from Merv, Turkmenistan, as a cultural and trading centre of prime importance on the Silk Road. Pottery from Merv has been studied at UCL – making the material accessible and comparable in terms of analytical strategies.

While the fabrics of all the sherds sampled do vary, the underglaze and ishkor wares are fairly uniform – red or buff earthenware with very small inclusions of quartz and other minerals and no temper. Analyses of the finer unglazed wares show similar chemical compositions to the glazed pottery, indicating that the most commonly found glazed wares were produced at or near Akhsiket.

6. FURTHER WORK

The research strategy for the present study is of course geared towards enabling further research based on sound preliminary data. Comparisons to

pre-Islamic pottery and 14th – 15th century Timurid glazes to investigate a wider chronology of technological change would need to be conducted, as well as analysis in greater quantity of the other types of glazed wares mentioned above to confirm preliminary estimates of relationships and provenance. Further comparison to glass remains would help determine whether there is any relation between glass-making materials and glaze. A pilot study on glasses (Jolley 2003) shows that so far there is some difference in composition between the glasses and the glaze, as is necessary due to the differing working conditions. Continued analysis of stylistic motifs and comparisons with other decorated material in the wider Islamic world is needed to complement any scientific analysis.

7. CONCLUSION

There is still a long way to go as far as data collection and analysis is concerned, but a basic characterisation of the pottery at Akhsiket is beginning to form. As with any comparable pilot study, the research questions are necessarily basic, being concerned mainly with interpretations of technology and chronology. While these questions assume the importance of glazed pottery to understanding the society of Akhsiket and hopefully the wider region, a higher order of interpretation may not be possible until further work can be done as mentioned above. However, the very existence of such pottery, its widespread use, and the possibilities of industry and/or trade bring up many interesting questions that will need exploring.

REFERENCES

Anarbaev, A.A. & Rehren, Th. *Akhsiket*. Unpublished.

Blue of Samarkand, 2000. in Proc. Symp. On Revitalization of Traditional Ceramic Techniques in Central Asia. UNESCO: Samarkand.

Jolley, C.L. 2003. *Analysis of Glass from Ahsiket, Uzbekistan*. MSc Dissertation, UCL.

Keblow Bernsted, A. 2003. *Early Islamic Pottery.* Archetype: London.

Kleinmann, B. 1986. 'History and development of Early Islamic Pottery Glazes.' In J.S. Olin & M.J. Blackman (eds.) *Proc. 24th Intl. Archaeometry Symp*, 73-85.

Papakhristu, O. & Rehren, Th. (2002) 'Techniques and technology of ceramic vessel manufacture – Crucibles for wootz smelting in Central Asia.' in V. Kilikoglou, *et al.* (eds.) *Modern Trends in Scientific Studies on Ancient Ceramics*. BAR Intl. Series 1011, 69-74.

Shirinov, T. Sh, *et al.* (1998) *Kubo: City in Akhmad Al-Fargoni.* FAN: Tashkent.

EUROPEAN GLASS TRADE BEADS, NEUTRON ACTIVATION ANALYSIS, AND THE HISTORICAL IMPLICATIONS OF DATING SEASONAL BASQUE WHALING STATIONS IN THE NEW WORLD

A. Herzog
Département d'histoire, Université Laval, Québec (Québec), Canada, G1K 7P4, anja@oricom.ca

J.-F. Moreau
Laboratoire d'archéologie et Département des sciences humaines, Université du Québec à Chicoutimi, Chicoutimi (Québec), Canada, G7H 2B1, jfmoreau@uqac.ca

1. GENERAL HISTORIC CONTEXT AND SPECIFIC RESEARCH PROJECT

Basque whalers were among the first Europeans to frequent northeastern North America from the early 16th century onwards and their seasonal sites known today can be found along the coasts of Eastern Canada (fig. 1). These sites, mainly clustered at the eastern fringe of the Gulf of St. Lawrence as well as further to the west, near the mouth of the Saguenay River, have proved difficult to date with precision, mainly due to the lack of chronologically short-lived artefact types. Written sources allow for a general dating to the period of 1540 to 1640, without further refinements. After this time, the Basque whale fisheries are said to have declined and virtually disappeared in the region. Basques have also played an active part in the development of the fur trade from the 1580s onwards. During the early 17th century, this trade became subject to successive monopolies granted by the king of France to trading companies in an effort to boost the establishement of a French colony in the St. Lawrence Valley, thus potentially depriving Basques of a lucrative source of income and affecting their seasonal activities in North America. One of the commodities traded in exchange for furs were glass beads, nowadays to be found on a regular basis on protohistoric sites in eastern North-America. In 2001, a new Basque settlement was discovered on Petit Mécatina Island, off Quebec's Lower North Shore (fig. 1; Fitzhugh, 2001). The artefact assemblage of this site differs from other Basque sites known and raises questions on the

possibility of a continous Basque presence in North America even after the implantation of a permanent French colony. Among the collection, there were several glass beads (fig 2).

Figure 1. 16th and 17th Century Basque Whaling Stations in Eastern Canada.

Figure 2. Glass Beads from the Petit Mécatina Collection.

2. THE STUDY OF GLASS BEADS

Over the past few decades, North-American archaeologists have used classifications based on morpho-typological characteristics and site contexts to date glass beads. By now, researchers also have successfully applied Neutron Activation Analysis to samples of monochrome beads taken from sites in eastern North America and Europe, in an effort to refine chronologies by comparing the elemental composition of beads belonging to the same colour group. Six of the Petit Mécatina beads were analysed and the results for five of them could be compared to existing data (fig. 2, tables 1 and 2).

Artefact #	Description	Condition	Diameter	Height
EdBt-3:274[1]	Black, round bead, with inset of three white alternating wavy lines	Fragmentary	11 mm	9 mm
EdBt-3:275	Black, round bead	Whole	7 mm	5 mm
EdBt-3:276	Red, round bead	Fragmentary	7 mm	6.5 mm
EdBt-3:277	White, circular bead (seed bead)	Whole	4 mm	3 mm
EdBt-3:278[2]	Navy blue, circular bead (seed bead)	Whole	3,5 mm	2 mm
EdBt-3:279	Turquoise, circular bead (seed bead)	Fragmentary	3,2 mm	2,1 mm
EdBt-3:280	Turquoise, circular bead (seed bead)	Fragmentary	2,5 mm	2 mm

1. This specimen could not be analysed as only monochrome beads yield reliable results for comparison.

2. Insufficient comparative data is available for navy blue beads for establishing chronological sequences.

Table 1. Technical Information on the Petit Mécatina Glass Beads.

2.1. Methodology of Analysis

In a nuclear reactor, the beads were irradiated serially for five minutes at 5 kW power with a neutron flux of 2.5 x 10^{11} neutrons cm^{-2} s^{-1}. After a delay time of five to seven minutes, each bead was assayed for five minutes for its gamma-ray activity using a Ge-detector based gamma-ray spectrometer to produce data for Al, Ca, Cl, Co, Cu, Mn, Na, and Sn. After one to three hours, they were recounted for 600 – 2000 s (depending on the level of K) to analyse for As, K, Na and Sb, with Na linking the two countings to ensure analytical credibility (Moreau *et al.*, 1997). The results are presented in table 2.

Bead \ Element	Al %	Ca %	Cl %	Co ppm	Cu %	Mn ppm	K %	Na %	Sn ppm	As ppm	Sb ppm
EdBt-3:277, white	0.83	7.12	0.7	≤ 51	≤ 0.031	2536	1.23	8.385	≤ 1286	≤ 127	27530
EdBt-3:279, turquoise	0.42	4.87	1.77	181	0.58	165	1.45	12.15	≤ 1109	≤ 168	≤ 266
EdBt-3:280, turquoise	0.28	3.38	1.07	222	0.66	272	1.22	10.03	≤ 880	≤ 254	≤ 381
EdBt-3:275, black	1.23	7.66	0.51	≤ 144	≤ 0.077	56990	0.99	7.86	≤ 6783	≤ 85	≤ 133
EdBt-3:276, red	1.75	4.88	0.92	55	0.5	4224	0.74	9.28	≤ 1948	≤ 69	980
EdBt-3:278, navy blue	0.95	6.7	0.37	490	≤ 0.03	374	2.13	9.16	≤ 995	297	17660

Table 2. Elemental Composition of the Petit Mécatina Glass Beads.

2.2. White and Turquoise Beads

The elemental composition of Petit Mécatina's white bead was compared to sequences established for the same type of bead in Québec (Moreau *et al.*, 2002). When justified by the size of the sample, the 50 year intervals used originally were replaced by 25 year intervals. The resulting time periods per element were compared and a manufacturing date situated between 1675 and 1730 was

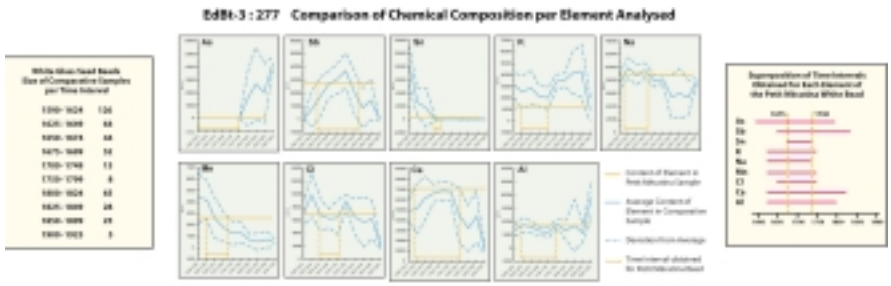

Figure 3. Analysis of the Petit Mécatina White Glass Bead.

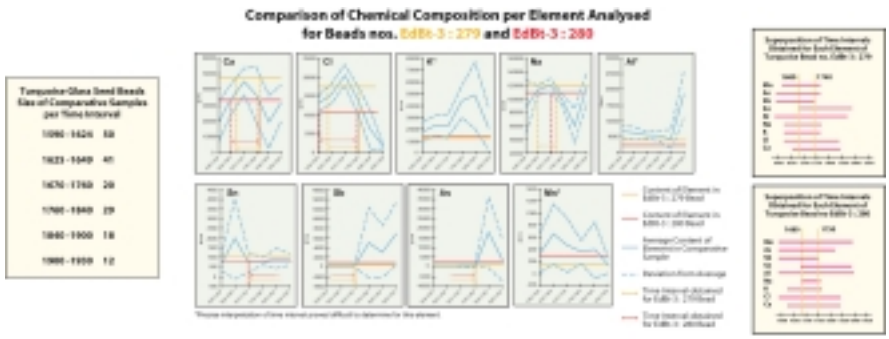

Figure 4. Analysis of the Petit Mécatina Turquoise Glass Beads.

obtained (fig. 3). Petit Mécatina's turquoise beads were compared to sequences of irregular intervals, necessary due to the great variability of the size of the samples available for these chronologies (Hancock *et al.*, 1996). The comparison of the resulting intervals per element lead to a date situated between 1680 and 1740 for bead EdBt-3:279, and between 1680 and 1750 for bead. EdBt-3:280 (fig. 4).

2.3. Black and Red Beads

For the black and red beads, no continuous sequences are available for comparison. For the black bead, samples come from Amsterdam and two sites in eastern Canada and the periods for which data is available are the early 17th century, the mid-17th century and the first half of the 18th century (Karklins *et al.*, 2002; Moreau *et al.*, 1997, 2002). Factor analysis using *Statistica* was applied to treat the data statistically. A table illustrating the relative importance of the different elements preceeds the diagram presenting the Petit Mécatina bead's relative position in this series. Being situated between the Amerstdam low and high K beads dated to ca. 1610 and the Sillery beads of the mid-17th century, this bead was tentatively dated to the decade of 1620 to 1630 (fig. 5). For the red bead, a large sample of 127 beads is available from the Amsterdam ca. 1610 context (Karklins *et al.*, 2002), and three smaller

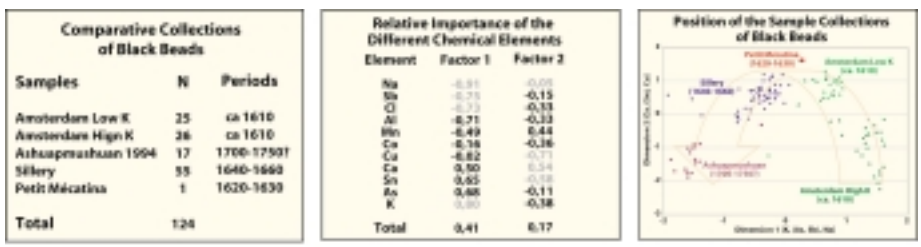

Comparative Collections of Black Beads

Samples	N	Periods
Amsterdam Low K	25	ca 1610
Amsterdam High K	26	ca 1610
Ashuapmushuan 1994	17	1700-1750?
Sillery	55	1640-1660
Petit Mécatina	1	1620-1630
Total	124	

Relative Importance of the Different Chemical Elements

Element	Factor 1	Factor 2
Na	-0,91	-0,08
Mg	-0,75	-0,15
Cl	-0,73	-0,33
Al	-0,71	-0,33
Mn	-0,49	0,44
Ca	-0,18	-0,36
Cu	-0,82	-0,71
Ca	0,50	0,34
Sn	0,65	-0,58
As	0,88	-0,11
K	-0,80	-0,38
Total	0,41	0,17

Position of the Sample Collections of Black Beads

Figure 5. Analysis of the Petit Mécatina Black Glass Bead.

samples come from Québec, two of which dating to about 1625-1650, and the third to a context dated after 1663 (Moreau *et al.*, 1997, 2002). This data was also analysed statistically and the Petit Mécatina bead unequivocally compares to the Chicoutimi post 1663 sample (fig. 6).

3. DISCUSSION

The combination of the results obtained for the white and turquoise beads date the Petit Mécatina site between 1680 and 1730, extensible to 1675-1750 (fig. 7). This result is further confirmed by the minimal date established for the red bead (post 1663). However, the manufacturing date of the black bead

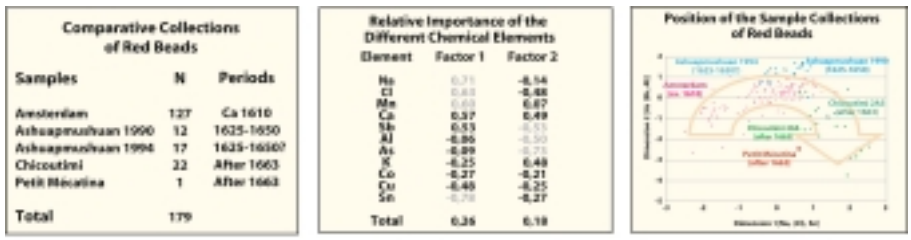

Figure 6. Analysis of the Petit Mécatina Red Glass Bead.

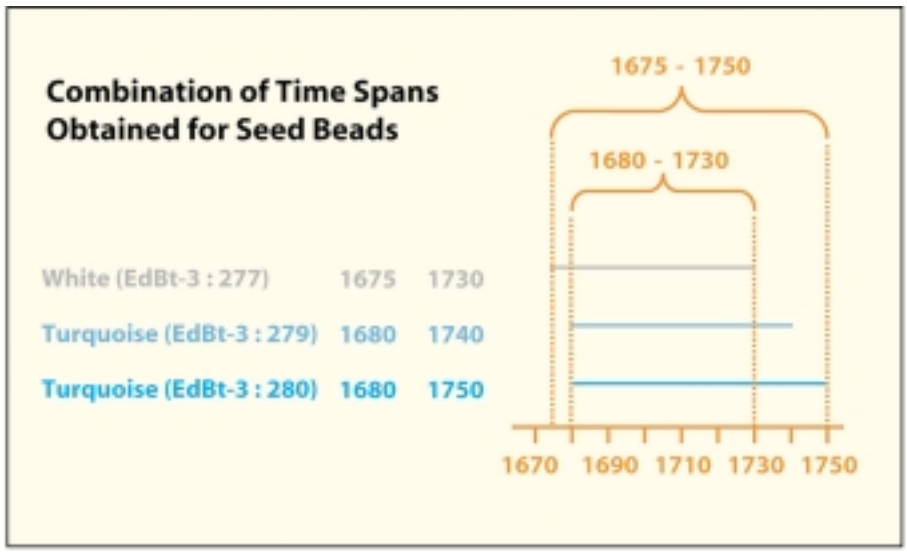

Figure 7. Date of Occupation of the Petit Mécatina Basque Site as Obtained from Analysis of the Seed Beads.

seems to predate the others by several decades, being possibly situated in the 1620s. Petit Mécatina's artefact assemblage does yield several other types of artefacts that may support the results for the majority of the beads. However, the use of some of these objects spans a much longer period starting in the early 17th century. Thus, also considering the early date for the black bead, the possibility of an earlier occupation on this site or a longer occupation period than that known for other Basque sites cannot be entirely excluded.

4. GENERAL CONCLUSION

The application of NAA to the Petit Mécatina site's glass bead collection has allowed for a clearer refinement of the dates of its

occupation than would have been possible by conventional dating data available for other artefact types. The later date of the site points to a Basque presence in the Gulf at a time when they are said to have largely ceased their activities in Eastern Canada. However, before the decline of the whaling industry in North America, this industry is said to have become more and more supplemented by activities like trade with indigenous people. With this trade becoming the monopoly of influential trading companies, incursions into the latter by European fishermen are sometimes mentioned as sources of conflict in the French colony's fur trade. Could Petit Mécatina point to the fact that Basque and other European fishermen might have had the opportunity to continue their trading activities in less controlled regions such as Quebec's Lower North Shore during the late 17th and early 18th century? The relative spatial "isolation" (see fig. 1) as well as the now established later date and the presence of glass beads on this particular Basque site could hint into this direction.

The study of glass beads has made tremendous progress over the past 15 years. The analysis of the chemical composition of various monochrome bead types by NAA has led to the development of chronological sequences that are constantly improving. The Petit Mécatina example, providing only a small sample of beads, has nevertheless shown the capacity of this field of research for providing an innovative dating technique for protohistoric North American archaeological sites. It has the potential of becoming largely independent of archaeological context and written evidence for dating purposes, and may thus help placing archaeological research into a better-defined time scale.

ACKNOWLEDGEMENTS

I am indebted to Dr. Jean-François Moreau, who kindly provided all the details and illustrations on the analysis of the Petit Mécatina glass beads and to Dr. Ron G. V. Hancock, who collected the neutron activation data at the MacMaster University Reactor Facility. Archaeological research on the Petit Mécatina Basque site is carried out by Dr. William W. Fitzhugh of the Smithsonian Institution in Washington, to whom I am grateful for giving me complete access to the archaeological collection. My gratitude also goes to Andrée Héroux, Geographer, who created the location map and edited all the illustrations. I would also like to thank my advisors, Dr. Réginald Auger and Dr. Laurier Turgeon, both of Université Laval, for their support. This project would not have been possible without the financial assistance of the Groupe d'archéométrie, the CÉLAT, the Département d'histoire, and AÉLIÉS, all at Université Laval, Québec.

REFERENCES

Fitzhugh, W. W. 2001, *The Gateways Project 2001: Archaeological Survey of the Quebec Lower North Shore, Gulf of St. Lawrence, from Mingan to Blanc Sablon*. Washington, Smithsonian Institution, National Museum of Natural History, Arctic Studies Center. Submitted to Ministère de la Culture et des Communications du Québec.

Hancock, R. G. V. *et al.* 1996, "Chemical Chronology of Turquoise Blue Glass Trade Beads from the Lac-Saint-Jean Region of Québec" in Orna, M. V., *ed.*, *Archaeological Chemistry. Organic, Inorganic, and Biochemical Analysis*. Washington, American Chemical Society, ACS Symposium Series n° 625, p. 23-36.

Karklins, K. *et al.* 2002, "Analysis of Glass Beads and Glass Recovered from an Early 17th-Century Glassmaking House in Amsterdam" in Jakes, K. A., *dir.*, *Archaeological Chemistry. Materials, Methods, and Meaning*. Washington, American Chemical Society, ACS Symposium Series n° 831, p. 110-127.

Moreau, J.-F. *et al.* 1997, "Taphonomical and Chronological Studies of a Concentration of European Glass Trade Beads from Ashuapmushuan, Central Québec (Canada)", *Iskos* (Finska Fornminnesföreningen) ", 11: 173-181.

—, 2002 "Late French (1700-1750) to Early English (1750-1800) Regime White Glass Trade Beads From A Presumed Decorated Bag Found at the Ashuapmushuan Site (Eastern Central Québec), Canada" in JEREM, E. and K. T. BIRO, *dir.*, *Archaeometry 98. Proceedings of the 31st Symposium*, 2 vol. British Archaeological Research, Coll. BAR International Series n° 1043, p.613-619.

Sempowski, M. L. *et al.* 2001, "Chemical Analysis of 17th-Century Red Glass Trade Beads from Northeastern North America and Amsterdam", *Archaeometry*, 43 (4): 503-515.

COMPARATIVE CERAMIC PETROLOGY OF *"AGUADA PORTEZUELO"* CERAMIC STYLE (*ca.* 650-900 A.D.): A TECHNOLOGICAL APPROACH FOR ITS STUDY AT THE CATAMARCA VALLEY (CATAMARCA VALLEY, PROVINCE OF CATAMARCA, NORTHWESTERN ARGENTINE)

Guillermo A. De La Fuente, Néstor Kristcautzky
Escuela de Arqueología, Universidad Nacional de Catamarca, Campus Universitario s/n, Belgrano N° 300, (4700) Catamarca, Argentina
email: gfuente@arqueologia.unca.edu.ar / nestorkris@yahoo.com

Gustavo Toselli
Laboratorio de Petrología, Facultad de Tecnología y Ciencias Aplicadas, Universidad Nacional de Catamarca, Belgrano 300, (4700) Catamarca, Argentina
email: gtoselli@tecno.unca.edu.ar

1. INTRODUCTION

The Aguada Portezuelo ceramic style (*ca.* 650-900 A.D.) from Northwestern Argentine region presents a great variation and complexity in the manufacture techniques employed by the ancient potters concerning the surface treatments and the decoration applied to the ceramic vessels (cf. Kush 1991, 1996-1997, González 1998). One of the highlight characteristics of these ceramics is their marked polychromy (figure 1 and 2), the motifs are elaborated in negative and positive and the colors used range from purple red, reddish, black and yellow, being this latter color unique in the archaeological ceramics from Northwestern Argentine (cf. González 1998). Sometimes, the colors have not been very well fixed by the firing and they appear as slight and without brightness, presenting also pre- and postfiring paintings (figure 3). Another of the technical decorative aspects very few studied for this ceramic is the existence of resistant negative paintings (cf. González 1998).

Additionally, a manufacture attribute of particular importance is the surface treatment. The internal surface of the vessels is sometimes of an

Figure 1. Aguada Portezuelo ceramic sherd. Postfiring paintings red, black, and brown on-white slip.

intense polished black color and in others it is burnished. Perhaps, it deals with a technical process of smoked of the internal surface of the vessels, but it is necessary to develop specific studies of the technique used to create this visual effect.

The main aspects related to the manufacture processes involved in the shaping and decoration of these vessels have not been fully investigated at the present. The macroscopic and microscopic (binocular microscope, 20X-40X) observations done until now allow to preliminary establish that these ceramic sherds present a very fine-grained and compact ceramic paste, mainly characterised by the presence of rounded quartz sands, biotite and muscovite as the principal mineralogical constituents (González 1998).

In this paper, we present the first results of a comparative ceramic petrology study carried out in a set of ceramic sherds assigned to Aguada Portezuelo style coming from several archaeological sites geographically located in the Catamarca valley (Kriscautzky and Togo 1996), with the main

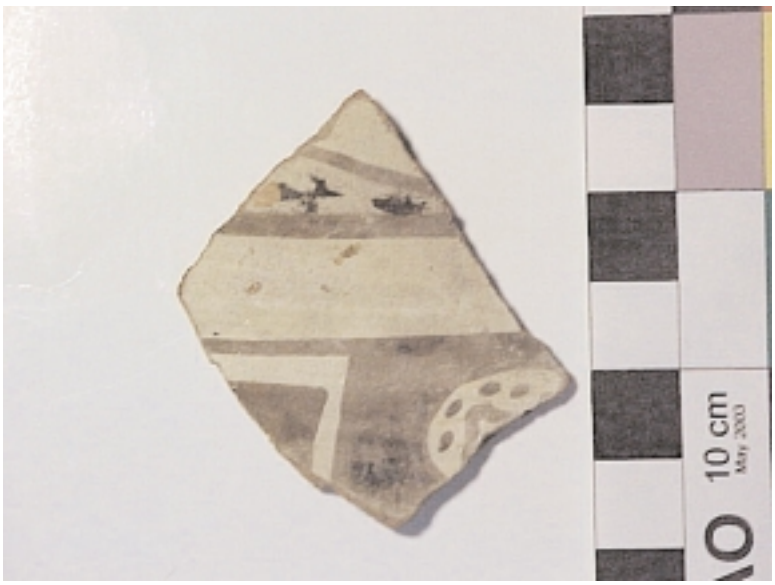

Figure 2. Aguada Portezuelo black-on-white sherd.

aim to discuss the technological characteristics and the manufacture process of this ceramic type and its modalities into the Catamarca valley. Qualitative variables such as type of matrix, porosity, roundness and microfractures, as well as quantitative variables –type of temper identified- are presented and discussed. Additionally, we discuss the utility of ceramic petrology to the study of the specific mineralogy of some kind of slips applied to surfaces of the ceramic vessels.

2. MATERIALS AND METHODS

Thirty-one ceramic sherds were analysed by ceramic petrology. The sherds come from stratigraphical excavations at six archaeological sites located geographically in the Catamarca valley, Province of Catamarca (figure 4). The archaeological sites are ^{14}C dated in the Middle Period (*ca.* 600 – 900 A.D.) belonging to the Aguada Culture of the Northwestern Argentine cultural chronology (cf. Kristcautzky 1996-1997: 27, Kristacautzky and Togo 1996, Gordillo 1996-1997: 23). Most of the sherds belong to subglobular vessels and bowls and they were used in funerary contexts.

The sherds were submitted to petrological analysis (high magnifications, 40X-100X); thus vertical thin-sections were elaborated and analysed by conventional methods applying the total counting area method for quantification of mineral inclusions and rock fragments (cf. Freestone 1991,

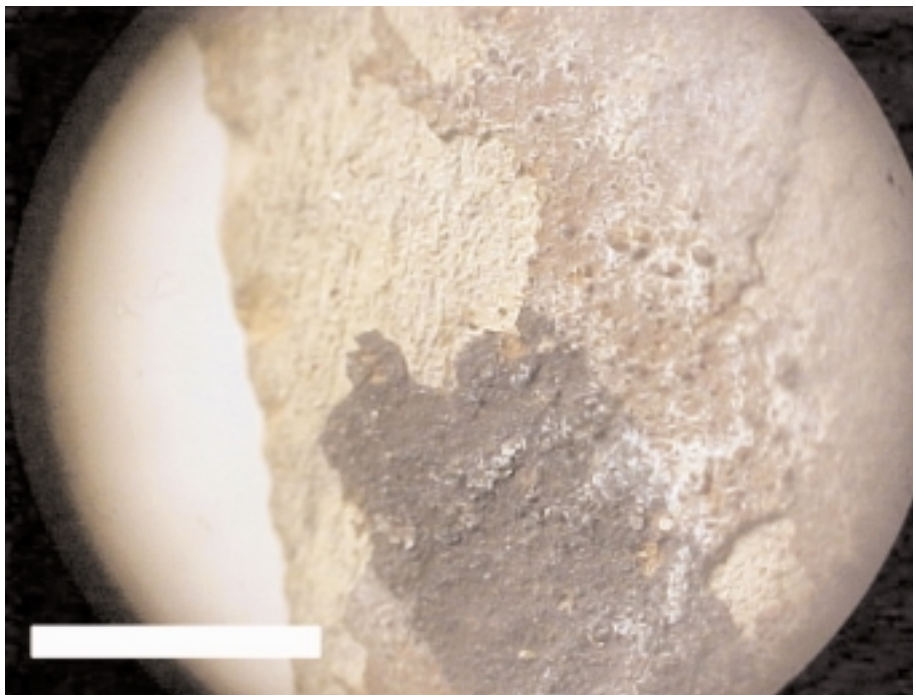

Figure 3. Microphotograph of decoration. Postfiring black and red paintings on white slip –magnification 20X- . Scale: 1 cm.

Middleton, Freestone, and Lesse 1985, Mathew, Woods, and Oliver 1991, Barraclough 1992).

3. RESULTS

The sherds analysed (N=31) present a very homogeneous fabric constitution characterised by a fine-grained compact fabric composed mainly by rounded monocrystalline quartz inclusions, biotite and muscovite. In less amounts there are inclusions of plutonic igneous rock fragments (basically granite) in medium size, primary and secondary calcite, and argillaceous rock fragments; sometimes combined with mafic materials such as amphiboles and pyroxenes with fine size. Polycrystalline quartz is also present in some sherds. All the sherds present a micaceous fine-grained matrix (mainly biotite and in a less extent muscovite).

Table 1 gives details of the temper distribution of a subset of ten (n=10) sherds, which are representative of the whole sample under analysis. The

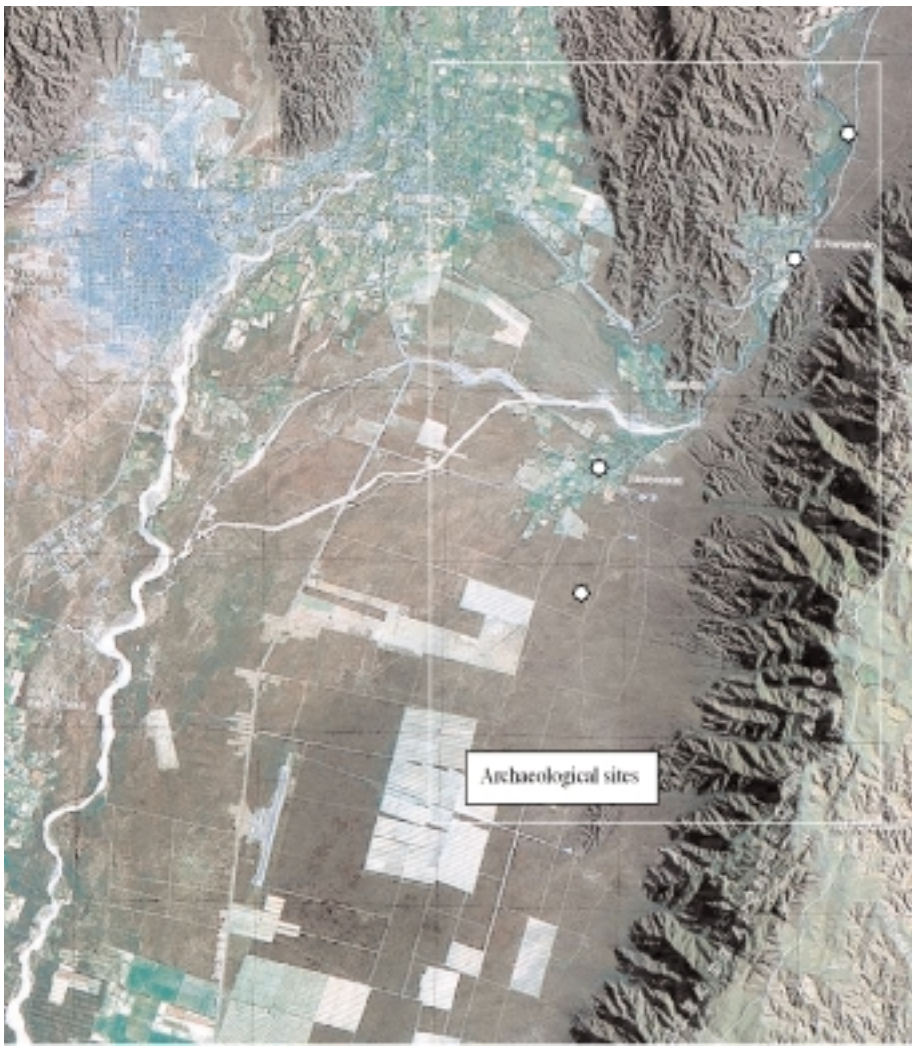

Figure 4. Satellital photograph of Catamarca valley showing the archaeological sites mentioned in the text.

values are expressed as relative percentages (%) of each temper. From this table, it can be observed that 100% of the sherds present rounded quartz grains (Q) as the main temper, combined mainly with biotite (B) and muscovite (M). Other inclusions present in lower proportions are plagioclase feldspar (FPL), igneous rock fragments –granite– (IRF), calcite (Ca), and argillaceous rock fragments (ARF) (figures 5, 6, 7, and 8).

For the whole sampling (N=31) the following observations were made:

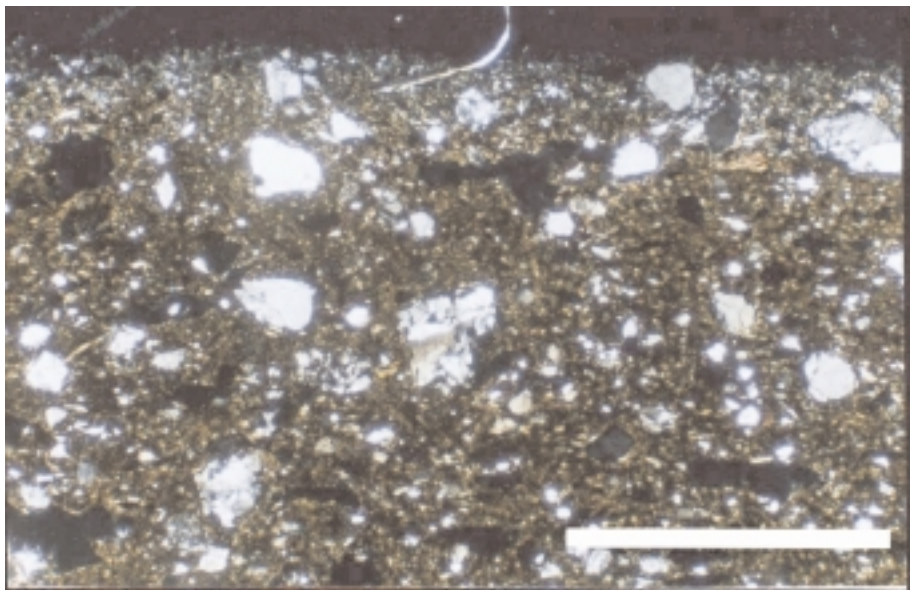

Figure 5. Microphotograph of Port. 001 sherd (XPL). Rounded quartz, biotite, muscovite, polycristalline quartz and igneous rock fragments. Scale: 2.5 mm.

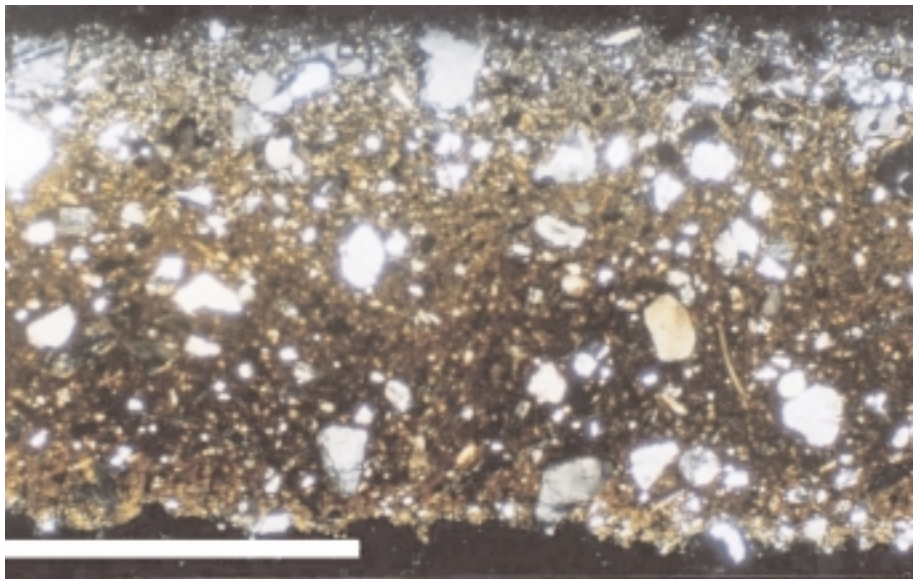

Figure 6. Micrograph of Port. 004 sherd (XPL). Detail of matrix, quartz, biotite, muscovite, and plagioclase feldespar. Observe the rounded quarzt inclusions present in the fabric. Scale: 2.5 mm.

a) Orientation of the inclusions: 25 sherds (80.6%) show a preferred orientation, and 6 sherds (19.4%) do not;

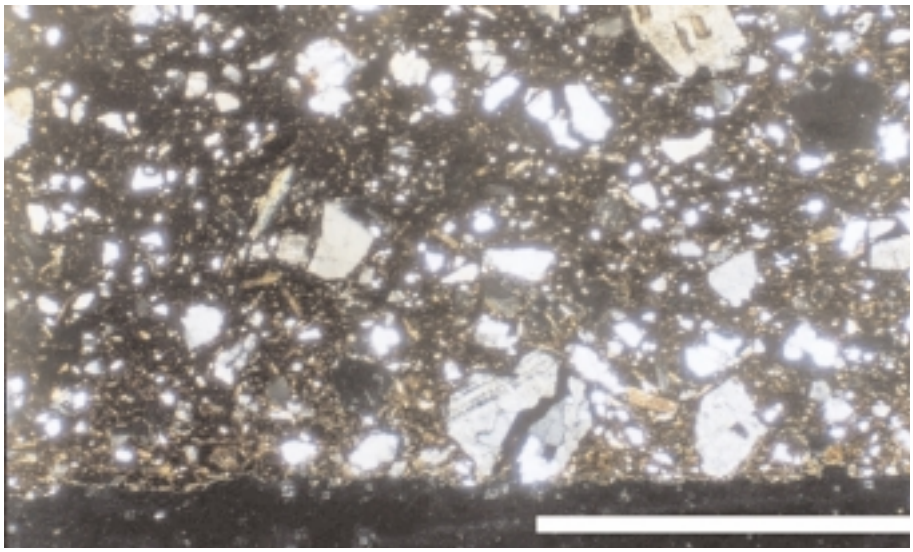

Figure 7. Microphotograph of LCCI 001 sherd (XPL). Matrix, quartz, igneous rock fragment, biotite, muscovite, and sericite-altered feldespar. Scale: 2.5 mm.

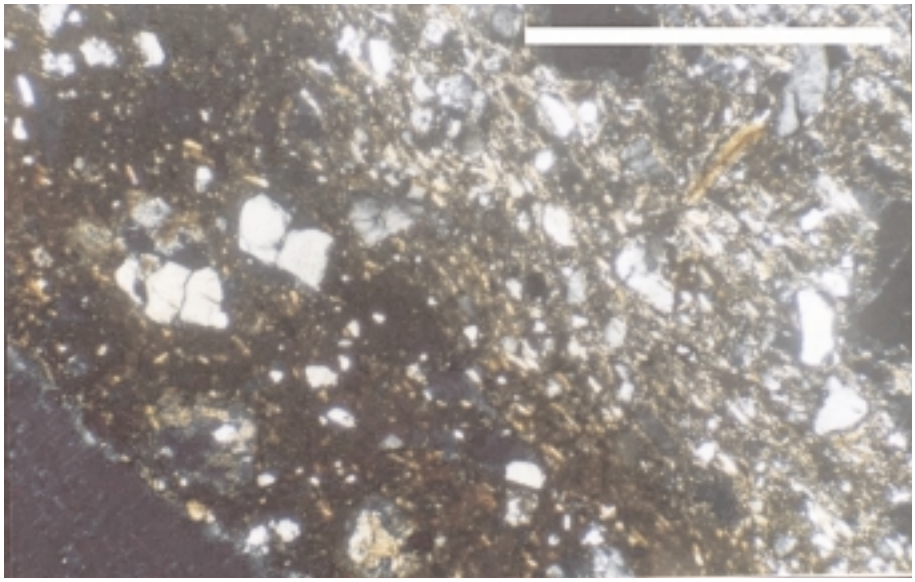

Figure 8. Microphotograph of TFS 750 sherd (XPL). Detail of matrix, quarz, polycristalline quartz, igneous rock fragment, biotite and muscovite. Scale: 2.5 mm.

b) Total proportion of inclusions: 27 sherds (87.09%) have 20% of inclusions by volume, 1 sherd (3.2%) has 15%, and 3 sherds (9.6%) have 10%;

c) Sorting: 19 sherds (61.3%) have fair sorting, 9 sherds (29%) have good sorting, 3 sherds (9.6%) have very good sorting;

d) Anisotropy: all sherds present anisotropic –optically active– characteristics in the matrix;

e) Composition at the bottom: 25 sherds (80.6%) have micaceous content (biotite and muscovite), and 6 sherds (19.3%) have micaceous content (only biotite);

f) The main range size recorded for quartz inclusions was fine (3-4 -0.063-0.25mm-) in the φ grain size scale.

Reference Code	Q	Pl. Q	FPl	B	M	IRF	Ca	ARF	Amph	Px
Port. 001	54	3.7		23	11	5.2				3
Port. 002	50	4.6		23.2	15.9	3.3	3.3(s)			
Port. 003	44		7	25	19	3	2.5(p)			
Port. 004	44.3		5	17	21	8		4.5		
LCCI 001	50	2.5	6.6	24.9	6.6	8.6				
TFS 750	39		7.7	24.5	12.5	7.8	6(s)	2.4		
TFS 548	47.5			27.8	19	5.5				
TFS 358	55				18.5	9.6	9(s)	7.8		
TFS 11	37.6		2	24	18.3	8.4	3	5.4	1.4	
TFS 334	52		5.7	36.3		6.4				

References: Q=quartz, Pl.Q= polycristalline quarz, FPl= plagioclase feldespar, B= biotite, M= muscovite, IRF= igneous rock frament (granite), Ca= calcite - (p) primary, (s) secondary-, ARF= argillaceous rock fragment, Amph= amphibole, Px= piroxene.

Table 1. Distribution of Temper in the sherds analysed.

In general, a good correlation was observed between the data obtained by petrological analysis and those from binocular microscope. Most of sherds analysed present different surface treatments as part of their decoration: (1) the external surface presents a prefiring white slip (10YR 8/1) with postfiring paintings in red (2.5YR 4/2), black (10YR 3/1), and brown (7.5YR 5/4) colors; (2) some of the sherds show a polished brown coloured external surface (7.5YR 6/4) with red (2.5YR 4/2) and black (7.5YR 4/1) postfiring paintings; (3) the internal surface generally present a polished surface of black colour (4/N).

Some sherds such as LCCI 001 and Port. 001 presented a brown slip (10YR 5/3) characterised mainly by the presence of great amounts of biotite

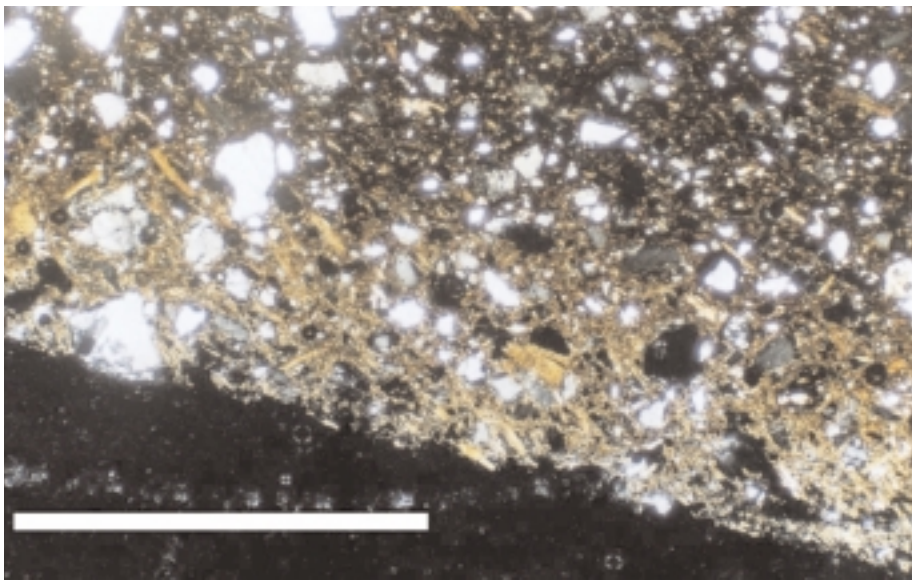

Figure 9. Microphotograph of LCCI 001 sherd (XPL). Matrix, and slip showing a differential mineralogy from the rest of the fabric. Scale: 2.5 mm.

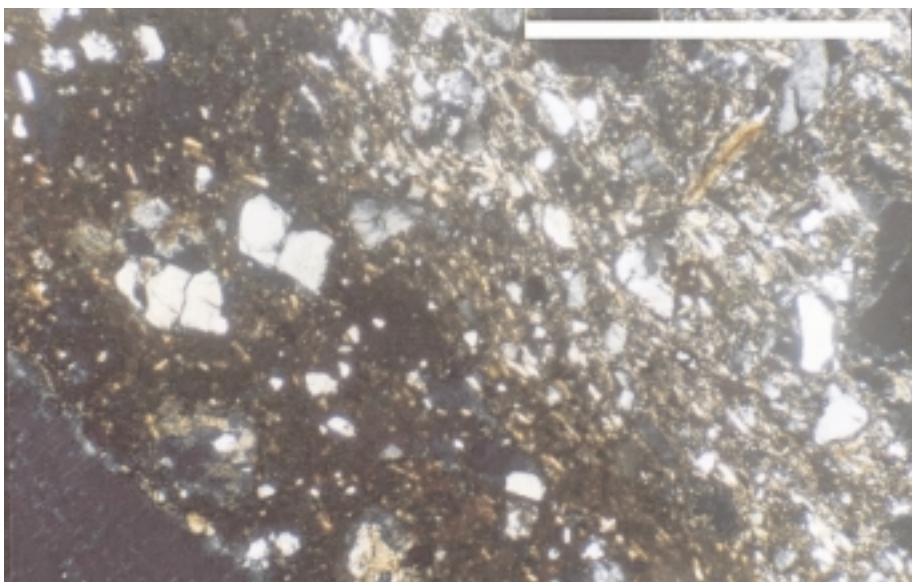

Figure 10. Microphotograph of Port. 002 sherd (XPL). View of the limit between the slip and the matrix. Scale: 1.2 mm.

preferentially oriented and with a different mineralogy from the rest of the fabric (figure 9 and 10). These slips were applied onto a vessel with a reduced fabric (5/N) and then fixed by a second oxidising firing of low temperature and short duration (figures 9, 10 and 11).

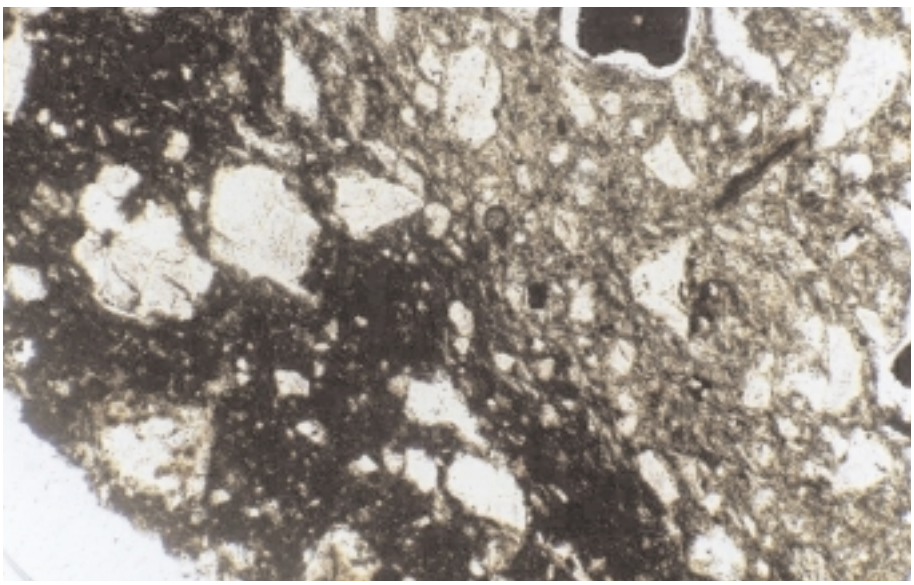

Figure 11. Idem fig. 10 in PPL.

4. DISCUSSION AND CONCLUSION

This preliminary study of comparative petrology revealed that the whole sample analysed (N=31) of ceramic sherds from six different archaeological sites located in the Catamarca valley presented an extremely homogeneous mineralogical composition, mainly characterised by the presence of rounded quartz inclusions –typically belonging to fluvial quartz sands–, biotite and muscovite, combined in lower proportions with igneous rock fragments (granite), plagioclase feldspars, and some mafic minerals such as hornblende and pyroxenes. This homogenous composition might be tentative related with the existence of one ceramic production centre located inside the valley for the Middle Period producing this ceramic type, although further chemical characterisation analyses must be performed to investigate this topic. Additionally, we could observe that ceramic petrology was successful in determining different technical stages in the manufacturing process of these ceramic vessels, involving a complex *"chaîne opératoire"* characterised by the existence at least of two firing stages with different atmospheres conditions (reducing and oxidising) and the fixation by oxidising firing of the decorative slips with a biotite-based mineralogy.

An ongoing analytical research project, throughout the application of SEM-EDS, involving the study of the pigments used by the ancient potters in the elaboration of the paintings/slips to decorate these ceramic vessels has preliminary concluded that most of the pigments are coming from inorganic sources (De La Fuente *et al.* 2004).

REFERENCES

Barraclough, A. 1992. Quaternary Sediment Analysis: A Deductive Approach at A-Level. *Teaching Geography* 17:15-18.

De La Fuente, G. A., Kritscautzky, N., and G. Toselli. 2004. Pigmentos, Engobes y Alfareros: una aproximación arqueométrica (SEM-EDS) al estudio tecnológico de pigmentos en cerámicas arqueológicas del Noroeste Argentino: el caso del tipo cerámico "Aguada Portezuelo" del valle de Catamarca. In *Libro de Resúmenes del XV Congreso Nacional de Arqueología Argentina*, Río Cuarto, 20-25 de septiembre de 2004, pp. 140. Universidad Nacional de Río Cuarto, Córdoba.

Freestone, I. C. 1991. Extending Ceramic Petrology. In *Recent Developments in Ceramic Petrology*, edited by A. P. Middletone and I. C. Freestone, pp. 399-410. British Museum Occasional Paper Nº 81. British Museum. London.

González, A. 1998. *Arte Precolombino. Cultura La Aguada. Arqueología y sus diseños.* Filme Ediciones Valero.

Gordillo, I. 1996-1997. Una Cuestión de Tiempo. *Shincal* 6: 15-25.

Kriscautzky, N. 1996-1997. Nuevos Aportes en la Arqueología del Valle de Catamarca. *Shincal* 6: 27-34.

Kriscautzky, N. and Togo, J. 1996. Prospección arqueológica en el Valle Central de Catamarca. Departamentos Valle Viejo, Capital, Fray Mamerto Esquiu, Paclin y Ambato. Actas y Memorias del *XI Congreso de Arqueologia Argentina (13° parte), Revista del Museo de Historia Natural de San Rafael, T. XXV (1/4): 141-153* . San Rafael, Mendoza.

Kusch, M.F. 1996-97. Estructura y diseño en la cerámica Portezuelo. *Shincal* 6: 241-248.

Kusch, M. F., M. Hoffman y C. H. Abal. 1997. "Variabilidad estilística en torno a la iconografía humano-felínica durante el Período Formativo (Catamarca y La Rioja). *Actas y Memorias del XI Congreso Nacional de Arqueología Argentina (4° parte), Revista del Museo de Historia Natural de San Rafael, T. XVI, (1/4): 183-202*. San Rafael. Mendoza.

Mathew, A. J., A. J. Woods, and C. Oliver. 1991. Spots before your Eyes: New Comparison Charts for Visual Percentage Estimation in Archaeological Material. In *Recent Developments in Ceramic Petrology*, edited by A. P. Middletone and I. C. Freestone, pp. 211-263. British Museum Occasional Paper Nº 81. British Museum. London.

Middletone, A. P., I. C. Freestone, and M. N. Lesse. 1985. Textural Analysis of Ceramic Thin Sections: Evaluation of Grain Sampling Procedures. *Archaeometry* 27(1):64-74.

THE "MYSTERY" OF THE POST-MEDIEVAL TRIANGULAR CRUCIBLES RECONSIDERED – A GLOBAL PERSPECTIVE

Marcos Martinón-Torres and Thilo Rehren
Institute of Archaeology. University College London

1. BACKGROUND

In 1677, the *chymist* Robert Plot examined some English crucibles manufactured by John Dwight, long time potter, experimental *chymist* and entepreneur, and concluded that "he hath discovered also the mystery of the Hessian wares, and makes Vessels for reteining the penetrating Salts and Spirits of the Chymists, more serviceable than were ever made in England, or imported from Germany it self" (Plot 1677). This secrect arguably unveiled in Dwight's workshop was indeed a long standing enigma: since the Middle Ages, crucibles manufactured in Hesse (Germany) had been widely traded across the world, thus indicating their renowned quality.

More than three centuries after Plot's observation, in 1992, John Cotter recaptured this "mystery" to raise awareness of the "remarkably little attention paid to the subject of post-medieval crucibles" and, particularly, to the triangular type (Cotter 1992: 256). Based on historical documents, he contended that literally millions of these had been imported into Britain alone.

The triangular or laboratory crucible is made by simply pushing inwards the upper walls of a beaker-shaped vessel, thus creating three pouring spouts (fig. 1). This simple tool was used in fire assays as well as in copper and brass metallurgy, for gold and silver working, glassworking and even in experiments in the quest for the philosophers' stone. Increasing numbers of these are recorded in different archaeological contexts but, until quite recently, they received little attention beyond vague attributions to the "Hessian type", particularly when they are sand-tempered and triangular.

2. RESEARCH QUESTIONS, MATERIALS AND METHODOLOGIES

This paper is a brief summary, necessarily short of bibliographic references, of a wider research project aimed at obtaining a more

Figure 1. "Nest" of triangular crucibles recovered in Hesse (Photo S. Häpe, by courtesy of H-G. Stephan).

comprehensive picture of this scenario and establishing the technological, historical and archaeological implications of this vessel type (Martinón-Torres 2005). Three basic questions were posed: (1) what is the "mystery" that made these crucibles so highly esteemed? (2) does the standard appearance of the vessels respond to a standard manufacture? and (3) were these crucibles primarily traded or was the triangular shape simply adopted progressively in different regions?

Accordingly, our research concentrated on three overlapping aspects: (1) the formal and material properties, as well as the performance characteristics, of these vessels, with a special focus on the choices made during their manufacture, consumption and use; (2) their process of manufacture; and (3) fabric grouping and provenance of different types.

The sources of information consulted were historical and archaeological. The former group included early modern technical treatises as well as documents regarding pottery production and trade. The archaeological data were obtained from the comparative analytical study by optical microscopy and SEM/EDX (following standard protocols in Martinón-Torres and Rehren 2002) of a range of crucible samples and ordinary ceramics obtained from ten

different sites in Germany, Britain, Portugal, Austria and Virginia (USA), together with a reconsideration of published examples.

This paper necessarily overlooks the potential of fine-grained chronological sequences and more detailed explorations into each case study (see Martinón-Torres 2005). However, it is hoped that it provides a general background where future finds and questions may be contextualised.

3. TRADITIONAL KNOWLEDGE: INFORMATION FROM TECHNICAL TREATISES

Cotter (1992) has provided a fine account of the best known written sources of information about the manufacture of triangular crucibles, namely the early modern century treatises and mining, metallurgy, alchemy and assaying. Using Cotter's sources, the resulting picture is that the best crucibles were made of light firing clay tempered with fine sand or crushed pebblestone and, occasionally, grog. The clay mixture could be shaped either on the potter's wheel or in brass moulds, and then fired in ordinary pottery kilns. Several provenances for the clay and/or the crucibles are cited, most of them in Central Europe. For example, there are references to the clays from Hildesheim and Waldenburg (Saxony), and to the crucibles from Ipps (Bohemia) and Vienna (Lower Austria) (cf. Cotter 1992). Occasionally, however, there are suggestions that crucibles could be produced outside this Central European focus, as is Biringuccio's mention of "Valencia clay" (Smith and Gnudi 1990: 72).

Remarkably, in the late 15th century, the alchemist Thomas Norton complained about the lack of suitable crucible makers "in any country of English grounde". Two hundred years later, Johann Glauber noted that "those [crucibles] of Hessia are still preferred before others, retaining better, metals and salts" (cf. Cotter 1992: 265-266).

Several technical qualities of the crucibles are appreciated. In some cases, their resistance to corrosion by hot metal oxides and fluxes seems to be the most important asset, as in Plot or Glauber's statements above. In other instances, a good refractoriness appears crucial (Sisco and Smith 1951: 180).

4. REVISED KNOWLEDGE: ARCHAEOMETRY AND WRITTEN DOCUMENTS

4.1. The light crucibles from Hesse

Contrary to widespread assumptions, neither all the triangular crucibles are Hessian, nor all the Hessian crucibles are triangular. It is true, however, that the triangular crucibles from Hesse played a major role in many sorts of

early modern pyrotechnological workshops. The large scale production of crucibles in the region of Hesse in Central Europe, particularly in Groβalmerode and Epterode, has been addressed in detail (Stephan 1995). Since the Middle Ages, these vessels were usually made of clay heavily tempered with sand, and massively traded. Nevertheless, information was missing with regards to the extent of this trade (but see Cotter 1993 and Stephan 1995) and the specific material properties and performance characteristics of these vessels.

Detailed analyses of samples across the world and spanning from the 16th to the 18th century reveal an extraordinary degree of homogeneity in the pastes. Hessian crucibles were invariably made with a remarkably lean and refractory clay, with alumina levels above 36 wt% and the sum of the alkalis below 2 wt% (table 1). The only noticeable mineral inclusions are occasional occurrences of iron oxides. The clay was tempered with 30-40 vol% of subangular or spheroid quartz grains, moderately well sorted (although this varies from sample to sample). These minerals are normally surrounded by large expansion voids. In some specimens, some possible grog fragments were observed, although the high degree of vitrification hinders a definite identification. The crucibles were thrown on the wheel, sometimes stamped

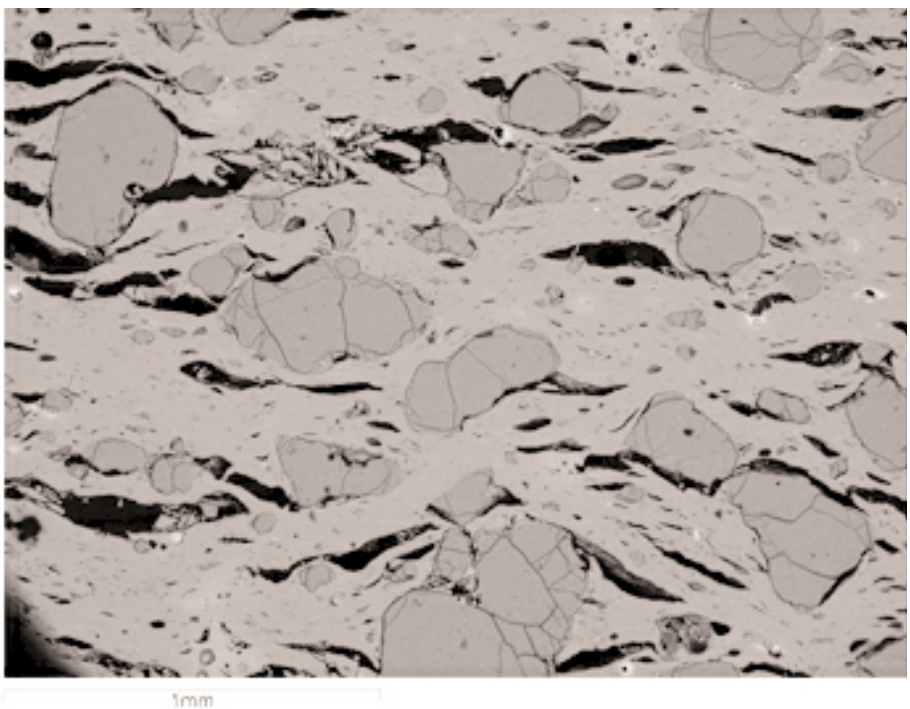

Figure 2. Backscattered electron image of a light Hessian crucible, showing sand temper shattered by thermal stress, expansion voids and a high degree of matrix vitrification.

in the base with a variety of motifs such as stars or initials, and fired to temperatures in excess of 1200 ºC, as indicated by the fact that, despite the high refractoriness, the clay matrix shows complete vitrification (fig. 2).

The abundant quartz temper substantially enhanced the toughness and the thermal shock resistance of the vessels (Tite *et al* 2001). The high temperature of the original firing would improve the vessels resistance to subsequent firings, while the homogenous glassy matrix would have augmented their tensile strength when handled whilst holding considerable weights. Even though the iron oxide inclusions often melted and thus fluxed the surrounding ceramic area, they are relatively rare and small, and would normally not have challenged the vessel's stability. All in all, the "mystery" of the quality of the Hessian wares seems to have been the selection of very refractory clays, well refined and mixed with fine quartz sand, and subsequently very high fired.

	Na_2O	MgO	Al_2O_3	SiO_2	P_2O_5	K_2O	CaO	TiO_2	FeO
Light Hessian (n=12)	0.2	0.5	36.7	56.9	0.2	1.4	0.3	1.9	1.8
Dark Bavarian (n=2)	0.7	0.9	28.3	56.9	0.3	2.6	0.9	1.3	8.1
Dark Austrian(?) (n=6)	0.2	0.7	32.4	57.3	0.3	2.1	0.7	1.3	5.0

Table 1. Average chemical composition by SEM/EDX, normalised to 100 wt%, of the ceramic matrices of different crucible types. From top to bottom: Hessian crucibles found at different sites; dark crucibles found in Obernzell and Oxford; dark crucibles found in Oberstockstall.

Although used samples may appear light grey or even black depending on the conditions of use, unused crucibles are very consistent in their appearance: the highly vitrified matrix is grey, but the areas surrounding the quartz grains, particularly those erupting through the surface, show orange shades. In addition, the texture of the surfaces is particularly sandy and pimply. These features make it relatively easy to single out a crucible as "Hessian" even before analysing it, as would have been the case in the past. This grainy surface, however, in addition to the substantial expansion voids within the paste, would have been a detrimental performance factor, facilitating the penetration of corrosive substances into the crucible body, which seems paradoxal in the light of the historical remarks of these vessels' resistance to corrosion.

Within this study, by comparison to samples from production centres, and given the consistent characteristics of the pastes, Hessian crucibles were identified or confirmed in contexts relating to bronze and brass metallurgy in Burgsteinfurt (Germany), coin minting in Porto (Portugal), the chymical laboratory at the Old Ashmolean (Oxford, UK), goldsmithing in Cripplegate (London, UK), and ore assaying and bronze metallurgy in Jamestown

(Virginia, USA). In addition, the stamps in the crucibles from the Archbishop's Mint in Trondheim (Norway), as well as others from Colchester and London (UK), could also be adscribed to Hesse.

4.2. The dark crucibles from Bavaria

A somewhat surprising discovery in the course of this study was the existence of another large scale producer of high-quality crucibles in post-medieval Europe, which was startingly overlooked in 16th-century treatises as much as in present-day studies (with the exception of a few notes in Cotter 1992).

From local historical documents and archaeological finds, it is known that, at least since the Middle Ages, potters from Bavaria and neighbouring regions competed for the exploitation of certain clays, which they used for the production of black wares in general, and crucibles in particular. These clays were referred to as *Eisentachen* or "iron clay", probably due to their metallic appearance, as they were naturally very rich in graphite inclusions. The most famous crucible producers in the area during early modern times were the potters from Obernzell, in the archdiocese of Passau, where the largest deposits of graphite in Europe are to be found. Other clay deposits in Bohemia and Upper Austria were exploited as well (Bauer 1976; Bauer 1983).

Bavarian crucibles are consistently wheel-thrown and fired dark grey or black in a smoky kiln, altough used samples range from brown through purple to orange. The clay matrices are rich in alumina (around 30 wt%), although they also show moderately high iron oxide levels (≥5 wt%) (table 1). They were fired to relatively high temperatures, in the range 950-1050 ºC, as noticed in the initial to intermediate degree of vitrification, together with the presence of residual plagioclase and the unaltered state of feldspar inclusions in unused vessels. The most remarkable feature of these fabrics is normally the presence of graphite speckles, in concentrations ranging from 20 to 70 vol% (fig. 3). As discussed elsewhere (Martinón-Torres 2005), graphite brings an excellent technical asset for the crucibles, enhancing to the utmost not only the toughness and the thermal shock resistance, but also the refractoriness, the tensile strength, the thermal conductivity and even the corrosion resistance of the crucibles. Only repeated firings in strongly oxidising conditions would progressively lead to the burning away of graphite and the subsequent weakening of the vessels.

The fact that graphite brings about specific material properties in the ceramic paste does not imply that all of these qualities were noticed or valued in the early post-medieval period, not even that the good quality was directly associated to the presence of graphite. In fact, the assemblage from the laboratory in Oberstockstall (Austria) shows the presence of non-graphitic crucibles that were reduced fired and used as the graphitic ones (Martinón-

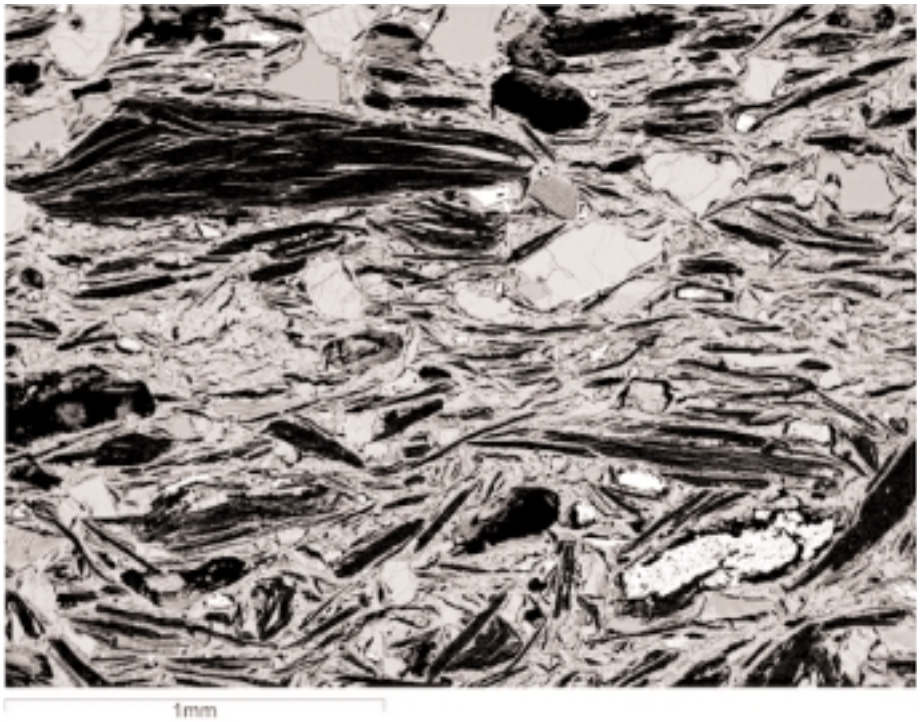

Figure 3. Backscattered electron image of a dark Bavarian crucible, showing abundant graphite speckles (black) as well as some silicate inclusions.

Torres *et al* 2003). Furthermore, graphite is not explicitly mentioned at all until the late 17th century (and even then it is referred to as *Wasserbley* or "liquid lead", still denoting an atypical understanding). In this sense, perhaps the better performance was originally related to the external quality, much more in line with the Renaissance mentality. Only by repeated experience, and through feedback between manufacturers and users, the link between graphite and good performance would have been fully realised. This would explain the concern with appearance, as all the crucibles produced in the region, graphitic or not, show a very smooth surface finish and black surface, resulting from a deliberately smoky firing.

Post-medieval dark crucibles, primarily graphitic, could be identified in the production centre of Obernzell, as well as in the laboratory in Oberstockstall (Lower Austria), the Ashmolean laboratory in Oxford (where, interestingly, Hessian ones are also present), some spot finds from London and Canterbury (UK), and the Imperial Mint in Rio de Janeiro (Brazil). Those produced in Obernzell sometimes show a compex stamp in the base, combining a symbol resembling a number 4, a cross and two initials inside an

elongate cartouche. The vessels found in Oberstockstall show a distinct 'T' stamp, and slightly different microstructure and composition.

5. CONCLUSIONS AND FURTHER WORK

This brief outline provides a preliminary picture of the crucible production and distribution in the post-medieval world. It has been shown that not only Hessian, once "mysteriously good", crucibles were produced and exported in large quantities, but also the historically less documented black crucibles manufactured in Bavaria, Bohemia and Upper Austria. The latter had generally equivalent material properties and performance characteristics, in spite of the different design and appearance. Other productions, possibly local, are present in several sites, and these are normally less refractory.

It seems reasonable to assume that both the main types co-existed and competed with each other in the international market. In this sense, their contrasting appearance and texture (light-coloured and sandy *versus* dark-coloured and smooth) may be highlighted as foremost factors potentially leading to their identification in the market as "one of a kind". It should be noted that shape, colour and texture, together with other external qualities, and not the material properties, are the features conditioning the choice of one pottery type or another (cf. Sillar 1997; Cumberpatch 1997; Jones 2004). Furthermore, the peculiar perception and understanding of graphitic clays in early times stresses the danger of assuming that past societies appreciated the same formal and material properties as we do today.

Given the variety of archaeological contexts where these crucibles are found, it will be interesting to determine the reasons behind the choice of each type of crucibles in each particular case, which specific features were noticed and valued, and details of the crucibles' performance in specific circumstances. In addition, questions arise as to the channels of this large scale commerce, and as to whether the flow of crucibles amongst different spheres of technology was accompanied by skills and ideas. These are aspects of ongoing research.

AKNOWLEDGEMENTS

We are most indebted to many colleagues who facilitated our access to samples for scientific analyses, including Paulo Dordio, Ian Freestone, Tom Freshwater, Rudolf Hammel, Carter Hudgins, Bill Kelso, Mark Norman, Alison Roberts, Fritz Salomon, John Shepherd, Hans-Georg Stephan, Sigrid von Osten and Gerd Weisgerber. Our work has substantially benefitted from feedback from Ingolf Bauer, Justine Bayley, Ian Freestone, Sigrid von Osten

and especially Bill Sillar, amongst others. Technical assistance by Kevin Reeves is also gratefully acknowledged. Generous funding has been granted by Área Sociocultural Caixanova; Dixon Studentship and Central Research Fund of the University of London; Arts and Humanities Research Board; Graduate School and Institute of Archaeology of University College London; and R. F. Tylecote Fund of the Historical Metallurgy Society.

REFERENCES

Bauer I 1976. Zur Geschichte der Schmelztiegelherstellung in Obernzell, *Volkstümliche Keramik aus Europa. Zum Gedenken an Paul Stieber*, 13-37. Munich: Deutscher Kunstverlag.

Bauer I 1983. *Handbuch und Führer zum Keramikmuseum Schlo? Obernzell, Zweigmuseum des Bayerischen Nationalmuseums* (2nd rev. edn.; 1st edn. 1982). Munich: Bayerisches Nationalmuseum.

Cotter J P 1992. 'The Mystery of the Hessian Wares': Post-medieval triangular crucibles. In D Gaimster and M Redknap (eds) *Everyday and Exotic Pottery from Europe c. 650-1900. Studies in honour of John G. Hurst*, 256-272. Oxford: Oxbow.

Cumberpatch C G 1997. Towards a phenomenological approach to the study of medieval pottery. In C G Cumberpatch and P W Blinkhorn (eds) *Not so much a pot, more a way of life. Current approaches to artefact analysis in archaeology*, 125-151. Oxford: Oxbow.

Jones A 2004. Archaeometry and materiality: materials-based analysis in theory and practice, *Archaeometry* 46: 327-338.

Martinón-Torres M 2005. *Chymistry and Crucibles in the Renaissance Laboratory: an Archaeometric and Historical Approach.* PhD thesis. University of London.

Martinón-Torres M and Rehren Th 2002. Agricola and Zwickau: a study of the theory and practice of Renaissance brass production in SE Germany', *Historical Metallurgy* 36(2): 95-111.

Martinón-Torres M, Rehren Th and von Osten S 2003. A 16th-century lab in a 21st-century lab: archaeometric study of the laboratory equipment from Oberstockstall (Kirchberg am Wagram, Austria). *Antiquity* 77(298) [http://antiquity.ac.uk/ProjGall/martinon/martinon.html].

Plot R 1677. *The natural history of Oxford-shire: being an essay toward the natural history of England*. Oxford.

Sillar B 1997. Reputable pots and disreputable potters: Individual and community choice in present-day pottery production and exchange in the Andes, in C G Cumberpatch and P W Blinkhorn (eds) *Not so much a pot, more a way of life. Current approaches to artefact analysis in archaeology*, 1-20. Oxford: Oxbow.

Sisco A G and Smith C S 1951. *Lazarus Ercker's Treatise on Ores and Assaying, translated from the German Edition of 1580*. Chicago: The University of Chicago Press.

Smith C S and Gnudi M T 1990. *The Pirotechnia of Vannoccio Biringuccio: The Classic Sixteenth-Century Treatise on Metals and Metallurgy* (1st edn. 1959). New York: Dover.

Stephan H-G 1995. *Großalmerode: Ein europäisches Zentrum der Herstellung von technischer Keramik. Die Geschichte der keramischen Gewerbe in Großalmerode und Epterode und die Entwicklung ihrer Produktion vom 12. bis zum 19. Jahrhundert, Teil II: Technische und Baukeramik…* Großalmerode: Glas- und Keramikmuseum.

Tite M S, Kilikoglou V and Vekinis G 2001. Strength, toughness and thermal shock resistance of ancient ceramics, and their influence on technological choice. *Archaeometry* 43: 301-324.

MAPPING AND CONFOCAL MICRORAMAN SPECTROSCOPY: NON-INVASIVE ANALYSIS OF WEATHERED STAINED GLASS WINDOWS

S. Murcia-Mascarós*, C. Domingo, S. Sánchez-Cortés and J. V. García-Ramos
Instituto de Estructura de la Materia, CSIC. C/ Serrano 121. 28006 Madrid
* smascaros@iem.cfmac.csic.es

A. Muñoz-Ruiz
Vetraria Muñoz de Pablos, S.L. Ctra. Arévalo, Km. 4. 40003 Segovia

ABSTRACT

Micro-Raman spectroscopy is an analytical method successfully used for the study of historical objects and pieces of art. It is a non-destructive and non-contact technique. Combining optical microscopy, which provides information on the morphology of the samples, and Raman spectroscopy, that gives information about molecular and crystal structures, it is possible to unequivocally identify the chemical composition of the samples even when its concentration is very low.

In this work, Raman spectroscopy was used to follow the processes taking place at surface of weathered glass as well as to aid to accurate restoration. In particular, Raman mapping technique has been used in combination with confocal method for characterizing small pieces of glass coming from stained glass windows (1495-1536) of the Cathedral of Avila (Spain). With these techniques we were able to detect the different material layers, to identify the corrosion, grisaille and glass compounds and the distribution of these components within the surface of the glass.

1. INTRODUCTION

Historic stained glass windows undergo a variety of corrosion phenomena (Fernández Navarro, 1996) like pitting (small conical depressions-craters) and crusting (corrosion layers having different compositions and textures). The principal factor of the decay of glass is water. In polluted atmospheric conditions, the pH of water is often acid thus inducing a superficial leaching of alkaline and alkaline earth elements in the irregular network of SiO_4 tetrahedra. It mainly depends on the glass chemical

composition: in particular, those potassium-rich are not highly resistant to weathering, whereas sodium-rich, are very durable.

The stained glass windows studied in this work show different types of corrosion, mainly crusting. The composition of crusts reflects the nature of the dominant gaseous pollutant present in the atmosphere at the time of crust formation (i.e. CO_2 and, in minor amount, SO_2 originating from combustion). The presence of crusts reduces the transparency of glass and modifies the colors perturbing the understanding of the iconography, the state of conservation is worring.

Artistically, these artworks are originally from several authors, diverse periods and very well differentiated styles (Vetraria, 2003). Juan de Valdivieso and Arnao de Flandes started the first stained glass window elaboration in 1495. In 1497 Juan de Valdivieso and Diego de Santillana placed four windows with the figures of St. James, St. John, St. Nicholas and St. Anne to the sides of altar. From this first group of windows, only one of them, representing to St. John, is conserved. In April 1498, other three windows with the scenes of the Nativity, the Epiphany and the Transfiguration were ordered to the same studio. Finally, Juan de Valdivieso and Diego de Santillana painted the windows of the north wall by the representation of St. Agatha, St. Agnes, St. Martha and St. Catherine. They also made the glasses of the Door of the Apostles, which represents the figures of eight of those saints, and the History of Resurrection.

Spectroscopic techniques have demonstrated to be very useful to artwork studies. In particular, Raman spectroscopy gives important molecular structure information of historical object materials (Smith, 2004). In this work, we report preliminary results to the study of historical stained glass windows using mapping and confocal Raman spectroscopy.

For increased sensitivity and selectivity, confocal configuration was used. In this way, the spatial resolution of the Raman measurements is increased along z axis and allows us to quantify the thickness of the corrosion layer.

2. EXPERIMENTAL

Different unprepared stained glass surfaces from Avila Cathedral were studied using a Renishaw Raman spectrometer. The Raman spectrum obtained by an argon ion laser (785 nm) was measured in a Renishaw RM2000 micro-Raman with an objective 50x. The laser power at the sample was 2 mW. The resolution was set at 4cm^{-1} and the geometry of micro-Raman measurements was 180º.

Maps were acquired with a step size of 1μm, consistent with the spatial resolution of the confocal microscope. Although data collection time

depended on several user-defined parameters, such as the image step size, number of steps, and spectral acquisition time, an entire Raman image was typically generated in 2–4 h.

In confocal configuration the CCD camera was closed to 3 pixels and slit to 50μm. The step size was of 2μm.

Figure 1. Detail of the panel 6 window sIII, Cathedral of Avila. Photographs were taken with transmitted and reflected light. A dense weathering crust is reducing the transparency of most glasses.

3. RESULTS AND DISCUSSION

According with historical data and artistic and technical analyses achieved during the restoration, we can conclude that Juan de Valdivieso painted the windows s-III and s-IV, Arnao de Flandes made the window sVI and Nicolás de Holanda is probably the author of the windows s-V, s-VII, S-VII and s-VIII. Contemporary windows were made from casa Maumejean among 1929-35 (Vetraria, 2003). The most important cause of degradation came from previous restorations. It is probably that glasses were treated with natural resins that suffer processes of transformation as oxidation or polymerisation. Some glasses are covered with a very sticky and dark layer. In the inside part, the glasses are also covered by powder and carbon from candles (fig. 1). Outside glasses are mostly covered by thin silica layer that

reduces transparency. Only down panels present a thick white layer of corrosion. Structural damages are also observed as broken glasses, absence of fragments and accumulation of bad placed mortars.

The average glass composition agrees with sodalime glasses (Fernandez Navarro, 1996) (wt% of oxides by ICP-AES):

SiO_2	Na_2O	CaO	K_2O	Al_2O_3	MgO	PbO	Fe_2O_3
59.2	11.60	9.82	4.64	5.92	3.53	1.12	1.52

This composition justified the absence of pitting on the glass surface, usually linked with potassium rich glasses. In the studied glasses, crusts are the most important damage. With the help of Raman Spectroscopy we observed the surface of the crust area (fig. 2) where it is possible to determine

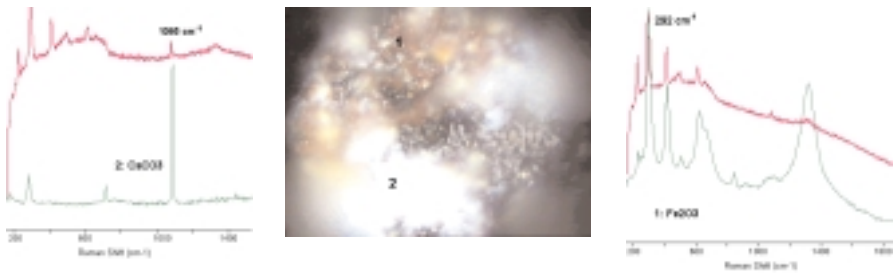

Figure 2. Micrograph of a small piece of glass and Raman Spectra recorded across the glass surface (in red). Components were identified by comparing with Renishaw Raman Library.

different components: carbonates, oxides, carbon particles and silica. In area 1, grisaille is present and Raman spectrum is correlated with hematite. In area 2, the Raman spectrum of the white crust reveals that the carbonate band at 1085 cm^{-1} corresponds to the calcite phase. Graphite and glass Raman spectra are also detected.

The same results were obtained in all the studied weathered areas. To determine the thickness of the carbonate crust we recorded confocal Raman along z-axis (fig. 3). We found a very wide range of crust thickness from 5 to 200 μm.

The characteristics bands at 1085 cm^{-1}, which is the most intense calcium carbonate Raman band and that at 294 cm^{-1}, due to hematite from grisaille, were followed to perform the Raman mapping, since these compounds represent the majority of these glass surface. The Raman maps display the distribution and intensity of these bands in a selected line of 34 μm (fig. 4).

Stained glasses were cleaned with very soft paintbrushes, distilled water and drying at 150ºC. The layer of carbonate has not been totally eliminated in

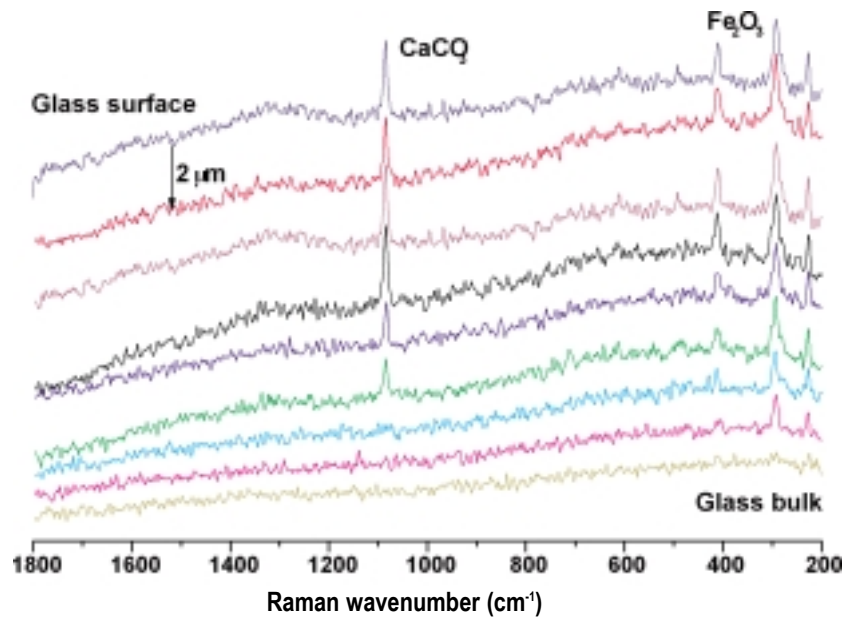

Figure 3. Confocal Raman from the SURFACE to the glass BULK along 16 µm. The thickness of the carbonate corrosion layer was estimated.

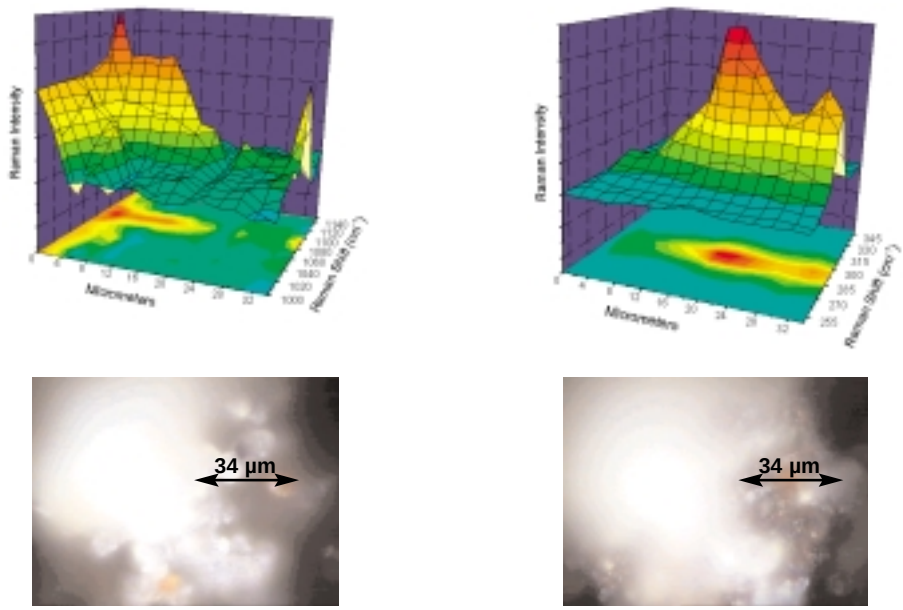

a) $CaCO_3$ (1085 cm^{-1}) **b) Fe_2O_3 (292 cm^{-1})**

Figure 4. Raman Mapping along a superficial LINE. The maps directly display the distribution of (a) calcium carbonate from the crust, covering (b) hematite from the grisaille.

order to avoid any damage. The Confocal Raman measurements have determined that residual thickness is not bigger than 5 μm. Even if that, this method gives the best results. Nevertheless, the stained glasses have recovered almost the whole original luminosity (Vetraria, 2003).

4. CONCLUSIONS

Raman spectral mapping is a powerful tool to obtain structural and chemical information about glass samples. Because Raman is a non-damaging technique, its use will be most probably increasing more and more to study historical stained glass windows. In this work, we show that this technique is excellent for studying samples which are difficult to characterize with other techniques. The big advantage is to have maximal spectral information condensed into an image. The combination of confocal Raman and Raman-mapping has a promising application in the study of weathered surfaces, and will be important for future archaeometry studies, as well as to test cleaning during restoration.

ACKNOWLEDGMENTS

This work has been partially financed by Comunidad de Madrid (Project 06/0134/2003). S.M.M thanks CSIC for the I3P contract of European Social Founds.

REFERENCES

Fernández Navarro, J.M. "Alteration processes of medieval stained glass windows. Study and protection treatments". *Materiales de Construcción*. 46 (1996) 5-20.

Smith, G.D. and Clark, R.J.H. "Raman microscopy in Archaeological Science". *Journal of Archaeological Science*, 31 (2004) 1137-1160.

Vetraria, S.L. *Report* to Ministerio de Educación, Cultura y Deportes. October 2003.

LUSTRE POTTERY IN INLAND SPAIN: ANALYTICAL STUDY OF THE CERAMIC DECORATION PRODUCED IN MUEL (ARAGON) IN THE 16th CENTURY

Josefina Pérez-Arantegui
Dept. Analytical Chemistry. Faculty of Sciences. University of Zaragoza.
50009 Zaragoza (Spain)

Ángel Larrea
Instituto de Ciencia de Materiales de Aragón. University of Zaragoza-CSIC.
50018 Zaragoza (Spain)

1. INTRODUCTION

In the Iberian Peninsula, the Crown of Aragon was one of the most flourishing ceramic production areas during the Middle Age and the Renaissance, and some towns are well known because of the production of beautiful pieces. Some documents told about an Islamic production of lustre pottery in Calatayud (Zaragoza) in the 12th century, but no workshops or objects have been found. However, during the 16th century in Aragon, one of the places known by its lustre pottery production was the town of Muel, close to the city of Zaragoza. The work, starting in the early 16th century, continued to the 18th century.

This lustre pottery is not an isolated case of decorated glazed ceramic in the area. It is part of the tin-glazed ceramic tradition in Aragon, from the case of Islamic tin-glazed pottery produced in Zaragoza and other towns during the 11th and 12th centuries, and through other Hispano-Moresque productions, like Teruel, and even linked to ceramic workshops of Valencia and Paterna (also belonging to the Crown of Aragon).

The aim of this study is to present some aspects of the characterization of lustre pottery produced in Muel, as microstructure, composition and raw materials, related to the production process. The study was mainly focused on the characterisation of the decoration, in order to recuperate the style and the way of producing ancient lustre. Therefore, to obtain a new similar object, we need to know the chemical composition of the body, the glaze

microstructure and its composition and the characteristics of the lustre, because all of them have some influence in the final aspect of the object.

2. ANALYTICAL STUDY

2.1. Ceramic bodies

First of all, the chemical composition of the ceramic bodies was determined by Inductively Coupled Plasma-Atomic Emission Spectrometry (ICP-AES). The results are shown in table 1 for the major elements and some minor elements. The main feature to be noted is that ceramic bodies have calcareous clays, because these clays produce yellow or white-buff colour, and they were used to be decorated with tin-glazes. This characteristic is common to other tin-glazed ceramic productions in closer areas, like Zaragoza, Teruel and Paterna (Valencia), always with calcareous-clay bodies, but they can be distinguished because of the proportions of some elements, as magnesium, for example, or some trace elements.

	Na_2O	MgO	Al_2O_3	K_2O	CaO	TiO_2	Fe_2O_3	MnO	Ba	Sr
Average value	0.70	3.10	17.3	2.84	13.6	0.71	6.12	0.0650	677	364
SD	*0.27*	*0.30*	*1.2*	*0.51*	*1.0*	*0.05*	*0.47*	*0.0090*	*53*	*35*

Table 1. Average chemical composition of ceramic bodies in lustre pottery from Muel and standard deviation (SD) (element oxides are given in weight% and Ba and Sr in $\mu g.g^{-1}$).

2.2. Lustre-decorated tin glazes

Tin-glaze microstructure was studied by Scanning Electron Microscopy (SEM). All glazes have similar thickness, 100 – 150 μm. All of them were put on biscuited bodies and a very thin layer can be distinguished between body and glaze. A variable number of quartz inclusions is observed in these glazes, that can improve their opacity.

Looking at the chemical composition of these tin glazes obtained by Energy-Dispersive X-ray (EDX) analysis, two similar groups can be observed, with slight differences in lead and potassium contents (see table 2). Once more, these tin glazes from Muel correspond to lead glazes with a small proportion of alkali elements, like other tin glazes produced in the Iberian Peninsula. If we compare tin glazes from Muel with other workshops (Islamic Zaragoza, Teruel or Paterna, geographically or chronologically closed to Muel), we can find not many differences in the composition of these glazes. They can be distinguished, but they correspond to the same type of glazes. We want to note only a feature, already observed in other studies of lustre pottery: it is the fact that tin glazes prepared to be decorated with lustre always have a higher proportion of potassium.

	Na_2O	Al_2O_3	SiO_2	K_2O	CaO	SnO_2	PbO
MUEL1	0.71	3.11	49.44	4.96	2.36	5.79	33.73
SD	*0.18*	*0.27*	*2.28*	*0.67*	*0.39*	*0.73*	*3.07*
MUEL2	0.62	2.80	44.75	3.05	2.06	6.45	39.56
SD	*0.09*	*0.23*	*0.83*	*0.41*	*0.91*	*0.73*	*1.88*

Table 2. Average chemical composition of tin glazes in lustre pottery from Muel and standard deviation (SD, in italic) (element oxides are given in weight%).

Coming now to the characteristics of the lustre, Muel workshops produced lustre pottery with very different colours: golden-yellow, red, reddish-brown, light-brown, etc. The question is now how potters produced the lustre in Muel, because objects have very diverse colours but also we find differences in the glossy or metallic lustre, with or without a true metallic shinning. The full answer to these questions is very complex, so, as part of a large project on lustre pottery, this paper is only focused on what potters used to produce lustre. The lustre of Muel was probably made by craftsmen coming direct from Valencia, but technical changes often occur when craftsmen move to new places and to re-establish a known method with somewhat different raw materials. Therefore, we divided this objective in three parts: the microstructure, the composition and the relation with possible raw materials.

On surface, lustre has a heterogeneous distribution, in colour and in presence, with areas with or without lustre. An examination of the surface by SEM (fig. 1) shows this heterogeneity, and even the evidence of the presence of small clusters of different composition, in backscattering images. The observation of the microstructure only in the first microns in depth confirms the presence of copper in the outer part, in this case, approximately in the first five-hundred nanometers. We can also observe a decreasing of some elements (like potassium and lead) in the outer part. Lustre observation in TEM displays a nanostructure with metallic particles of different sizes (fig. 2), this nanostructure is common to lustre produced in other workshops like Paterna, under a thin glassy layer, and with a first layer of big particles of metallic copper.

If we study the chemical composition of lustre on surface by EDX, we observe a distribution of the two main elements responsible of lustre (copper and silver). Considering the aspect of the lustre and the proportion of these elements, we can divide them in three groups. Due to the small thickness of the lustre and the analytical method used, we think that it is more interesting to consider not the simple values but the proportion of both elements in the possible recipes. So, we find again the same division in three different groups: the first one with a relation Cu/Ag less than 1; the second between 1 and 2; and the third one, with a proportion higher than 2.5.

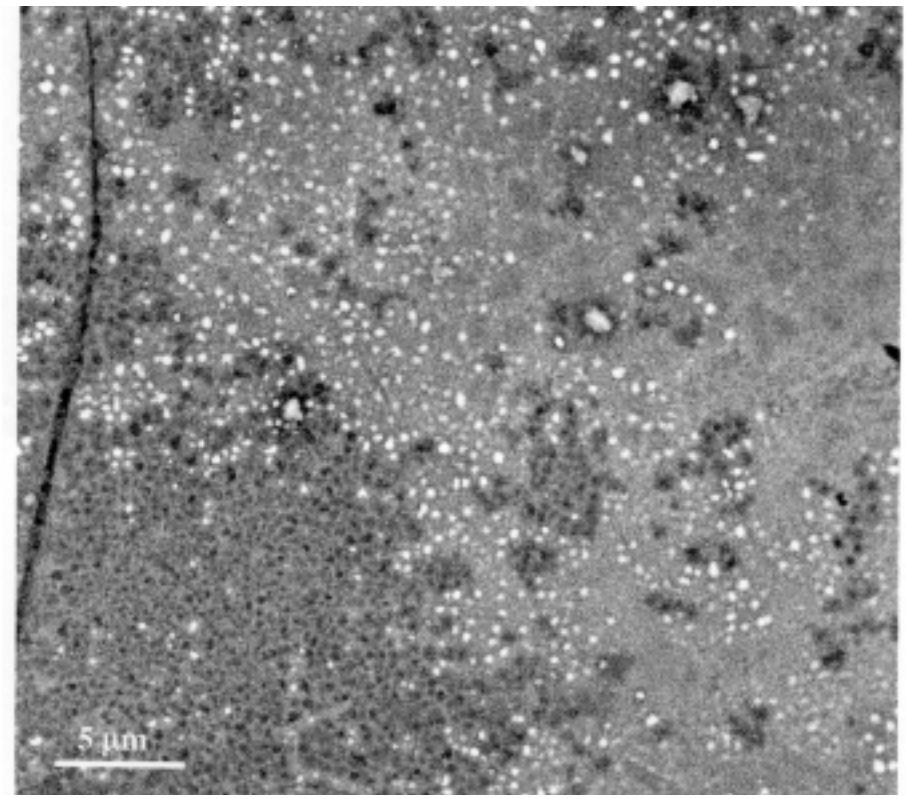

Figure 1. Backscattered electron image of a lustre surface.

Coming back to the relation between these elements and the ancient recipes, historical documentation collects some raw materials, recipes and procedures on the production of ancient lustre pottery in Muel, describing the use of different compounds in several proportions: in this case, silver coins, vermillion, vinegar and alum. "Then, in order to make all the pottery golden, they take very strong vinegar with which they mix two silver reales (small silver coins) which have been powdered, and vermillion (mercuric sulphide) and vinegar and a little "*alambre*" (translated as alum: aluminium-potassium sulphate, or as copper), and when it is completely mixed together they draw whatever they wish with a pen on the dishes and bowls, and place them a third time in the kiln so that they finish with a golden colour,…". The lustre recipe used in Spanish medieval workshops seems to be very similar, that is clay, iron oxides, copper and silver compounds and cinnabar. Therefore, at this moment of the research, the ancient recipe could agree with the first of Cu/Ag proportions, or with the others depending on the last ingredient (*alambre*). The presence of potassium was also verified and that of mercury is not possible to prove because of the elimination of this metal during firing.

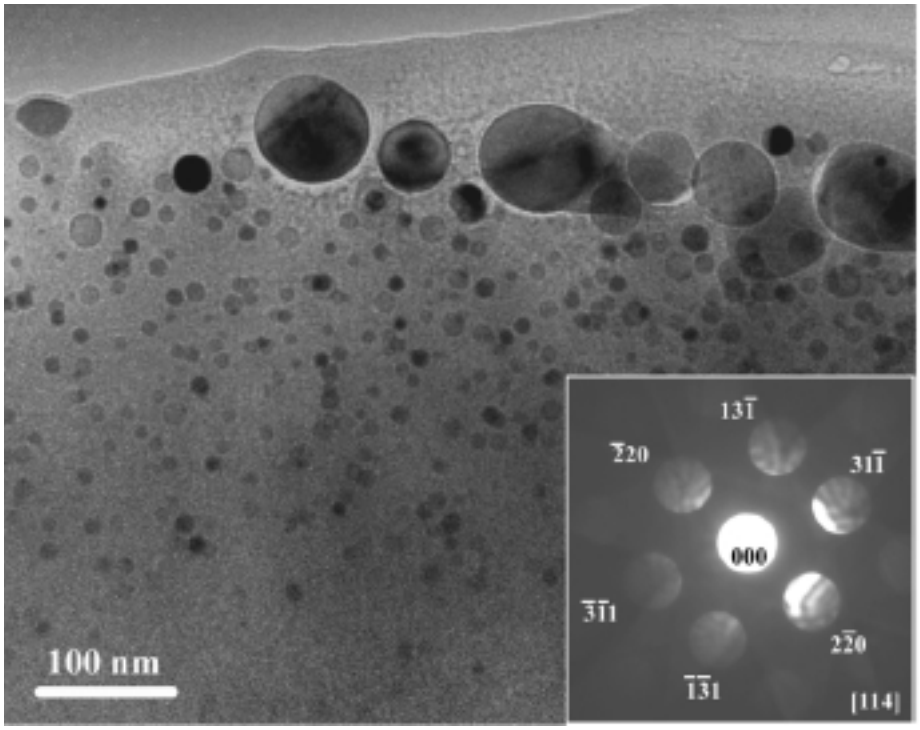

Figure 2. Lustre cross-section image by Transmission Electron Microscopy (*inset*: Electron Diffraction pattern of a copper particle).

ACKNOWLEDGEMENTS

This study is supported by 02/COOPERA/ES1368 research project in the INNOVARAGON program of the European Union (FEDER), Diputación General de Aragón (Aragonese Government), and Instituto Tecnológico de Aragón, Spain.

REFERENCES

Alvaro Zamora, I., 2002, *Cerámica aragonesa*. Vol. 1, 2 et 3, Ibercaja, Zaragoza.

Caiger Smith, A., 1985, *Lustre pottery: Technique, tradition and innovation in Islam and the Western World*, Faber & Faber, London.

Molera, J.; Mesquida, M.; Pérez-Arantegui, J.; Pradell, T.; Vendrell, M., 2001, Lustre recipes from a medieval workshop of Paterna, *Archaeometry*, **43** (4), 455-460.

Molera, J.; Pérez-Arantegui, J.; Pradell, T.; Vendrell-Saz, M., 2002, La céramique musulmane et mudéjare à reflets métalliques: une approche technique, *Le calife, le prince et le potier. Les faïences à reflets métalliques*, Réunion des musées nationaux, Paris, 214-219.

Molera, J.; Vendrell-Saz, M.; Pérez-Arantegui, J., 2001, Chemical and textural characterization of tin glazes in Islamic ceramics from eastern Spain, *Journal of Archaeological Science*, **28** (3), 331-340.

Pérez-Arantegui, J.; Larrea, A., 2003, The secret of early nanomaterials is revealed thanks to transmission electron microscopy, *TRAC-Trends in Analytical Chemistry*, **22** (5), 327-329.

Pérez-Arantegui, J.; Larrea, A.; Molera, J.; Pradell, T.; Vendrell-Saz, M., 2004, Some aspects of the characterisation of decorations on ceramic glazes, *Applied Physics A*, **79**, 235-239.

Pérez-Arantegui, J.; Molera, J.; Larrea, A.; Pradell, T.; Vendrell-Saz, M.; Borgia, I.; Brunetti, B.G.; Cariati, F.; Fermo, P.; Mellini, M.; Sgamelotti, A.; Viti, C., 2001, Luster pottery from the 13th to the 16th century: a nanostructured thin metallic film, *Journal of the American Ceramic Society*, **84** (2), 442-446.

Pradell, T., Molera, J., Vendrell, M., Pérez-Arantegui, J., Pantos, E., Roberts, M., DiMichiel, M., 2004, Role of cinnabar in luster production, *Journal of the American Ceramic Society*, **87** (6), 1018-1023.

Rose-Albrecht, J., 2002, Aragon et Catalogne, *Le calife, le prince et le potier. Les faïences à reflets métalliques*, Réunion des musées nationaux, Paris, 140-151.

Smith, A.D.; Pradell, T.; Molera, J.; Vendrell, M.; Marcus, M.A.; Pantos, E., 2003, Micro EXAFS study into the oxidation state of copper coloured Hispano-Moresque lustre decorations, *Journal de Physique IV (France)*, **104**, 519-522.

NON-DESTRUCTIVE QUANTITATIVE DETERMINATION OF TRACE ELEMENTS IN FINE CERAMICS BY USING A PORTABLE BEAM STABILITY CONTROLLED XRF SPECTROMETER (BSC-XRF)

Francesco Paolo Romano, Giuseppe Pappalardo*, Lighea Pappalardo, Francesca Rizzo*
INFN, Laboratori Nazionali del Sud, LANDIS, Via S. Sofia 44, 95123 Catania, Italy
*Università di Catania, Dipartimento di Fisica e Astronomia, Viale A. Doria 6, 95123 Catania, Italy

Salvatore Garraffo, Rossella Gigli, Antonella Pautasso**
CNR, Sezione di Catania dell'Istituto per i Beni Archeologici e Monumentali, Via A. di Sangiuliano 62, 95100 Catania, Italy
**CNR, Istituto per le Tecnologie Applicate ai Beni Culturali, Via Salaria Km. 29.3, Montelibretti, 00016 Rome, Italy

1. INTRODUCTION

At the LNS/INFN laboratories of Catania (Italy), in the framework of the Agenzia2000 special project of the Italian CNR, a new portable XRF spectrometer with a beam stability control (the BSC-XRF spectrometer) has been designed and realised (Romano et al. 2004).

The system has been used for the quantitative non-destructive determination of some trace elements (Rb, Sr, Y, Zr and Nb) in 10 fine pottery artefacts belonging to the votive deposit of San Francesco in Catania (Italy).

Concentrations of Rb, Sr, Y, Zr and Nb have been determined by using a multi-linear regression method developed at the LNS/INFN laboratories (Pappalardo et al. 1995; Gigli et al. 2002; Grasso et al. 2003).

Additionally, in order to test the homogeneity of the material composing artefacts, i.e. to test if the non-destructive approach is meaningful for the analyses of fine archaeological pottery, a small portion of the potsherds has been powdered and analysed by using the BSC-XRF system.

The comparison between non-destructive and destructive approach is presented and discussed.

2. THE PORTABLE BEAM-STABILITY-CONTROLLED XRF SPECTROMETER (BSC-XRF SPECTROMETER)

The BSC-XRF spectrometer is shown in fig. 1; the system consists of a portable X-ray tube coupled to an ancillary Si-PIN detector to control the energy and intensity stability of the primary X-ray beam; a second Si(Li) detector is used to acquire the characteristic X-ray spectra emitted by the sample being analysed.

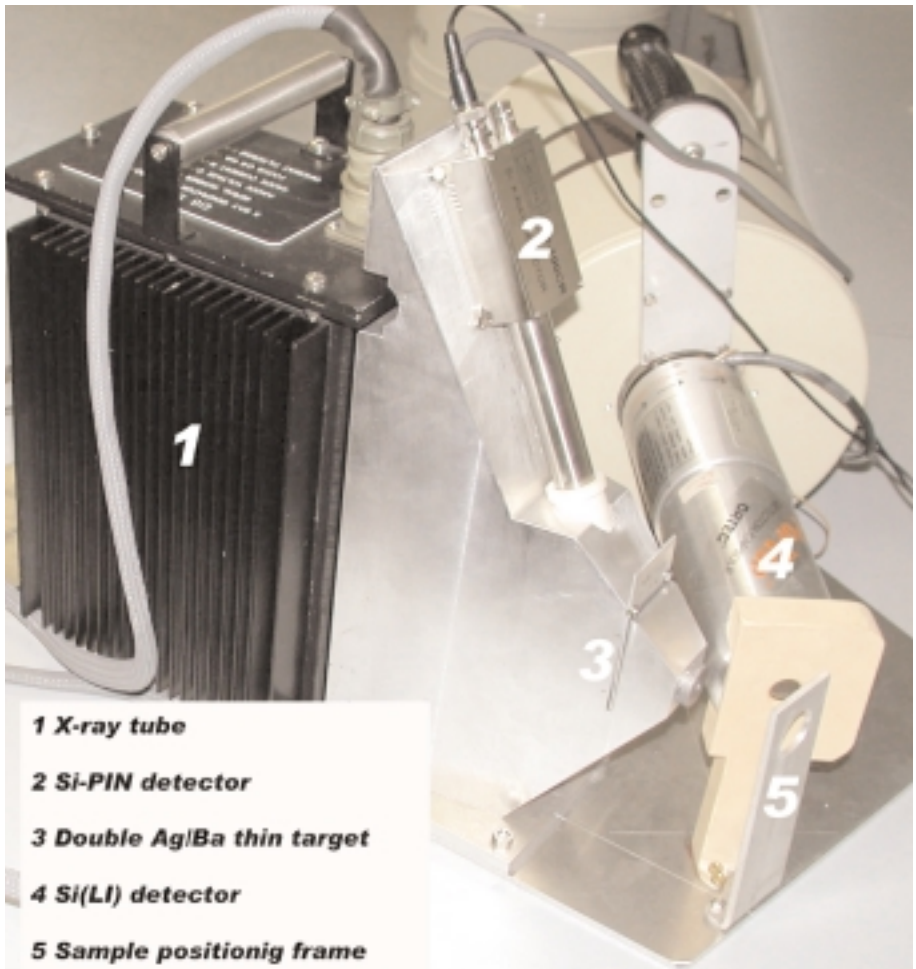

Figure 1. The new portable BSC-XRF spectrometer of the LNS/INFN laboratories.

During a measurement the X-ray beam crosses a double thin target of Ag and Ba, placed between the X-ray tube and the sample to be analysed. Monitoring the characteristic fluorescence of Ag and Ba with the Si-PIN

detector and determining the ratio R=Ag-Kα/Ba-Kα, it is possible to evidence every variation of the maximum energy of the excitation beam. Additionally, the sum I=Ag-Kα+Ba-Kα can be used to monitor the intensity of photons incident on the double thin target.

In order to operate in stable experimental conditions, the tube high voltage must be controlled in such a way as to maintain the parameter R at a constant value.

The proposed method allows to control stability of the energy and intensity of the X-ray primary beam to within an about of 1-1.5% (Romano et al. 2004).

3. QUANTITATIVE DETERMINATION OF SOME TRACE ELEMENTS CHARACTERISING FINE POTTERY

The portable BSC-XRF system has been used for the non-destructive quantitative determination of Rb, Sr, Y, Zr and Nb in 10 potsherds from the votive deposit of San Francesco in Catania. Their content can be considered as indicative of the composition of the clay pastes employed for the realisation of the artefacts and it can be used to highlight the differences between different classes of pottery and to classify doubtful samples.

Figure 2 shows a typical X-ray spectrum obtained from a pottery sample by using the BSC-XRF spectrometer.

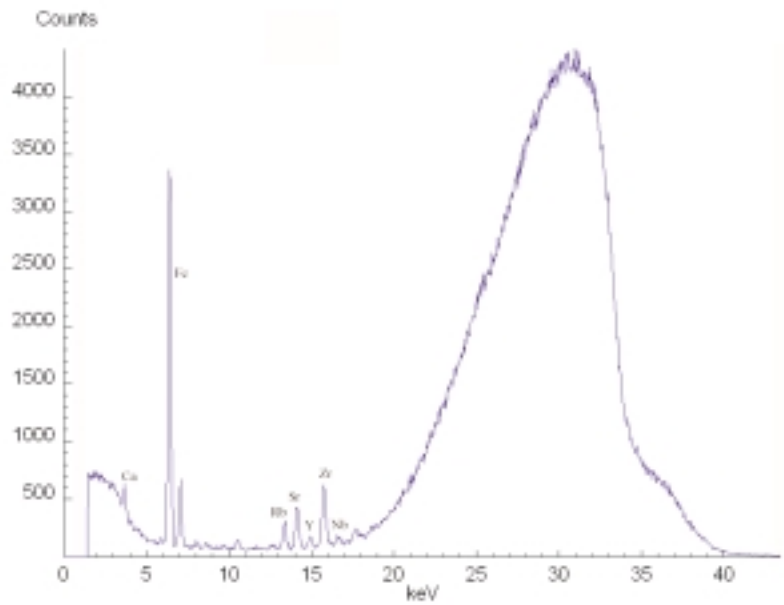

Figure 2. A typical X-ray spectrum obtained by measuring a potsherd.

The compositional data of the trace elements have been obtained by using a multi-linear regression method, developed at the LNS/INFN laboratories (Pappalardo et al. 1995; Gigli et al. 2002; Grasso et al. 2003). The analytical procedure has been previously tested by using different geological standards; the accuracy is 11% for Rb, 12% for Sr, 20% for Y, 11% for Zr and 12% for Nb.

Table 1 summarises quantitative data for the 10 analysed potsherds.

Sample	Rb	Sr	Y	Zr	Nb
L2	99 (115)	142 (151)	21 (22)	133 (146)	12 (14)
L8	153 (155)	251 (268)	27 (26)	161 (171)	14 (15)
L33	100 (105)	271(208)	26 (27)	26 (247)	24 (20)
L36	96 (91)	256 (257)	20 (22)	213 (212)	16 (14)
L39	91 (91)	235 (250)	20 (18)	214 (243)	18 (16)
L57	157 (145)	412 (412)	23 (18)	120 (114)	7 (9)
I14	199 (193)	158 (148)	19 (20)	164 (161)	18 (13)
T66	156 (147)	221 (202)	15 (21)	192 (159)	19 (18)
T78	159 (172)	418 (362)	17 (25)	184 (191)	18 (20)
T109	136 (124)	683 (622)	33 (16)	196 (156)	13 (14)

Table 1. Quantitative results in ppm obtained from the non-destructive and from the destructive (in parenthesis) analysis of the 10 fine potsherds. Errors in the data are of the same order of the accuracy.

4. NON-DESTRUCTIVE AND DESTRUCTIVE ANALYTICAL APPROACHES: COMPARISON BETWEEN SURFACE AND BULK QUANTITATIVE RESULTS

The non-destructive quantitative approach for the analyses of the 10 fine potsherds gives meaningful quantitative data only when they can be considered homogeneous.

In fact, the XRF technique is a surface method and the characteristic fluorescence emitted by elements composing archaeological pottery, comes from a limited thickness under the sample surface.

In order to test the homogeneity of the samples under investigation, a small portion of the 10 potsherds has been powdered, carefully homogenised and pressed to a disk-shaped pellet. The powders have been measured with the BSC-XRF system and analysed by using the quantitative method reported on the previous section.

Table 1 reports in parenthesis quantitative results. Differences in percentage between non-destructive and destructive XRF data are 6% for Rb, 9% for Sr, 28% for Y, 9% for Zr, 13% for Nb.

5. CONCLUSION

The portable XRF spectrometer (the BSC-XRF system) with a control of the energy and intensity stability of the primary beam has been briefly described.

The system is suitable to determine the presence of some trace elements in ancient pottery. Non-destructive measurements of Rb, Sr, Y, Zr and Nb have been performed in 10 potsherds belonging to the founds of the San Francesco votive deposit in Catania; their absolute content has been determined by using a multilinear regression method.

Finally in order to test the homogeneity of the analysed samples, a small portion of artefacts has been powdered and measured by using the BSC-XRF system. Non-destructive and destructive results show a good agreement, suggesting the use of a non-destructive approach for the fine pottery characterisation.

REFERENCES

Gigli R, Pappalardo L, Pautasso A, Romano FP, Pappalardo G, Carastro A. *Identification of a class of pottery within the votive deposit of Demetra Sanctuary in Catania by using a non destructive XRF method*. In Proceedings of 33th International Symposium on Archaeometry: 22-26 April 2002, Amsterdam, in press.

Grasso L, Pappalardo L, Romano FP. *Non destructive quantitative XRF analysis on greek archaic pottery of the Alaimo's Santuary in Lentini (Sicily).* In press in British Archaeological Reports, special issue of "Proceedings of the 4th Symposium on Archaeometry of the Hellenic Society of Archaeometry", National Hellenic Research Foundation, Athens 28-31 Maggio 2003.

Pappalardo G, Loreto G, Musumarra A, Pettinato S, Rizza G, Fichera V, Marino RM, Cirrincione R, Pappalardo L. *Non destructive determination of trace-elements in Greek pottery by use of a XRF portable system*, in Proceedings of the 1st International Congress on "Science and Technology for the Safeguard of Cultural Heritage in the Mediterranean Basin", December 1995 Acireale (Italy). Tipolitografia Luxograph: Palermo (Italy),1998; 803-806.

Romano FP, Calvi G, Furia E, Garraffo S, Marchetta C, PappalardoG, Pappalardo L, Rizzo F, Rovelli A. *X-Ray spectrometry.* Accepted on April 2004, in press.

TEM-EELS INVESTIGATION OF ANCIENT CERAMICS

Ph. Sciau, S. Relaix and Y. Khin
CEMES-CNRS, 29 rue J. Marvig, 31055 Toulouse Cedex, France

1. INTRODUCTION

Transmission electron microscopy (TEM) can be a powerful tool to characterize the thin decorated surfaces of ancient ceramics. It has been successfully used to image the metallic nanoparticles present in medieval glazes of lustre ceramics. Moreover, other information can be obtained with a resolution of a few nanometers such as: structural identification of nanocrystals, the local chemical composition, valence state and local atomic environment around specific atoms by electron energy loss spectroscopy (EELS). In this paper, these capacities are combined with the X-ray diffraction to study the nanostructure of the slip of *Terra Sigillata* ceramics.

Terra sigillata pottery is the most famous fine ware of the Roman period. It is characterised by the redness of its body (or paste) and slip (or gloss), similar to the colour of the clay (*terra*), and by the use of stamps (*sigilla*) in some cases. *Terra sigillata* production involves a complex process developed by potters in the Italian Peninsula and adopted, with greater or lesser success, all over the areas where this pottery was produced (Madrid Fernandez and Buxeda i Garrigos, 2002). Understanding how the production of high quality sigillata started in two important South Gaulish workshops (La Graufesenque and Montans) interests us. During the first century AD, these workshops produced enormous quantities of *sigillata*, which were sold all over the Roman Empire. The chemical and mineral composition of these ceramics (body and slip) have been analysed by many techniques such as XRF (Picon *et al*., 1975, Schneider, 1978), Microprobe (Picon, 1997, Sciau *et al*., 2004) or XRD (Vendier, Sciau and Dooryhee, 2002). In these two workshops different clays were used for body and slip preparation. The slip was obtained from a non-calcareous clay whereas a calcareous clay was used for the ceramic body. The firing temperatures were estimated both from the mineral composition of the bodies and from dilatometry measurements.

2. ARCHAEOLOGICAL SAMPLES AND EXPERIMENTAL METHODS

On the basis of the archaeological information given by Th. Matin and A. Vernhet, and for the good quality of the slip, three samples were selected from La Graufesenque (TSG…) and two from Montans (TSM…). These samples are dated between 20 and 80 AD. The investigations were carried out with a Philips CM20 electron microscope equipped with an EELS spectrometer. The ceramics were thinned first by mechanical grinding, then by using a PIPS (Precise Ion Polishing System). The X-ray diffraction patterns were recorded using a Seifert 3000T diffractometer equipped with a post-sample graphite-monochromater (λ=CuK$\alpha_{1,2}$).

3. TEM-EELS INVESTIGATION

At the nanometer scale, the slip of the five samples shows the same structure: small crystals dispersed in a glass matrix (fig. 1). EELS measurements were made in order to determine the composition of the matrix and the crystals. The matrix contains mainly Al, Si and O. The mole ratio Al/Si is around 1/5 for all samples (table 1). In each sample the composition of the glass matrix is rather homogeneous. Two populations of crystals can be easily identified. First, for crystals with well-delimited straight edges (noted H, in the figure 1), electron diffraction shows that the bigger crystals of this type have the hematite structure. EELS shows that all these crystals contain, in addition to O and Fe, a small amount of Ti and Al. The absence of Si K-edge in the spectrum on the figure 1 (curve a), confirm that the matrix surrounding the crystal were not analysed. Al is present in the crystal and not due to the contribution from the matrix. The O K-edge is typical to the iron oxides and similar the O K-edge of hematite. From the area surface peaks, the proportion of substitution on the Fe-sites can be evaluated with an accuracy of about 10%. In the fives samples, the hematite crystals contain Ti and Al in similar proportions (table 1). Crystals of the second type (C) are smaller with curvilinear edges. Only the crystals in very thin zones can be analysed alone without the matrix. In the majority of cases, the analysed volume is larger that the crystal, like as for the curve b of the figure 1. Compared to the analysis of the matrix alone, the ratio Al/Si and the shape of Al K-edge are very different. These crystals contain Al in significant proportions. The iron is also present in weak proportions. From XRD (Cf. §4) and micro-Raman investigations, the main mineral phases are hematite, corundum and quartz. A few rutile crystals were also found in some slips by micro-Raman. Among these phases, only the corundum is in agreement with the EELS analysis. Crystals of the second type are corundum and contain a small amount of Fe, which can be estimated around 7% (table 1). In the TSG50aa sample from La Graufesenque, few spinel crystals were found. These crystals contain Mg, Al, Fe and O but in different proportions.

	Matrix			Hematite				Corundum		
Sample	**Al (%)**	**Si (%)**	**N**	**Fe (%)**	**Al (%)**	**Ti (%)**	**N**	**Al (%)**	**Fe (%)**	**N**
TSMTH1	23 (4)	77 (4)	3	88 (4)	8 (2)	5 (1)	3	94 (3)	6 (3)	2
TSMTH3	22 (4)	78 (2)	2	87 (3)	9 (2)	4 (1)	3	93 (2)	7 (2)	3
TSGGL6	21 (4)	79 (4)	4	87 (4)	9 (2)	6 (2)	4	94 (3)	6 (3)	4
TSGGL10	19 (3)	81 (3)	3	87 (4)	8 (2)	5 (2)	4	94 (3)	6 (3)	3
TSG50aa	19 (2)	81 (2)	5	87 (4)	8 (2)	5 (2)	5	93 (4)	8 (3)	2

Table 1. EELS analysis. The two first samples are from Montans. The atomic concentrations are in mole and the standard deviations are given in parenthesis. N is the number of analysis.

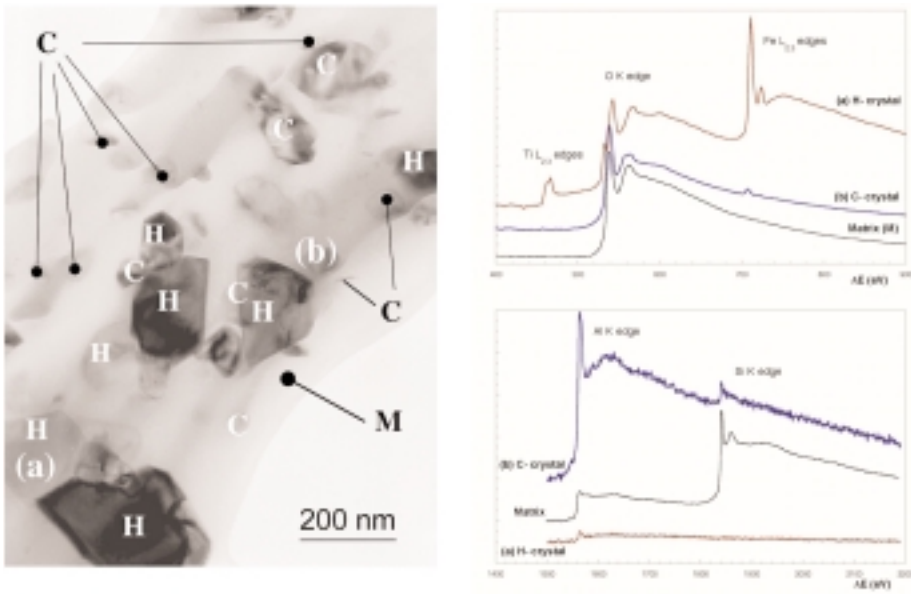

Figure 1. Bright field image of the TSGGL6 slip. The EELS spectra of the matrix (zone M), and of the (a) and (b) crystals are given on the right.

4. XRD STUDY

The diffraction patterns of the five samples are similar to those published in previous studies (Vendier *et al.*, 2002, Sciau *et al.*, 2004). The main crystalline phases are quartz, hematite and corundum. Rulite is present but only in very small amounts, in agreement with the micro-Raman study where few rutile crystals have been detected in the slip of samples from La Graufesenque and Montans. The strong diffraction lines of anorthite were observed for two samples with thin slip (<15µm). We have already discussed this point (Sciau *et al.*, 2004) and it is due to the diffraction signal of the

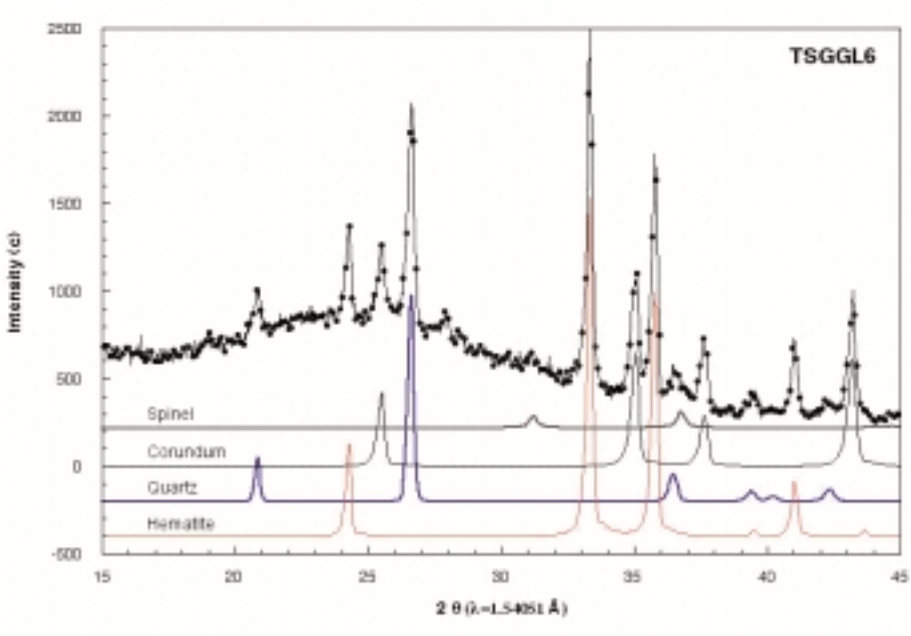

Figure 2. Observed powder diffraction pattern for the TSGGL6 sample in a limited 2θ range with the calculated contribution of different phases.

anorthite present in the body. Weak and very large peaks are also observed at the positions of a spinel phase. The diffraction patterns were fitted using the Rietveld method. The structures of the quartz, hematite, corundum, rutile and spinel phases were introduced. In a first step, the scale for each phase and the background were refined. However, in all samples, the amount of rutile was too weak (< 1%) to be refined. In a second step, the rutile phase was removed and the cell and the profile parameters of other phases were also refined (fig. 2). The experimental profile was introduced in order to determine the crystal imperfection broadening for each phase. The reflection lines of corundum are strongly broadened and the analysis show that this is mainly due to the crystal size in good agreement with the TEM observations, which showed that the corundum crystals are the smallest with a size of few tens nanometers. The line broadening is weaker for the hematite due to the larger crystal size. For quartz the broadening is mainly due to strain. The amount of spinel is too weak to provide an analysis of the diffraction profile and a determination of the origin of the line broadening. However, the diffraction lines are very large and it is clear that this phase is poorly crystallised. The cell parameters of the hematite are very similar from one sample to another but they are smaller than the cell parameters of the pure phase (Fe_2O_3), in agreement with a substitution of Fe by Al. The Al

substitution was estimated from the a-parameter (Perinet & Laffon, 1972). The cell parameters of the corundum are larger than in the pure phase (Al_2O_3) in all samples. In the same way, the Fe-substitution was determined from the difference of the cell parameters (table 2).

	Hematite			Corundum			Quartz			Spinel
Sample	**W (%)**	**S (nm)**	**Al (%)**	**W (%)**	**S (nm)**	**Fe (%)**	**W (%)**	**St. (%)**	**S (nm)**	**W (%)**
TSMTH1	26 (1)	45 (5)	5.5 (4)	51 (2)	29 (5)	8 (1)	21 (2)	0.85	80 (20)	2 (1)
TSMTH3	34 (1)	44 (5)	5.5 (4)	38 (1)	18 (4)	10 (1)	28 (2)	0.86	80 (20)	< 1
TSGGL6	30 (1)	33 (4)	5.5 (4)	53 (1)	22 (5)	8 (1)	15 (2)	1.1		2 (1)
TSGGL10	36 (1)	44 (5)	3.8 (4)	33 (1)	17 (4)	9 (1)	26 (2)	0.75	40 (10)	5 (1)
TSG50aa	37 (1)	54 (6)	5.7 (4)	34 (2)	24 (5)	9 (1)	28 (2)	0.95		1 (1)

Table 2. Rietveld results. W and S are respectively the relative weigh and the crystal size of the analysed phase. The atomic substitutions are in mole with the deviations given in parenthesis.

5. CONCLUSION

The analysed slips of the sigillata from La Graufesenque and Montans have the same specific microstructure: a glass matrix containing sub-microscopic hematite and corundum crystals. The glass matrix is mainly made of silicon and aluminium oxide. Iron or other metallic ions are not present so it is certainly transparent. The colour is given by the hematite crystals and to a lesser measure by the corundum crystals, which contain iron. So it is essential to determine the size, the composition and the distribution of these crystals. The colour of hematite depends on the crystal size. The bulk crystals are black and when the size decreases (< 1μm) the colour shifts to red. The fraction of aluminium has a similar effect (Barron & Torrent, 1984). The presence of iron in corundum gives a light yellow colour to these crystals. The two crystal populations are homogenously dispersed in the matrix and, together, they give the red-orange colour to the sigillata.

REFERENCES

Barron, V.; Torrent, J. (1984). *Clays and Clay Minerals*, **32**, 157-158.

Madrid Fernández, M.; Buxeda i Garrigos, J. (2002). Modern Trends in Scientific Studies on Ancient Ceramics, *BAR International Series*. **1011**, 287-298.

Perinet, G.; Laffon, R. (1972). *C.R. Acad. Sci. Paris*, **275**, 1021-1024

Picón, M. (1997). *Revue d'Archéométrie*. **21**, 86-96.

Picón, M.; Carré, C.; Cordoliani, M.L.; Vichy, M.; Hernández, J.A.; Micnard, J.L. (1975). *Archaeometry*, **17 (2)**, 191-199.

Schneider, G. (1978). *Berliner Beiträge zur Archäeometrie*. **3**, 63-122.

Sciau, Ph.; Languille, M. A.; Dooryhee, E.; Martín, Th.; Vernhet, A. (2004). IPA - Archaeological Portuguese Institute, *Proceedings of the 7th European Meeting on Ancient Ceramics* (to be published).

Vendier, L.; Sciau, Ph.; Dooryhee, E. (2002). *J. Phys. IV France*. **12**, Pr6 189-196.

EARLY NEOLITHIC POTTERY PRODUCTION IN HUNGARY: A COMPARATIVE ARCHAEOMETRICAL STUDY OF KÖRÖS AND STARČEVO CERAMICS

György Szakmány, Katalin Gherdán
Department of Petrology and Geochemistry,
Eötvös L. University, Budapest, Hungary

Elisabetta Starnini
Department of Archaeology and Classical Philology,
University of Genova, Italy

1. INTRODUCTION: ARCHAEOLOGICAL BACKGROUND

This interdisciplinary research project started some years ago in order to characterize the oldest pottery production in Hungary from the Early Neolithic Körös and Starčevo cultures, dated to the first half and middle of the VIth millennium B.C. (Makkay 1989; 1992; Bökönyi 1992; Kalicz et al. 1998; Whittle et al. 2002).

The Starčevo culture represents the westernmost unit of the large Early Neolithic archaeological complex, comprising towards the east Körös culture and even more to the east, Criş culture, representing the first food-producing communities in the Carpathian Basin. In Hungary, the Körös culture spreads in the Great Hungarian Plain, while Starčevo occupies the southern part of Transdanubia, reaching its northernmost borders at Lake Balaton (fig. 1.)

The two cultures show strong similarities in their material culture. The characteristic pottery of the period is homogenous in form and macroscopic features over a wide area, suggesting a high degree of cultural contacts and transmission of technological skills.

The research concentrates on pottery raw material as well as production technology.

Representative pottery samples were studied from five different Neolithic settlements of the Körös culture – located near Endrőd and Szarvas – and compared to those coming from one Starčevo culture site, Vörs. For comparison other fired clay artefacts (net weights) were also studied from Körös culture.

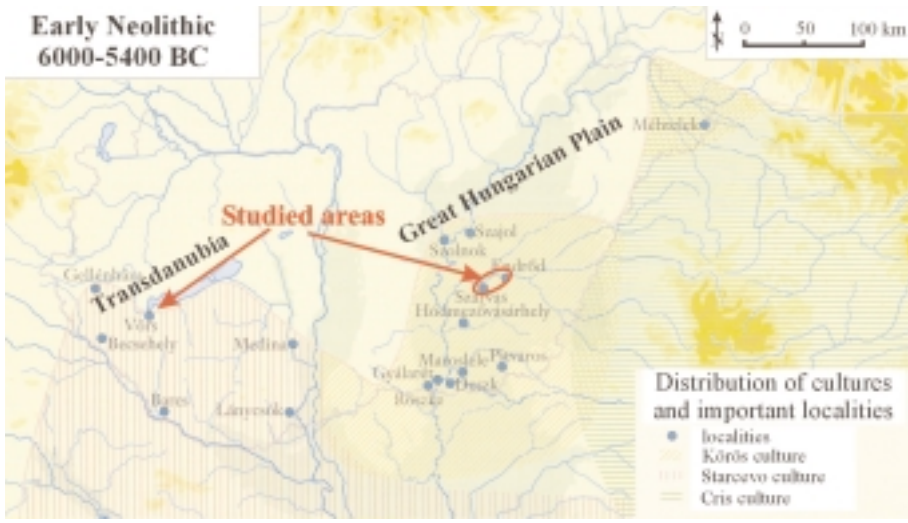

Figure 1. Studied area and localities of the collected samples.

2. METHODS

50 pottery samples, accompanied by 8 net weight samples of the Körös culture and 17 samples of the Starčevo culture were subjected to analyses. Sherds were examined under the binocular microscope and petrographic analysis was carried out under the polarizing microscope. Fabric analysis and quantitative analysis (volume percent) of the non-plastic material was done. Mineralogical composition of the paste was revealed with the help of X-ray powder diffraction analysis.

X-ray fluorescence analysis (XRF) and instrumental neutron activation analysis was used to determine the following major and trace elements: Si, Ti, Al, Fe, Mn, Mg, Ca, Na, K, P, Rb, Sr, Ba, Pb, Th, Zr, Hf, Nb, Y, V, Cr, Co, Ni, REE.

The small, rounded nodules present in the pottery samples were examined under the scanning electron microscope; their chemical composition was determined by the electron microprobe.

3. RESULTS

3.1. Petrography

The results of petrographic and X-ray powder diffraction analyses of both Körös and Starčevo culture samples were already shown in detail (Szakmány et al, in press; Gherdán et al, in press). Potteries of both cultures are dominantly very porous and fine grained, having serial (in few cases

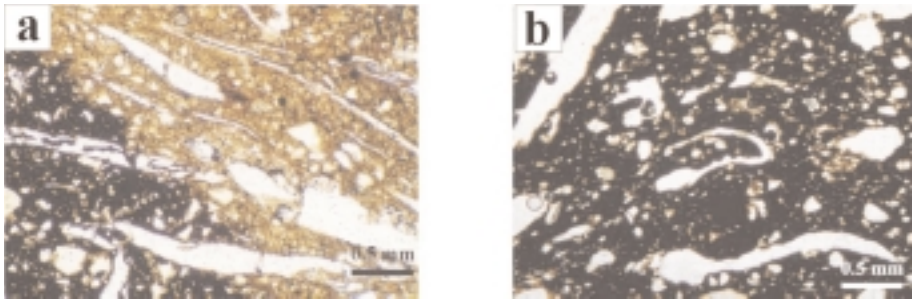

Figure 2. Thin-section micrograph of a tipical Körös Culture (a) and Starčevo Culture (b) potteries.

hiatal) fabric. Vegetal material – most probably chaff – was used as tempering material. Other non-plastic material involves: mono- and polycrystalline quartz, plagioclase, K-feldspar, mica and accessories (tourmaline, zircon, rutile etc.). These mineral fragments are mainly angular. In some Starčevo culture samples well rounded clay pellets and angular–sub rounded argillaceous rock fragments are also present. The amount of non-plastic material is little in both cultures' potteries, not exceeding 15 volume percent (fig. 2).

Macroscopically all potsherds have a "sandwich-like" structure, i.e. the surface and the margin of the pottery fragments is red–brownish red, while their core is black. Separate X-ray powder diffraction analyses of the cores and the margins showed compositional differences between the parts. The most striking feature is the presence of chlorite in the core and its absence in the margin. These results compared to Livingstone's ethnoarchaeological survey of firing types, show that the potteries were fired at low maximum temperatures (700–750°C), with high heating rates and short soaking times.

3.2. Fe-rich nodules

In some samples of both Körös and Starčevo pottery products rounded, pebble-like, almost opaque nodules, with a diameter of some millimetres (max. 15 mm) can be found as inclusions. Under the polarizing microscope these nodules are brownish red or almost opaque, containing mineral inclusions, dominantly quartz. The nodules were investigated under the scanning electron microscope and their geochemical composition was determined with the help of the electron microprobe. Backscattered electron images show that the nodules usually have similar concentric structure. Geochemical analyses revealed that iron poor (4–5%) and iron rich (30–40%) zones can be distinguished. The contact lines between the zones are sharp, at the borderline iron content can be extremely high (60–70%) (Fig. 3).

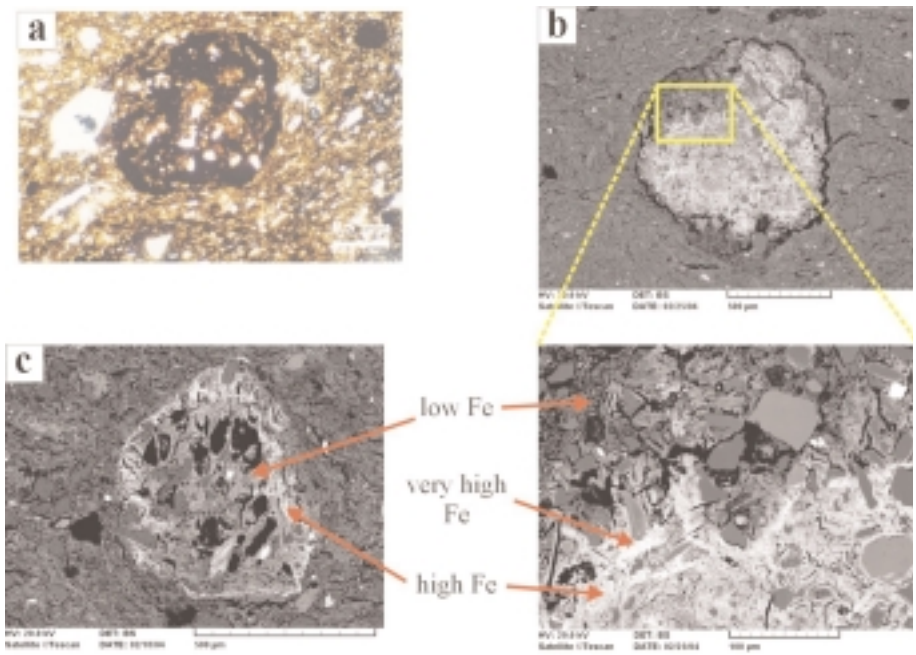

Figure 3. Microscopic and SEM images of the rounded nodules. a) Polarising microscopic photo from Körös Culture (Szarvas 23 site); b) and c) SEM images of the iron rich nodules in Körös Culture (a) and Starčevo Culture (b).

Structures similar to those discussed above are common in clay rich soils of marshlands or floodlands or in meadow soils (Szendrei 2001). This suggests that ancient potters of the Körös and Starčevo cultures used this kind of raw material.

3.3. Geochemistry of ceramics

Representative samples of both Körös and Starčevo culture potteries and one net weight sample from Szarvas were subjected to "whole pottery" (major and minor elements composition and REE-s) geochemical analyses. Multi element diagrams were used to recognize similarities and differences among samples. Geochemical data were normalized on the composition of post-Archean Australian Shale, PAAS (Taylor and McLennan 1985, McLennan 2001) and – in case of REEs – on chondrite composition (Nakamura 1974).

Major element patterns are very similar in case of SiO_2, TiO_2, Al_2O_3, Fe_2O_3, MgO and K_2O, also close to the composition of the PAAS. MnO, CaO and Na_2O contents vary in wider ranges, but samples from the same site keep

together. The only exception is the net weight sample from Szarvas. Phosphorus content – especially in case of Starčevo samples – is extraordinarily high, which is most probably due to contamination.

Minor element patterns are also similar, with greater differences in LIL element (Sr, Ba) composition. Rare Earth Element patterns follow the trend characteristic of fine grained sediments.

4. SUMMARY AND CONCLUSIONS

(1) This study compared the pottery productions of two Early Neolithic cultural groups (Körös and Starčevo) of the Carpathian Basin, using petrologic and geochemical methods.

(2) In both cultures potteries have similar macroscopic features and also similar mineralogical and geochemical composition. Based on the presence and geochemical composition of iron-rich nodules it is suggested that argillaceous silt or silty clay already subjected to pedogenesis was tempered with vegetal material and used as raw material in pottery manufacturing. X-ray powder diffraction analyses of the paste showed that potteries were fired at low maximum temperatures (700–750°C), with high heating rates and low soaking times.

(3) Data available so far seem to confirm the great homogeneity, already noticed at stylistic level, of the ceramic production (raw material, firing) of the early Neolithic in Hungary throughout a long period, most probably indicating cultural transmission within groups belonging to a traditionally structured, technologically stable society.

ACKNOWLEDGEMENTS

This research is conducted in the framework of the Hungarian-Italian Intergovernmental Science & Technology Cooperation Program 2004–2007. The authors are grateful to János MAKKAY and Katalin T. BIRÓ for the permission to analyse samples from their excavations, and to Kamilla G. SÓLYMOS, Heinrich TAUBALD, Farkas PINTÉR for analyses of the samples.

REFERENCES

Bökönyi, S. (ed.) 1992: Cultural and landscape changes in South-east Hungary. I. Reports on the Gyomaendrőd Project, Archeolingua 1. Budapest, 382 p.

Gherdán, K. – T. Biró, K. – Szakmány, Gy. in press: Petrologic studies on Early Neolithic Pottery from Vörs, SW Hungary. – Acta Mineralogica-Petrographica.

Kalicz, N. – Virág, Zs. – T. Biró, K. 1998: The northern periphery of the Early Neolithic Starčevo culture in south-western Hungary: a case study of an excavation at Lake Balaton. – Documenta Praehistorica XXV, pp. 151-187.

Makkay, J. (ed.) 1989: Békés megye régészeti topográfiája. A szarvasi járás IV/2. [The Archaeological Topography of Békés county, the Szarvas district IV/2] Magyarország Régészeti Topográfiája 8, Budapest, 500 p.

Makkay, J. 1992: Excavations at the Körös culture settlement of Endrőd-Öregszőlők 119 in 1986-1989. In: Bökönyi, S. (ed.) 1992: Cultural and landscape changes in South-east Hungary. I. Reports on the Gyomaendrőd Project, Archeolingua 1. Budapest, pp. 121-193.

McLennan, S. M. 2001: Relationships between the trace element composition of sedimentary rocks and upper continental crust. Geochemistry, Geophysics, Geosystems, **2**, 2000GC000109 (electronic publication).

Szakmány, Gy. – Starnini, E. – Raucsik, B. in press: Preliminary archaeometric investigation of Early Neolithic pottery of the Körös Culture (Hungary). In: Proceedings of the 33nd International Symposium on Archaeometry, Amsterdam, 2002.

Szendrei, G. (2001): Micromorphology of inland soil types. – Budapest 156p. (in Hungarian).

Taylor, S. R. – McLennan, S. M. 1985: The Continental Crust: its Composition and Evolution. Blackwell, Oxford, 312 p.

Whittle, A. – Bartosiewicz, L. – Borić, D. – Pettitt, P. Richards, M. 2002: In the beginning: new radiocarbon dates for the Early Neolithic in northern Serbia and south-east Hungary. – Antaeus 25. Budapest, pp. 63-117.

ARCHAEOMETRICAL INVESTIGATION OF POTTERY OF THE 10th CENTURY, EDELÉNY, NORTH-EAST HUNGARY

Veronika Szilágyi, György Szakmány
Eötvös Loránd University, Department of Petrology and Geochemistry
e-mail: szilagyi.vera@vipmail.hu

Mária Wolf
Hungarian National Museum, Department of Medieval Archaeology

Tamás Weiszburg
Eötvös Loránd University, Department of Mineralogy

1. LOCALITY AND IMPORTANCE

This study deals with the archaeometric investigation of ceramic finds of a 10th century (period of the Hungarian Conquest) archaeological settlement, Edelény.

The earthwork of Borsod on the castle hill lies on the bank of river Bódva in the town of Edelény 30 km North of Miskolc, North-East Hungary (fig. 1).

Figure 1. Location map of the castle hill of Borsod.

Figure 2. Typical forms of vessels from Edelény.

Excavations directed by Mária Wolf were going on here from 1987 to 1999. Archaeological research has proved that there was a fortress here at the time of the foundation of the Hungarian State (at the end of the 10th or at the beginning of the 11th century) which functioned as the county town of the newly formed Borsod County of the new state.

There was a Hungarian village in the 10th century on the castle hill before the building of the earthwork. This settlement – according to archaeological evidence – burnt down and eleven houses destroyed by the fire were found. Under the ruins a great variety of archaeological finds came to light among which pottery has an overriding importance. Up to now only pots coming from graves could give information on contemporary Hungarian pottery technology. It is now the first time that there is possibility for analysis of ceramics of a closed context from that period (Wolf 1996, 2003).

2. ARCHAEOLOGICAL CONTEXT AND EXPERIMENTALS

More than 100 complete pots and a large number of fragments of vessels made by slow throwing were found during the archaeological excavation. To a large extent pottery was used as a cooking implement (fig. 2). The ceramic

assemblage contains several sherds whose shape (so-called ribbed-necked ceramics) has connection with the Eastern culture of Saltovo that involved the early home of the Hungarians. On the surface of some of the sherds signs of high temperature alterations (blisters) can be detected.

The aim of our study was to determine the provenance of the raw material (whether the sherds showing a different shape are imports), the method of manufacture and to observe ceramics suffered secondary firing (conflagration).

The analytical program was based on macroscopic and thin-section petrography, accompanied by X-ray powder diffraction and X-ray fluorescence analysis of the pottery samples. Besides the pottery assemblage, a natural, clay rich sediment, collected in the vicinity of the excavation, was also examined with the same methods. Petrographic analysis by polarizing microscope was applied for study of the temper material and the fabric, X-ray powder diffraction analysis (XRPD) for phase identification and bulk (major and trace) element analysis by X-ray fluorescence method (XRF) for getting to know chemical composition of ceramics. To characterize sherds with blistered surface the scanning electron microscope equipped with an energy dispersive spectrometer (SEM-EDS) was used.

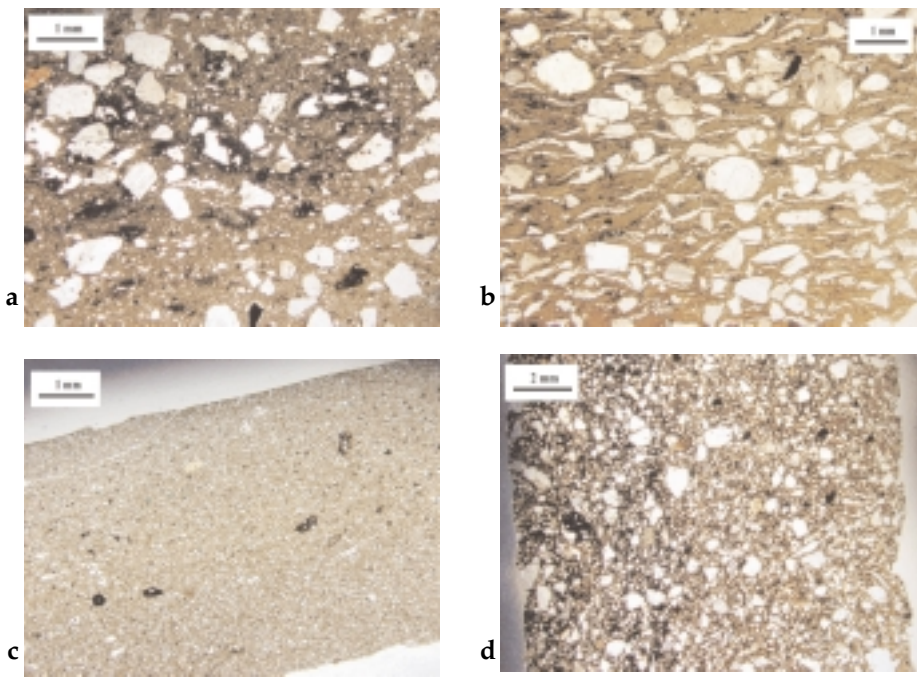

Figure 3. Thin section photos of type I and the fabric subgroups of ceramics.

3. PETROGRAPHIC INVESTIGATIONS

Microscopic investigations were aimed at the classification of ceramics on the basis of the composition of the non-plastic inclusions and secondly of the fabric. Pottery samples form three groups, each of which contains textural subgroups (hiatal, serial).

Group I (fig. 3) has a non-plastic component composition consisting mainly of acidic-neutral low grade metamorphic litho- and mineral fragments (quartz, feldspar, muscovite) and argillaceous rock fragments. In addition to this, sedimentary (radiolarite, carbonatic) and magmatic lithofragments were found in small quantities. There are 4 fabric subgroups inside this group: the most frequent one is a hiatal fabric with silty clay matrix (fig. 3a), more rare is a hiatal fabric with pure clay matrix (fig. 3b), while a few sherds have serial fabric (fine- or medium-grained (fig. 3c-d)). In most cases the use of temper can not be proved, although there are few samples that show signs of tempering or levigation.

Group II has a similar composition to the previous group concerning temper, except for the complete or almost complete absence of detrital mica and mica bearing metamorphic lithofragments (fig. 4).

Group III contains dominantly calcite, poly- and monocrystalline quartz and metamorphic lithofragments as temper grains (fig. 5).

Each pottery considered to be an outlier from an archaeological point of view (so-called ribbed-necked ceramics) belongs to group I.

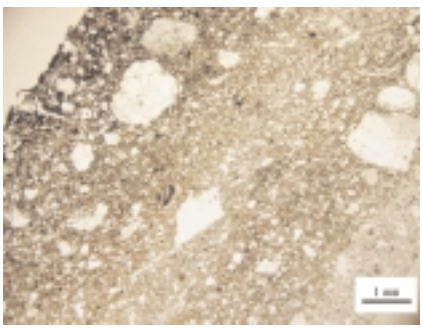

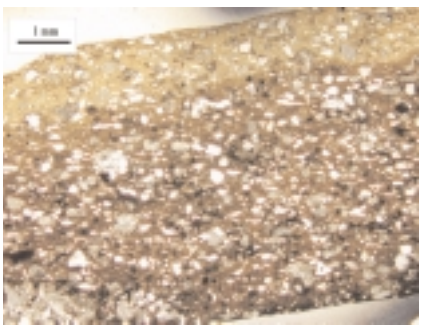

Figures 4-5. Thin section photos of ceramics of type I and II.

4. MINERALOGICAL (XRPD) ANALYSIS

X-ray powder diffraction was applied in order to identify mineral phases especially the clay matrix. The analyzed samples generally consist of mica type (10Å) phyllosilicate, quartz and feldspar (as expected on the basis of the microscopic observations). In the case of group II the phyllosilicates are not detected while in group III calcite can be detected. We had the opportunity to

collect samples from the local sediment (unmanufactured red clay). Its XRPD spectrum shows the same phases detected in fired ceramics. Mineral assemblage, especially the presence of calcite, suggests that ceramics were fired at relatively low maximum temperatures (<750˚C).

5. GEOCHEMICAL ANALYSIS

We had the opportunity to analyze both the ceramic samples and the potential raw material by XRF analysis. To present the main differences between the raw and the fired material we applied values normalized to the raw clay. Major and trace element composition of the potteries and a local, clay rich sediment shows great similarity, strengthening the hypothesis that potters used local raw material. In spite of this fact there are smaller differences. There is positive anomaly of CaO and P_2O_5. The divergences of the P_2O_5 can indicate an effect of the manufacture or use of the ceramics. The high CaO content characterizes group III.

6. ON TRACK OF THE CONFLAGRATION

Samples affected by overfiring got blistered on their surface and the remaining material looks like slag (large bubble-like pores and isotropic vitrified material around) (fig. 6). Backscattered electron images of the vitrified material show an interesting fabric (fig. 7). Light grey material is a Si-Al-alkali-rich vitrified phase while dendrite-like skeletal crystals are Fe-Si-rich minerals (fayalite). The presence of skeletal crystals suggests a very fast cooling that could not have happened if the pots had been overfired in a kiln (so they are not wasters). This fabric is an evidence for alteration of pots in a quick, very intensive fire.

7. CONCLUSION

With the help of the petrographic and instrumental analitical investigations it can be stated that ceramics of the 10th century from Edelény form 3 groups on the basis of the material of the non-plastic grains. The non-plastics of the ceramics are mostly polimict and a little part of them is monomict. These clasts seem to be similar to the geological environment according to their composition (mainly low grade metamorphic rock fragments and granitoid magmatic, sedimentary rock and limestone fragments to a smaller extent), so the potter may have used local raw material. Moreover, the potential area of the provenance, the gathering ground of river Bódva, has got a complex geology that can create a polimict feature to our ceramics. In spite of the fact that there are smaller differences between the groups the pottery assemblage does not contain import pots. In

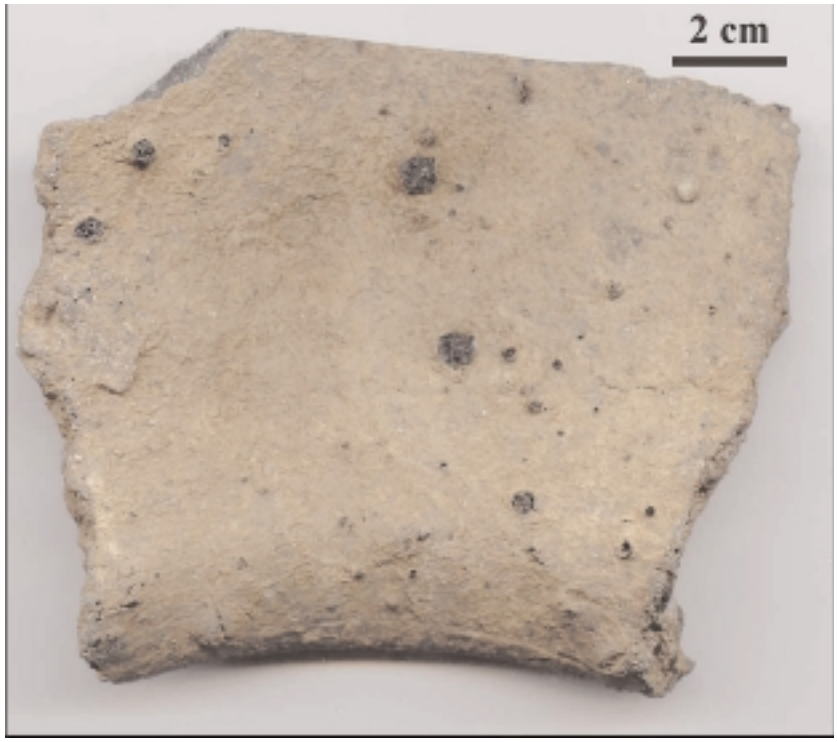

Figure 6. Blistered surface of a ceramic suffered secondary overfiring.

some cases pots suffered secondary overfiring when the settlement burnt down and got blistered on their surface. Vessels were manufactured by tempering or not the local clay with local alluvial sand (mainly metamorphic, granitoid magmatic and limestone rock fragments) after that were fired on a medium temperature (<750ºC). The potter was unable to control the firing atmosphere in the chamber (of a kiln or a pit).

AKNOWLEDGEMENTS

The authors are grateful to Gy. Lovas, J. Király, K. Gál-Sólymos (Eötvös Loránd University), H. Thaubald and F. Pintér (University of Tübingen) for their help in laboratory work. This work and our participation on the "Archaeometry 2004" Conference was supported by "Pro Renovanda Cultura Hungariae" Foundation and Eötvös Loránd University, Faculty of Sciences.

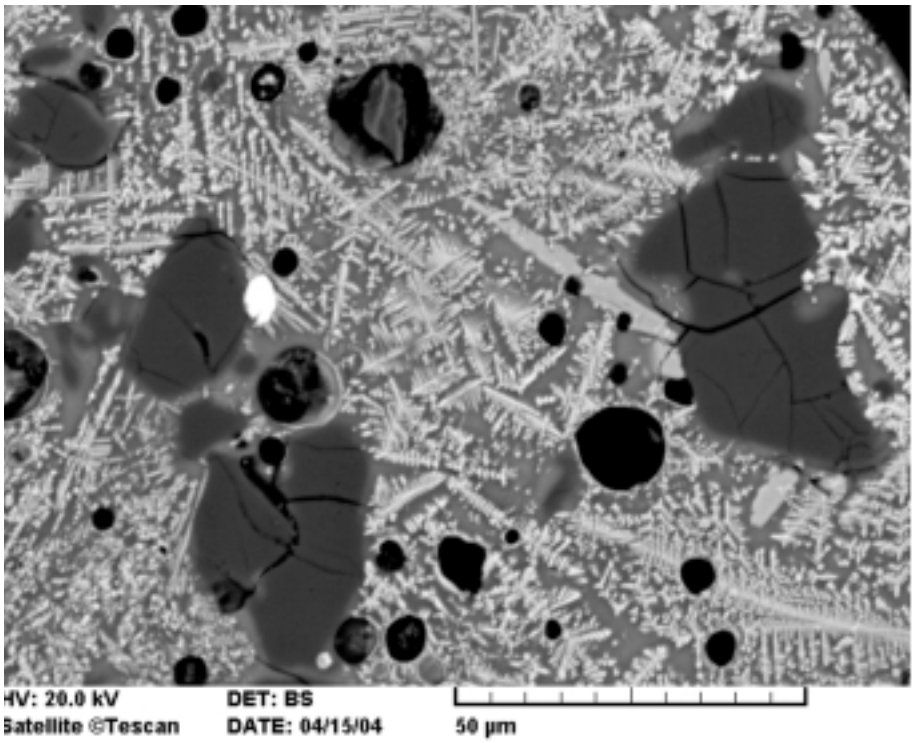

Figure 7. Backscattered electron image of a blistered pore.

REFERENCES

Wolf, M. 2003: New results on the Hungarian ceramic production of the 10th century. Evidences of the finds of Borsod. In: XLII. Almanach of the Herman Ottó Museum of Miskolc, pp. 85-108.

Wolf, M. 1996: Edelény - Fortress of Borsod. In:The Ancient Hungarians – Exhibition Catalogue, Hungarian National Museum, p. 417-423.

THE WANDERING SCIENTIST, OR THE QUEST FOR INTERCALIBRATION

S.Y. Waksman
Laboratoire de céramologie, CNRS UMR 5138,
Maison de l'Orient et de la Méditerranée, 7 rue Raulin, 69365 Lyon cedex 7, France,
waksman@mom.fr

1. INTRODUCTION

Intercalibration has been a long-standing concern, which arises as soon as different laboratories wish to compare their analytical results (e.g. Yellin *et al.* 1978, Hatcher *et al.* 1980, Harbottle 1982, Jones 1986, Tomlinson 2002, Hein *et al.* 2002) or when a given laboratory is moving from one analytical method or protocol to another (e.g. Hatcher *et al.* 1995). It also comes out when a given scientist happens to move from one lab to another - a situation that most beginning scientists experience - and intends to use his/her own data in a cumulative way. Although analytical results tend in general to be more reliable, analytical shifts between different setups are still observed. It is thus desirable to try to correct these shifts, or at least to be aware of them when one has to interpret results of various origin.

We would like to mention the intercalibration procedure we have been using over a number of case studies. Our main motivation was the simultaneous use in clustering analysis of data we acquired in different laboratories, in the framework of provenance studies of ceramics (Chervinsky *et al.* 1996, Waksman 2002, Waksman and François forthcoming). These data were obtained by methods as diverse as WD-XRF (Laboratoire de céramologie, Lyon, France), PIXE (Centre de Recherches Nucléaires, Strasbourg, France and Harvard University, Cambridge Mass., USA), INAA (Centre de Recherches Nucléaires, Strasbourg, and Hebrew University, Jerusalem, Israel), ICP-AES and ICP-MS (Geological Survey of Israel, Jerusalem). Collaborative programs with laboratories in Oxford (analyses by ICP-AES carried out by H. Hatcher) and in Beirut (PIXE) also required intercalibration (Waksman *et al.* 2001, Roumié *et al.* forthcoming). For each setup, the initial optimization and performance characteristics had been independantly determined with the help of certified standards (Waksman *et al.* 1995, Waksman 1995, Megaw *et al.* 2003, Roumié *et al.* 2004).

2. INTERCALIBRATION PROCEDURE

The procedure starts as usual with the analysis in the two systems to be intercalibrated of a common batch of samples or standards. The results are then compared to evaluate if they are significantly different, taking into account the respective precision of the analytical setups. If they are, we try to determine whether corrections may be applied using a simple, empiric model based on linear least squares regression. For a given element, three cases are distinguished, which are illustrated in figure 1 and related data (table 1).

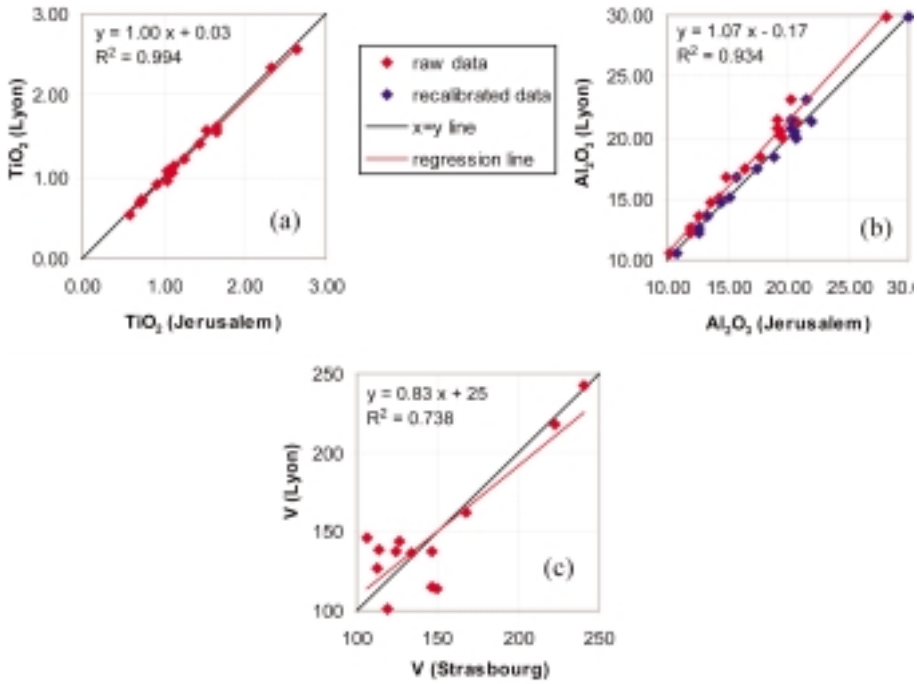

Figure 1. Analytical results obtained on the same samples in different laboratories: raw data and associated regression line, x=y line and recalibrated data (case b). The coefficients of the regression line are indicated, as well as the squared coefficient of correlation R^2. TiO_2 and Al_2O_3 are in weight pourcent, V in ppm.

– The results are not significantly different. The analyses of the intercalibration batch in setup 1 (x coordinate) plotted against the analyses of the same batch in setup 2 (y coordinate) closely correspond to the x=y line (fig. 1a);

– The results are significantly correlated but the regression line between the two series of analyses is not the x=y line (fig. 1b);

	TiO_2 (%)			Al_2O_3 (%)				V (ppm)		
	Lyon	Jeru.	certif. raw	Lyon	Jeru. raw	Jeru. recal.	certif.	Lyon	Stras. raw	certif.
σ/m	< 1%	< 1%		< 1%	< 1%			5%	>20%	
DRN	1.070	1.04	1.11	18.35	17.74	18.81	17.89	218	223	225
BEN	2.644	2.57	2.69	10.49	10.24	10.79	10.39	243	240	242
SRM679	1.055	0.95	1.050	23.06	20.33	21.59	22.64			
ECRM776	1.526	1.57	1.63	29.80	28.18	29.98	29.44			
KNsherd	0.738	0.72	*0.77	15.11	14.32	15.15	*15.0			
BYZ 1	0.724	0.70		17.49	16.50	17.49		115	146	
BYZ 2								101	119	
BYZ 3								114	150	
BYZ 4								127	113	
BYZ 5	1.142	1.14		21.34	20.68	21.96		137	146	
BYZ 6								136	134	
BYZ 7	1.114	1.06		20.69	19.11	20.28		162	168	
BYZ 8	0.920	0.92		19.89	19.56	20.76		139	114	
BYZ 9								144	126	
BYZ 10	0.704	0.69		20.46	19.42	20.61		137	124	
BYZ 11	0.584	0.53		21.44	19.15	20.32		146	106	
BYZ 12	1.266	1.22		13.53	12.62	13.33				
BYZ 13	1.658	1.62		12.59	11.97	12.64				
BYZ 14	1.665	1.54		16.69	14.94	15.82				
BYZ 15	1.457	1.40		14.70	13.71	14.50				
BYZ 16	2.323	2.33		20.27	19.35	20.53				
BYZ 72	1.048	1.07		12.27	11.97	12.64				
	Fig. 1a			Fig. 1b				Fig. 1c		

Jeru.: Jerusalem; Stras.: Strasbourg; recal.: recalibrated; certif.: certified; * : indicative; σ/m : estimated precision.

Table 1. Intercalibration data obtained in Lyon, Jerusalem and Strasbourg laboratories corresponding to biplots (fig. 1). The "BYZ" series corresponds to ceramics samples, others are standards.

– The results are significantly different and not significantly correlated, although the coefficient of correlation R may be high (fig. 1c).

In the first case, no correction is applied. In the third case, the element is not considered fit for use in statistical analysis involving data from the two systems. In the second case, we use the regression line to calculate recalibrated data. Data are calibrated against one of the system which is chosen as the "reference system", or the "reference lab". Our choice was not *a priori* based on the performance characteristics (precision, accuracy, detection limits, long term reproducibility) of the respective setups. Still, the reference system is *a minima* expected to present reasonably good precision and long term

reproducibility, features much more critical here than accuracy. It is the case for data accumulated over the last 25 years or so at the "Laboratoire de céramologie" in Lyon, which has been chosen as reference laboratory also for practical reasons as the one where our analyses are still on going, as opposed to analyses carried out elsewhere in the framework of limited projects.

The aim of the intercalibration is to predict values as close as possible to those which would have been obtained in the chosen reference setup. Thus, the latter is taken in fig. 1 as the y coordinate. The slope a and intercept b of the regression line obtained from the (x,y) batch are used to calculate recalibrated data (x_recal) : x_recal = ax + b. The binary plot (x_recal,y) shows how the points have been brought back to the x=y line (fig. 1b). When the corrected (x_recal) values are globally closer to the (y) values than the (x) values, the same correction is applied to the whole batch of samples analyzed with setup (x) to be intercalibrated, before they are used in statistical treatments together with samples analyzed with setup (y).

This procedure is able to take into account systematic shifts as well as shifts which vary linearly with the concentration within the range considered. Surprisingly, it seems to have been hardly ever used in the literature, as corrections are often limited to the multiplication by a single average ratio (Hein *et al.* 2002, Tomlinson 2002). It is also possibly due to the fact that it requires the analysis of a more extensive intercalibration batch.

3. INTERCALIBRATION BATCH

A careful choice of the intercalibration batch is required. We used to include certified geological standards. However, it appeared that the possibility to refer to "absolute" concentrations mattered less than samples which fully represent the range of values under consideration. Commercial certified standards are actually rarely representative of the ceramics we are dealing with both by their matrix and by the concentrations in trace elements. Whenever possible, we now think it preferable in the case of a finite number of data to select within the samples to be calibrated a sub-sample representative of its variability to be re-analyzed in the other system. This batch should ideally be chosen such as:

– for each element, compositions cover the whole interval of values to be calibrated;

– for each element, points are evenly distributed over the whole interval (and thus not fit for modelling as a normal distribution, hence our designation of "empiric model");

– the intercalibration batch contains as few samples as possible.

Figure 1c illustrates a case where the intercalibration batch is not quite appropriate. High values of vanadium (V) in geological standards DR-N

and BE-N (Geostandard Newsletter 1989) lead to a fairly high, statistically significant, R^2. However, points corresponding to ceramics samples show a large dispersion (to be related to the low precision of V (Strasbourg)) which excludes the use of this element for the pair of setups and the range of concentration considered (65<c<190 ppm). In general, outlying points may induce R values which do not reflect the actual correlation of the whole batch.

The choice of the intercalibration batch is of course more delicate when one is dealing with two on-going databases. Samples representative for different types of clay material (kaolinitic, highly calcareous, derived from ultrabasic rocks, etc.) may be included to cover as much as possible of the potential geochemical variations.

4. CONCLUDING REMARKS

This procedure improves the comparability of data for elements showing significantly correlated results in a properly chosen intercalibration batch. The intercalibration of the 6 setups we considered requested the examination of a large number of biplots and related data, all of which can not be extensively presented here. Neither is it possible to extend on the subsequent use of recalibrated data in multivariate statistical treatments and the trends observed in different situations of clustering (features of inter-group and intra-group variability, direct versus indirect intercalibration via the reference setup, etc.). The procedure we described may seem rather tedious, as clear-cut differences will in general be visible independantly of the quality of the intercalibration, whereas in delicate cases of attribution doubts may always remain. It may however clear up several situations in-between. Probably its prime virtue is to make us aware of the limits of compatibility of the data, and, in the framework of provenance studies based on compositional data, to help us interpreting how significant chemical differences are.

REFERENCES

Chervinsky, J., Waksman, S.Y., and Scott, J.A., 1996, A new PIXE-RBS setup at Harvard University: application to the analysis of Byzantine glazed ceramics from the excavations of Sardis, unpublished poster presented at Archaeometry '96 (Urbana, Illinois, USA).

Geostandard Newsletters, 1989, **13**, Special Issue.

Hatcher, H., Hedges, R.E.M., Pollard, A.M., and Kenrick, P.M., 1980, Analysis of Hellenistic and Roman fine pottery from Benghazi, *Archaeometry*, **22**, 133-151.

Hatcher, H., Tite, M.S., and Walsh, N., 1995, A comparison of inductively-coupled plasma emission spectrometry and atomic absorption spectrometry analysis on standard reference materials and ceramics, *Archaeometry*, **37**, 83-94.

Harbottle, G., 1982, Provenience studies using Neutron Activation Analysis: the role of standardization, in *Archaeological Ceramics*, Smithsonian Institution Press, Washington D.C., 67-77.

Hein, A. Tsolakidou, A., Iliopoulos, I., Mommsen, H., Buxeda i Garrigos, J., Montana, G., and Kilikoglou, V., 2002, Standardisation of elemental analytical techniques applied to provenance studies of archaeological ceramics: an interlaboratory calibration study, *The Analyst*, **127**, 542-553.

Jones, R.E., 1986, *Greek and Cypriot pottery. A Review of Scientific Studies*, Fitch Laboratory Occasional Paper 1, British School at Athens, Athens.

Megaw, A.H.S., Armstrong, P., Hatcher, H., 2003, Zeuxippus Ware: an analytical approach to the question of provenance, in *VIIe Congrès International sur la Céramique Médiévale en Méditerranée*, Athens, 91-100.

Roumié, M., Atallah, C., Nsouli, B., and Waksman, S.Y., forthcoming, Application of PIXE funny filter for cluster analysis of Byzantine amphorae from Beirut, *Nuclear Instruments and Methods in Physics Research B*.

Roumié, M., Nsouli, B., Zahraman, K., and Reslan, A., 2004, First accelerator based ion beam analysis facility in Lebanon: development and applications, *Nuclear Instruments and Methods in Physics Research B*, **219-220**, 389-393.

Tomlinson, J.E., 2002, Comparison of the results of neutron activation analysis on ancient pottery at two laboratories: N.C.S.R. "Demokritos" & the University of Manchester, in *Modern Trends in Scientific Studies of Ancient Ceramics*, BAR International Series 1011, 35-43.

Waksman, S.Y., and François, V., forthcoming, Vers une redéfinition typologique et analytique des céramiques byzantines du type *Zeuxippus Ware*, *Bulletin de Correspondance Hellénique*.

Waksman, S.Y., 2002, Céramiques levantines de l'époque des Croisades: le cas des productions à pâte rouge des ateliers de Beyrouth, *Revue d'Archéométrie*, **26**, 67-77.

Waksman, S.Y., Hatcher, H., and Armstrong, P., 2001, Recherches sur les céramiques byzantines: intercalibration et harmonisation des bases de données analytiques française et anglaise, Rapport final de programme franco-britannique CNRS – Royal Society, unpublished report.

Waksman, S.Y., 1995, Les céramiques byzantines des fouilles de Pergame. Caractérisation des productions locales et importées par analyse élémentaire par les méthodes PIXE et INAA et par pétrographie, unpublished Ph.D. thesis, University of Strasbourg.

Waksman, S.Y., Pape, A., and Heitz, C., 1995, Precision and accuracy in standards analysis by PIXE, *Journal of Radioanalytical and Nuclear Chemistry*, **196**, 135-142.

Yellin, J., Perlman, I., Asaro, F., Michel, H.V., and Mosier, D.F., 1978, Comparison of neutron activation analysis from the Lawrence Berkeley Laboratory and the Hebrew University, *Archaeometry*, **20**, 95-100.

6. BIOMATERIALS

INDEX

ANATOMO-PATHOLOGICAL STUDY OF THE HUMAN REMAINS COMING FROM THE DOLMEN DE CAÑADA REAL HOUSED AT THE ARCHAEOLOGICAL MUSEUM OF SEVILLE (SPAIN)

Rosario Cabrero García
Departamento de Prehistoria y Arqueología, Universidad de Sevilla.
E-mail: cabrero@us.es

Assumpciò Malgosa Morera, Santiago Safont Mas ,
M. Eulàlia Subirà de Galdàcano
Departament de Biologia Animal, de Biologia Vegetal i d'Ecologia, Unitat d'Antropologia, Universitat Autònoma de Barcelona.
E-mail: Assumpcio.Malgosa@uab.es ; Santi.Safont@uab.es ; Eulalia.Subira@uab.es

Ezequiel Gómez Murga
Licenciado en Historia. E-mail: egomezmurga@yahoo.es

1. INTRODUCTION

The human remains whose analysis we present in this *34th International Symposium of Archaeometry* come from the archaeological excavation carried out in 1967 by the Professor of «Prehistory, Ancient History and Middle Ages of Spain», Juan de Mata Carriazo y Arroquia (1899-1989) –at that time Delegate of Area of the National Service of Excavations–, in the denominated Dolmen de Cañada Real (Los Molares, Seville).

The Dolmen de Cañada Real belonged to an outstanding megalithic necropolis, of at least six L-shaped tombs, also well-known as tombs of bent corridor, dated by absolute dating method in the first half of the IV millennium B.C. (*El Palomar*).

Atmospheric data from Stuiver et al. (1998); OxCal v3.8 Bronk Ramsey (2002); cub r:4 sd: 123 prob usp (chron).

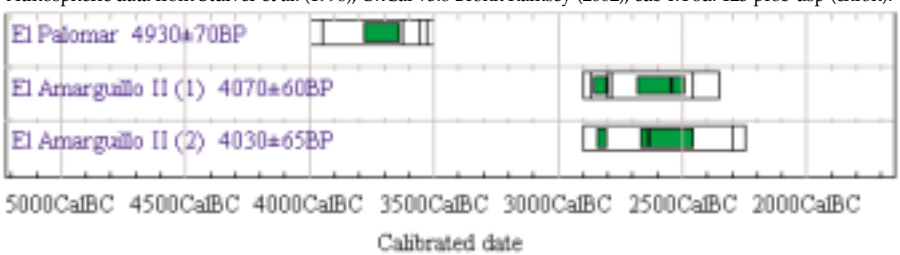

Members of the Department of Prehistory and Archaeology of the Faculty of Geography and History of the University of Seville have recently discovered, next to this necropolis, remains of the ancient settlement.

At that time the outlet of the river Guadalquivir was a great marine gulf whose coast was located about 15 kilometers to the W of our necropolis (Arteaga, Schulz, Ross 1995).

The architectural elements of the *Dolmen de Cañada Real* are built out of sandstone, very abundant in the area. However, many of the materials found in their interior are carried out in raw materials of distant origin (variscite, serpentine, diabase,...).

The pottery is also of high interest, as some forms and decorations are reminiscent of those considered traditionally of the Andalusian neolithic of the «Culture of the Caves», and because in one of them, an inclusion (temper), a small metal ball (made up of copper, zinc, lead and iron), has been identified.

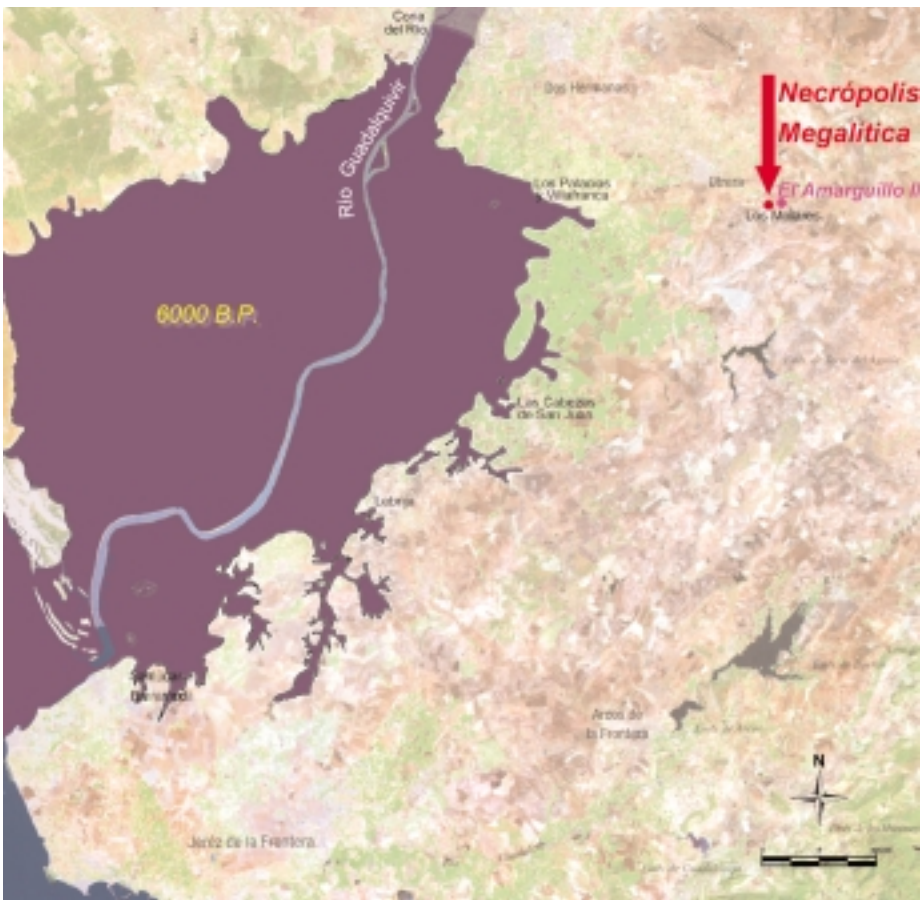

New perspectives would open up with the recovery and restoration of this megalithic tomb, because it would allow us to study new data related with its architecture and symbolic elements (concrete origin of the raw materials, quarry work, or possible presence of paintings, engravings...).

Not much more than a kilometre of distance of this archaeological place, we find another settlement, *El Amarguillo II*, in the same municipal term, with several tombs of different typologies (single graves and megalithic constructions) that have a later chronology (mid-III millennium B.C., by two dates based on C14). The site was discovered and dug by members of the Department of Prehistory and Archaeology of the University of Seville. It is an agricultural and cattle settlement, with a landscape in which grasslands proliferate between the arboreal formations of *Pinus* and *Quercus*, and where metalwork was carried out. In other recent studies, they highlight the latest discoveries of shapes related with the "typical schematic art".

2. ANALYSIS

The human remains of the *Dolmen de Cañada Real* were contained under five different numerations. Archaeological reference does not exist for the excavation that relates each bone group with a different burial. However, it seems logical to show off their ownership *a priori* to 5 burials (14315, 14316, 14317, 14318 and 14320) each one of which it has been studied independently.

R.E.P. 14315

Under this numeration belong cranial fragments, vertebrae, tibia, tarsus and metatarsus that seem to indicate the presence of a single individual. The size and thickness of the bone pieces as well as the welded epiphysis of the metatarsals and metacarpals indicate the individual's mature age. On the other hand, a fragment of lambdatic suture is conserved, located among the parietal bone and the occipital one that it has begun to be obliterated, process that habitually takes place starting from the 30 years which confirms the individual's mature age. Contrarily, the superior and inferior rims of the body of the vertebrae that are conserved are quite complete without alterations nor arthritis, more typical of a relatively young individual.

Regarding the individual's sex, the bones have a quite robust aspect and, baring in mind that no long bone is intact to be able to be assigned to a concrete sex, the size of the bones of the foot would seem more characteristic of a masculine individual. The cranial fragments are also fairly thick with the presence of strong muscular attachments and of a supramastoidal crest, characteristic usually associated with the masculine sex.

It is interesting to highlight the presence of two pathological vertebrae (LM-5 and LM-8). Both bones present nodules of Schmorld, lesions of variable size that are observed in the vertebral bodies in form of furrows or small sinkings and that they are usually produced by muscular strains on the spine that lead to microtraumatisms and sinkings of the external faces of the vertebral bodies. Also, you can appreciate an entesopathy in the tendon attachment of the astragalus LM-2 whose cause could possibly be a strain of the musculature of the first toe. The vertebral lesion and the entesopathic relate well with the robustness of the bones and the individual's sex, reflecting the possible hardness of the individuals way of life but of his age.

R.E.P. 14316

These initials correspond to a very fragmentary individual, represented by part of a femur as well as diverse bone chips. As it is logical, the individual's scarce representativeness does not allow its assignment to any age nor sex; only you can record the thickness of the femur fragment that would allow to attribute a mature age to the individual.

R.E.P. 14317

Not a single complete bone is conserved here, only fragments of various sizes whose anatomical study reveals the existence of two individuals: an adult and a sub-adult. This last one has been diagnosed starting from a rib whose dimensions cannot be related with the same individuals other bone fragment. It is not possible to indicate the age of this sub-adult individual since it lacks the distal end of the rib, although it would probably belong to a boy.

Regarding the mature individual, the remains could be attributed to a graceful, and therefore possibly feminine individual, as one can deduce from the fragment of left clavicle as well as from the gracile nature of the muscular attachments in the diaphysis of the bones of the forearm and in the fibula.

R.E.P. 14318

In this burial fragments of long bones, of scapula and of coccyx have been identified, as well as of the tarsus. All the bones present a state of not very favourable conservation for their reconstruction and diagnosis, but in spite of this the remains cannot be attributed to more than one individual. It is necessary to highlight the presence of an incinerated bone fragment (LM-CR-II-17) of which the conservation of the original structure of the bone, the absence of traverse fractures as well as the coloration of the bone seems to

indicate that the temperatures suffered by the bone were not excessive; everything leads to think of an accidental incineration of the bone more than in a differential funerary treatment.

In general the bone that better allows to carry out an approach of the sex and the individual's age is the coccyx since it is one of the bones that presents the biggest sexual dimorphism. In R.E.P. 14318 a fragment of left pubis was located that presents a quite closed pubic angle which allows us to assign it, in principle, to the masculine sex. This observation should not be considered as absolute since it is derived from a single character and not from a whole bone. In any case, the robustness of the fragments diaphysary, the size of the distal epiphysis of the femur and of the bones of the tarsus seem to confirm this diagnosis. In the same way, the general aspect of the scapula seems masculine, but the dimensions of the glenoid cavity (21,6 x 10,4 mm) would indicate an individual of feminine sex.

Regarding the age, the fragments of iliac crest of the coccyx bone and the distal epiphysis of a proximal phalange of the foot they show the individual's mature age. The pubic simphysis, used as age indicator shows a quite young individual (20-25 years) since the formation of bony borders is not observed in the simphysis.

R.E.P. 14320

These initials correspond to a varied bone group that includes diaphysis fragments and epiphysis of long bones, phalanges and other fragments (vertebrae, ribs, clavicles and scapulas). The morphological analysis of the bones indicates the presence of at least two individuals, deducible from the proximal and medial phalanges of the third finger of the hand that present different characteristics of size and robustness so that they do not match each other. At the same time, two ulna fragments (LM-CR-I-50 and LM-CR-I-60) are sufficiently different as for robustness, muscular impressions and size as to allow to differentiate between two individuals.

Since the epiphysis of the previously mentioned phalanges is welded with the diaphysis one can affirm the mature age of the two individuals. The same indication is provided by the state of the iliac crest. The only opposing inferior molar presents very little waste that which would indicate a 17-25 year-old individual.

In connection with the pathological study, the molar does not present cavities nor dental tartar, also, the observation of the root cavity confirms the absence of periodontal illness and consequently of periostitis, everything is more characteristic of a young individual.

On the other hand, in the fragment of sacrum (LM-CR-I-3) one can observe the presence of a discal hernia product of a lumbo-sacral deformity that which is indicative of an overload in the back.

3. CONCLUSIONS

The anthropological analysis confirms that these megalithic constructions harboured collective burials (7 in the *Dolmen de Cañada Real*). It is necessary to highlight the presence of an infantile individual, although their representation is tiny, and six adults of different sex but not of very advanced age.

However, working without of the references that accompanied the bones, one can only deduce the presence of a minimum of three individuals, two adults, probably of both sexes, and a sub-adult. Relatively young individuals are exposed to hard conditions of life, since these lesions are associated with the overload of muscular type and microtraumatisms caused by heavy loads in the back.

REFERENCES

Arteaga, O.; Schulz, H. D.; Roos, A. M.: «El problema del 'Lacus Ligustinus'. Investigaciones geoarqueológicas en torno a las marismas del Bajo Guadalquivir», *Tartessos, 25 años después*, Jeréz de la Frontera, 1995: 99-135.

RECONSTRUCTING THE DIET OF RANCHO DEL RIO'S INHABITANTS BY PALEOECOLOGICAL AND ARCHAEOLOGICAL APPROACHES

Alison Diefenderfer, David Small
Dept. of Sociology and Anthropology Lehigh University, Bethlehem, PA 18015, USA

Zicheng Yu
Dept. of Earth & Environmental Sciences Lehigh University, Bethlehem, PA 18015, USA

Aaron Shugar
Archaeometallurgy Laboratory Lehigh University, Bethlehem, PA 18015, USA
Smithsonian Center for Materials Research and Education, Suitland, MD 20746, USA

Within Archaeology, pollen analysis studies are used to determine the environmental conditions that existed during the time that of a site's inhabitance. Pollen analysis examines soils found in situ looking for and identifying microfossil, macrofossil, and phytolithic evidence from foliage over time providing information concerning past localized ecology, plant life. In addition, and more relevant to this study, pollen analysis can aid in the reconstruction of past diet by determining agricultural subsistence and local food sources available to the inhabitants. The investigation of ancient diets has interested archaeologist since it can aid in formulating hypotheses concerning aspects of ancient social and cultural activity including the rise, structure, and downfall of civilizations (such as what might have occurred in Latin America with the Mayan Civilization), issues of health, and evidence for local resource specialization. Agricultural crises, food shortages, and starvation could all be possible motives for a group to leave a particular village area or for the direct downfall of a complex society.

Although successful pollen analysis and archaeobotanical studies have been done in Latin America particularly at the Mayan site of Ceren, El Salvador (Sharer 1994:445), in Highland Guatemala (Islebe and Hooghiemstra 1996) and at the site of Laguna de Cocos in northern Belize (Hansen 1990), there has been limited success in northwestern Honduras. Part of our current investigation was to see if these types of studies could be done successfully at Rancho del Rio, a rural site in northwestern Honduras inhabited from pre 8th century A.D. to late 9th century A.D. based on pottery

analysis (Urban and Schortman) lacing it contextually in the Late Classic and Early Postclassic. In addition, based on the ceramic assemblage, it appears that Rancho del Rio was involved in producing ceramics on a large scale. We believe that Rancho del Rio may be a resource specialized site producing ceramics which would be traded for other stable goods, including food. The pollen analysis may also provide evidence of this theory.

What we hope to gain from this investigation is an understanding of the assemblage during inhabitance and what types of food the inhabitants produced, used, and consumed. Some elements of dietary restrictions/limitations have been noticed in human bone remains from this site (for example, Iron deficiencies). Were the inhabitants of Rancho del Rio cultivating exclusively maize, a staple crop in Maya society or were they supplementing their diet with other foodstuffs? Was this region farmed as it is currently? Were they even cultivating at this site or was food gathered elsewhere or even traded for? These are only some of the questions we hope the pollen assemblage could help answer.

Since there is not a lake nearby to take core specimens from, the pollen samples were taken from the excavation lots and floated in a flotation bucket. Thirteen samples (n=13) were collected along a section 20 to 80 cm below ground surface (BGS). This was inclusive of the time before, during, and after occupation as derived from the artifact collection. The actual period of inhabitance roughly correlates to the depth interval between 35 and 45 cm BGS. In total, four soil strata were distinguishable upon color, texture and general composition. These four layers were the topsoil and most contemporary layer (0-20 cm BGS), a gray and clayey layer (20-35 cm BGS), the mineral-rich layer corresponding with the floors of the site structures (35-45 cm BGS), and lastly, the dark brown sandy layer preceding inhabitance (45-80 cm BGS).

Since our archaeobotanical study occurred during the first year of Rancho del Rio's excavation in 2003, there was not a systematic and even intervaled sampling for flotation samples. Rather, we discriminated several general locales that we would expect minimal stratigraphic disruption (i.e. away from tree roots) and regions that would have been frequently used areas for food preparation and trash disposal (i.e. courtyards, trash middens) per Mayan cultural practices. We did not sample from areas where teeth and bones were found, although some of the soil samples collected were from a suboperation that later included skeletal remains. This last exclusion is due to the fact that pollen evidence would be disturbed, possibly discarded or destroyed by the sifting process necessary to find any other teeth or small skeletal remains not always noticeable at first glance.

With each of the 13 soil samples, a five phase investigation followed: (1) soil collection at the site, (2) flotation of samples, (3) chemical processing of

the filtered material, (4) analysis of the microfossil (on slide mounts) and macrofossil evidence (in plastic petri dishes), and (5) comparison of pollen to identification reference books.

The flotation of the samples was done so that the organic materal would be brought to the surface while the denser materials would sink to the bottom. The denser material includes clay and other material not necessary for paleoecological work. The organic-rich material was captured in a cloth coffee bean filter. With the samples where there was a great deal of organic material, more than 1 filter was used. In total, 14 subsamples resulted from the flotation.

In the laboratory, a 4-mL subsample was removed from each filter. Each subsample was sieved through 180 and 10-micrometer nylon mesh. The portion of each sample for macrofossil analysis was the portion sieved that was larger than 180 micrometers. This material was stored in petri dishes for microscopic analysis. This macrofossil evidence could include fish vertebra, flowers and leaves. The material between 10 and 180 micrometers was processed using standard procedure, removing non-desired material from the soil sample piecemeal. In turn, the microfossil material was pretreated with HCl (to remove carbonates), KOH (to remove humid acid), HF (to remove silicates) and acetolysis (to remove other organic material). Pollen concentrations were placed on slide mounts. These were counted under 400x magnification, and between 25 and 100 pollen grains/spores were counted per sample. Preliminary identifications were then made using comparison of the slides to two pollen catalogs, the *Key to the Quaternary Pollen and Spores of the Great Lakes Region* (McAndrews et al 1973) and the *Pollen Key for the Venezuela Guayana* (Rull 2003).

The following graphic depicts the prominent pollen types found. In total, there were 25 different classified types with 13 of these types being discovered in totals of less than 10 spores. This table shows the 12 most prevailing taxa found in this investigation. There were 9 unknown types per comparison with the two catalogs. Further comparison will need to be done in hopes of determining the source and taxa involved in these unknowns. Since this preliminary study was done without a spike (a non-native pollen taxa for concentration reference) because it was unknown what plants would have been native at the time nor was the soil weighed prior to flotation, this data is raw and uncontrolled for over or under-representation.

Overall, there were good preservation levels of the pollen, particularly during the time of Rancho del Rio's inhabitance. The main types of pollen identified consisted of grasses (*Poaceae*), herbs, shrubs, and *Lycopodium*. The microfossil findings from our study correlate well to findings of *Poaceae* in Highland Guatemala (Islebe and Hooghiemstra 1996:1091-1099) and a fair amount of *Gramineae* and *Chenopodiaceae* at the interval 0-1 m BGS in northern Belize (Hansen 1990:174-175).

Site	Depth (cm)	A	B	C	D	E	F	G	H	I	J	K	L	T. Count
1	80	8	0	10	0	3	1	0	1	0	0	0	0	**24**
4	37	8	8	24	2	12	3	3	1	1	7	3	0	**78**
	40	1	2	4	0	39	0	9	6	3	2	29	4	**100**
	70	3	2	8	1	0	1	2	0	3	1	2	0	**25**
5	40	3	2	10	2	8	2	3	3	2	0	7	2	**50**
6	26	5	3	23	0	6	1	0	1	3	0	4	3	**50**
	26	7	1	11	1	7	2	1	2	4	0	2	3	**51**
	26	1	0	20	1	12	0	1	0	1	3	5	0	**51**
	65	13	0	13	0	11	1	0	5	4	0	1	0	**50**
	65	6	0	7	0	6	0	0	4	1	0	1	0	**25**
8	20	3	1	8	0	2	2	0	2	2	1	3	0	**25**
	40	0	5	11	1	10	2	1	1	11	3	0	0	**46**
	40	5	3	7	0	3	0	3	0	2	0	0	1	**25**
	40	2	5	6	3	2	0	2	0	3	0	1	0	**25**
	Grand Totals	**65**	**32**	**162**	**11**	**121**	**15**	**25**	**26**	**40**	**17**	**58**	**13**	**625**

Note: The total count column is the total number of all pollen types counted for that particular soil sample.

Pollen Types in table 1	
A = *Poaceae*	G = Unknpown 1
B = *Cyperaceae*	H = Unknown 2
C = *Lycopodium*	I = Indeterminable
D = *Chenopod*	J = Unknown 5
E = *Myrsine guianesis*	K = Unknown 6
F = *Xyris* type	L = *Tepuianthus ayuantepuyensis*

Table 1. Prominent Pollen Types.

An additional important finding was the complete absence of maize and corn from the fossil assemblage. At first glance this might seem to support the concept of a resource specialized site producing ceramics and trading for food. However, there are manos and metates (stone grinding tools used in food preparation) in artifact assemblage indicating some level of food processing occurring on site and as such, some level of evidence in the pollen record should exist. It is also possible that the used agricultural field lies outside the collection area or that the evidence of maize was destroyed over time. The evidence might still be present in phytoliths and further research might prove this to be true.

More systematic pollen studies combined with the examine the teeth found at the site for tooth decay as Clark Larsen did in Georgia (Renfrew and Bahn 2000:307) or even systematic analysis for the change in ^{13}C in soil humus looking for signature changes pointing towards maize cultivation (Webb et al 2004:1039-1040) may provide more detailed information concerning the production of maize on the site.

Therefore, although our study was only a preliminary one, some general information has been added to the archaeological depiction of life at Rancho del Rio. At face value, this study has aided in drawing together possible hypotheses regarding agriculture, trade, and usages of this region during the late Classic and early Postclassic time periods even if it has not fully answered our earlier questions about dietary resources.

REFERENCES

Hansen, B.C.S. (1990) Pollen Stratigraphy of Laguna de Cocos. In Ancient Maya Wetland Agriculture, Excavations on Albion Island, Northern Belize. M.D. Pohl, ed. Boulder, CO: Westview Press, 155-186.

Islebe, G.A. and H. Hooghiemstra (1996) Recent Pollen Spectra of Highland Guatemala. *Journal of Biogeography* 22(6):1091-1099.

McAndrews, John H., Albert A. Berti, and Geoffrey Norris (1973) Key to the Quaternary Pollen and Spores of the Great Lakes Region. Toronto: The University of Toronto Press for the Royal Ontario Museum [out of print].

Renfrew, Colin and Paul Bahn (2000) Archaeology: Theories, Methods, and Practice (Third Edition). New York: Thames and Hudson, Inc.

Rull, Valentí (2003) Pollen Key for the Venezuela Guayana. Internet. http://einstein.uab.es/vrull/Guayana_key/initial.htm (originally an abbreviated published piece in *Palynology*, 27:99-133).

Sharer, Robert J. (1994) Ancient Maya (Fifth Edition). Stanford: Stanford University Press.

Urban, Patricia and Edward Schortman (2003) Pottery Dating at Rancho del Rio (field activity)

Webb, Elizabeth A., Henry P. Schwarcz, and Paul F. Healy (2004) Detection of ancient maize in lowland Maya soils using stable carbon isotopes: evidence from Caracol, Belize. *Journal of Archaeological Science 31*: 1039-1052.

COOKING ACTIVITIES IN A BUILDING YARD DURING THE MIDDLE AGE. ORGANIC RESIDUES IN POTSHERDS RECOVERED FROM THE CARMINE CONVENT IN SIENA

Alessandra Pecci, Francesca Grassi
Dipartimento di Archeologia e Storia delle Arti, Università di Siena

Laura Salvini, Gianluca Giorgi
Centro di Analisi e Determinazioni Strutturali, Università di Siena

1. INTRODUCTION

Lipid analysis is very useful in the identification of vessel contents, because lipids are contained in virtually all human food, both plants and animals. Moreover, lipids, in particular fatty acids, are very well preserved even in the archaeological context (Rottlander 1990:37).

In order to obtain information about the Middle Age dietary, efforts were made in the analysis of organic residues absorbed within the ceramics. In particular we present here the results of the study of the organic residues absorbed in nine potsherds taken from some vessels recovered from the Carmine Convent in Siena.

During the restauration of the Convent carried out at the beginning of 2001, a voult built at the beginning of the XIV th. century was discovered and it showed a very interesting filling. Hundreds of ceramic vessels were placed to fill the space between the vault and the upper floor (figure 1). The Medieval Archaeology Area of the University of Siena realized, in agreement with the Soprintendenza Archeologica and the Soprintendenza ai Beni Ambientali e Architettonici of Tuscany, an emergency excavation of half of the vault, digging and digitally documenting the work (Francovich, Valenti 2002).

Most of the pottery found was discarded material obtained from the ceramic workshops present in the area around the Convent. Some of them were instead fragments of jars and pans probably used by the workers for cooking their meals or as food containers. They were characterized by a coarse ware and burnt traces. It could be reasonably supposed that these

Figure 1. Filling material of the vault.

vesels preserved some organic residues of the food cooked or stored in them. Nine sherds were sampled: four jars, two lids, three pans, one of which had holes in the bottom (sample 9).

2. EXPERIMENTAL

Spot tests developed in the Archaeometric Laboratory of the UNAM, Mexico, were performed following Barba et al. 1991.

Afterward the samples were extracted and saponified following previously reported procedures (Regert et al. 1998) and analysed by gas chromatography-mass spectrometry (GC/MS).

The analyses were performed using a mass spectrometer Saturn 2000 (Varian, Walnut Crick, CA) equipped with a 30 m x 0.25 mm (i.d.) fused silica capillary column coated with a DB5 stationary phase (0.25 μm film thickness).

For the lipid extract, the column temperature was held isothermally at 50°C for 1 min immediately after injection, then was increased from 50°C to 300°C at 5°C/min and held for 10 min.

The temperature program for the saponified samples consisted of a 1 min isothermal hold at 40°C followed by a ramp from 40°C to 300°C at 3°C/min (held for 20 min).

The mass spectrometer was operated in the electron ionization mode (70 eV). The injector and the transfer line temperatures were 280°C and 170°C respectively. The mass spectrometer was scanned over the *m/z* 40-650 range.

3. RESULTS AND DISCUSSION

According to the results obtained by the spot tests two different groups of samples were identified. The first one characterized by high amount of fatty acids (group A) and the second (group B) by their absence. The gas chromatograms obtained from the lipid extraction of the analysed samples showed the presence of different classes of compounds. Although it was not possible to identify all the peaks of the chromatograms, we were able to establish the nature of most of them. In particular, the fatty acids detected are those usually used in literature to trace animal and vegetable origin of the fats (Evershed et al. 2002, Mottram at al. 1999). In fact the most abundant were saturated and monounsaturated fatty acids with 16 and 18 carbon atoms. Also saturated fatty acids with shorter chain were detected.

On the basis of their organic contents, the samples were divided into three main groups. The first two correspond to group A characterized using the spot tests.

The first group is constituted by samples showing the predominance of saturated fatty acids especially palmitic ($C_{16:0}$) and stearic($C_{18:0}$) acids even if different isomers of monounsaturated $C_{18:1}$ were present (figure 2, left). The origin of these organic residues can be related to degraded animal fats, due to the high amounts of the saturated $C_{18:0}$ fatty acid.

The samples can be further differentiated on the basis of the ratio $C_{16:0}/C_{18:0}$. In three samples the abundance of the $C_{18:0}$ and $C_{16:0}$ components

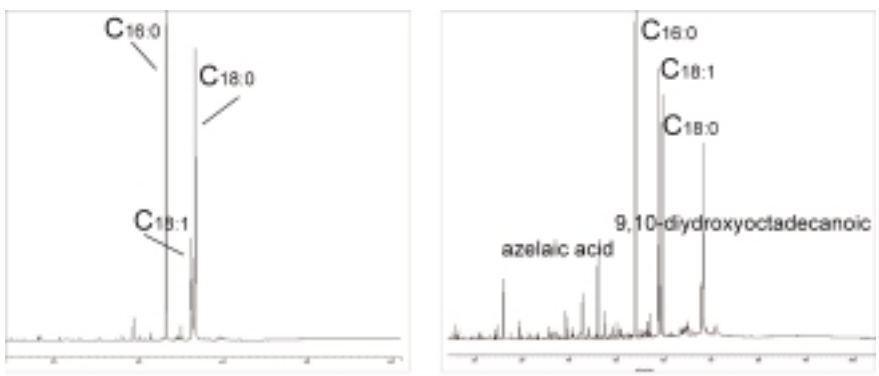

Figure 2. Partial gas chromatogram of the total lipid extract of one of the samples that showed the presence of animal fat (left). Alkaline treatment of the insoluble residues of the sample of the jar which probably contained olive oil (right).

is similar. The ratio $C_{16:0}/C_{18:0}$ close to 1 is characteristic of "cauldron" potsherds analysed by Mottram (Mottram et al., 1999). These are general purpose cooking vessels that are supposed to contain lipid residues of mixed origin.

The presence of odd number fatty acids, such as $C_{15:0}$ and $C_{17:0}$ and their branched forms, produced by ruminant animals through the activities of gut bacteria, suggests that among the animal meat cooked there were ruminants (Mottram et al., 1999).

In another sample from this group the $C_{16:0}$ component was more abundant than the $C_{18:0}$. No odd number fatty acids were detected, suggesting that no ruminant animals were cooked in it.

The alkaline treatment of the insoluble residues, besides the free fatty acids observed also in the solvent extraction (discussed above), yielded appreciable amounts of oxygenated fatty acids derivatives. In particular a series of α,ω–dicarboxylic acids, ranging from C_7 to C_{12}, have been identified, together with α- and ω-hydroxy acids. All these components are the result of complex decomposition processes of fatty acids occurring during the use and the burial of the potsherds.

The second group is formed of only a jar. The GC-MS chromatogram of the total lipid extract of this sample shows the presence of high amount of the monounsaturated $C_{18:1}$ fatty acid and small amounts of saturated components such as $C_{16:0}$ and $C_{18:0}$. The predominance of $C_{18:1}$ suggests that mainly vegetable oil have been stored in this jar. Furthermore the alkaline treatment of the insoluble residues of the sample shows the predominance of the azelaic acid, a bicarboxylic acid with nine carbon atoms, and high amounts of 9,10-dihydroxyoctadecanoic acid (figure 2, right). These acids are related with the decomposition of the oleic acid (Regert et al. 1998). It is known that oleic acid is the main component of olive oil. This suggest that probably the jar contained olive oil. Laboratory degradation experiments performed on olive oil absorbed in ceramic potsherds showed a lipid profile similar to the one obtained for the sample analysed (Dudd, Regert, Evershed 1998).

The third and last group (correspondig to the group B of the spot tests) is composed of the three samples. In this case the presence of fatty acids was undetectable. This is an interesting result from the archaeological point of view because it shows that the vessels were not used to contain vegetable or animal oils nor any other liquid rich in fats. It is then possible to suppose that two of them were probably used to contain or boil water and possibly cereals. The pan with holes on the bottom might have been used as a colander, but the burnt traces on the external part suggest that it was exposed to the fire. These elements point to the possibility that it was used to roast chestnuts, a very common food during the Middle Age.

Figure 3. Pan with holes on the bottom.

4. CONCLUSIONS

This study showed that different and specific amounts of fatty acids are present in the samples analysed. The differentiation of fatty acid profiles, depending on the nature of the ceramic samples, suggested a different use of these objects.

On the basis of the total lipid profiles, three groups of objects were distinguished. One of these was formed of samples that did not show any presence of fatty acids. This suggests that they were used for containing or boiling water or other substances not rich in fats. In particular, sample 9 might have been used as a colander or to roast chestnuts. The second group is formed of a sample of a jar that might have been used to contain olive oil. The other samples might have been used to cook different kinds of foodstuff, including animals.

The information provided by the spot tests concerns only the presence-absence of fatty acids. Nevertheless the correlation between the results

obtained applying the spot tests and the GC-MS analysis showed the validity of the first technique, expecially for a first screening on a big amount of samples.

REFERENCES

Barba, L.; Rodríguez, R.; Córdoba, J.L., 1991, *Manual de técnicas microquímicas de campo para la arqueología*, IIA, UNAM, Mexico.

Dudd, S.; Regert, M.; Evershed, R., 1998, "Assessing microbial lipid contributions during laboratory degradations of fats and oils pure triacylglycerols absorbed in ceramic potsherds" *Organical Geochemistry*, vol. 29 n.5-7:1345-1354.

Evershed, R.; Dudd, S.; Copely, M.; Berstan, R.; Scott, A.; Mottram, H.; Bulley, S.; Crossman, Z., 2002 "Chemistry of Archaeological Animal Fats", *Accounts of Chemical Research*, vol 35, n.8:660-668.

Francovich, R., Valenti, M. 2002 *C'era una volta. La ceramica medievale nel convento del Carmine*, Polistampa, Firenze.

Mottram, H. R.; Dudd, S. N.; Lawrence, G. J.; Stott, A. W.; Evershed, R. P., 1999 "New chromatographic, mass spectrometric and stable isotope approaches to the classification of degraded animal fats preserved in archaeological pottery", *Journal of Chromatography A*, n. 833:209-221.

Regert, M.; Bland, H. A.; Dudd, S.; van Bergen, P.; Evershed, R., 1998 "Free and bond fatty acid oxidation products in archaeological ceramic vessels", *The Royal Society B*, vol. 265, pp. 2027-2032.

Rottlander, R., 1990 "Lipid Analysis in the identification of vessel contents", in W. Biers, P. McGovern *Organic contents of ancient vessels: material analysis and archaeological investigation*, MASCA, University of Pennsylvania, Philadelphia, pp. 37-40.